2 items in back pocket

TECTONO-STRATIGRAPHY AND EVOLUTION OF THE MESOZOIC PINDOS OPHIOLITE AND ASSOCIATED UNITS, NORTHWEST GREECE.

GREGORY JONES

SUBMITTED FOR THE DEGREE OF DOCTOR OF PHILOSOPHY

UNIVERSITY OF EDINBURGH

1990

ABSTRACT

The northwest Pindos Mountains of Greece expose a sequence of Mesozoic and Tertiary thrust sheets, which include the Jurassic Pindos ophiolite, composed of ultramafic and mafic oceanic crust and mantle. Regional mapping has established the tectonic order of these units from top to base as follows: i) a mainly ultramafic ophiolitic thrust sheet (Dramala Complex of the Pindos Ophiolite Group) and basal metamorphic sole (Loumnitsa Unit of the Pindos Ophiolite Group); ii) Late Cretaceous platformal limestones (Orliakas Group); iii) dismembered intrusive and extrusive ophiolitic rocks (Aspropotamos Complex of the Pindos Ophiolite Group); iv) tectonic melange and olistostromes, dominated by Triassic-Jurassic volcanic and sedimentary rocks (Avdella Melange); v) coherent thrust sheets of Late Jurassic-Late Cretaceous deep-water sediments (Dio Dendra Group); vi) Early Tertiary flysch (Pindos Flysch). Immobile trace-element studies indicate that the Triassic and Jurassic extrusives of the volcanic-sedimentary melange, formed mainly at within-plate through to mid ocean ridge settings. By contrast, the structurally overlying ophiolitic extrusives include boninite series volcanic rocks and depleted island arc tholeiites, indicative of a supra-subduction zone origin. Initial displacement of the ophiolite (ca 165 Ma) is recorded in the formation of a metamorphic sole, passing structurally downwards from a basal peridotite mylonite zone into amphibolite and greenschist facies rocks. The sole rocks in general have MORB and WPB trace-element chemical affinities, although a limited number of samples are more depleted in high field strength elements, and can be correlated with rocks of island arc origin, including boninites. Petrological and structural comparisons suggest the Pindos ophiolite is regionally continuous beneath the Meso-Hellenic trough with the Vourinos ophiolite to the east. This ophiolite, similarly has a supra-subduction zone chemical signature, and is also underlain by fragmentary metamorphic sole and melange units.

In the favoured tectonic model, the Pindos ophiolite formed above a Early to Mid Jurassic westerly-dipping intra-oceanic subduction zone. Continuing subduction produced a thick accretionary complex, now represented by the Avdella Melange that underlies the Pindos ophiolitic units. During the Late Jurassic, the supra-subduction zone ophiolite was emplaced as a relatively undeformed sheet, northeastwards onto the Pelagonian Zone, an assumed microcontinent. The "fore-arc" crust situated immediately above the subduction zone was detached and overthrust by the remainder of the ophiolite sheet during this emplacement stage. Following this, the Pindos ocean remained partly open to the west as a remnant basin, undergoing deep-water and marginal carbonate deposition from the Late Jurassic to Late Cretaceous. In Early Tertiary time (?Palaeocene-Eocene), this basin began to close. The Pindos ophiolite was sliced, and together with the dismembered fore-arc, Jurassic melange and younger deep-water sediments, was thrust westwards over a flexural foreland basin (Pindos Flysch), and then onto the Apulian continental margin as an inboard-propagating thrust stack. Inferred footwall structures (old palaeogeographic features?) and/or late stage folding were mainly responsible for the formation of large orthogonal (e.g. Armata-Milea corridor) and transverse (e.g. Perivoli corridor) culminations. Final thrusting was accompanied by extension behind the deformation front, leading to the formation and infilling of the Meso-Hellenic molasse basin.

up unannounced. Similarly, patrons of the Milionis and Perdhiki hotels are thanked for their hospitality at various times. Sarandis Dimitiradis is thanked for his logistical support, particularly during the first field season. Also, I would like to thank the friends I made in Perivoli for adopting me as one of their own, especially, Litsa, Katerina, Yannis and Vangelitsa and the multitudinous members of their family, and to Virgil and Becky Marco for introducing me to them all.

In Edinburgh, I would like to thank the members of the "Tethyan Group" for their companionship and deep discussions on Tethyan geology during my time there! and particularly Pete Clift, with whom much of this adventure has taken place, despite the car. The attic mob (1987 vintage) are duly acknowledged. Geoff Angel, Dodie James, Diana Baty, Yvonne Cooper, and John Miller have been particularly helpful teaching me laboratory techniques, and Euan Clarkson kindly allowed me use his laboratory facilities. Many other people have helped me out at various stages of this project, particularly the indispensible Helena, Heather and Denise, and I give them a collective "thank you".

The last few years would not have been the same without Eva, and I thank her for putting up with me during this time. Finally, I would like to thank my parents and my brother for their support during my whole higher education, it is all down to them that this thesis exists. I hope I can share the rare beauty of the north Pindos Mountains with them one day.

CONTENTS

List of Figures

Chapter 1

Chapter 2

Chapter 3

List of Plates

CHAPTER 1

INTRODUCTION TO THE GEOLOGY OF THE NORTH PINDOS MOUNTAINS, WITHIN THE FRAMEWORK OF THE EASTERN MEDITERRANEAN

1.1 Introduction

The tectonic setting, genesis and emplacement of ophiolites and related former deep-sea units in the Mesozoic Tethyan orogenic belt, has attracted the interest of geologists for many years. One key area within the Tethyan system is the Pindos ophiolite, situated in the northern Pindos Mountains of Greece. The Pindos Mountains, part of ancient western Macedonia, form an elongate north-south chain, found in western mainland Greece, and northwards into Albania.

The topography is dominated by flat-topped mountains, separated by deeply incised river valleys. The highest mountains are found in the north, where the twin peaks of the Smolikas Mountains reach a maximum height of 2637 m, and several other peaks also exceed 2000 m. The mountains give way to lower-lying (up to 1000 m), rolling hills to the east, in the Grevena district. The mountain vegetation is dominated by extensive pine forest, mostly black pine, which grows up to 2300 m, and the beech is also common in certain areas. The fauna and flora of the Pindos Mountains are the richest in Europe, with greater than 6000 species present, including the European brown bear, the wolf, the Golden Eagle and the Lammergeyer. The major centres of population are the towns of Grevena in the east, and Ioanina in the west, in both of whose provinces the north Pindos Mountains lie. Within the mountains themselves, the Koutsovlach transhumant and permanent villages of Metsovo, Vovousa, Perivoli, Avdella, Samarina and Dhistraton are busiest in summer.

1.2 Geotectonic setting of the north Pindos area.

The Greek area forms part of the Early Tertiary Alpine orogenic system, which is represented in this area by the parallel tectonic belts that constitute the Hellenides (Fig. 1.1). This zone of continental collision represents the result of final closure of the Tethys Ocean (Neumayr 1875), which had existed as an embayment into the Pangean supercontinent since the Late Palaeozoic. In palaeogeographic reconstructions of the Tethys, two distinct oceanic realms are distinguished in time: a mainly Palaeozoic ocean (Palaeotethys), and the Mesozoic to Early Tertiary Neotethys (Dercourt et al. 1986; Robertson and Dixon 1984). Neotethys formed by rifting of the continent of the Permo-Triassic Gondwana supercontinent, perhaps following the closure of Palaeotethys (e.g. Sengor et al. 1984).

Critical to the understanding of the Hellenides, is the reconstruction of the various palaeogeographic elements which existed over time. Neotethys, with which we are primarily concerned here, was thought to have consisted of a series of continental fragments separated by small ocean basins (Fig. 1.2). These microcontinental slivers probably rifted away from the northern margin of Gondwana, during the Middle Triassic break up of this continent (e.g. Robertson and Dixon 1984). The primary site of the closure of Neotethys within Greece, was believed to be represented by the units of the Vardar Zone, of the "internal" (i.e. northeasterly) Hellenides (Fig. 1.3). However, closure of other small Tethyan basins was also demonstrated in the external Hellenides (e.g. the Othris Ocean, Smith 1975), both areas displacing oceanic basement (ophiolites) onto continental margins.

1.3 Subdivisions of the Greek Hellenides

The geology of Greece (summarised in Aubouin et al. 1970, 1977; Smith and Moores 1972) essentially consists of a series of northwest-southeast-trending parallel tectonic belts, the "isopic zones" of Aubouin (1959; Fig. 1.3). These are areas of variable lithology and structural/metamorphic histories, brought into contact along major tectonic boundaries. The isopic zones are therefore in some ways comparable to tectonostratigraphic terranes defined in other regions (Howell, 1989). The main difference is that the Greek isopic zones often have many stratigraphic and tectonic features which can be

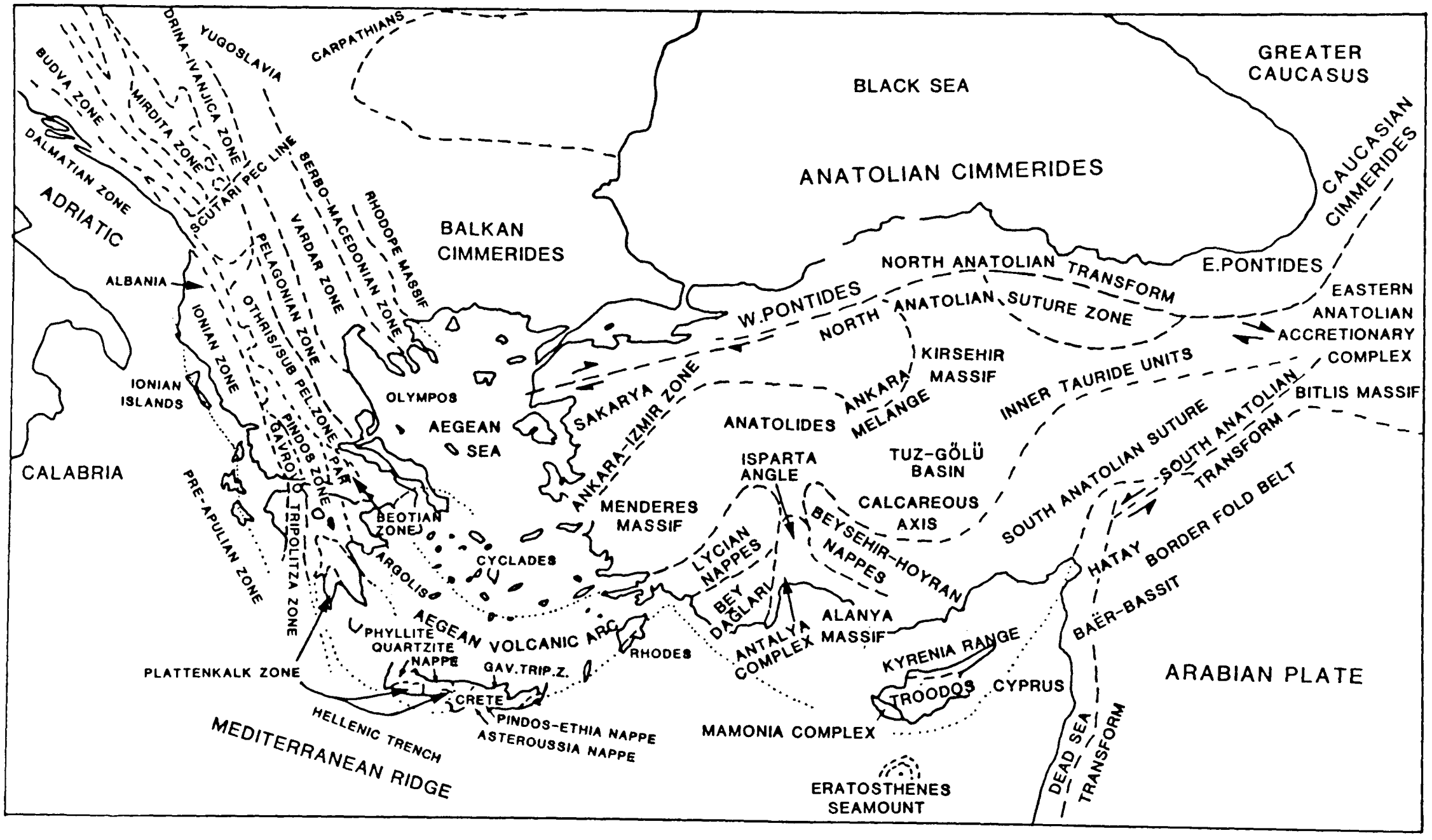

Fig. 1.1 Tectonic elements of the Eastern Mediterranean and near East region, based on Robertson and Dixon (1984). Note the position of the "internal" and "external" Hellenides, and the continuation of the tectonic belts to the north and east of Greece.

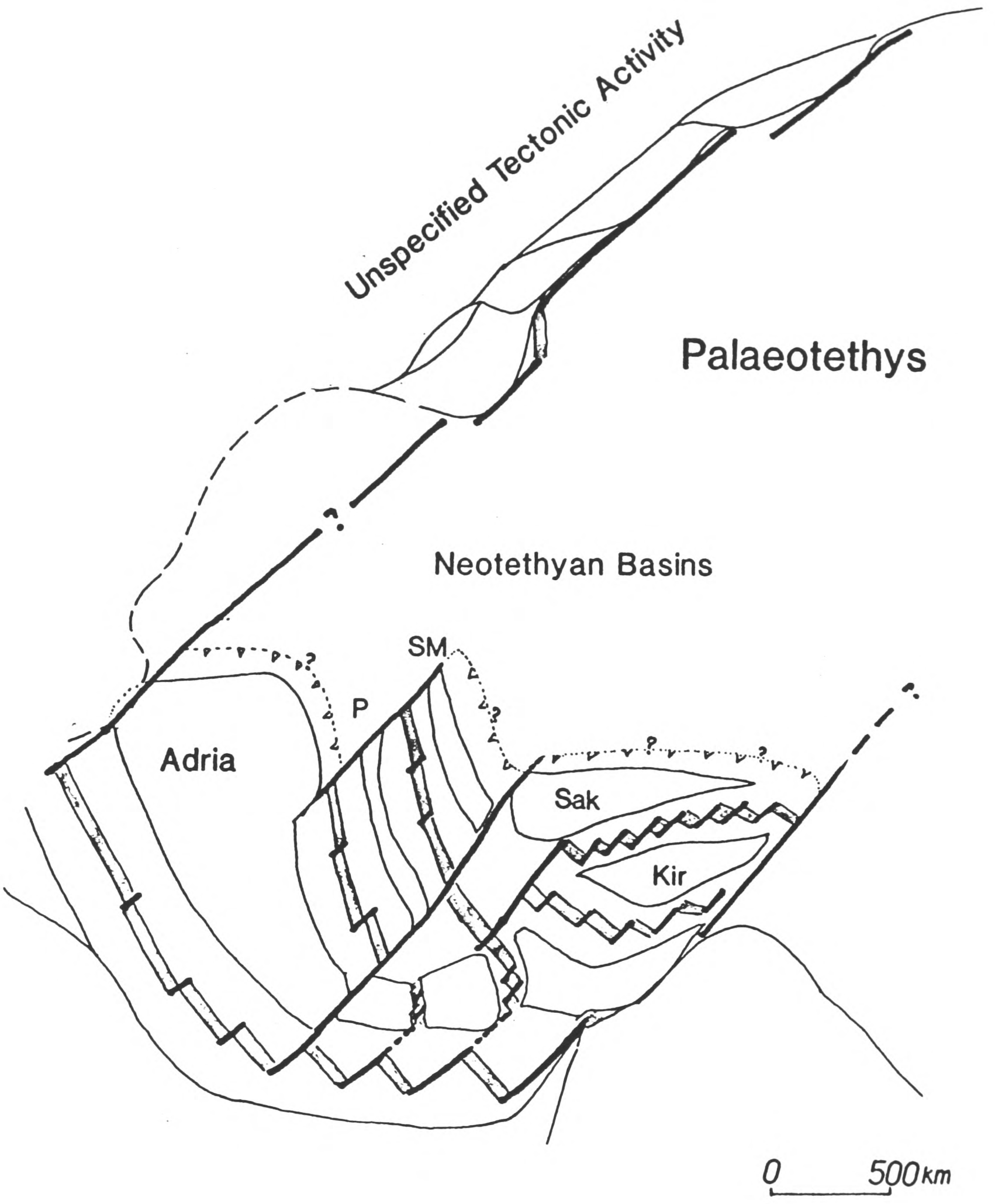

Fig. 1.2 Palaeogeographic reconstruction of the northern margin of Neotethys during the Jurassic, showing the positions of various small ocean basins (including the Pindos or Othris ocean) and rifted continental fragments (e.g. the Pelagonian). After Robertson and Dixon (1984).

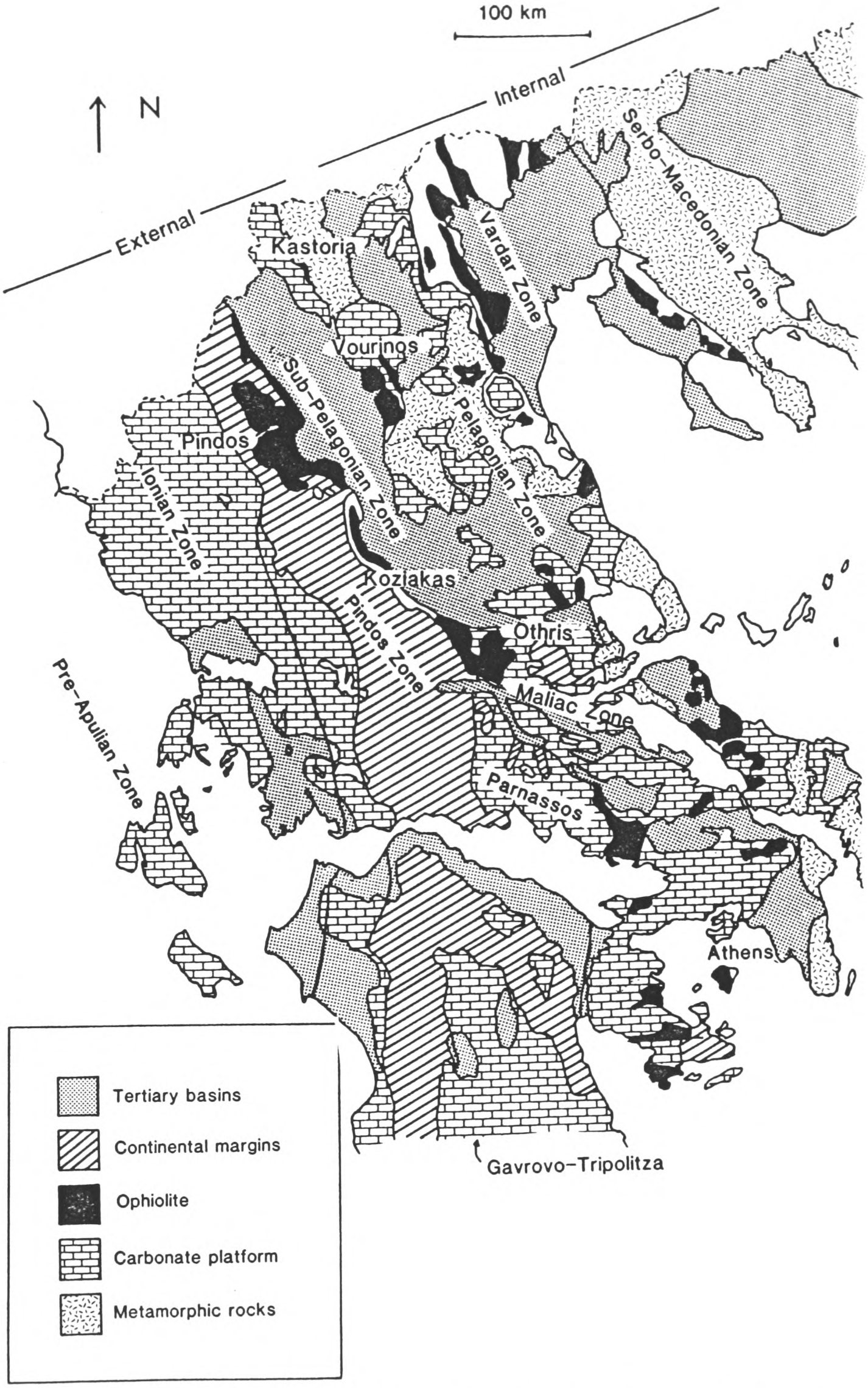

Fig. 1.3 Tectono-stratigraphic zones of Greece ("Isopic Zones" of Aubouin 1959), modified after Vergely (1984). The main outcrops of ophiolitic rocks are also shown. Note the position of the study area, located within the Pelagonian, Sub-Pelagonian, and Pindos Zones of the external Hellenides.

correlated across zone boundaries, implying that the amount of lateral motion between them is probably limited (Jones et al. 1988). The concept of isopic zones is therefore primarily limited by the "cylindrical" view of Greek geology which it advocates.

The study area (Fig 1.4) encompasses three of the isopic zones of Aubouin (op. cit): the Ionian, Pindos and Sub-Pelagonian Zones. These will be described below, along with other Zones relevant to the geological evolution of the region (refer to Figs. 1.1. and 1.3 for the position and extent of each isopic zone).

The *Ionian Zone* in western Greece represents (Figs. 1.3; 1.5) part of the Apulian continent (*Pre-Apulian Zone* in Greece), which was probably located at the northeastern edge of the African plate, which finally collided with Europe during the Tertiary. The Ionian Zone consists of probable continental basement and carbonate cover sequences (Permian-Tertiary) of intra-platform basinal facies, overlain by Tertiary Flysch (IGME/IFP 1966; Aubouin et al. 1970). In central and southern Greece, the *Gavrovo-Tripolitza Zone* is of true platform carbonate facies, and is overthrust by the Pindos Zone sequences. All these sequences were deformed primarily during Alpine collision.

As classically defined, the *Pindos-Olonos Zone* consists of a series of deep-water carbonate and terrigenous sediments of ?Mid Triassic to Tertiary age (Aubouin 1959; Fleury 1980; Green 1983; Fig. 1.5), considered to be the continental margin and basinal sequences of an ocean formed west of the Ionian platform (Othris ocean, Smith 1975). The Pindos Zone sequences are thought to be allochthonous in central Greece, and similarly in southern Greece they form a far-travelled nappe. In the study area, the Pindos Zone is represented only by flysch and deep-water carbonate sequences of Latest Jurassic to Eocene age, older sediments not being exposed. The ophiolites and melanges of the Sub-Pelagonian Zone overthrust the sediments of the Pindos Zone, and were thus emplaced southwestwards in the Late Eocene.

The *Sub-Pelagonian Zone* (Othris Zone; Smith et al. 1975) is complexly tectonised, consisting of major ophiolite complexes (e.g. Pindos, Vourinos, Othris), and associated tectonic and sedimentary melanges, containing a large variety of oceanic and continental margin sediments, together with abundant volcanic rocks. In the study area, the Pindos ophiolite is associated with thick

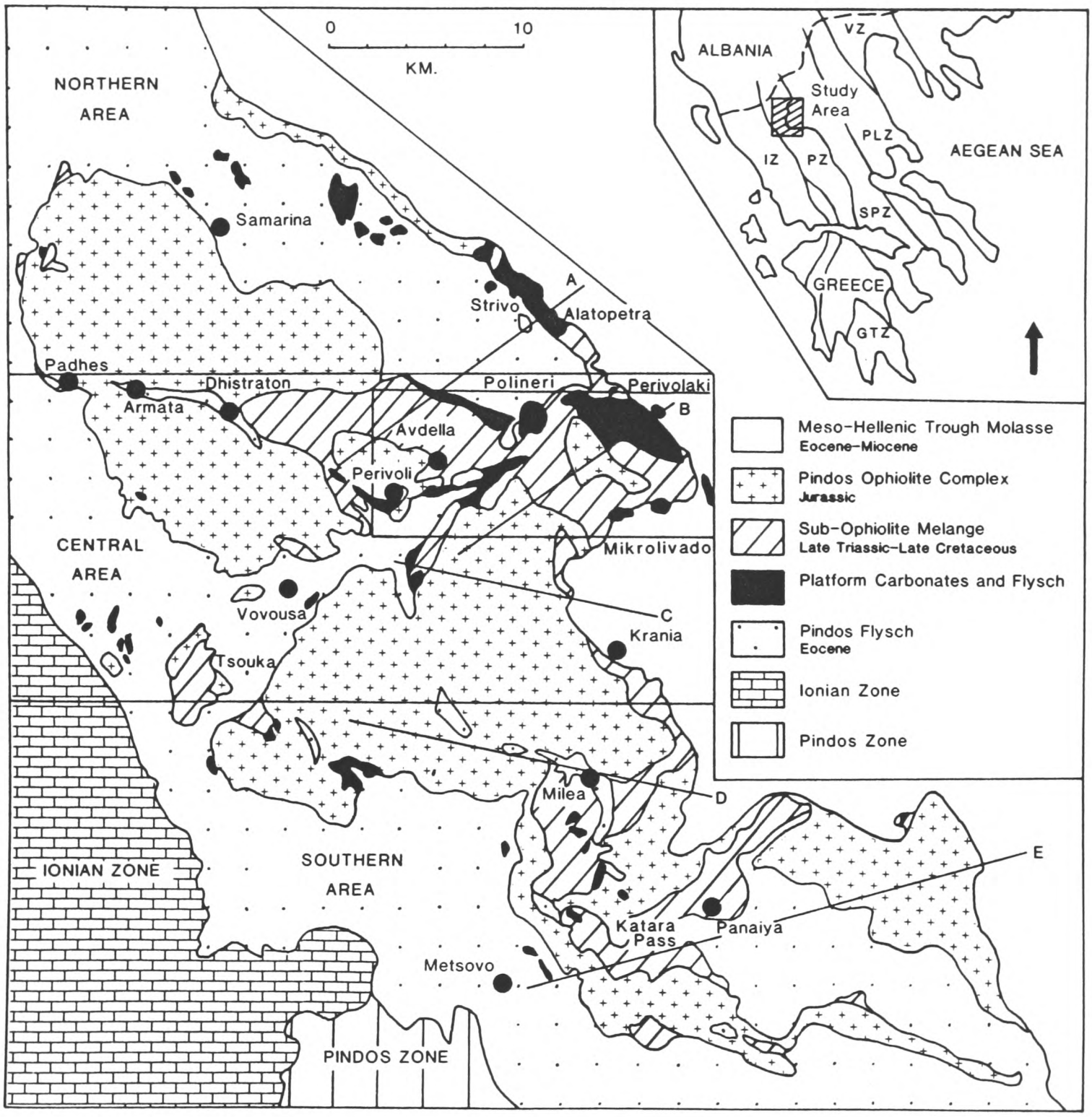

Fig. 1.4 Outline geological and locality map of the north Pindos Mountains. Modified after Brunn (1956).

A

Radiolarite
Mudstone
Sandstone
Evaporite
Replacement chert
Carbonate platform
Rift volcanics and volcaniclastics
Dolomite
Rift clastics
Metamorphic basement

500
metres
0

Pelagonian
Othris
Ionian
Pindos
Euboean
Parnassos
Gavrovo

Ol
Eo
Pal
UCr
LCr
UJu
MJu
LJu
Tr

IONIAN

Pal
Ma
UCr
LCr
UJu
LJu
Tr

GAVROVO–
TRIPOLITZA

Pal
UCr
LCr
UJu
LJu
UTr

PINDOS
OLONOS

Pal
UCr
LCr
UJu
LJu
No
Ca
An
LTr

VARDOUSSIA

Pal
UCr
LCr
UJu
MJu
LJu
UTr

PARNASSOS

LCr
UJu
MJu
UTr

BEOTIA

Tith
UJu
LJu
UTr
LTr
UPm
Z Z

OTHRIS

Tith
UJu
MJu
LJu
UTr
MTr

EUBOEA

UJu
?UJu
?MJu
?LJu
?Pm

N.PELAGONIAN
METAMORPHIC

B

100
m
0

Radiolarites
Ma
Da
Redeposited
carbonates
No
Ca
Radiolarites
Basalts

From Ferrière 1982

Fig. 1.5 a) Summary of the stratigraphy of the Ionian, Pindos, Sub-Pelagonian and Pelagonian Zones (after Robertson et al. in press). b) The stratigraphy of the Koziakas Mountains.

tectonic and sedimentary melange. The Koziakas Mountains area, located west and southwest of Kalambaka contains overthrust sequences which are sedimentologically considered transitional between Sub-Pelagonian Zone and Pindos Zone sequences (Ferriere 1982; Lekkas 1988; Jones and Robertson 1990; Fig. 1.5)

The *Pelagonian Zone* (Figs 1.3; 1.5) forms the boundary between the internal and external Hellenides, and is fundamental to the understanding of the whole system. The Pelagonian Zone consists of Palaeozoic metamorphic basement and granites, with a cover of Late Palaeozoic and Early Mesozoic clastic sediments, with Triassic-Jurassic metamorphosed and non-metamorphosed platform carbonates (e.g. Kastoria area; Mountrakis 1986). The ophiolites and melanges of the Sub-Pelagonian Zone overthrust the Pelagonian zone, and are transgressed by Late Jurassic to Late Cretaceous cover sequences (Brunn 1956), therefore also indicating a Late Jurassic emplacement event for the ophiolites ("Eohellenic orogeny", Jacobshagen et al. 1976).

The *Vardar Zone* (Fig. 1.3) represents an extensive suture zone, formed during the closure of a more easterly Neotethyan basin, the Vardar Ocean (Brunn 1956; Mercier 1966; Vergely 1984). The zone comprises similar units to the Sub-Pelagonian Zone, including dismembered ophiolite sheets, arc volcanic units and extensive melange of pre-Cretaceous age (e.g. Edessa region; Mercier and Vergely 1972). Closure of the Vardar Zone is considered by several authors (Aubouin et al. 1970; Bernoulli and Laubscher 1972; Vergely 1976, 1977, 1984), to have been responsible for the Jurassic emplacement of the Sub-Pelagonian ophiolites across the Pelagonian Zone, into the Othris (or Pindos) ocean. The Olympus "window" on the eastern Pelagonian margin (Godfriaux 1962; Barton 1976), has revealed that Eocene carbonates of the Olympus sequence are overthrust by Pelagonian basement nappes, and in addition, extensive blueschist formation has occured (Godfriaux and Schmitt 1982). Further to the northeast, the complexly deformed basement and cover sequences of the *Serbo-Macedonian and Rhodope Zones* are found.

The *Maliac Zone* (Ferriere 1972, 1976; Smith et al. 1975), is defined as the zone of transition between the Othris ophiolite and Sub-Pelagonian sequences of central Greece, and the sedimentary Pindos Zone. However, the Maliac

Zone essentially can be considered part of the Sub-Pelagonian Zone, as it seems to contain sequences essentially similar to this Zone in other parts of Greece, including the study area. West of the Maliac Zone, and east of the Pindos Zone is the *Beotian Zone*, as defined by Celet and Clement 1971). This zone was based on the occurrence of Late-Jurassic to Early Cretaceous flysch sequences, and extended from the Argolis peninsula to the north Pindos area. The construction of this zone was criticised (e.g. Papanikolaou and Sideris 1979), because it did not represent a palaeogeographic entity.

One other palaeogeographic entity which is relevant to this discussion is the *Parnassos platform*, consis ting mainly of ?Norian to Mid Eocene neritic limestones (Celet 1962), now thrust and folded. Parnassos lies to the west of the Othris ophiolite in southern central Greece (and thus west of the Maliac Zone), and probably represents a rifted fragment of the Gavrovo-Tripolitsa platform (Fleury 1980).

1.4 Tethyan ophiolites

Ophiolites (Greek for "snake rock") are fragments of oceanic crust and mantle which have been emplaced onto continents during collisional tectonic episodes. Tethyan ophiolites, due to their size and abundance, have received an enormous amount of attention over the past twenty years, since it was realised that ophiolites represent on-land fragments of oceanic crust (Gass 1968). Two Tethyan ophiolites in particular, the Troodos ophiolite of Cyprus, and the Semail ophiolite of Oman have been, and continue to be, the subject of intense scientific study (Gass 1990). These ophiolites present an unparalleled opportunity to view a part of the earths crust and mantle, which otherwise remains virtually inaccessible. Also of equal interest, has been the question of how these great ophiolite bodies were displaced from ocean basins onto continents during orogenesis.

A general map of Tethyan ophiolites (Fig. 1.6) shows the distribution of these bodies across Europe and Asia. The Pindos ophiolite is therefore part of a long fragmentary chain of ophiolites, interpreted as having been displaced from a series of small oceans, which together constitute the Tethys Ocean.

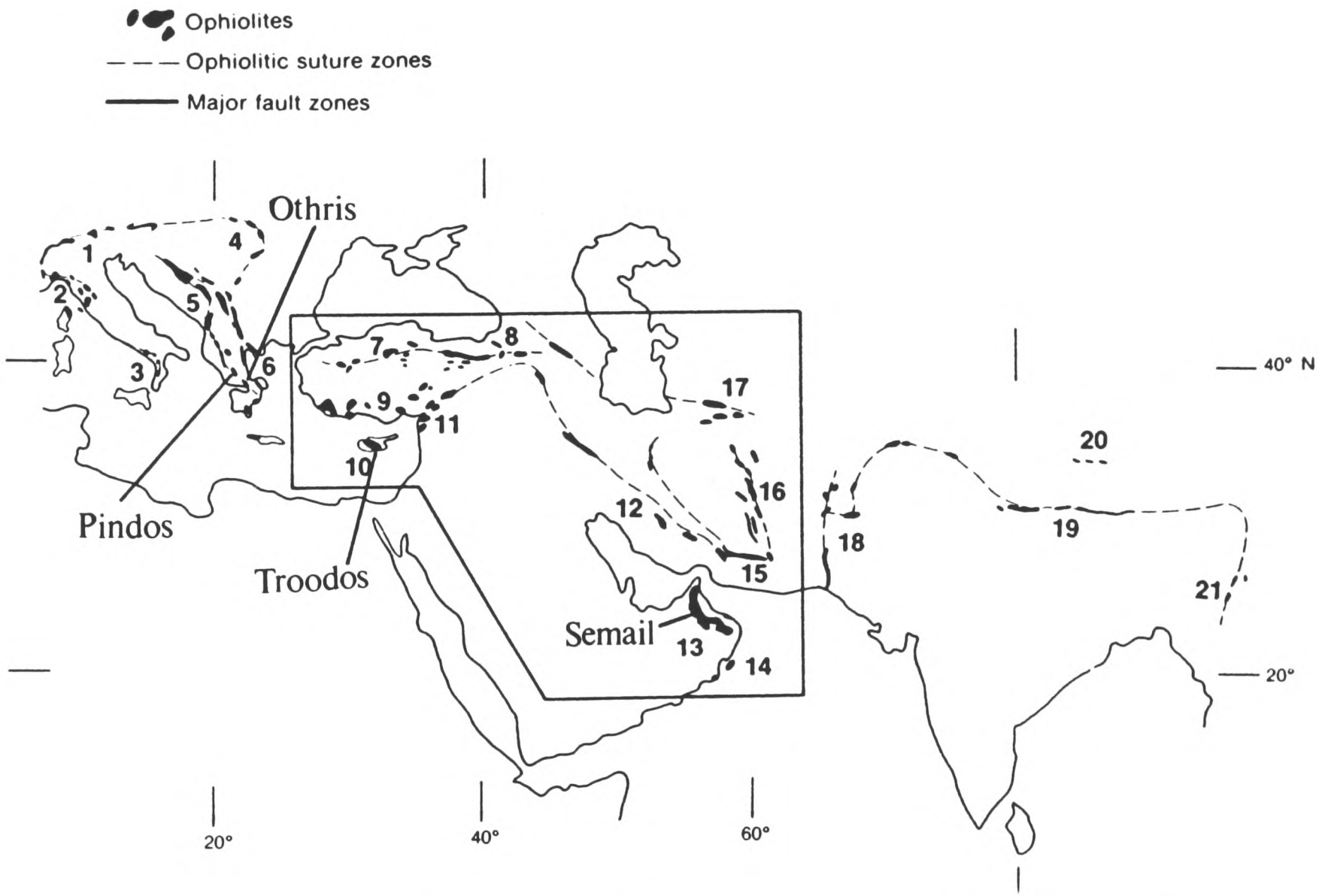

Fig. 1.6 Sketch map showing the distribution and occurrence of the ophiolite bodies of the Tethyan belt in the Eastern Mediterranean and near East. The position of the Pindos ophiolite is indicated. From Lippard et al. 1986.

Ophiolites in the Greek area are found mainly within two distinct belts which continue north into Albania and Yugoslavia; the Vardar Zone in the northeast and the Sub-Pelagonian zone in the west (Fig. 1.3). In southeastern Greece, the distinction between these two belts is less clear. In Yugoslavia, there is a difference in the basic lithologies of ophiolites from each zone: the western ophiolites are predominantly lherzolitic, and the eastern ophiolites are harzburgitic (Pamic 1983). However, south of the Scutari-Pec transform fault, the ophiolites of both belts are more or less harzburgitic. In Greece, the Pindos Vourinos and Evvia ophiolites are harzburgitic, whereas Othris contains both lherzolites and harzburgites.

1.5 Previous studies

The first travellers into the Pindos Mountains to make geological observations were Phillipson (1893) and Hilber (1894). The first major contribution was made by Renz, during a stratigraphic study of the Dinarides and the Hellenides, who traversed the Pindos Mountains and the Meso-Hellenic Trough in 1928. In general, the detailed geology of the northern Pindos Mountains is poorly known. Brunn (1956) made the first comprehensive geological map of northwestern Greece, including the northern Pindos Mountains, at a scale of 1:100,000. This map was subsequently enlarged and published as several 1:50,000 sheets (e.g. Metsovo sheet; IGME 1960). Subsequently, numerous authors have described aspects of the ophiolite (Parrot 1967, 1969; Terry 1974; Capedri et al. 1980, 1981, 1982; Ross & Zimmerman 1982; Kostopoulos 1989); the metamorphic sole (Whitechurch & Parrot 1978; Roddick et al. 1979; Spray & Roddick 1980; Thuizat et al. 1981; Spray et al. 1984); and the palaeontology and sedimentary history (Terry 1971, 1975; Terry & Mercier 1971; Lorsong 1977, 1979). Kemp & McCaig (1984) mapped a small area, the Perivoli corridor, in more detail (1:5,000) and produced an outline tectonic model.

1.6 Tectonic models for the evolution of northern Greece

The tectonic evolution of Greece has been the subject of some debate over the past 20 years, since the advent of plate tectonic theory. The main points of contention have concerned the origin of the great ophiolite

complexes, and the spatial reconstruction of the various palaeogeographical units (see a review in Robertson and Dixon 1984). Previous tectonic interpretations of the region recognise an important Late Jurassic ("Eohellenic") tectonic event (Aubouin et al. 1970), which affected both the Pindos and Sub-Pelagonian tectonic zones in northern and central Greece (Figs. 1.3; 1.7; Brunn 1956; Aubouin 1959; Kemp & McCaig 1984), and the Vardar zone of northeast Greece. This event is thought to have resulted in emplacement of ophiolites (Pindos, Vourinos and Kastoria) onto the continental margin of the Pelagonian Zone. The direction of emplacement of these ophiolites is uncertain: they were either rooted far to the east in the Vardar Zone, and were thrust over the Pelagonian Zone (Aubouin et al. 1970; Bernoulli & Laubscher 1972; Jacobshagen 1978; Vergely 1976, 1977, 1984), or rooted nearer their present position, within the Pindos-Othris Zone (Naylor & Harle 1976; Smith 1979; Smith et al. 1979; Kemp & McCaig 1984; Fig. 1.7).

Vergely (1984), in a comprehensive study of the tectonic evolution of the Hellenides, considered that two basins with oceanic basement were in existence. One was sited to the east of the Pelagonian continent, within the Vardar Zone, and the other to the west, within the Maliac Zone (Fig. 1.8). He considers that the Othris ophiolite was derived from the Maliac Zone, during Late Jurassic to Early Cretaceous closure of this basin (tectonic phases Je1-2). He also proposed that the Pindos and Vourinos ophiolites were derived from the closure of the Vardar Zone, also at this time. Thus, in this model, the Othris ophiolite was emplaced to the northeast, and Pindos and Vourinos southwestwards. The model also preserves the idea that the western belt ophiolites are at least partly lherzolitic in Greece (i.e. Othris), and the harzburgitic ophiolites now found in that belt are more allochthonous.

The pre-Late Jurassic tectonic history of the Pindos ophiolite and associated units, is therefore critical to an understanding of the geological evolution of the Hellenides. The main reason for this, is that the units of this age may preserve evidence that the Sub-Pelagonian Zone, and perhaps even the Pindos Zone, was floored by oceanic basement, and therefore a probable source of the Pindos and Vourinos ophiolites. The Pindos ophiolite is believed to be continuous with the Vourinos (Moores 1969) and Kastoria (Mountrakis 1986) ophiolites beneath the Meso-Hellenic molasse trough, and perhaps also with the Othris and Koziakas ophiolites along strike to the south (Smith 1979 Ferriere 1982; Fig. 1.3).

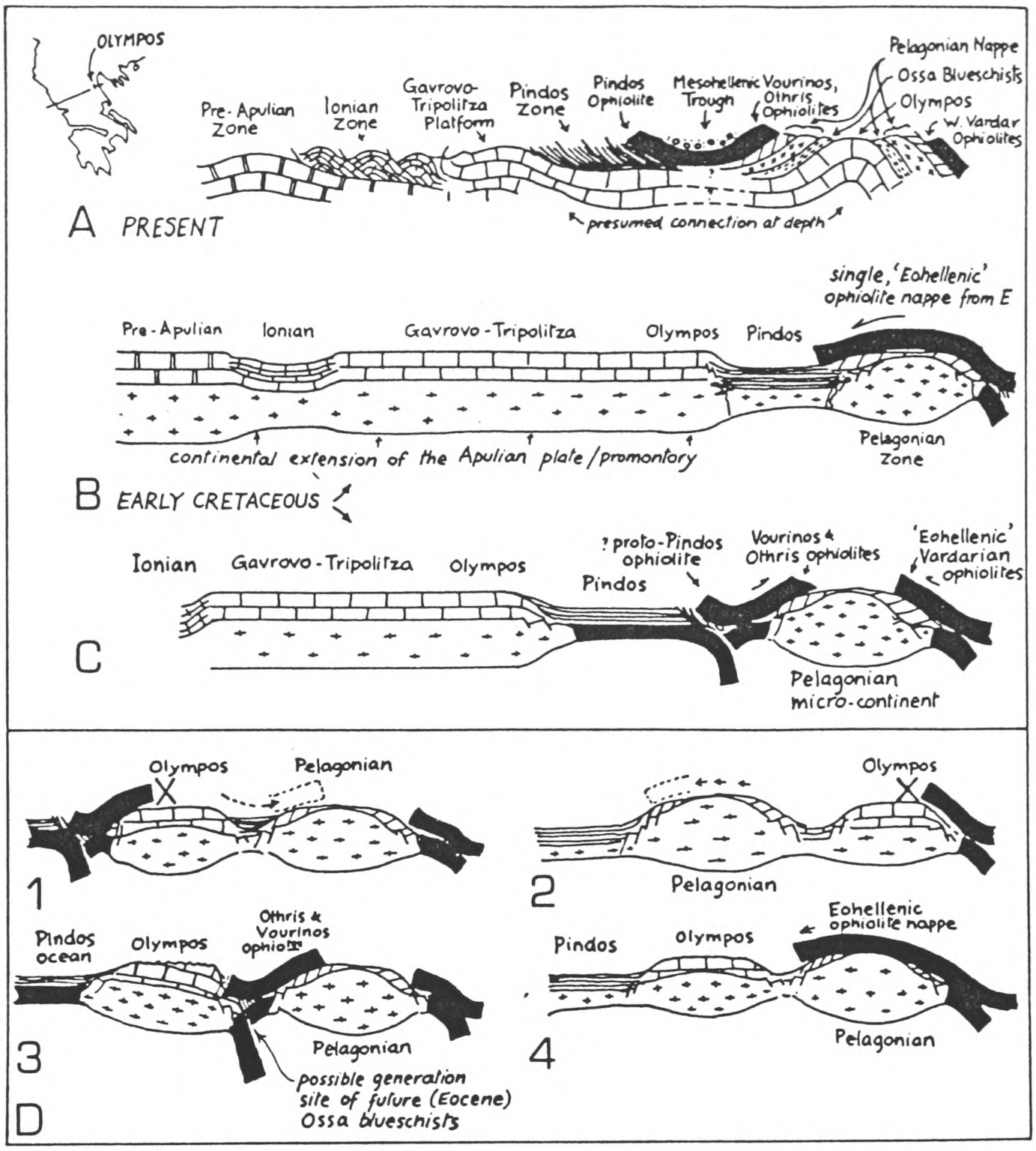

FIG. 12. Principal alternative models for ophiolite emplacement in northern mainland Greece. *A*. Present structural section across the northern mainland (schematic), after Jacobshagen, 1977. The Olympos carbonate sequence is assumed to be a continuation of the Gavrovo-Tripolitza carbonate platform and the Pindos and Vourinos ophiolites are assumed to be continuous beneath the Mesohellenic molasse trough. *B*. *Single*, Vardarian, root-zone model for ophiolites emplaced onto the Pelagonian zone and its carbonate cover in the Late Jurassic-Early Cretaceous ('Eohellenic') event. After Jacobshagen, 1977. *C*. *Double* (Pindos & Vardar) root-zone model favoured by Ferrière and Vergely 1976, Smith *et al*. 1979, Bébien *et al*. 1980, and others. Vourinos is attributed variously to E or W derivation. The Pindos-Othris ophiolite emplacement mechanism illustrated is based on the **Smith & Spray** roll-back/roll-to principle (see Figs 9g and 10c): other authors may favour alternative methods from the same western source. See Fig. 18 for the subsquent eastward Tertiary thrusting models. *D*. Alternative possibilities for an *internal* Olympos carbonate-bank, east of the Pindos basin, and their implications for ophiolite emplacement in the Late Jurassic-Early Cretaceous. Each section assumes that the Olympos platform cannot have been overthrust by an ophiolite in the Triassic to Palaeocene interval. Along-strike continuity of the Olympos platform is here assumed but may not be real (see text). *1* and *3*—Oceanic Pindos basin as in *C*. *2* and *4*—Stretched-continental Pindos basin and single, eastern ophiolite root zone, as in *B*. *1* and *2* appear to be impossible: the Olympos sequence bars the way to west Pelagonian ophiolites in *1* and

Fig. 1.7 Schematic cross-sections showing possible modes of ophiolite emplacement during the Late Jurassic, in northern Greece. From Robertson and Dixon (1984).

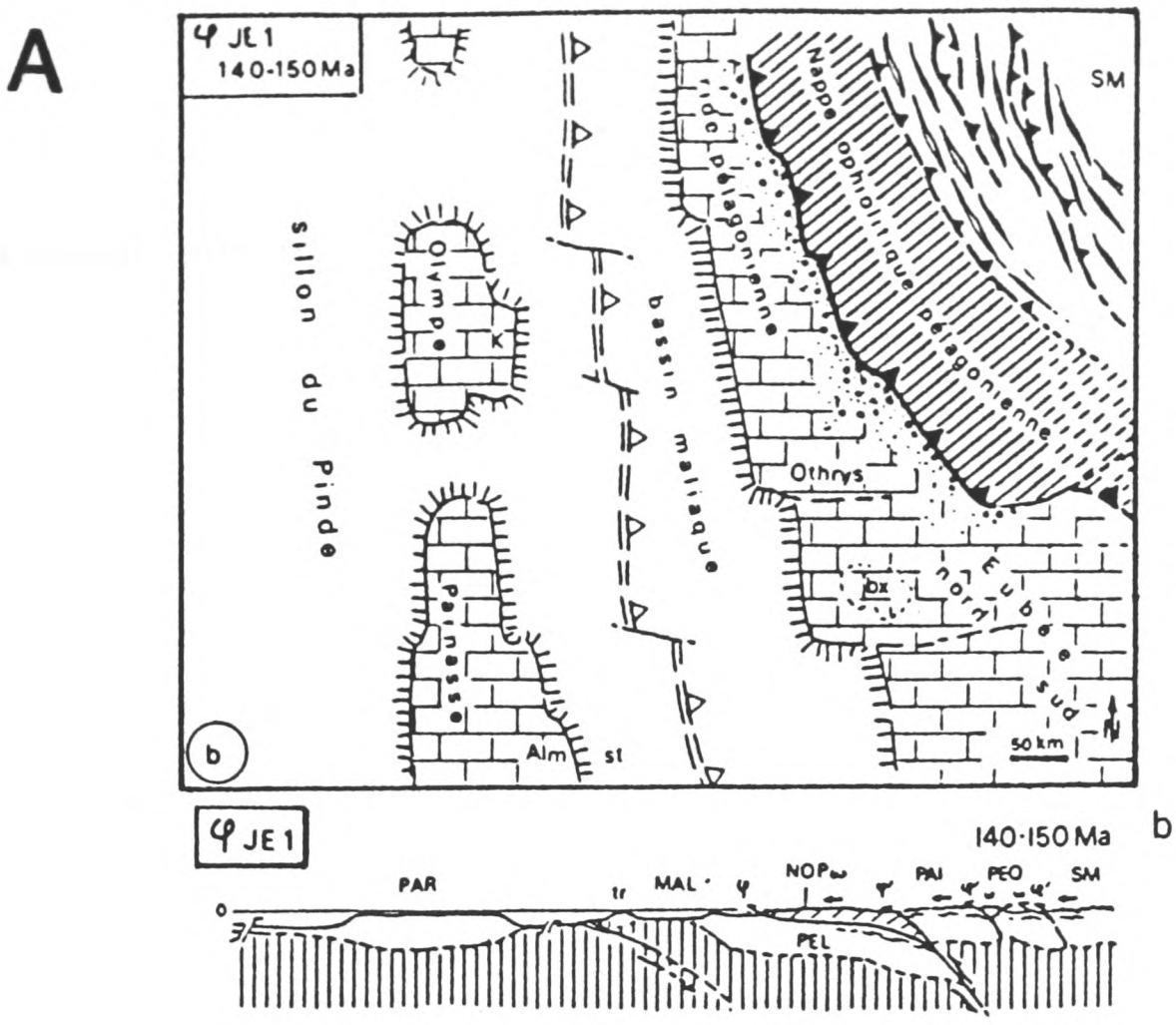

Fig 1.8 Tectonic evolution of the Greek region during the a) Late Jurassic and b) Early Cretaceous; from Vergely (1984). Note the position of the Maliac basin, essentially the lateral equivalent of the Sub-Pelagonian Zone in central Greece, and the external (Pindos Zone) origin of the Olympos platform (see text).

1.7 Objectives and approach

This study has concentrated on the collection of new structural, sedimentological and geochemical data, with the aim of reconstructing the Mesozoic and Tertiary evolution of the northern Pindos region, for comparison to other parts of the Hellenides. The basis of this study was the construction of a tectonic stratigraphy, using established principles of thrust tectonics. To accompish this, several periods of regional reconnaissance were undertaken, partly in conjunction with A.H.F. Robertson, J.R. Cann, and also A. Rassios and G. Migiros of the Greek Geological Survey. The primary objectives were to ensure the consistency of the stratigraphy on a regional scale, and to allow the construction of regional cross-sections. Also, more detailed structural mapping was undertaken where necessary, particularly along the complex refolded structure of the Perivoli corridor. An important part of the stratigraphic work was to improve the age data set for the sequences present. This was mainly achieved using radiolarian biostratigraphy. Despite detailed igneous geochemical coverage for the central part of the ophiolite, elsewhere there was little data available. A programme of geochemical reconnaissance of the ophiolitic intrusives and extrusives in other areas was therefore undertaken. The study has also attempted to understand the processes responsible for the resultant features (e.g. Jones et al. 1990).

1.8 Tectono-stratigraphy

The northwestern Pindos Mountains expose a sequence of thrust sheets that were finally tectonically emplaced onto a continental margin during the Early Tertiary Alpine orogeny. Five major tectono-stratigraphic units are distinguished (Fig. 1.9): the Pindos Ophiolite Group (Jurassic), the Avdella Melange (Late Triassic-Late Jurassic), the deep-sea sedimentary Dio Dendra Group (Late Jurassic-Late Cretaceous), and the shallow-water limestone Orliakas Group (Late Cretaceous). These thrust sheets were emplaced over the terrigenous Pindos Flysch of Maastrichtian to Eocene age. Each tectonic unit is bounded by a major thrust contact, which generally dips eastwards towards the Meso-Hellenic trough (Fig. 1.3). Details of each unit are given in Appendix (1).

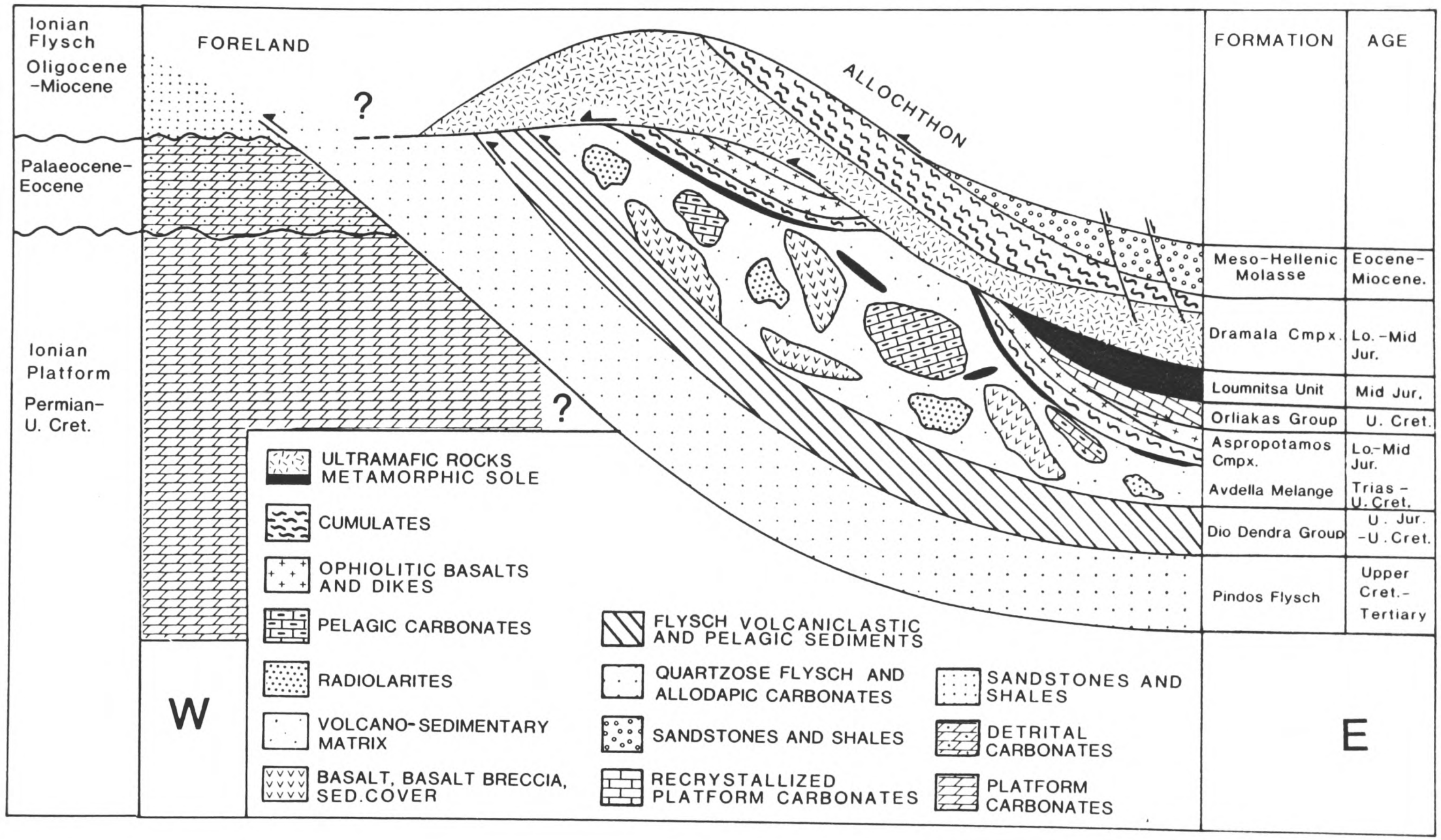

Fig. 1.9 Schematic tectono-stratigraphy of the north Pindos Mountains thrust stack (Jones and Robertson in press).

The major thrust sheets occur in a constant tectonic stacking order (Fig. 1.9; Brunn 1956; Kemp & McCaig 1984), although out-of-sequence thrusting, and large-scale folding of the thrust stack complicates the tectonostratigraphy in some areas. The structurally highest units in the region belong to the Pindos Ophiolite Group (Fig. 1.9, and Appendix 1). Three main tectonic units are distinguished: i) the Dramala Complex, a dismembered ultramafic thrust sheet; ii) the Aspropotamos Complex, comprising ultramafic and mafic cumulate, intrusive and extrusive rocks, and minor sedimentary rocks; iii) the Loumnitsa Unit, a basal metamorphic sole found beneath the ophiolitic units.

The uppermost tectonic unit is the *Dramala Complex*, which overlies the other units along a major out-of sequence thrust, the Achladi thrust (new name). Well developed sections of the Dramala Complex are found in the Smolikas Mountain range in the north, generally within the central area (e.g. Dramala Mountain), and in the area east of Metsovo in the south (Fig. 1.4). The Dramala Complex locally passes structurally downwards into a basal metamorphic sole, the *Loumnitsa Unit*, which consists primarily of amphibolite to greenschist facies metabasites and metasediments. The Loumnitsa Unit also occurs at other structural levels (see below), due to out-of-sequence thrusting within the Pindos Ophiolite Group. Tectonically beneath the Dramala Complex, and locally the Loumnitsa Unit, is the *Aspropotamos Complex* (Pindos Ophiolite Group). This complex consists of a structurally dismembered sequence of basic extrusives, intrusives and cumulate ophiolitic rocks, which is well known from the Aspropotamos River (Fig. 1.4; Parrot 1967; Capedri et al. 1980; Kostopoulos 1988), and has since been recognised throughout the region. The Loumnitsa Unit is found at the base of the Aspropotamos Complex in several areas. Locally, the Late Cretaceous platform carbonates of the *Orliakas Group* overthrust the Aspropotamos Complex (Fig. 1.9; see Chapter 7).

The Pindos Ophiolite Group is structurally underlain by the *Avdella Melange*, a tectono-sedimentary melange unit, over 1.5 km thick (Fig. 1.9). Below this comes the *Dio Dendra Group* (Late Jurassic to Late Cretaceous), consisting of a series of turbiditic carbonate and terrigenous sediments. Beneath all these units is a several kilometre-thick turbiditic sequence of Maastrichtian-Eocene age, the *Pindos Flysch*, which forms the footwall to the thrust stack across the region. Finally, later Tertiary post-orogenic

transgressive "molasse" deposits of the Meso-Hellenic trough mantle the thrust sheets to the east.

1.9 Thesis organisation

The following chapters consider firstly the Pindos Ophiolite Group (Chapters 2 and 3), the Avdella Melange (4), and Cretaceous sediments of the Dio Dendra and Orliakas Groups (5), as defined above. The penultimate chapter (7), deals mainly with the structural geology of the region, and the final chapter (8), concludes with an outline tectonic model for the evolution of the Pindos ocean basin. A summary of the work carried out in this study is in press at the time of writing (Jones and Robertson 1990 in press).

A standard format has been used throughout for structural measurements consisting of a three figure number (the vector), followed by a two figure number (the amount of dip), and finally the direction of dip (e.g. 213/65/SE). When vectors only are given, they are as three figure numbers (e.g. 040^{o}), or when quoted, may be given in the format 'N80E'.

CHAPTER 2

THE PINDOS OPHIOLITE GROUP: OCEANIC CRUST AND MANTLE

2.1 Introduction

The Pindos ophiolite (Figs. 2.1, 2.2) is one of a series of emplaced oceanic crustal and mantle fragments which, together, form the Tethyan ophiolite belts of the Eastern Mediterranean region. These ophiolites mark the tectonic sutures formed by the progressive closure of the Mesozoic Neotethyan ocean, and include the Semail ophiolite (Oman), the Troodos Complex (Cyprus), the Antalya Complex (S.W. Turkey), the Hatay and Baer-Bassit ophiolites (Turkey and Syria), the Zlatibor ophiolites (Yugoslavia), and the Vourinos, Othris and Evvia ophiolites of central mainland Greece (Chapter 1). The Pindos ophiolite is believed to have formed during the Jurassic, based on radiometric dating of the metamorphic sole (165 $\pm$ 3 Ma.; Spray et al. 1984; see Chapter 3). Consideration of the structure and lithologies of the Pindos ophiolite, has additionally provided the basis for a new plate tectonic model for the origin of the Pindos and Vourinos ophiolites (Chapter 8; Jones and Robertson 1990; Jones et al. 1990).

The Pindos ophiolite was first studied by Brunn (1956), as part of a regional mapping programme in northern Greece. He established the presence of an igneous association, which he interpreted as resulting from crystallisation of a giant submarine magma effusion on to the seafloor (Brunn 1960). The mapping of Brunn also incorporated the more easterly Vourinos ophiolite, which is now believed to be continuous with the Pindos ophiolite beneath the Tertiary sediments of the Meso-Hellenic trough (Chapter 1; Smith 1979). Subsequently, Parrot (1967, 1969) studied the ophiolitic rocks of the lower Aspropotamos River area, and published an outline map of the eastern central margin of the region. Parrot and Verdoni (1976) undertook further petrological and geochemical studies of the ophiolite suite. Terry (1974, 1979) also carried out petrological studies, and proposed an outline model for the mutual relationships and evolution of the ophiolitic rocks.

A

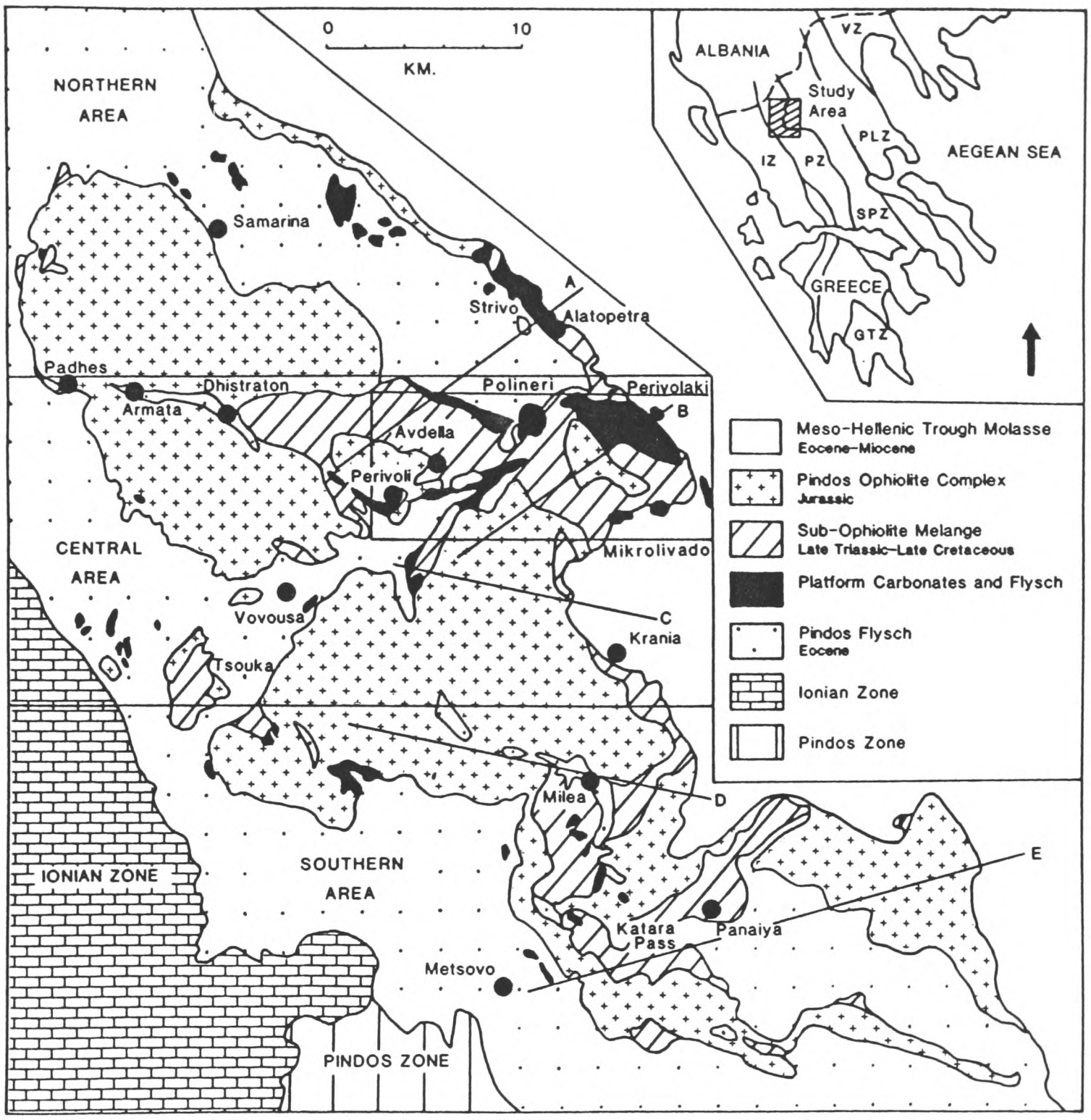

Fig. 2.1 General geological map showing the Pindos ophiolite (undifferentiated), and its relationship to adjacent tectonic units. Northern, central and southern sectors are outlined. b) The geographical position of other presumed related ophiolite bodies in Greece, Othris, Koziakas, Vourinos, and Kastoria.

B

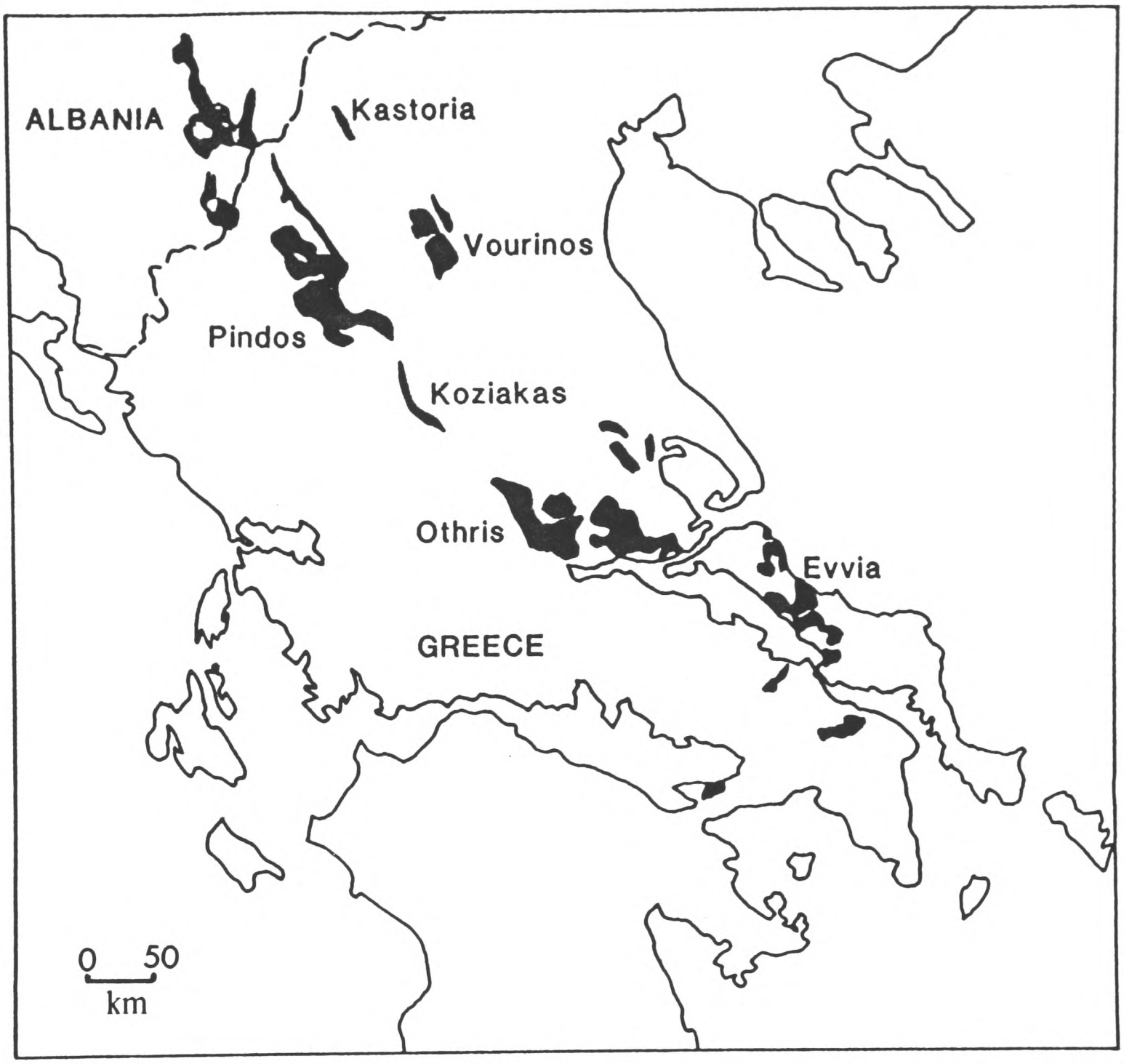
ALBANIA
Kastoria
Vourinos
Pindos
Koziakas
Othris
Evvia
GREECE
0 50
km

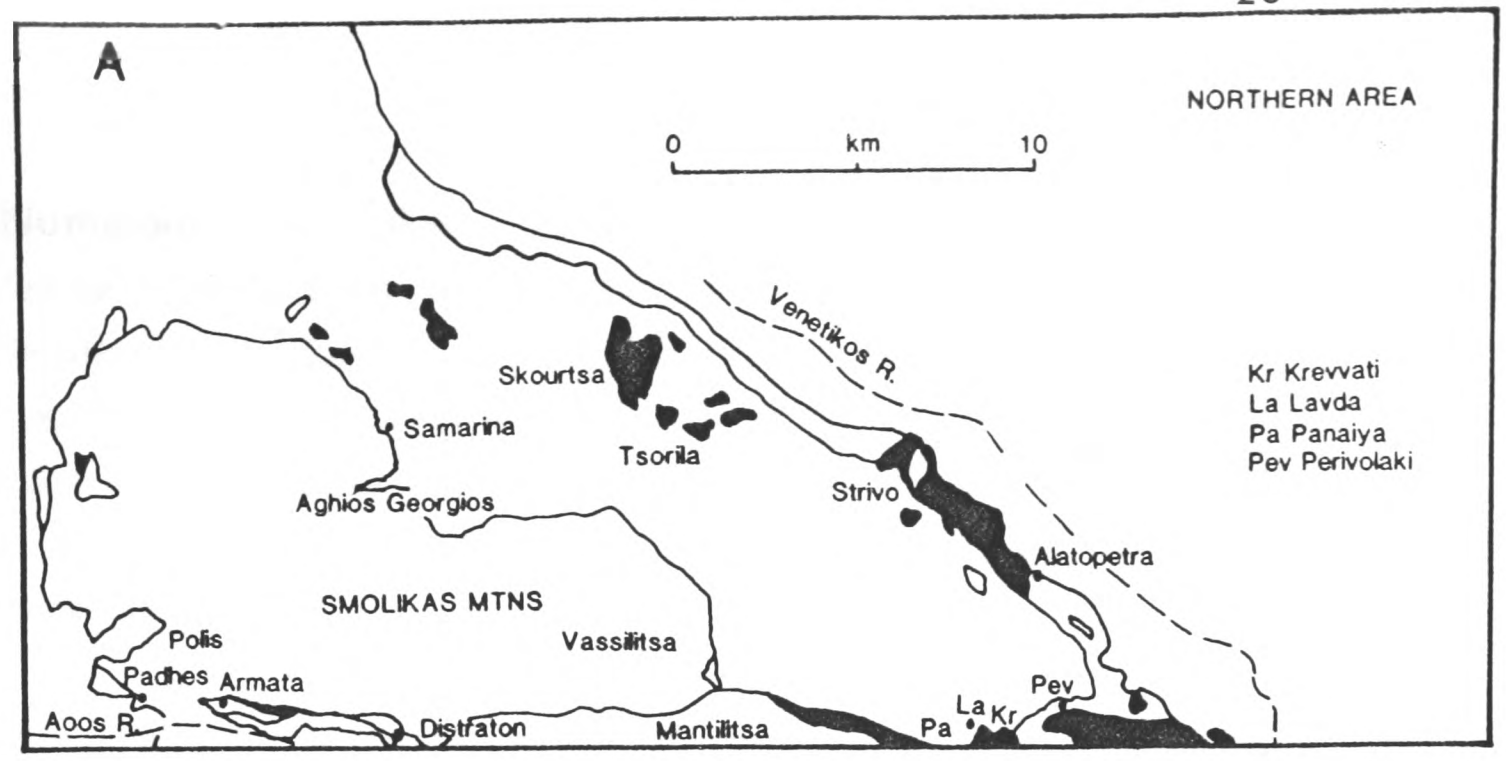

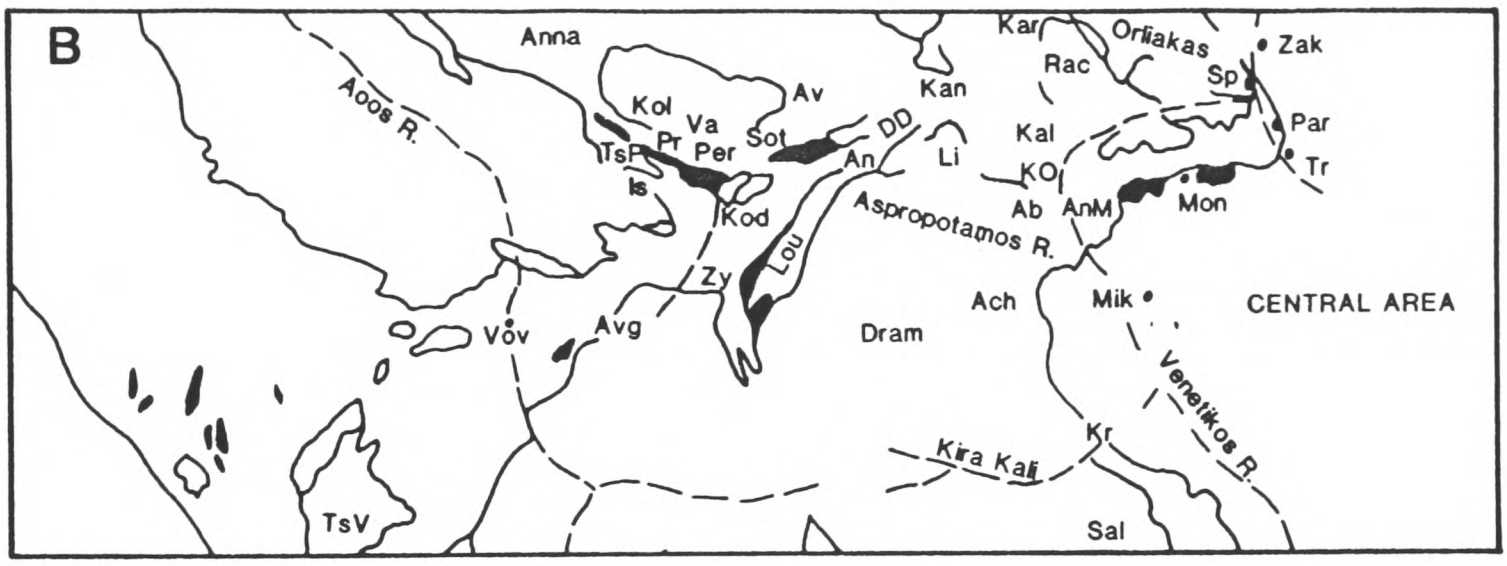

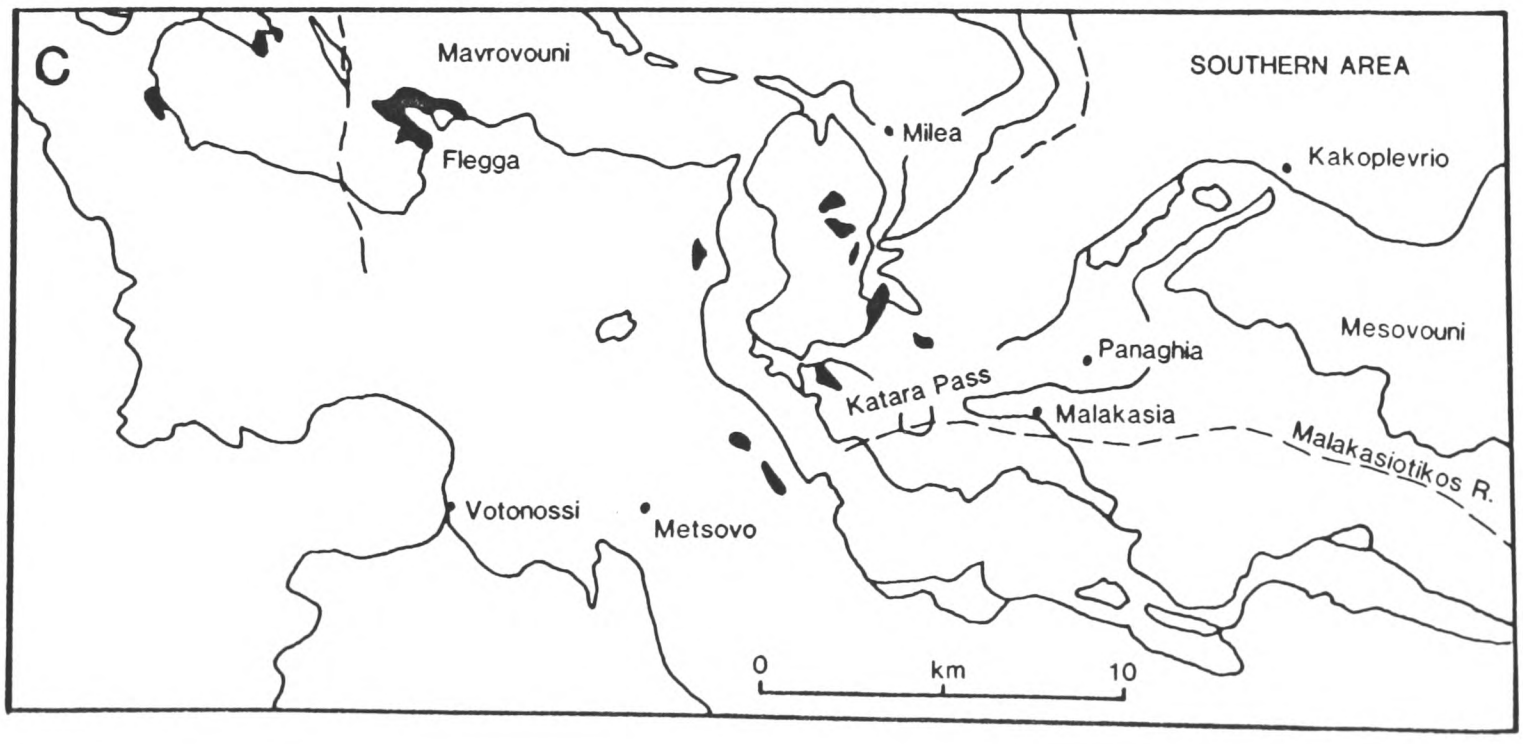

Fig. 2.2 Locality maps for the northern, central and southern regions of the Pindos Mountains (see Fig. 2.1).

Numerous other volcanic geochemical studies (Montigny et al. 1973; Pearce 1979; Richard and Allegre 1980; Capedri et al. 1980, 1981, 1982; Bertolani 1982; Dupuy et al. 1984; Kostopoulos 1989) have been carried out. Most of these studies were completed only within the lower part of the Aspropotamos Valley, and produced variable interpretations for the origin of the ophiolite, reflecting the igneous and structural complexity present.

This study has not concentrated primarily on the ophiolite crustal and mantle lithologies of the north Pindos area. However, one aim was to undertake geochemical reconnaissance of the volcanic and intrusive rocks in other areas of the mountains, in order to identify new localitites for comparison with data from the Aspropotamos Valley type area. Therefore, this Chapter will summarise observations made during regional reconnaissance of the Pindos ophiolite, and from a small number of more detailed studies of the crustal rocks. Comparisons with other Greek ophiolites, particularly Vourinos, are critical to an overall understanding of the tectonic evolution of the central Greek area, and are summarised below.

2.2 Tectonic framework of the Pindos ophiolite within Greece

In the tectonic model based on this study (Chapter 8), the western Greek ophiolites, which include Othris (Smith et al. 1976, 1979), Vourinos (Moores 1969; Wright 1986), Kastoria (Mountrakis 1984, 1986), Koziakas (Ferriere 1982; Capedri et al. 1985) and Pindos, were emplaced generally eastwards (Naylor and Harle 1976; Smith 1979; Jones and Robertson 1990), onto the margin of the Pelagonian Zone (see Chapter 1). The alternative view, i.e. westwards emplacement (Vergely 1976, 1977, 1984; Jacobshagen et al. 1978) is discussed in Chapter 8. The timing of emplacement of the Vourinos ophiolite is constrained by the presence of Late Jurassic (Kimmeridgian-Tithonian) transgressive sediments (located at the Krapa Hills, W. Vourinos; Mavrides et al. 1979).

Following initial Jurassic emplacement (see Chapter 1), the Pindos thrust sheets were further deformed by the Early Tertiary collision of Apulia with the Pelagonian microcontinent, part of the broad zone of

collision between the African and Eurasian plates. The collision resulted in the telescoping of the ophiolite and its associated sedimentary sequences, and emplacement of these units southwestwards onto the marginal sediments of the Ionian platform (see Chapter 1). In summary, the Pindos ophiolite is believed to have undergone a two-stage emplacement history, a conclusion which is critical to an understanding of the present day disposition of the ophiolite, and of the structures present within the region.

2.3 Tectono-stratigraphy

The gross structure of the Pindos ophiolite has already been considered in detail; Brunn (1956) produced generalised cross-sections across the mountains, which were supplemented by sections of the eastern margin of the ophiolite, presented by Parrot (1967), and by Jones and Robertson (1990). A structural interpretation of the ophiolite is presented later in this thesis (Chapter 7).

The formal stratigraphic name for the units which comprise the "Pindos ophiolite" is the Pindos Ophiolite Group (Chapter 1 and Appendix 1). The group has been further subdivided into three tectonic units (Jones and Robertson 1990; Fig. 2.3), which are, from the top downwards, the Dramala Complex, the Aspropotamos Complex and the Loumnitsa Unit. This Chapter is concerned with the first two of these units, and the following Chapter deals with the Loumnitsa Unit in more detail.

The Dramala and Aspropotamos Complexes comprise the ophiolitic crustal and mantle rocks of the Pindos ophiolite, which are found exposed over an area of some 3000 km^2. These rocks are complexly tectonised by several stages of deformation, during formation of the ophiolite and initial emplacement (Jurassic), and during subsequent re-thrusting (Early Tertiary; see Chapter 7). The Dramala Complex is defined on tectono-stratigraphic grounds as forming the uppermost thrust sheet in the region, and consists lithologically of oceanic mantle and lower crustal sequences. The Aspropotamos Complex tectonically underlies the Dramala Complex over much of the region. These two are separated by a major out-of-sequence thrust, the Achladi thrust (Jones and Robertson

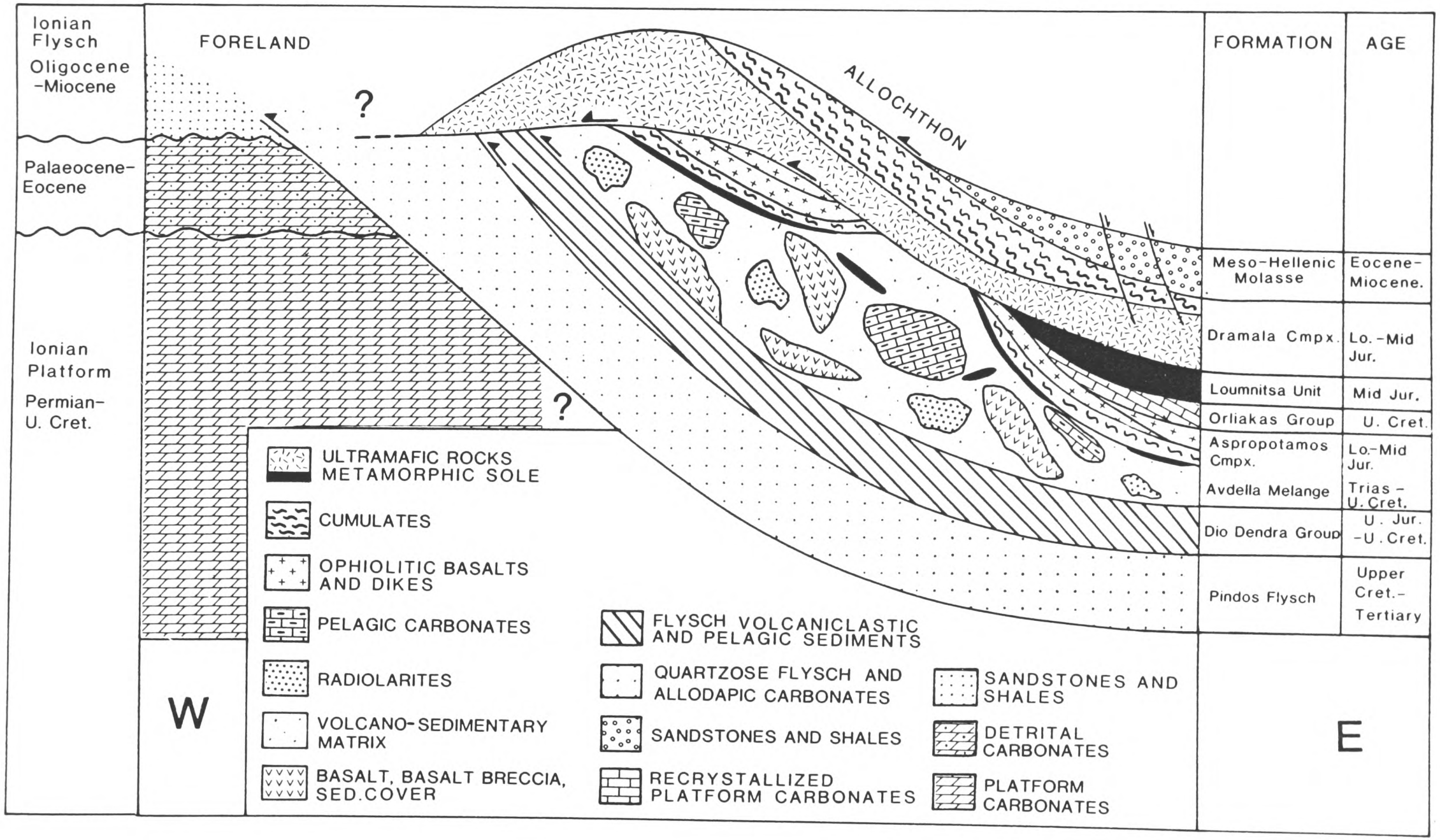

Fig. 2.3 Tectonostratigraphy of the north Pindos Mountains. (see text and Chapter 1 for explanation). Note the position of the Dramala Complex and the Aspropotamos Complex.

1990), which is named after the locality on the northeastern slopes of Dramala Mountain (Fig. 2.2), where the thrust is well exposed (see Chapters 1, 7).

2.4 THE DRAMALA COMPLEX

2.4.1 Lithologies

The Dramala Complex (see Appendix 1) primarily consists of variably serpentinized harzburgite tectonite restite (i.e. depleted mantle harzburgite). Subordinate, but locally abundant, lithologies include dunite, pyroxenite and a range of ultramafic and mafic cumulate rocks. Previous studies of the Pindos peridotites have led to confusion regarding their nature. Lherzolite has been reported as the dominant mantle lithology, (e.g. Lippard et al. 1986; Spray 1990), whereas mantle lherzolites are in fact, extremely limited in occurrence (e.g. Vassilitsa area; Terry 1974), and the ultramafic part of the ophiolite is therefore almost exclusively harzburgitic.

Rassios (in prep.) distinguishes six main lithological associations within the Dramala Mountain area: 1) harzburgite, with some dunite as small pods and layers; 2) harzburgite with pyroxenite dykes or boudins; 3) harzburgite with gabbroic veins and dykes; 4) harzburgite with significant dunite pods and larger bodies; 5) a mixed zone of harzburgite and cumulates; and 6) a sequence of cumulates (in the Kira Kali River area; Fig. 2.2). The cumulates are dominantly troctolites, with subordinate wehrlite and plagioclase dunite. In the opinion of Rassios (in prep.), the mixed zone, which varies from 300 to 3000 m in thickness, corresponds to the position of the petrologic Moho. This may be comparable to the "transition zone" recognised within parts of the Semail ophiolite of Oman (Culeneer et al. 1988).

Serpentinised, banded ultramafic mylonites (up to 40m thick), are found immediately above the Achladi thrust, and contain a fabric which parallels the amphibolites of the underlying metamorphic sole (e.g. Loumnitsa Valley, Fig. 2.2; see Chapter 3). Similar lithologies have been reported from the base of the Semail ophiolite, Oman (Searle and Malpas

1980), and are thought to relate to the emplacement phase of the ophiolite. The Dramala Complex also posesses a basal serpentinite unit, locally up to 300 m thick, which is described more fully elsewhere (Chapter 3).

Massive chromite is rare within the Dramala Complex, although it may be locally more abundant as disseminated grains within cumulate rocks. The largest chromite discovery made to date is some 150 m long and 10 cms thick (on Dramala Mountain; A. Rassios pers. comm. 1989).

2.4.2 Regional distribution of the Dramala Complex

During regional reconnaissance studies of the Pindos Mountains (partly in conjunction with J.R. Cann), brief observations of the Dramala peridotites were made, and are presented here.

a) *Northern area*

The northern area (Fig. 2.2) contains large areas of mapped ultramafic and mafic rocks (e.g. Konitsa sheet; IGME 1985). In the Vassilitsa-Mantilitsa area, harzburgite tectonites are partly serpentinised and contain rodingitised gabbro dykes, isoclinally folded along sub-vertical axes (1 km S.W. of the ski centre). West of this locality, on the track towards Dhistraton, further extensive areas of harzburgite are visible both to the north and south. To the east side of Dhistraton village, lower crustal cumulates are exposed including dunite cumulates. From Dhistraton northeastwards to Samarina, a thick section of cumulate plagioclase dunite, dunite, gabbro, anorthosite and troctolite is exposed. These lithologies are highly folded and intersheared, with associated cross-cutting foliations. Locally, a strong foliation has deformed pre-existing gabbro dykes. The gabbros are often pegmatitic and strongly flasered. Individual gabbroic dykes are isoclinally folded along sub-horizontal axes.

North of Samarina, strongly foliated harzburgite is present. The roadside sections exposed west of Armata village (Fig. 2.2), show thick sections of harzburgite, with a several hundred metre-thick basal serpentinite unit. The serpentinite cliffs contain spectacularly exposed

sections of rodingitised gabbro dykes. These dykes are folded along sub-horizontal axes, and shearing and boudinage are intensely developed. Harzburgite tectonite is exposed on the western slopes of the high Smolikas range (Fig. 2.2). Much of the remainder of this northern area is unexplored, particularly the northern Aoos Valley, north of Vovousa and south of Armata, where peridotites are extensively exposed.

b) *Central area*

The main exposures of peridotite are found in the Dramala-Salatoura area, where it is best documented (Rassios in prep.). Other significant peridotite occurrences are in the Valia Kalda region, the Avgo-Vovousa region and northwest of Perivoli in the Koleo-Anna region (Fig. 2.2). These areas mostly consist of mantle tectonites (harzburgite, dunite and pyxroxenite), with local sections encompassing the petrological Moho (e.g. Kira Kali-Salatoura area; A. Rassios in prep; J. R. Cann pers. comm. 1988; S. Miller, M. Solbe unpublished data). The Moho appears to dip at a moderate angle towards the southeast in this area. Crustal cumulate rocks are exposed along the road between Mikrolivado and Milea, as well as in valleys east of the road.

c) *Southern area*

West of Milea, peridotites are extensively exposed in the Mavrovouni-Flegga areas (Metsovo sheet, IGME 1959), to the south in the Katara Pass east of Metsovo, and the Mesovouni massif exposed north of the main road between Panayia and Kalambaka (Panayia sheet IGME 1980; Fig. 2.2). The section exposed along the road is composed mostly of strongly deformed mantle harzburgite, and exceeds 5 km in thickness.

2.4.3 Mantle tectonite fabrics of the Dramala Complex

The Dramala Complex harzburgites and dunites commonly contain a strong planar foliation defined by the alignment of orthopyroxene and spinel crystals. Additionally, these crystals, particulary the spinels, may be

individually elongate and define a lineation within the plane of the foliation. A preliminary structural study of the Dramala Mountain peridotites (Ross and Zimmerman 1982; Rassios, in prep.) has helped to distinguish those structures formed during spreading within the oceanic environment, from those which were the result of emplacement-related processes. Critically, the study of Ross and Zimmerman (1984) shows that a phase of mylonite development with a north-north-eastward (towards 016^{o}) overthrust sense occurred, at low temperatures (800-750^{o}) at depths of 30-35 km, probably relating to obduction of the peridotite. The results indicate that an early high temperature (i.e. 1200-900^{o}) foliation (strike 125/50/S), also with associated mylonites, is deformed by a lower temperature foliation (strike 040/60/S) which also affects the cumulate rocks (Rassios in prep.). Brittle faults and shears trend from the 040^{o} direction around to a 125/30/N trend. These structures are consistent with those measured in peridotites of the Vourinos ophiolite as summarised below (Ross et al. 1980; Grivas et al. 1986; Wright 1986; Roberts et al. 1988; Moat 1990). Indeed Ross and Zimmerman (op. cit.) state that "It is probable that the two ophiolites (Pindos and Vourinos) shared a common origin, and an identical early obduction history"

2.4.4 Summary of the Dramala Complex

The Dramala Complex represents an extensively exposed mantle harzburgite-dunite sequence, which upwards, passes via a locally preserved petrological Moho, into ultramafic and mafic crustal cumulates. Mylonitic deformation within the mantle sequence is generally intense, with the development of strong pervasive foliations. The structures within the peridotites are believed to have developed in response to one or more of the following: 1) mantle flow at a spreading ridge; 2) initial displacement and subsequent obduction of the ophiolite; and 3) Tertiary thrust re-imbrication and/or extensional faulting. These structures are at present not fully documented in the Pindos area (except in the Dramala area), although the Vourinos peridotites are now well described (e.g. Roberts et al. 1988).

2.5 THE ASPROPOTAMOS COMPLEX: A DISMEMBERED OPHIOLITIC THRUST SHEET

2.5.1 Introduction

The Aspropotamos Complex (see Appendix 1; Jones and Robertson 1990) consists of thrust slices of geochemically and lithologically complicated ophiolitic cumulate, intrusive and extrusive rocks (Parrot 1967, 1969; Montigny et al. 1973; Capedri et al. 1980, 1981, 1982; Dupuy et al. 1984; Kostopoulos 1989; Fig. 2.4). The complex has been previously described in detail only along the lower Aspropotamos River section (Abelia area, Fig. 2.2), and from Avdella (Fig. 2.2). The best preserved successions are found on the eastern margin of the central region, around the villages of Spileo, Monahiti, Mikrolivado and Krania (Fig. 2.2).

This study has included geochemical reconnaissance to document the variation present in the other parts of the ophiolite belt where the Aspropotamos Complex has been newly recognised (see below; Jones and Robertson 1990). Kostopoulos (1989), in a detailed study of the lower Aspropotamos and Avdella sections, described and named the igneous units present (Fig. 2.5). He additionally subdivided the Aspropotamos Complex into Western and Eastern areas, but discovery of the complex in numerous other parts of the Pindos Mountains (Jones and Robertson 1990; Jones et al. 1990) has subsequently invalidated this localised sub-division. Also uncertain is the applicability of individual unit names (Fig. 2.5) to other lithological sequences of the Aspropotamos Complex. Problems may arise when, for example, boninitic dykes (the "N50E unit" of Kostopoulos op. cit.) trend at right angles to this direction elsewhere. Additionally, the section exposed west of Spileo (Fig. 2.2), not studied by Kostopoulos (op. cit.), is in many ways better preserved, particularly with regard to the original igneous contacts within the upper part of the crustal section.

In outcrop, these ophiolitic rocks occur as thrust slices of variable dimensions (up to 2.5 km thick and several km long). Although tectonised, the complex preserves many original igneous and sedimentary contact relationships. All of the major lithological boundaries found within typical oceanic crust are present within the complex, but not all can be found at any one locality.

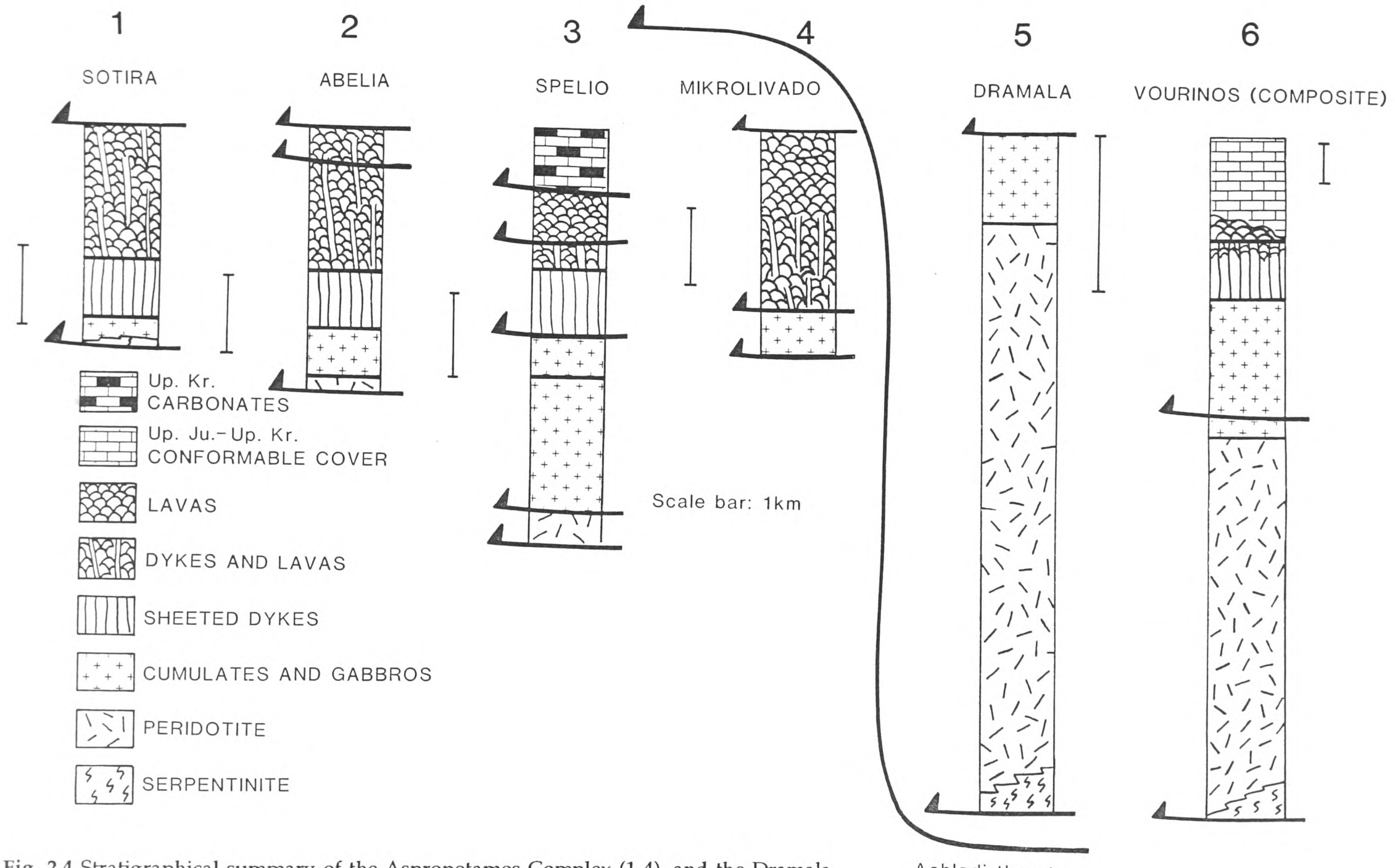

Fig. 2.4 Stratigraphical summary of the Aspropotamos Complex (1-4), and the Dramala Complex (5) at key localities (see Figs. 2.1, 2.2). The Vourinos ophiolite is also presented for comparison (after Rassios et al. 1983).

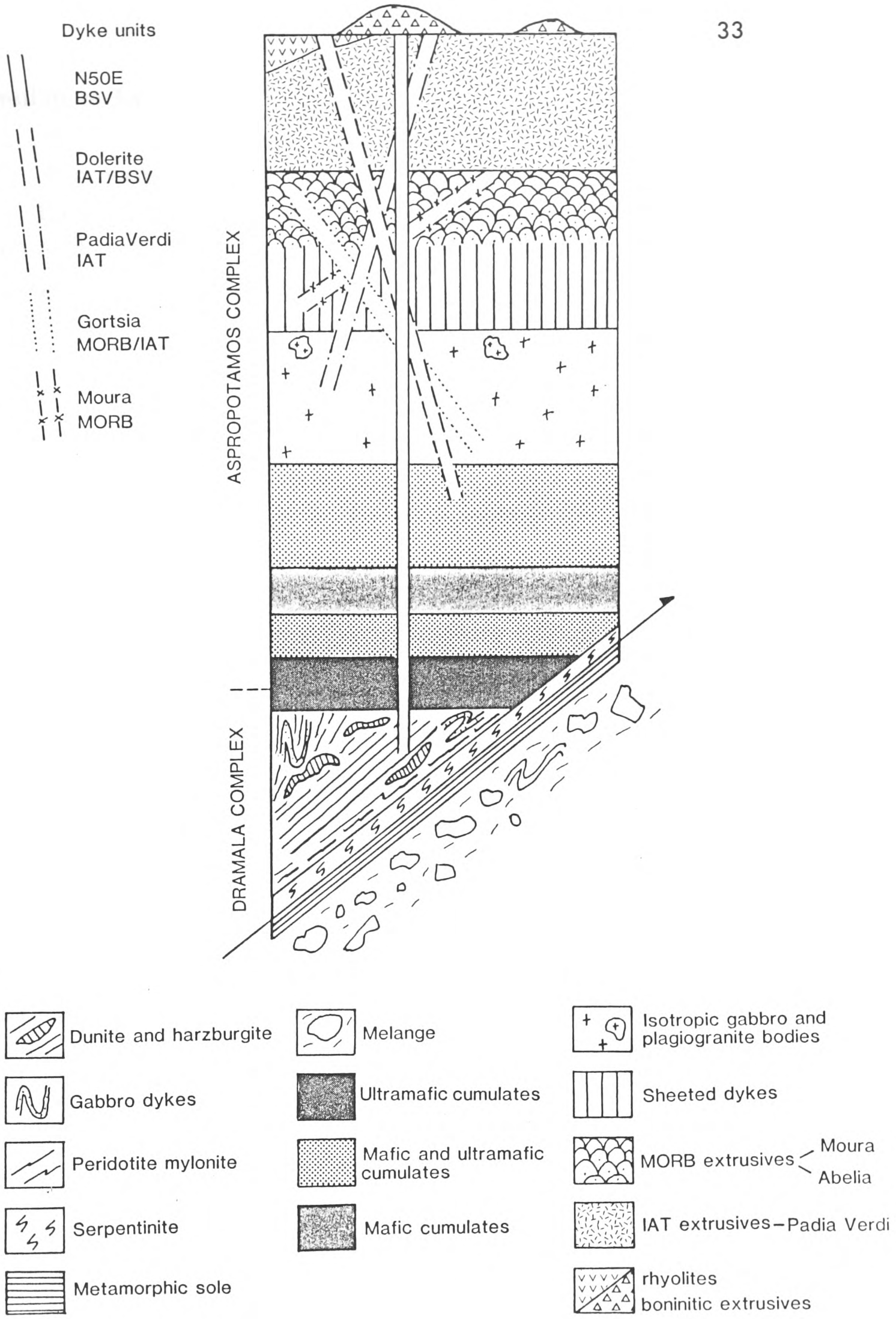

Fig. 2.5 Diagrammatic representation of the stratigraphy of the Pindos ophiolite (modified after Kostopoulos 1989).

2.5.2 Cumulate rocks

The Aspropotamos Complex contains a variety of cumulate lithologies, thought to represent the residua of the once active magma chamber(s) of the Pindos ophiolite. These cumulates were classified into three main groups (Fig. 2.5) at one locality (Abelia, Fig 2.2; Kostopoulos 1989). From the base up, they are dunite-wehrlite-olivine gabbro (Layered Ultramafic Group; 120 m thick), dunite-anorthosite-troctolite-gabbro (Layered Mafic-Ultramafic Group; 150 m thick), and layered gabbro (Layered Mafic Group; 300 m thick) cumulates. These cumulate rocks usually form the lowest exposed parts of the Aspropotamos Complex, and are locally structurally underlain by sheets of serpentinite (e.g. S.E. of Avdella, Fig 2.2), or metamorphic sole rocks (Chapter 3). In well preserved sections, these cumulate rocks are reported to pass upwards into high-level isotropic gabbros (e.g. Abelia, Fig. 2.2; Kostopoulos 1989). Cumulate plagioclase dunite, with abundant chrome spinel, is interlayered with wehrlite, flaser gabbro and troctolite in the area west of Spileo village (Rachi Kerasias; Fig. 2.2). In general, the cumulate rocks are comparable to those found associated with the Dramala Complex, suggesting that it is genetically linked with those of the Aspropotamos Complex.

2.5.3 High level gabbros

Isotropic, or high-level, non-layered gabbros are present at several localities within the central and southern areas of the north Pindos Mountains. Isotropic gabbros, containing plagiogranites, are found at the contact with the sheeted dyke complex (e.g. W. of Spileo; Fig. 2.2). Here, several tens of metres of light grey, weathered gabbro with felsic veins, contain anastomosing plagiogranite veins and screens up to 30 m long. Isotropic gabbros crop out extensively in the lower Aspropotamos River area (Isotropic Mafic-Intermediate Group of Kostopoulos 1989), where they are reported as being 370 m-thick, and of clinopyroxene-plagioclase-magnetite mineralogy (Kostopoulos op. cit.). Southwards from this locality, towards Mikrolivado, these gabbros continue, and have been mapped as a belt several hundred metres wide, but have only been observed by the author at one locality, southeast of Achladi (Fig. 2.2; Parrot 1967) and thus require further study. Isotropic gabbros were also

discovered in the Katara Pass area, where they are cross-cut by individual hydrothermally metamorphosed basaltic dykes.

2.5.4 Plagiogranites

Plagiogranites (e.g. those at Spileo, see above) are found within the isotropic gabbros and rarely the sheeted dykes of the Complex. They are quartz-feldspar-hornblende-chlorite rocks. Plagiogranites have been discovered in two other localities, associated with the Aspropotamos volcanic sequences exposed to the southwest and southeast of Avdella. Southwest of the village on the Perivoli road, gabbros and sheeted dykes contain elongate pods and veins of plagiogranite. A prominent block of white plagiogranite is also found on the track south of Avdella, approximately 100 m west of the Avdella stream valley. This block is enclosed within basal serpentinite, which underlies cumulates, dykes and volcanics of the Aspropotamos Complex. In thin section these rocks contain quartz, plagioclase, hornblende (altering to chlorite or biotite) accessory sphene, zircon and epidote.

2.5.5 The sheeted dyke complex

The sheeted dyke complex is thought to be the most convincing evidence for ophiolite complexes having been formed at a oceanic spreading axis (Moores and Vine 1971). Sheeted dykes have been recognised in most of the major ophiolite complexes of the world (e.g. Oman, Pallister 1981; Troodos, Kidd and Cann 1974), where their thickness and chilled margin relationships have been studied in some detail. Sheeted dykes are only well exposed locally within the Aspropotamos Complex, and are at an early stage of study. Where present, they are 100% sheeted, with well preserved chilled margins (Plate 2.1). The best locality for viewing the dyke complex occurs west of Spelio, to the north of the Venetikos valley (Fig. 2.2). There, the dykes are individually up to 2 m-thick (Plate 2.1). The transition upwards into the volcanic sequence, demonstrated by the appearance of screens of pillowed and massive basalt, and downwards into the high-level gabbros are both

locally preserved. An approximate minimum thickness estimate for the sheeted complex in this area is 500 m.

The majority of sheeted dykes at Spileo trend approximately NW-SE (Fig. 2.6), and are of MORB, or evolved-MORB chemical type (see below). There, and at nearby localities (e.g. Abelia; Kostopoulos 1989), boninitic dykes are observed to cross-cut the MORB and other more depleted dykes (MORB-IAT and IAT). The younger, more chemically depleted dykes trend subparallel (i e. NNE-SSW) to highly discordant (i e. SW-NE), with respect to the predominant sheeted dyke trend (NW-SE). Tectonically-sheared dyke complexes of MORB composition are found at several other localities (e.g. east of Armata, Katara Pass, Fig. 2.2), where they are also cross-cut by later, more geochemically depleted dykes.

The sheeted dykes exposed elsewhere (e.g. Perivolaki; Ziakas-Perivoli road; Sotira Mountain, Avdella; Fig. 2.2), are entirely of IAT and boninitic geochemical affinities (Plate 2.1, 2.2). These dykes tend to be thinner on average than the MORB dykes described above (1.5-2 m; see Plate 2.1). Near the village of Perivolaki (Fig. 2.1, 2.2), high level gabbros and sheeted dykes pass locally upwards into boninitic pillow lavas with abundant weathered glassy rims (Plate 2.2).

At Avdella, (Sotira Mountain; Fig. 2.2) a kilometre-thick succession shows cumulate gabbros passing into sheeted dykes and extrusives, which include pillowed lavas and pillow breccias. All of these units are of boninitic affinities (Western Aspropotamos Complex of Kostopoulos 1989; see below), and appear to form an isolated unit, separate from any earlier MORB-type dykes. Similar IAT and boninitic sheeted complexes are found on the Avdella-Perivoli track (2 km S.W. of Avdella; Fig. 2.2), and in the Venetikos Valley area, south of Spileo (E. Valsami pers. comm. 1989). Individual boninitic dykes have also been observed intruding the cumulate sequence, where it is well exposed.

Further south, in the Koziakas area, a boninitic dyke has also been discovered intruding harzburgite, further providing evidence of their late-stage intrusion (Capedri et al. 1985).

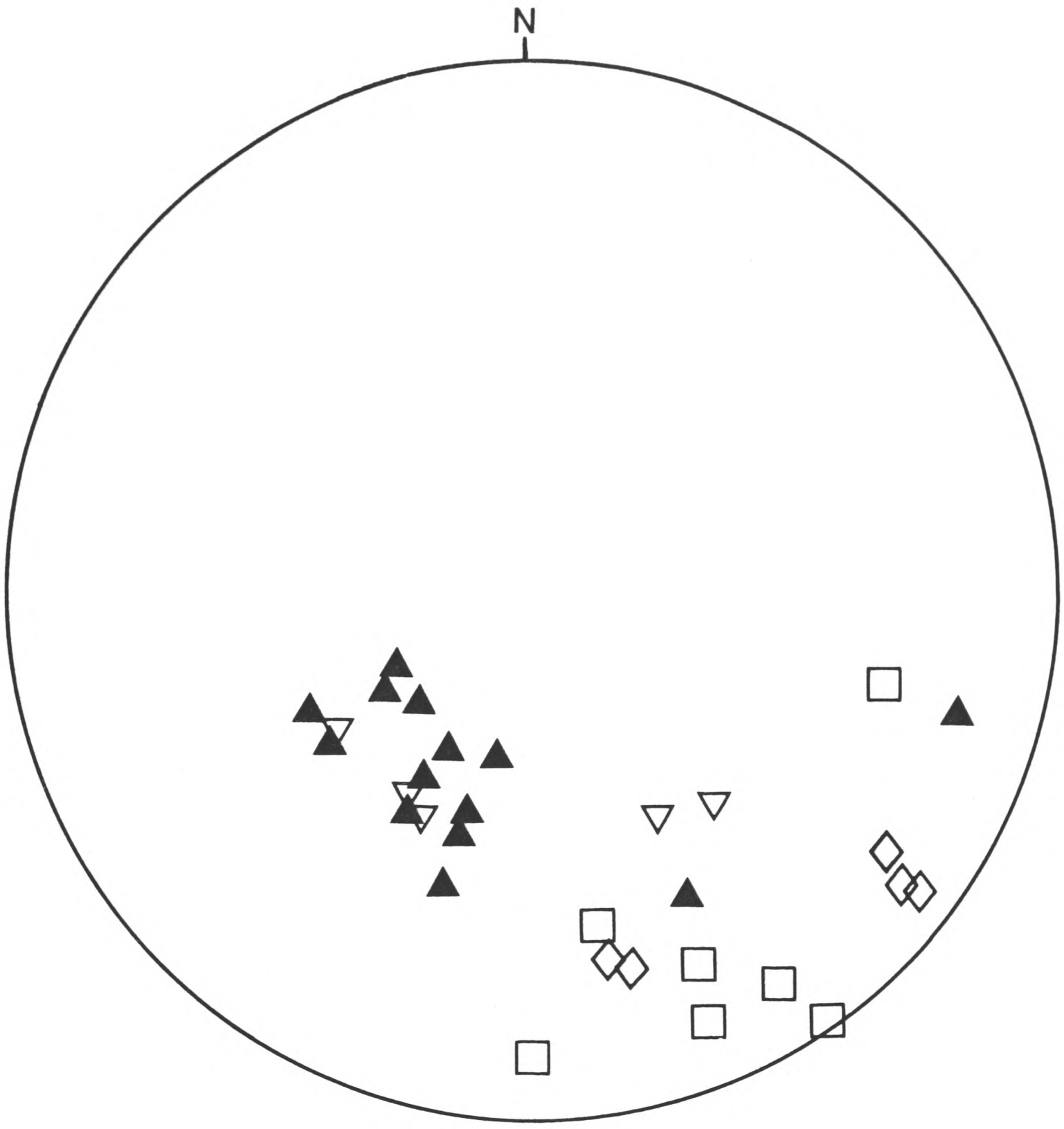

▲ Spelio and Karamoula, sheeted MORB

▽ Spelio individual and sheeted IAT–BON

◇ Perivolaki sheeted IAT–BON

□ Karamoula sheeted IAT–BON

Fig. 2.6 Equal-area stereographic projection of poles to dyke trends. Spileo, Karamoula and Perivolaki localities (Fig. 2.2). MORB= mid ocean ridge basalts; IAT= island arc tholeiites; BON= boninites.

2.5.6 The extrusive sequence of the Aspropotamos Complex

The extrusive units of the Aspropotamos Complex (up to 2 km thick; Fig. 2.3, 2.5) consist of pillow lavas (up to 3 m long; Plate 2.3), massive lavas, basalt breccias and hyaloclastites, with common cross-cutting intrusive rocks (Plate 2.3). The lavas are usually micro-phyric to vesicular, and are dark green, dark grey, or blue-grey when fresh. Their mineralogy when fresh is albite and augite, with accessory chlorite, calcite, quartz and rare zeolites. Epidote is extremely common, either as a vein mineral, filling vesicles, or within the mesostasis. The petrology and geochemisty of the extrusives has been discussed at length elsewhere (e.g. Kostopoulos 1989), and will not be considered in detail here. The Aspropotamos Complex extrusive sequences are extremely variable. There is a general compositional change within the volcanic sequence, with a predominance of basaltic andesites and andesites being found towards the exposed upper part. Also present locally are both rhyolites and high-Zr rhyolites, containing abundant vesicles (e.g. W. of Paroreio village, Fig. 2.2).

2.5.7 Volcanic stratigraphy

The large number of geochemical analyses (see below) now available for the Pindos intrusive and volcanic units allows a tentative reconstruction of the volcanic stratigraphy to be made. This has been attempted by Kostopoulos (1989) for the lower Aspropotamos Valley. This stratigraphy has been modified here, using additional field and geochemical evidence (Fig. 2.5). A complex series of volcanic and intrusive events is present, in which a general pattern of progressively more depleted and evolved volcanics is erupted.

The volcanic stratigraphy of the Aspropotamos Complex is somewhat similar to that observed within the Oman ophiolite, where MORB-IAT transitional volcanic units (Geotimes Unit) are intruded and overlain by successively more depleted units (Lasail, Alley and Clinopyroxene-phyric Units; Alabaster and Pearce 1982). No rocks specifically comparable to boninites are found in Oman, although the clinopyroxene-phyric unit is transitional from IAT to BSV. The Troodos

(Murton 1990) and Hatay ophiolites (Piskin et al. 1986) similarly show more depleted extrusives, including boninites, towards the top of the succession.

2.5.8 Hydrothermal metamorphism

The Aspropotamos Complex extrusives have experienced intense hydrothermal metamorphism (e.g. Valsami and Cann in prep.) while they were within the oceanic environment. Virtually all of the lavas display assemblages typical of lower to upper greenschist facies oceanic metamorphism, with zeolite facies rocks being uncommon. Amphibolite facies assemblages are also present within the sheeted dyke complex. Well developed epidosites occur within both the extrusive and intrusive units (E. Valsami pers. comm. 1989), and many of the basalts are metamorphosed to transitional quartz-chlorite-epidote and quartz-chlorite rocks. Good examples of the extrusives can be seen along the road linking Mikrolivado with the Aspropotamos valley (Fig. 2.1). At many localities, individual dykes and local dyke swarms are found cross-cutting the extrusives (e.g. N.W. of Monahiti, Fig. 2.2). Minor sulphide deposits have also been discovered at several localities (e.g. east of Perivoli, Dhistraton-Armata area Fig. 2.2).

2.5.9 Sediments associated with the Aspropotamos Complex

Sediments intercalated with extrusives of the Aspropotamos Complex comprise radiolarian chert, cherty mudstone, metalliferous oxide-sediments (Robertson and Varnavas 1990), siltstone, mudstone and rare marl. Conformable contacts with the extrusives are extremely rare, but thrust-bounded sediment packages within the volcanics, up to 45 m thick, are relatively common. Umberiferous sediments within pillow lavas exposed west of the Venetikos River (near Trikomon, Fig. 2.2), contain quartz, white mica and haematite. The extrusives from this locality also contain a silicified volcaniclastic horizon as a thrust intercalation. This rock has detrital fragments of quartz (including polycrystalline quartz clasts) and volcanic material, set in a glassy chloritic matrix. A small valley on the eastern bank of the Venetikos River (W. of Trikomon), exposes thin,

pink pelagic interpillow limestones, which have unfortunately not yielded any fauna.

2.6 GEOCHEMISTRY OF THE ASPROPOTAMOS COMPLEX

2.6.1 Introduction and previous studies

Previous work on the volcanic rocks of the north Pindos Mountains (Parrot 1967, 1969; Montigny et al. 1973; Terry 1974, 1979; Parrot and Verdoni 1976; Pearce 1979; Capedri et al. 1980, 1981, 1982; Kostopoulos 1989) highlighted the variety of chemical types present within the ophiolite crustal sequences. Further work was necessary, however, to confirm the regional extent of this chemical variation, and to discover new localities. A wide range of igneous geochemical signatures are consistently displayed by the basic rocks of the Aspropotamos Complex throughout the northern Pindos region. This complexity is best displayed in the well-preserved sections within the Aspropotamos Valley, where successively intruded dykes exhibit a general trend towards greater geochemical depletion in high field strength elements. At one key locality (Abelia, Fig. 2.2), six stages of dyke intrusion are observed, showing a progressive trend from MORB to IAT, and then BSV (Boninite Series Volcanics; Kostopoulos 1989). Elsewhere, dyke and lava sections may be of a single type (BSV; e.g. Sotira, Fig 2.2; Kostopoulos 1989).

2.6.2 Tectonic discrimination diagrams

The chemistry and petrogenetic evolution of the Pindos ophiolitic units from the central area has been described in some detail by Kostopoulos (1989). The data presented here have been collected from other areas of the Pindos Mountains, and are summarised below. These data (Appendix 3) are presented as geochemical discrimination and multi-element diagrams (Figs. 2.7-2.15), mainly using immobile trace elements to highlight the chemical variations present. They extend geochemical coverage of the Pindos ophiolitic rocks. The discrimination diagrams also help to indicate the possible tectonic environment of origin for the volcanic units, based on comparison of data from modern day oceanic

settings. The diagrams are usually divided into fields consisting of within plate basalt (WPB), characteristic of ocean islands and areas of continental rifting, mid-ocean ridge basalts (MORB), typical of Mid Atlantic-type constructive plate boundaries and also back-arc basins, and island arc tholeiites (IAT) typical of oceanic arcs formed above destructive plate boundaries, and certain back-arc basins. A particular type of supra-subduction zone magma type is boninite (BSV or Boninite Series Volcanics), which represent high magnesium and silica andesites, enriched in compatible trace elements and depleted in titanium and other high field strength elements.

The discrimination diagrams utilised are the Ti-Zr-Y (Pearce and Cann 1973), Zr/Y-Zr, Ti-Zr (Pearce 1980), Cr-Ti and Cr-Y diagrams (Figs. 2.7-2.9), and the Nb-Y and Rb-Nb+Y plots for plagiogranites (Fig. 2.10). The Ti-Zr-Y, Ti-Zr and Zr/Y-Y diagrams are useful for separating within plate basalts, and partially for separating MORB and IAT basalts from other magmas. The Cr-Y, Cr-Ti and MORB-normalised multi-element diagrams (Figs. 2.11-2.15) are particularly useful for illustrating any subduction component that may be present. For a detailed description of the potential of each diagram, the reader is referred to Pearce and Cann (1973), Pearce (1980, 1982), Wood et al. (1979) and Kostopoulos (1989) for the Pindos volcanics.

The most important feature of the geochemistry is that a complete range of volcanic geochemistries is preserved. If the associated volcanics from the Avdella Melange (Chapter 4) are also taken into consideration, a sequence from alkalic WPB through to boninites, including all intermediate varieties, are present. This is well displayed by the Cr-Y diagrams shown in Fig. 2.9. Also plotted on this diagram are the fields for the intrusive and extrusive rocks of the Vourinos ophiolite, which plot almost exclusively in the island arc tholeiite field of Pearce (1980).

The plagiogranites (n=6) have been analysed geochemically, and are shown to be highly acidic rocks, with silica values ranging from 64% to 77%. The analyses have been plotted on the Rb-Y+Nb and Nb-Y discrimination diagrams (Fig. 2.10; Pearce et al. 1984b). These diagrams are used in the tectonic classification of granitic rocks, which are sub-divided into syn-collision (Syn-COLG), volcanic arc (VAG), ocean ridge (ORG) and

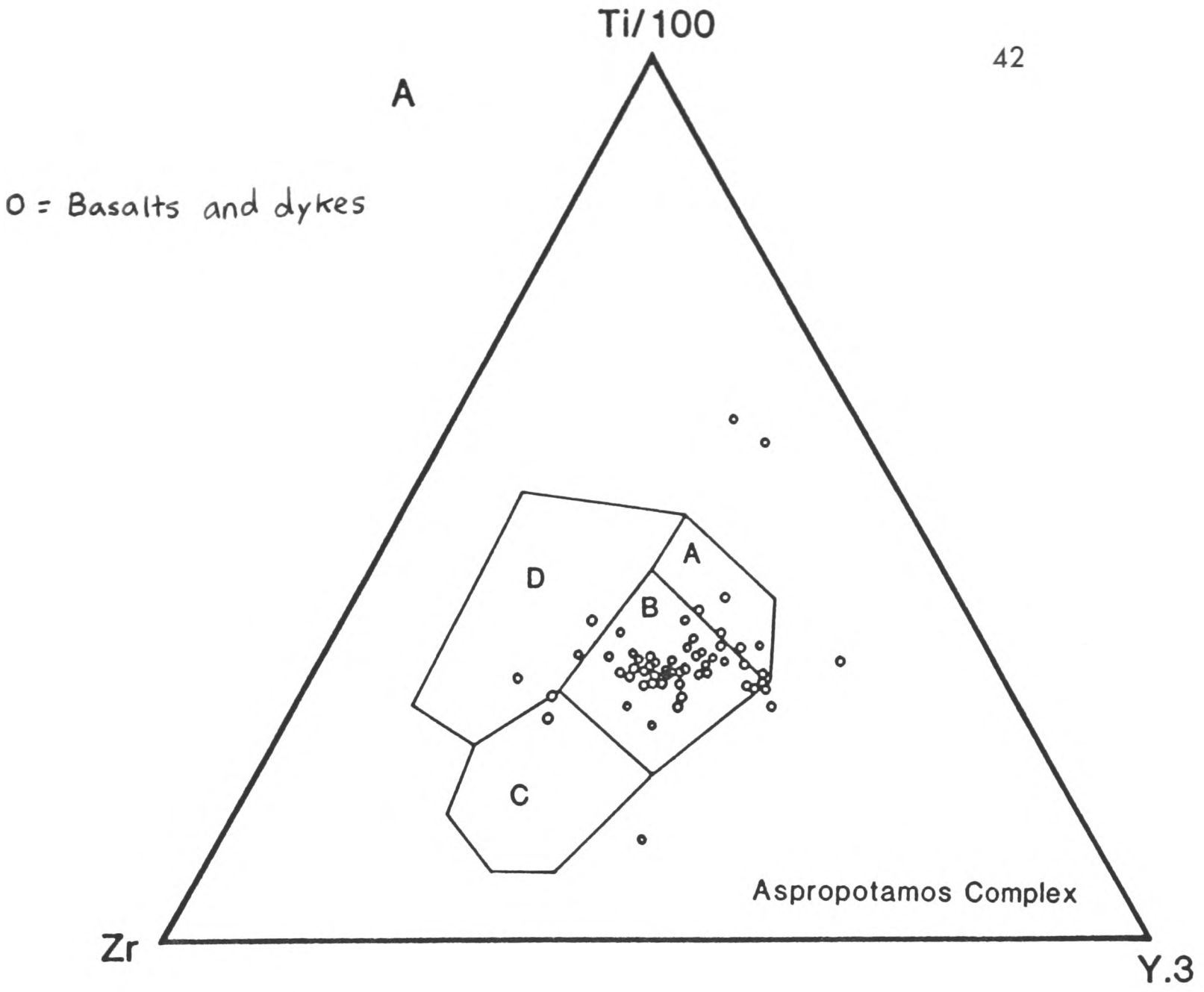

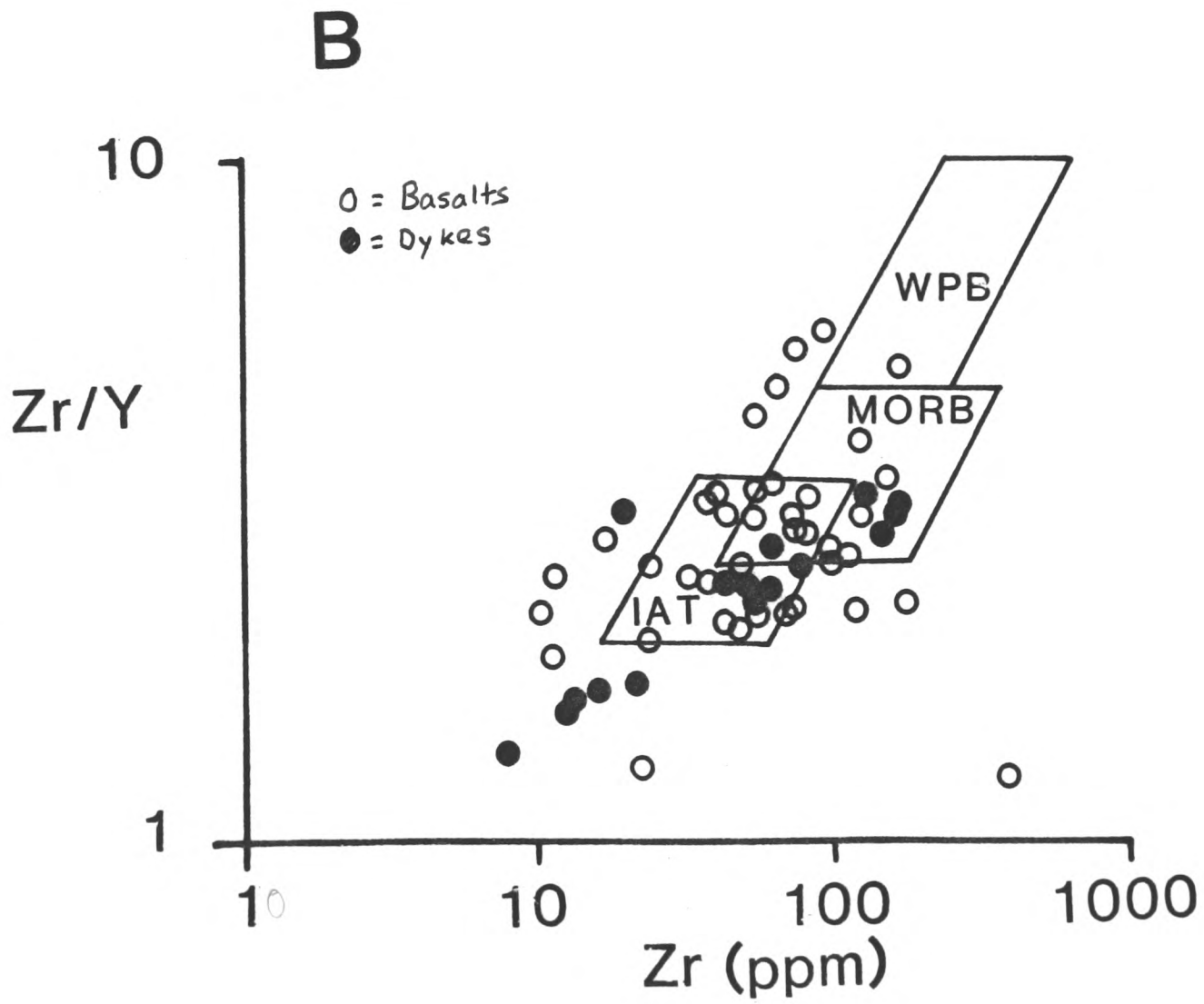

Fig. 2.7 a) Ti-Zr-Y triangular plot for the Aspropotamos ophiolitic rocks analysed by XRF in Edinburgh. Fields A+B= island arc tholeiites; B= mid ocean ridge basalts; B+C= calc-alkaline basalts; D=within plate basalts (after Pearce and Cann 1973). b) Zr/Y-Zr plot for the Aspropotamos Complex. WPB= within plate basalts; MORB= mid ocean ridge basalts; IAT=island arc tholeiites (after Pearce 1975).

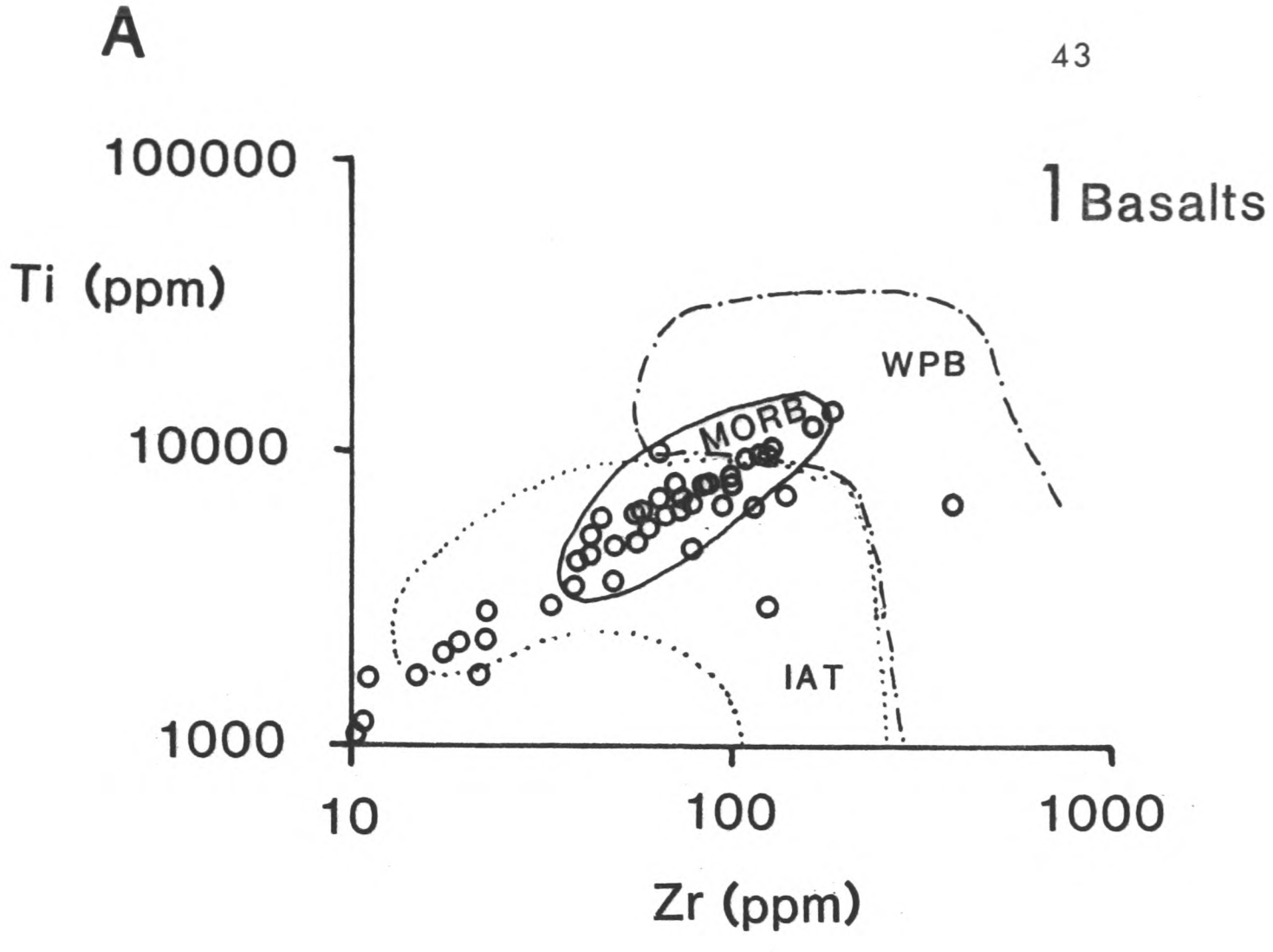

Fig. 2.8 A) Ti-Zr plot for the Aspropotamos Complex. 1) basalts; 2) dykes. WPB= within plate basalts; MORB= mid ocean ridge basalts; IAT=island arc tholeiites (after Pearce and Cann 1973). B) Cr-Ti plot for the Aspropotamos Complex. 1) basalts; 2) dykes. Fields after Pearce (1975).

B

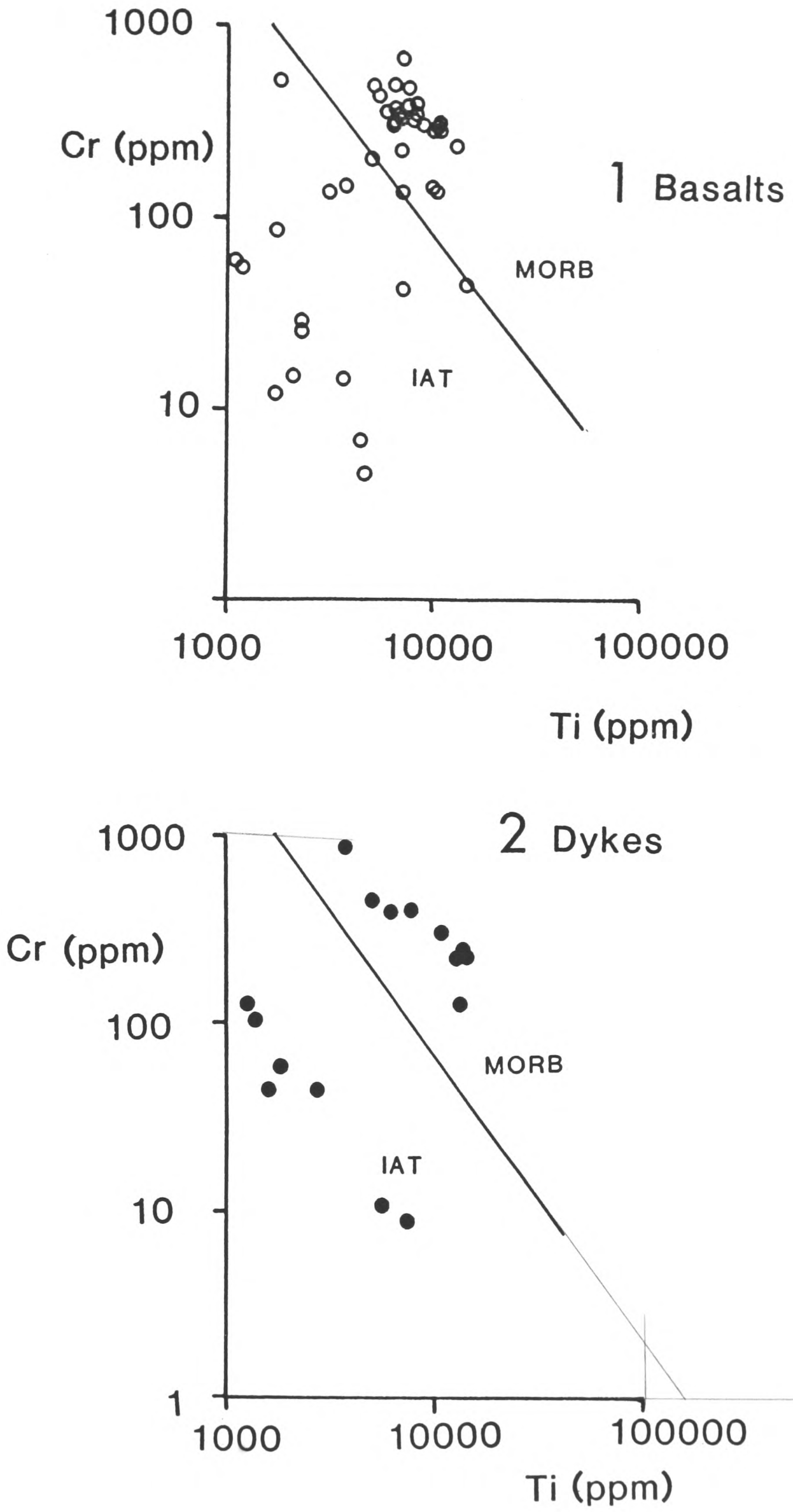
1000
Cr (ppm)
100
10
1
1000
10000
100000
Ti (ppm)
1 Basalts
MORB
IAT
2 Dykes
MORB
IAT

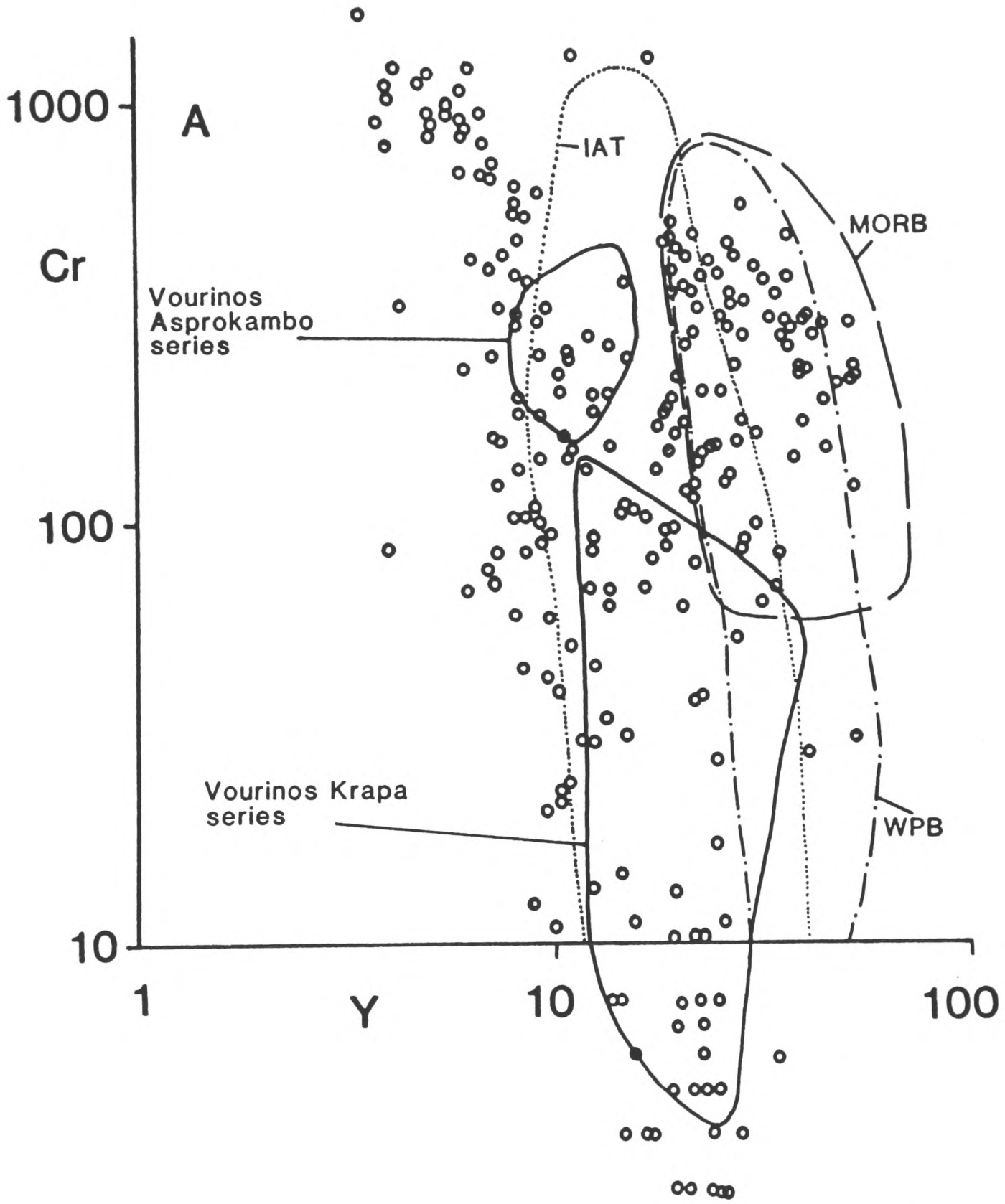

Fig 2.9 Cr-Y diagram for the Aspropotamos Complex. Data from this study, and Kostopoulos (1989). Key as in Fig 2.7.b. Fields for the Vourinos ophiolite intrusives (Asprokambo series) and extrusives (Krapa series) are superimposed, based on data from this study, Beccaluva et al. 1984 and Noiret et al. 1981.

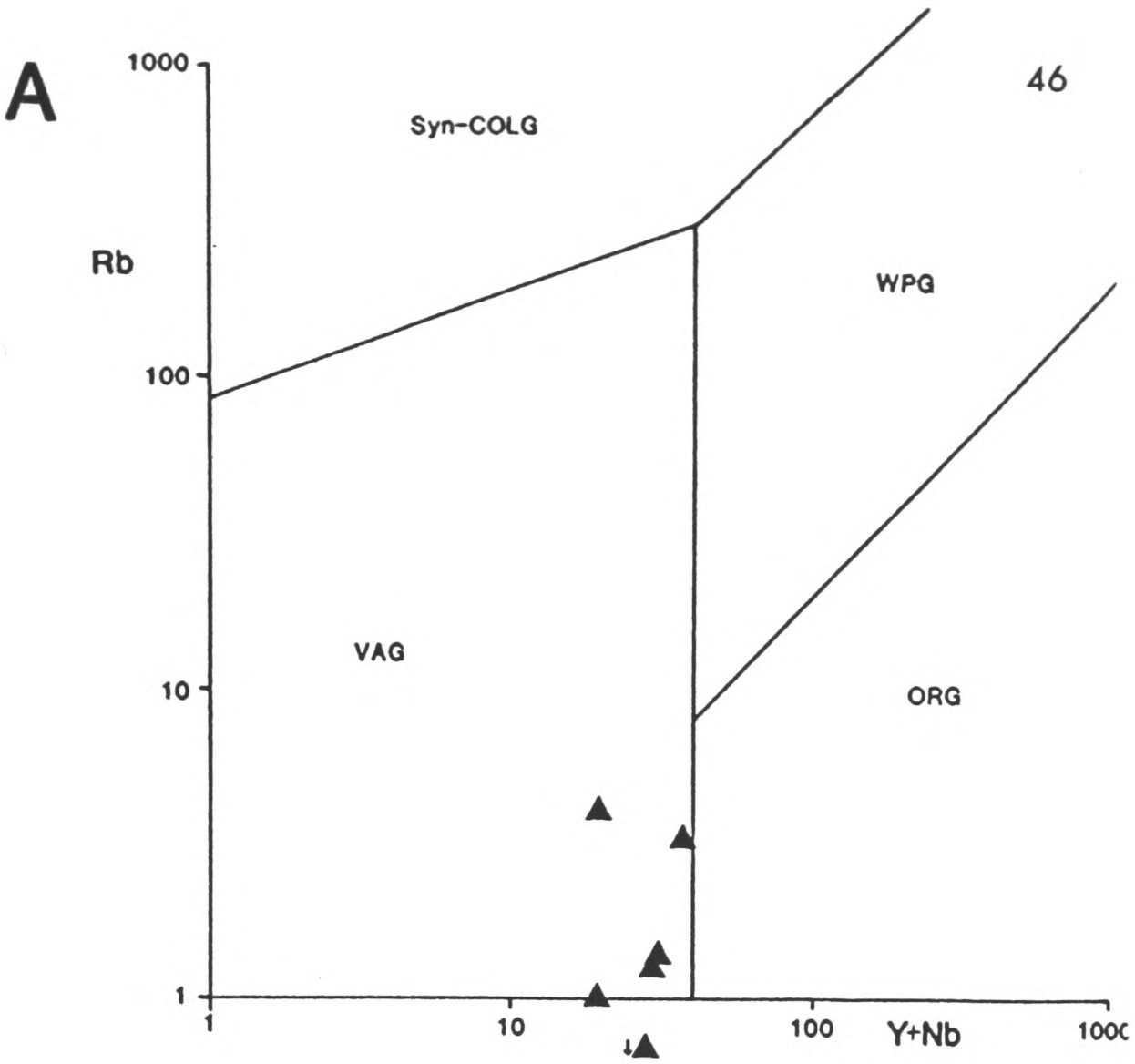

Fig. 2.10 a) RB-Y+Nb and b) Nb-Y tectonic discrimination diagrams (after Pearce et al. 1984b) for oceanic plagiogranites of the Pindos ophiolite (closed triangles). Syn-COLG= syn collision granite; VAG= volcanic arc granite; ORG= ocean ridge granite; WPG= within plate granite. Fields for Oman, Troodos, Antalya and Vourinos after Pearce et al (1984b).

within plate granite (WPG). The Pindos plagiogranites plot within the VAG fields in these diagrams, and not the ORG field, as might have been expected. It can be seen from the Nb-Y diagram that there is some correlation between the Pindos values and the values obtained for Vourinos, which also plot, along with the other main Tethyan ophiolites, mainly in the VAG field. It is worth mentioning that both Troodos and Oman do overlap into the ORG field, but this may, perhaps, be a function of sample size. The plagiogranites were also plotted on multi-element plots (Fig. 2.11), normalised against the ORG values of Pearce et al. (1984b). These show a trend similar to those presented for Troodos and Oman volcanic arc granites by Pearce et al. (1984), although direct comparison is difficult, as different trace elements are utilised.

2.6.3 Geochemical reconnaissance of the Aspropotamos Complex

The Aspropotamos Complex has been recognised in numerous other parts of the Pindos Mountains, as well as in the Aspropotamos Valley type area, based on reconnaissance geochemical analysis (e.g. Vovousa, Armata, Dhistraton, and Katara Pass, Fig. 2.1), suggesting that it forms a regionally extensive thrust sheet. The ophiolitic units found elsewhere usually comprise tectonised cumulates, intrusives and extrusives, and all show comparable geochemical sequences to the type area, including units showing depletions in immobile high field strength elements.

Geochemical data for the southern region of the Pindos Mountains also illustrates the geochemical spectrum present, as shown on MORB-normalised multi-element diagrams (normalising values: Sr=120 ppm, K_20=0.15%, Rb=2 ppm, Ba=20 ppm, Nb=4 ppm, La=4.5 ppm Ce=10 ppm, Nd=8 ppm, P=0.12%, Zr=90 ppm, Ti=1.5%, Y=30 ppm, Sc=40 ppm and Cr=250 ppm). For example, in the Metsovo area (the Katara Pass; Fig. 2.2), IAT and boninitic-type volcanics are found. Sample 97/88 (Fig. 2.12a) is a low Cr, transitional IAT-BSV rock, depleted in high field strength elements and Ti. This rock does not have the high magnesium content of boninites, but does have a high silica content (Appendix 3). At one prominent locality, immediately adjacent to the main Metsovo-Kalambaka road, these boninitic lavas are overlain by Late Cretaceous pelagic limestones,

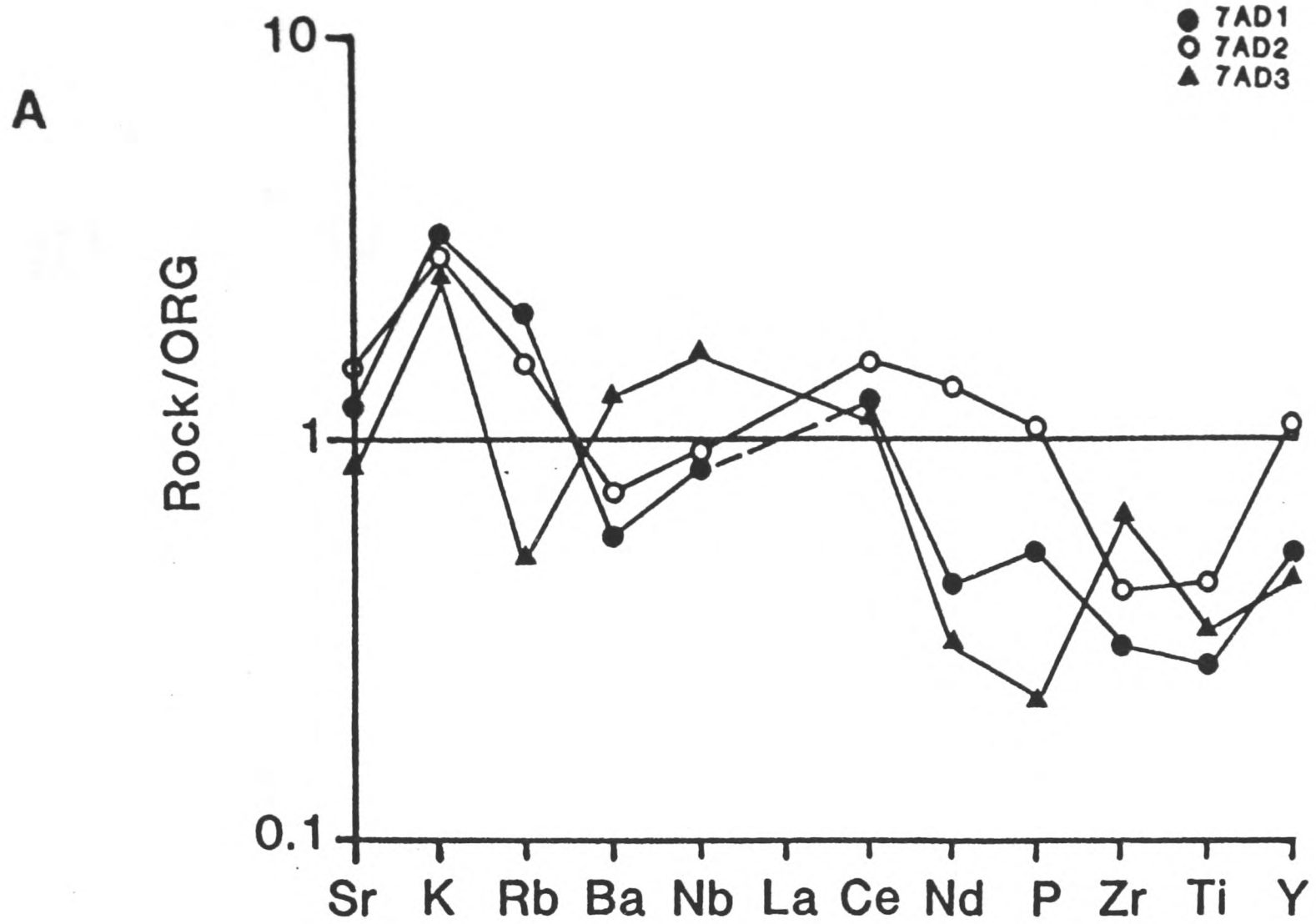

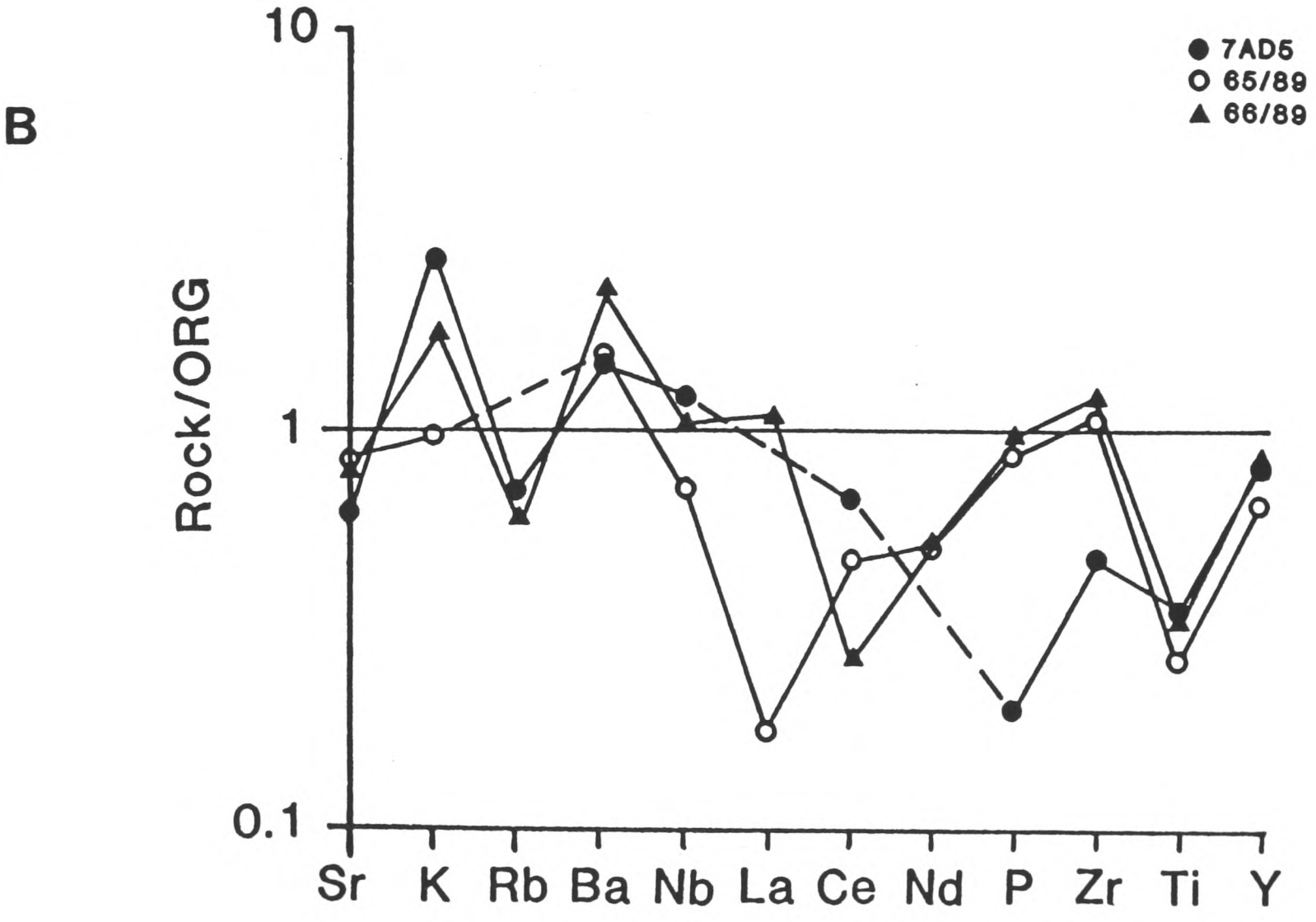

Fig. 2.11 Multi-element plots of Aspropotamos Complex plagiogranites, normalised to average ocean ridge granite (values from Pearce et al. 1984b). See text for explanation.

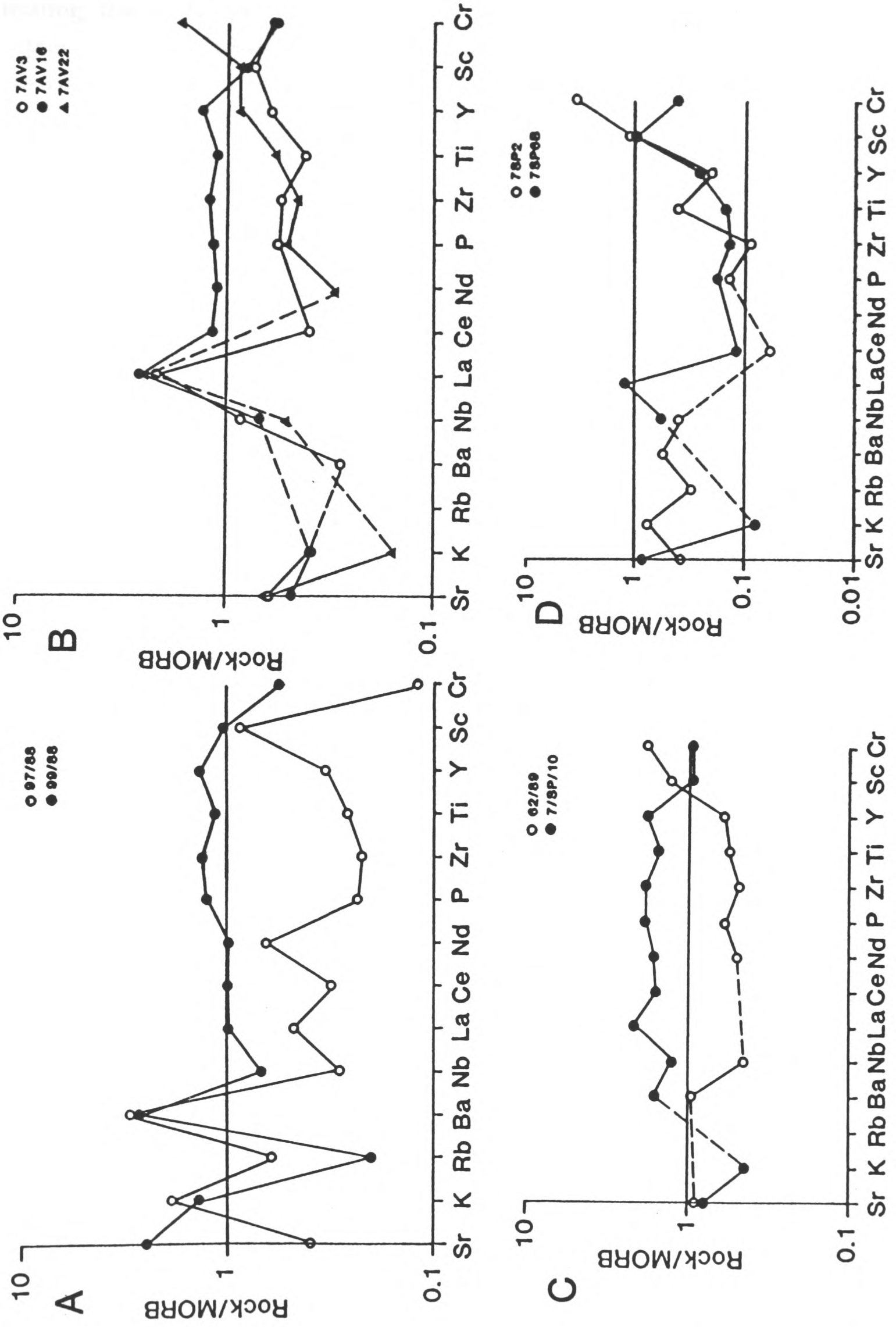

Fig. 2.12 Multi element plots for the intrusive and extrusive rocks of the Aspropotamos Complex. a) Basalt flows from the Metsovo-Kalambaka road, western Katara Pass, 10 Km east of Metsovo. b) Basalts, Aoos Valley, 7 Kms N. of Vovousa. c) Dykes, Venetikos valley, 5 kms W. of Spileo village. d) as for c). See text for explanation.

indicating that they were exposed on the seafloor during this time (Chapter 5). These extrusive thrust slices are relatively uncommon in the southern area, except in the Katara Pass. MORB-type sheeted dykes, gabbros and extrusives are also found in this area (e.g. sample 99/88; Fig. 2.12a).

In the western-central area, extrusives are exposed in the Aoos Valley (N. of Vovousa, Fig. 2.1). Notably, these basalts demonstrate a range from N-MORB to transitional MORB-IAT and true IAT signatures (Fig. 2.12b), similar to basalts in the lower Aspropotamos area and elsewhere. This is illustrated by Ti values below 1 %, and associated low Zr (minimum 42.6 ppm) and Nb (minimum 2.1 ppm) values. Y varies between 18.4 ppm and 39.4 ppm. Sample 7AV16 is a somewhat evolved MORB, sample 7AV3 is a more depleted MORB-IAT with particularly low Ti, and 7AV22 is an IAT with somewhat elevated Cr (Fig. 2.12b). Extrusives exposed south of Vovousa (12 Km S. on the Metsovo road) are of MORB-type, similar petrographically to rocks from Spileo.

Some of the most extensive areas of exposed extrusive rocks, with local sheeted and individual dyke swarms, occur to the west of Spileo. As mentioned above, the sheeted dykes are of evolved MORB-type (e.g. 7SP10; Fig. 2.12c), or more depleted MORB and transitional to IAT (e.g. 62/89; Fig. 2.12c). The boninitic dykes which are also found in this sequence have a characteristic dish-shaped pattern, extremely depleted in HFS elements, and may be either somewhat Cr enriched or depleted, relative to normal MORB (e.g. 7SP2, 7SP6B; Fig. 2.12d).

Basalts from the immediately overlying volcanic sequence, show a wide range of compositions over a small horizontal distance (several tens of m). Some of these rocks are evolved MORB's, similar to the dykes (e.g. 7SP13; Fig. 2.13a). Others are slightly evolved N-MORB, which are occasionally depleted in rare earth elements (e.g. 57/89; Fig 2.13a). Additionally, rocks transitional between MORB and IAT (e.g. 63 and 64/89; Fig 2.13b) are also present.

South and southwest of the Spileo area (Fig. 2.2), extensive volcanics are exposed, interpreted as belonging to the upper units of the Aspropotamos Complex, which originally overlay the lower crustal

lithologies already described. These rocks are the subject of a study by Valsami (1990), and are exclusively of IAT and boninitic chemistry (southern slopes of the Venetikos Valley, approx 3 km southwest of Spileo, Fig. 2.2). Also, some parts of the volcanic sequence (i.e. towards the exposed top) contain highly evolved andesites and rhyolites, which are locally extremely vesicular (e.g. W. of Paroreio, Fig. 2.2). The geochemical variation is displayed over relatively small distances in the field (10's to 100's of metres), and supports the complexity seen within the intrusives.

East of Perivolaki (Fig. 2.2), some sheeted dykes are low in Cr, and are of IAT-type (e.g. 106/89; Fig. 2.13c), others being more boninitic. Basalts here are also boninitic (108/89; Fig. 2.13d). At Krania, both E-MORB (e.g. 67/89; Fig. 2.13d) and transitional MORB-IAT (e.g. 68/89; Fig. 2.13d) volcanics were discovered. In the Venetikos valley west of Trikomon (Fig. 2.2), basalts have MORB (e.g. 87A/89; Fig. 2.14b and see Appendix 3), and primitive E-type MORB (90/89, Fig. 2.14b; 92 and 93/89, Fig. 2.14c) characteristics. Similar primitive E-type MORBs, with a small but consistent P enrichment, were also found at the confluence of the Venetikos and Aspropotamos Rivers (7VE36 and 7VE37; Fig. 2.14d). To the southwest and southeast of Avdella, depleted volcanics of boninitic type are present (7AD8, 95/89; Fig. 2.15a), as shown by Kostopoulos (1989). Again, variation occurs in the absolute abundance of elements, particularly Cr, between basalts and dykes from the same area.

In the northern area, basalts and dykes of the Aspropotamos Complex have only been found in the region east of Armata (Fig. 2.2). There, the dykes were of N-MORB chemistry (e.g. 38/89; Fig. 2.15b), and the sampled basalts were IAT (e.g. 35/89; Fig. 2.15b).

2.6.4 Summary of the Aspropotamos Complex

The Aspropotamos Complex comprises a tectonised sequence of ultramafic to mafic cumulate, intrusive and extrusive rocks. These lithologies together form part of a thrust sheet, several kilometres thick, which tectonically underlies the mainly ultramafic rocks of the Dramala Complex. The oceanic crustal intrusive and extrusive units contain a variety of rock types, which range from gabbros and dolerites, through to

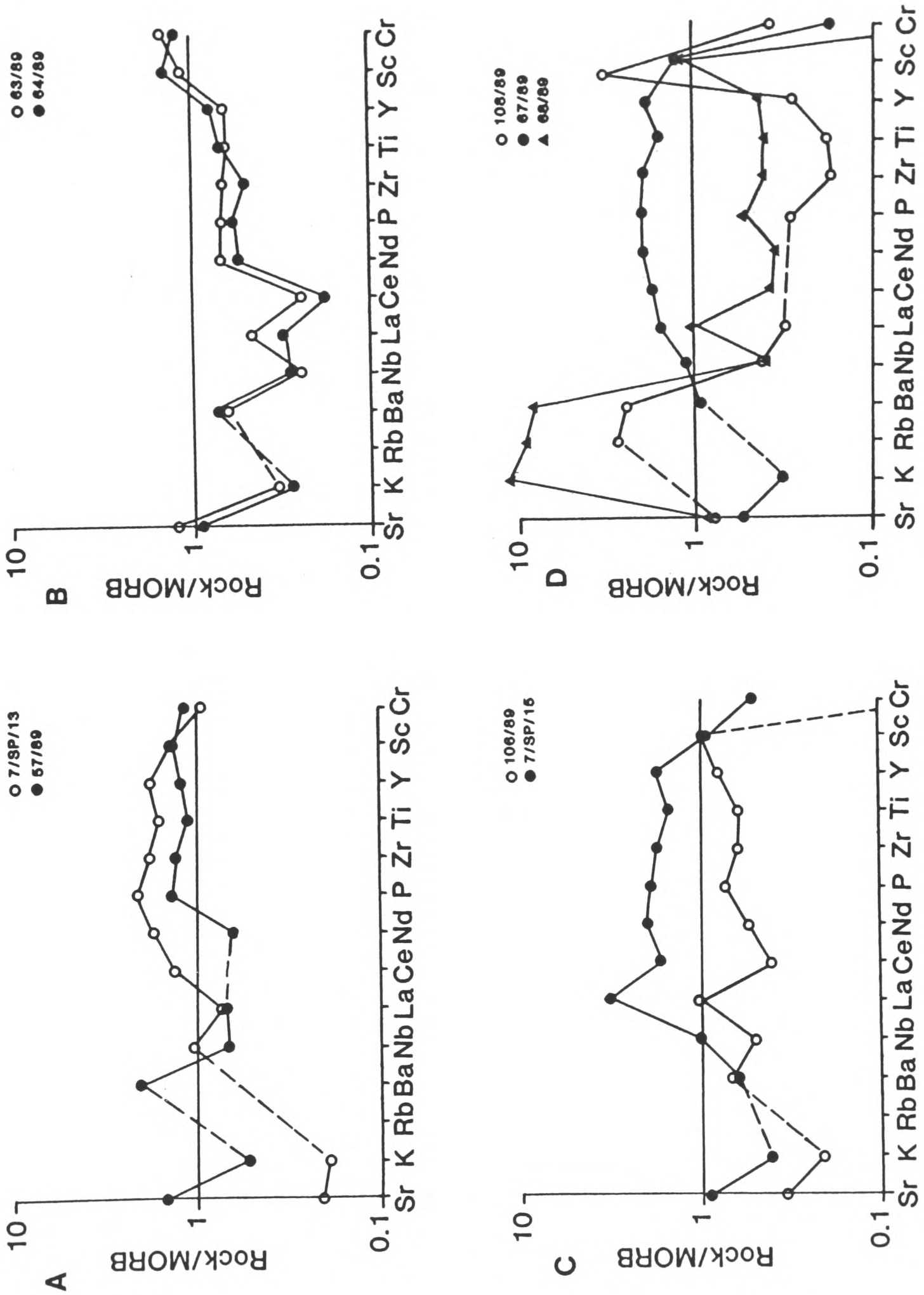

Fig. 2.13 Multi-element plots; a) Basalts, 5 kms W. of Spileo village. b) as for a). c) Road 4 kms east of Perivolaki village (sheeted dyke, 106/89; basalt, 108;89; Plate 3.3). d) Pillow basalts, Kranea village.

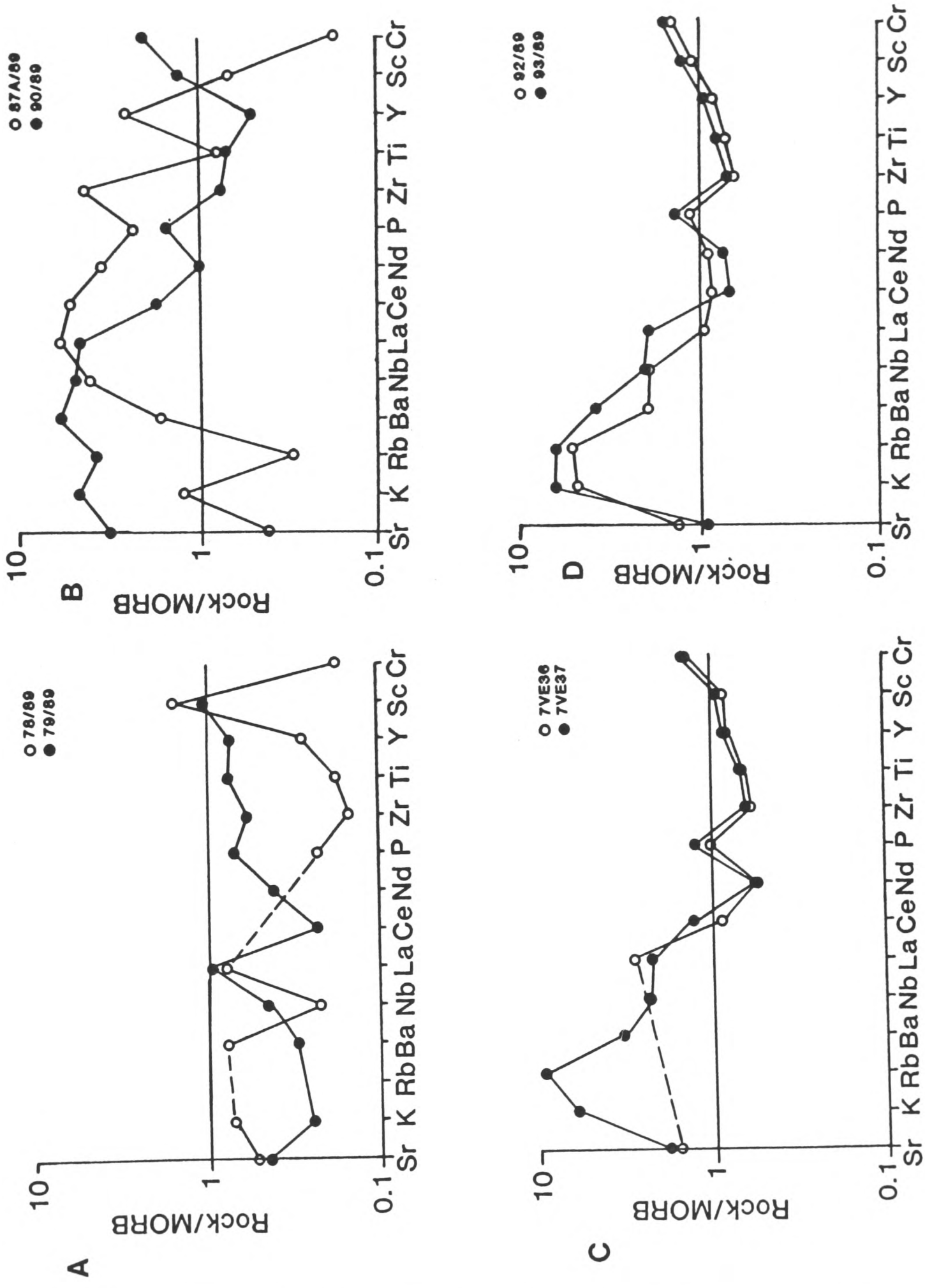

Fig. 2.14 Multi-element plots; a) Karamoula, 5 kms S.W. of Zakas village (both dykes). b) Aspropotamos bridge , 3 kms W. of Trikamon (both pillow basalts; 87A/89, N.of bridge; 90/89, S. of bridge). c) Pillow basalts (large bolster-type pillows) roadside W. of the Aspropotamos bridge, 4 kms W. of Trikamon village. d) Pillow basalts, confluence of the Aspropotamos and Venetikos Rivers, near Agios Nikolaos (Monahiti; Fig. 2.2).

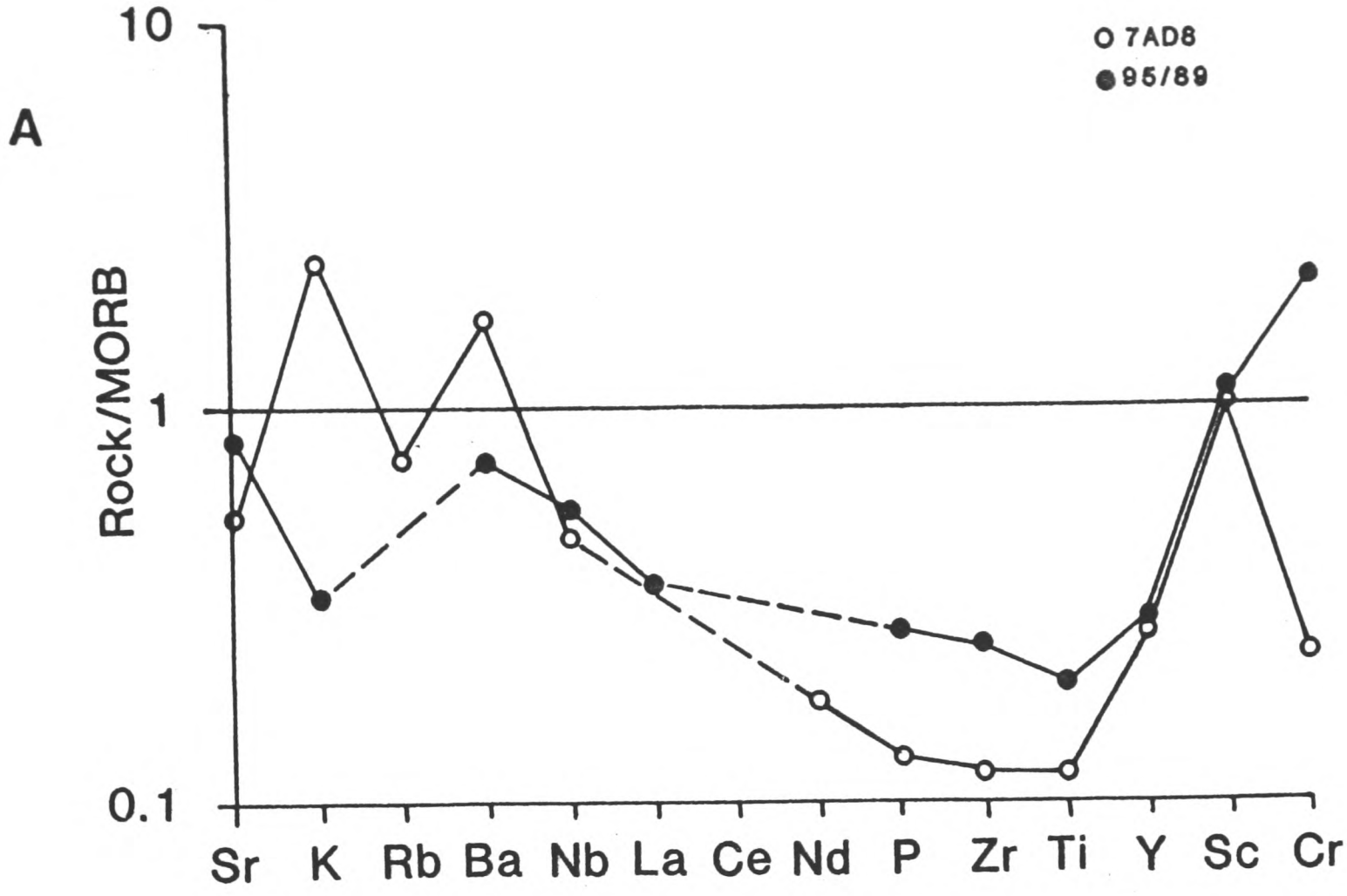

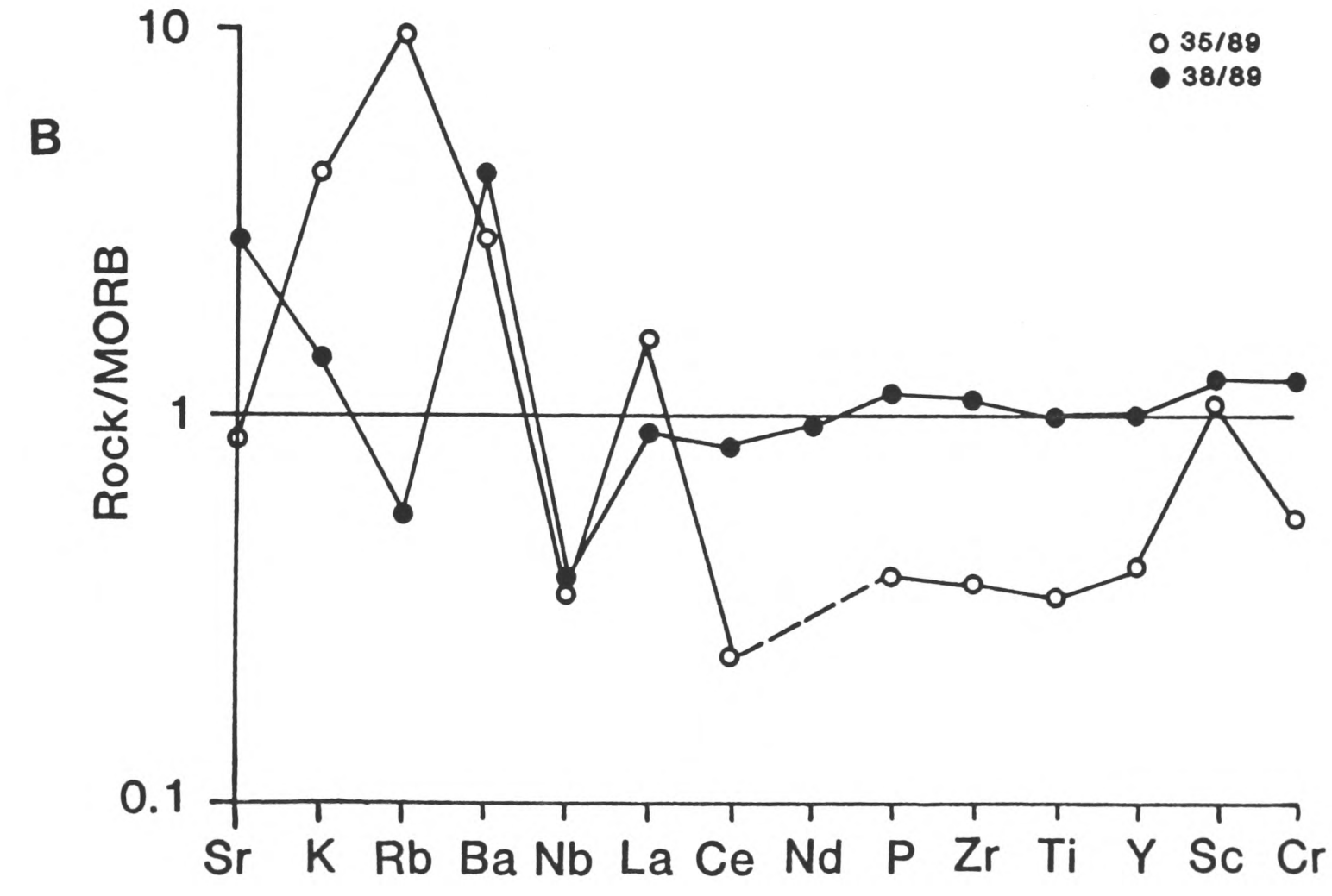

Fig. 2.15 a) Massive flow, hillside 2 kms S.W. of Avdella village, N. of the track to Perivoli (7AD8). Dyke, part of sheared sheeted complex, 5 kms S.W. of Avdella village, roadside on track to Perivoli (95/89). b) Sheeted dykes, 2 kms E. of Armata village.

basalts andesites and rhyolites. The basic rocks contain a wide range of geochemical compositions, which are found consistently displayed across the entire Pindos Mountains. The geochemistry suggests that these rocks were formed in tectonic settings which included a mid ocean ridge through to a "fore-arc" above an active subduction zone (Kostopoulos 1989; Jones and Robertson 1990).

2.7 COMPARISONS WITH OTHER TETHYAN OPHIOLITES

The Pindos ophiolite has numerous features in common with other ophiolites of the "Tethyan" belt (see Chapter 1). The Semail ophiolite of Oman and the Troodos ophiolite of Cyprus are two of the best known and best exposed Tethyan ophiolites. A brief summary of their inferred origins are presented below. The Vourinos ophiolite (Chapter 1), is believed to be part of the same section of oceanic lithosphere as the Pindos ophiolite, and is therefore critical to an understanding of the formation and setting of the Dramala and Aspropotamos Complexes.

2.7.1 The Vourinos ophiolite

Numerous lines of evidence suggest that the Vourinos and Pindos ophiolites were part of the same original oceanic system (Smith 1979; Fig. 2.16), not least the fact that they are in such close geographical proximity. The earliest integrated study of the Vourinos ophiolitic rocks was that of Moores (1969), who produced a geological map and suggested four possible origins for the complex. Noiret et al (1981) produced geochemical and isotopic data which led them to suggest that the Vourinos ophiolite was probably of island arc origin. Accumulated lithological, geochemical and structural evidence gathered subsequently are summarised below. These data further strengthen the comparison between the Pindos and Vourinos ophiolites, and allow construction of a possible tectonic model for their common origins.

2.7.1.2 Vourinos mantle and cumulate sequences

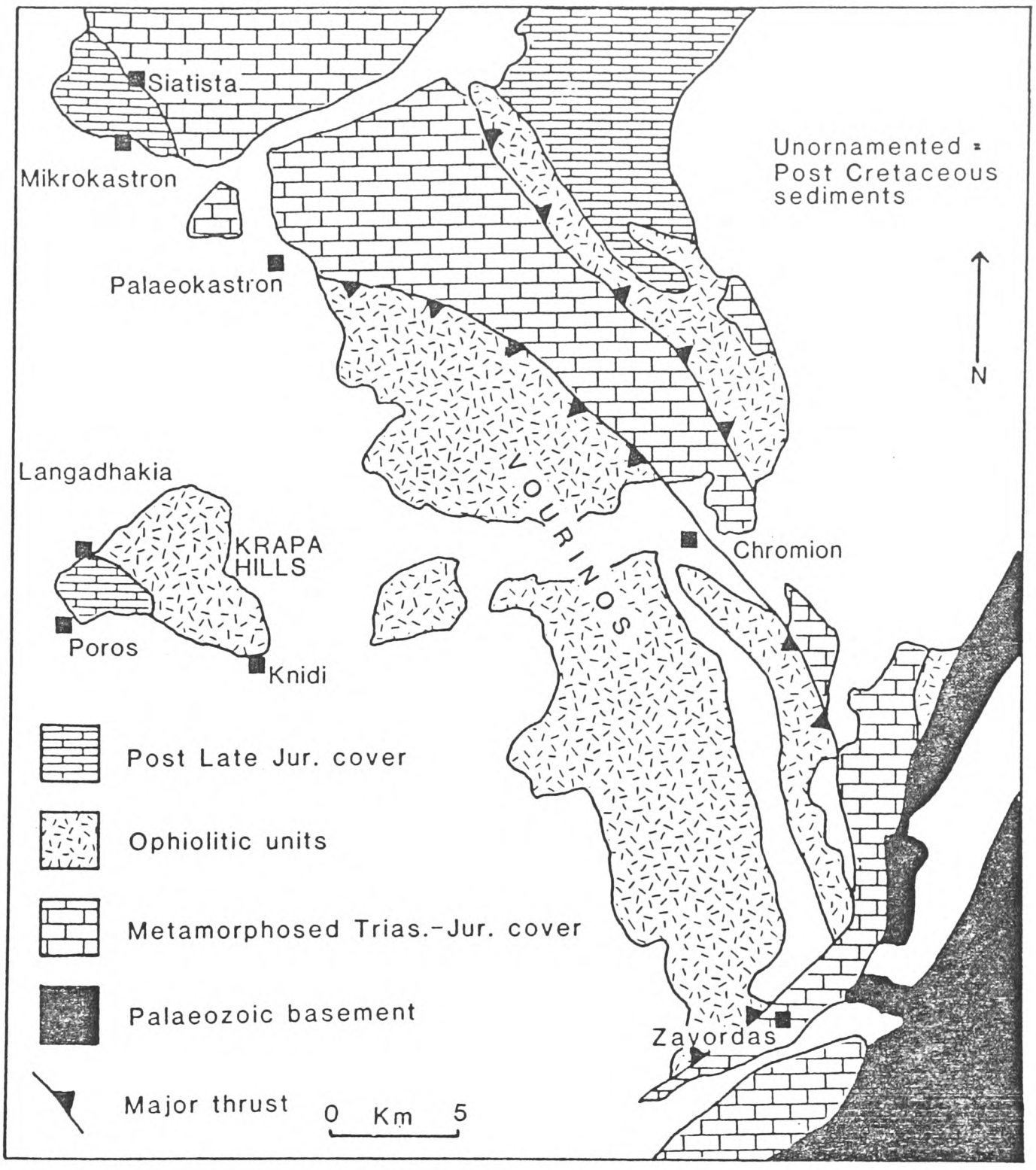

Fig. 2.16 Locality map for the Vourinos ophiolite (modified after Vergely 1984). See Fig 2.1 for locality of Vourinos.

The Vourinos mantle and lower crustal sequences (Moores 1969) consist of harzburgite-dunite dominated peridotites, with overlying layered crustal cumulates (Jackson et al. 1975). The ophiolite was interpreted as representing a spreading centre (Jackson et al. 1975; Harkins et al 1980; Ross et al. 1980), based on the following lines of evidence:

1) The presence of dunite bodies, both deformed and undeformed, within the harzburgite, implies multiple intrusion of magma at a constructive margin (Harkins et al. 1980). A magmatic origin is required for these dunites because of sharp contacts with their host rocks.

2) Structural studies of the olivine fabrics within the peridotites, together with pyroxene thermobarometry and paleopiezometry, has led to the interpretation of Vourinos as a remnant of a mantle diapir and overlying magma chamber, located at a spreading ridge (Ross et al. 1980). These authors demonstrate that a subsequent mylonitic deformation was superimposed on the early diapir-related fabric. According to their model, the mylonites formed at 30 km depth, away from the spreading centre, and their sense of overthrusting is towards the north and north-north-east. Notably, peridotite foliations (formed at 60 km depth) rotate towards the horizontal, within the upper part of the mantle sequence, similar to peridotite fabrics seen in areas interpreted as representing fossil spreading axes within the Semail peridotites of Oman (Culeneer et al. 1988; Nicolas et al. 1988).

3) From a study of the cyclic cumulates, combined with other lithological evidence, Jackson et al. (1975) suggested an origin by magmatic crystallisation in a large magma chamber at a mid-ocean ridge.

4) Parts of the Dramala Complex and perhaps also the Vourinos ophiolite correspond to a "transition zone" between mantle and crustal rocks where harzburgite abundance generally decreases and dunite increases, and where the Moho is therefore indistinct (Moores 1969; Rassios in prep.). Locally, in southern Vourinos, a pyroxenite dyke swarm cuts the transition zone (Moores op. cit.), and in the Dramala area, pyroxenite and gabbroic dykes are particularly common (Rassios in prep.). This may be comparable to the transition zone found within the Oman peridotites, in which magmatic activity, chromite pods and magmatic impregnation

characterise a similar zone, interpreted as primary residual mantle, remaining after diapiric rise at a spreading centre (Culeneer and Nicolas 1985; Benn et al. 1988).

Mantle tectonite studies of the Vourinos ophiolite show that high-temperature mantle fabrics trend north-north-west and dip towards the southwest at approximately 50^{o} (Grivas et al,1986). This fabric is cross-cut by mylonite zones, along which thrust displacement towards the present north-east has occurred (e.g. Ross et al. op.cit.; Wright 1986). These fabrics are therefore identical to those found in the Dramala Complex (see above), and critically define the emplacement of both ophiolites towards the northeast. This emplacement may have been accommodated along 040^{o}-trending transform faults, for example the central valley fault of Vourinos, into which mantle fabrics are found to rotate (Moat 1990).

2.7.1.3 Intrusive and extrusive sequences.

Within the Vourinos ophiolite, the extrusives (Krapa series) are entirely of IAT geochemical type, and are cross-cut by transitional to boninitic-type intrusive dykes (Asprokambo series; Beccaluva et al. 1984), similar to those found within the Aspropotamos Complex. The Cr-Y diagram presented (Fig. 2.9), shows that the Vourinos volcanic and intrusive rocks correlate with the more depleted rocks of the Pindos suite, although the Pindos boninitic rocks show a greater overall depletion of the high field strength elements (e.g Zr, Nb, Ti). The intrusion of the Asprokambo dykes into the Krapa series volcanics is significant because it provides independent evidence for the timing of the intrusion of the boninitic magmas, already shown in the Aspropotamos Complex.

From accumulated evidence therefore, the Vourinos ophiolite is interpreted as representing crust and mantle formed originally at a supra-subduction zone spreading centre, which produced only chemically depleted magmas. Subsequently, the ophiolite was thrust towards the present north and nort-north-east whilst still within the oceanic environment.

2.7.2 Semail ophiolite of Oman

The Late Cretaceous Semail ophiolite of Oman is interpreted as having formed in a similar tectonic environment to the Pindos ophiolite. The volcanic and intrusive stratigraphy of both ophiolites is partly comparable (see above). The Semail ophiolite is also a harzburgite and dunite-dominated peridotite, with numerous sections preserving the petrological Moho. According to the model of the Open University team (Lippard et al. 1986), the Semail ophiolite originated as a supra-subduction zone ophiolite above a northeast-dipping subduction zone, north of the Arabian continental margin during the Mid to Late Cretaceous (subduction zone initiated at 110 Ma; Fig 2.17). Prior to this, an earlier ocean basin had existed in the region from Permian times, following continental break-up of Gondwanaland.

The newly formed SSZ lithosphere of the Semail ophiolite was initially displaced in the oceanic environment at 93 Ma (Lanphere et al. 1981), to form the metamorphic sole. It was subsequently emplaced onto the margin as a relatively coherent sheet, and transgressed by cover sediments. An alternative model for the origin of the Semail ophiolite has been presented by Nicolas et al. (1988a), which suggests that the ophiolite formed at a fast spreading ridge, not in a supra-subduction setting.

2.7.3 The Troodos ophiolite of Cyprus

The Troodos ophiolite (e.g. Gass, 1979) has been studied extensively since the early 1970's, and is thought to represent an ophiolite still in the process of being emplaced onto a continental margin (e.g. Robertson et al. in press). The ophiolite is relatively coherent, and forms a concentric outcrop pattern radiating from the centre of the island. There, the exposed peridotite is mainly serpentinised harzburgite (Laurent 1990), with local dunite and chromite bodies. The sequence continues through ultramafic and mafic cumulates (pyroxenites, dunites, wehrlites, troctolites), into high-level gabbros. The sheeted dykes are extremely well exposed, and are the subject of numerous studies (e.g. Kidd and Cann 1974). The extrusive sequence (Pearce 1975; Robinson et al. 1983, Rautenschlein 1985) was interpreted as having formed by spreading above a subduction zone. Most

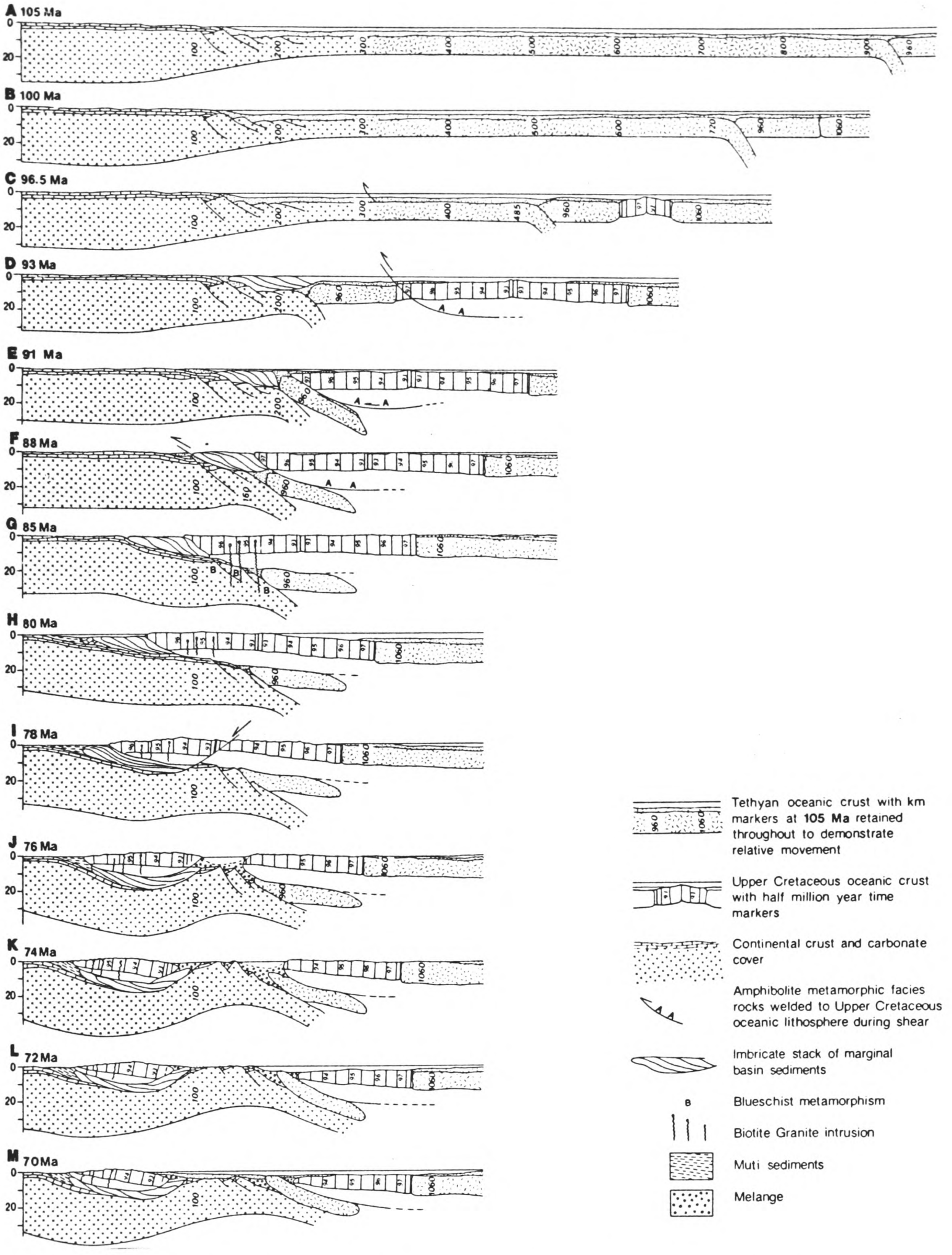

Fig. 2.17 Model for the evolution of the Semail ophiolite, Oman (after Lippard et al. 1986). Note the formation of an ophiolite complex above a subduction zone (B, C; approx. 97 Ma), following earlier rifting and spreading. During compression, the ophiolitic crust and mantle is displaced (D; 93 Ma) along the boundary between pre-existing ocean crust and newly generated supra-subduction zone crust. In contrast to the Pindos ophiolite, the isolated fore arc crust is not seen in Oman, and is shown as being subducted and overridden during ophiolite emplacement in this model (E, F).

of the volcanic units present are more high field-strength element depleted than MORB, and the most depleted IAT-type lavas are generally found towards the top of the succession. Locally within the Arakapas fossil transform fault (Limassol Forest area), boninitic-type volcanics are also present (Simonian and Gass 1978; Murton 1986, 1990).

2.7.4 Summary

The tectonic setting of the Pindos ophiolite has been partly clarified by the extensive igneous geochemical database. The severe thrust and fold deformation present within the Pindos area is not, however, found in the Troodos and Semail ophiolites, and therefore spatial relationships of the ophiolite rocks are not easily reconstructed. In general terms, the mantle and crustal sequences are comparable to the Semail and Troodos examples. The volcanic stratigraphy of the Troodos ophiolite does not contain basal MORB-type lavas, and the Semail ophiolite is more comparable in this respect. However, the Semail rocks differ in detail from MORB, as they have low values of the compatible element Cr. Similarly, the Troodos boninitic dykes and volcanics are spatially limited to the Transform Sequence of the Limassol Forest area, whereas the Pindos and Semail boninites are apparently more widespread.

2.8 INTERPRETATIVE MODEL FOR THE EVOLUTION OF THE DRAMALA AND ASPROPOTAMOS COMPLEXES

2.8.1 Mantle sequences

Following regional rifting and break-up during the Mid-Late Triassic, the Pindos basin developed oceanic crust during the Latest Triassic and Earliest Jurassic (see Chapter 4). The crust formed during these stages is now found partly preserved within the Avdella Melange, and partly within the crustal sections of the Aspropotamos Complex.

The Pindos ophiolitic units are inferred to represent the mantle (Dramala Complex) and mainly crustal (Aspropotamos Complex) sections of a developing supra-subduction-type tectonic setting, similar to those

observed today in the Western Pacific region (e.g. Eocene history of the Marianas forearc). In common with many Tethyan ophiolites, no true volcanic arc was ever formed, or is found preserved today. This has been explained by development of the ophiolites by pre-arc spreading (Pearce 1982), prior to the development of a volcanic chain. A possible model for the development of the Pindos and Vourinos ophiolites has been developed as part of this study (Fig. 2.18; Chapter 8). The evidence for this model provided by the Pindos ophiolitic units is presented here.

The Dramala Complex is thought to be of supra-subduction-type, because it is a harzburgite-dunite dominated, peridotite mantle sequence (Pearce et al. 1984a). It is here interpreted to represent mantle which was located away from the above subduction-zone spreading axis during the time of obduction. This is because the Dramala Complex lacks abundant massive chromites, those present being elongate and thin (e.g. 150 m long, 10 cms wide; A. Rassios pers. comm. 1989). This may imply that convective mantle flow away from the ridge (therefore off-axis) apparently streaked out the original chromite diapiric pods, as in the model of Culeneer et al. (1988). Also the Pindos ophiolite contains rare areas of lherzolite, similar to the Othris ophiolite, indicating that complete depletion of the mantle sequence had not occurred, unlike that of Vourinos. The presence of abundant refractory chromites within the Vourinos peridotites (Moores 1969; Rassios and Roberts 1986; Moat 1990) is in stark contrast to the Dramala Complex, and Vourinos is therefore assumed to represent a lateral (i.e. located nearer to an above-subduction zone spreading axis at the time of displacement and obduction) equivalent of the Dramala Complex (Jones and Robertson 1990).

The structures present within the Dramala and Vourinos peridotites are significant for several reasons. The high temperature fabrics probably represent structures produced by diapiric spreading at a ridge axis, and/or during ductile thrusting. The Dramala Complex peridotites contain a high-temperature foliation which strikes northwest-southeast, and dips at approximately 50^{o} to the southwest (Ross and Zimmerman 1982; Rassios in prep.). The Vourinos high temperature foliation is extremely comparable (50-60^{o} to the S.W.), suggesting that either the foliation in these peridotites was formed during spreading at the same side of a ridge axis, or it was "frozen in" at high temperatures during

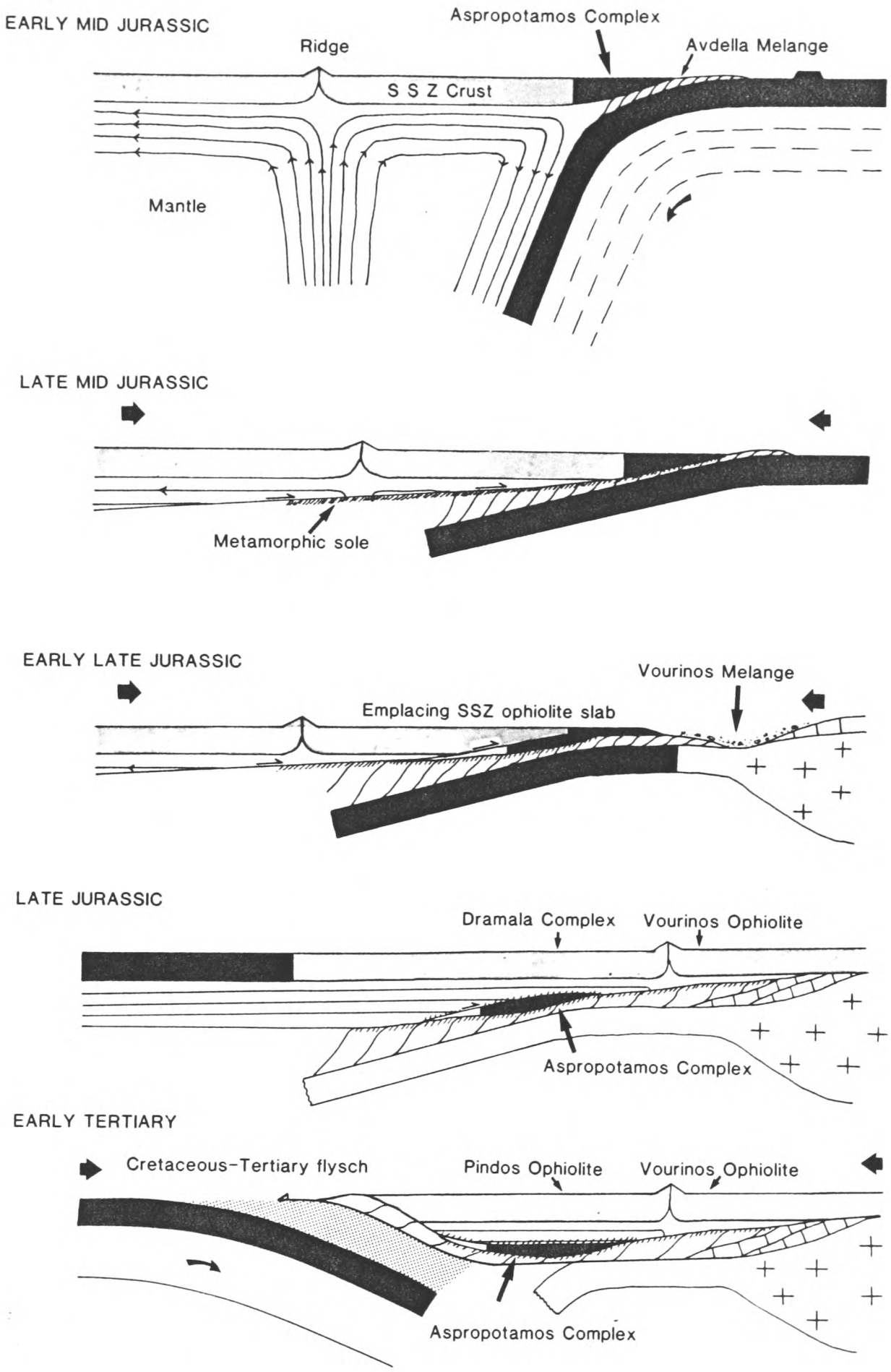

Fig. 2.18 Model for the evolution of the Pindos and Vourinos ophiolites during the Mesozoic and Tertiary. Development of supra-subduction zone crust, followed by displacement and overthrusting of the fore-arc region. See text for further explanation.

the initial displacement of the peridotite to the northeast. The latter is the interpretation favoured here (Fig. 2.18), because the foliation is accompanied by parallel mylonite zones, and by perpendicular shear fabrics, formed at both higher and lower temperatures, which also affect crustal units (Ross et al. 1980). Indeed, this interpretation has been proposed previously (Roberts et al. 1988) who state that "emplacement strain geometry (i.e. initial ophiolite displacement) is established very early in the history of the ophiolite, and is difficult to distinguish from mantle fabrics formed at a spreading centre". Further thrusting would result in the cooling of the peridotite and the formation of the lower temperature mylonites, during progressive obduction (Fig. 2.19). The critical observation is that these mylonites have a sense of overthrusting towards the northeast in both the Dramala Complex and Vourinos ophiolite (Ross and Zimmerman 1982), perhaps the best evidence for Jurassic emplacement vectors obtained thus far.

Sometimes, high-temperature foliations rotate into structures interpreted as oceanic transform faults (040^{o}-trending structures; Moat 1990). Brittle faults measured in the peridotites represent late-stage thrust-related "cold" deformation, probably Tertiary rethrusting towards the southwest (Chapter 7). These data together indicate that the Dramala Complex and the Vourinos ophiolite were produced at a northwest-southeast-trending ridge axis, and were thrust shortly after formation towards the northeast, along high-temperature ductile mylonite zones (i.e. ophiolite displacement and obduction phase). This thrusting was accompanied by movement along 040^{o}-trending shear zones (transforms?). This was followed, perhaps much later, by brittle thrusting towards the southwest, with associated 040^{o}-trending shears (i.e. Tertiary emplacement structures). The data obtained from studies of the peridotite therefore agree remarkably well with structural evidence obtained from other units in the Pindos-Vourinos area (Chapter 7).

The overlying crustal cumulate sequence of the Dramala Complex displays a variety of layered ultramafic and mafic lithologies. Wehrlites, thought to be the plutonic equivalent of depleted boninitic and IAT extrusive rocks, are found as part of this layered sequence. Their relationship to the IAT and BSV dykes and extrusives is described by Kostopoulos (1989). This situation is in contrast to that found in Oman,

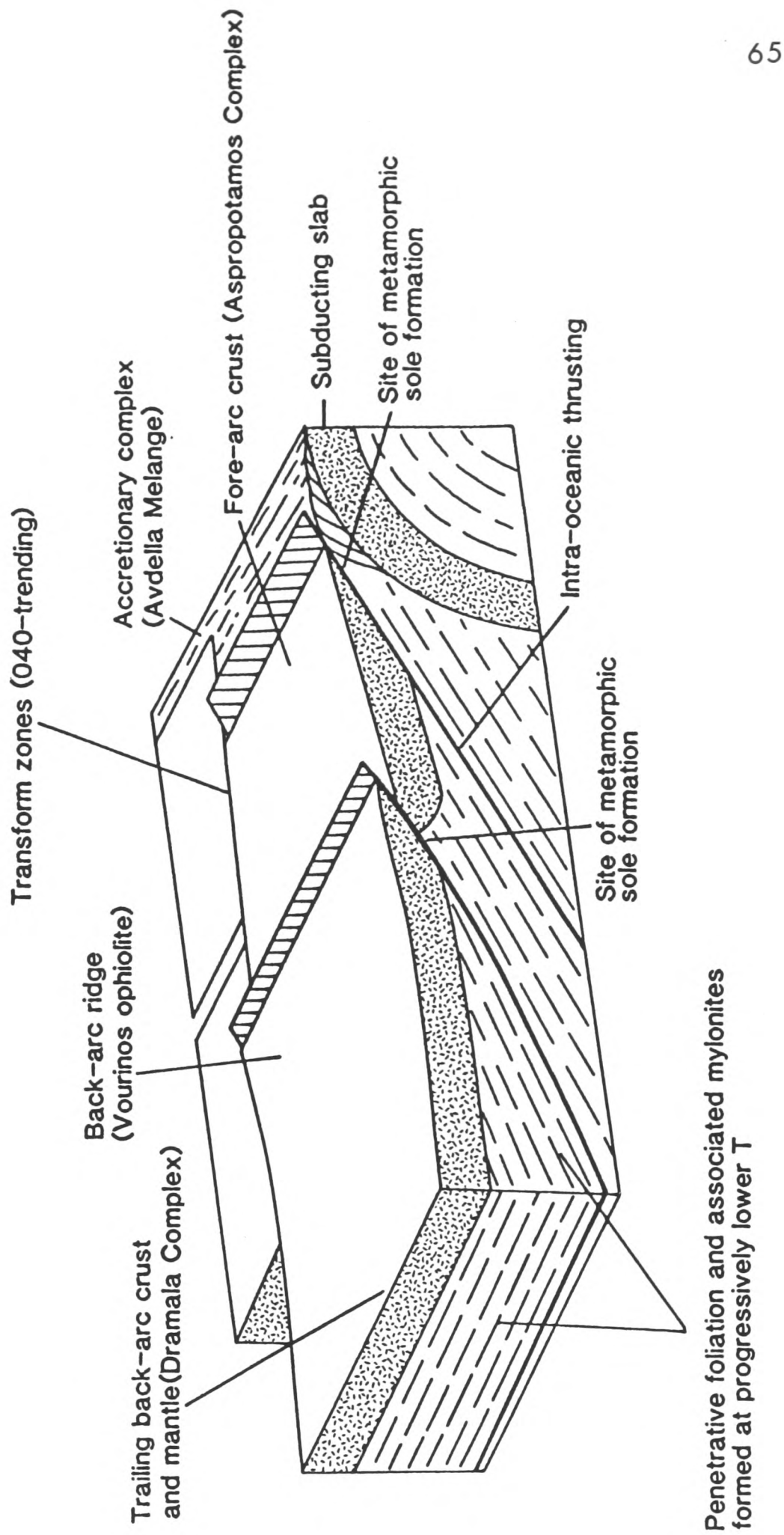

Fig. 2.19 Diagram to explain one possible method of formation of high temperature foliations with the Dramala Complex and Vourinos ophiolite mantle sequence. Initial compression of the newly formed supra-subduction zone (SSZ) crust forms a high-temperature "displacement" penetrative mantle foliation within the proto-Pindos and Vourinos ophiolite peridotites. Parallel mylonites form at high temperatures, and subsequently during progressive thrusting at lower temperatures (see text). This latter stage also led to the formation of the metamorphic sole, probably along the major thrust dislocations at the SSZ ridge, and along the subduction zone (see Chapter 3). Previous oceanic transform systems are reactivated (trending approximately 040°), to account for some foliations seen within the Vourinos ophiolite, and perhaps parts of the Dramala Complex.

where wehrlites and associated cumulates form large intrusive bodies into earlier-formed cumulates, which can be traced to the surface (Juteau et al. 1988).

2.8.2 Crustal evolution

The Aspropotamos Complex has been shown to contain a stratigraphically lowest unit of MORB-type extrusives and intrusives (including extensive sheeted dykes), which are accompanied by crustal cumulates interpreted as the residues remaining after the extraction of such melts (plagioclase dunite-troctolite-anorthosite-gabbro; Kostopoulos 1989). The complex also contains intrusives and extrusives of a more depleted nature, and these too have probable cumulate equivalents (Dunite-wehrlite-pyroxenite; Kostopoulos 1989). These cumulates must have crystallised at the base of the same magma chamber by complex open system fractionation processes.

As discussed in Chapter 8, the Pindos ophiolitic rocks may have formed in a pre-existing ocean basin (Mid-Atlantic-type), which was subsequently influenced by subduction processes, or as a rifted back-arc basin (Sea of Japan-type), under the influence of an external subduction zone. Furthermore, a combination of these possibilities is possible. Evidence for the presence of a pre-existing ocean basin is as follows: i) Triassic MORB-type lavas are known in the melange of the Pindos area (Kostpouolos 1989); ii) melange sediments indicate the presence of a deep-water basin in the area as early as Mid Triassic times; iii) the occurrence of extensive MORB-type volcanics (and sheeted dykes) at the base of the volcanic sequence, the age of which is unclear (i.e. possibly Triassic); iv) indirect evidence from radiometic age dating of similar MORB-type sequences in the Othris ophiolite (Roddick et al. 1979).

Data from this study, and from the Pindos Zone of southern and central Greece (Piper 1982), infer that the Pindos ocean may have opened as a "back-arc" basin due to eastward-directed subduction. However, no oceanic crust is thought to have existed to the west of the Pindos Zone during the Mesozoic (A. Robertson, pers. comm. 1990). Subduction of a Palaeotethyan ocean (see Chapter 1) beneath the eastern margin of the

Pelagonian microcontinent seems the most plausible cause. Geochemical analysis, including rare earth element data, has shown that some Triassic volcanic rocks in southern Greece are depleted in high field strength trace elements (Piper 1982), suggesting that a subduction-related component was present in the mantle during rifting of the Pindos ocean. A similar phenomenon has been discovered during the present study, where rocks with an IAT-type signature have depositionally overlying turbidites, dated as Late Triassic (see Chapter 4).

It is proposed, from the above evidence, that the Pindos basin developed oceanic crust during the Late Triassic, subsequent to a regional (Mid Triassic?) rifting episode. These MORB-type volcanics are found partly within the Avdella Melange and within the basal part of the Aspropotamos Complex. This Triassic ridge system may have become very slow spreading, or possibly extinct at a later stage. The causal mechanism for the cessation of spreading is unknown. As the heat source was now removed from the ridge, it would presumably have cooled and subsided. This would then be an ideal situation for the initiation of a subduction zone by ridge-collapse, or a similar mechanism (Robertson and Dixon 1985).

The subduction zone must have developed prior to the formation of the metamorphic sole (Bathonian; and see Chapter 3). Further supporting evidence for a Lower-Mid Jurassic age for the ophiolite, is the fact that boninitic lava clasts were not discovered in sediments older than Bathonian (see 4·7·6 p186). Subduction may eventually have been triggered due to relative plate motions following the opening of the north Atlantic at this time (Livermore and Smith 1985). Formation of a subduction zone would then have led to the development of the trace-element depleted Pindos ophiolitic units, by extension caused by "roll-back" of the subducting slab (Smith and Spray 1984) and hydration of the overlying mantle wedge. An unusual feature of the Pindos ophiolitic units is the presence of locally abundant dykes and lavas of evolved MORB chemistries. Rocks of similar chemistry are found at fast spreading ridges within present-day oceans, related to propagating ridge segments (e.g. East Pacific Rise; Pearce et al. 1986). There is at present no evidence for the time of formation of these units, other than they are found in the basal section of the volcanic sequence. They may therefore have formed during

the initial propagation of a spreading ridge in the Late Triassic, or at the start of above-subduction zone crustal formation.

The crustal sections of the Aspropotamos Complex appear anomalously thin (2-3 km), and may well represent "fore-arc" crust formed adjacent to the active subduction zone (Kostopoulos, 1989). This crust may in part have been tectonically thinned during subduction or later emplacement, but in the Aspropotamos Valley the crustal sequence is interpreted as complete (Kostopoulos op. cit.). The extensive southeast-trending MORB dykes exposed near Spileo are interpreted to represent the trend of the spreading ridge axis (i.e. approximately N.W.; Fig. 2.6), assuming no severe block rotations occurred during thrusting. This dyke trend is also found within more depleted rocks in this area (E. Valsami pers. comm. 1990).

The Aspropotamos Complex demonstrates a clear influence of subduction in its sequential geochemical depletion of the intrusive and extrusive units (N-MORB, MORB/IAT, IAT; Kostopoulos 1989), culminating in the production of boninitic lavas and dykes, typical of modern day fore-arc settings (Cameron et al. 1980; Crawford et al. 1982; Hickey and Frey 1982). Boninites observed in present-day fore-arc settings, are poorly understood in terms of their temporal distribution (Murton 1990). The situation is clearer within ophiolites, although a complete range of spatial and temporal associations are present. For example, the Betts Cove ophiolite in Newfoundland contains highly depleted rocks as the earliest volcanic event (Jenner et al. 1990). This situation is reversed in Oman, where progressively more depleted rocks are found higher in the sequence, and in the Troodos ophiolite where the boninites are found within a transform-type structural setting (Murton 1990).

The Pindos boninites can be demonstrated to have formed as the latest volcanic event within much of the ophiolite (Kostopoulos 1989), but occurrences at other stages cannot be ruled out. For example, the temporal relationships of the boninites found near Avdella are unknown, and depleted dykes are found trending sub-parallel to MORB dykes in the Spileo area. Possible explanations for boninite development in the Pindos ophiolite are: i) remelting of a previously depleted mantle source under hydrous conditions during "roll-back" of a subduction zone, and therefore

potentially generated at several stages during supra-subduction zone crustal development; ii) they conceivably could have developed at a late stage during "roll-forward" and tectonic disruption during the initial phases of intra-oceanic displacement (at the trench and/or at transforms). In the case of the Pindos ophiolite, the late stage boninitic dykes mostly show contrasting trends to earlier less-depleted dykes, perhaps relating to crustal rotation. Such rotation could have taken place along a "leaky" transform fault (Kostopoulos 1989), which was however, related to oblique subduction or incipient emplacement, as mentioned in point (ii) above.

Supra-subduction zone ophiolite genesis was followed soon afterwards by intra-oceanic detachment and formation of the metamorphic sole. Evidence that the Dramala Complex may have partially overthrust along transform-type offsets, is shown by the presence of breccias of harzburgite and jasper, cemented by ophicalcite, found at Smolikas Mountain (Chapter 4). A possible model for this feature, and to explain the occurrence of sole rocks on thick cumulate sections of the Dramala Complex is presented in Chapter 3. This invokes along-strike, out-of-sequence thrusting along the basal detatchment, perhaps away from the fore-arc region, and utilising transform lineaments now placed in compression.

The Pindos ocean was sutured further north in Albania and Yugoslavia (Karamata 1988; Shallo 1980) during the Late Jurassic collisional event, and subduction ceased at this time further south in northern Greece. As a result, the Dramala Complex and the Aspropotamos Complex remained stranded in the eastern part of the Pindos ocean during the Cretaceous and Early Tertiary. These units were emplaced onto Apulia during Early Tertiary convergence, and final closure of the remnant Pindos ocean. This two phase emplacement (Jurassic and Early Cretaceous) may explain why the Aspropotamos Complex "fore-arc" sliver was preserved, unlike the comparable section in Oman (Lippard et al. 1986).

Plate 2.1 (a) MORB-type sheeted dykes dipping to the northeast, track along the Venetikos valley to the west of Spileo village (Fig. 2.1). Field of view approximately 150 m. (b) Close-up of sheeted dykes shown in (a). Notebook (circled) is 20 cms long. (c) Irregularly intruded basaltic dyke intruding hydrothermally veined isotropic gabbros, track west of Spileo, as above. (d) Pyroxene-phyric andesitic dyke (boninite) intruded parallel to the MORB-type dykes shown in (a) above, near Spileo. Chilled margin is indicated (A).

Plate 2.2 (a) Curving sheeted dykes (A) of IAT and boninitic affinities, at Karamoula (Fig. 2.2). Hammer for scale. Note that these dykes are considerably thinner than MORB-dykes from Splieo (Plate 3.1). Note also the occurrence of an earlier dyke (B), dipping more steeply. (b) Dyke swarm (IAT), somewhat sheared, cutting basalt screens, Karamoula. Hammer for scale (circled).

Plate 2.3 (a) Pillow basalts (boninites), showing characteristic altered glass-rich inter-pillow material (G). Part of an extrusive sequence, probably associated with sheeted dykes of Karamoula (Plate 3.2). Road to Perivolaki (Fig. 2.2). (b) Dykes (D; MORB-IAT) cross-cutting screens of pillowed basalt (P; mainly MORB), track west of Spileo. (c) Large pillows and bolsters of IAT extrusives (road to Mikrolivado, N.E. of Achladi (Fig. 2.2).

2.1

2.2

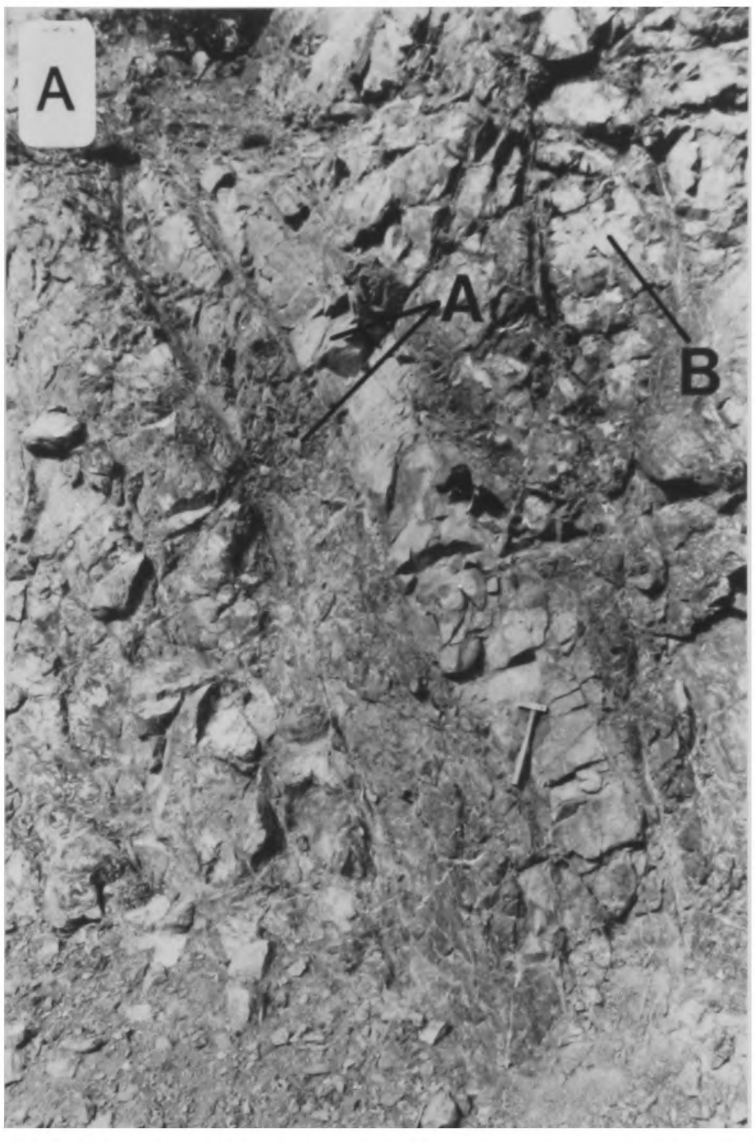

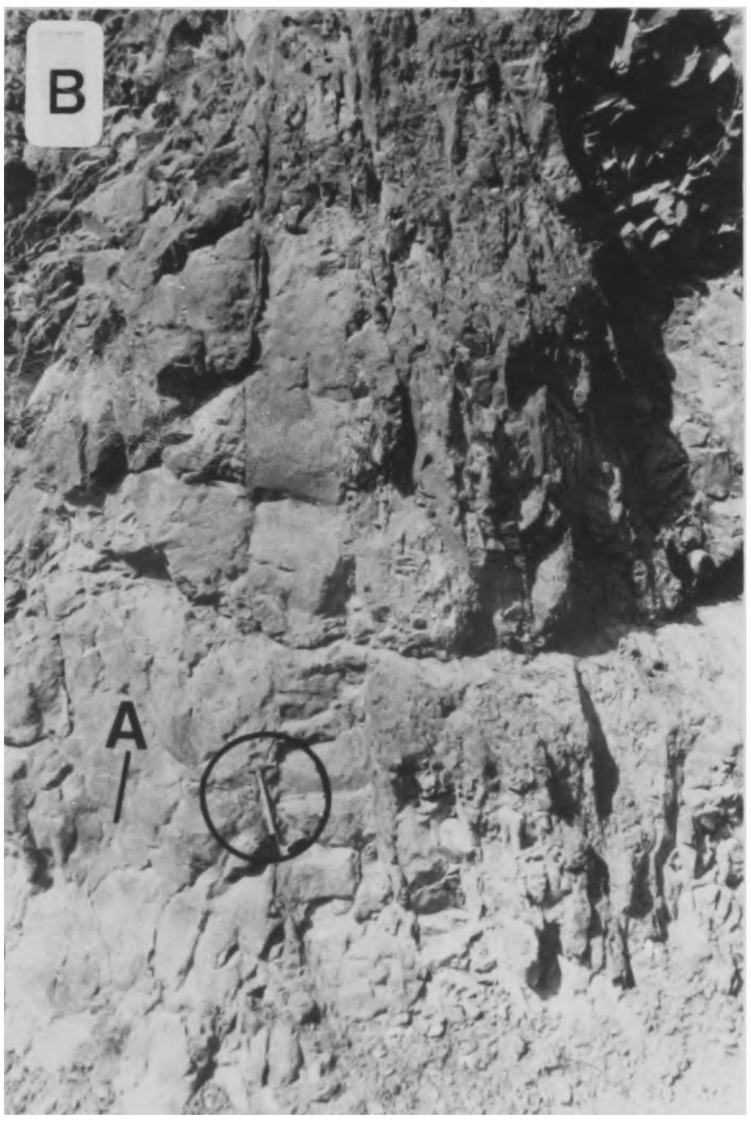

2.3

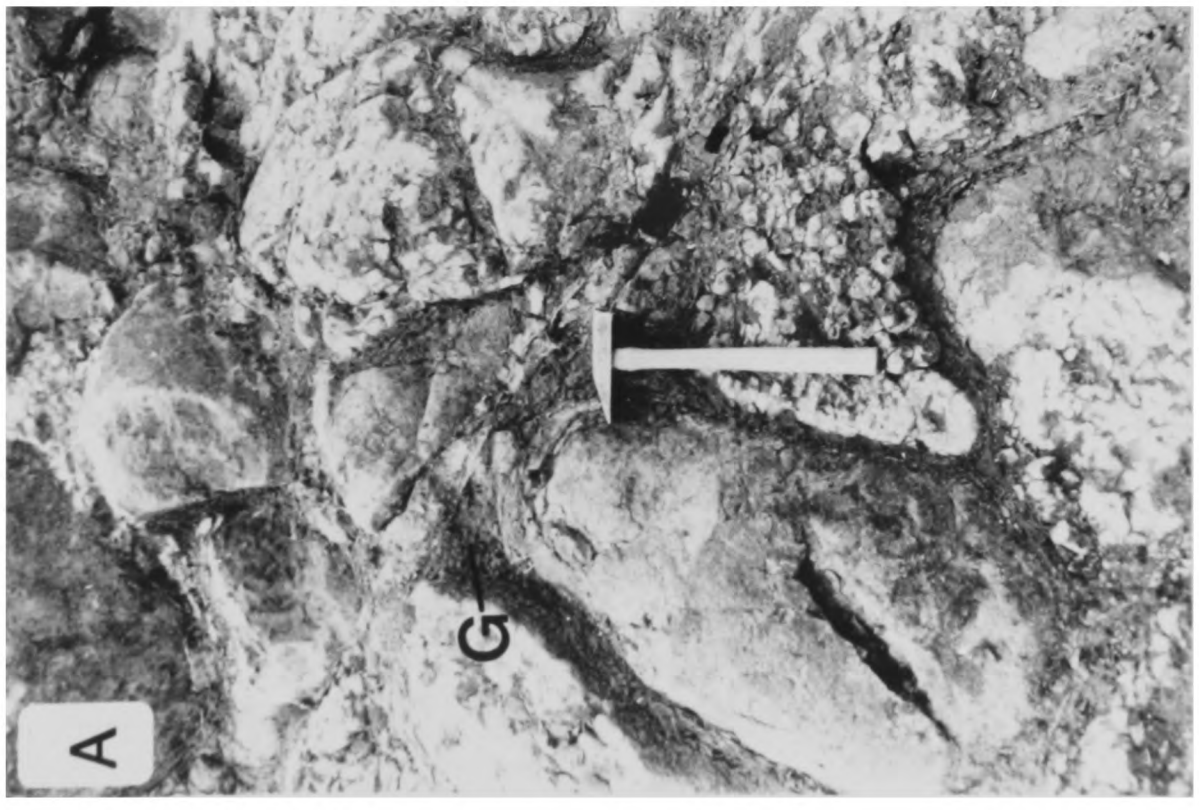

CHAPTER 3

THE LOUMNITSA UNIT: METAMORPHIC SOLE OF THE PINDOS OPHIOLITE

3.1 Introduction

Metamorphic rocks found in the north Pindos Mountains were named the Loumnitsa Unit (Jones and Robertson 1990; this work), from the type section found in the Loumnitsa Valley, 5 km east of Perivoli (see Appendix 1; and Fig. 3.1). These rocks were initially considered to represent Palaeozoic basement by Brunn (1956), but have since been re-interpreted as metamorphic "aureole" units formed during the Mesozoic (Williams and Smyth 1973; Whitechurch and Parrot 1978). Several previous studies have been attempted on the metamorphic rocks of the region (Whitechurch and Parrot 1978; Spray and Roddick 1980; Kemp and McCaig 1984), focusing on one aspect of their genesis, or on specific localities. A comprehensive study of this unit is presented in this chapter, based on detailed studies and widespread reconnaissance of the region.

3.2 Metamorphic rocks associated with other ophiolite belts

The Loumnitsa Unit closely resembles metamorphic rocks found in other Tethyan Mesozoic ophiolite belts (Woodcock and Robertson 1977), and those found associated with Palaeozoic ophiolitic complexes (e.g. Bay of Islands Complex, Newfoundland; Williams and Smyth 1973; Malpas et al. 1973; Jamieson 1977, 1979; Malpas 1979). The ophiolites of central and southern Greece have well preserved, though often fragmentary, metamorphic soles (e.g. Vourinos, see below). In the Othris ophiolite (see Chapter 1), the metamorphic sole outcrops only sporadically, but where exposed consists of garnet amphibolite and feldspathic amphibolite, preserved beneath serpentinised peridotites (e.g. near Lamia; Spray and Roddick 1980; Ferriere 1982). The Evvia ophiolite of eastern central Greece (Spray and Roddick 1980; Simantov et al. 1988), has garnet amphibolites and a variety of greenschist facies metabasites and metasediments occurring as a sole beneath serpentinised harzburgites, in the west of the island.

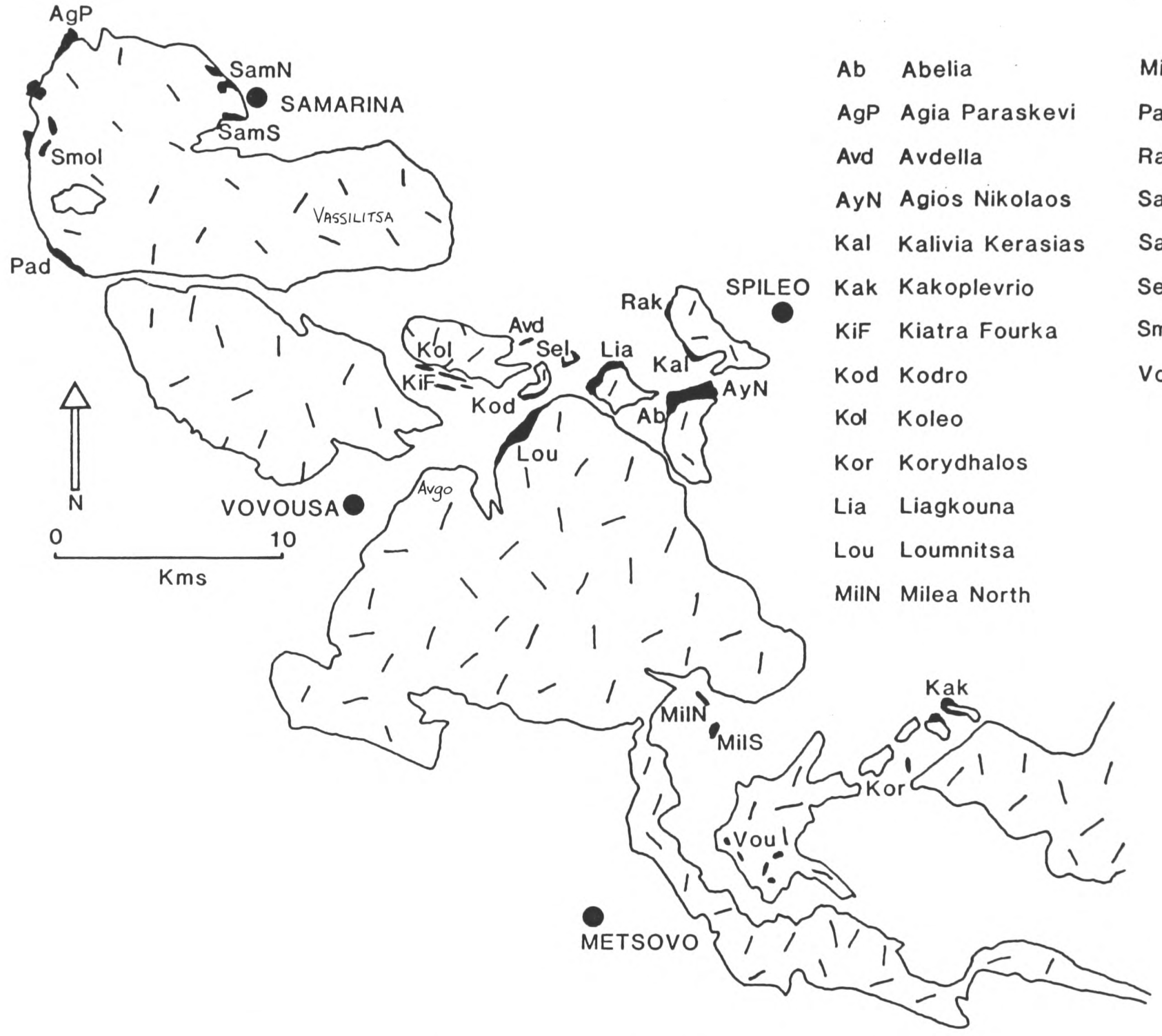

Ab	Abelia	MilS	Milea South
AgP	Agia Paraskevi	Pad	Padhes
Avd	Avdella	Rak	Rachi Kerasias
AyN	Agios Nikolaos	SamN	Samarina North
Kal	Kalivia Kerasias	SamS	Samarina South
Kak	Kakoplevrio	Sel	Selloma Lakkou
KiF	Kiatra Fourka	Smol	Smolikas
Kod	Kodro	Vou	Voulgaris
Kol	Koleo		
Kor	Korydhalos		
Lia	Liagkouna		
Lou	Loumnitsa		
MilN	Milea North		

Fig. 3.1 Locality map showing the main exposures of the metamorphic sole (Loumnitsa Unit) in the north Pindos Mountains.

The Semail ophiolite of Oman provides a good example of a well developed metamorphic sole beneath a peridotite thrust sheet, and was recently studied in detail (e.g. Searle 1980; Searle and Malpas 1980, 1982; Ghent and Stout 1981). In the ophiolite complexes of Turkey, metamorphic sole rocks have been observed in a similar tectonic position to those of the Loumnitsa Unit (Juteau 1975, 1980; Thuizat et al. 1981), as have sole rocks identified in Baer-Bassit, Syria (Parrot 1973, 1974). The major ophiolite bodies of Yugoslavia also display extensive occurrences of sub-ophiolitic metamorphic rocks (Pamic et al. 1973; Karamata 1975; Lanphere et al. 1975; Dimitrijevic and Dimitrijevic 1980), as do their continuations to the south in Albania (Aubouin and Ndojaj 1964; Shallo 1978; Turku 1986), here interpreted as representing metamorphic soles.

3.3 Characteristics of metamorphic soles

General models have been constructed for the stratigraphy and mode of formation of metamorphic soles, based on their observed field characteristics (e.g. Spray 1984; Fig 3.2). In broad terms, metamorphic sole rocks from a number of ophiolites and Alpine-type peridotites have been shown to have several features in common, as defined by Searle and Malpas (1980):

a) Metamorphic rocks occupy a constant stratigraphic position at the base of the ophiolite, and underlie a thick ultramafic unit.

b) They exhibit decreasing metamorphic grade with depth beneath the peridotite.

c) The metamorphic complexes characteristically have a narrow width, suggesting a high geothermal gradient.

d) There is a general lack of intrusive phenomena (e.g. dykes, xenoliths and chilled margins) associated with the contact between the ultramafic and the metamorphic rocks.

A

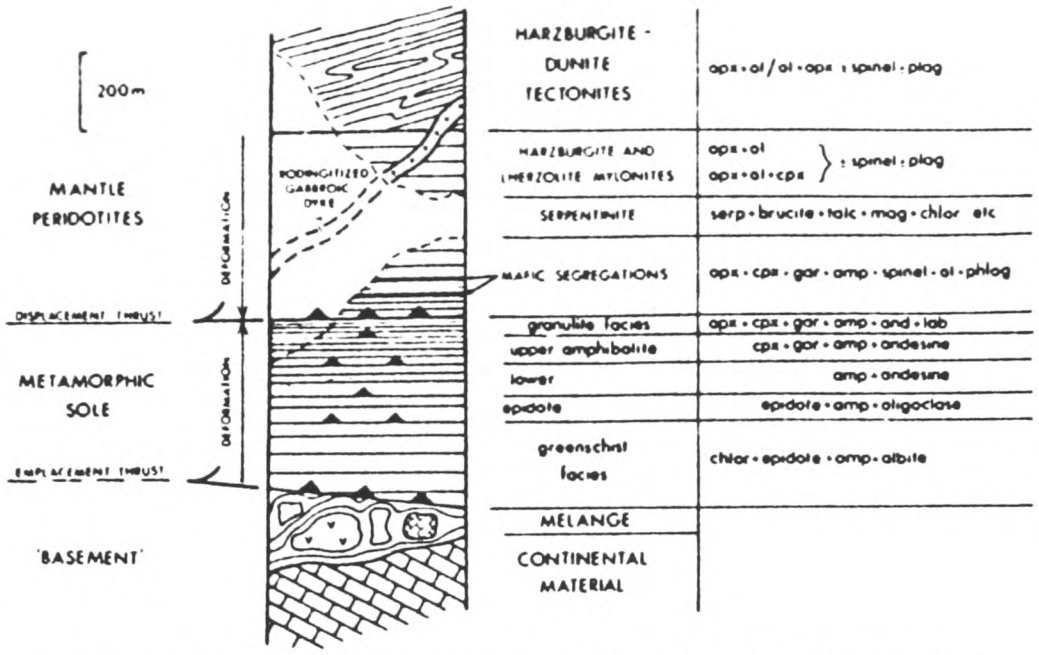

FIG. 2. Idealized cross-section of the base of an ophiolite showing relationship between metamorphic sole and overlying mantle peridotites. Variation in metamorphic grade and diagnostic parageneses for a mafic protolith for the sole are also shown. If present, metasedimentary lithologies would normally be restricted to the lower parts of the sole and yield, for example, quartz-albite-epidote-mica schists (metapelites), quartzites (meta-arenites) or calc-silicate assemablages (impure carbonates). Overlying mantle peridotites show a 'mirror' style of deformation at their base which overprints earlier tectonite fabrics. Lherzolite containing mafic segregations is also prevalent in the basal region. Varieties of pyroxenite, dunite and gabbroic dykes and sills may intrude the main lithologies. (The granulite-facies unit of the sole is shown enlarged for clarity, in reality it is likely to be ≪10 m thick.)

B

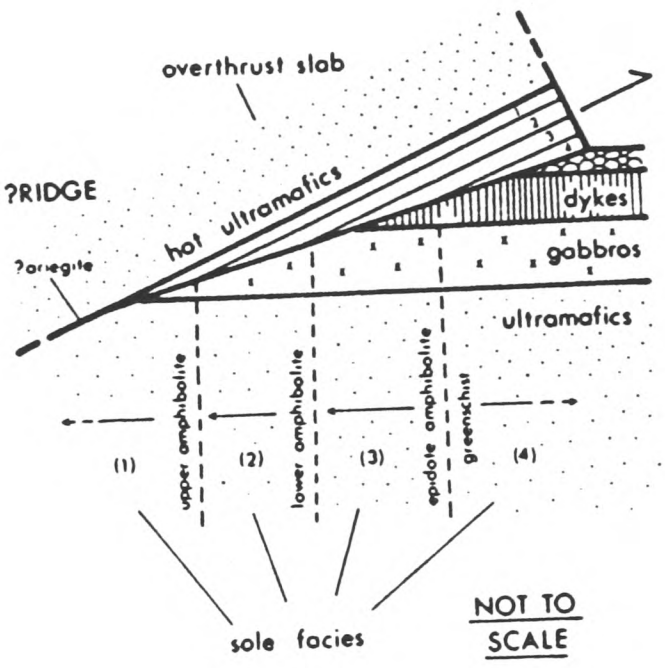

FIG. 3. Simplified model for the formation of a metamorphic sole along a thrust fault penetrating oceanic crust and upper mantle. The sole is shown divided into four arbitrary '*PT* planes' ranging from greenschist to upper amphibolite-granulite facies. The sole is only complete when all four *PT* planes are tectonically juxtaposed. This obviates the necessity of having extremely high thermal gradients existing through the whole thickness of the complete sole. As thrusting and metamorphism continue, lower-grade rocks are progressively 'welded' onto the hanging wall such that the locus of shearing moves downwards and away from the peridotite.

Fig. 3.2 a) Generalised stratigraphy of metamorphic soles. b) Model for the formation of ophiolite metamorphic soles. Both after Spray (1984).

e) Where there has been no dismemberment, orientations of metamorphic fabrics and the conditions of their formation are essentially the same in the basal ultramafic rocks and the metamorphic rocks.

In general, the Pindos metamorphic sole rocks conform to these features. However, one aspect of the Loumnitsa Unit is that sole rocks are found at the base of not only ultramafic rocks (as in 1, above), but also cumulate and possibly intrusive units of the ophiolite, a feature not previously been recognised from other ophiolite belts. The aim of this chapter is to document the occurrences of the sole in the Pindos Mountains, and to present new geochemical and petrological data from each locality. This data is then used to suggest a model for the generation and tectonic setting of the Loumnitsa Unit, and possibly other comparable ophiolite soles.

3.4 Radiometric ages

Hornblende crystals from amphibolites of the Loumnitsa Unit exposed south of Milea (Fig. 3.1) have been dated by the K-Ar method (Thuizat et al. 1981), as 172±5 Ma (Mid. Jurassic). ^{40}Ar-^{39}Ar dating of similar rocks at Kiatra Fourka, N.W. of Perivoli (Roddick et al. 1979; Spray and Roddick 1980) gave ages of 173±3 and 172±3 Ma ages (corrected to 165± 3 Ma; Spray et al. 1984). This corresponds to the Bathonian stage of the Mid Jurassic on the Harland et al. (1989) timescale.

3.5 Distribution

The Loumnitsa Unit is distributed widely, but discontinuously throughout the north Pindos Mountains, as shown on Fig. 3.1. In the northern sector, the unit occurs as localised outcrops, such as those in the Smolikas Mountains (I.G.M.E. Konitsa sheet, 1984; e.g. in the Padhes and Samarina areas, Fig. 3.1). In the central area, the unit is more widespread, particularly along the Perivoli corridor, where the main localities have been studied in some detail. Exposures have also been studied in the southern sector (e.g. Milea, Korydhalos, Fig. 3.1), but occurrences in this

area are in general, poorly known. Each of the important main localities will be described, and summarised in a later section.

3.6 Field occurrence

The Loumnitsa Unit is found at three main tectonic levels within the north Pindos thrust stack (Fig. 3.3):

i) Beneath ultramafic mantle units of the Dramala Complex.

ii) Beneath ultramafic and mafic crustal units of the Aspropotamos Complex (see below).

iii) Within the Avdella Melange, as isolated tectonic blocks.

The Loumnitsa Unit lithologies are most commonly found within the Avdella Melange (Chapter 4) as blocks of variable dimensions (less than 1 m to several hundred m thick). However, several important sections occur where the transition downwards from the Dramala Complex and the Aspropotamos Complex is still preserved intact. The Loumnitsa Unit is apparently best preserved where the overlying peridotite is folded or overturned, commonly where there has been re-imbrication of the sole. The predominant metamorphic foliation is usually steeply dipping as a result. At these localities, a general decrease in metamorphic gradient from amphibolite through to greenschist and unmetamorphosed lithologies is present, although thrust repetiton of these sequences often complicates this picture.

The best preserved localities discovered, where an intact sole is present on the base of the Dramala Complex, are the Loumnitsa Valley to the east of Perivoli, and Liagkouna Mountain (Fig. 3.1). Several well-exposed sections where the sole is found attached to the Aspropotamos Complex are found along the Veneticos Valley, between Abelia and Spelio, (Fig. 3.1). Other relevant localities (e.g. S. of Samarina; Padhes Village, Kodro Mountain) will also be described later.

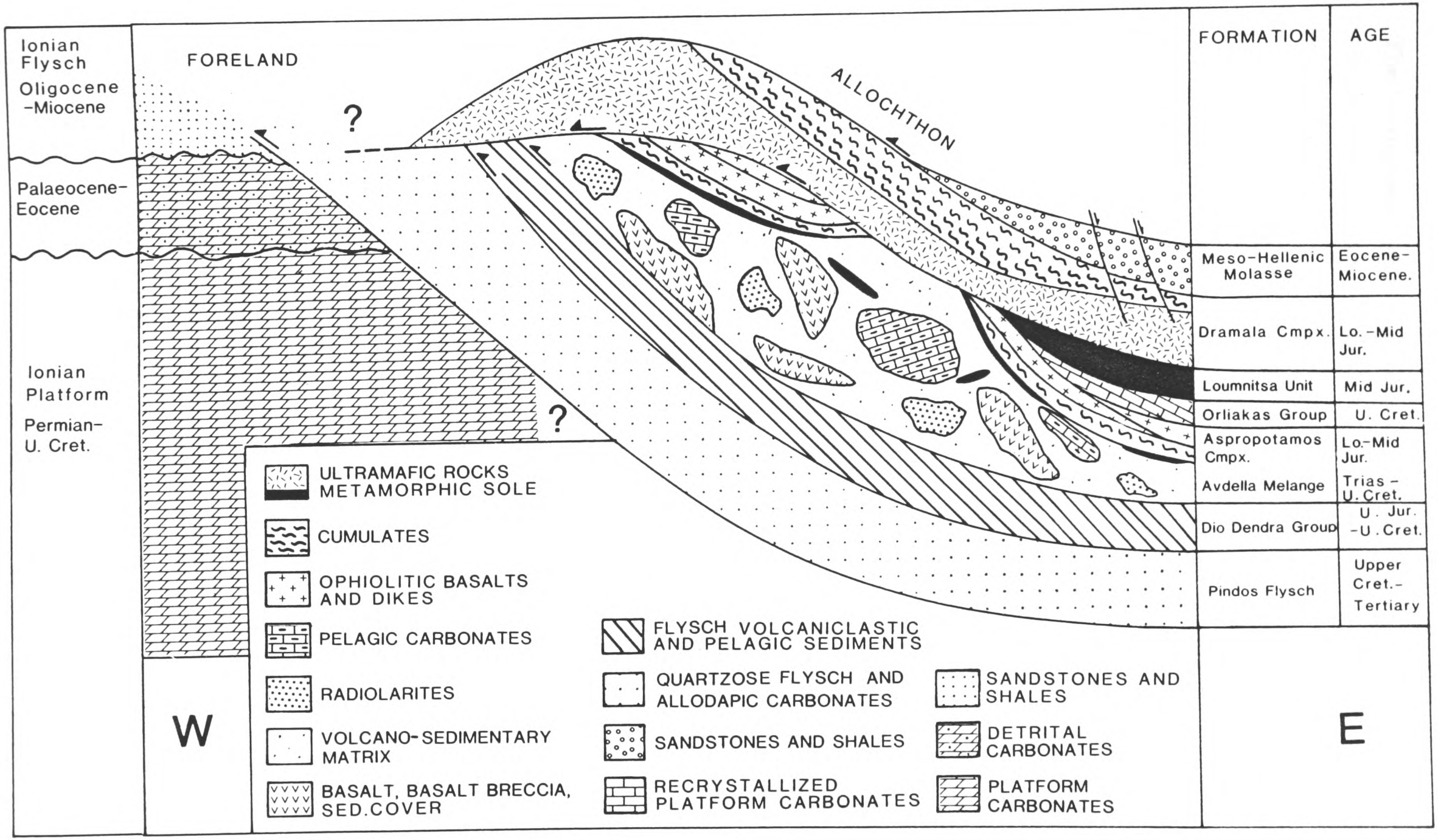

Fig. 3.3 Tectono-stratigraphy of the north Pindos Mountains, showing the position of the Loumnitsa Unit beneath the Dramala and Aspropotamos Complexes (Jones and Robertson 1990).

The Loumnitsa Unit is separated from the overlying ophiolitic units by a major tectonic contact, the Achladi thrust (Jones and Robertson 1990). This is comparable to the tectonic position of the Semail thrust of Oman, which similarly separates the Semail ophiolite from the basal metamorphic sheet (Searle and Malpas 1980). A basal peridotite mylonite unit is found above the Achladi thrust (see below), which is considered here to be part of the metamorphic assemblage. A true maximum thickness of approximately 300 m for the Loumnitsa Unit is reached in the Loumnitsa Valley. Structural cross-sections of the basal part of the ophiolite and the sub-ophiolite melange are presented in Chapter 7. The sections show that the sole is demonstrably thrust over the Avdella Melange, and where only detached sheets of sole are present, probably marks the top of this tectonic unit.

3.7 ASSOCIATED LITHOLOGIES OF THE DRAMALA COMPLEX

The basal metamorphic rocks of the Pindos Mountains can be divided into three mappable units:

1) Basal serpentinite and peridotite mylonite ("banded unit") of the Dramala Complex (with rodingites).

2) Amphibolite facies metamorphic rocks (Loumnitsa Unit), with localised rodingites.

3) Greenschist facies metamorphic rocks (Loumnitsa Unit).

These units are usually all present only in the best preserved sections. Over much of the region, the sole and basal mylonite are missing or detached, and only the basal serpentinite is found.

3.7.1 Basal serpentinite of the Dramala Complex

The Dramala Complex, in common with other ophiolites (e.g. Vourinos, Moores 1969; Semail, Lippard et al. 1986), posesses a basal zone of more complete serpentinisation, in comparison to the remainder of the

peridotite sheet. This unit is not a part of the metamorphic sequence, but, as it forms the basal unit of the ophiolite across much of the region, it is considered at this stage. This basal unit is up to several hundred metres thick, and is normally present where an intact metamorphic sequence is absent. The contact of the basal serpentinite with the underlying units (i.e. the Achladi thrust) is typically undulatory (e.g. E. side of Avgo Mountain, Fig. 3.1). At numerous localities, individual sheets (10 m to 80 m thick) of serpentinised peridotite have been detached from the Dramala Complex, tectonically incorporated, and subsequently folded into the underlying melange (e.g. at Kiatra Fourka; Fig. 3.1).

The degree of serpentinitisation is variable, and often completely serpentinised harzburgite will pass over a short distance (i.e. within several m) into fresh peridotite (e.g. Loumnitsa Valley). Patches of less altered harzburgite, with relict bastites formed by the replacement of orthopyroxene, may be found within more completely serpentinised rock. The serpentinites are generally of two main types; a blue-grey fibrous type which weathers to a dark greenish-grey, and dark green serpentine which weathers to a rust-brown colour. Rarely, wholesale alteration to a light-grey talc occurs (e.g. at Kalivia Kerasias; Fig. 3.1).

3.7.2 Basal peridotite mylonite of the Dramala Complex

This highly deformed zone is recognisable within the Dramala Complex peridotites at several localities where a downwards progression into the Loumnitsa Unit is preserved (e.g. Loumnitsa Valley, Liagkouna, S. Samarina; Fig. 3.1). The thickness of this unit is difficult to assess, as in most cases it passes upwards into similarly highly foliated peridotites of the Dramala Complex. However, rocks with a predominant high-temperature fabric orientated sub-parallel to the amphibolite foliation, occur up to 40 m above the Achladi thrust plane (e.g. Loumnitsa Valley, Fig. 3.4).

In the Semail ophiolite, Oman, a similar "banded ultramafic unit" is present above the Semail thrust, and "forms an integral part of the metamorphic assemblage" (Searle and Malpas 1982). This unit is up to 150 m thick (Searle and Malpas 1980), although according to Boudier and

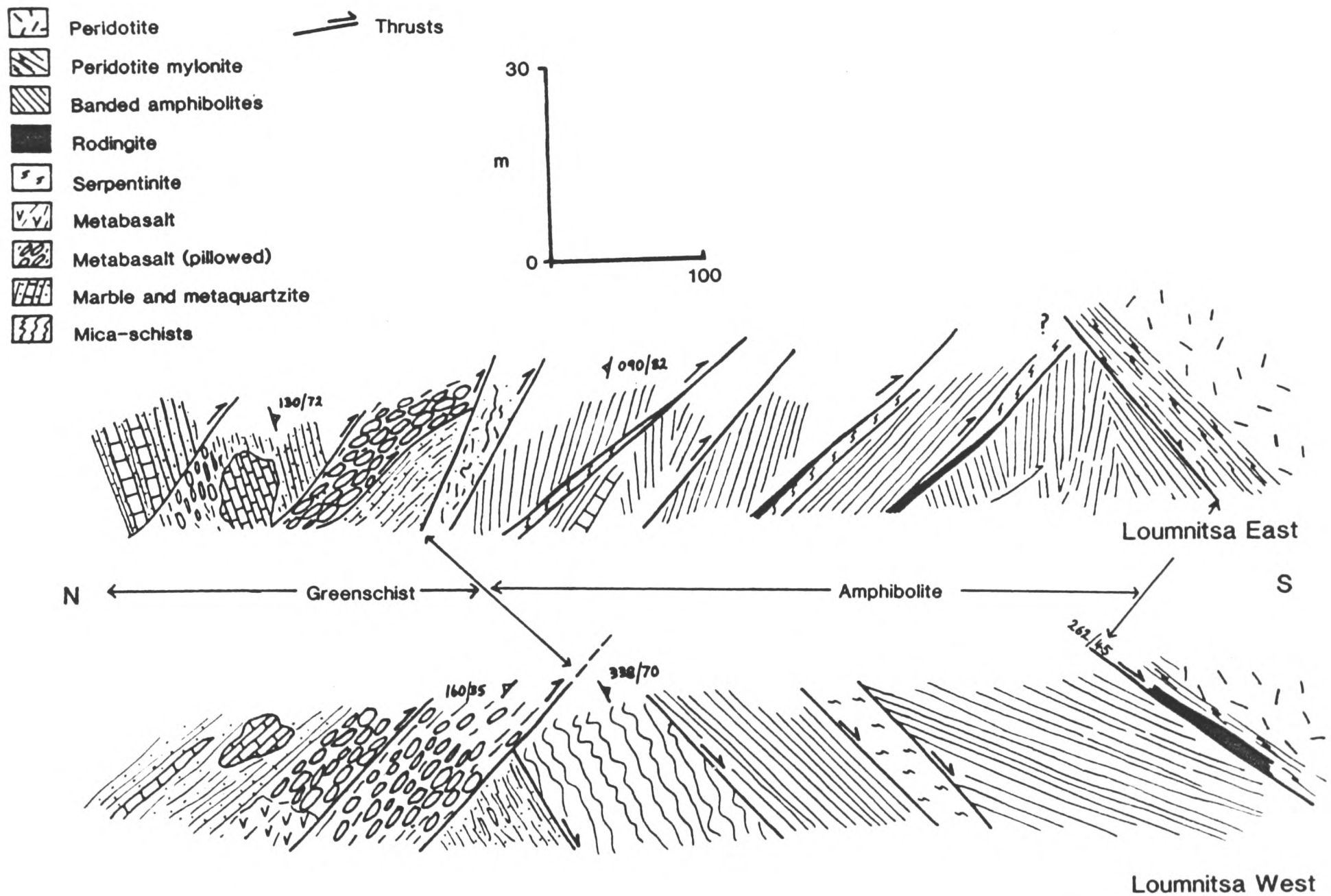

Fig. 3.4 Sketch structural sections along roadside exposures in the Loumnitsa Valley (Fig. 3.1).

Coleman (1981), thrust related deformation is still present in peridotite microfabrics at least 500 m above the Semail thrust plane, and perhaps up to 2 km above it. The banding in this unit is, however, on a much larger scale (tens of metres) than that observed in the Pindos examples. In the Bay of Islands ophiolite, Newfoundland, a centimetre-banded basal peridotite mylonite unit (approx 40 m thick), contains recrystallised and deformed olivine and orthopyroxene crystals, which are up to 60 modal % serpentinised olivine (Williams and Smyth 1973; Malpas 1979) This unit is therefore of similar dimensions to the Pindos basal mylonite.

The Dramala Complex basal peridotite shows intense mylonitic deformation within ultramafic lithologies, mainly serpentinised harzburgite. Peridotite mylonite from Liagkouna Mountain (187/88) shows well developed banding in hand specimen and thin section. The bands are 1 mm to 1 cm thick, and are alternately green-brown and light-grey in colour. The green-brown bands were originally olivine-rich (dunitic) layers, which are mostly altered to mesh-textured serpentinite. The essentially euhedral olivine crystal outlines are defined by an opaque mineral, probably chromite. The lighter-coloured bands are more highly deformed, and more completely serpentinised, and were probably originally more orthopyroxene rich. Anastomosing thin shear zones of elongate serpentine, are seen separating areas of euhedral tabular serpentine. This band is also characterised by patches of zoisite. The serpentine crystals in both bands show undulose extinction, and probably replaced previously strained olivine and pyroxene crystals. Chrome spinels do not appear to conform to the boundaries of these bands, but are similarly concentrated in layers, and individual crystals are elongate.

3.7.3 Hydrothermally altered rocks (Rodingites)

At two localities (the Loumnitsa Valley and Liagkouna, Fig. 3.1), the peridotite mylonite of the Dramala Complex is locally transformed into a thin zone (maximum 5 m thick) of intense hydrothermal alteration (Fig. 3.4). These mainly fine-grained rocks can be described as rodingites, (metasomatised mafic and ultramafic rocks; Coleman 1963), and lie immediately beneath the Achladi thrust on the west side of the Loumnitsa Valley (Fig. 3.4). On the east side of the valley, they are found in a similar

position, repeated beneath an imbricated serpentinised peridotite/sole contact (Fig. 3.4). Another altered rock-type occurs beneath the basal peridotite at Liagkouna (Fig. 3.1). The rocks are light-grey/green and crystalline, composed mainly of pyroxenes with skeletal texture, set in a fine-grained matrix of intergrown radiating chlorite laths and serpentine. This rock is more strongly banded, and was probably initially a peridotite mylonite. The specimen collected in the Loumnitsa Valley (128/88), is of variable grain size, with large amounts of well crystallised prehnite, and some quartz and plagioclase crystals (up to 5 mm in length). Banding is not easily discernable in thin section. Prehnite crystals are commonly sutured together along their margins, and show several features which suggest they represent *in situ* alteration of orthopyroxenes. Firstly, they may show traces of exsolution lamellae typical of a high temperature pyroxene, and secondly they commonly display undulose extinction, as they are replacing highly deformed crystals from the basal mylonite of the peridotite. Crystals of red-brown chrome spinel are present, and appear unaffected by the wholesale alteration around them.

In the Samarinotikos River Valley (N. of Samarina; Fig. 3.1) the basal serpentinite passes into a thin (2 m) lens of highly rodingitised amphibolite, immediately before passing into less altered banded amphibolite. In thin section, this gabbro has extensive veins and matrix areas of prehnite and zoisite/clinozoisite, which form a hard, white matrix to the amphibole crystals. Rodingitic rocks are found at several other localities (e.g. at Kodro; Fig. 3.1). There, a 80 cm long veinlet of calc-silicates with diopside, prehnite and clinozoisite is found within the upper part of the amphibolite section.

A similar zone of hydrothermal metamorphism is found in the aureole of the Bay of Islands complex (Malpas 1979). The rodingites described by Malpas (op. cit.) from there are, in general, comparable mineralogically and geochemically to those described from the Loumnitsa Unit above. In the Bay of Islands, prehnite, xonotlite, calcite, epidote and clinozoisite are very common, with original garnets altering to hydrogrossular and chlorite.

The occurrence of these rodingites appears to be due to the presence of mainly low-temperature, carbonate-rich hydrothermal waters

affecting the original metamorphic assemblage. They represent alteration which formed after initial high temperature metamorphism, as evidenced by undeformed veins which cross-cut the amphibolite schistosity. It can be shown that this alteration also occured at least partly prior to Early Tertiary re-imbrication of the thrust sheets, as rodingitised gabbro dykes are folded at the base of the ophiolite in the Armata area (see below). A further phase of serpentinisation must have taken place during the Tertiary re-thrusting, as serpentinite is presently found along tectonic contacts of this age.

Coleman (1977), in summarising the nature and occurrence of rodingites, stated that calcium metasomatism is a normal by-product of serpentinisation. He also suggested that mylonitisation of some rodingites indicated that deformation may have accompanied metasomatism. It would appear from textural evidence however, that the basal peridotite mylonitic fabric in the Pindos ophiolite was formed during oceanic thrusting at high temperatures, and rodingitisation significantly postdated this event. The metasomatic fluids appear to have been channeled at the base of the serpentinised peridotite, along the contact with the amphibolite facies rocks, which subsequently led to wholesale alteration of the earlier peridotite mylonitic fabric. Serpentinisation must have taken place whilst the peridotite still retained some remnant heat, as an upper greenschist facies mineral assemblage was developed. This may indicate that this was sometime during, or soon after, initial ophiolite emplacement.

3.8 THE LOUMNITSA UNIT

3.8.1 Amphibolites

Where best preserved, the Loumnitsa Unit amphibolite facies rocks are found directly beneath the Achladi thrust, passing structurally downwards from serpentinised ultramafic rocks of the Dramala Complex. The amphibolites are usually dark and light grey colour-banded (amphibole-feldspar compositional banding), or dark grey homogenous amphibole-rich rocks (Plate 3.1), and are generally of basic origin. Plagioclase may also be intergrown with the amphiboles at some localities. Texturally, they range from coarse and granular, through to fine grained

and schistose. Quartz and calcite veining is found commonly within the amphibolite facies rocks (e.g. Veneticos Valley; Fig. 3.1; Plate 3.1).

The amphibolites are composed mainly of usually strongly pleochroic, (green to colourless) hornblende, and plagioclase feldspar (Plate 3.2). The grain size (up to 6 mm) and degree of alteration is extremely variable, both within and between exposures. Some samples contain green amphiboles showing strong pleochroism, and moderately to highly albitised plagioclases, which have an inclusion-rich "dusty" appearance. A wide variety of accessory minerals occur, including epidote, clinozoisite, apatite, sphene, and zircon. Albitisation of the feldspars (Plate 3.2) has frequently occured (An_{20-25}; Whitechurch and Parrot 1978; An_{23-32}, Spray and Roddick 1980), and other retrogressive alteration minerals include widespread prehnite along veins, or throughout the matrix (Plate 3.3). A hornblende analysed from the Loumnitsa Unit (Kiatra Fourka; Fig. 3.1) by Spray and Roddick (1980), was calcic in composition (ferroan-pargasitic hornblende).

In contrast to other Tethyan metamorphic soles, garnets are not present in amphibolites from the Loumnitsa Unit. Amphiboles from the Loumnitsa Unit are also usually light green to colourless, indicative of comparatively low temperatures of crystallisation. Brown amphibole was found at one locality (S.W. of Alatopetra; see Chapter 2 for locality), but the rock was strongly retrogressed, and no garnets were present.

3.8.2 Greenschists

The greenschist facies rocks of the Loumnitsa Unit comprise a variety of metasediments, including quartz schists, phyllites, graphitic schists, marbles, meta-cherts and garnet-mica-schists (Plates 3.3, 3.4). These metasediments are sometimes intercalated with metabasic rocks, usually epidote-amphibolites. In the lower greenschist facies, highly sheared meta-lavas and meta-gabbros, with preserved pillow forms and relict igneous textures are common (e.g. Agios Nikolaos area, Monahiti; Fig. 3.1). Metabasic rocks of the greenschist facies typically contain assemblages of actinolite, chlorite, epidote, albite and minor quartz.

Garnet-mica schists contain quartz-muscovite-biotite-garnet-opaques-rutile-apatite-sphene (chlorite) assemblages (Spray and Roddick 1980). These authors report that the garnets present are syn-tectonic, sub-idioblastic almandines ($Alm_{73}Gr_{07}Py_{15}Sp_5$). They are of two different varieties; larger (maximum 6 mm) porphyroblasts with overgrown rims and inclusion trails (quartz and opaques), and smaller (< 0.2 mm) crystals with no trails (Plate 3.4). The first type show chemical zoning towards their rims (Fe^{2+} and Mg increase, and Ca and Mn decrease outwards). The smaller garnets have a similar composition to the rims of the larger ones, suggesting they formed later (Spray and Roddick 1980; Plate 3.4).

At Korydhalos (Fig. 3.1), a greenschist facies chloritic schist was found interbedded with chert, and probably represents a metamorphosed impure tuffaceous horizon, of mainly basaltic composition (see below). At Agios Nikolaos (Monahiti) epidote-chlorite-plagioclase metagabbros with relict ophitic texture occur, together with phyllites, and graphitic schists. Many of the metamorphic sole basalts are in the greenschist facies. Some of these basalts could be confused with low grade metabasalts affected by ocean-floor metamorphism (See previous chapter), but their structural position within mainly coherent sole sequences argues against this origin (e.g. as seen at S. Samarina, Fig. 3.1). Unfortunately, the distinction becomes less clear within disrupted sole sequences, or where the sole grades into thick ophiolite or melange basalts (e.g. Agios Nikolaos (Monahiti), Fig. 3.1). These basalts contain assemblages of chlorite, albite, relict pyroxenes, epidote, sphene, actinolite and quartz. Iron-manganese-rich sediments (umbers) overlying these basalts (S. Samarina) contain muscovite mica, haematite and quartz.

In general, the metasediments found at other localities conform to the mineralogical and textural features described above. However, at one locality (Selloma Lakkou; Fig. 3.1), euhedral clinozoisite crystals are found aligned parallel to the schistosity, as well as within inclusion trails of the large (6 mm) garnets present (Plate 3.3). This specimen also contains less common crystals of epidote and zircon.

3.8.3 Marbles within the metamorphic sole

A common feature of the Loumnitsa Unit is the presence of marble blocks enclosed in the basal serpentinite of the Dramala Complex, or within the metamorphic sole. These meta-carbonates usually have no preserved internal structures, but occasionally, traces of bedding are seen. North of Samarina, an 80 m-thick marble is enclosed in an imbricated serpentinite slice. Numerous marbles and limestones are mapped as cropping out at the base of the peridotite sheet in the northern mountains (e.g. S. of Agia Paraskevi, Fig. 3.1; IGME Konitsa sheet 1987). At the village of Kakoplevrion, N. of Kalambaka, white coarsely crystalline marbles of Jurassic age (with *Thaumatoporella parvovesiculifera*, a shallow-water alga; IGME Panayia sheet, 1980) are enclosed in the basal serpentinite (Plate 3.5). Structurally beneath, unmetamorphosed, thick-bedded shallow-water carbonates and associated radiolarites are present (Plate 3.5). Northwest of the village of Padhes (Fig. 3.1), a thick shallow-water carbonate sequence (Early Jurassic; Konitsa sheet, IGME 1987) is found inter-thrust with sheets of serpentinite, near the base of the main peridotite sheet in this area (see below; Fig. 3.5). Marbles are also found within the greenschist and lower amphibolite rocks here (Plate 3.5 see below).

3.9 RELATIONSHIP OF THE LOUMNITSA UNIT TO THE PINDOS OPHIOLITIC UNITS

As mentioned above, the Loumnitsa unit is found in thrust contact with *both* the mantle harzburgite sheet and the crustal sections of the Pindos ophiolite, a feature which may be unique in ophiolites. Several very well exposed localities illustrate this phenomenon, displaying metamorphic sole sequences in original thrust contact with cumulates, intrusives and even extrusives of the ophiolite suite. The localities where these sequences are present will now be described.

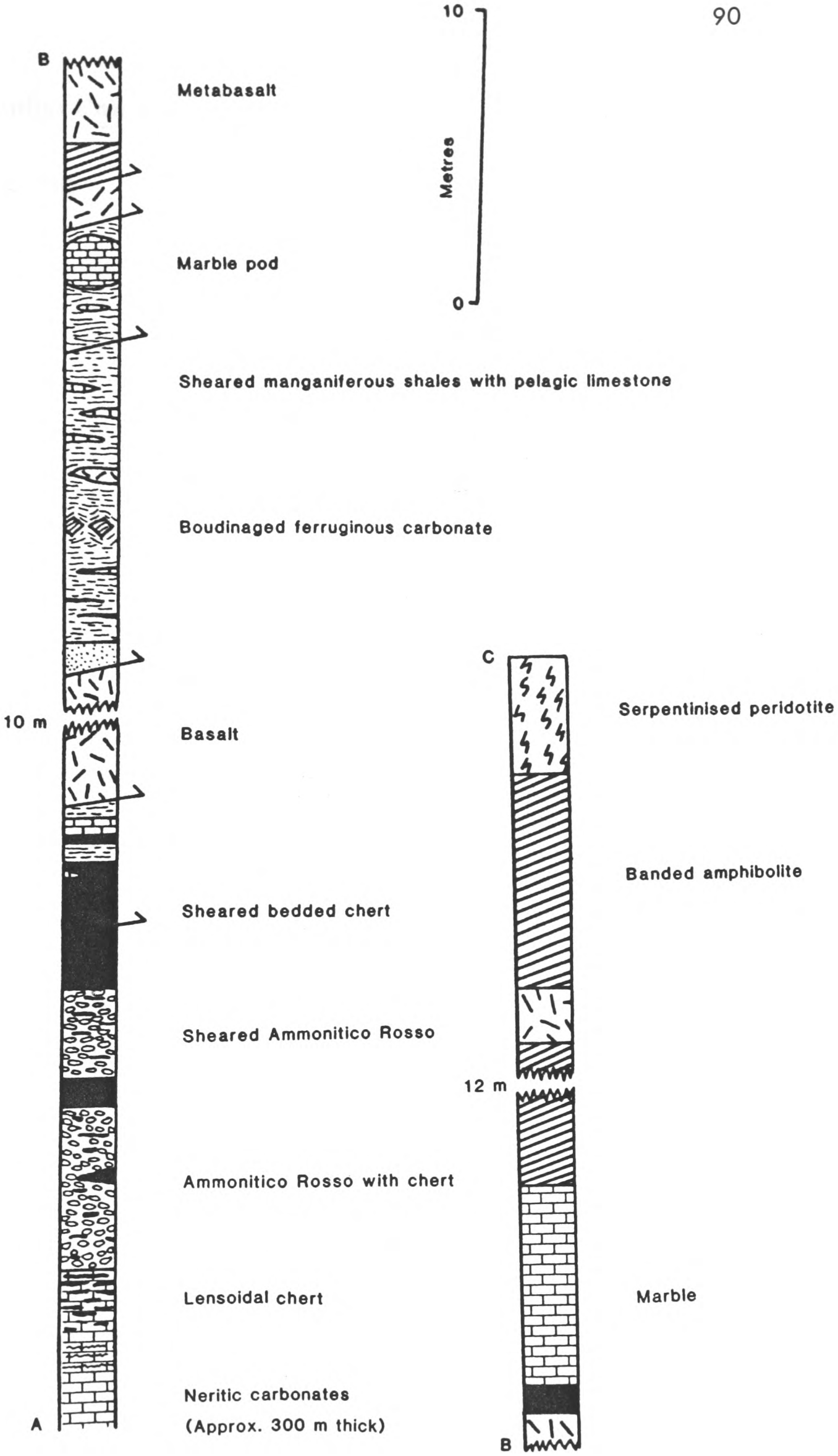

Fig. 3.5 Outline section of the metamorphic sole section exposed 100 m west of the village of Padhes (see Fig. 3.1). Of particular note is the basal greenschist and sub-greenschist facies shallow water carbonate sequence, interpreted as forming by emplacement of the ophiolite over a continental margin (see text for details).

3.9.1 Loumnitsa Unit and the Dramala Complex

a) *Loumnitsa Valley*

The Loumnitsa Valley (E. of Perivoli, Fig. 3.1) is the type locality for the Loumnitsa Unit, and exposes a complex section of metamorphic rocks, which occur in thrust contact with mantle harzburgites of the Dramala Complex. Detailed transects along the valley are presented in Figure 3.4, and only an outline of the main features will be described here. A structural thickness of more than 500 m of metamorphosed Loumnitsa Unit rocks are present.

The mantle rocks are exposed approximately 2.5 km to the south along this north-south-trending valley, and consist of thick mantle harzburgites and dunites, which contain strong foliations, believed to be primarily the result of plastic flow within the mantle (see Chapter 1). A basal peridotite mylonite occurs above the Achladi thrust, which is poorly exposed on both sides of the valley. The thrust dips to the northwest at 50^{o} at this locality. On the west side of the valley, the fabric in the underlying amphibolite facies rocks is approximately parallel to the thrust, whereas on the east side, it is only locally parallel, and is then tectonically disrupted, and consequently dips mainly to the north.

Banded feldspathic amphibolites are the most common lithology, although near the peridotite contact on the east side, an unusual black, coarse-grained and deeply weathered amphibolite occurs. Several imbricate slices of serpentinite are found within the amphibolites, with local metasomatised peridotites being found along these thrust planes (see above). The main thrusts are indicated on the sketch section (Fig. 3.4), and the folding present is described below. In detail, the sequence is complexly deformed. Amphibolite facies metasediments (mainly quartzitic schists) are found towards the contact with the greenschists. This contact dips to the north on both sides of the valley, and passes in that direction into slivers of amphibolite facies metasediments and pillowed greenschist-facies metabasalts. The basalts are recognisable on both sides of the valley, and are associated with meta-sediments of pelagic origin, including marbles, cherts and red shales. The section continues into poorly metamorphosed, and thrust-deformed Avdella Melange, composed

essentially of similar pelagic shales and cherts, redeposited limestones, and basalts.

b) *Liagkouna Mountain*

Several sections of metamorphic sole are exposed on Liagkouna Mountain, particularly on the southwest and northwest sides of the peridotite body which caps this mountain (Fig. 3.1). This section again exposes the primary peridotite/sole contact. The Achladi thrust dips towards the northwest, but the subsequent thrusts and foliations are variably dipping. Over 200 m of banded amphibolites, with particularly spectacular ductile folds, pass northwestwards into amphibolite facies metaquartzites and garnet-mica schists, displaying strong boudinage. Metasediments and metabasites of the greenschist facies at this locality include almost 50 m of light grey, bedded radiolarite, calcareous rocks, a variety of phyllites and graphitic schists, together with epidote amphibolites and greenschist metabasalts. The originally underlying melange has been re-thrust over the southeast-dipping sole along a northwest-dipping later thrust, as seems to be the pattern for several of the sole sections (e.g. N.W. side of Liagkouna).

c) *Samarina south*

South of the village of Samarina on the road to Dhistraton (near Agios Georgios church; Fig. 3.1.), a spectacular section, several km thick, is comprised of cumulate dunites with rodingitised pegmatitic gabbro dykes (commonly folded and intersheared into the dunites), troctolites and anorthosites. Towards the base, schistose serpentinites pass downwards into banded amphibolites (approx 30 m) and greenschists (150 m), displaying several interesting features. The greenschist-facies rocks are highly sheared, layer-parallel extended and thrust-imbricated, and include cleaved red and grey shales, together with limestones and shales which still preserve their original depositional contacts. Several thrust slices of basalt (WPB and MORB) are found within this section. Within the lower part of the section, sheared gabbros, interpreted as original sheeted dykes, and pillow lavas (1 m size pillows) are found. The pillows in one outcrop

have overlying metalliferous sediments, with an undulating depositional contact.

d) *Samarina north*

In the eastern Smolikas Mountains, to the north of Samarina, (Fig. 3.1), foliated serpentinised harzburgites of the Dramala Complex are faulted along a neotectonic fault scarp, against highly sheared serpentinite. The serpentinite passes eastwards into 20 m of coarse-grained, rodingitised amphibolites. More serpentinite surrounds a large marble block, which is found above a tectonic contact between the sole and the Pindos flysch at this locality.

e) *Padhes village*

Immediately west of the village, several hundred metres of unmetamorphosed to weakly metamorphosed massive light-grey carbonates (see 3.8.3 above; Fig. 3.5) sometimes with algal structures, are locally interthrust with serpentinite. At the top of the carbonate succession, a thin interval (3 m) of nodular chert passes into nodular carbonate of "Ammonitico Rosso" facies. Above this come mildly deformed greenschist facies shales and cherts, followed by thrusted and tectonically boudinaged metalliferous sediments, pelagic limestones, black shales, and eventually metabasalts. The sequence continues with a variety of amphibolite facies metabasalts, marbles and schists. Finally, banded amphibolites pass into a major thrust contact with serpentinised peridotites of the Dramala Complex. This well preserved sequence illustrates several important points which will be discussed later.

3.9.2 The Loumnitsa Unit and the Aspropotamos Complex

a) *Kalivia Kerasias south*

This section is exposed on the track which runs west of Spileo village, along the Venetikos Valley at river level. An imbricated and

downfaulted section of gabbros, sheeted dykes and lavas, is faulted against a sequence of layered cumulates to the west. These consist of coarse-grained gabbros and troctolites with minor wehrlites, and pass westwards into cumulate dunites, with inter-cumulus plagioclase and abundant chrome spinels. At the base of this cumulate section, serpentinite several metres thick has an attached metamorphic sole sequence. All of the cumulate contacts, and the schistosity within the metamorphic sole, dip to the east at approximately 30 degrees.

The metamorphic sole is composed mainly of meta-sediments, although immediately beneath the contact a brown, fine-grained schist (40 m thick), of probable meta-basic origin occurs (Plate 3.5). Then, a 70 m-thick unit consisting of marbles, red and grey meta-marls, mica-schists, meta-cherts and quartzites passes into unmetamorphosed or poorly metamorphosed sediments beneath. The metamorphic sole sequence is probably of upper greenschist facies at this locality, although grade is not easily determinable. Flattening has occurred, as shown by well developed boudinage, and a strong sub-parallel foliation. Folds and kink bands are common, as are low-angle shears and discrete thrusts. The underlying sediments contain red marls (with a Mid Triassic ammonite fauna; see Chapter 4), cherts, large limestone olistoliths, together with serpentinite sheets and thin basalts. Although several small thrusts are found between these and the higher grade rocks, they are not believed to have large displacements. This locality therefore records a transition from cumulates with an attached metamorphic sole, into almost unmetamorphosed material which appears to have formed the protolith.

b) *Rachi Kerasias*

Immediately south of the main track between Ziakas and Perivoli at Rachi Kerasias (Fig 3.1), a thin sequence of banded amphibolites and quartzose schists are exposed, which are in contact with the basal serpentinite of the cumulate dunites described above at Kalivia Kerasias. Here, quartz veins are common within the foliation of the schists and phyllites, and the sequence is thrust over deformed sediments of the melange. Greenschists are not preserved here, and the section shows

metre-scale folding and imbrication of the amphibolite foliation along northwest-southeast trending axes.

c) *Kodro Mountain*

Immediately east of Perivoli village, on Kodro Mountain, a metamorphic sole sequence is found underlying a sheet of serpentinite. A northwards-dipping foliation is present in the section. This locality has been previously described by Whitechurch and Parrot (1978), who measured more than 30 m of garnet, epidote and plagioclase amphibolites, garnet-mica schists, quartzose schists, and epidote rich rocks. In fact, the section here is much thicker, in the order of 200-300 m structural thickness. Whitechurch and Parrot (op. cit.) state that the maximum temperature/pressure conditions reached are at the greenschist-lower amphibolite boundary (T 450-500 C; P> 2 Kb).

Work on this section shows that it is again thrust-imbricated, but 3 km north of the church at Kodro, a contact with basal serpentinised peridotite mylonite is exposed. This peridotite is interpreted as forming part of the Aspropotamos Complex, which detailed mapping has shown to continue northwards beneath the ophiolite crustal section exposed at Sotira Mountain (see previous chapter). Further small outcrops of the metamorphic sole near Avdella are probably also underlying this thrust sheet, but have become imbricated along a steeply-dipping, to overturned northwestern contact of the Sotira Mountain sequence. These rocks include banded amphibolite blocks, and a variety of schists and marbles exposed in the area to the northeast of Avdella (see detailed map in Chapter 4).

d) *Venetikos-Agios Nikolaos (Monahiti)*

This area of metamorphic sole is exposed in the Venetikos River bed, and in the area around, and leading to, the church at Agios Nikolaos (Monahiti). The sequence dips south-south-east, and is dominated by metabasalts (with cross-cutting dykes), gabbros, phyllites, calc-schists and greenschists, which are commonly folded and thrust deformed. At the

junction of the Venetikos and the Aspropotamos Rivers, banded amphibolites are present. Meta-sediments are extremely common, and include nodular and platy pelagic limestones, redeposited limestones rich in platform-derived debris, abundant radiolarite with well preserved radiolaria, and a variety of shales and marls. At several outcrops, these meta-sediments can be seen conformably overlying the extrusives.

Thrust contacts and fold axes (Tertiary emplacement related) trend E-W within the river section, and NW-SE or NE-SW in other parts of the section. Thrusting is towards the south locally within the metamorphic sheet, and the section is highly imbricated (Fig. 3.6). Serpentinite is found within these imbrications, usually a schistose fibrous type, but locally, hard crystalline pods of harzburgite and dunite are recognisable. The serpentinite contains a strong foliation, which generally parallels tectonic contacts in the section.

The metabasalts are grey and red-brown in colour, and commonly preserve pillow forms. Within the basalts, ductile folds are present, generally plunging quite steeply to the west or east, mainly recognisable where quartz veins are present. The early metamorphic fabric (S1) dips moderately toward the southeast, where it is not refolded during late-stage brittle thrusting. Strong axial planar cleavages are associated with these early high-temperature folds (S2), and locally, crenulation of these earlier cleavages can be seen (S3). Small scale thrusts with minor displacements also trend sub-parallel to these fold axes. Steeply dipping and vertical strike-slip faults trend perpendicular to the predominant foliation, as shown in water-worn outcrops in the Venetikos river. These faults also have small displacements (<1 m).

The metabasalts (and schistose metabasites) are of MORB and WPB geochemistry (see section 3.10), and are generally of greenschist facies. The mineral assemblages include plagioclase, pyroxene, and variable alteration to chlorite, epidote, zoisite, white mica, calcite, quartz and opaques. Chlorite and serpentinite veins are present in some specimens. Other basalts preserve much of their original mineralogy and texture. Within the greenschist part of the sole, gabbros with preserved ophitic textures are common, sometimes as dyke swarms intruding basaltic flows. They contain serpentinite after olivine, and sericitised albites. Elsewhere (e.g.

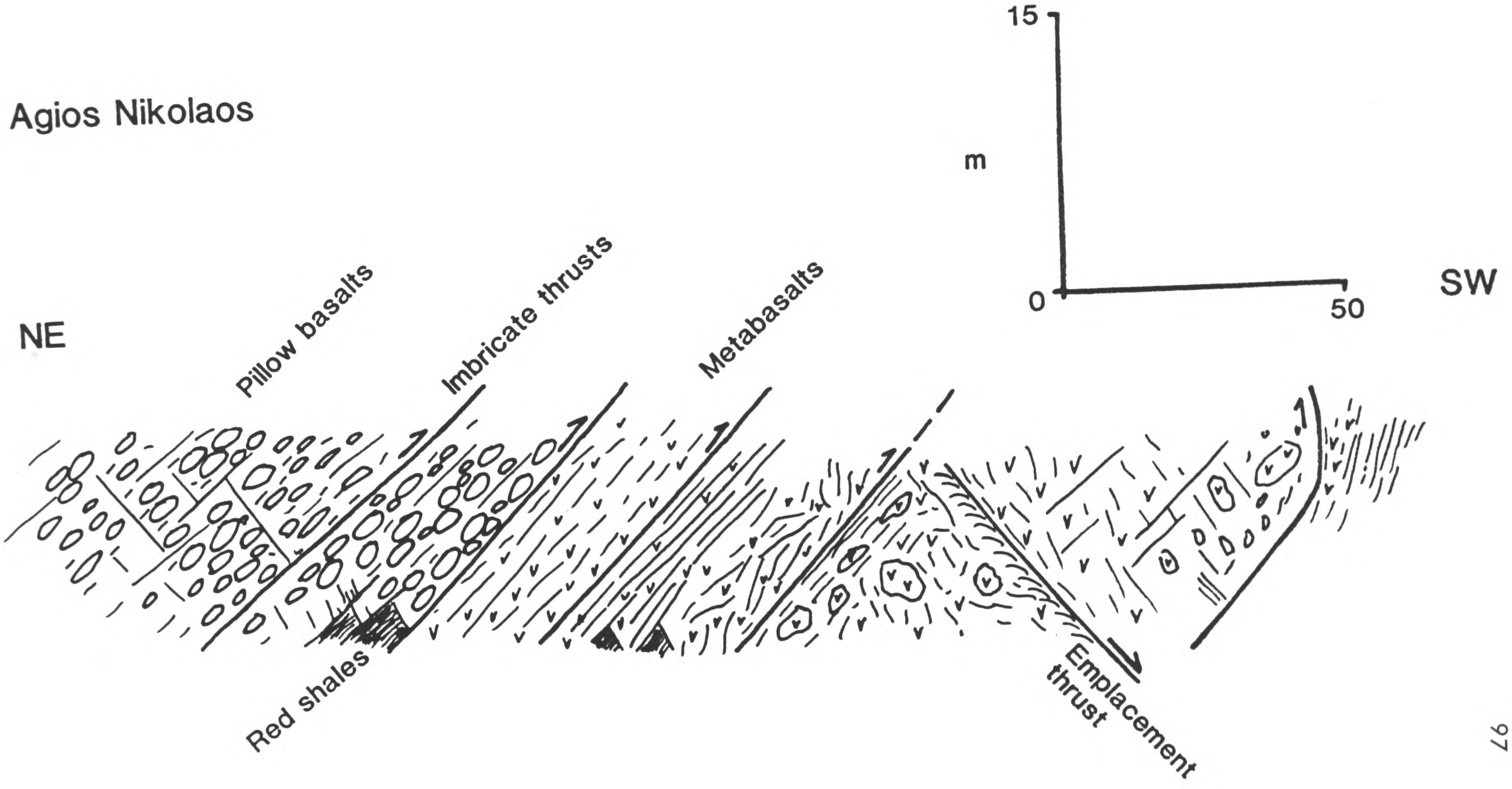

Fig. 3.6 Sketch section along a track showing the greenschist part of the Loumnitsa Unit, 500 m N. of Agios Nikolaos church (Monahiti, Fig. 3.1).

Venetikos river bed), coarse grained feldspathic-rich gabbros have uncertain contacts with the surrounding rocks, but may originally have been localised intrusive bodies.

The meta-sediments represent mainly deep-water pelagic sediments, which are common within parts of the Avdella Melange (see Chapter 4). Quartz-schists, garnet-mica schists, calcschists, and meta-cherts are common. The cherts here are of Late Triassic age (P. De Wever, pers. comm., 1990), based on the the radiolaria present (see Chapter 4). The associated sediments are also similar to those dated as Late Triassic at Avdella (i.e. red marls and nodular limestones). In addition, blocks within the river bed, presumably of local derivation, contain Late Triassic Megalodontid bivalves. Within the lava sequences, thin (10-60 cms) marble lenses, and more extensive beds (several metres) are found. One of these marbles contains abundant well preserved ooids, with a sparite cement, which was probably redeposited as a calciturbidite from a shelf environment.

The metamorphic sole at this locality is interpreted as underlying the ophiolitic crustal rocks of the Abelia-Moura stream area (see Chapter 2). The contact is preserved at the confluence of the Aspropotamos and Veneticos rivers, and to the northwest on the hillside of Kopanes (See main map, enclosure 1), where banded amphibolites with serpentinite slices, are faulted against ophiolitic lavas, distinguished by more depleted geochemical signatures (evolved plagiorhyolites and IAT). The ophiolitic lavas pass with some structural complication westwards into sheeted dykes and then high level gabbros. More remnants of metamorphic sole (amphibolites and meta-basalts) occur on the hillside to the northwest of Abelia and the Aspropotamos Valley, where a sheet of serpentinite occurs before the contact with the ophiolitic rocks

3.10 GEOCHEMISTRY OF THE LOUMNITSA UNIT

3.10.1 Introduction

One of the primary objectives of the study of the metamorphic sole lithologies was to compare their geochemistry with unmetamorphosed basaltic rocks found in other tectonic units of the north Pindos Mountains, and to determine any relationships between them. Evidence from igneous petrology (Winchester and Floyd 1976; J. A. Pearce, pers. comm. 1988), and studies of other sole units (Malpas 1979), suggests that certain trace elements (eg Ti, Zr, Cr) remain immobile in the lower amphibolite pressure/temperature field, thus allowing a direct comparison to be made. However, by the upper amphibolite facies, this may not be the case, especially if signs of partial melting are visible in the field or in hand specimen. As none of the Loumnitsa Unit amphibolites are of high grade, mobility of elements due to this factor is not considered likely.

The data gained from whole-rock XRF analysis of metabasites (Appendix 2) can be plotted on standard geochemical plots (e.g. Pearce and Cann 1973; Pearce 1982), and used to interpret the likely tectonic environment of formation, in the case of metabasic lithologies. Particular caution must be applied to those elements which may commonly be found in abundances near, or below the detection limit of the analytical equipment used (see Appendix 2). This particularly affects the light rare earth elements (LREE) and Nb. Where this is a limiting factor, the elements have been omitted from multi-element plots presented below.

3.10.2 Rodingites

Geochemically, these rocks are characterised by a low silica and titanium content, and a moderate to high CaO content. Aluminium, magnesium and iron oxides comprise most of the remaining major elements. The most abundant trace elements are chromium, nickel and vanadium, with a general depletion of all other elements. The Loumnitsa Valley (128/88; Appendix 4) and Liagkouna samples (184/88; Appendix 4) compare well, the latter being particularly chromite rich. Both are

probably highly metasomatised ultramafic rocks. The sample analysed from Kodro (2/27/8; Appendix 4) has more than 23% CaO, and correspondingly lower MgO and Na_2O than usually found in a metabasic analysis. The TiO_2 value is low, as are the Zr, Nb and Y values. This rock is probably a rodingitised basic rock, either originally a gabbro or a basalt. Several of the other metabasites analysed have relatively high CaO values (see Appendix 4), and can be more or less considered as rodingites. The effect of rodingitisation on "immobile" trace elements is unclear. From a consideration of analyses in this study, it would appear that the effect is probably minimal, as rodingitised and unaltered metabasites from the same locality show comparatively small variations in immobile trace element values. For example, samples 2/27/8 and 4/27/8 from Kodro Mountain, are rodingitised, but contain comparable immobile element values to less altered metabasites at this locality (e.g. 5/27/8; see below).

3.10.3 Amphibolites

A large number (40; Appendix 4) of amphibolite-facies rocks from numerous localities in the Pindos Mountains have been analysed to determine the nature of the protoliths. Most of the amphibolites analysed from the Loumnitsa Unit are of metabasic origin, as suggested by the major element chemistry and immobile trace elements. The analyses of the amphibolites are relatively uniform throughout the whole region (Appendix 4), despite the variable mineralogical contents and degrees of alteration present.

Several geochemical discrimination diagrams are particularly useful in classifying the amphibolites (see Chapter 2). These include the Ti-Zr-Y, Zr/Y-Zr, Cr-Y, Ti/Y-Nb/Y and MORB-normalised plots. These are presented as Figures 3.7 to 3.9. The Ti-Zr, Ti-Zr-Y and Zr/Y-Zr plots are used to distinguish MORB from WPB-type lavas. Cr-Y is useful for separating IAT from other, less evolved lavas, and Ti/Y-Nb/Y separates most lavas into tholeiitic, transitional or alkalic varieties. The MORB-normalised plots (Figs. 3.10-3.14) show the variation of each basalt from typical oceanic tholeiitic MORB values, and emphasises relative enrichments or depletions of the chosen elements within individual samples.

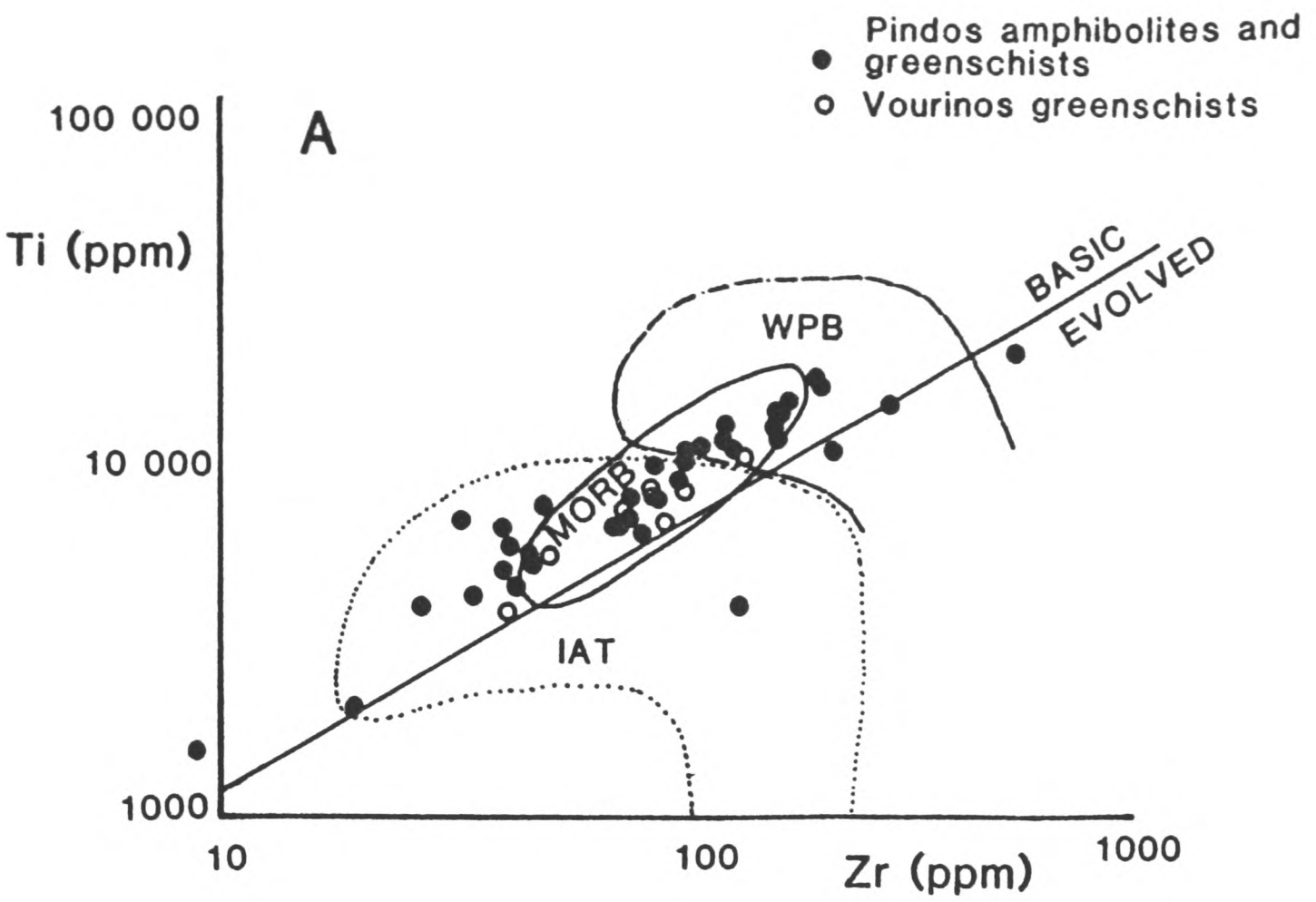

Fig. 3.7 a) Ti-Zr plot for the Loumnitsa Unit, after Pearce and Cann (1973). WPB= within plate basalt; MORB= mid ocean ridge basalt; IAT= island arc tholeiite; Closed circles: Loumnitsa Unit amphibolites and greenschists. Open circles: Vourinos greenschist basalts. b) Zr/Y-Zr plot for the Loumnitsa Unit after Pearce (1975). Key as for a).

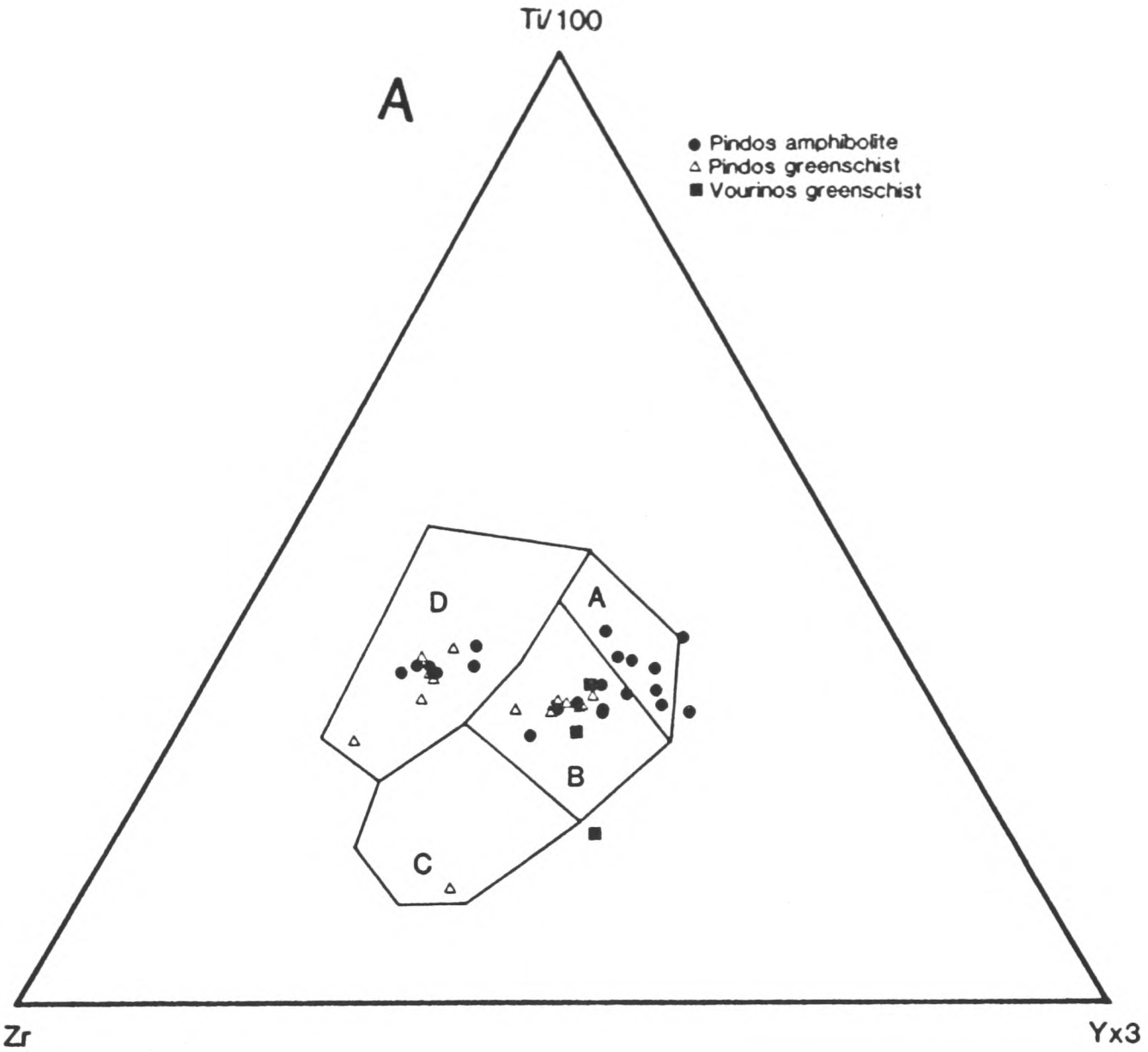

Fig. 3.8 a) Ti-Zr-Y plot for the Loumnitsa Unit, after Pearce and Cann (1973). Within plate basalts plot in field D, calc-alkaline basalts in fields Band C, mid-ocean ridge basalts in field B, and island arc tholeiites in fields A and B. b) Ti/Y-Nb/Y plot for the Loumnitsa Unit, after Pearce (1982). Fields as in Fig. 3.7a. Thol= tholeiitic; Trans= transitional; Alk= alkaline basalts.

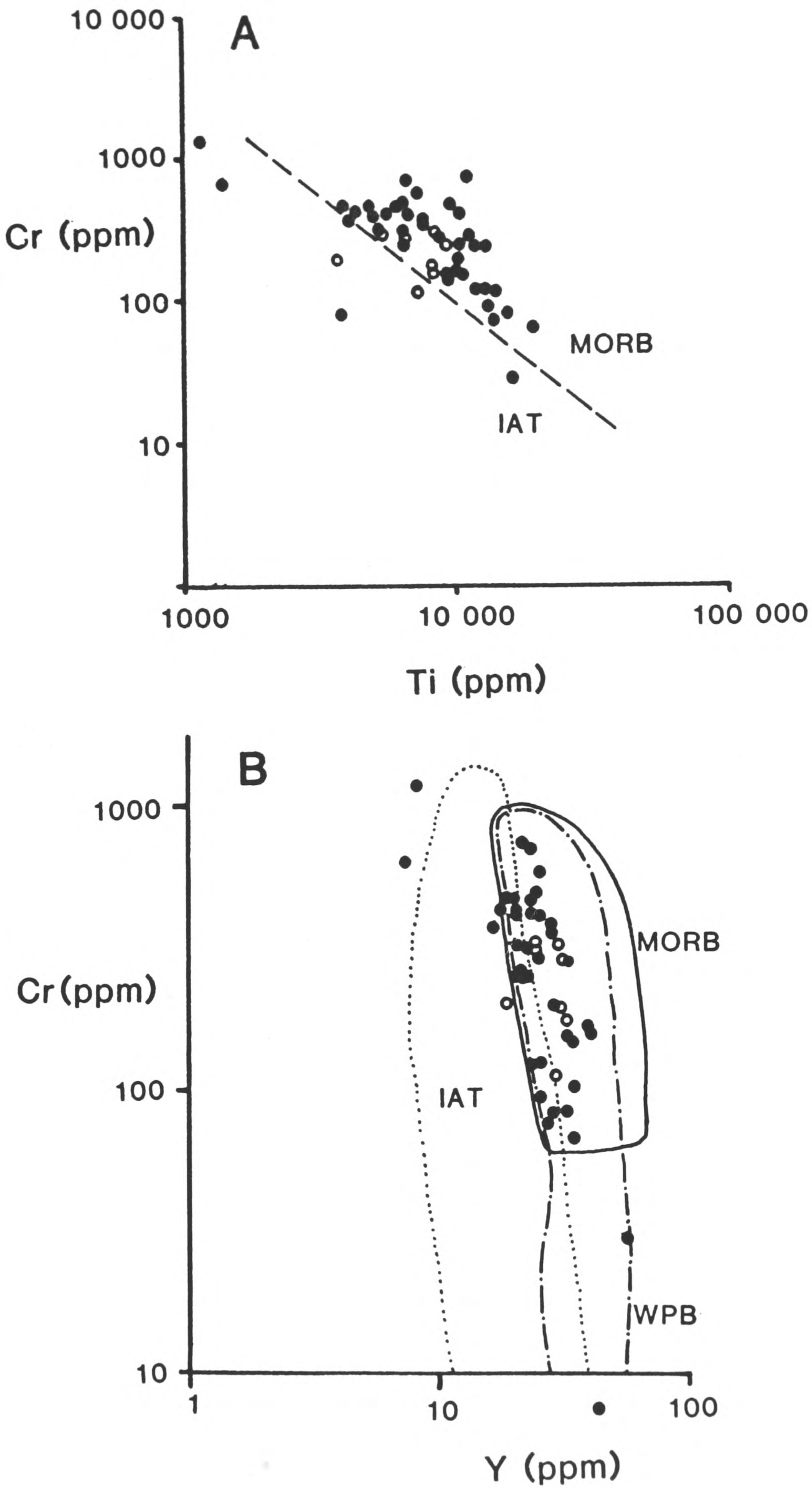

Fig. 3.9 a) Cr-Ti plot for the Loumnitsa Unit (after Pearce 1975). b) Cr-Y plot for the Loumnitsa Unit, after Pearce (1975). Key as in Fig. 3.7.a

The amphibolite facies metabasic rocks have been separated from those of other origins (i.e. ultramafics, metasediments) and are the only type considered here. The SiO_2 values vary from 38.7% to 54.5% showing the range of variation present within the major elements. Other major element contents also vary considerably as a result of mobility during and after metamorphism. Calcium contents vary according to the amount of metasomatic alteration present. The rocks with high CaO contents (i.e. rodingitic metabasalts; see above), tend to have correspondingly lower $Si0_2$ values (43-45%; see Appendix 4). The values of the immobile element titanium range from 0.65 to 2.24, indicating a wide variation in the source magmas which formed the initial basalt liquids. Within the trace element analyses, chromium values are moderately low (<100-400 ppm), but range up to over 700 ppm. Zr values range from 42 to 169 ppm, and Y from 18 to 29 ppm.

The data from these rocks presented on the trace element variation diagrams shows that the amphibolites are mostly, but not exclusively of within plate basalt (WPB) and MORB geochemical type. On the Ti-Zr diagram (Fig. 3.7.a), the range of Ti and Zr values is usefully displayed. Most of the analysed rocks are also shown to be basic and not evolved. A notable feature is that a group of the analyses fall only in the IAT field (see below). This is further emphasised on the Zr/Y-Zr diagram (Fig. 3.7.b), in which three distinct chemical groups begin to emerge. The Ti-Zr-Y triangular plot (Fig. 3.8.a) similarly shows a scatter of the data from the WPB through MORB and into the IAT (or low-K tholeiite) fields. Two distinct geochemical groups are displayed by the Ti/Y-Nb-Y diagram (Fig. 3.8.b), one of WPB-type alkaline and transitional basalts, and a second group dominantly of MORB and/or IAT-type basalts.

Diagrams particularly useful for separating rocks of possible IAT affinities include Cr-Ti and Cr-Y. When drawn for the metamorphic sole rocks (Fig. 3.9. a, b), it can be seen that most of the analyses fall in the MORB and WPB fields, and only a small number of analyses are found in the IAT field. These analyses are significant, however, and will be discussed further below.

A number of geochemical groups can be distinguished from a study of the multi-element variation diagrams plotted for the Loumnitsa Unit amphibolites. A group of rocks showing strong within plate basalt-type signatures (e.g. 123/88, Fig. 3.10.a), are characterised by a general enrichment of elements relative to MORB (Group 1). Variations in the content of the incompatible elements and Cr, distinguish how relatively primitive or evolved these metabasalts are. A second geochemical group (Group 2) can be distinguished, in which the general pattern is flat, or slightly U-shaped, in other words of MORB or depleted relative to MORB-type. This is probably the most common type present, and is found at many of the localities studied (Figs. 3.10, 3.11). This group includes metabasalts showing metasomatic alteration (e.g. 124/88, 127/88, from the Loumnitsa Valley, Fig. 3.10.a; 186/88, from Liagkouna, Fig. 3.10 b; 1/27/8, 2/27/8, from Kodro Mountain, Fig. 3.11.a), and metabasalts showing little or no Ca metasomatism (e.g. 5/27/8 from Kodro, Fig. 3.11.b). These rocks show depletions in P, Ti, Zr and Y, and enrichment in Cr, relative to normal MORB. Due to analytical uncertainties regarding the light rare earth elements, a subduction-zone origin cannot be proven for the more depleted basalts of this group. The patterns do, in general, compare well with chemical patterns from island arcs, (e.g. S. Sandwich Islands; Pearce unpublished manuscript, see also Chapter 4).

The most depleted samples relative to normal MORB in terms of their trace element content, are directly comparable to rocks from volcanic arcs (Group 3). Sample 33/89 from Padhes in the northern Pindos Mountains (Fig. 3.1), shows a clear light rare earth element enrichment (Fig. 3.12.a). This enrichment can only have been derived from secondary enrichment by subduction-influenced melts. This amphibolite was collected close (i.e. within 10 m) to the contact with the ultramafic rocks of the Dramala Complex.

One amphibolite collected from immediately beneath the Dramala Complex at Liagkouna (183/88; Fig. 3.10b), has a chemistry almost identical to immobile trace element-depleted high magnesian andesites (boninites), found in the ophiolitic Aspropotamos Complex of the Pindos Mountains (Chapter 2). This rock has been somewhat rodingitised, as it has a CaO value of 18.7 %, and a low SiO_2 content (44 %), although calcium silicate minerals are not particularly abundant in thin section.

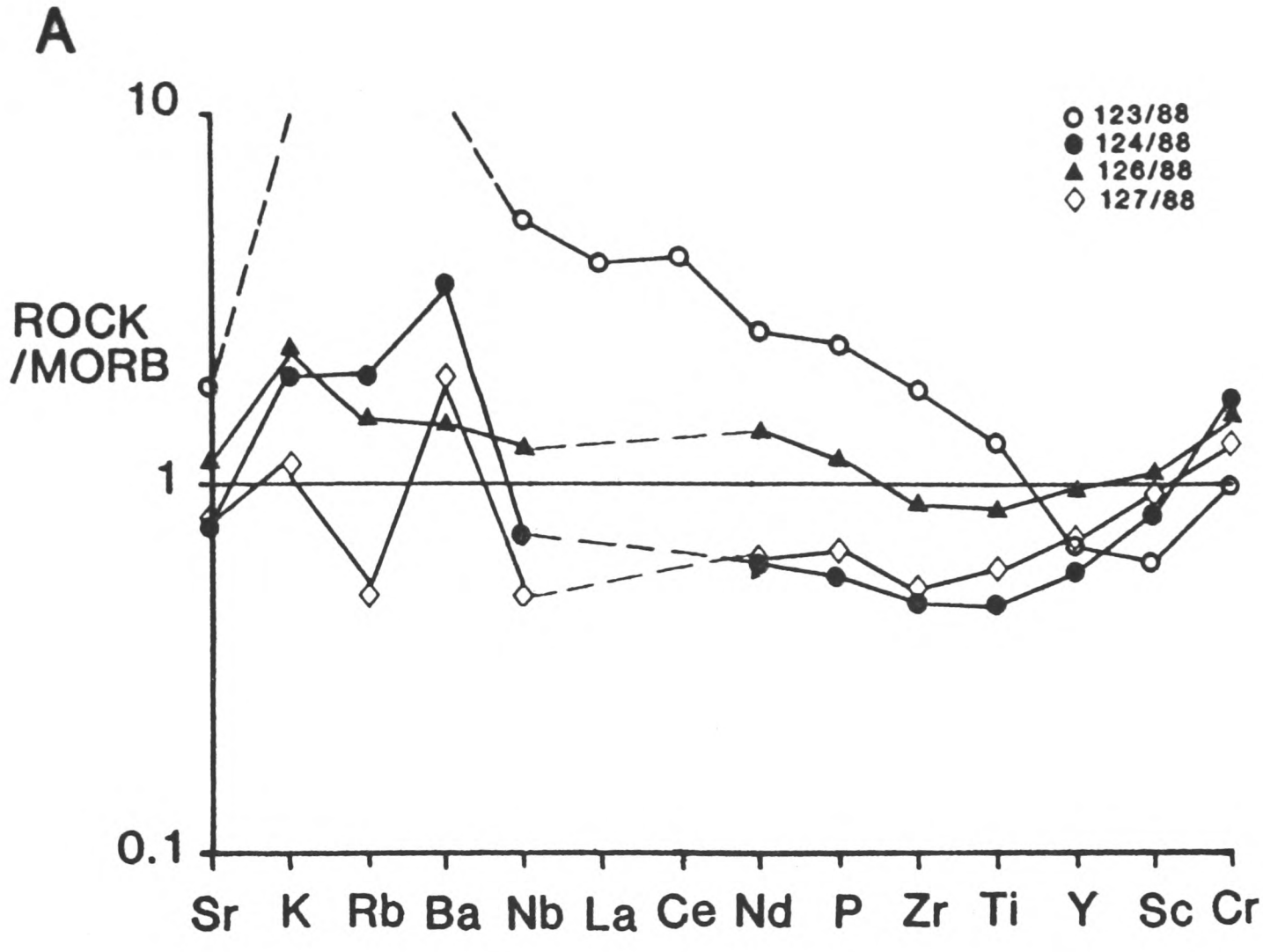

Fig 3.10 MORB-normalised multi-element plots (Pearce 1975) for the Loumnitsa Unit; a) Loumnitsa Valley amphibolites; b) Liagkouna Mountain amphibolites and greenschists (22/88). Normalising values (partly after Pearce 1980); Sr=120 ppm, K_2O= 0.15%, Rb= 2.0ppm, Ba= 20 ppm, Nb=4 ppm, La= 4.5 ppm, Ce=10 ppm, Nd= 8 ppm, P= 0.12%, Zr= 90 ppm, Ti= 1.5 %, Y=30 ppm, Sc= 40 ppm, Cr= 250 ppm.

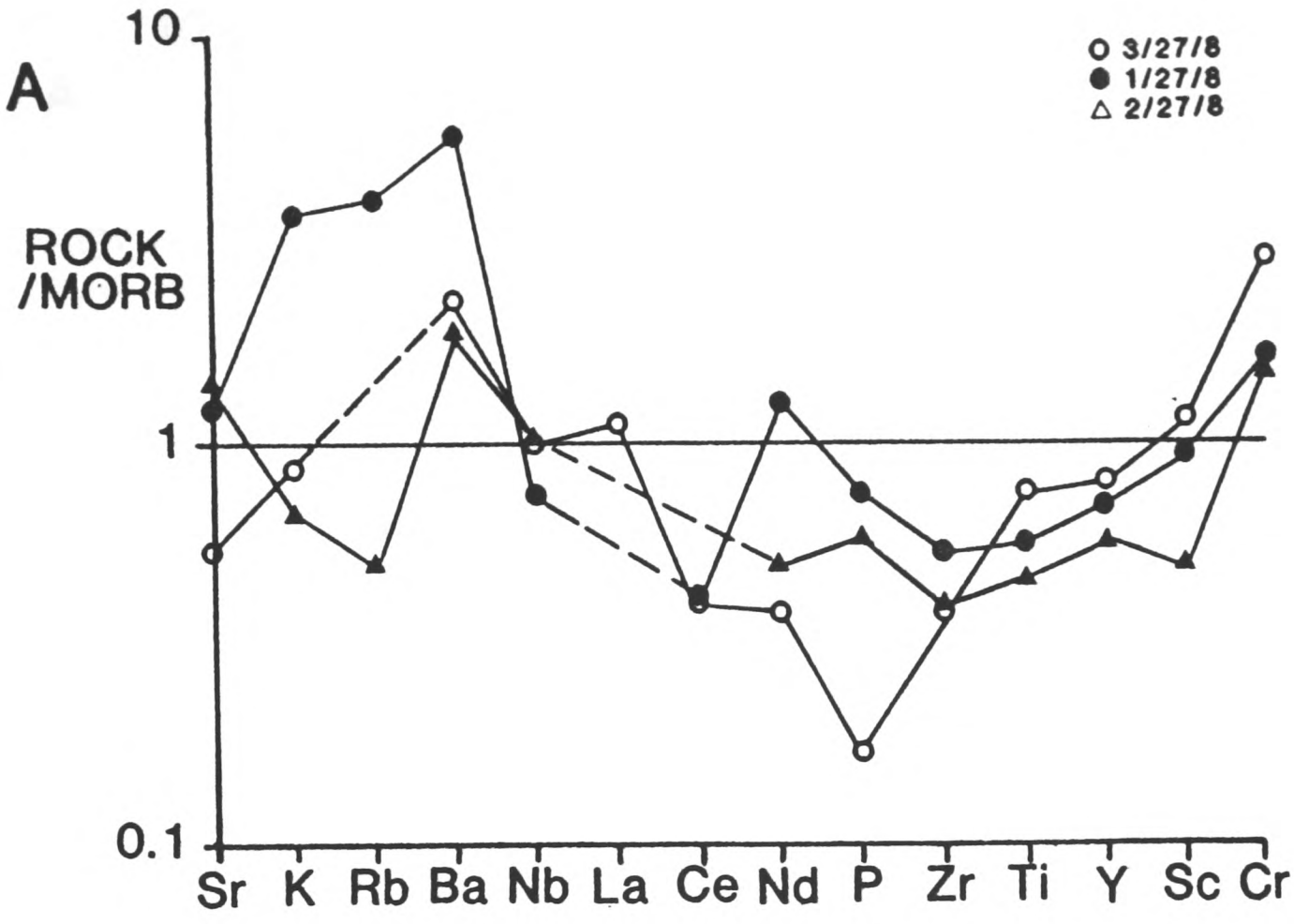

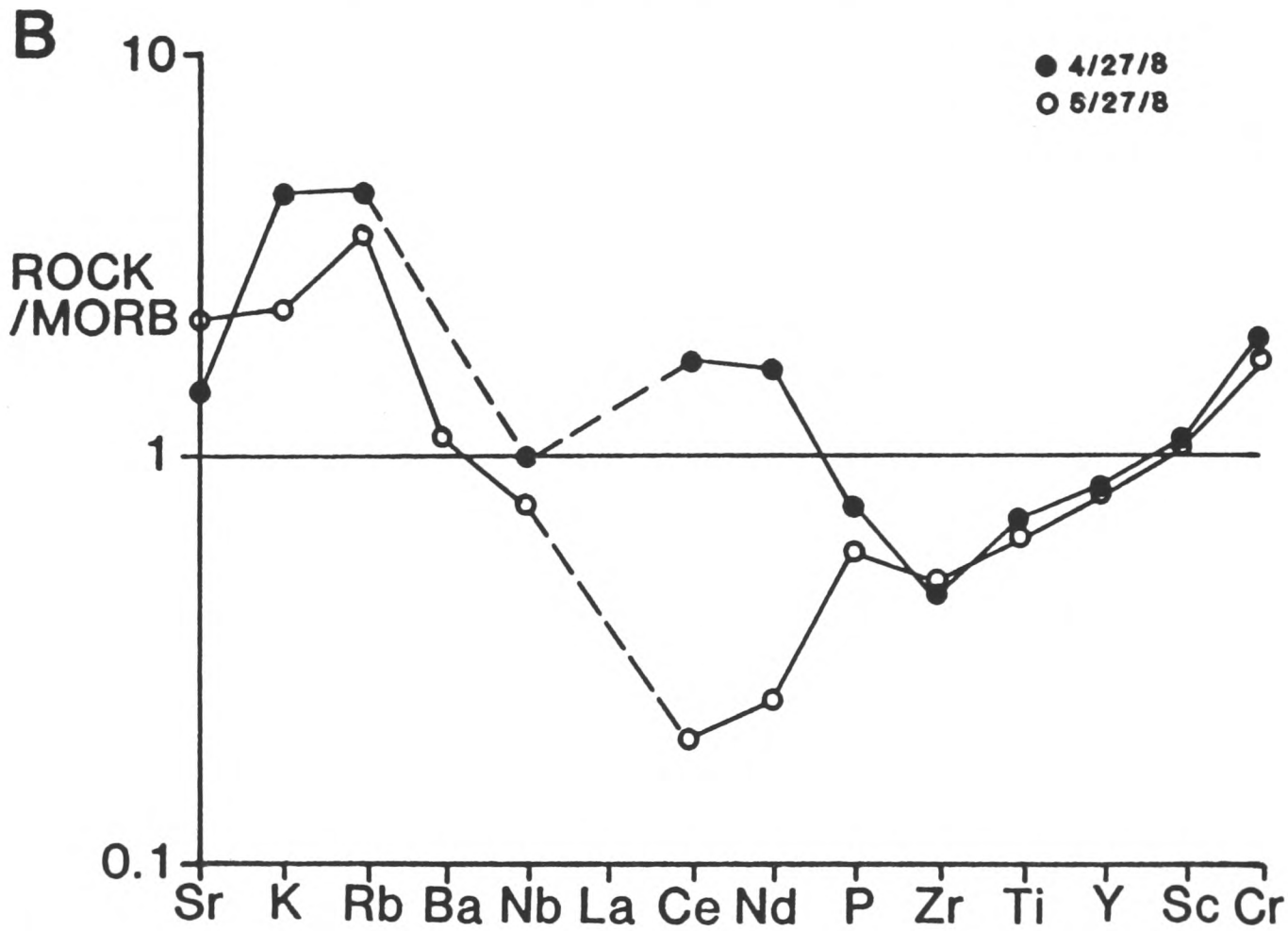

Fig. 3.11.a,b; Multi-element plots for Kodro Mountain amphibolites. Normalised as for Fig. 3.10.

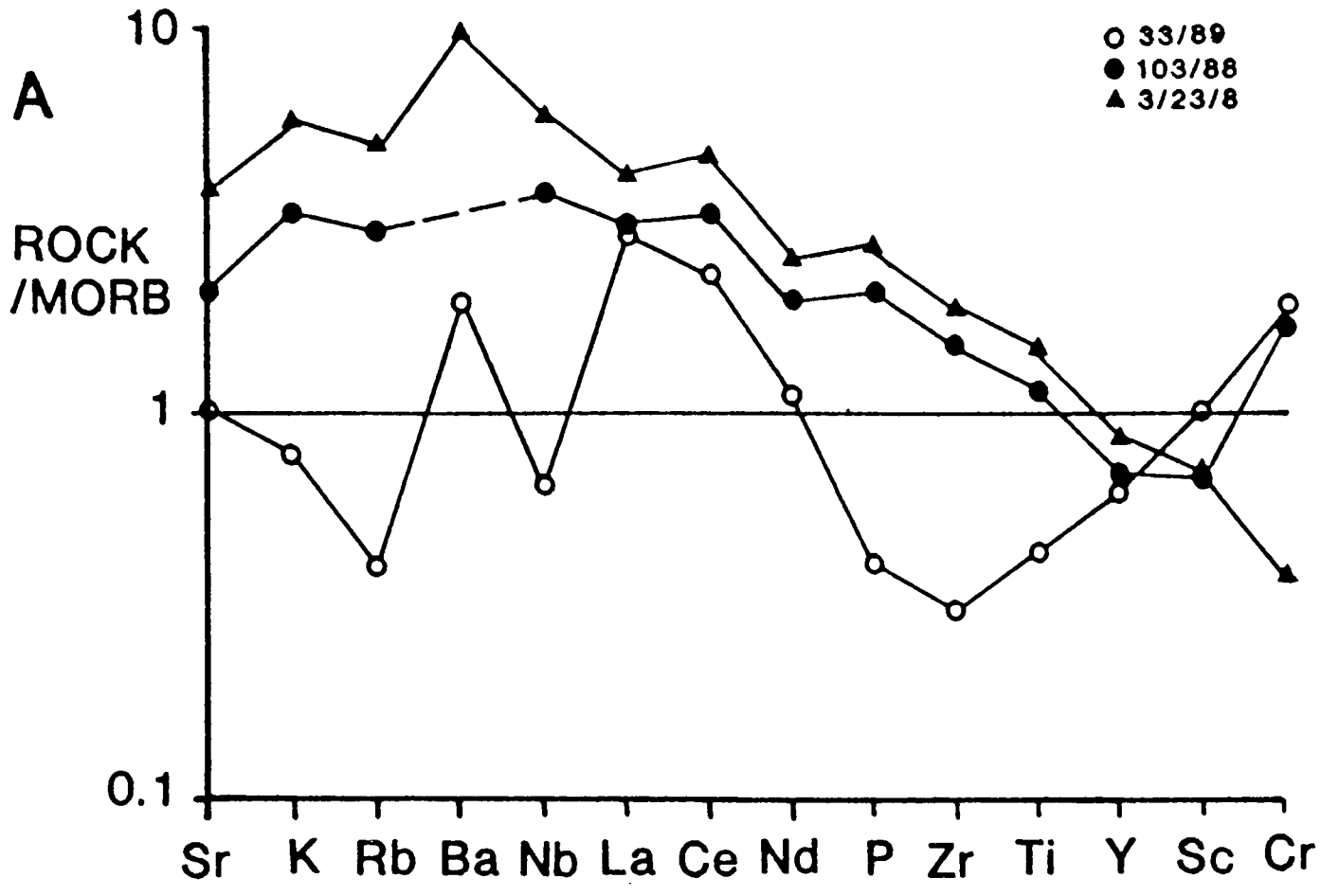

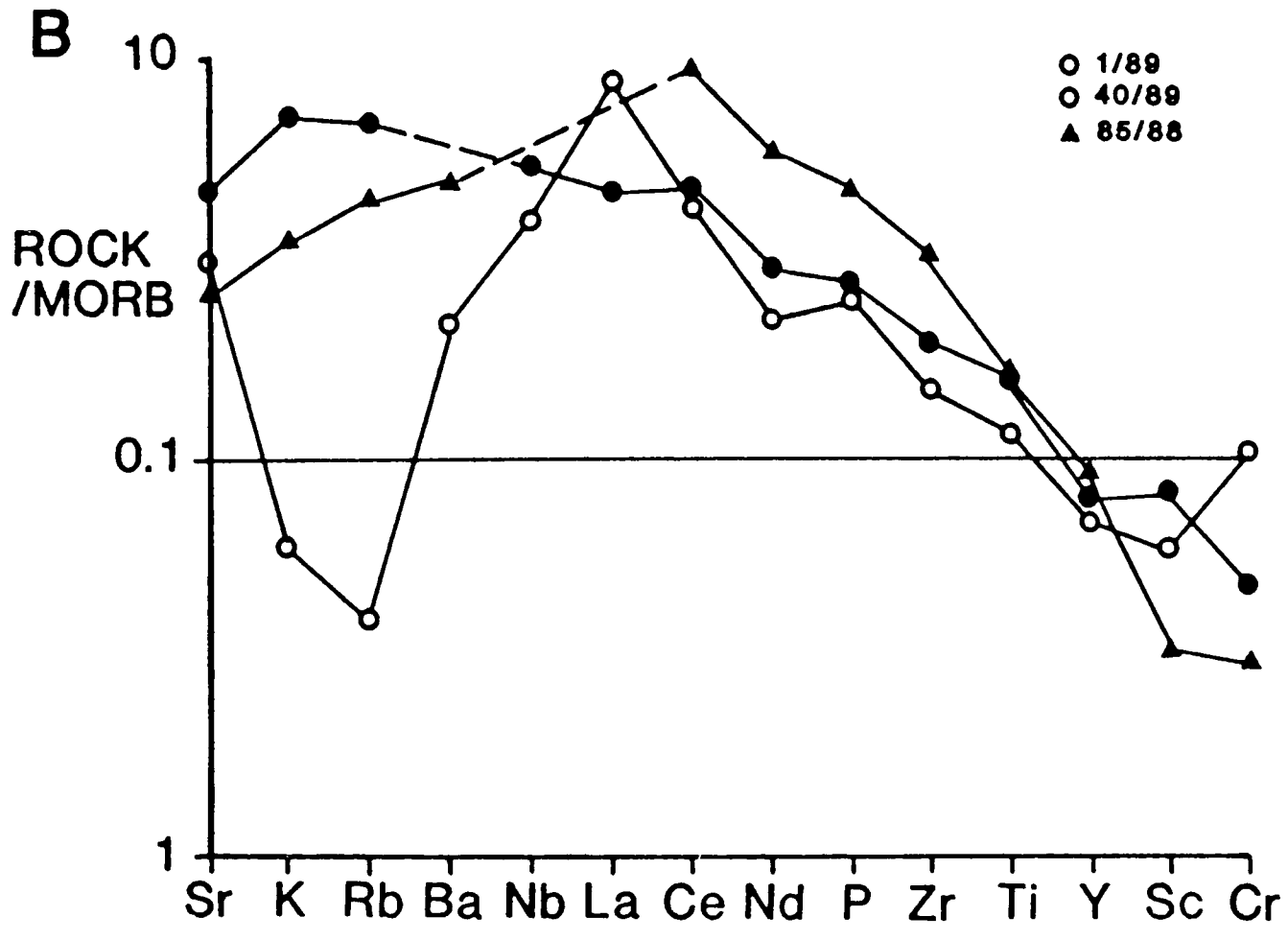

Fig. 3.12 Multi-element plots for: a) Padhes amphibolite (33/89); Avdella amphibolite (3/23/8); Milea amphibolite (103/88); b) Greenschist clast from an olistostrome conglomerate, near Alatopetra Village (1/89); greenschist from the east side Vassilitsa Mountain (Fig. 3.1, 40/89); Greenschist interbedded with radiolarite, Korydhalos (Fig. 3.1, 85/88). Normalised as for Fig. 3.10.

Also noticeable is the high MgO content (12 %), and very low Ti (0.25), characteristic features of boninites. The incompatible trace elements and rare earth elements are all depleted (e.g. Zr 12 ppm; Nb 1 ppm; Y 7 ppm), with a corresponding increase in compatible elements, particularly Cr (720 ppm). The multi-element plot (Fig. 3. 10b) shows a typical dish-shape, and may be compared to boninitic rocks shown in Chapter 2. These rocks are only known from the fore-arc regions above subduction zones in modern ocean basins (see Chapter 2).

Trace-element depletions in these amphibolite-facies rocks could result from either: 1) some mobility of trace elements may have occurred during high-temperature metamorphism; 2) the earliest basalts accreted onto the peridotites during thrusting (i.e. those found immediately adjacent to the peridotite) were originally of somewhat more depleted chemistries than normal MORB; 3) there has been trace-element mobility during metasomatic alteration of these amphibolites. The major element contents of samples 183/89, 33/89 and 5/27/8 do not suggest that any mobility has taken place during high-temperature metamorphism. Additionally, although many of the most depleted rocks present have major element analyses and mineralogies affected by low-temperature metasomatism (at 500^{o} or less; Coleman 1977), this is not considered likely to have affected trace elements such as Zr, Ti and Y, which are considered to be almost totally immobile at such temperatures. It is concluded therefore, that some of the rocks of the Loumnitsa Unit were primarily depleted in certain trace elements, and these are presently found at or near the contact with peridotites of the Dramala Complex. It is unlikely that hydrothermal alteration also concentrated along the base of the peridotite has significantly altered the abundance of "immobile " trace elements. Some caution should however be applied, and mineralogical assemblages taken into account, paticularly when dealing with higher metamorphic temperatures.

3.10.4 Greenschists

The greenschist facies lithologies consist of a wide range of meta-sedimentary and metabasic rocks. These will be considered in turn.

a) *Metabasites*

Greenschist metabasites either occur as truly schistose chloritic rocks, or as recognisable meta-basalts or meta-gabbros with relict igneous textures. The analyses show both WPB and MORB affinities, and not the more depleted traces associated with the higher grade rocks. SiO_2 values range from 41.9 % to 50.7 %. and TiO_2 ranges from 0.64 % to 3.3 %. Trace element values are also variable, Zr ranges from 75 to 294 ppm, and Y from 21 ppm to 56 ppm. A chloritic greenschist from Korydhalos (85/88) gives a strongly WPB signature (Fig. 3.12.b). Other greenschist-facies metabasalts from the Venetikos Valley and Agios Nikolaos (Monahiti), are both of MORB (1/20/8/D; Fig. 3.13.a) and WPB-type (8/AN/10; Fig. 3.13.b), although structural complexities at this locality mean that distinguishing greenschist rocks of the sole from ocean-floor metamorphosed melange basalts is difficult. In summary, the greenschist facies rocks may be either of N-MORB or WPB geochemical affinities, but WPB-type volcanics are most common.

(b) *Metasediments*

Analyses of metasediments are presented in Appendix 4. A variety of rocks are present, including calc-schists (e.g. Agios Nikolaos; 14/24/8), mica schists, phyllites, marbles, and cherts. These rocks are characterised by high SiO_2 or CaO values, and high values of some trace elements; e.g. Ba, Sr.

3.10.5 Summary

In summary, it is concluded that amphibolites of the Loumnitsa Unit from the sampled localities, have original geochemistries which can be categorised as follows:

1) Enriched within-plate basalts, with steeply sloping multi-element patterns, from Nb or Ba through to Y. Some of these rocks are primitive

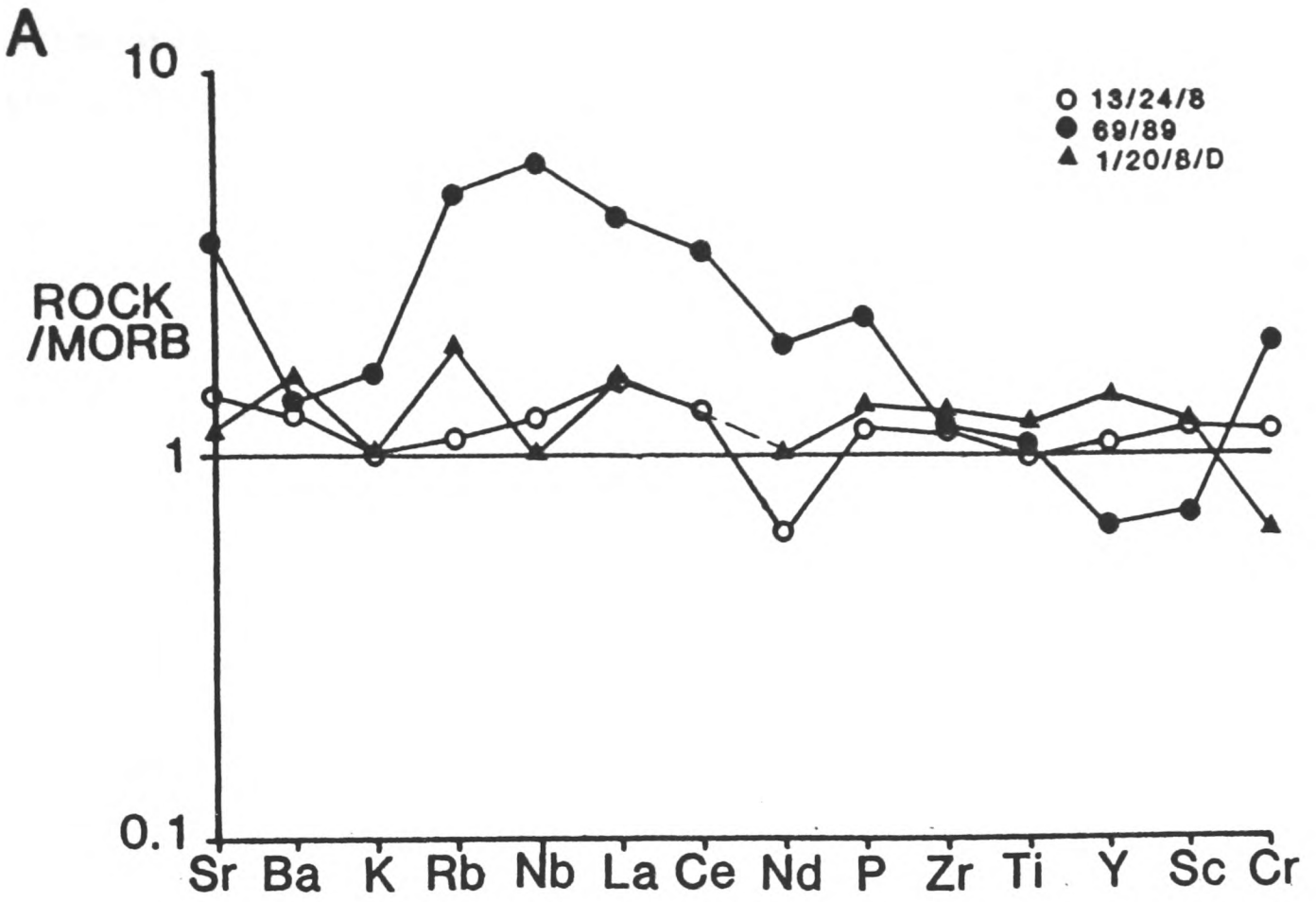

Fig. 3.13 a) Greenschists from Agios Nikolaos, Monahiti (13/24/8 and 69/89) and the Venetikos Valley (1/20/8/D). b) Greenschists from the Venetikos Valley at Agios Nikolaos, part of the same metamorphic sole sequence as that at Agios Nikolaos.

(103/88), and some are more evolved (3/23/8), as shown by the lower Cr and higher incompatible element content.

2) Numerous examples of rocks which range from MORB-type values, to slightly more depleted than MORB. The multi-element patterns vary from being almost horizontal along the MORB base line, through to mildly U-shaped below this line. These rocks probably do not show a light rare earth element enrichment, although the values of these elements are too close to detection limits to be certain. They represent aggregate high degrees of melting. Despite a multi-element pattern resembling IAT-type basalts, a subduction origin cannot be proven based on this analytical data.

3) A limited number of samples (e.g. 33/89), with a clear light rare-earth element enrichment and associated high Cr values, showing a quite strongly sinusoidal multi-element trace. This indicates a definite secondary enrichment in light ion lithophile elements, typical of rocks from island arc suites.

4) Samples which are strongly depleted in all elements except compatibles (Sc and Cr), which have deep U-shaped multi-element traces. These rocks have close affinities with high magnesian volcanics (boninites), only known from fore-arc teconic settings.

In general terms, the greenschist facies rocks are of within plate or MORB chemistry, and the amphibolite facies sole shows the more depleted signatures. There seems to be no correlation between the chemistry of the sole, and its occurrence beneath either of the Aspropotamos and Dramala Complexes. Similarly, sampling was not sufficiently detailed to distinguish true chemical differences between each locality.

3.11 Geochemical comparisons of basic rocks from the metamorphic sole and Avdella Melange

The geochemical characteristics of the Loumnitsa Unit were compared to the regionally associated volcanic rocks of the Aspropotamos

Complex and the Avdella Melange, to establish if there is a genetic relationship present. In the Semail ophiolite, Searle and Malpas (1982) concluded that there was no exact correlation with either the underlying melange volcanics (Haybi Complex), or the volcanics of the Semail ophiolite, from a consideration of the sole amphibolite chemistry (Fig. 3.14). However, Lippard et al. (1986) emphasised that there is a correlation between the amphibolites and the transitional-tholeiitic lavas of the Haybi Complex, especially when the rare earth elements are considered, and thus they cannot be discounted as possible protoliths. Metamorphic rocks from the St. Anthony Complex of Newfoundland (Jamieson 1981) contain a variety of amphibolite chemistries. Metabasites from the Goose Cove Schist and Green Ridge Amphibolite are tholeiitic at the contact with the peridotite, and become more transitional and alkaline downwards. The associated volcanics (Ireland Point Volcanics) range from alkaline to tholeiitic basalts, apparently of WPB and WPB-MORB transitional type, that may also therefore have formed part of the protolith.

Generally, the metabasalts and amphibolites of the Loumnitsa Unit are comparable to basalts of the Avdella Melange. This is demonstrated by the Cr-Y discrimination diagram presented (Fig. 3.15), which compares the analyses from the two units. They show that a large degree of overlap is present between them. The main differences appear to be that a greater proportion of alkaline basalts (WPB) are present within the melange, although several of the "sole" basalts are also clearly of this type. Individual analyses can also be compared to one another. For example, a greenschist analysed at Korydhalos (85/88; Fig. 3.16a), compares to a melange basalt from Liagkouna Mountain (147/88), both being WPB-type basalts. An amphibolite from Milea (109/89) also compares to a basalt from the Dio Dendra Valley (218/88; Fig. 3.16.b).

3.12 Geothermometry and geobarometry

The metamorphic rocks of the Loumnitsa Unit were previously reported as being of lower amphibolite metamorphic facies (Spray and Roddick 1980), and upper greenschist facies (Whitechurch and Parrot 1978). Extensive sampling across the region has indeed established that lower amphibolite is the maximum grade attained, based on the absence

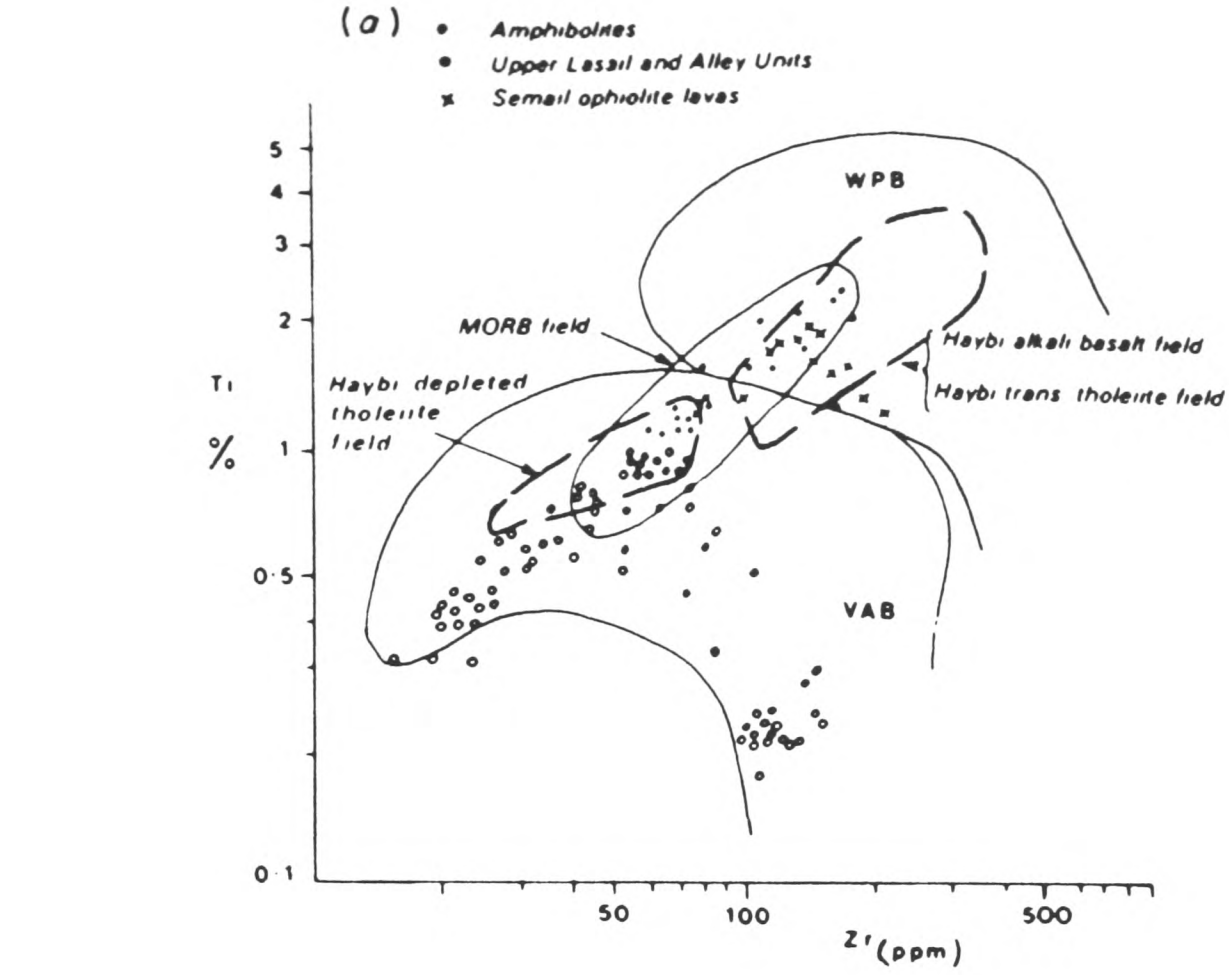

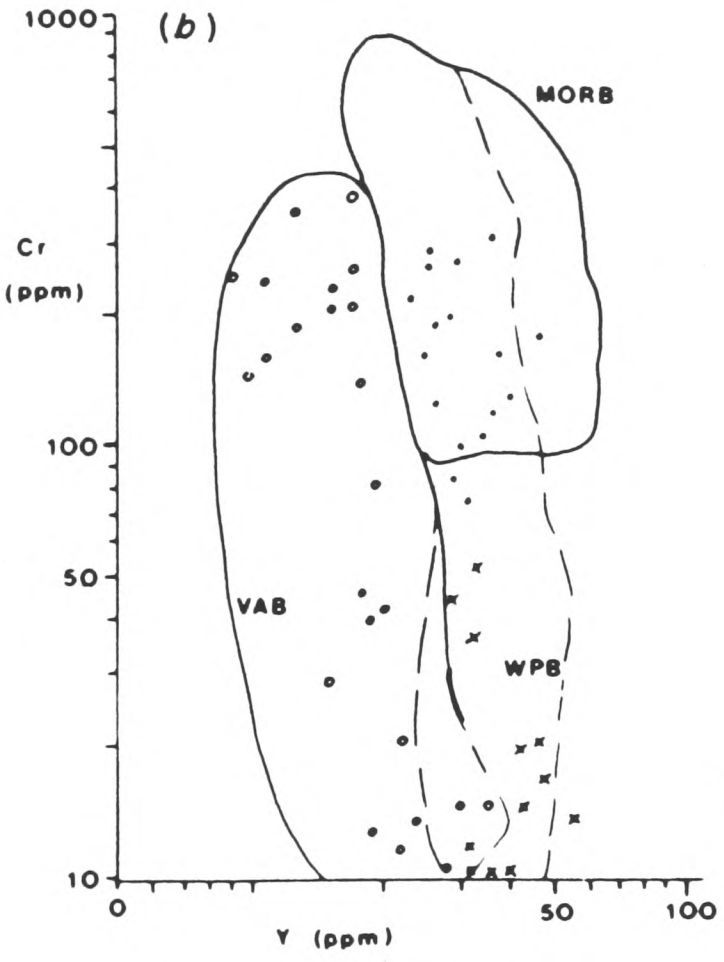

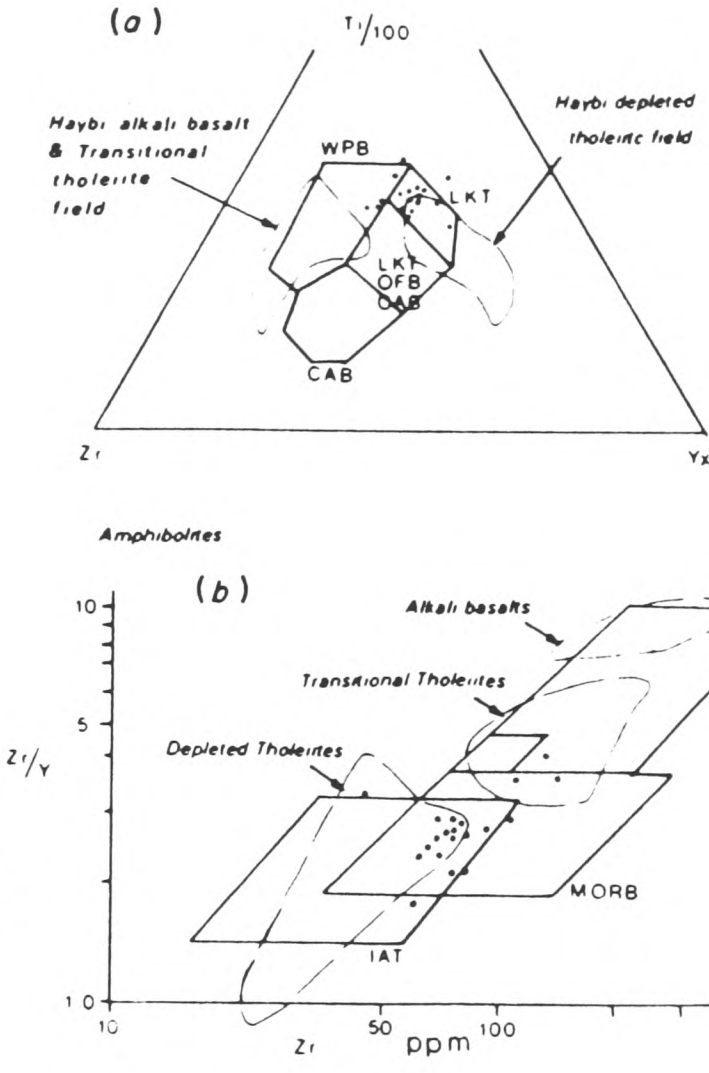

Fig. 3.14 Geochemical discrimination diagrams from the metamorphic sole of the Semail ophiolite, Oman (from Searle and Malpas 1982). Note the position of the amphibolite facies rocks, in comparison to the data presented above for the Loumnitsa Unit.

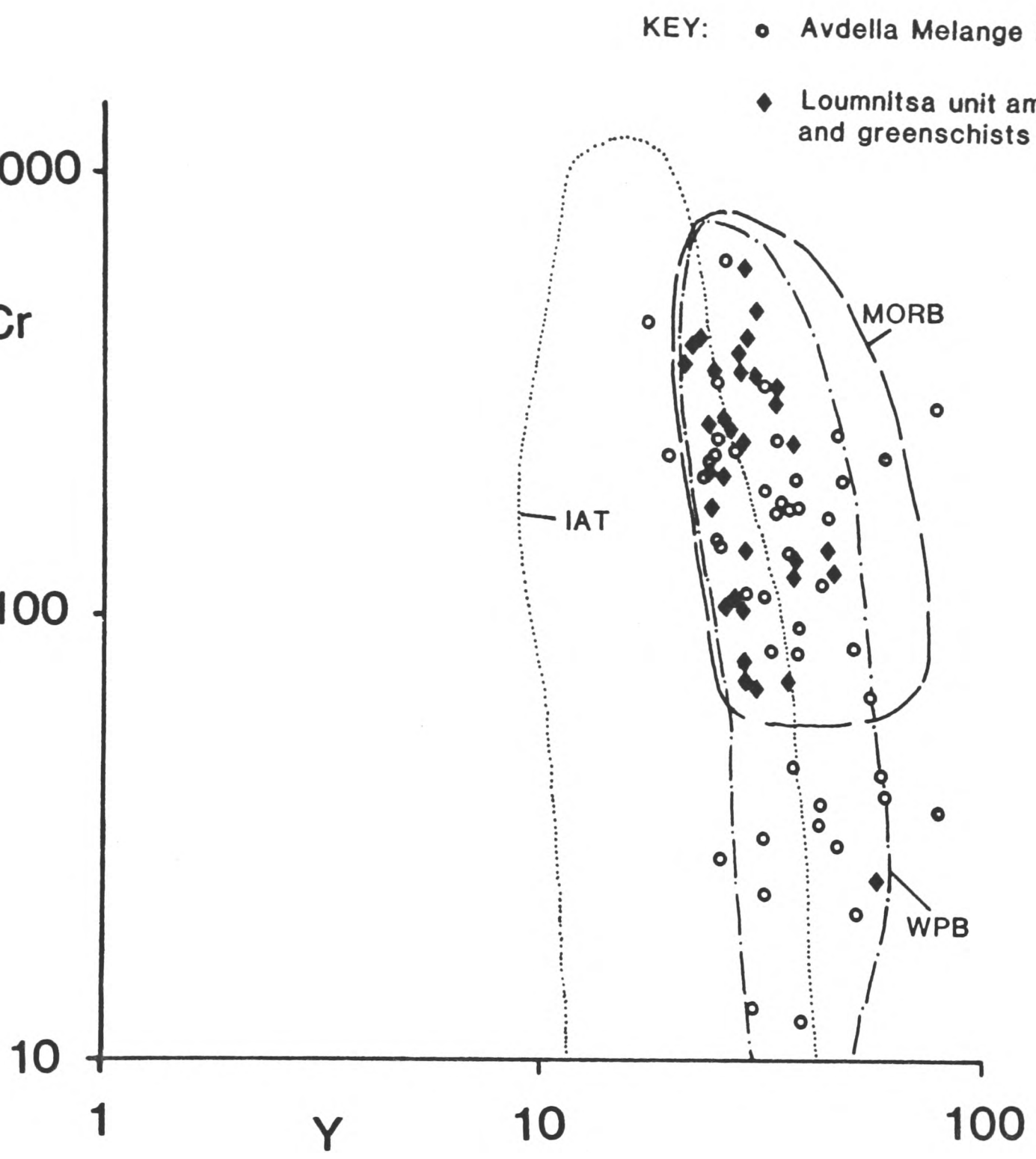

Fig. 3.15 Cr-Y plot comparing amphibolites and greenschists from the Loumnitsa Unit with the tectonically underlying Avdella Melange (see Chapter 4).

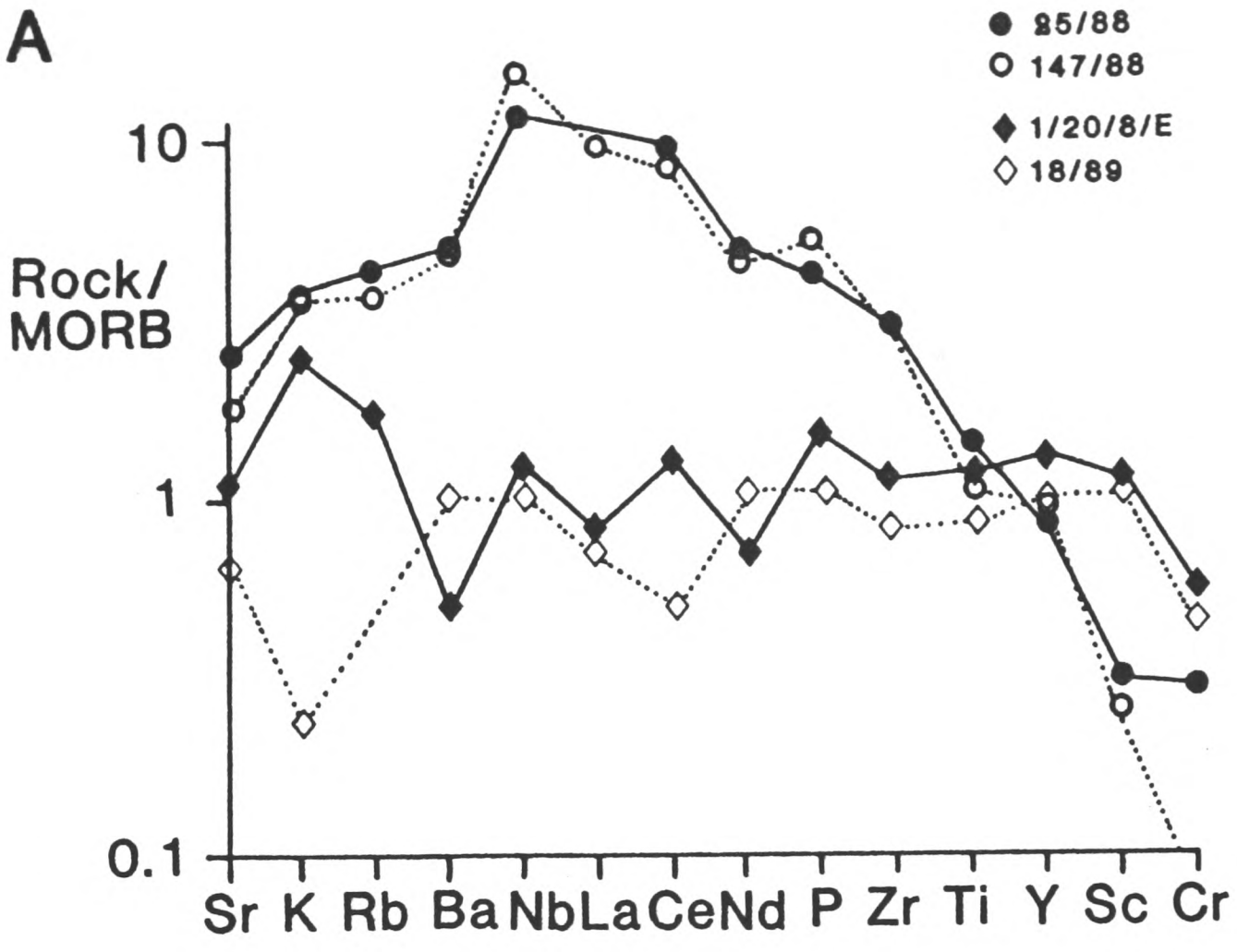

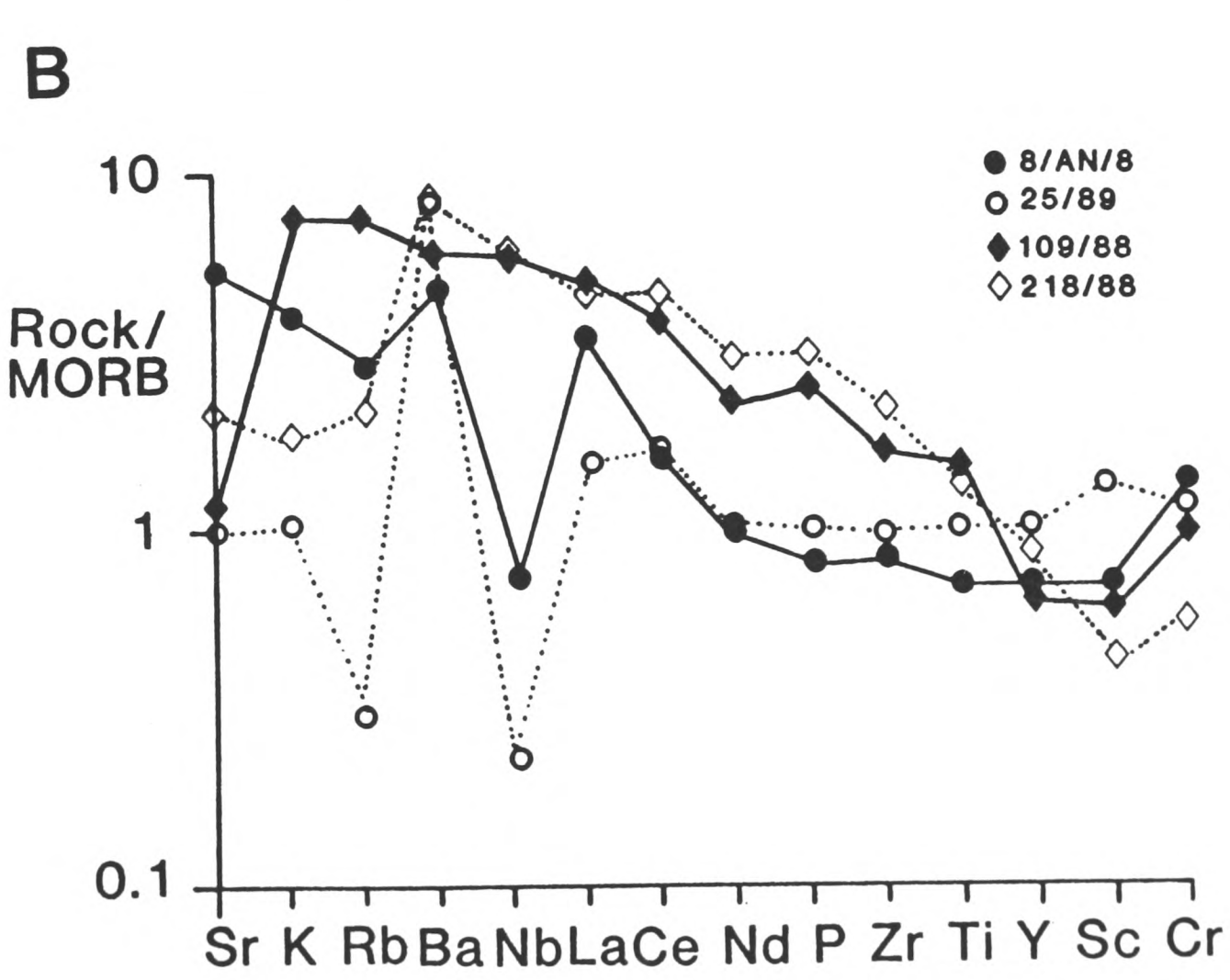

Fig. 3.16 Multi-element plots comparing amphibolites and greenschists of the Loumnitsa Unit with unmetamorphosed basalts from the Avdella Melange (see Chapter 4). a) greenschist, Korydhalos (85/88); melange basalt, Liagkouna (147/88); greenschist, Venetikos Valley, (1/20/8/E); Melange basalt, S. of Samarina (18/89). b) Greenschist basalt, Venetikos Valley (8/An/8); basalt, Smolikas Mountains (25/89); amphibolite, Milea (109/88); basalt, Dio Dendra (218/88). For normalising values see Fig. 3.10. Note the similarities in the analyses, suggesting that the basalts form the protoliths for the metamorphic rocks.

of garnets and metamorphic pyroxene, and the presence of green hornblendes. Many of the amphibolites studied have been altered at lower temperatures, and now contain minerals typical of the greenschist facies. The pressure estimates for metamorphic sole formation are probably in the order of 2-4 Kb, although this is not well constrained.

3.13 DEFORMATION OF THE LOUMNITSA UNIT

3.13.1 Internal deformation of the amphibolites and greenschists

The metamorphic rocks of the Loumnitsa Unit have undergone multiphase deformation. Structures present within them were studied in detail, in an attempt to understand the timing and nature of the deformation, and to identify fold vergences.

The main deformational events are summarised in Table 3.1. These are grouped into two categories: (1) probable Mid Jurassic structures; (2) probable Early Tertiary structures. The earlier structures range from high-temperature metamorphic fabrics and isoclinal folds, through to brittle fractures. The later structures are usually larger-scale brittle-type folds and faults, related to thrust emplacement.

One of the most important features of the metamorphic sole is that it may preserve a record of the initial displacement vector of the Pindos ophiolite, within high-temperature, and therefore early-formed folds. These are present as spectacular small-scale (0.02-2 m) tight to isoclinal, intrafolial folds, found mainly within the amphibolite facies rocks (Plate 3.6). Analysis of these folds is complicated by refolding and thrusting that has taken place during the Tertiary. The most difficult problem is to restore the folds to the horizontal, parallel to the inferred direction of thrust emplacement. Using the premise that the related lithologies of the basal ultramafic rocks indicate the way-up with respect to the amphibolite and greenschist sole rocks, the effects of Tertiary large-scale folding and re-imbrication can theoretically be removed.

Four main localities were studied where the sole is still attached to the Dramala Complex (Loumnitsa, Liagkouna, Kodro, Samarina; Fig. 3.1).

TABLE 3.1

ROCK TYPE	STRUCTURES	AGE
AMPHIBOLITES	Regionally extensive S1 high-temperature foliation, axial planar to F1 fold axes. Folds are tight to isoclinal. Small scale extensional structures, displacing S1 fabric, on centimetre scale.	Probable Mid-Jurassic structures
GREENSCHISTS	S1 axial planar foliation. F1 isoclinal folds, usually visible within quartz bands. Boudinage of competant layers. Local S2 foliation, axial planar to F2 folds, both moderately steeply dipping. S3 crenulation cleavage locally developed. Elsewhere, symmetrical and asymmetrical kink folds (F3?) deform S1, and possibly S2.	
STRUCTURES IN BOTH UNITS	Metre-scale folding of early fabrics, usually tight to isoclinal, with steeply-dipping to vertical axial planes, which trend NW-SE. Axial planar cleavage locally developed. Sub-horizontal to moderately-dipping thrust planes, variably dipping. Vertical to steeply-dipping faults, probably wrench faults. Trend approximately 040^{o}.	Early Tertiary

The folds from Samarina occur in a series of banded amphibolites, in which the plagioclase-rich bands are deformed by small (1 cm or less) folds. These folds plunge steeply towards the northwest and verge towards the northeast (Fig. 3.17). The amphibolites are part of a conformable sole sequence, which passes down from cumulate dunites of the Dramala Complex and basal serpentinite, into amphibolites and greenschist-facies metabasites and metasediments, finally passing into a narrow thrust slice of melange (see 3.9.1.c). The amphibolite foliation is dipping uniformly to the southwest at this locality, with little subsequent deformation, and so only northeastward vergence seems to be indicated by this locality.

At Liagkouna Mountain, the folds show some pattern in relation to the direction of dip of the schistosity, despite extensive fold and thrust-related deformation (Fig. 3.17). In general, where the foliation dips to the north, 'S'-type minor folds are developed, and when the foliation is southward dipping, 'Z'-type folds are found, in the direction of plunge. However, this cannot be related to the general structure here, as the base of the peridotite forming the upper limit of the sole is overturned to the southeast.

The Loumnitsa Valley section contains well-exposed folds which are found within a steeply-dipping primary schistosity (S1). This schistosity is trending variably due to imbrication of this section (Fig. 3.4), and is visibly folded by steep to vertically plunging concentric folds at the southern end of the section. The folds here are thus difficult to interpret. Similar problems were encountered at Kodro Mountain, where lack of suitable exposure and later deformation has confused the structural history. Here, folds are either neutral, or give opposing vergence senses.

In summary, a lack of strong lineations and extensive Tertiary folding and thrusting has made minor fold interpretation difficult. In the least deformed locality, at Samarina, northeastward vergence was indicated, as it was at the more deformed Liagkouna. The sections at Loumnitsa and Kodro were considered unreliable as indicators of initial thrust vergence.

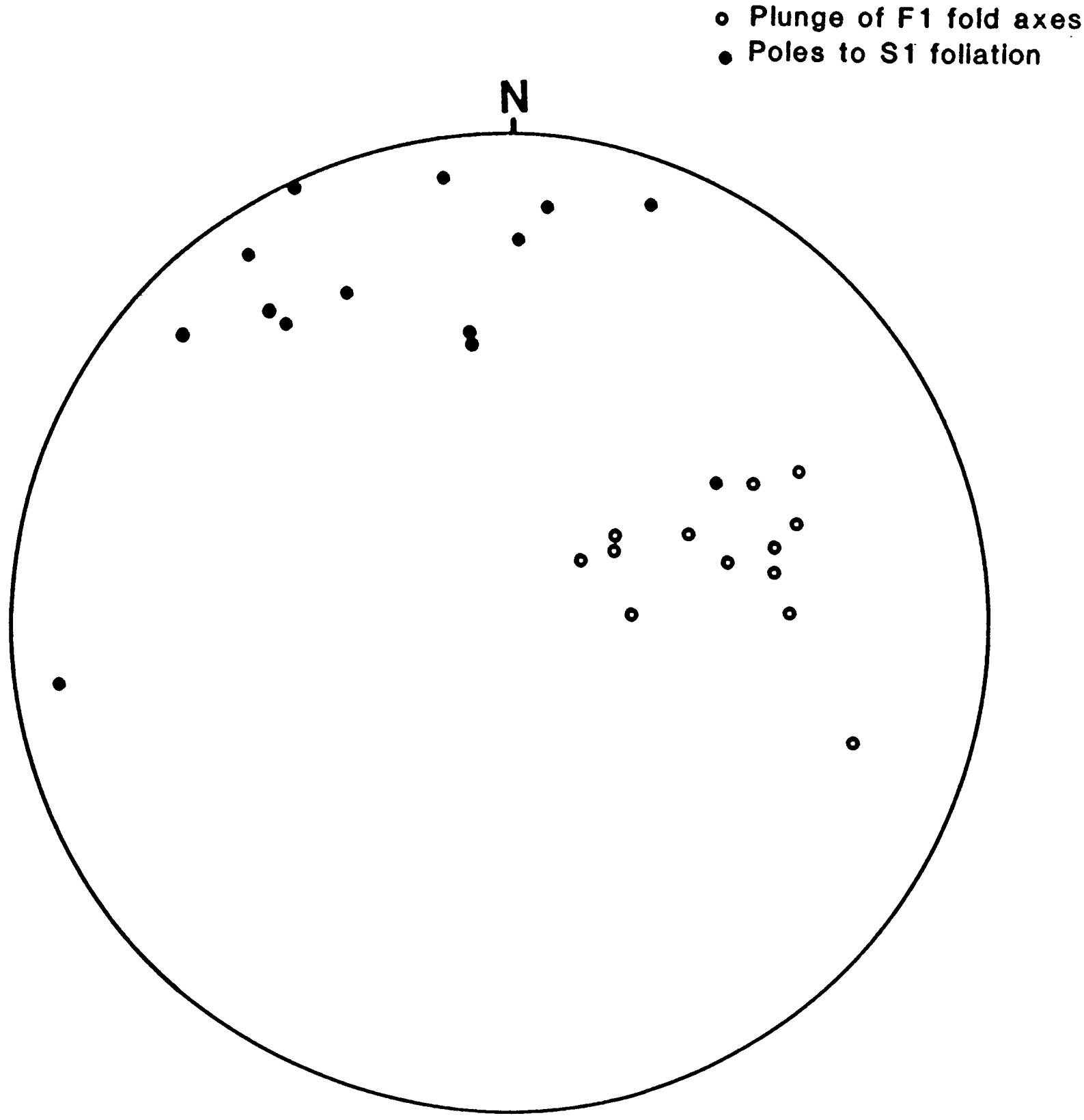

Fig. 3.17 Plunge of high-temperature foliation and fold axes within the Loumnitsa Unit amphibolites, Liagkouna Mountain (see text for explanation).

3.13.2 Large-scale structure of the metamorphic sole

The sole rocks are often highly imbricated beneath the peridotite sheet, probably associated with late-stage southwestward-directed rethrusting (see Chapter 7). At several localities, the underlying melange has been re-thrust over the sole (e.g. Loumnitsa; Fig. 3.4). The sole outcrop pattern is strongly controlled also by Tertiary folding, as shown in the structural cross sections. Thrusting has detached large slabs of the metamorphic sheet from the base of the peridotite, and left them stranded on top of the melange. This may have occurred both during the Jurassic and the Tertiary thrusting episodes. These slabs were then folded according to the local and regional structures.

3.14 Comparison with the Vourinos metamorphic sole

The Vourinos ophiolite is reported to posess a basal amphibolite facies metamorphic sole, not visited in this study, which is best exposed in the Aliakmon River section, at the southern margin of the ophiolite (Pichon and Brunn 1985). The ophiolite and amphibolites overthrust a metamorphosed "melange" unit (Moores 1969; Zimmerman 1972), which was visited briefly during this study, and is further described in Chapter 4. This "melange" is here interpreted as representing the greenschist facies of the metamorphic sole. Consequently, a brief description of the geochemistry of the Vourinos greenschist facies metabasic rocks is presented here, for comparison to those of the Loumnitsa Unit.

The sub-ophiolite sequence was described by Pichon and Brunn (1985), as consisting of sequences (up to 240 m thick) of amphibolite interthrust with serpentinite, passing into greenschist metasediments (quartzites, marbles, cherts), meta-tuffs and pillow lavas (up to 1 m diameter), with a downward-decreasing metamorphic gradient. The amphibolites at this locality are of upper amphibolite facies, in contrast to the Loumnitsa Unit amphibolites. They are thrust against the basal serpentinite of the Vourinos peridotites, and the base of the sole was in turn thrust onto Early Mesozoic neritic platform carbonates towards the south. These carbonates were observed by the author (in the Zavordas Monastery area, southern Vourinos, Fig. 3.18) to be highly

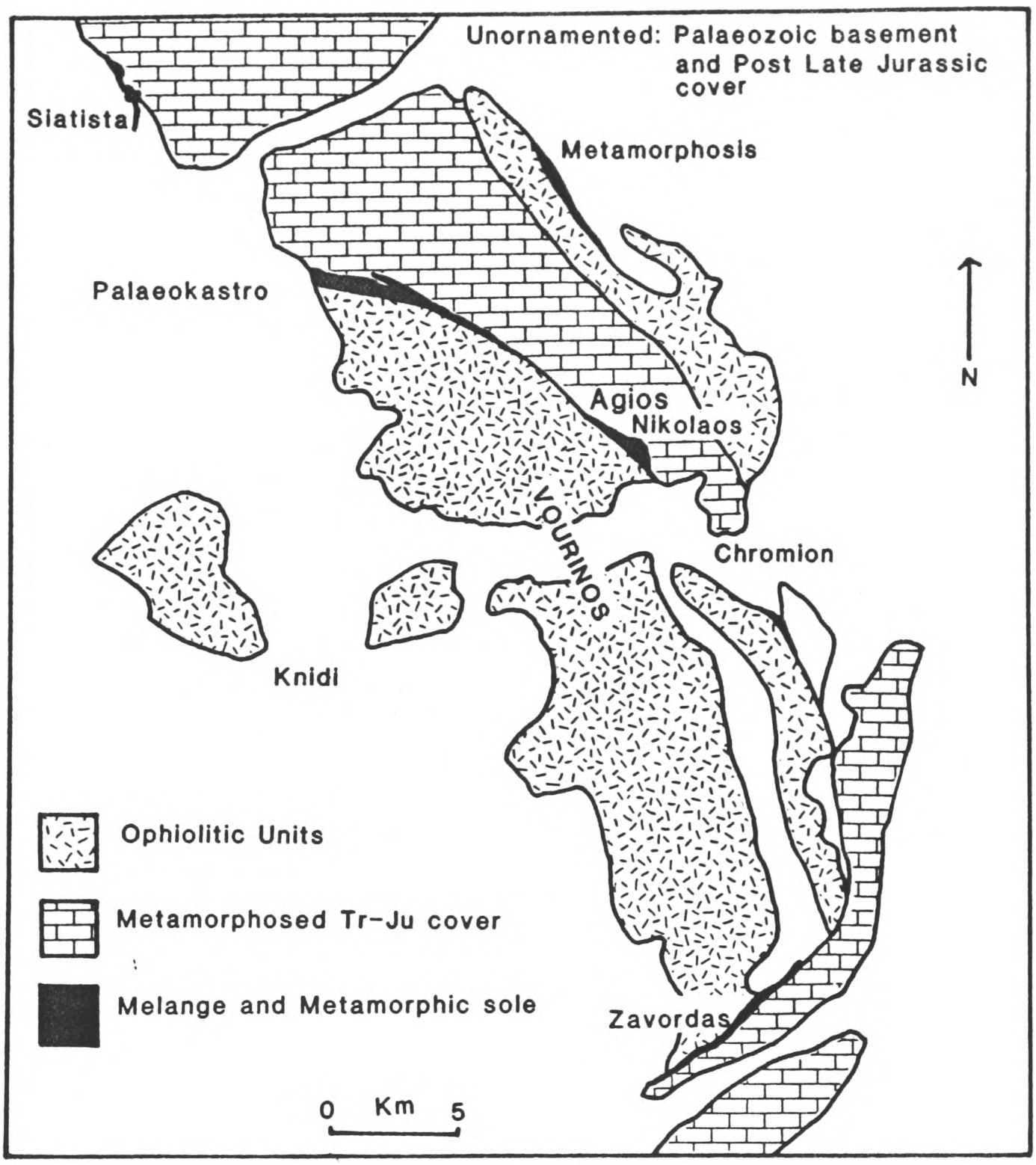

Fig. 3.18 Map of the Vourinos ophiolite showing the main outcrops of greenschist facies melange, and greenschist and amphibolite facies metamorphic sole rocks described in the text.

metamorphosed, near the contact with the peridotite. The main lithology is a banded mylonitic marble, with spectacular high-temperature folds, interpreted as having formed in a dextral shear zone (see Chapter 4; Wright 1986). Also present at Zavordas are coarse-grained and rodingitised gabbroic dykes, meta-conglomerates, and meta-tuffs. Importantly, Brunn (1956) has described glaucophane from the Aliakmon River area.

3.15 Geochemistry of metabasalts from the Vourinos metamorphic sole and melange

Previous workers (Spray and Roddick 1980) presented a analysis of an amphibolite from the Agios Nikolaos valley (5 km N.W. of Chromion), which is of WPB-type. This is the only chemical data for the amphibolite facies of the Vourinos sole. Greenschist facies basic rocks from the Vourinos melange are mainly carbonatised, chlorite-rich, schistose rocks. Metasediments, particularly phyllites and schists are particularly common. Samples of metabasic rocks were collected from several localities within the Vourinos area (e.g. Palaeokastron, Zavordas, Agios Nikolaos Valley; Fig. 3.18). These were analysed by X-ray fluorescence (see Appendix 2), and the results are presented in Appendix 4.

The basic rocks analysed were geochemically of MORB-type (Fig. 3.7-3.9; Fig. 3.19.a,b); no WPB-type signatures were discovered. Phyllitic greenschists from near Zavordas Monastery (26/88 and 27/88; Fig. 3.19.a) are of MORB-type. Samples from the Agios Nikolaos Valley, near Chromion (37 and 39/88), plot near or in the IAT field on several discrimination diagrams (e.g. Ti-Zr), but are more probably of somewhat depleted MORB, and transitional to IAT-type. The geochemistry of the Vourinos melange and sole rocks, therefore contrasts quite sharply with the available data from the Vourinos ophiolite extrusives and intrusives, which are exclusively of IAT and boninitic-type (see Chapter 2).

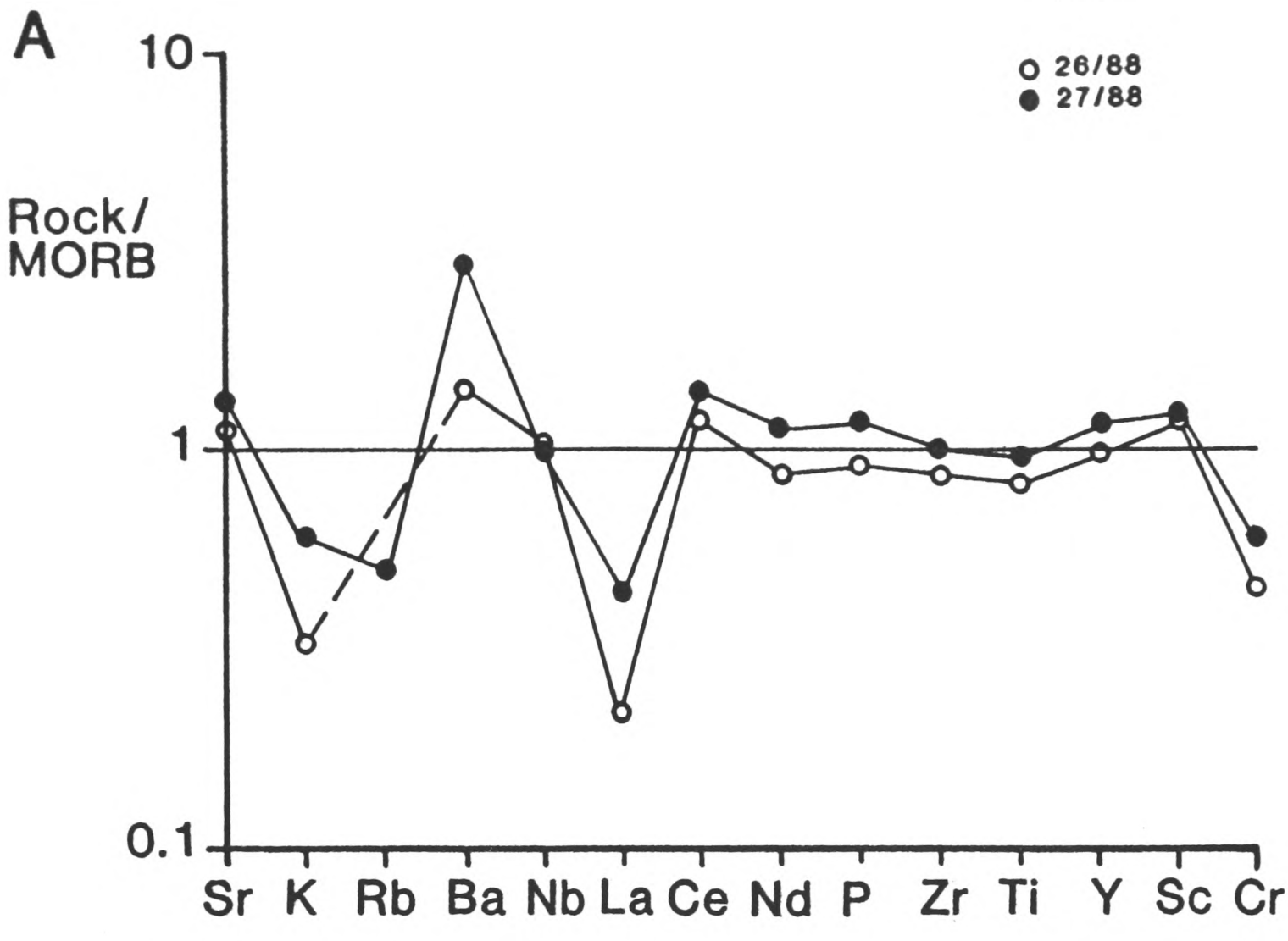

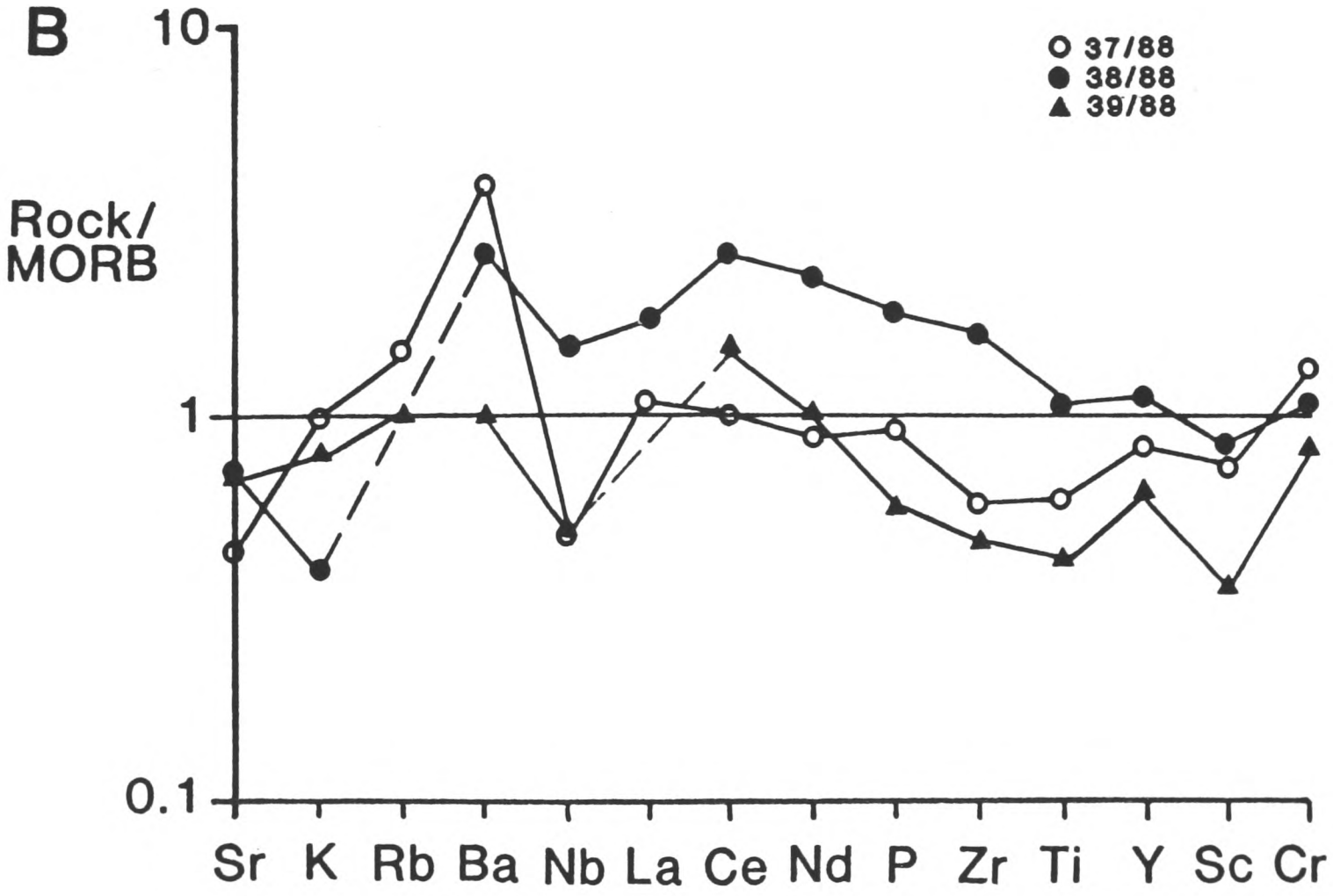

Fig. 3.19 Multi-element diagrams for greenschist facies basalts from the Vourinos melange. a) Phyllitic greenschists, Zavordas Monastery. b) Greenschist basalts, Agios Nikolaos Valley, near Chromion. For normalising values, see Fig. 3.10.

3.16 FORMATION AND EVOLUTION OF THE LOUMNITSA UNIT

Early work on metamorphic soles (see a review in Coleman 1977) suggested that they originated as a result of contact metamorphism by rising ultramafic magmas (e.g. Brunn 1956; Smith 1958). More recently, it has been demonstrated that they represent high temperature shear zones, formed during the tectonic emplacement of ophiolite bodies onto continental margins (Williams and Smyth 1973; Searle 1980). Discussion still revolves around the exact location or locations within the oceanic environment where these rocks might have formed (e.g. ocean ridge, subduction zone), the origin of the protoliths, and the stage during the obduction process when the metamorphism takes place.

One of the most well established facts is that the age of amphibolites within metamorphic soles corresponds very closely with the age of crystallisation of the host peridotites (Searle and Malpas 1980; Tilton et al. 1981). However in Oman, it has been shown that although the amphibolite facies rocks (approx. 90 Ma) are of similar age to the ophiolite, they are older than the subjacent greenschists (approximately 80 Ma; see Searle and Malpas 1980). This, together with the fact that they are polyphase deformed, suggests that the soles were progressively assembled in time and space, under variable P/T paths (Spray 1984). The possible heat sources for the formation of the soles have been discussed at length elsewhere (e.g. Woodcock and Robertson 1977; Searle 1980; Spray 1984), and probably include a combination of residual heat from the ophiolite, frictional heating during thrusting and serpentinisation. Interestingly, Spray (1984) considers that the most important of these is probably residual heating, which led to his conclusion that the site of initial tectonic decoupling must have been in the proximity of a spreading centre (see below).

3.16.1 Models of metamorphic sole formation.

Several models have been proposed for the site of initial displacement of ophiolite complexes within the oceanic environment, and therefore the site of metamorphic sole formation. These models are summarised in Fig. 3.20. The first model invokes thrusting along the

A Decoupling along elastic/plastic limit in a subduction zone

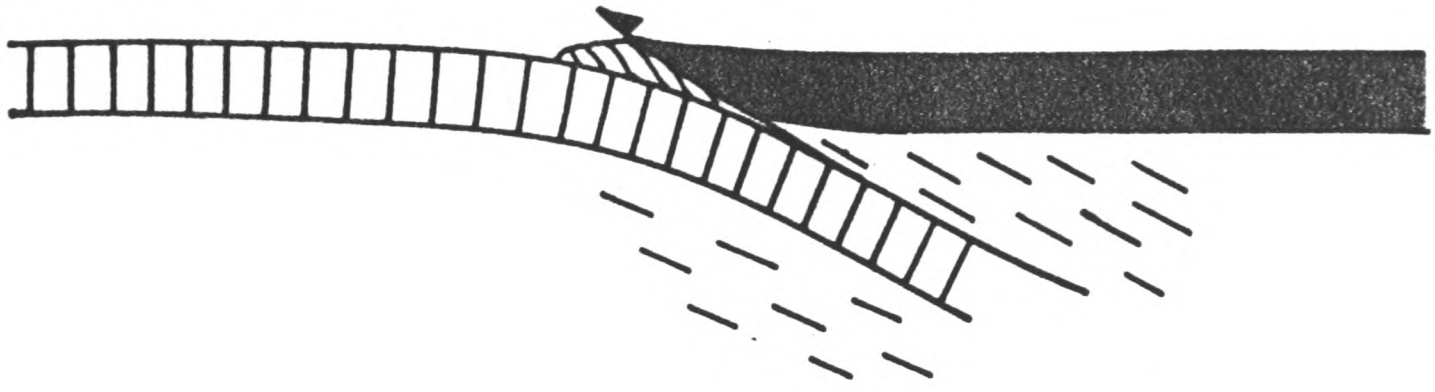

B Decoupling along lithosphere/asthenosphere boundary at a ridge

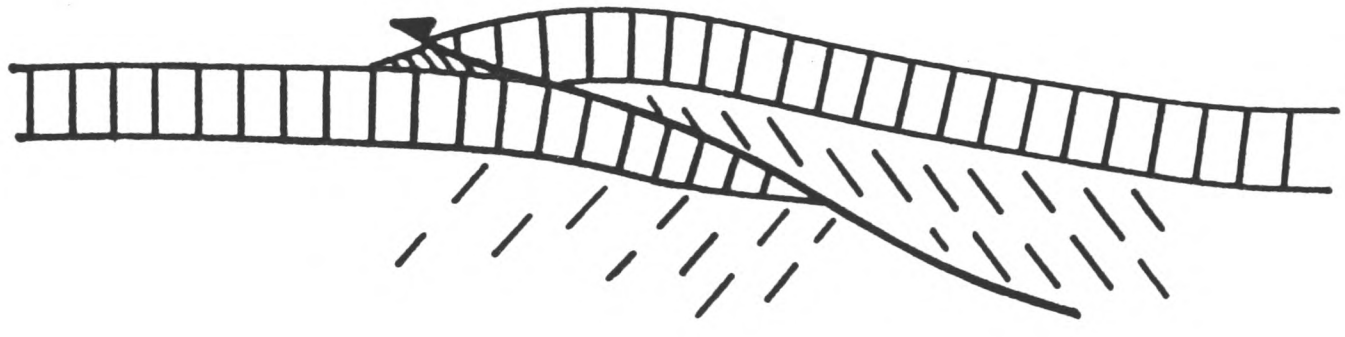

C Decoupling along the boundary between old and new oceanic lithosphere

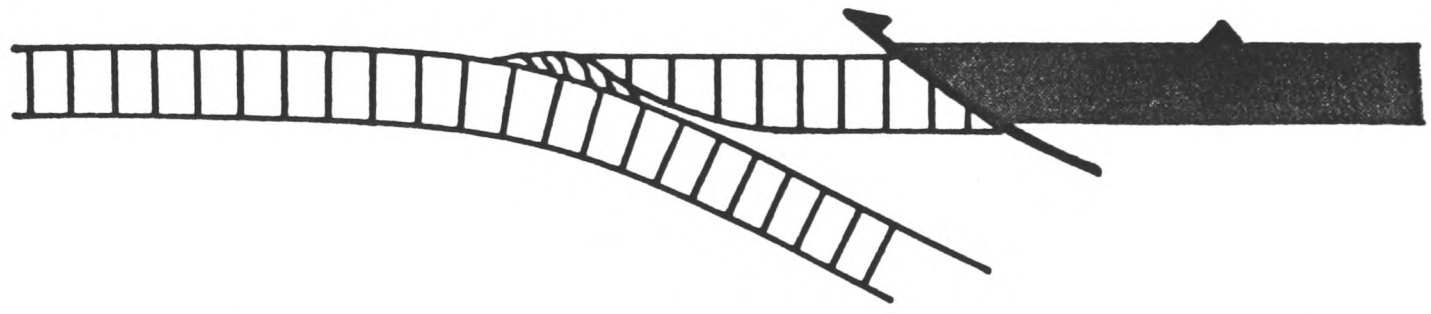

Fig 3.20 Possible oceanic environments for the site of ophiolite displacement and metamorphic sole formation. A) After Nicolas and Le Pichon (1980). B) after Nicolas and Le Pichon (1980); Boudier et al. (1982); Spray (1984); C) After Lippard et al. (1986).

elastic-plastic boundary within a fully developed subduction zone (Nicolas and Le Pichon 1980). This origin was suggested previously for the Loumnitsa Unit by Whitechurch and Parrot (1978). The second model suggests that overthrusting took place at a spreading ridge, along the lithosphere-asthenosphere boundary (Nicolas and Le Pichon, op. cit.). The spreading centre may have been of MORB-type, or supra-subduction zone-type within a marginal basin. This has become a widely accepted model for the formation of metamorphic soles and the sole of the Semail ophiolite in particular (Boudier and Coleman 1981; Ghent and Stout 1981; Boudier et al. 1982). Spray (1984), considered that ophiolite displacement and sole formation took place along the lithosphere-astheonosphere boundary, a mechanically weak boundary. This was envisaged as occurring in the vicinity of an ocean ridge, where sufficient heat was present. He also pointed out that ophiolites are mostly less than 15 km thick, and there must therefore be a fundamental discontinuity at this depth. Also, the presence of granulite facies rocks at the top of some soles suggests that temperatures up to 1000^{o} were needed, which approximated to the temperature along the lithosphere-asthenosphere boundary. Malpas (1979) suggested that a high heat flow was also necessary, and proposed that this may be present at a ridge, above an oceanic "hot-spots" and in marginal basins.

A third model was proposed by Lippard et al. 1986 for the formation of the sole of the Semail ophiolite, in which they considered that the supra-subduction zone crust and mantle was displaced along the boundary between the hot newly formed crust and the marginal fore-arc crust. One problem is that the fore-arc crust as envisaged in this model, is not found preserved in Oman, and its nature is therefore unknown. It is however, considered unlikely by this author that the fore-arc was not also influenced by supra-subduction zone spreading processes, from a comparison with the volcanism of present-day fore-arc regions. Therefore, amphibolite facies rocks from Oman should show evidence of a supra-subduction geochemical signature, which is not the case from those samples analysed (Searle and Malpas 1982). This model still remains as a possible site for the initiation of ophiolite displacement, as thrusting may theoretically have taken place in any part of the above-subduction zone crust (Fig. 3.20).

Fourthly, metamorphic soles may possibly have formed during the initiation of subduction within an ocean basin (Casey and Dewey 1984), either at a ridge, or along a ridge-transform intersection. The sole would be plastered onto the base of the overriding plate, and preserved until emplacement occurred. This model would seem to require that subduction related volcanic rocks would intrude the sole during subsequent spreading. Indeed, this has been shown to be true of ophiolites of the Taurides (see below).

3.16.2 Relationship of metamorphic soles to ophiolite volcanism

In general, metamorphic soles are formed shortly after ophiolite volcanism has ended. This is the case for the Pindos and Vourinos ophiolites, and numerous other ophiolite complexes of the Tethys region and elsewhere. However, in some ophiolites, intrusive rocks have been documented cross-cutting the sole. This is well documented in the Semail ophiolite, where diabase dykes are seen to cross-cut the amphibolites and basal peridotites of the ophiolite, but are truncated at greenschist level (Pallister and Knight 1988). These dykes have been shown to be geochemically related to the uppermost volcanic unit of the ophiolite, the Salahi Group (Alabaster et al. 1982), which are within plate alkaline lavas, in contrast to the immediately underlying Clinopyroxene-phyric lavas of the ophiolitic sequence (see Chapter 2). Other igneous rocks cross-cut the metamorphic sole in Oman. These are acidic intrusives, mainly biotite granites (Lippard et al. 1986). Both these granites and the dolerite dykes are therefore products of obduction-related magmatism, and are related to continental margin crust remelting during ophiolite emplacement. The field relationships present also further prove the late-stage accretion of the greenschist facies rocks of the metamorphic sole.

Other Tethyan ophiolites also contain soles with late intrusive phenomena. The Late Cretaceous Pozanti-Karsanti ophiolite of Turkey (Cakir et al. 1978) is reported as containing hundreds of low-K tholeiitic dykes, which intrude both the tectonites and the sole. A similar feature has been reported from the Lycian nappes of southern Turkey (Cakir et al. 1978), and seems to be a common occurrence within the Tauric ophiolites. This contrasts sharply with the chemistry and lithologies described from

Oman, and indicates the complexity of the volcanism associated with oceanic thrusting.

3.16.3 Application of theoretical models to the Loumnitsa Unit

It can be seen from the model presented for the formation of the Loumnitsa Unit (Fig. 3.21), that a multi-stage evolution is necessary to explain the field relations present (Malpas 1979; Searle and Malpas 1980). In reality, the situation was probably highly complex, and much more petrological, structural and geochemical data, particularly from Vourinos, are needed before the problem can be fully resolved. However, sufficient information is available for construction of a possible tectonic model (Fig. 3.21).

The model proposes that two stages of metamorphic sole formation took place within the Jurassic Pindos ocean, after the last documented volcanic event within the ophiolite. An amphibolite facies metamorphic sole was first accreted during initial deep-seated displacement of crust and mantle, probably along the boundary between the newly formed back-arc crust (represented by the Vourinos ophiolite and Dramala Complex), and the fore-arc region (Aspropotamos Complex; Fig. 3.21.b; see Chapter 2). This would account for the presence of amphibolites with depleted trace-element geochemistries found at the base of the Dramala Complex, by accretion of supra-subduction related volcanics of the fore-arc to peridotite, and possibly also cumulate ophiolitic rocks. This site is preferred to that of a spreading ridge, as proposed by Spray (1984; back-arc ridge in the case of Pindos and Vourinos), as this would imply that the sole of the Dramala Complex would have been of high temperature and pressure, in fact higher grade than that of the Vourinos sole, in all probability (Fig. 3.21). Furthermore, a large amount of material with more depleted chemistries would have been accreted to the upper part of the amphibolite facies sole, compared to the limited volume apparently present today.

The second stage of major displacement (Fig. 3.21.b) took place along the roof thrust of the subduction zone during sequential thrusting, leading to metamorphism of material from the accretionary prism

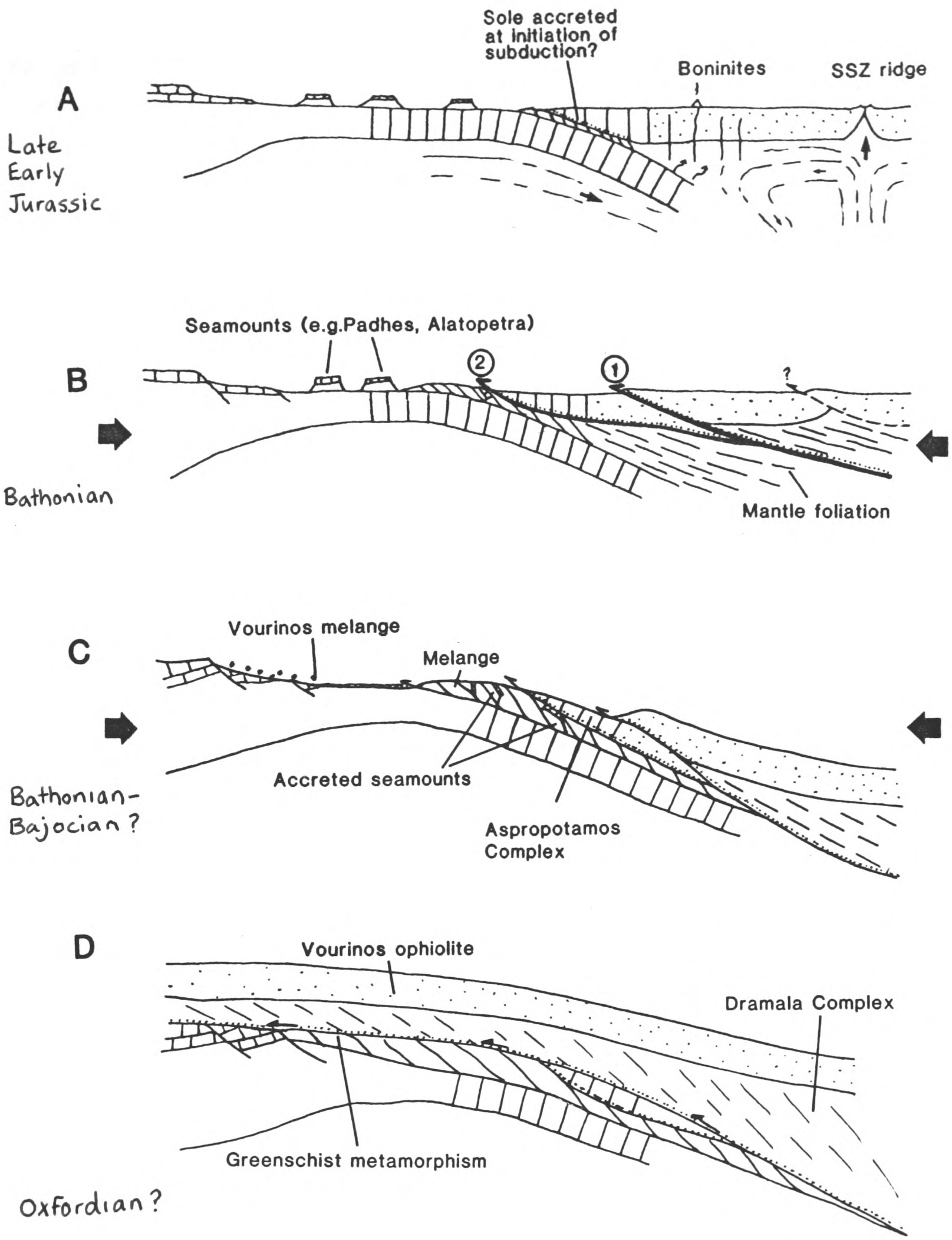

Fig. 3.21 Proposed two-dimensional model of formation of the Loumnitsa Unit, within the Pindos ocean basin. a) Formation of supra-subduction zone crust and mantle. Possible initial phase of sole formation, at the initiation of subduction, not considered likely for the Pindos-vourinos ophiolites. b) thrusting at the boundary of older fore-arc and supra-subduction zone crust and mantle (1), displacing the Vourinos ophiolite and the Dramala Complex towards the northeast. Displacement at the ridge is also possible, but considered less likely (see text). A second thrust develops along the subduction zone (2), forming a further sole on the Aspropotamos Complex. c) Underplating of the Aspropotamos Complex occurs during overthrusting onto the continental margin, greenschists accreted, thrusting transfers to lower levels. d) The Aspropotamos Complex is overthrust by the remainder of the ophiolite, which causes greenschist facies metamorphism of the platform carbonates, from the excess residual heat from the ridge. Along-strike variations are not shown, but may be significant.

(Chapter 4) by still hot fore-arc crust. This explains the comparatively low temperatures and pressures found within the sole of all the Pindos rocks, and perhaps the higher temperatures and pressures described from the Vourinos sole, due to the former presence of a ridge. The Aspropotamos Complex preserves very little mantle material (mainly serpentinite), and is envisaged to have been detached along the crust-mantle boundary during progressive thrusting (Fig 3.21.c). Finally, the whole thrust stack was emplaced onto the continental margin, metamorphosing both the platform carbonates and the Vourinos melange. The Aspropotamos Complex, with its preserved metamorphic sole, was overridden by the main peridotite mass (Fig. 3.21.d). This model implies that the obduction process took place in a manner similar to that of a "piggy-back" thrust sequence, seen in continental thrust belts, the most distal thrust being the oldest. The main lines of evidence for this model are:

1) Vourinos is interpreted as representing crust and mantle located at or near a supra-subduction zone ridge within this system at the time of obduction, whereas the Pindos ophiolitic units are i) mantle and crust situated away from the ridge (Dramala Complex); and ii) "fore-arc" crust immediately above a subduction zone (Aspropotamos Complex) respectively.

2) The Vourinos sole is apparently of higher temperature (upper amphibolite), and possibly pressure (e.g. presence of glaucophane locally) than the Pindos sole. Further investigation of the Vourinos sole is needed, to establish if the sole could have formed by overthrusting at the ridge, as proposed by Spray (1984), and Nicolas and Le Pichon (1980; Fig. 3.21.b).

3) The sole at the base of the Aspropotamos Complex is apparently geochemically only of MORB- and within plate-type. The Dramala Complex sole does contain locally more chemically depleted amphibolites (e.g. at Padhes and Liagkouna; see above), and some of the Vourinos greenschist basalts are also transitional to IAT. This crust may therefore have had the opportunity to accrete more chemically depleted fore-arc crustal material, by overthrusting during emplacement.

4) The sole is present on cumulate, and possibly intrusive crustal rocks of both the Aspropotamos and Dramala Complexes (see below).

It should be noted that the model of Casey and Dewey (1984) may have applied to the Loumnitsa Unit, as an alternative to the second phase of thrusting in the model outlined above (Fig. 3.21.b). In this model, the sole may have accreted to the Aspropotamos Complex during initial subduction (Fig. 3.21.a), not during the second stage of sole formation as outlined above. Subsequent underthrusting then took place at deeper structural levels, to form the accretionary complex. Indeed, there may be some evidence for this, as at some localities (e.g. Kalivia Kerasias, Fig. 3.1), metamorphic sole rocks are of extremely similar lithology to subjacent poorly metamorphosed melange sediments. One major problem of this model is that the Loumnitsa Unit would almost certainly have been cross-cut by later volcanism. This model may, however, apply to ophiolites such as Pozanti-Karsanti as described above (Cakir et al. 1978), where early formed metamorphic soles are cross cut by the later products of supra-subduction zone volcanism. The observation regarding the similarity between greenschist facies, rocks and immediately underlying melange rocks can be explained by thrusting taking place at progressively lower levels during emplacement. The ophiolite firstly metamorphoses a distal part of the sedimentary sequence during greenschist facies metamorphism, and then the active thrust decollement transfers to a lower level, transporting more proximal, now unmetamorphosed, parts of the same sediment sequence towards the continental margin.

As mentioned above, many of the metabasites of the Loumnitsa Unit sampled are not of depleted trace element chemistries, in contrast to the overlying volcanics. A similar pattern has emerged from other ophiolites (e.g. Semail ophiolite basal amphibolites showed no similarities to the overlying volcanic sequence; Searle and Malpas 1982), suggesting an allochthonous origin for the ophiolite. Data from the Loumnitsa Unit and the Semail ophiolite does, however indicate that the higher-grade sole rocks are mostly tholeiitic and of MORB-type or more depleted chemistry, suggesting that the initial accretion of amphibolite-facies rocks took place far out in the ocean, away from the continental margin. Interestingly, amphibolites sampled from the sole of the Evvia ophiolite of eastern central Greece (Simantov et al. 1988) appear to be mainly of IAT affinities.

The presence of abundant metasediments and shallow-water carbonate blocks may indicate that the lower-grade rocks were accreted near, or at the continental margin (Fig. 3.22.a). This story is confirmed by the sole sequence found at Padhes, where the progressive accretion of firstly amphibolites, oceanic basalts and pelagic sediments, followed by marginal and shallow-water carbonates is strikingly displayed. The greenschist-facies rocks of the Loumnitsa Unit are mostly WPB-type, indicating they were probably accreted closer to the continental margin.

The marbles found in the Pindos sole are in many ways comparable to the so called Oman "exotic" limestones of Permian and Triassic age (Glennie et al. 1974; Graham 1980a; 1980b), which are similarly found within the greenschist facies metamorphic sole and melange units (Haybi Complex; Searle and Malpas 1980). These rocks form large (up to 300m by 600 Km^2) olistoliths within the Haybi Complex (e.g. in Wadi Hawasina). The "exotics" are mainly of shallow-water origin, the Permian blocks forming in an uncertain palaeo-tectonic position, probably on off-margin highs or intra-continental shelves. The Triassic blocks probably formed as more extensive carbonate platforms, away from the continental margin. The Pindos carbonate blocks are of similar facies, and occur in a similar structural position to the Oman blocks, and both must have been accreted at a late stage as the ophiolite impinged onto the continental margin (Fig. 3.22.a), as similarly envisaged in the model of Searle and Malpas (1980; Fig. 3.22.b).

The Loumnitsa Unit further extends our knowledge of the nature of metamorphic sole rocks, because in the Pindos Mountains they are found attached not only mantle peridotites, but also to crustal cumulates and possibly even intrusive rocks, a feature previously unrecognised in other ophiolites. Several tectonic situations might account for this feature (Fig. 3.23): (1) the sole may have formed directly along the bounding thrust of a subduction zone, where the oceanic lithosphere thins towards the leading edge (Casey and Dewey 1984); (2) the sole might have formed by the basal detachment thrust cutting up-section during emplacement, at any position within the oceanic lithosphere; (3) the sole may be accreted onto crustal rocks along oceanic transform faults, particularly if they have undergone compression.

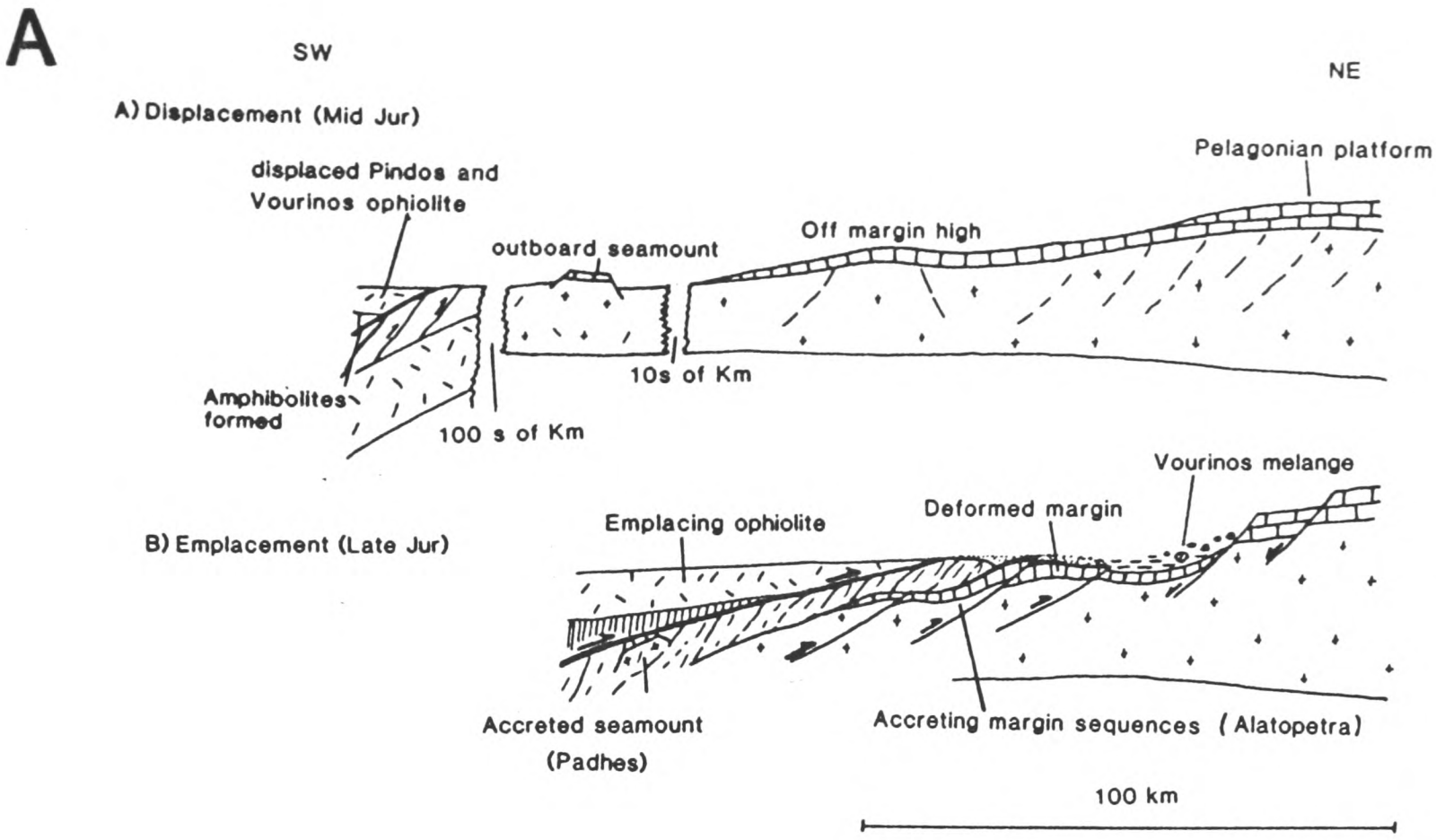

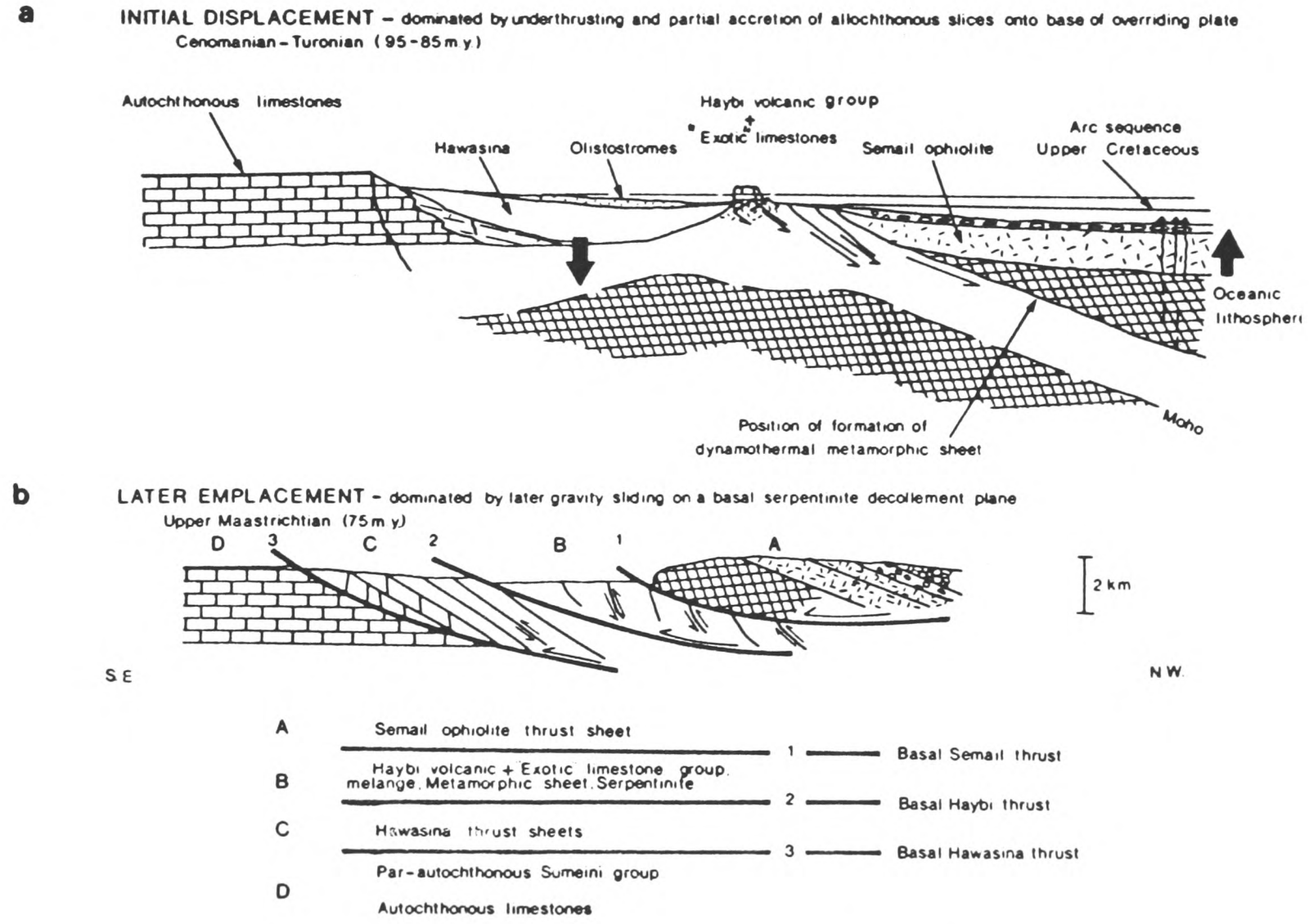

Fig. 3.22 a) Model for the accretion of greenschist facies marbles into the Loumnitsa Unit, during emplacement onto the Pelagonian margin. b) Model for the emplacement of the Semail ophiolite, Oman, showing continental margin carbonates about to be accreted into the metamorphic sole. After Searle and Malpas 1980.

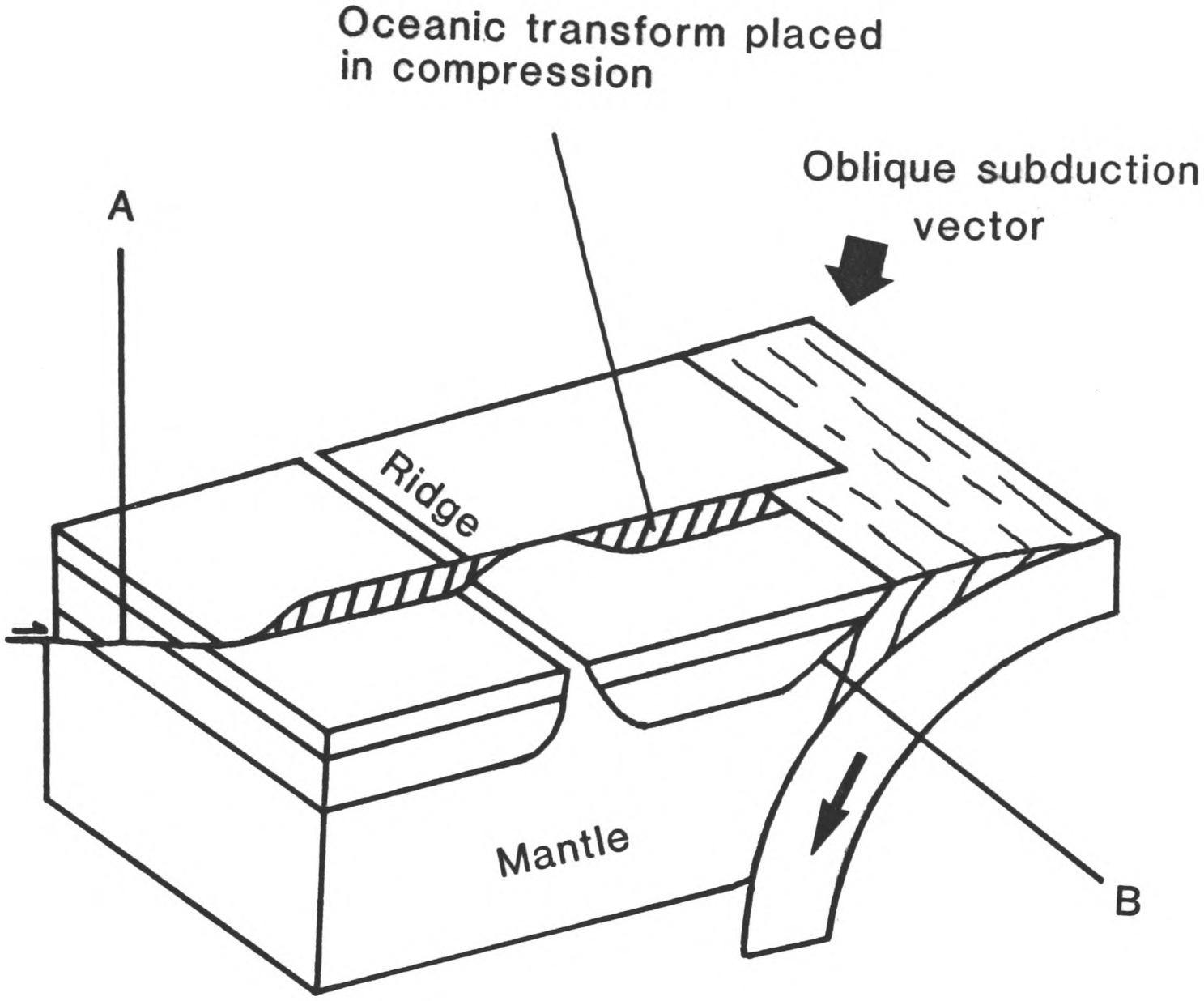

Fig. 3.23 Block diagram to show two possible oceanic environments for the formation of metamorphic soles on ophiolite cumulate rocks. A) Oceanic transform placed in compression, causing local overthrusting of the crustal succession. B) Thrusting occurs along a basal detachment (basal thrust of a subduction zone?), cutting up-section through the crustal sequence during initial intra-oceanic displacement.

Evidence for all three of these situations is present within the Pindos area. Consideration of the reconstructed thicknesses and geochemistry of the crustal rocks of the ophiolite, seems to suggest an origin as thinned "fore-arc" crust, formed adjacent to a subduction zone (Kostopoulos 1989; Jones and Robertson 1990). As has already been described, these thin crustal sequences have sole rocks in basal thrust contact, perhaps suggesting that they formed along the "roof thrust" of a subduction zone as in (1) above. In many cases, however, an origin by out-of-sequence thrusting, as in (2) above, cannot be discounted. The presence in some areas of calcite-cemented harzburgite-jasper breccias immediately beneath the peridotite (see Chapter 4) is interpreted as possibly representing displacement along transforms, as suggested in (3).

Plate 3.1 Field photographs of the amphibolite facies rocks from the Loumnitsa Unit. a) Steeply dipping S1 foliation, immediately beneath the basal peridotite mylonite of the Dramala Complex, Loumnitsa Valley (crook is approximately 1 m long). b) Multiphase folded banded plagioclase amphibolite. Note late-stage brittle faulting affecting the banding. Loose block in the Aspropotamos River, foot of the Loumnitsa Valley. c) Partly rodingitised amphibolite with quartz veining, Kodro Mountain. d) Folded quartz veins in lower amphibolite facies metabasalt, Venetikos River Valley, 1 km north of the confluence with the Aspropotamos River.

Plate 3.2 Thin section photomicrographs of amphibolites. a) Poorly banded epidote amphibolite, with albitised plagioclase feldspars (P), green pleochroic hornblende crystals (H), and abundant high relief epidote (E). (123/88, Loumnitsa Valley; x40 PPL). b) Large green hornblende (H) with included epidote crystals, surrounded by smaller hornblende crystals and plagioclase (3/23/8, N.W. of Avdella; field of view 6 mm, PPL). c) Rodingitised amphibolite, showing albitised feldspars, amphiboles and large patches of clinozoisite (Z) in the matrix (5/27/8, Kodro Mountain; field of view 6mm, XPL). d) Fold in fine grained epidote amphibolite (15/88, Liagkouna Mountain; x10 PPL).

Plate 3.3 a) Garnet-mica-schist, with large euhedral garnet porphyroblast (G), enveloped by the foliation. The garnets have inclusions of zoisite and albite (A). The matrix contains low birefringence biotite (B), abundant epidote and zoisite/clinozoisite (Z) crystals, plus quartz, albite and white mica (131/88, Selloma Lakkou; x32, PPL). b) Coarsening inwards prehnite vein (P) cross cutting amphiboles, with further patches of prehnite in the matrix (20/88, Liagkouna Mountain; x46, XPL). c) Calc-schist, with banded calcite, white mica, biotite and pyrite (14/24/8, Agios Nikolaos Monahiti; field of view 6 mm, PPL). d) Plagioclase-quartz vein (P) in amphibolite, with later formed fibrous amphibole needles. Albite, sphene and hornblende are found on the margin (123/88, Loumnitsa Valley; x64, XPL).

Plate 3.4 Greenschist facies metasediments; a) Garnet-mica-schist, with euhedral garnets showing quartz trails, and clear rims. Note also the small euhedral garnets, of similar composition to the overgrowths (see text). Quartz-muscovite-albite matrix (1/21/8 Kodro Mountain; field of view 6 mm, PPL). As above, showing matrix foliation (scale as above; XPL). c and d) Garnet-mica-schist, with small garnet porphyroblasts in a quartz and mica-rich, strongly compositionally banded matrix (c=PPL; d=XPL; both views x9).

PLATE 3.5 a) Marble (M) enclosed in basal serpentinite of the Dramala Complex harzburgites (H), Kakoplevrion Village (Fig. 3.1). Equivalent unmetamorphosed limestones (L) and cherts, are also seen at this locality. b) Marble (M) within upper greenschist/lower amphibolite facies sole at Padhes Village (Fig. 3.1) c) Banded marbles (M), red phyllites (P) and greenschist metabasites (G), S.E. Kalivia Kerasias. This section is found at the base of ophiolite cumulate rocks. Note hammer for scale.

PLATE 3.6 A variety of intrafolial folds within the Loumnitsa Unit amphibolites. a) Loumnitsa Valley. b) and c) amphibolites, Liagkouna Mountain. d) Folded schistosity in greenschists, Liagkouna Mountain.

3.1

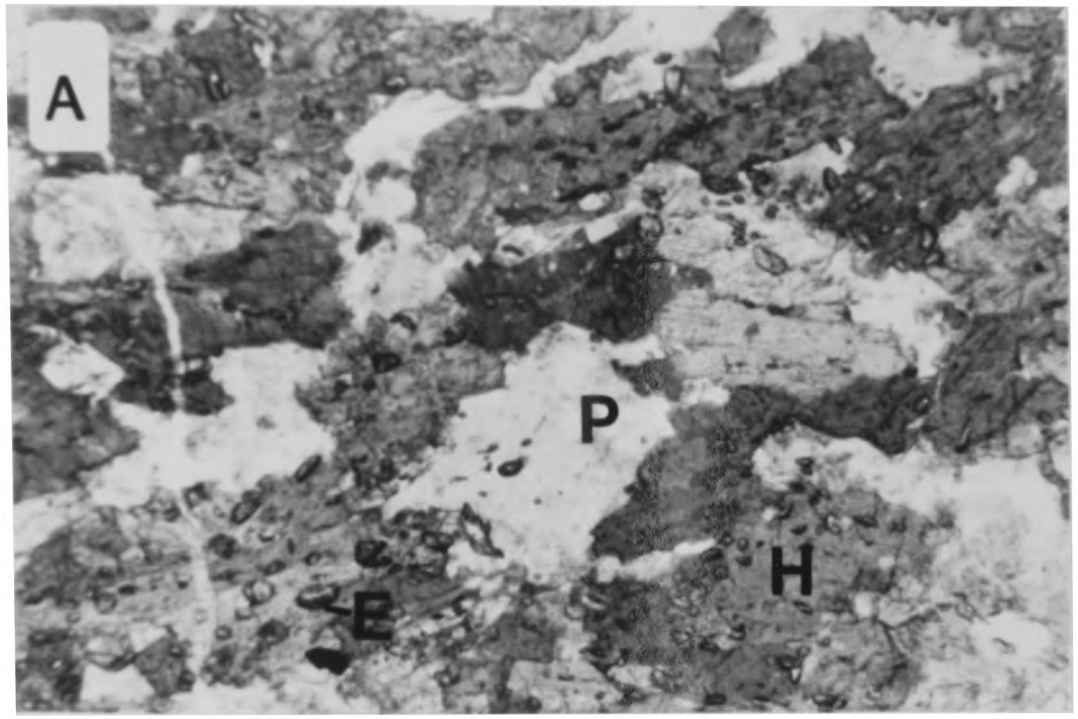

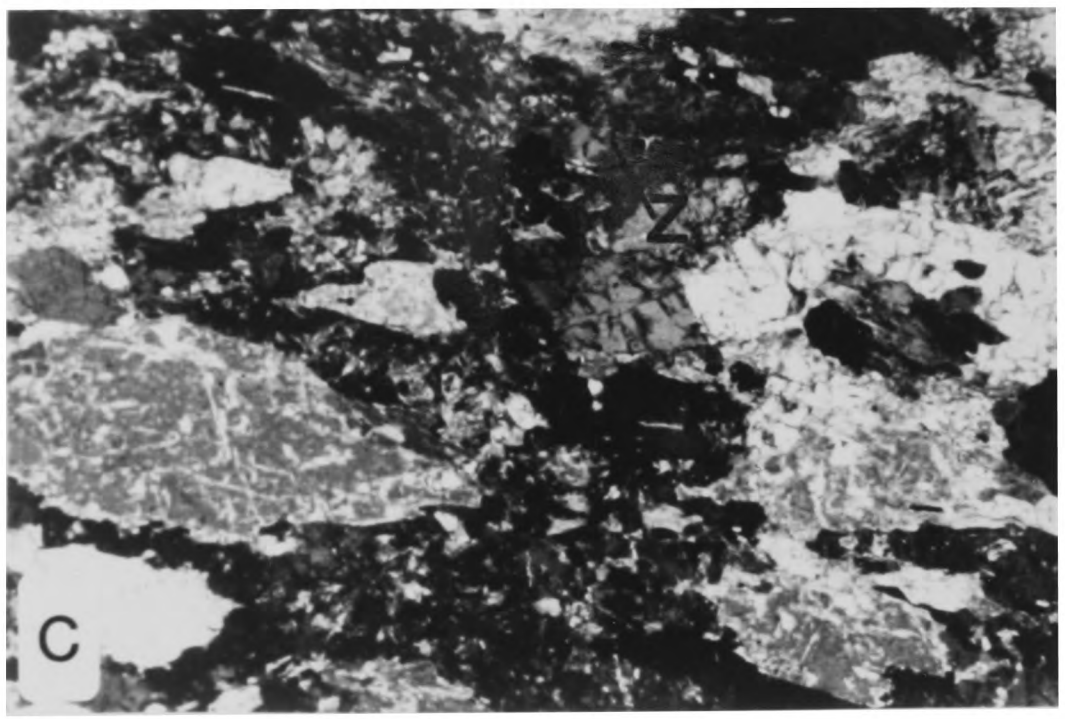

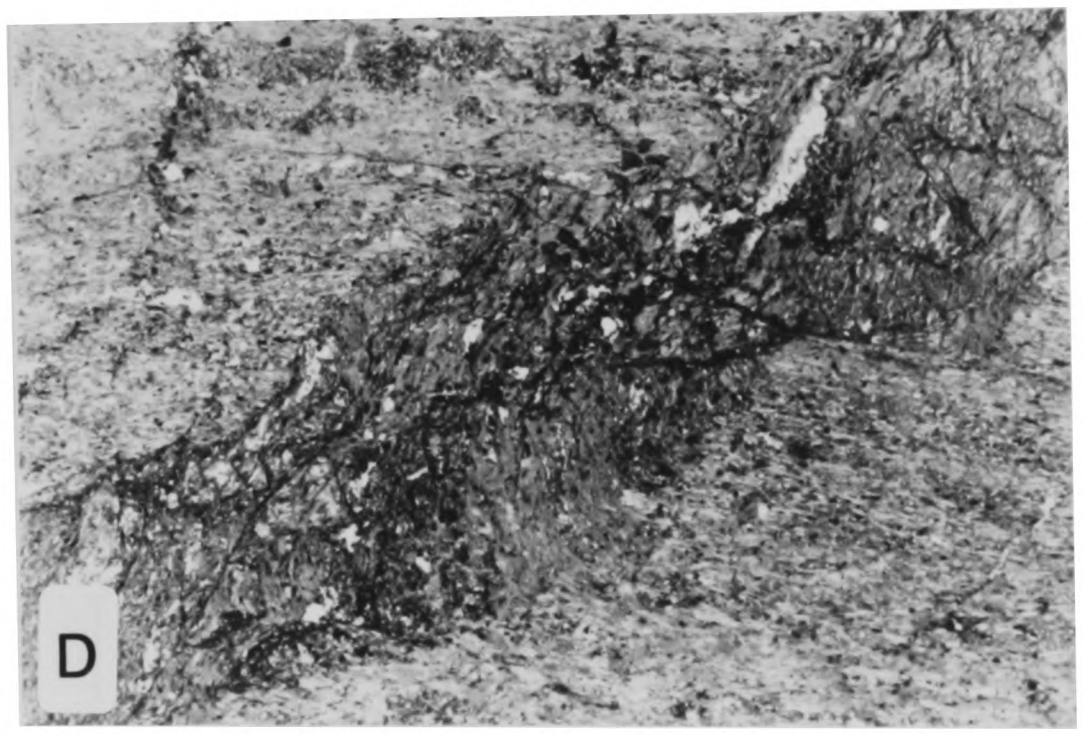

3.2

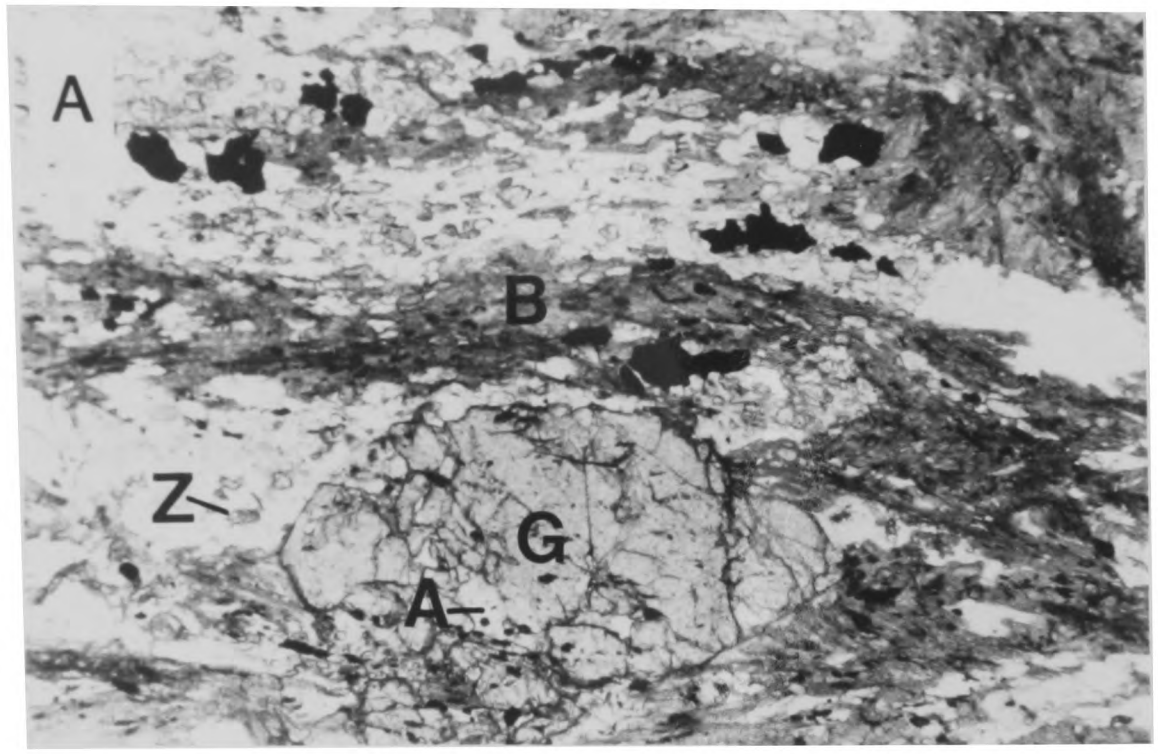

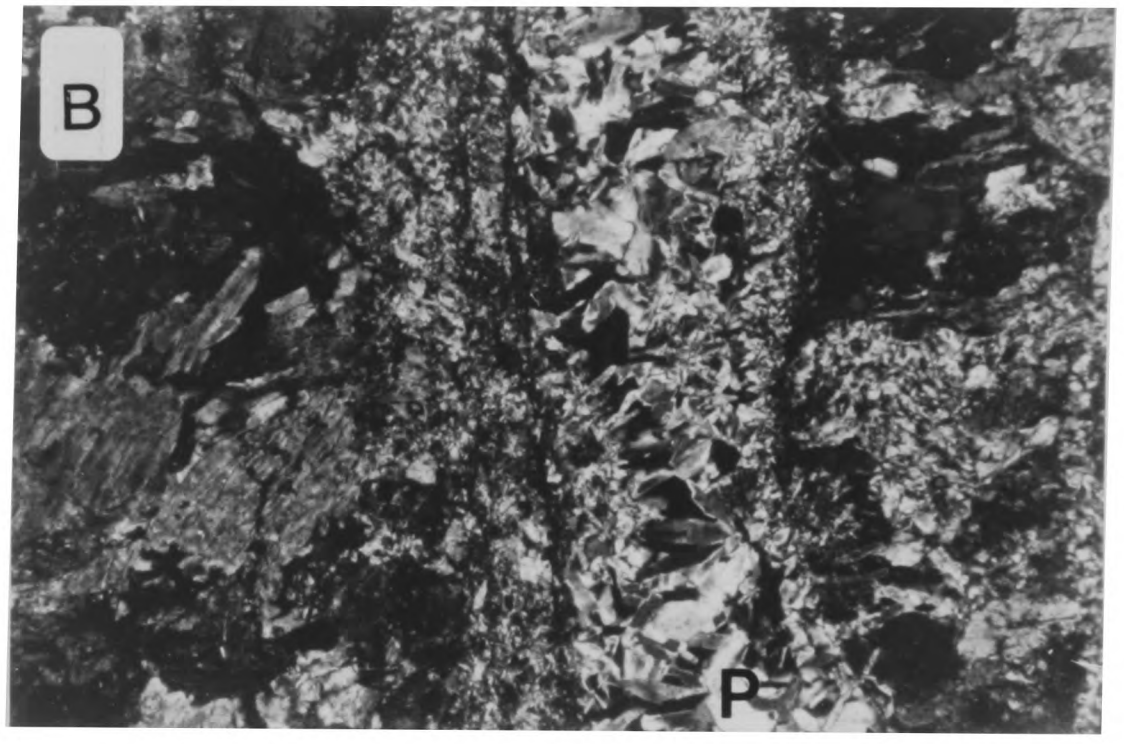

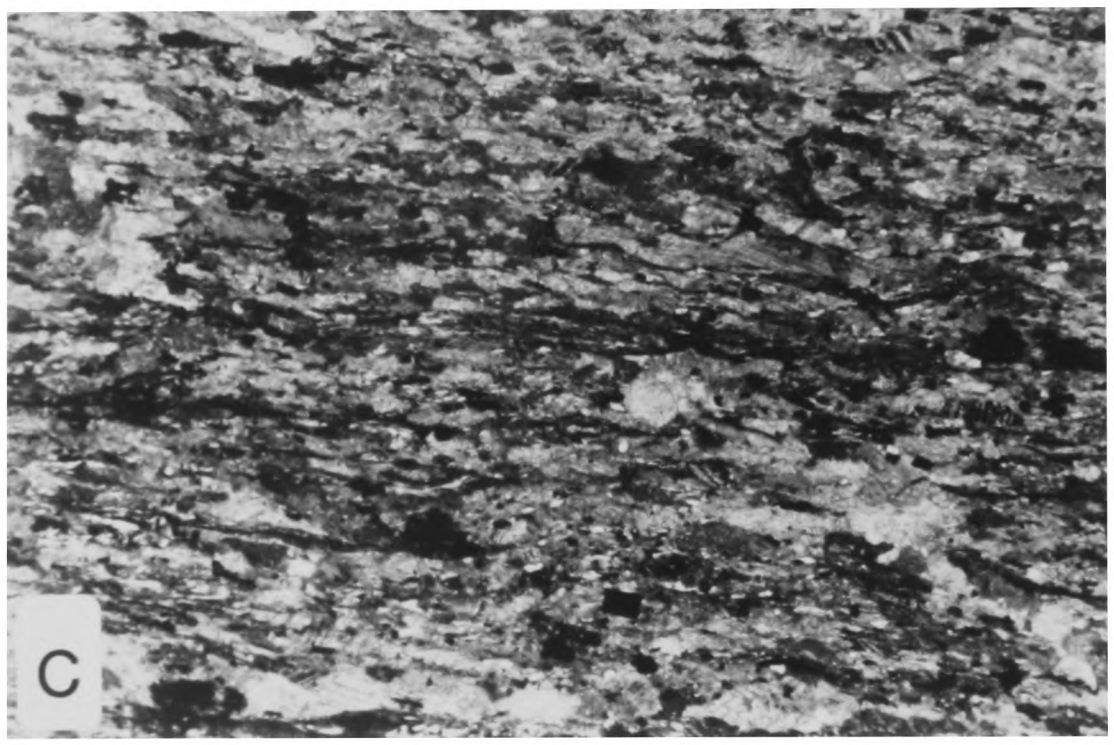

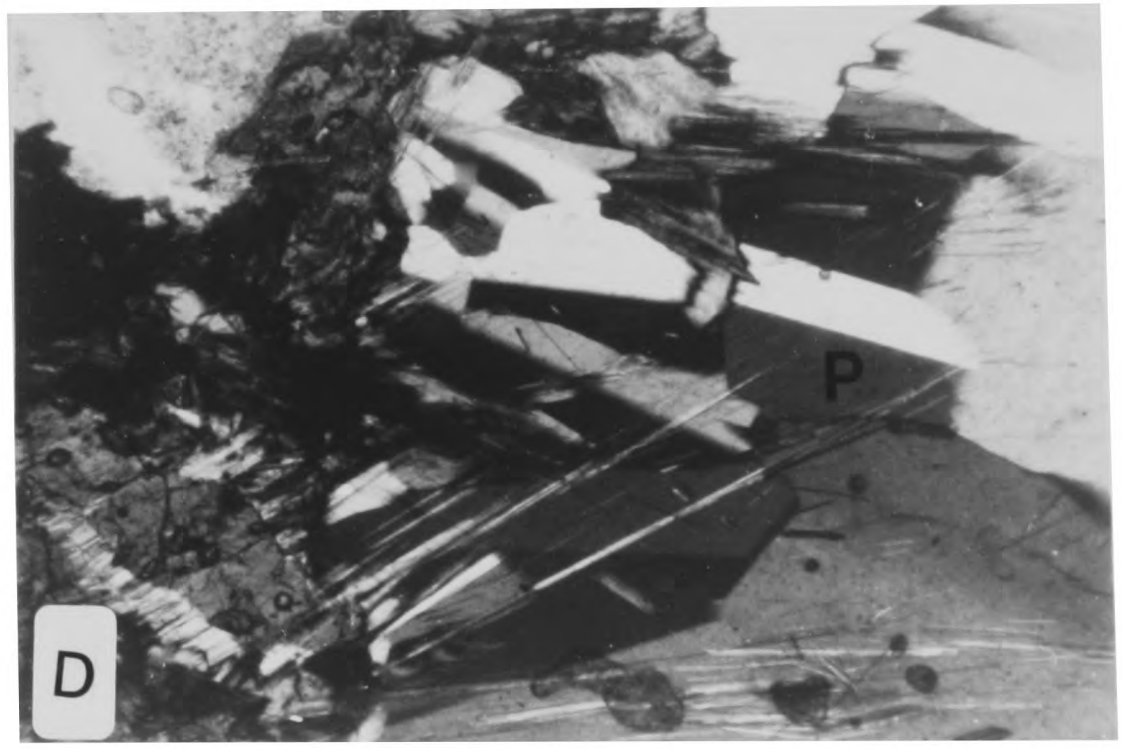

3.3

3.4

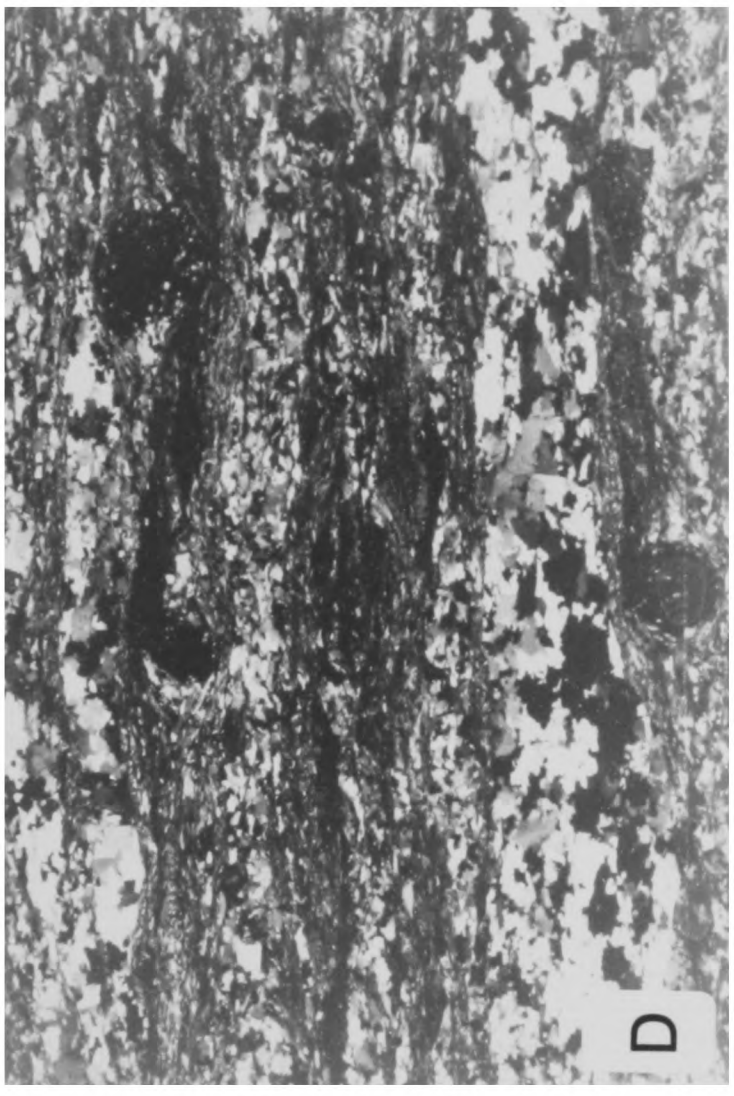

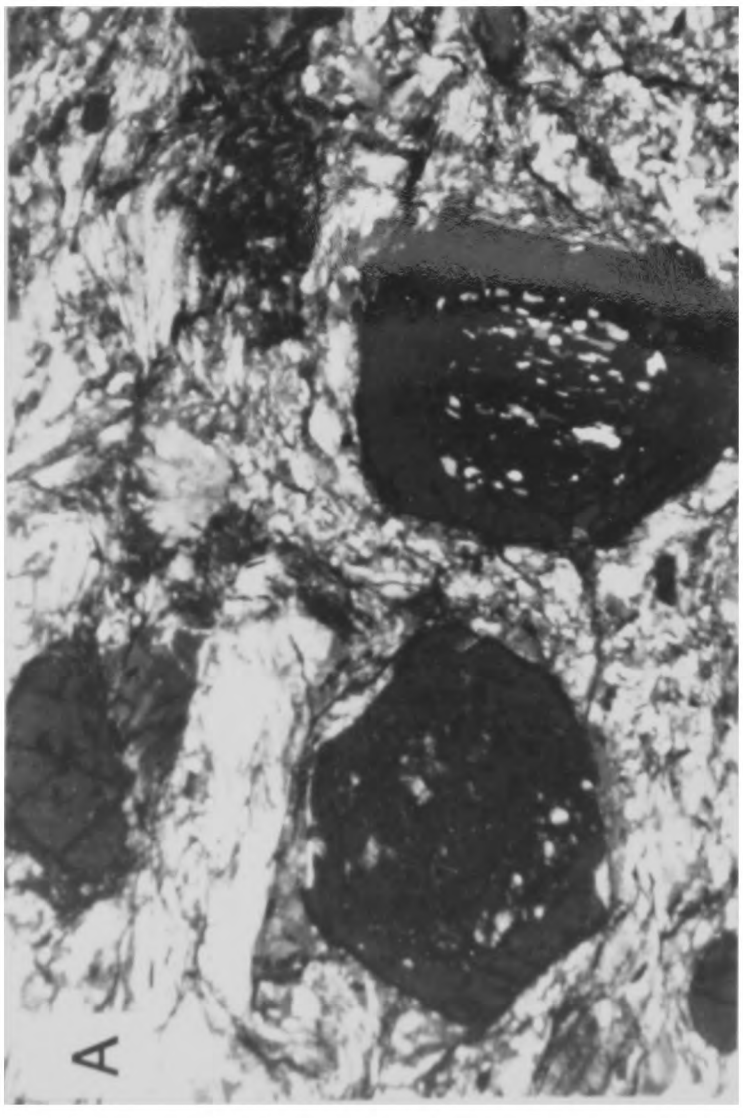

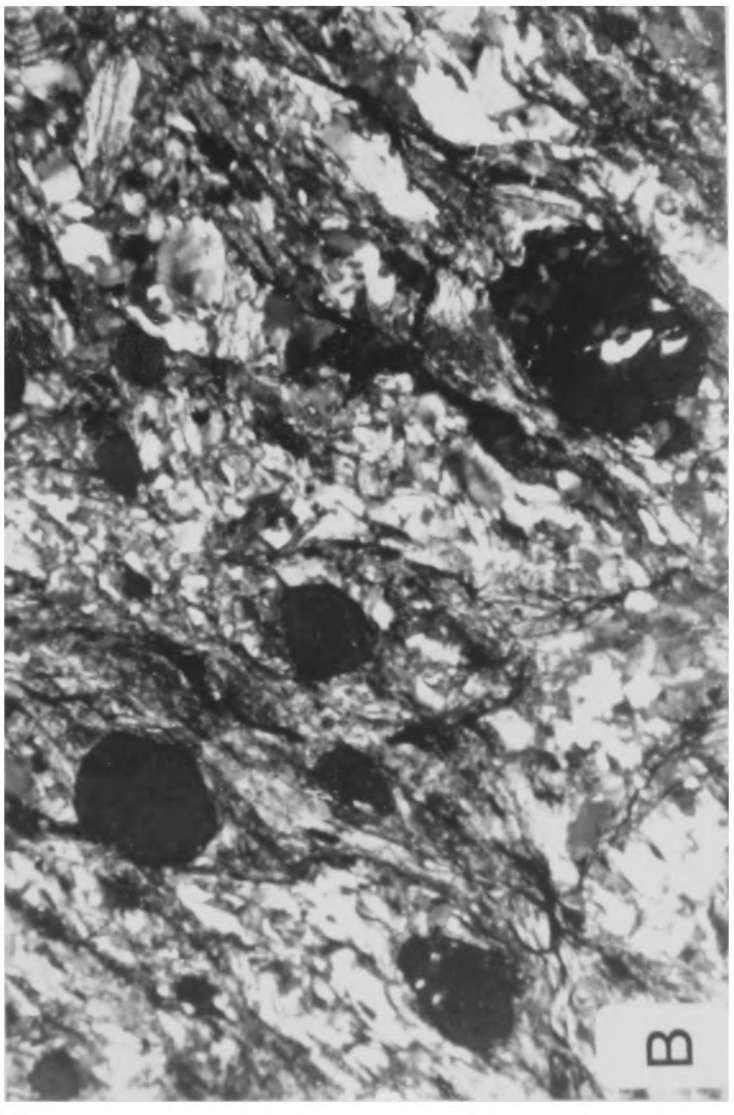


3.5
A
H
M
L


B
M

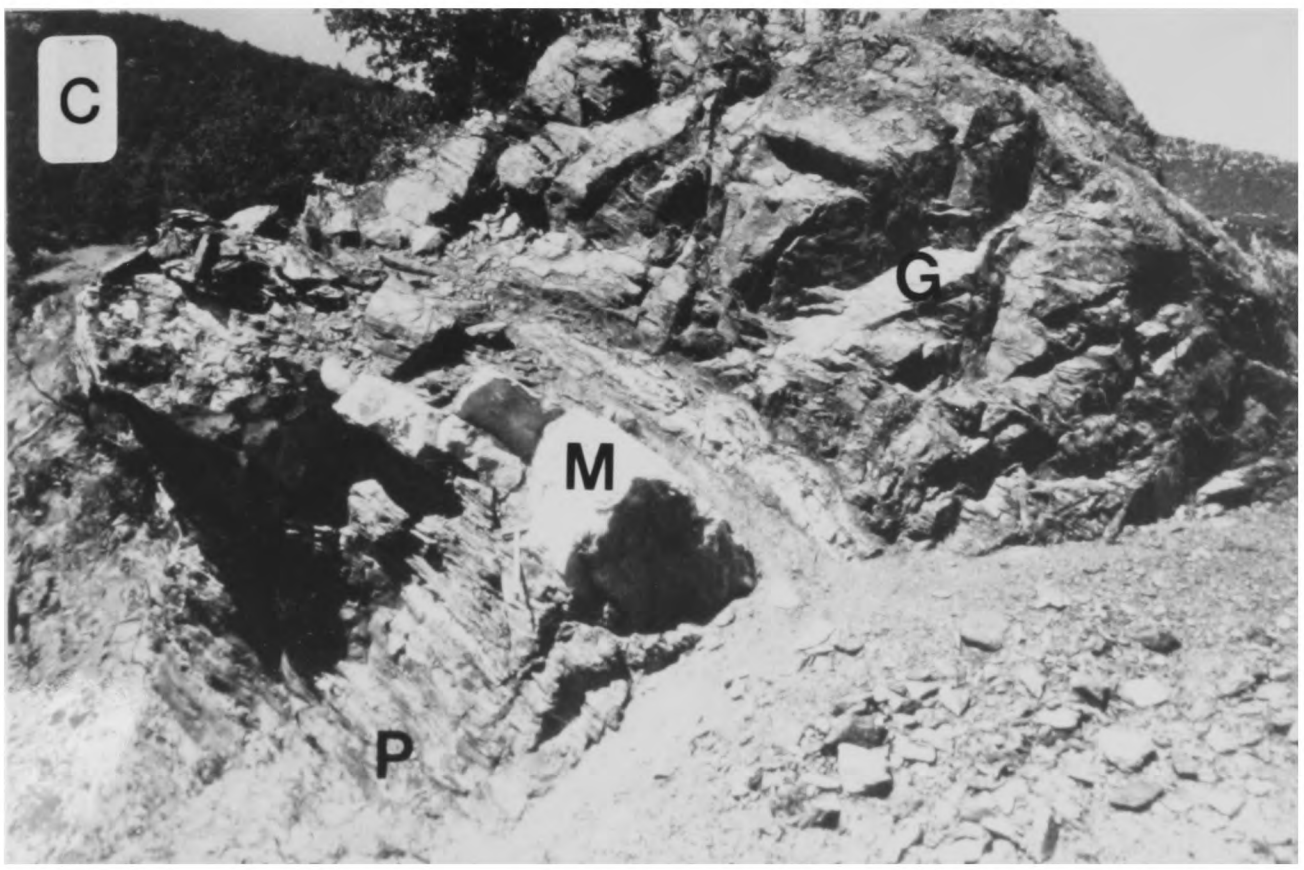
C
G
M
P

3.6

CHAPTER 4

THE AVDELLA MELANGE: TECTONIC AND SEDIMENTARY MELANGE

4.1 Introduction:tectonic setting of the Avdella Melange

The Avdella Melange (see Appendix 1; Fig. 4.1) forms part of an extensive north-south trending melange belt found in Greece, Albania and Yugoslavia (Diabase-Chert Formation; Karamata 1988). The Avdella Melange incorporates the Perivoli Complex, described previously by Kemp and McCaig (1984), and the Anilion Complex of Lorsong (1977, 1979). Regionally, the melange consistently underlies the units of the Pindos Ophiolite Group (Fig. 4.2), except where out-of-sequence thrusting has occurred. Over much of the area the unit consists of "block-in-matrix"-type melange, mainly composed of basalts and sediments, with subordinate metamorphic blocks detached from the tectonically overlying Loumnitsa Unit. This can be seen at the type area, 1 km northeast of Avdella (Fig 4.2). Wide areas of a single lithology may also be found, which are mapped as discrete tectonic slices (e.g. Stragopetra, N.E. of Avdella; Fig. 4.1). The matrix is dominated by incompetent sedimentary lithologies, mainly shale, marl and sandstone.

The melange varies in structural thickness up to a maximum of >1000 m, north of Avdella (Fig. 4.1). Fossil evidence from this study, particularly radiolaria, suggest a mainly Late Triassic and Jurassic age for the melange (see below; Terry 1971; Terry and Mercier 1973). Evidence from one locality (S. of Milea; Fig. 4.1), where transgressive pelagic sediments are found overlying block-in-matrix melange sequences, indicates a pre-Late Jurassic deformation event affected the melange sequences. Cretaceous blocks are also present in the melange, indicating subsequent Tertiary rethrusting. Primary sedimentary and/or igneous contact relationships are occasionally preserved within blocks or slices, allowing local stratigraphies to be constructed. Serpentinite sheets form a significant part of the melange in some areas (e.g. Perivoli, Milea; Fig. 4.1), and are commonly found as sheets or blocks interthrust with other units.

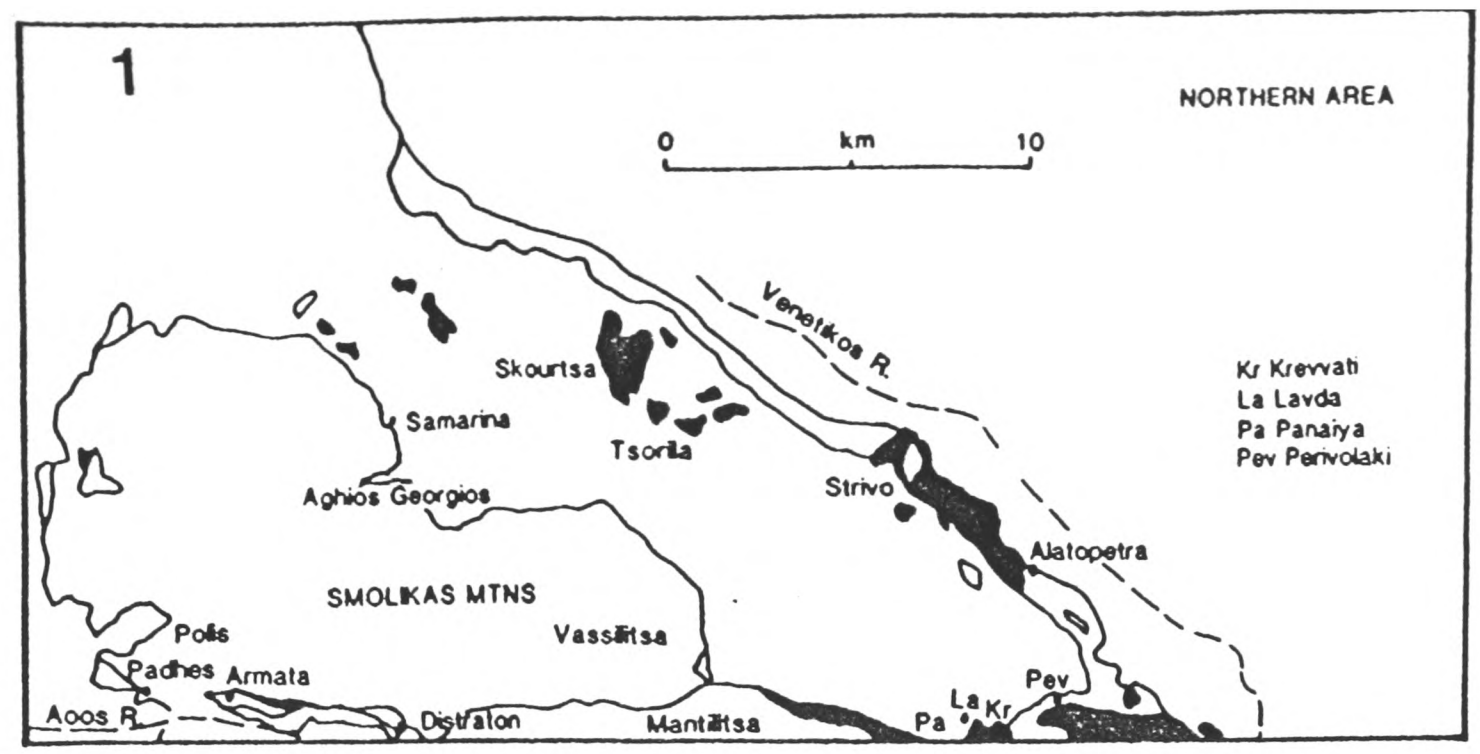

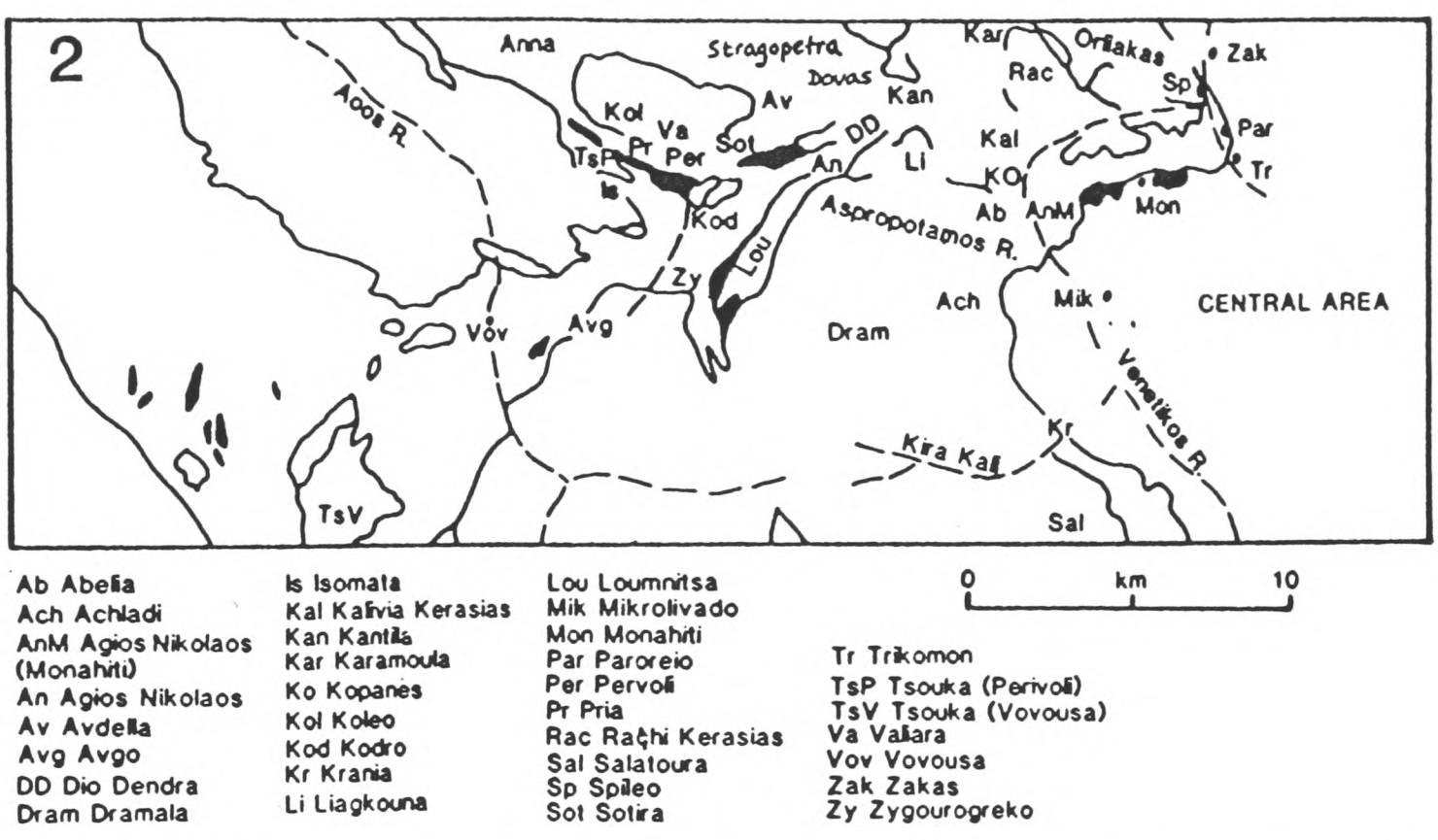

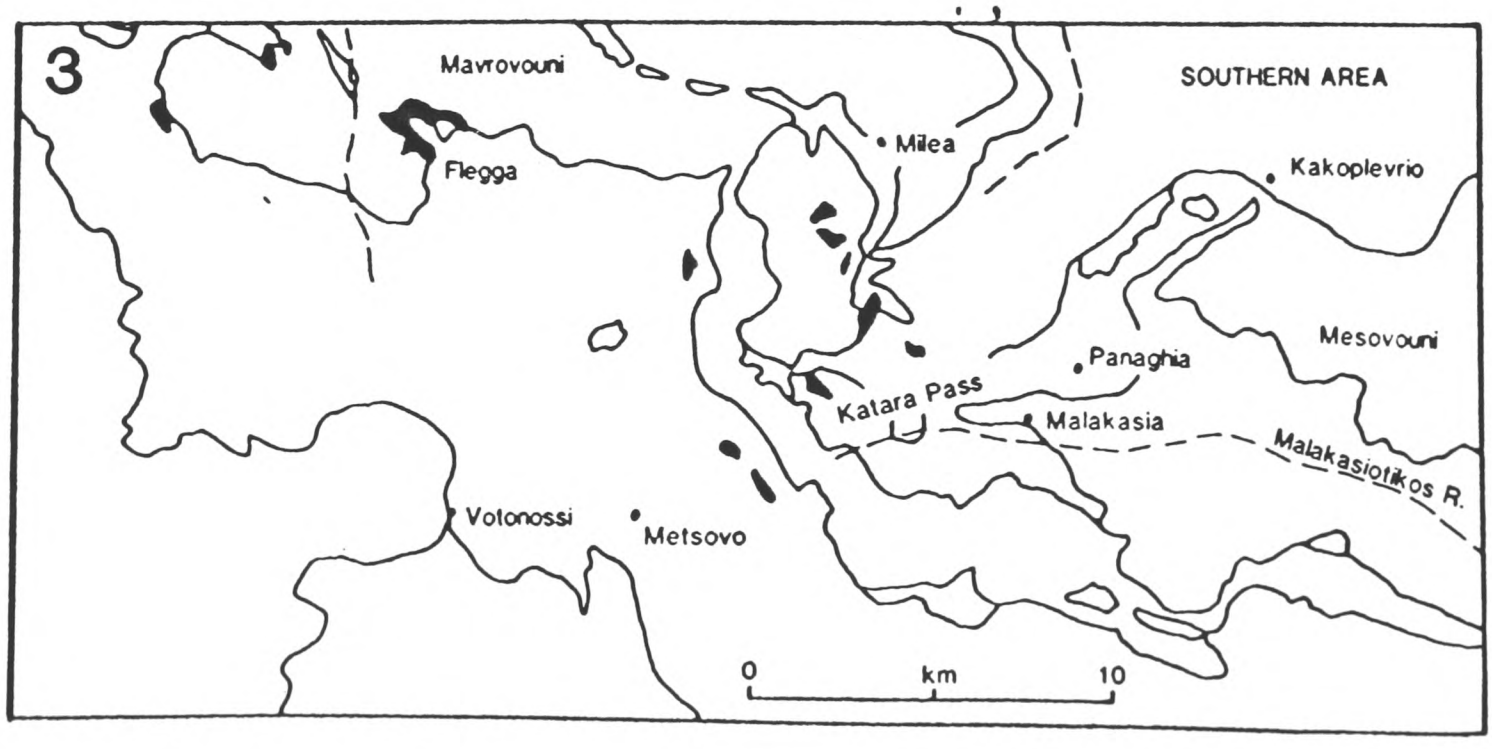

Fig. 4.1 a) Regional locality maps for the Avdella Melange. 1) northern area 2) central area 3) southern area. b) Detailed map of the central area. Refer to Chapter 2, Fig. 2.1 for the division of each area and the location of the central area map.

B

SIMPLIFIED GEOLOGICAL MAP,
CENTRAL NORTH PINDOS MOUNTAINS, GREECE.

ARKOUDOPETRA
AVDELLA
STRAGOPETRA
SOTIRA
PERLEKI
DIO DENDRA
Papaliapi
Megali Pedias
Agios Nikolaos
PERIVOLI
KODRO
ZYGOUROGREKO
Loumnitsa
DRAMALA
SELLOMA LAKKOU
Aspri Petra
Panaiya
Dovas
KANTILA
KREVVATI
KARAMOULA
Rachi Kerasias
Kalivia Kerasias
ORLIAKAS HILLS
ZIAKAS
SPELIO
Megali Plagia
Veneticos River
LIAGKOUNA
Aspropotamos River
Agios Nikolaos
Megali Petra
MONAHITI
Abelia
Achladi
MIKROLIVADO

Dramala Complex
Loumnitsa Unit
Aspropotamos Complex
Avdella Melange
Dio Dendra Group
Orliakas Group
Pindos Flysch
Molasse
Extrusives
Intrusives
River

Major thrust: certain
" " uncertain
Thrust: certain
" uncertain
Contact certain
" uncertian
Normal Fault cert.
Normal Fault uncert.

0 1
KM
N

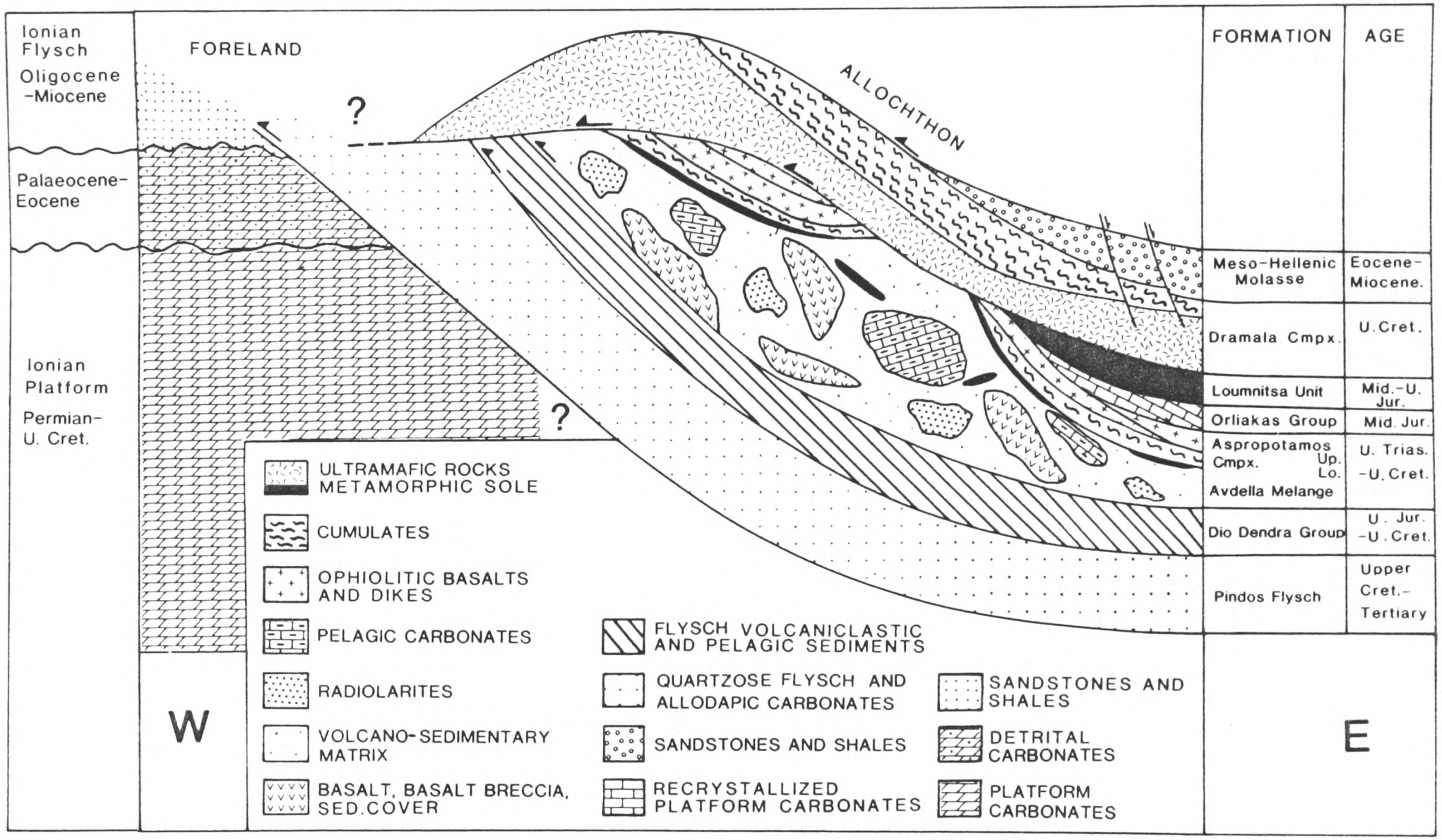

Fig. 4.2 a) Tectonostratigraphy of the north Pindos Mountains; note the position of the Avdella Melange, which occur structurally beneath the units of the Pindos Ophiolite Group. b) Geological map of the region 1 km N.E. of Avdella, the type area for the Avdella Melange.

GEOLOGICAL MAP OF THE AREA N.E. OF AVDELLA VILLAGE

Serpentinite
Massive basalts
Pillow basalts and breccia
Amphibolite
Schist and marble
Quartzo-feldspathic arenites

Radiolarite
Carbonates, variably metamorphosed
Poor exposure and melange undiffrerentiated
Basalt-sediment tectonic mixtures

Unmade road
Tectonic contact or block limit
Normal contact

0 20 40
M

N

STRAGOPETRA

AVDELLA

B

4.2 Definition of "melange"

The term melange has previously been used in several senses to describe chaotic mixtures of rocks found at outcrop. The term was first applied by Greenly (1919), to the Gwna Melange of Anglesey, North Wales. Since then, attempts to categorise "melange" (e.g. Raymond and Terranova 1984) have, in general, failed to provide a satisfactory working definition which can be applied in a wide variety of terrains. Problems have centred, for example, on the presence or absence of "exotic blocks" within a sequence, and the relative contributions of tectonic and sedimentary processes. It is therefore necessary to construct a working definition of the term melange for application to the Pindos Mountains as follows:

" The term melange is used to describe a mappable unit (commonly, but not exclusively, of block-in-matrix type), which is composed of a wide variety of igneous, metamorphic and sedimentary lithologies, usually in tectonic contact with each other. Within individual blocks ("olistoliths") or tectonic slices, intact conformable sequences may be present. Those units believed to have formed entirely by sedimentary mass-wasting processes, are given the name "olistostromes".

The lithologies of the Avdella Melange are summarised in Table 4.1. The relationships of these units to each other in the field will now be discussed below.

4.3 IGNEOUS ROCKS OF THE AVDELLA MELANGE

4.3.1 Extrusive volcanic rocks

Particularly important are thick, pillowed and massive, vesicular spilitic lava sequences, associated with basalt breccia and hyaloclastite (e.g. N.E. of Avdella, Fig. 4.1; Plate 4.1; Terry 1971). These lavas occur as blocks (up to 200 m thick) within a more extensive matrix, and as thrust sheets with little or no adjacent matrix (up to 2 km thick; e.g. Stragopetra, N.E. of Avdella; Fig. 4.1). The extrusives are locally interbedded with,

and/or overlain by pelagic carbonates containing *Halobia*, indicating a Late Triassic age (Terry 1971). The volcanics have been described previously (Kostopoulos 1989), who distinguished three main field units, based on weathering and geochemical characteristics: the Avdella (WPB; purple weathering), Aspri Petra (S. of Kantila, Fig. 4.1; T-MORB; purple-green) and Stragopetra (N-MORB; yellow-brown) units (Fig. 4.1; see geochemistry section below).

Several points need to be made regarding the naming and geochemical distribution of these volcanics, following further structural and geochemical work by the author:

(1) The volcanics are, in fact, commonly of more than one geochemical variety at the type localities described by Kostopoulos (1989), thus rendering the locality names for each chemical variety obsolete. At Avdella, WPB and T-MORB are present and at Stragopetra, volcanics of WPB, T-MORB and N-MORB affinities are interthrust. At Aspri Petra, slices of volcanics with an IAT signature are also present. In general terms, the basalts are complexly interthrust, and the concept of "type" localities for a geochemical affinity may not be valid.

(2) The lavas weather to distinctive colours in the field, which does, in general, reflect their chemical composition (see below), but this must be considered unreliable as a mapping tool. An example occurs in the Dio Dendra Valley (1 km S. of Aspri Petra; Fig. 4.1) which proves this point. Here, at a roadside outcrop, purple-red vesicular lavas, with interpillow haematitic marls are overlain by a more extensive bed of marl. Above the marl comes a sequence of strongly yellow-brown weathering lavas. Geochemically, however both basalt units are of transitional MORB-type, thus illustrating the difficulty of mapping basalt units based on weathering colour in the field.

(3) Volcanics of N-MORB-type discovered at Kopanes and Stragopetra-Avdella (Fig. 4.1) usually occur immediately beneath the ophiolitic units of the Aspropotamos Complex or interthrust with the metamorphic sole. These lavas form large bolster-like pillows, in contrast to the smaller pillows of the tectonically underlying volcanics. However, there is a possibility that these N-MORB volcanics may form an imbricate thrust

sheet derived from one or the other of these latter two units (where N-MORB's are also found), and therefore do not form part of the Avdella Melange.

The extrusive rocks are usually vesicular feldspar-phyric basalts and andesites (Plate 4.2). In many specimens, fine-grained haematitic material is abundant in the matrix, giving the distinctive red-brown colour. In general, these lavas are highly spilitised, commonly altering to chlorite, and carbonate. No fresh pyroxene is usually preserved, and opaque minerals are abundant, particularly pyrite and magnetite. The vesicles are commonly large (up to 1 cm), and are infilled with chlorite, quartz and opaque minerals. Some of the basalts found contain epidote and prehnite in abundance, and may also be strongly brecciated (Plate 4.2).

4.3.2 Intrusive rocks

Intrusive rocks are rare, mainly restricted to medium to coarsely crystalline basic sills (up to 1.2 m-thick), which locally intrude turbidite sequences (e.g. at Kokkina Litharia, Fig. 4.1b). These are generally ophitic gabbros and localised differentiates. At Tsouka (N.W. of Perivoli), a coarse grained (6 mm) gabbroic sill occurs (approx 1 m wide), with chilled margins and a baked contact with surrounding sediments. The gabbro is highly weathered, and has intruded pelagic grey mudstones, carbonate breccias, marls and cherts, already affected by small-scale, soft-sediment extensional faulting. The sills at Kokkina Litharia are coarsely-crystalline melanogabbros, leucogabbros and dolerites containing mainly zoned and twinned albite, altering to white mica. Sodic clinopyroxene (usally aegirine) and orthopyroxene is present. Rare orthoclase crystals occur in these rocks. Minor phases include abundant magnetite (sometimes aligned) and apatite. The pyroxenes are altered in most cases to patches of chlorite, but sometimes to to a highly pleochroic biotite.

The gabbroic rocks from other localities are found as isolated blocks in the melange (e.g. Liagkouna; Pria, N.W. Perivoli), and are extremely similar mineralogically to those described. At Avdella however, a gabbro of this type (samples 75 and 76/88) has a conformably overlying carbonate

cover. In the west of the Smolikas Range, northwest of Polis (Fig. 4.1), coarsely crystalline gabbro blocks are present within the Avdella Melange, and similar gabbroic rocks occur in several other localities, probably related to the volcanic sequences.

4.3.3 Geochemistry of melange basalts

An extensive data base now exists for the Avdella Melange volcanic rocks following new analyses (28 basalts, 11 gabbros, see Appendix 4, and Kostopoulos 1989). The analyses mainly indicate WPB, WPB-MORB transitional and MORB compositions, typical of stretched continental lithosphere through to mid ocean ridge-type tectonic settings. As mentioned above, three geochemical groups were identified by Kostopoulos (1989): WPB alkaline basalts; T-MORB tholeiitic basalts and N-MORB tholeiitic basalts. New data collected during this study (Appendix 5), shows that these geochemical types are present regionally within the Avdella Melange. An important new observation is that basalts sampled from the melange may locally show a depletion of high field strength trace elements, more typical of rocks associated with island arcs, as described below. The additional data have somewhat merged the boundaries between the three units described by Kostopoulos (op. cit. see above), further supporting a gradual evolution of the chemistry of the melange volcanics.

The Avdella Melange basalts have been plotted on standard chemical discrimination diagrams to show these variations (Figs. 4.3 to 4.5). Coarsely-crystalline lavas and gabbros (see above) are also included on the scatter diagrams for completeness, but only basalts are discussed here. The diagrams show that the melange contains mainly basic tholeiitic volcanics, commonly enriched in all elements except those compatible with garnet lherzolite (Cr, Sc, Y). The majority of the melange volcanics therefore are of WPB-type, as shown by the convex patterns present in the MORB-normalised multi-element plots (Figs. 4.6, 4.7). Most of the basalts fall in the MORB field on the Ti-Zr diagram (Fig. 4.3.a), with a scatter into the WPB field also being prominent. Six analyses lie in the IAT field, three of these being basaltic andesites from Alatopetra, which are evolved lavas, and two are gabbros. The remaining IAT-type basalt is discussed below

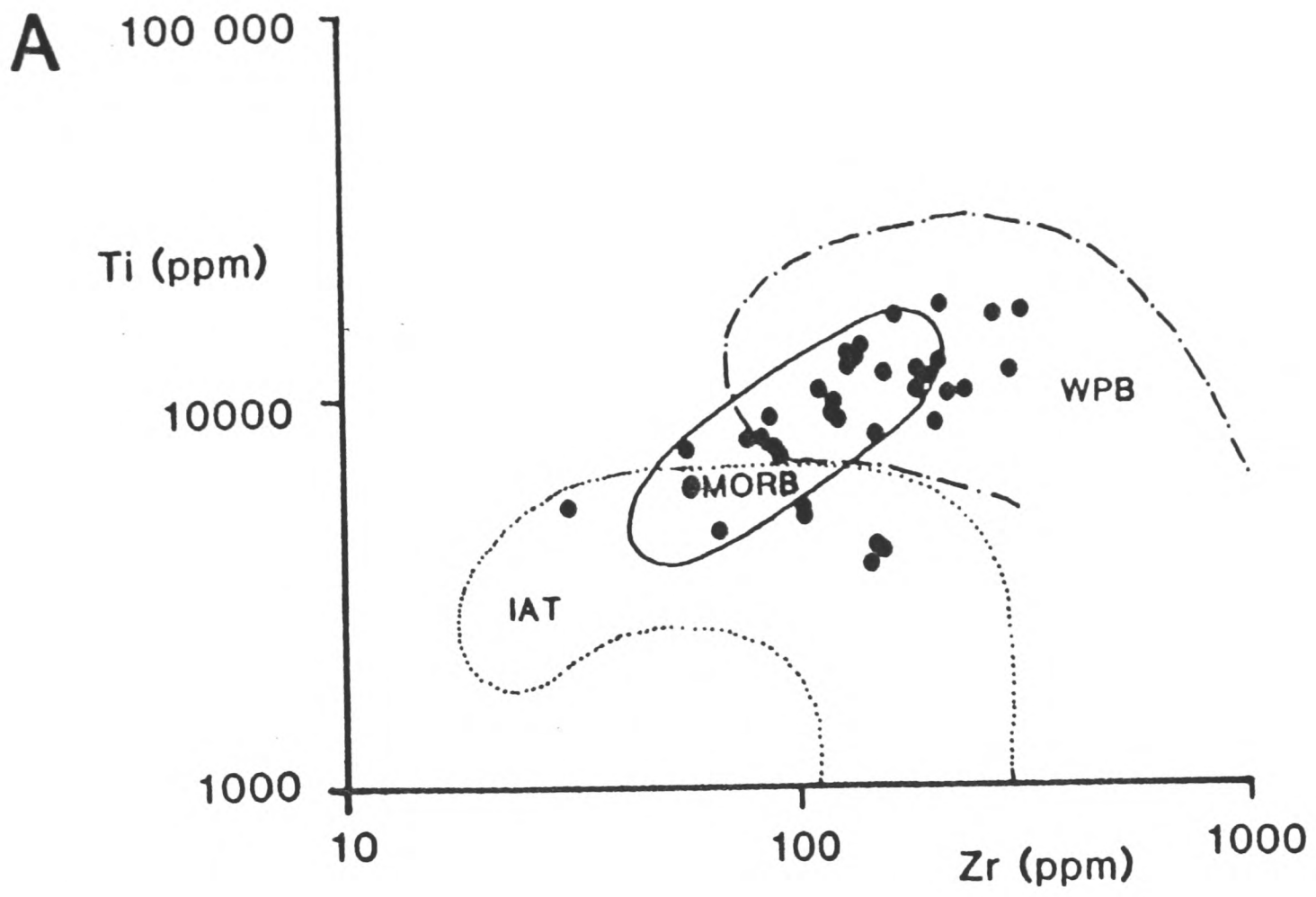

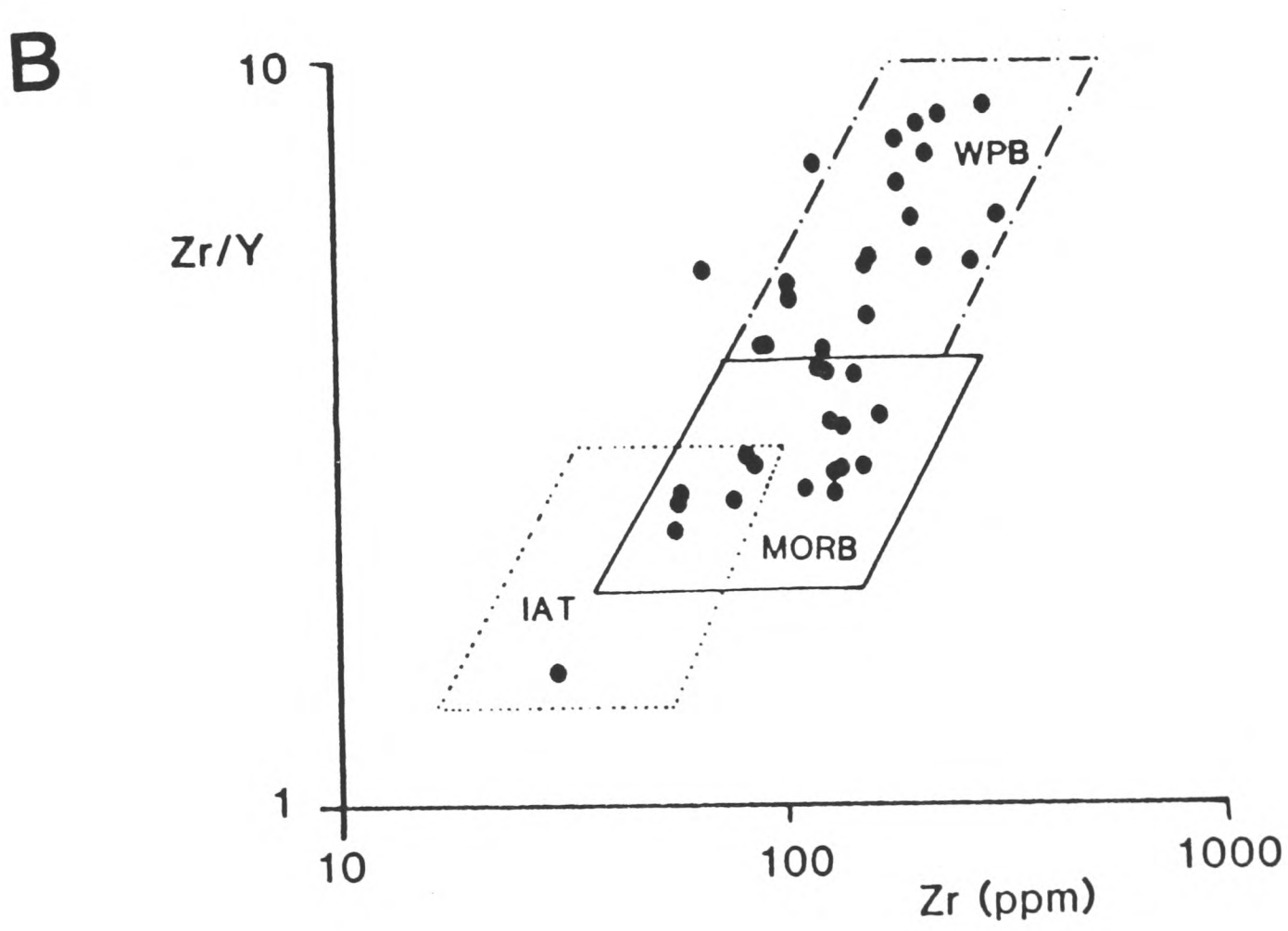

Fig. 4.3 a) Ti-Zr diagram for the Avdella melange basalts. WPB= Within Plate Basalt; MORB= Mid Ocean Ridge Basalt; IAT= Island Arc Tholeiite (After Pearce and Cann 1973). b) Zr/Y-Zr diagram. fields as for a) above.

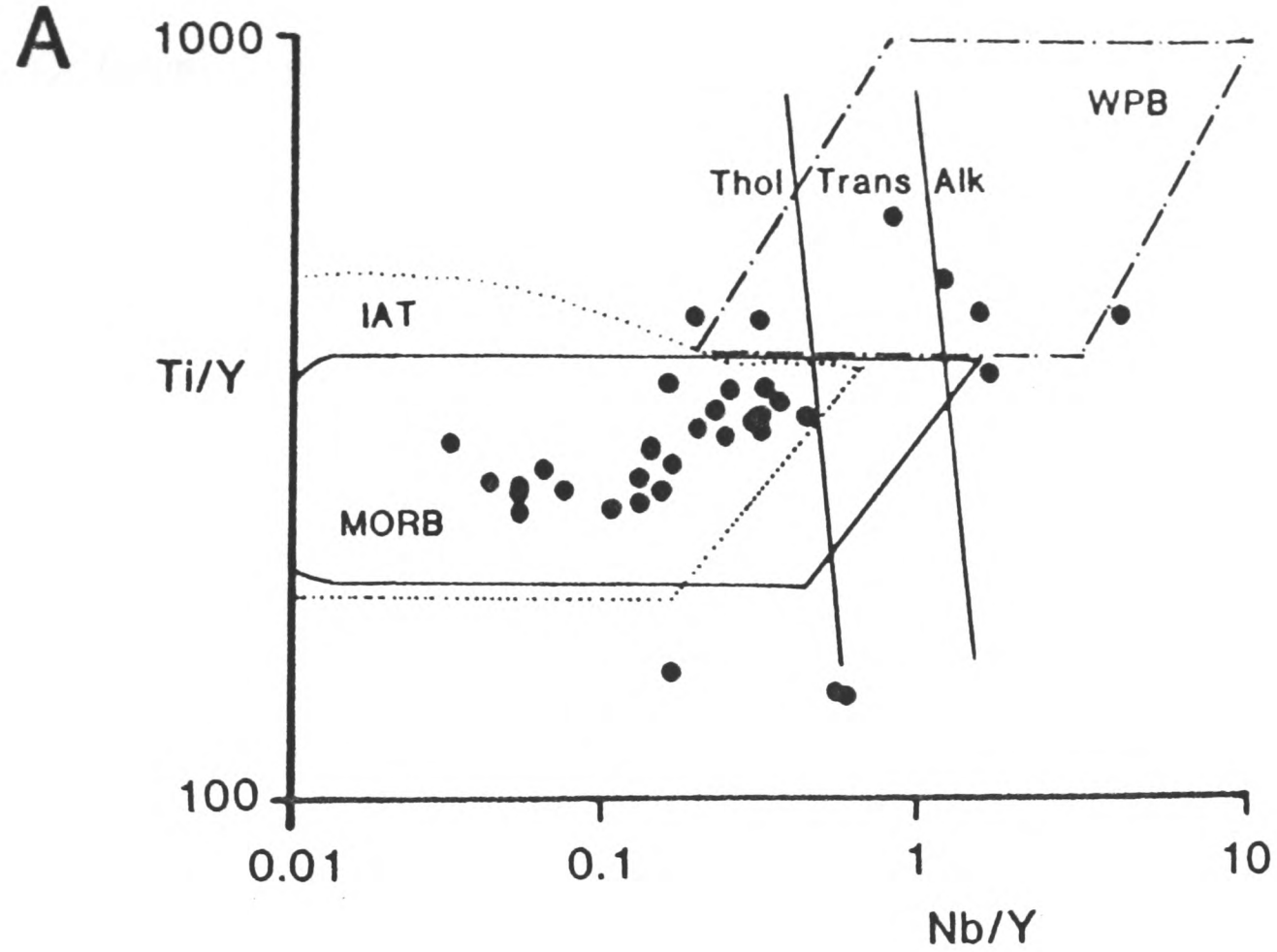

Fig. 4.4 a) Ti/Y-Nb/Y plot (after Pearce 1982). Fields as in Fig. 4.3; Thol= tholeiitic basalt; Trans= transitional basalt; Alk= Alkaline basalt. b) Ti-Zr-Y plot for Avdella Melange basalts. Fields; A+B= IAT; B= MORB; B+C= calk-alkaline basalts; D= Within Plate Basalts.

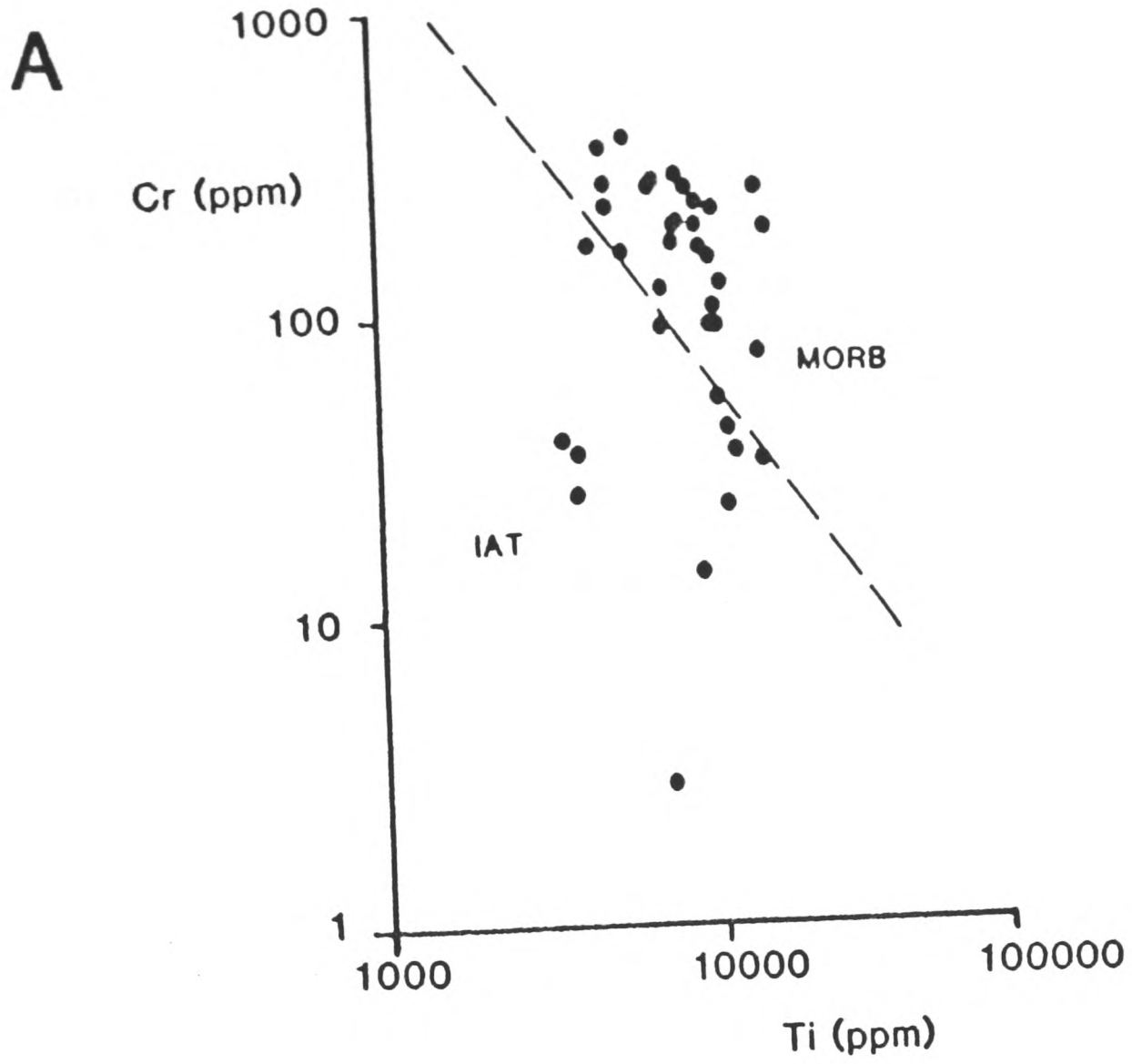

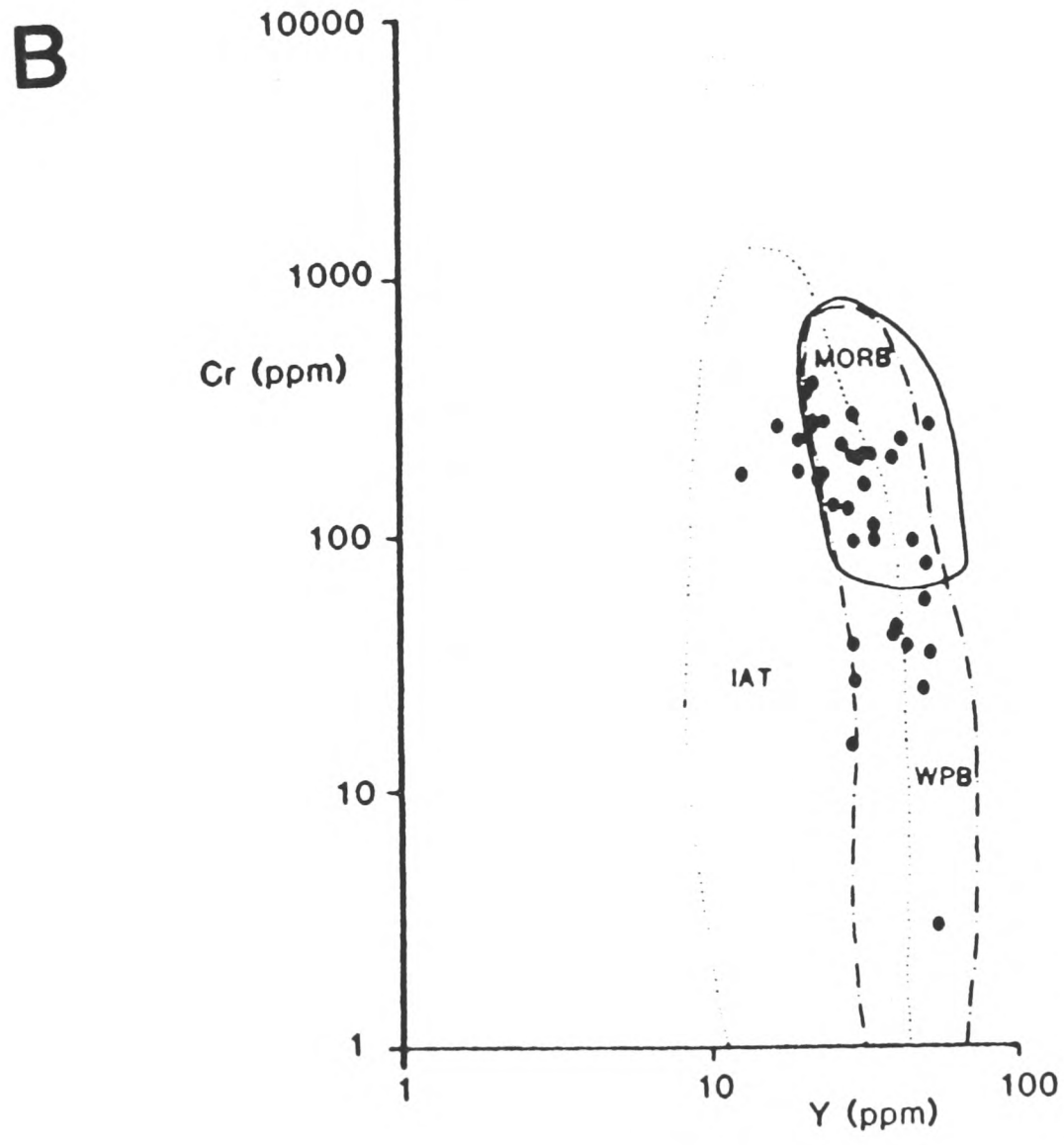

Fig. 4.5 a) Cr-Ti plot for Avdella Melange basalts (after Pearce 1975). MORB= Mid Ocean Ridge Basalt; IAT= Island arc tholeiite. b) Cr-Y plot for the Avdella Melange basalts (after Pearce 1982). Fields as for Fig. 4.3).

(86/89). The Zr/Y-Zr diagram (Fig. 4.3.b) illustrates the high contents of Zr relative to Y present in many of these rocks. The Ti/Y-Nb/Y diagram (Fig. 4.4.a) also shows the relatively low Ti/Y ratios, and the tholeiitic nature of most of the samples analysed. The Ti-Zr-Y triangular plot (Fig. 4.4.b) shows a spread of data, concentrated in the ocean floor field. The Cr-Ti and Cr-Y diagrams (Fig. 4.5) show that most of the analyses, excepting gabbros, plot in the MORB and WPB fields on these diagrams, which tend to highlight any IAT-type signatures present. Some of the volcanics analysed are of somewhat different chemistries to those described. At Alatopetra, where good stratigraphic control is available, evolved basaltic andesites are particularly low in titanium (0.63-0.70) and other transition elements (e.g. Ti, Cr, Ni, Cu, Zn, V, Co, Sc), whereas HFSE (Zr, P, Nb) are moderately high (Fig 4.6.b).

The multi-element plots provide an ideal way to see the variation of these rocks relative to normal MORB (for normalising values see Chapter 2). A selection of analyses are presented here, mainly on a locality basis. The basaltic rocks from Tsouka Mountain (Fig. 4.1) are of within-plate, and evolved MORB-type (Fig. 4.6.c). A dyke found cross-cutting these volcanics (47/89; Fig. 4.6.d) is probably also of evolved MORB-type, shown by a relatively flat chemical trace, and a particularly strong depletion of Cr. A basalt found interbedded with (probably overlying) sediments here, has a very strong WPB pattern (52/89; Fig. 4.6.d). Fig. 4.7.a shows WPB signatures from the Dio Dendra Valley, (S. of Aspri Petra, 218/88 and 219/88; Fig. 4.1), and an enriched MORB from Stragopetra (233/88; Figs. 4.1, 4.7.a).

North of Liagkouna Mountain, on the main Perivoli to Grevena road, melange basalts (Aspri Petra unit of Kostopoulos 1989) are well exposed. Here, transitional to MORB-type lavas are common within the melange (e.g. 85/89, Fig. 4.7b). However, on the southern part of Kantila hillside, purple-grey and green-brown basalts more typical of depleted MORB and IAT chemical affinities are present (86/89, 87/89; Fig 4.7.b). These basalts are conformably overlain by rudites and arenites rich in volcanic detritus. These sediments are part of a disrupted turbidite sequence which crops out extensively in this area (see Liagkouna section below). Bedded radiolarite blocks (5-8 m thick) collected 200 m south of the basalts described, form a disrupted but probably originally continuous

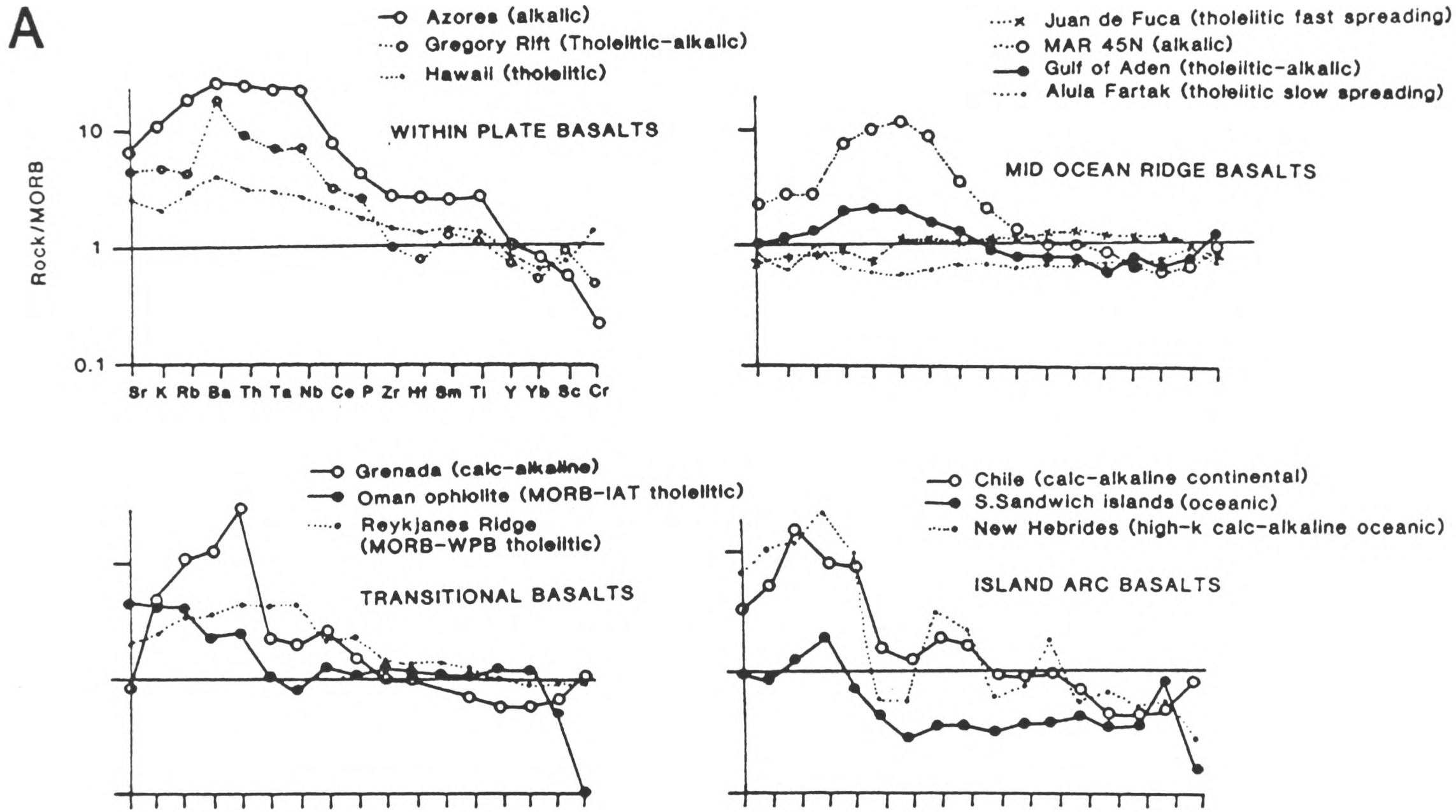

Fig. 4.6 a) Typical trace element multi-element plots for typical within plate transitional, MORB and IAT basalts, for comparison to Avdella Melange basalts (after Pearce unpublished manuscript). b) Multi-element plots for evolved basaltic andesites from Alatopetra (evolved WPB, with low Ti; Fig 4.1). c) Basalts from Tsouka, 15 kms S.W. of Vovousa (42 and 45/89) similar to transitional MORB-WPB tholeiitic basalts from the Reykjanes ridge (see Fig. 4.6a). d) Dyke from swarm cross-cutting the basalts in c) above (47/89; more evolved than 42 and 45/89), and strongly within-plate basalt from tectonically overlying thrust sheet (52/89).

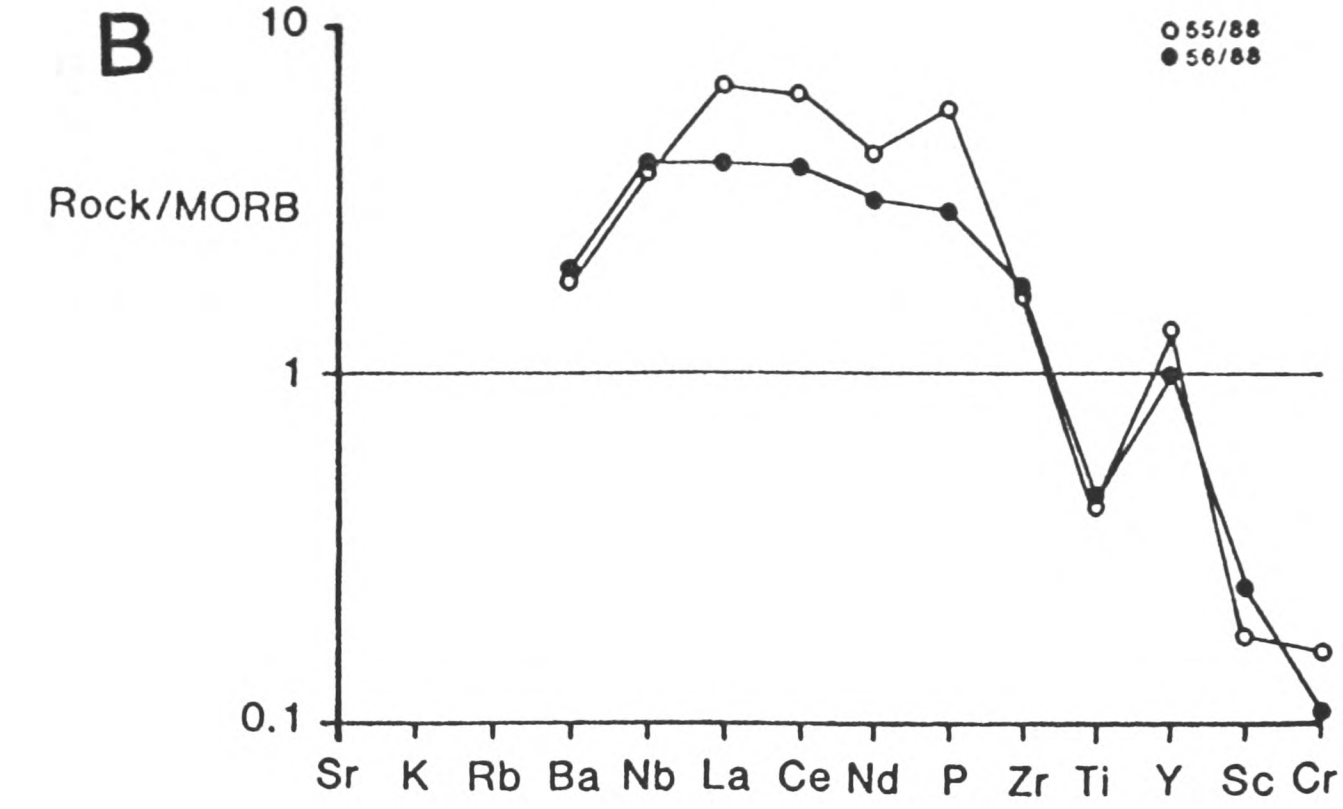
B
10
1
0.1
Rock/MORB
○ 55/88
● 56/88
Sr K Rb Ba Nb La Ce Nd P Zr Ti Y Sc Cr

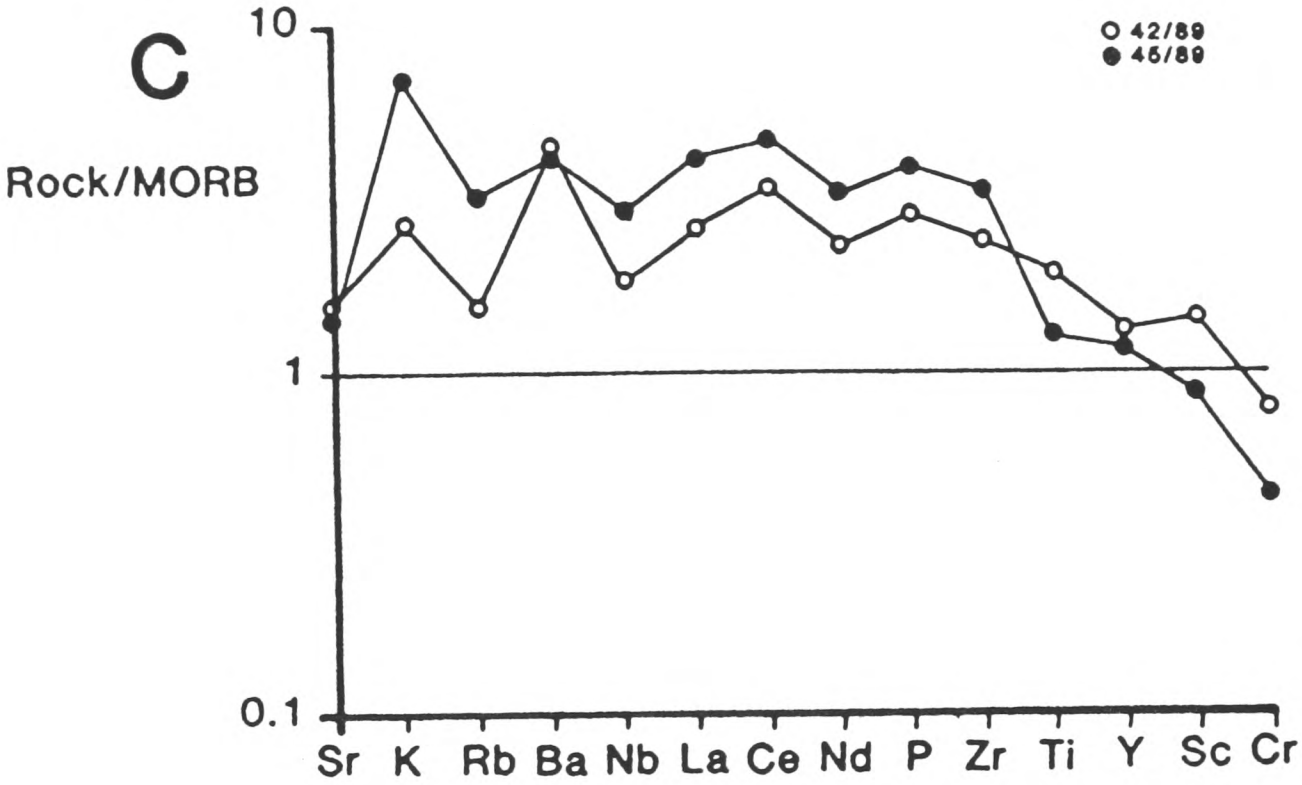
C
10
1
0.1
Rock/MORB
○ 42/89
● 45/89
Sr K Rb Ba Nb La Ce Nd P Zr Ti Y Sc Cr

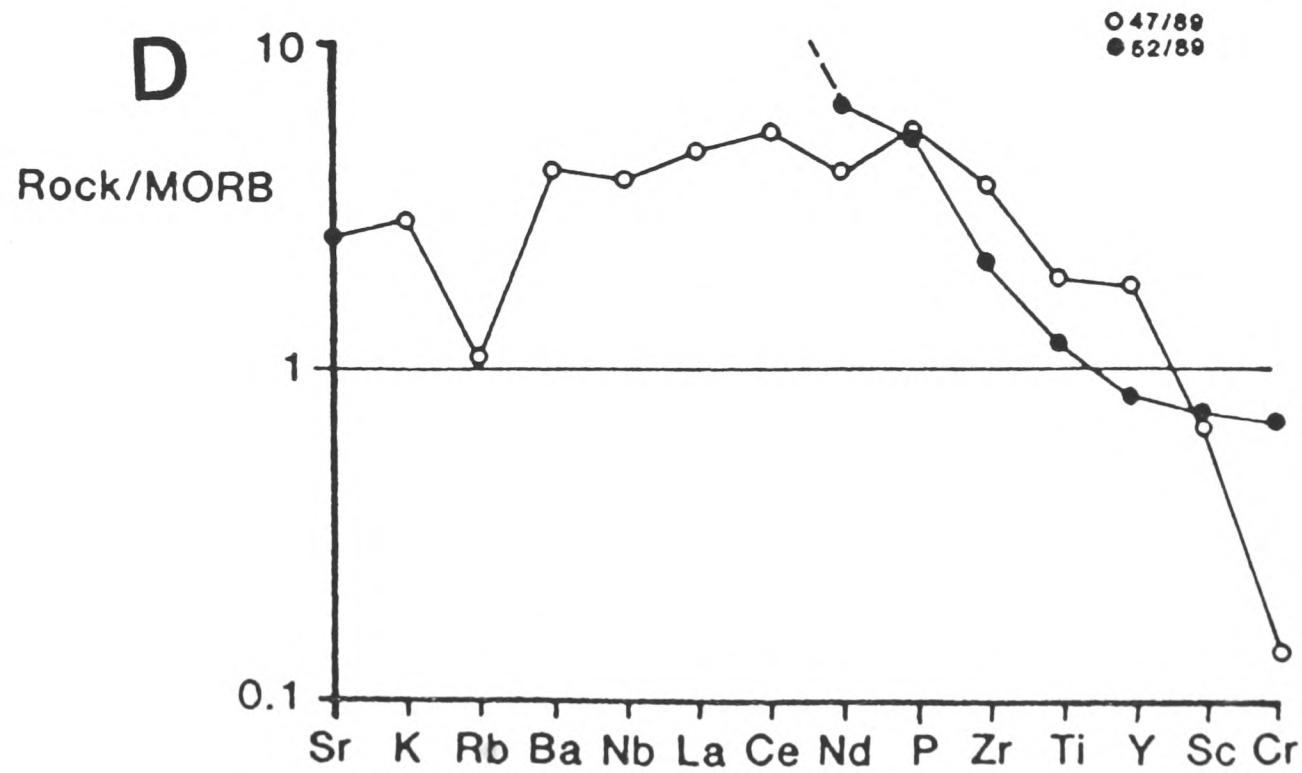
D
10
1
0.1
Rock/MORB
○ 47/89
● 52/89
Sr K Rb Ba Nb La Ce Nd P Zr Ti Y Sc Cr

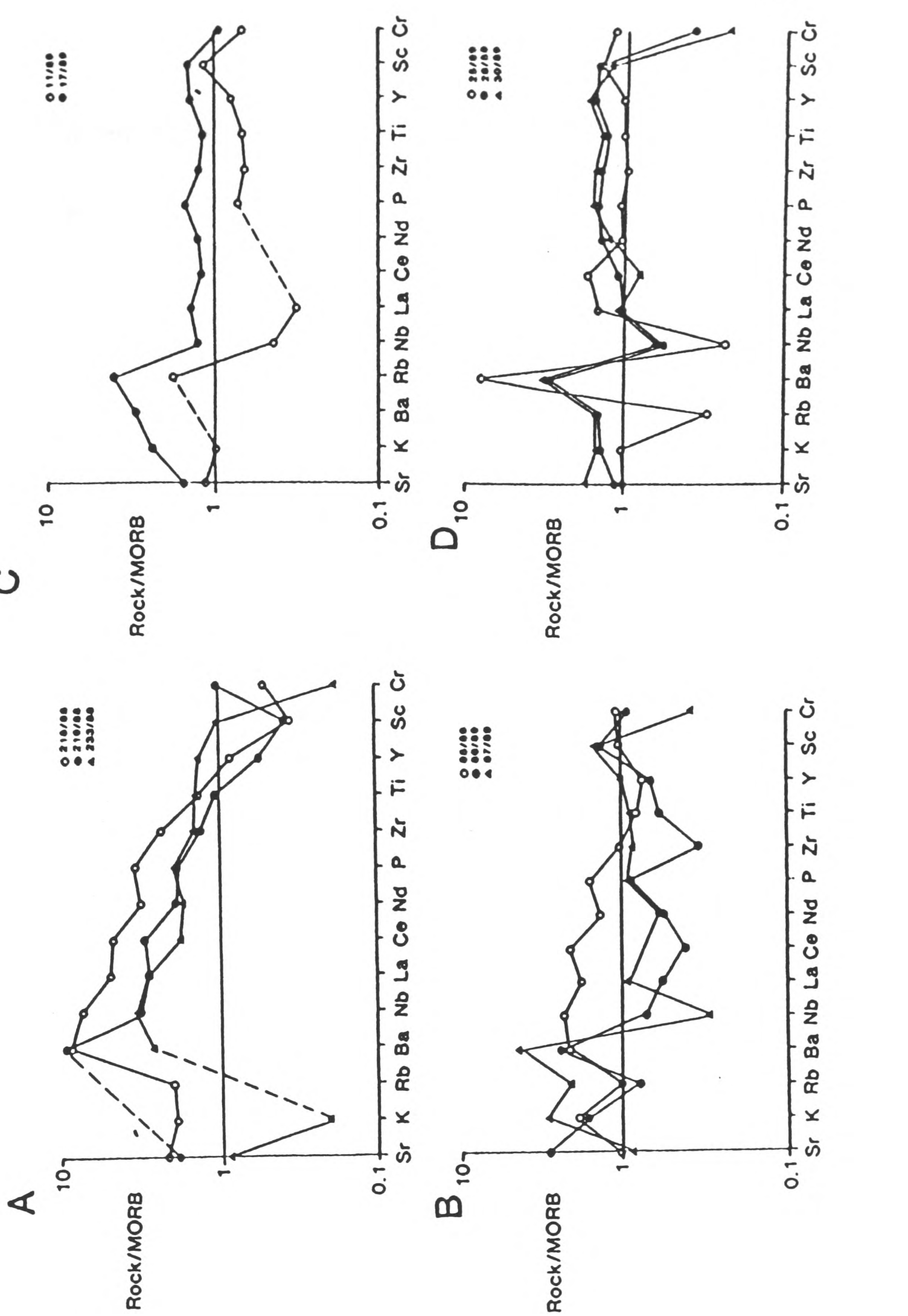

Fig. 4.7 Multi-element plots, see Fig. 4.1 for localities. a) central Dio Dendra Valley, 3 kms S.W. of Aspri Petra (218 and 219/88; tholeiitic WPB, similar to Hawaiian basalts Fig. 4.6a) and Stragopetra Mountain (233/88; E-type MORB). b) Basalts from Aspri Petra (85/89; slightly evolved MORB), and S. Kantila Hill (86 and 87/89). Note the island arc signature of these latter two basalts, which are overlain by Late Triassic turbidite sequences. c) Basalts from melange beneath greenschist facies metamorphic sole (6 kms S.W. of Samarina). Evolved MORB (11/89) and depleted MORB (MORB-IAT transitional; 17/89). d) Basalt from W. Smolikas (25/89; MORB-IAT transitional). Basalts from W. of Armata (28/89 and 30/89) are MORB-IAT transitional, with low contents of compatible elements.

unit (40 m outcrop length) within this sequence. These blocks contain Late Triassic radiolaria (e.g. *Capnuchosphaera* sp.; see below). Similar interbedded siliciclastic and carbonate turbidites from northwest Liagkouna, some 300 m to the south of this outcrop, were also dated as Late Triassic. These field relations suggest, therefore, that these IAT-type basalts are part of the melange sequence. In the southern Pindos Zone, similar volcanic rocks of IAT-type have been discovered within Triassic melange in the Peloponessos region of southern Greece (Piper 1982; Degnan and Robertson 1990).

Melange basalts from the northern region are also of variable chemical types. Rocks collected partly in the lower greenschist facies of the Loumnitsa Unit and partly from underlying melange (S. of Samarina; Fig. 4.7.c) show similar chemical traces, but one sample (11/89; Fig. 4.7.c) is depleted in most immobile trace elements, relative to normal MORB, and the other is slightly enriched (evolved MORB). A basalt from the western Smolikas Mountains (25/89; Fig. 4.7.d) is again of somewhat variable chemistry, but essentially displays a MORB trace. Other samples collected west of Armata (28 and 30/89; Fig. 4.7.d) are also somewhat Nb depleted, and are classified as evolved MORB. These basalts may also be partly transitional to IAT, as shown by the low Nb and Cr values present.

4.3.4 Summary

The melange basic volcanic rocks show a range of chemical features which range from common within plate alkaline basalts, through to less abundant MORB-type basalts. Also present in some areas are basalts which are of IAT type, and others with depletions of certain HFS elements, which are transitional to IAT. The melange basalts found at Samarina are chemically of evolved MORB type, and are indistinguishable from rocks in the basal part of the Aspropotamos Complex ophiolitic units.

4.4 INTACT OCEANIC SEDIMENTARY SEQUENCES WITHIN THE AVDELLA MELANGE

A wide variety of sedimentary lithologies are present within the Avdella Melange. They occur as detached blocks ("olistoliths") up to 400m^2 (e.g. at Dovas, Fig. 4.1b), as more extensive thrust bounded packages (e.g. Liagkouna), and as a dismembered matrix to the olistoliths (e.g. Mantilitsa-Vassilitsa area). The main lithologies present are summarised in Table 4.1. Here, the more intact sequences discovered are described in more detail, and the more dismembered olistolith blocks are considered later.

4.4.1 Pelagic and volcaniclastic turbidite sequences

a) *Alatopetra*

Large melange blocks at Alatopetra (Figs. 4.1, 4.8, 4.9) preserve conformable sedimentary sequences of Triassic and Jurassic age (Fig. 4.10). Volcanic extrusives, including resedimented volcaniclastics (Plate 4.1), have an intact cover of grey condensed carbonates (probably Triassic). The volcanics are highly vesicular purple andesites, and along the contact with the overlying limestones, a red-brown, strongly haematitic, siliceous marl is developed. Some of the volcanics have been reworked, and form coarse basaltic turbidite units, with well-developed graded bedding (Plate 4.1). The overlying carbonates contain palaeo-extensional faults with small displacements (maximum 80 cms), forming a horst and graben structure within one of the blocks (Plate 4.1). These carbonates are overlain by pink nodular limestones (ammonitico rosso), along a gradational contact (Plate 4.1). These rocks consist of somewhat elongate carbonate-rich nodules, joined along stylolitic suture lines. Parts of this unit have a more clay-rich haematitic matrix which encloses the nodules (Plate 4.4). In thin section, both matrix and nodules are dominated by micritic calcite, the nodules being mostly unfossiliferous, but the matrix contains fragments of thin-shelled bivalves, recrystallised radiolaria and cephalopod fragments. These nodular limestones contain several localized phosphatic hardgrounds towards the upper part of the unit (Plate 4.4). These contain sparse shell lags of mainly fragmentary belemnite guards, together with

TABLE 4.1

MELANGE BLOCK LITHOLOGY AND OCCURRENCE	AGE	THICKNESS (MAXIMUM APPROX.)
Purple, green, red-brown vesicular basalts, often pillowed, with basalt breccias and hyaloclastites. found as blocks and sheared thrust sheets.	?Mid-Late. Triassic	1 km+
Yellow-brown weathering basalts, dark green when fresh. Commonly forming large pillows and bolsters or massive units. May be vesicular.	Late Trias.- Early Jur.	100 m
Gabbros and olivine gabbros, found as sills and small intrusive bodies, poorly exposed mainly.	?Trias	Several metres
Pink, hematitic fine-grained pelagic carbonates. Contain thin shelled pelagic bivalves and recrystallised radiolaria. Found overlying alkali volcanics.	Late Trias.	Several tens of metres
Pink to light grey nodular carbonates of "ammonitico rosso" facies. Contain stylolites and seams of red marl. Fossiliferous including belemnites, foraminifera and radiolaria. Localised hardgrounds.	Late Trias.- Early Jur.	20 m
Grey or pink fine-grained, thick bedded, carbonates, with replacement chert nodules, extensional faults and neptunian dykes. Alkali basalt basement.	Late Trias- Early Jur.	50 m +
Calcirudites and calcarenites. (e.g. Loumnitsa) Interbedded with radiolarian chert. Fossiliferous packstones and biosparites, with occasional oosparites (e.g. Alatopetra). Calcilutites, commonly redeposited (e.g. Dovas).	Late Trias- Jurassic	1 m-300 m
Fine-grained, thick, regularly bedded micritic carbonates (e.g. Kakoplevrion, Padhes). Platformal-type.	Late-Trias.- Jurassic	300 m +

Fossiliferous carbonates, with shallow-water fauna, mainly bivalves and stromatolites.	Late Trias.	40 m
Radiolarian chert. Red-brown and green ribbon chert. Often interbedded with shales and marls.	1)Late Trias. 2)Mid.-Late Jur.	Tens of metres
Black, red and grey shales and marls. Some siliceous shales and manganiferous shales.	Late Trias-Jurassic	?Tens of metres
Fine rudites, arenites and silts, composed of metamorphic quartz, feldspar, mica. Occasional mafic clasts. Turbiditic origin.	?Trias.	10-40 m
Clastic turbidites, ranging from coarse pebble rudites to black shales. Contains abundant ophiolitic debris, plus chert and fine-grained limestones, and minor quartz and feldspar.	Mid Jur?	250 m
Amphibolites, greenschists, quartz-schists etc. Detached parts of the metamorphic sole.	Mid Jur	300 m

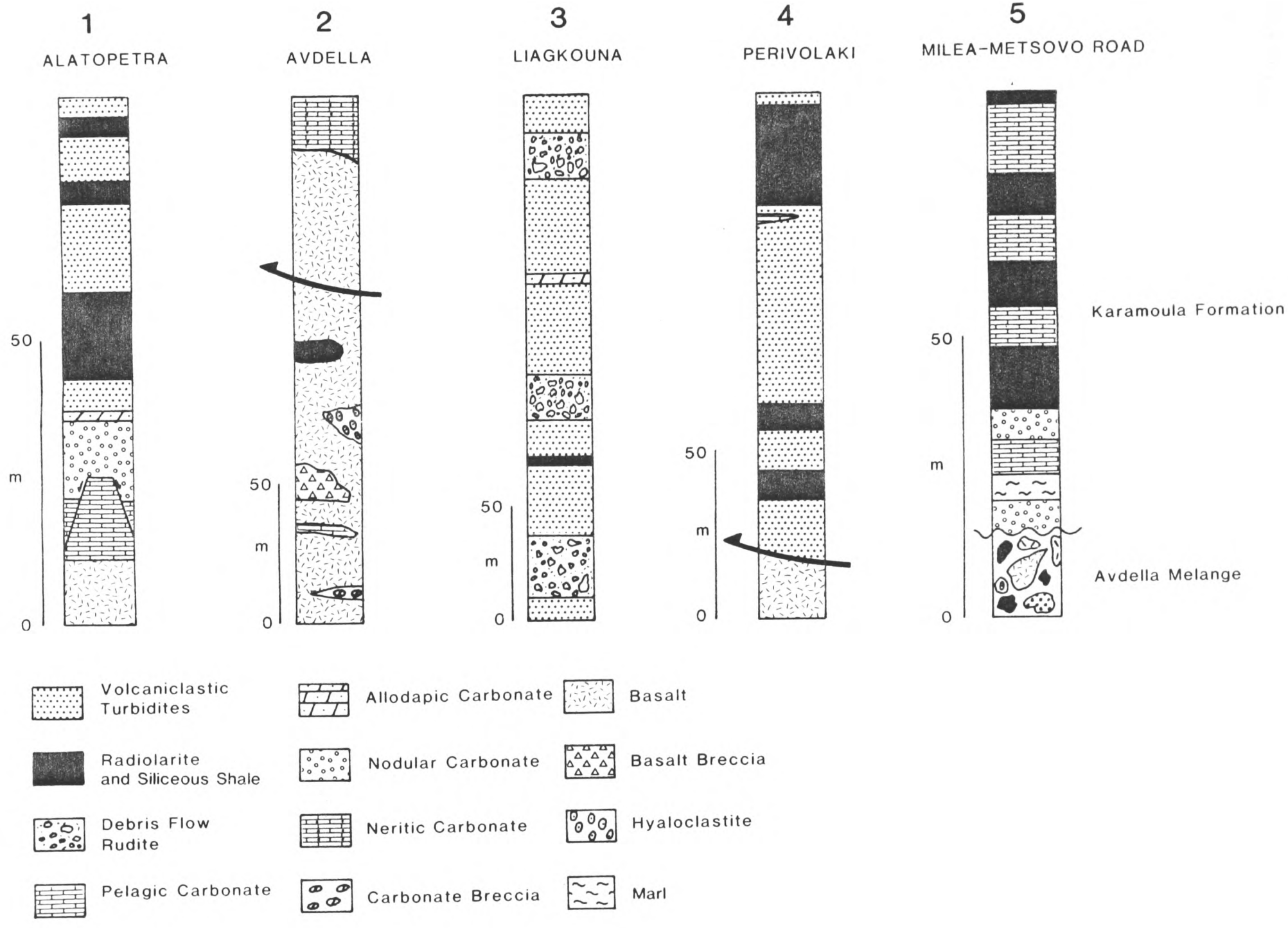

Fig. 4.8 Generalised stratigraphic columns for coherent melange sedimentary sequences (see Fig. 4.1). Column 5 shows the Avdella Melange transgessed by a Late Jurassic-Early Cretaceous sequence at Milea.

borings and dissolution striae. No preserved ammonites were found at this locality.

On the blocks where a full sequence is developed (Fig. 4.9), a thin (10-70 cm) grey bioclastic calcarenite overlies the ammonitico rosso (Plate 4.5). This contains derived shallow water material, particularly ooids and echinoid fragments. Other bioclasts include algae, brachiopod valves, pelletoidal material and miliolinid foraminifera (Plate 4.6). Some blocks do not have the above calcarenite, and pass directly into a pink calcilutite, which locally may directly transgress the faulted, thick-bedded carbonates. These calcilutites also contain fragmentary belemnite guards. Deposition of these sediments appears to have been partly syn-tectonic, as thickness changes occur across the fault plane. On one of the blocks, the succeeding unit is a recrystallised radiolarite horizon (15 cms-thick). This unit has an undulating base, interpreted as having formed due to differential compaction. Upwards, this passes into a purple, laminated calcilutite, before a transition into several metres of manganiferous and siliceous mudstones.

A red-brown haematitic shale horizon follows these manganiferous mudstones, and a major horizon of radiolarian chert is present above this unit (Plate 4.5). The radiolarites were sampled for radiolarian age dating, but unfortunately yielded no well preserved specimens. However, they are of probable Bajocian to Tithonian age, compared with data from radiolarites of the Pindos Zone of central and southern Greece (De Wever and Cordey, 1986; De Wever, 1989). The radiolarites are, in turn overlain by and partly interbedded with, ophiolite-derived turbidite successions (Figs. 4.8, 4.10). Notably, this sequence is overlain by calcarenites and terrigenous sediments of the Pindos Flysch at this locality.

b) *Perivolaki*

Northeast of Perivolaki Village (Fig. 4.1), a deformed but partly coherent sequence (Fig. 4.8) preserves at the base, ribbon radiolarites with interbedded terrigenous quartzo-feldspathic fine-grained sediments. These sediments are partly thrust deformed. They pass upwards into

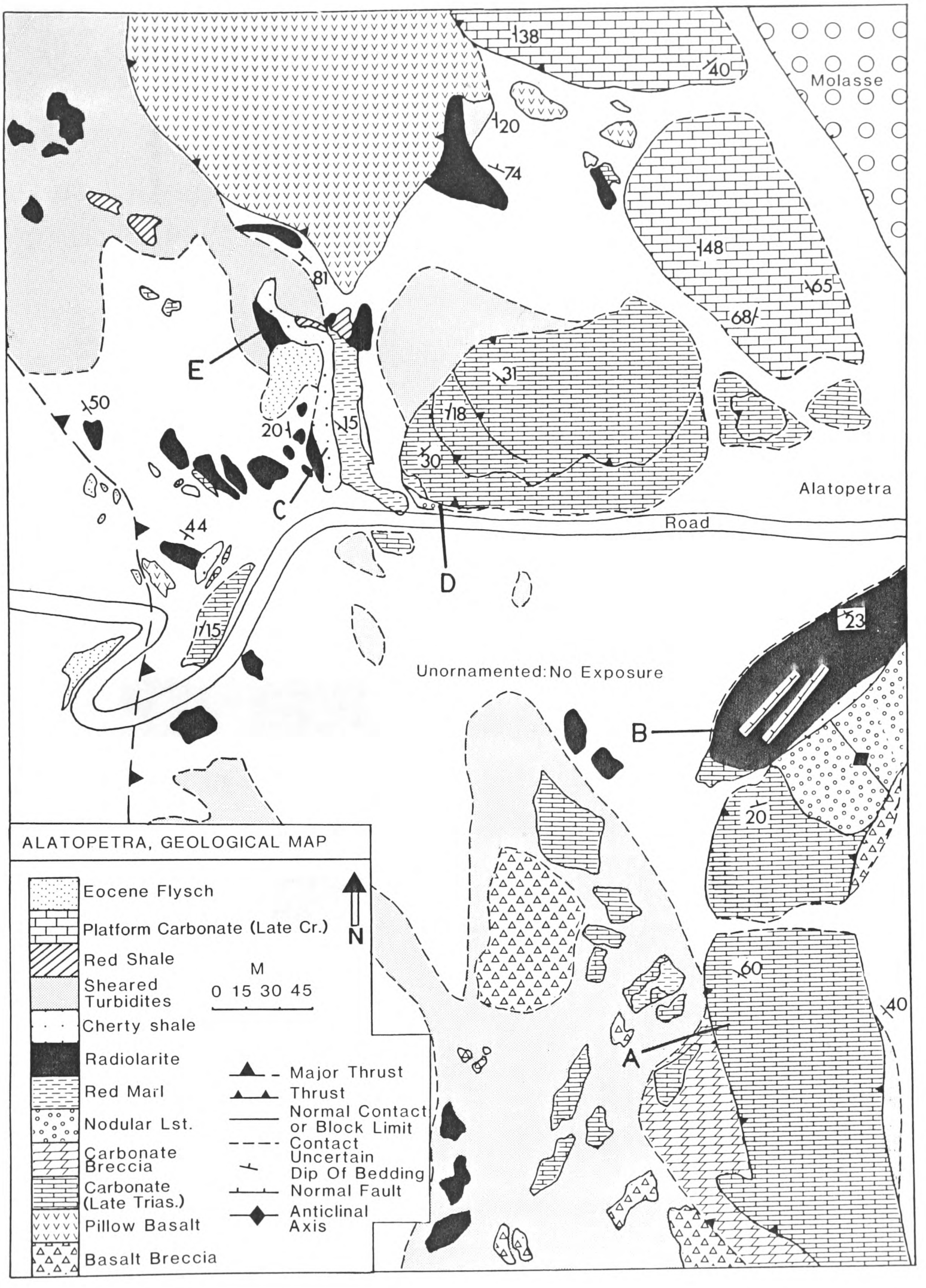

Fig. 4.9 Geological map of the Avdella Melange in the area immediately W. of Alatopetra Village. Numbers refer to stratigraphic logs of melange blocks (Fig. 4.10).

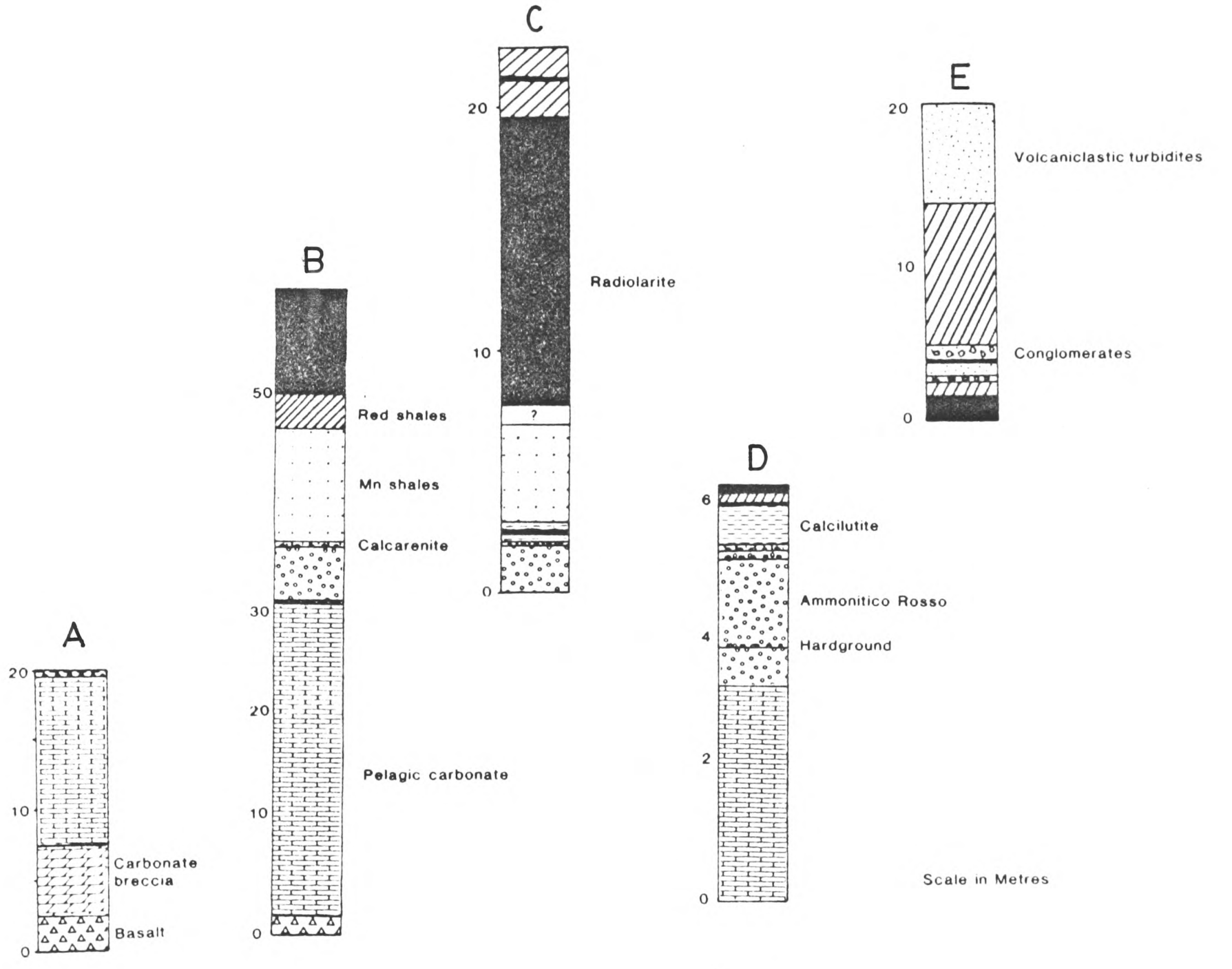

Fig. 4.10 Stratigraphic logs of individual sedimentary sequences preserved within melange blocks at Alatopetra (see Fig. 4.9 for localities).

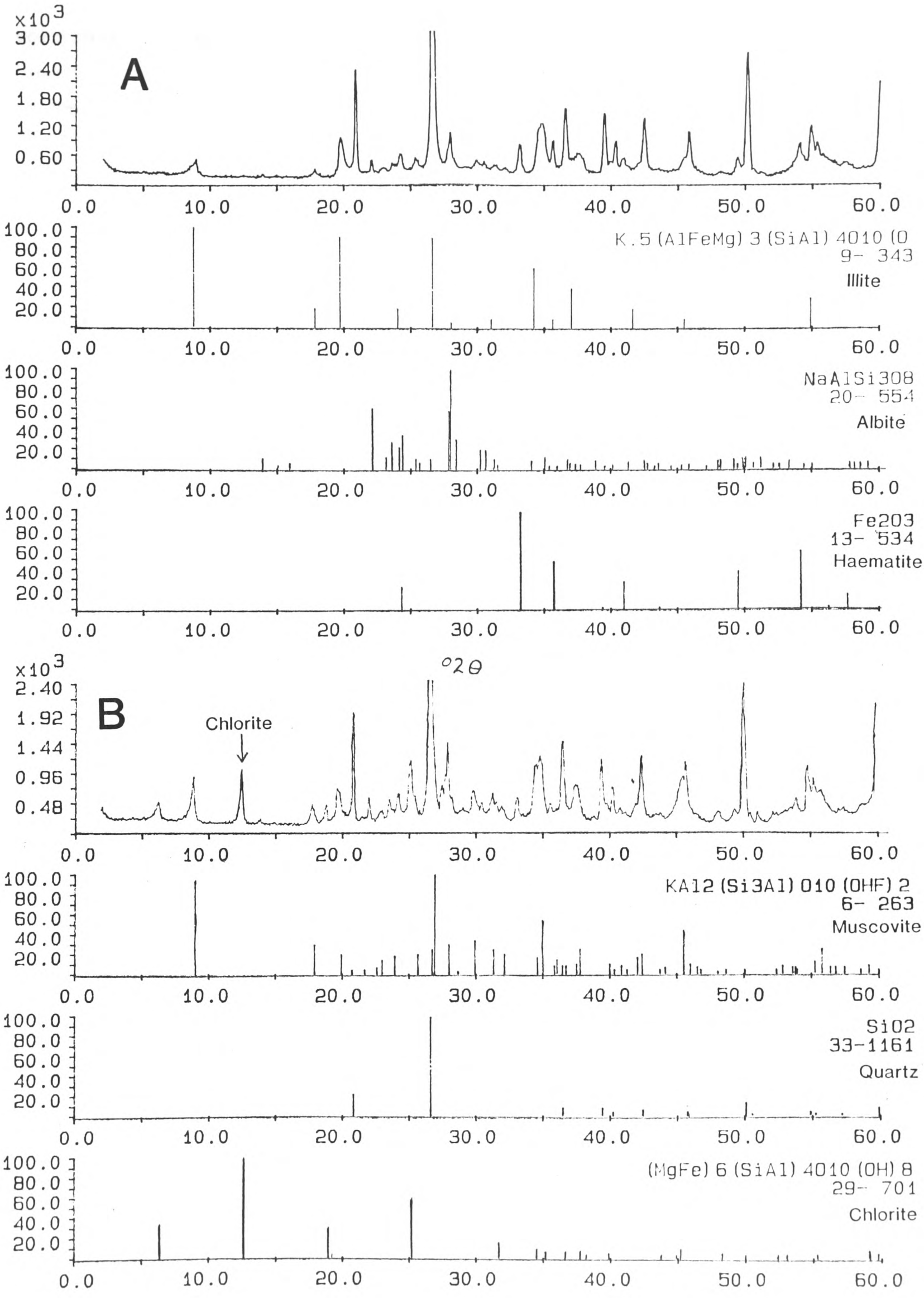

Fig. 4.11 X-Ray diffraction plots for the transition from shales with continentally-derived material (a), through to immediately overlying volcanically derived material (b), marked by the influx of chlorite (see Fig. 4.15).

volcaniclastic turbidites, containing thin, discontinuous, pelagic limestones, together with abundant black mudstones and manganiferous shales (Plate 4.1). The contact from apparently terrigenous mica-quartz-feldspar detritus to volcanic detritus (i.e. containing chlorite) is sharp. X-ray diffractograms for this transition are presented in Fig. 4.11, showing the incoming of abundant chlorite into the sediment sequence. The turbidites contain phacoidal arenaceous beds, which contain basalt and chert clasts in abundance. Towards the top of the sequence, several radiolarite horizons, up to 5 m thick, are present. The uppermost of these was dated, using radiolaria, as being of Late Callovian to Late Oxfordian age (see below; and Appendix 7). This succession thus demonstrates a transition from continental to volcanic-derived deep-sea sediments, not observed elsewhere.

c) *Tsouka Mountain*

At this locality (Tsouka, S.W. of Vovousa; Fig. 4.1), disrupted sheeted dykes and pillow lavas of mainly WPB affinities (Plate 4.7; see above) pass, with some tectonic disruption, up into interbedded volcaniclastic turbidites, thin pelagic cherty limestones, radiolarites and siliceous mudstones. Also present are continentally-derived siliciclastics and ammonitico rosso-type carbonates (as slide blocks). Further up the sequence, a 20 m-thick channelised carbonate unit cuts erosively into basaltic-derived sediments. Several of the dykes cross-cut red-brown pelagic carbonate and recrystallised radiolarites, with well preserved chilled margins (Plate 4.7). These radiolarites have been dated as Late Triassic using radiolaria (Jones et al. in prep; see below). Additionally, lava units of WPB-type occur as contemporaneous sheets within the turbidite sequence. Melange olistolith blocks at this locality contain clasts of pink and grey pelagic carbonates, with obtrusive blocks of basalt, up to 1 m in length (Plate 4.7).

d) *Liagkouna Mountain*

At Liagkouna Mountain, a coherent melange sequence comprises coarse-grained debris flow units ("olistostromes"), and finer-grained

turbidites (Fig 4.8, section 3). This sequence contains clasts of many of the lithologies of the Avdella Melange, including quartzo-feldspathic sandstones. The turbidites and olistostromes are found both as well-bedded sequences (e.g. N.W. Liagkouna, Fig. 4.1), and as disrupted tectonic blocks elsewhere in the melange (e.g. E. Kalivia Kerasias, Fig. 4.1). Clasts of basalt (WPB-and MORB-type lava clasts appear to dominate), chert and pelagic limestone, up to 40 cm in diameter, are common. Thin sections reveal gabbro, dolerite, vesicular phyric basalt, pyroxene crystals, serpentinite, brecciated basalt, quartz-arenite, pink and grey micritic limestone, chert and calcified chert. This sequence also contains a 80 cm-thick carbonate turbidite unit, containing rare clasts of gabbro, basalt and chert at its ruditic base, and grading-up into fine grained carbonate. This carbonate unit also contains a variety of shallow-water-derived bioclasts. These include abudant algal thalli, brachiopod valves and echinoid fragments.

An interval of bedded radiolarite (11 m-thick; Fig. 4.8) is present within the sequence, presumably representing the background pelagic sedimentation at this time. This is dated as Late Triassic (Jones et al. in prep; see below). As mentioned above, radiolarites from within similar, but more tectonised turbidites, 300 m to the north, also contain a Late Triassic fauna.

e) *Smolikas Mountains*

Well-bedded, undeformed turbidite sheets are exposed at Polis in the western part of the Smolikas range. Here extensive (several hundred m^2) sedimentary fans of volcaniclastic and pelagic sediment (Plate 4.8), contain graded rudaceous and arenaceous units (1-2 m thick), interbedded with haematitic, siliceous and manganiferous shales and marls. Fine-grained sediments analysed by XRD from this locality revealed and the presence of chlorite, quartz, albite and haematite.

f) *N.W. Perivoli*

In the Valiara valley and in surrounding areas to the northwest of Perivoli, several exposed sections of melange volcaniclastic turbidites are

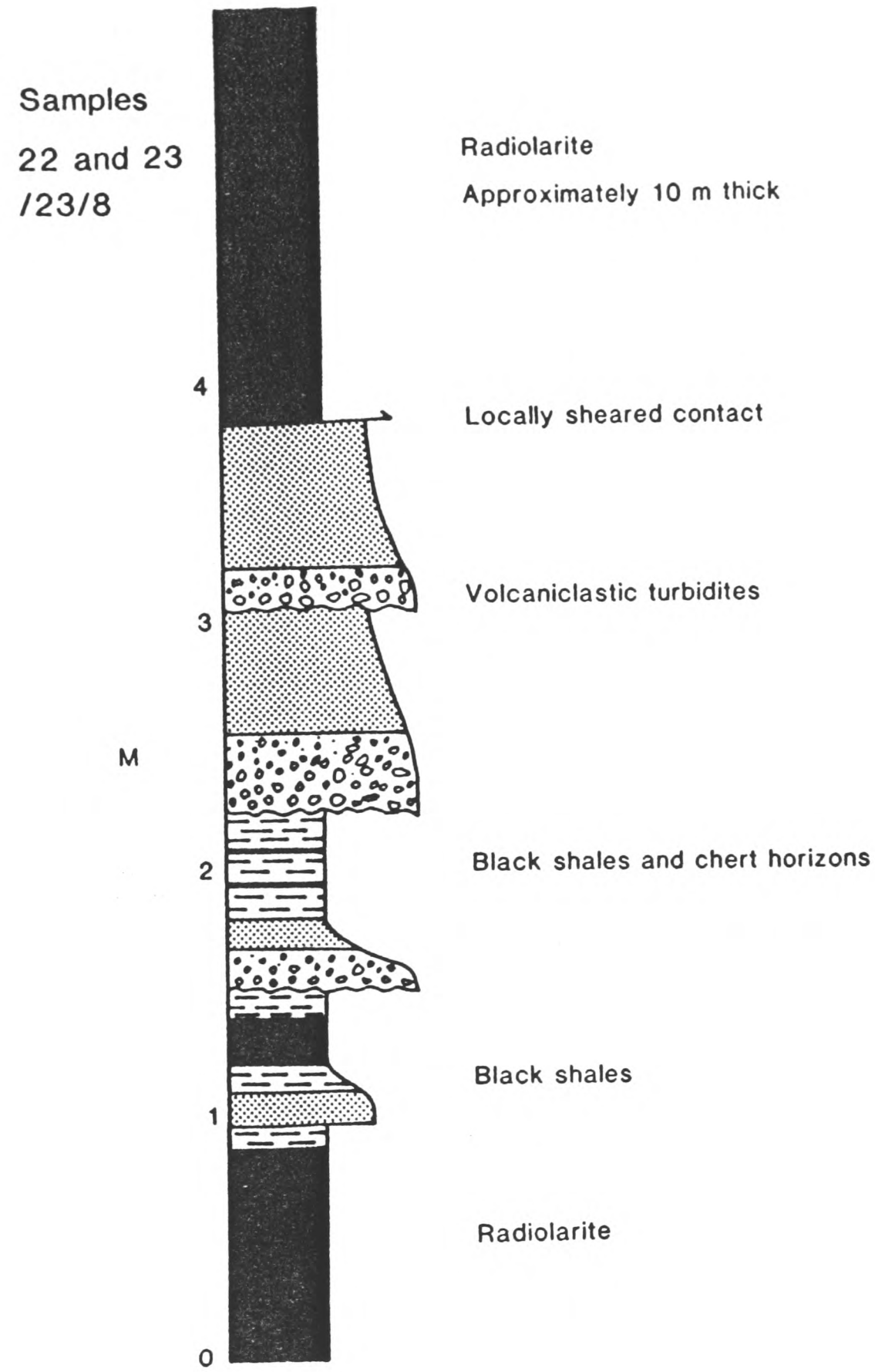

Fig. 4.12 Stratigraphic log of a melange volcaniclastic turbidite block at the Aspropotamos Bridge, Perivoli (Fig. 4.1). Samples refer to radiolarian cherts which yielded an age of Mid to Upper Jurassic (see text for further detail).

found (Plate 4.8). This region was mapped by McCaig (1978; unpublished data) who later published an outline description of some of the sediments present (Kemp and McCaig, 1984). The clasts in the debris flow units can sometimes be lithologically correlated with large blocks within the melange. For example, a clast of distinctive algal limestone depositionally overlying gabbros at Avdella (see above), was discovered in a debris flow, north of Perivoli (Fig. 4.1). One basic extrusive clast, 2 m in diameter, was analysed from this debris flow and found to be of boninite series volcanic (BSV) affinites. This implies that these sediments were deposited after the Pindos ophiolite was formed, as boninitic volcanics are the last igneous intrusive event found within the ophiolite sequence. This is backed-up by new age data (see below), which suggests that these volcaniclastics were deposited in post-Bathonian times.

The olistostromal sequences exposed here show evidence of soft-sediment deformation structures, as described by Kemp and McCaig (op. cit.; see Chapter 7). They quote the occurrence of slump folds, and slump horizons with slide blocks. Sediments from the Valiara valley also include horizons where limestone blocks lie in a black shale matrix. Both the carbonates and the shales show evidence of deformation before lithification, perhaps in overpressured water-saturated sediment. The limestone blocks have boundary indentations and pinch and swell-type structure. The shales may show a "scaly" fabric caused by planar alignment of clay minerals. Similar structures are seen, for example, in the accretionary belts of Japan (e.g. Shimanto Belt; Pickering et al. 1988). Microfossils from melange turbidites of this type were dated as Mid-Late Jurassic (Terry 1975) at one locality in the southern area (near Panaghia; Fig. 4.1).

4.4.2 Quartzo-feldspathic turbiditic sediments

In several areas, the Avdella Melange contains thrust-bound coherent turbidite sequences, composed of terrigenous, fine-to medium-grained, carbonate-cemented sandstone and shale. Along the Aspropotamos valley at Kokkina Litharia (S.W. Liagkouna; Fig. 4.1) these sequences are locally up to 150 m thick. Fine rudites and coarse arenites are present in individual beds up to 1.5 m thick, which display extreme

layer-parallel-extension, shearing and folding (see Chapter 7). The clasts include fine-to medium-grained plagiclase-phyric acidic volcanics and intrusives, quartzose schists and other quartzo-feldspathic metamorphic clasts, and also re-eroded clasts of quartz arenite (Plate 4.3). The metamorphic clasts show evidence of a complex deformational history, and include polycrystalline quartz with sutured grain boundaries and undulose extinction, and kink-folded quartz schists. Rare epidote grains, and more abundant chlorite are present in the matrix. The clasts are mostly angular to sub-angular, but some well-rounded smaller quartz clasts were discovered. A calcite cement is present in many of the samples studied, with individual calcite plates up to 3 mm in diameter. The clasts may also have clay rims, or more commonly clay is combined with carbonate in the matrix. Siltstones and shales are present as interbeds. X-ray diffractograms of these shales, show the dominant presence of quartz-feldspar and white mica. Plant material is present within the hemipelagic shales. These sediments are intruded by basic sills at this locality (see 4.3.2 above).

More usually, these successions form part of the melange matrix, and are found as blocks or poorly preserved thrust slices between basalt thrust sheets of inferred Triassic age (e.g. at Stragopetra; Fig 4.1). These turbidites are also spatially associated, and sometimes interbedded with, recrystallised radiolarites, although they have not been found in depositional sedimentary contact with the basalts. Blocks and thin-bedded sequences of similar lithologies to those described above, are common in the melange across the region. These sediments are probably the protoliths for the metaquartzites of the metamorphic sole. Only one thin rudaceous horizon (20 cms thick) has so far been encountered (N.W. of Avdella, Fig. 4.1). Basalt, gabbro (ophitic dolerite) and chert fragments are extremely rare. Pyrite crystals up to 5 mm in diameter, are found in arenites from Avdella (Plate 4.3). They are grown around several individual quartz clasts, and they suggest that the turbidites were perhaps originally deposited beneath the Carbonate Compensation Depth in some cases.

A cathodoluminescence study of specimen 14/23/8 showed an abundance of brownish luminescing metamorphic quartz, containing small zircons and apatites. Some of the schistose clasts were calcified

along the foliation during the cement phase. Feldspars are generally greenish suggesting Mn substitution for Ca has taken place.

In summary, these sediments are distal turbidite sequences composed of quartzo-feldspathic grains derived from a granitic and/or metamorphic source area, presumably the basement of the Pelagonian Zone, to the east. They probably pass upwards into radiolarites of Late Triassic age. A similar story has been described from the Oman Mountains (Cooper 1990), where continentally-derived sandstones pass upwards in to Late Triassic radiolarites (Zulla Formation, Hamrat Duru Group, Jebel Misht area, central Oman Mountains).

4.5 OLISTOLITH BLOCKS OF THE AVDELLA MELANGE

The Avdella Melange contains a variety of olistolith blocks, which generally consist of the more competent lithologies present such as carbonates and radiolarites. These blocks are too numerous to document individually, and only representative lithological varieties will be mentioned. The olistoliths have been classified into their probable depositional environment of formation for the purposes of description. In general, redeposited sediments (turbidites) and pelagic sediments dominate, but some important occurrences of shallower-water sediments are also found. The olistoliths are believed to represent Mid-Late Triassic to Late Jurassic sediments, but the ages are, in general, not well known. The Melange also contains Cretaceous olistolith blocks, which are described in Chapter 5.

4.5.1 Platform and platform margin sediments.

Sediments of shallow-water facies are comparitively rare within the Avdella Melange, compared to the abundance of these sediments found on the now adjacent Ionian and Pelagonian carbonate platforms (Brunn 1956). Several interesting occurrences of shallow-water sediments of Triassic age exist. Jurassic shallow water carbonates are not present within the melange, but are found within the metamorphic sole (Chapter 3). Near the village of Panaghia (Fig 4.1), a fossiliferous olistolith block of Late

Triassic age (after Marcoux, quoted in Pichon and Brunn 1985) contains current-sorted bioclastic carbonate beds rich in brachiopods (Rhynchonellids and Terebratulids, listed in Brunn 1956), and other shallow water material. Semi-circular mounds of algal material (stromatolites) are also present. In thin section, algae and brachiopod valves are abundant. Also present are benthic foraminifera, corals and sponges. Clasts of micritic carbonate with fenestrae are present, within a more sparitic matrix containing a greater proportion of bioclasts. This shallow-marine carbonate was deposited therefore in an an off-reef or slope environment.

Isolated out-of-situ blocks discovered in the Venetikos River valley west of Agios Nikolaos church (Monahiti), contain large Megalodontid bivalves, characteristic of Triassic shallow-water carbonates throughout Alpine Tethys. These occur in white fine-grained carbonates showing internal bioturbation structures (diplocraterion-type with internal spreite, and a local pelletoidal carbonate infill). The bivalves are typically 6-8 cms in length, with a characteristic heart-shape cross-section.

North of Samarina, carbonate blocks several tens of metres in diameter contain localised coral build-ups, of presumed Late-Triassic age (Plate 4.8). These blocks occur in thin melange exposed in this area beneath harzburgitic peridotite of the Dramala Complex, and are probably related to similar blocks described from the Loumnitsa Unit (Chapter 3).

4.5.2 Slope and pelagic sediments

The majority of the sedimentary olistoliths found within the Avdella Melange are of turbiditic or pelagic origin. Commonly these are carbonates, but radiolarites are also found as individual blocks, or interbedded with the carbonates. The most common lithology present is thinly-bedded, pink or light grey micritic carbonate. These sediments are found in association with a variety of other carbonate sediments, many of which are redeposited. They are believed to have been deposited over a wide time interval (Late Triassic-Late Jurassic). For example, at some localities (e.g. Dovas; Fig. 4.1), the distinctive Upper Jurassic pelagic crinoid *Saccocoma* sp. is present, whereas elsewhere, Triassic bivalves are

common. More thickly-bedded, fine-grained carbonates with abundant replacement chert nodules are also present.

Thin-shelled bivalves (e.g. *Halobia, Posidonia;* Plate 4.9) are found within micritic carbonates, typical of the "filament limestones" described from other parts of Greece (Brunn 1956; Bernoulli and Jenkyns 1974; Green 1982). Radiolaria, usually recrystallised to calcite, are present in abundance within these sediments. Red haematitic marls from Avdella are laminated, recrystallised micritic rocks. Evidence for pressure-solution processes is provided by haematite-rich stylolites, which cross-cut the laminae. Rare benthonic foraminifera and shallow-water derived clasts, such as echinoid or algal fragments may also be encountered. Pelagic carbonates intercalated with basalts and hyaloclastites contain *Halobia* bivalve fragments, and spalled basaltic material, mainly volcanic glass (Plate 4.9). These sediments are also normally haematite-rich.

Pink and grey nodular limestones known as "ammonitico rosso" from other areas of the Alpine System are also present within the melange (Bernoulli and Jenkyns 1974). They are preserved within an intact sequence at Alatopetra (see above), and their stratigraphic position suggests they are of Late Triassic-Early Jurassic age. In other areas of the melange, this facies may be present as isolated small blocks (e.g. Avdella). Lithologicaly, the rocks consist of grey or pink fine-grained carbonate nodules (up to several centimetres in diameter commonly) within a haematitic clay-rich matrix. The nodules are joined along stylolitic pressure-solution contacts. The amount of carbonate in relation to the matrix varies considerably, more pelagic varieties probably containing greater amounts of clay. The nodules are commonly fossiliferous, with thin-shelled bivalves and radiolaria. Rare benthic foraminifera are present. These rocks may contain fragments of cephalopods (ammonites and belemnites), although more complete ammonite specimens were not discovered.

At the southern extremity of Kalivia Kerasias (Fig. 4.1), recrystallised red-brown ammonite-bearing haematitic marls contain ammonites of Mid-Triassic (Anisian-Carnian) age (M.K. Howarth pers. comm. 1990). The species present include *Sageceras* sp. *Monophyllites* sp. *Arcestes* sp. and *Michelinoceras* sp., an orthocone nautiloid. The section also

contains mildly metamorphosed carbonate breccias forming large (30 m) olistoliths. Other pelagic sediments, including cherts, red shales and marls, and interthrust basalts are also found here. North of this locality (W. of Rachi Kerasias; Fig. 4.1), several thrust and folded carbonate blocks are exposed. These include pink and light-grey thinly-bedded (5-8 cms) pelagic limestones, with rare red radiolarite interbeds. Similar facies rocks were discovered at Koleo, (N.W. of Perivoli; Plate 4.10).

At Tsouka (Fig. 4.1), an olistolith block debrite containing clasts of pink and grey micritic carbonates (up to 2 m), basalt (up to 60 cms) and chert are shown to be of likely Triassic age, by the presence of *Halobia*-type bivalves within the carbonate clasts. At this locality also, a Triassic turbidite sequence is found mostly tectonically overlying oceanic basement (see above).

Fine-grained carbonate clasts are extremely abundant within carbonate breccias in the melange. The breccias are typically clast-supported, and adjacent clasts have stylolitic contacts (Plate 4.10). Examples are found on Stragopetra mountain, where clasts contain thin-shelled bivalves, and are sometimes found with blocks of vesicular purple basalt, of Triassic age. Elsewhere, carbonate turbidites are associated with sediments of Jurassic age, and are found as part of deep-water radiolarite-black shale volcaniclastic sequences, often just beneath the greenschist rocks of the Loumnitsa Unit. In the Loumnitsa Valley (Fig. 4.1), clasts of compressed, elongated grey fine-grained carbonate are up to 50 cms in length (Plate 4.10).

Partially *in-situ* examples of pelagic carbonates are found at Liagkouna Mountain. There, cherty porcellanous limestones (Plate 4.10) occur as a bedded sequence, with associated ferruginous mudstones, volcaniclastic sediments and radiolarite. This limestone can be traced for several km along the western flank of the mountain.

At Aspri Petra (Fig. 4.1), carbonate breccias and fine-grained carbonate turbidites are found cross-cutting terrigenous clastic turbidites containing chert, basalt and serpentinite clasts. This probably represents a redeposition of slope carbonate material basinwards, during the Mid-Late Triassic.

The melange also contains abundant radiolarian chert (see below; Jones et al. in prep; De Wever 1989), often recrystallised and calcite-veined (e.g. at Alatopetra; Fig. 4.8, section 1; Fig. 4.10). The radiolarites are commonly associated with manganiferous and ferruginous shales (e.g. Perivolaki, Fig. 4.1). The radiolarite occurs as isolated blocks, as more extensive tectonic slices, and within conformable sedimentary sequences (e.g. Alatopetra, Plate 4.5; see above). It is regularly bedded (2-6 cm thick on average), generally red-brown, red or green, except where local reduction to light grey or green occurs has taken place, particularly along thrust planes.

One of the more abundant sediment types found as melange blocks are volcaniclastic sequences, similar to those described from Alatopetra, Valiara, and Smolikas above. At the Aspropotamos bridge near Perivoli, conglomeratic to muddy volcaniclastic turbidites are interbedded with radiolarites of Bathonian-Lower Callovian age (see below; Fig. 4.12), which therefore mainly post-date metamorphic sole formation, and pre-date the most likely age of ophiolite emplacement onto the continental margin. The turbidite units (Bouma Tb-e) are composed of ophiolitic detritus, including altered serpentinite, gabbro and chloritised and fresh basalt in abundance Plate 4.11). Angular to sub-rounded radiolarite clasts are extremely common. Angular quartz grains are also present, probably indicating involvement of Pelagonian basement at this stage. Each turbidite unit grades upwards into hemipelagic black shales, which have strong penetrative scaly fabrics, and are cut by sub-horizontal shears and thrusts. Some of the degraded serpentinite fragments contain mylonitic sygmoidal foliations, developed around chrome spinel porphyroblasts.

Other sediments to be found rarely within the melange include serpentinite breccias, which at one locality (S.W. of Alatopetra; Fig. 4.1) were found conformably overlying an amphibolite block in a sheared olistostrome sequence. In the western Smolikas Mountains, (Polis; Fig. 4.1), hydrothermal calcite and jasper forms the cement to ultramafic (mainly harzburgite) breccias, up to 20 m thick, found immediately beneath the Dramala Complex peridotites.

4.6 DIAGENESIS AND METAMORPHISM OF MELANGE SEDIMENTS

In general, the basaltic and associated sedimentary rocks of the melange have undergone only deep burial diagenesis. Often, particularly near the metamorphic sole, extensive areas of lower greenschist facies lava-sediment units may occur. The distinction of melange lithologies from greenschist facies rocks of the metamorphic sole is often difficult. At some localities (e.g. Agios Nikolaos, Monahiti; Fig. 4.1) pillowed and massive basalt with cross-cutting dykes, conformably overlain by thin, recrystallised pelagic limestones, red marls and radiolarites, are very similar to sequences found in the melange elsewhere. One 4 m-thick redeposited oolitic carbonate (containing rare serpentinite grains; Plate 4.12) from this locality, is similar to redeposited carbonates found at Alatopetra and Stragopetra (Fig. 4.1).

Cathodoluminescence studies of some melange carbonates revealed several generations of cement phases. For example, a calcarenite form Alatopetra (see Plate 4.6) contains a dark, poorly luminescent marine cement on echinoid and crinoid fragments, and a bright luminescent calcite cement, related to a vein network. Additionally, extra cements are found within a series of vuggy fenestrae. Diagenesis of melange carbonates is clearly a complex story, which would require greater study.

4.6.1 Illite crystallinity studies

To attempt to quantify the grade of metamorphism present within the melange sedimentary sequences, an illite crystallinity (reviewed by Frey 1987) study was carried out on almost 150 melange shales and other fine-grained sediments. The sediments were collected along a transect between Alatopetra village and west of Perivoli (see Fig 4.1), approximately along the Tertiary emplacement vector. The experimental method follows that of Weber (1972) and is given in Appendix 6. It essentially involves X-ray diffraction studies of a known grain size of sediment, and comparison to an external quartz standard. The crystallinity of the 10 Angstrom illite mica peak is dependent on temperature, and therefore an index of crystallinity is used to define low-temperature metamorphic gradients. Many of the samples collected contained some

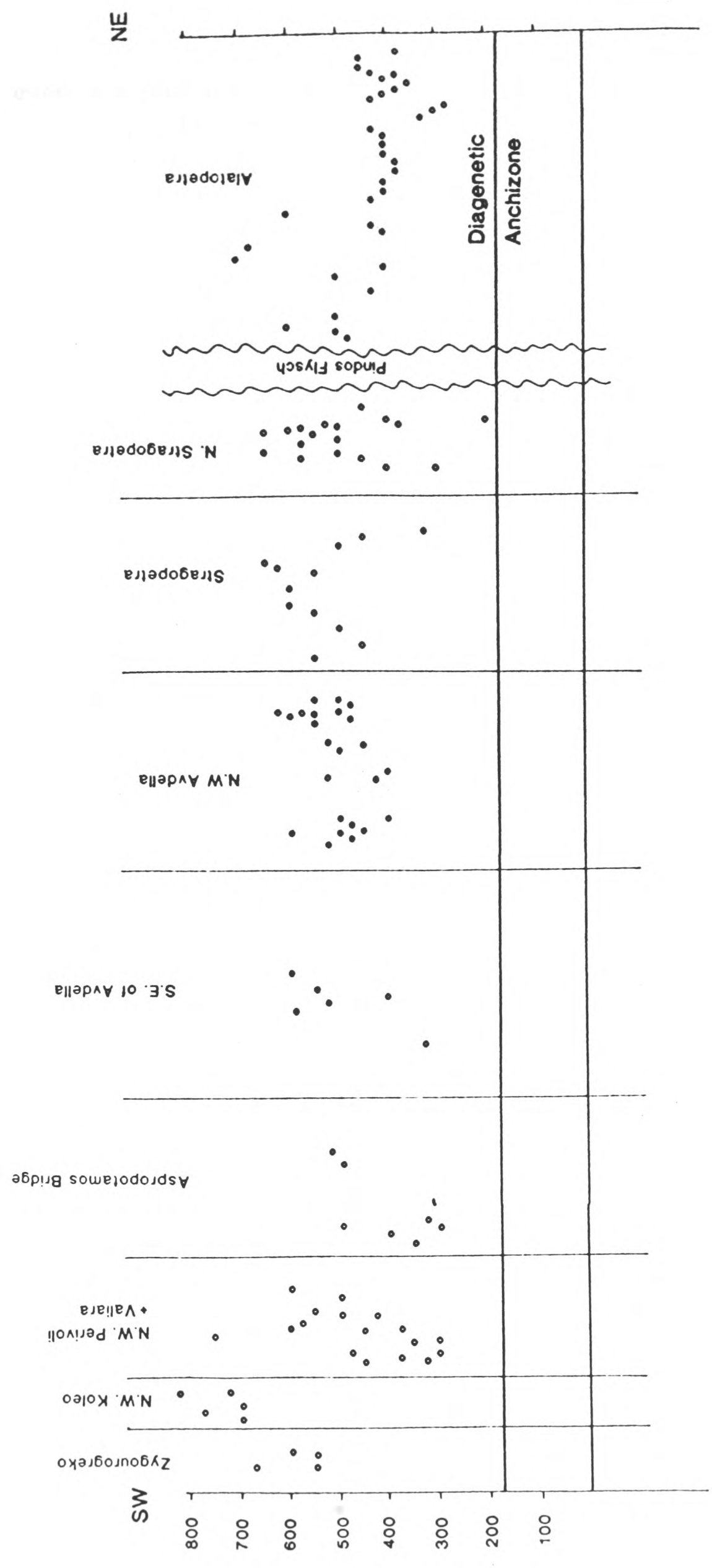

Fig. 4.13 Diagram showing the results of an illite crystallinity profile across the Avdella Melange. Localities are shown on Fig. 4.1. Note that due to field sampling difficulties, the samples are plotted at random within each grid for a particular locality, and therefore no spatial relationship exists between them. Comparisons of grade can therefore only be made between each major locality. See text for further discussion.

illite. However, a significant proportion of the samples were not of sufficient crystallinity to be measured, as only gave broad and indistinct peaks, more typical of illite-smectite mixed layer clays.

The results of this study are presented in Fig. 4.13. They show that the melange sediments are mainly in the high diagenetic grade of metamorphism, and therefore essentially unmetamorphosed. No samples reached the anchizone, which is defined at 175 Hb_{rel} (Kisch 1987), and characterised by relatively sharp, narrow diffractogram peaks. This suggests that the melange was not buried to great depth, despite being quite extensively thrust deformed, and therefore the preserved sequences were accreted at comparatively high levels.

The samples could not be collected continuously along the traverse, and so inferences about the position of metamorphic discontinuities related to faulting cannot be made. Only a general estimate of the crystallinities at any one locality are possible. For example, in the Tsouka area, near Perivoli, the values are higher than those obtained on Stragopetra, on average.

4.7 RADIOLARIAN BIOSTRATIGRAPHY OF THE AVDELLA MELANGE

A program of biostratigraphical dating of radiolarian cherts was initiated during an integrated study of the geological evolution of the Pindos ophiolite and its associated sedimentary sequences (Jones and Robertson 1990). As mentioned previously, evidence from south of Milea (Fig. 4.1; Plate 4.7) shows that the melange was transgressed by the Upper Tithonian (see Chapter 5). The overall objective was to establish the age range of radiolarites associated with the Pindos ophiolite, and to date more accurately the individual melange sequences present. The implications of these data for the Mesozoic evolution of this part of Neotethys will be considered in Chapter 8.

4.7.1 Regional correlation within Greece

An important aspect of the radiolarian age data is a comparison of the data obtained from northern Greece with the presumed synchronous, but generally lesser deformed, sedimentary and volcanic sequences of the Pindos and Sub-Pelagonian "tectono-stratigraphic" zones of central and southern mainland Greece (Aubouin et al. 1970). The Sub-Pelagonian zone comprises ophiolitic ultramafic and mafic rocks, usually of harzburgitic type (e.g. Othris, Vourinos, Euboea ophiolites; Fig. 4.14). A range of rift and early spreading-related volcanics and associated sediments, including radiolarites, are usually found in tectonic association with the ophiolites. Traditionally, the Pindos ophiolite and the Avdella Melange are considered as being part of this zone.

The Pindos Zone exposes mildly deformed, turbiditic and pelagic sediments, interpreted as continental margin and ocean basin sequences. Bedded radiolarite and other oceanic sequences from the Pindos Zone have been well described and dated previously (Dercourt et al. 1973; De Wever et al. 1979; Fleury 1980; De Wever 1982; De Wever and Origlia-Devos 1982a, 1982b; Green 1983; De Wever and Cordey 1986) providing an extensive data base. The Dio Dendra Group and the Pindos Flysch of the study area are considered as being part of the Pindos Zone.

4.7.2 Radiolarian biostratigraphy of the Sub-Pelagonian and Pindos Zones of central and southern Greece

Biostratigraphic work from the Pindos Zone has established with some precision the ages of the radiolarite intervals within that sequence. There, a thin Liassic interval (De Wever and Origlia-Devos 1982a), and a thicker Mid-Upper Jurassic interval (?Bajocian-Tithonian), the radiolarite series *sensu stricto*, are both present (De Wever and Cordey 1986). Within the Sub-Pelagonian Zone, Late Triassic radiolarites are associated with volcanic rocks and within sedimentary sequences in the Othris region (Fig. 4.14). Radiolarites of Norian age are found between pillow lavas (Tourla series, De Wever 1982; Ferriere 1982), and within sedimentary sequences (Loggitsion series, Ladinian-Carnian; Ferriere 1982). Kimmeridgian-Tithonian radiolarites are also found within the Othris area (Origlia-Devos

Fig. 4.14 Map of the Greek area showing the main occurrences of radiolarites, as mentioned in the text.

in Ferriere 1982). Southeast of Othris, on the island of Eubeoa, interpillow cherts contain an Oxfordian fauna (Baumgartner 1984). Additionally, an Oxfordian-Mid Kimmeridgian date was found in sedimentary sequences in northern Evvia (Baumgartner 1984; Ferriere 1986). In the eastern Peloponessos (Argolis Peninsula), radiolarites are of Mid Callovian or Early Oxfordian age (Baumgartner 1984).

4.7.3 Previous biostratigraphical studies in the north Pindos Mountains

The sedimentary sequences of the north Pindos Mountains are for the most part poorly dated. Previous biostratigraphic work in the region (Brunn 1956; Terry 1971, 1975; Terry and Mercier 1971) provided an outline of the range of sediment ages present (Late Triassic to Tertiary), mainly using rare macro-fossils and foraminifera. In particular, turbiditic sediments from the melange were dated near Panaghia (Fig. 4.1) as Mid-Late Jurassic (Terry and Mercier 1971), using calcareous microfossils.

4.7.4 Radiolarites of the Avdella Melange

The sediments of the Avdella Melange are assumed to have been deposited as the along-strike equivalents of the Sub-Pelagonian volcano-sedimentary sequence of the Othris and Euboea areas. They are, in turn, also interpreted as forming distally (i.e. to the present day NE) in relation to the passive margin sediments represented by the Pindos Zone (Ferriere 1982; Green 1983).

Radiolarites are most commonly found within the melange as blocks, due to their greater competence relative to other sediments, but they are also occasionally found within more coherent sedimentary sequences, where they are most able to provide useful age data.

The Avdella Melange contains sediments which differ markedly to those found further south, reflecting the contrasting tectonic regimes operating within the Pindos ocean during the Mesozoic. In particular, thick sequences of volcaniclastic turbidites, associated with interbedded radiolarites and redeposited carbonates occur (see above). These

volcaniclastic sediments are lithologically diverse, but are generally rich in detritus which includes serpentinised ultramafic material, basalt, gabbro, pelagic limestone and radiolarite. However, not all of this detritus was necessarily derived from emplaced ophiolites. Material from older, pre-ophiolite emplacement sequences (e.g. ridge flank breccias, trench turbidites) may also be present. In the southern Pindos Zone, ophiolitic detritus is found only in Lower Cretaceous sediments (Green 1982; Fleury 1980).

4.7.5 Field collection of samples, and laboratory study techniques

The samples collected were initially scrutinised in the field, with the aim of collecting specimens which contained unrecrystallised radiolarian tests. However, many of the samples collected (approx 90) were barren due to recrystallisation, and only 15 samples yielded identifiable radiolaria. The radiolaria were extracted from their host cherts by successive etching with very dilute hydroflouric acid, according to standard processing techniques (Pessagno and Newport 1972; De Wever et al. 1979; De Wever 1982). The residues were then viewed under reflected light, the individual radiolarian tests were picked, and subsequently studied and photographed under the Scanning Electron Microscope in Edinburgh (Cambridge Instruments). Identification to species level was then undertaken where possible. Thin sections of some of the more critical samples collected unfortunately did not reveal any further identifiable forms.

4.7.6 Synthesis of the radiolarian ages.

Six samples yielded radiolaria of Mid-Late Triassic age, (Carnian-Norian; Plate 4.13; see Appendix 7). Three of these samples are from the same locality (Veneticos River valley at Agios Nikolaos; Fig. 4.1), and provide good age control for this locality. Characteristic genera include *Capnuchosphaera* sp. and *Xiphotheca cf karpenissionensis*. Another other locality (S.W. Kandila hill, Fig. 4.1) provides a probable Late Triassic age for turbidites in this area. Other localities where radiolaria of this age were found include Tsouka Mountain (S.W. of Vovousa; Fig. 4.1), where

radiolarites conformably overlie pillow basalts, and both are intruded by later basic dykes (see above). At Armata, slices of radiolarite interthrust with basalts in the Avdella Melange also yielded Triassic forms (Plate 4.13).

The second interval of northern Pindos radiolarite deposition recorded by the fauna is Mid to Late Jurassic (Plate 4.14), comparable to the radiolarites of the Pindos Zone of central and southern Greece (De Wever 1989). The radiolarites of this age in the study area were associated with turbiditic sediments, mainly of ophiolitic derivation. The melange block from Perivoli (Fig. 4.12) yielded a well preserved fauna from four samples, which can be assigned to an age of Bathonian-Lower Callovian, by the presence of *Unuma echinatus* and *Hsuum maxwelli* gp.

The most abundant radiolarian fauna was obtained from a bedded radiolarite from northeast of the village of Perivolaki, within a folded but coherent melange turbidite sequence (Fig. 4.15). This sample (200D/88) came from near the top of this sequence, and provided an age of Late Callovian to Late Oxfordian, based on *Tripocyclia trigonum* and *Hsuum maxwelli*.

A melange radiolarite block from Megali Pedias (25/23/8) yielded *Tricolocapsa plicarum*, with a range of (Bajocian?) Bathonian-Lower Middle Oxfordian. Another block from Milea (107/88) contained *Hsuum maxwelli* gp. of Bathonian-Oxfordian (possibly earliest Kimmeridgian) age. A further melange block from this locality (100/88) yielded a wide age range of Bajocian to latest Tithonian, based on *Hsuum brevicostatum*. Similar wide-ranging Late Jurassic ages were gained from a radiolarite imbricate slice from Kodro Mountain (120/88), and from metamorphosed radiolarite interthrust, and partly overlying basalts at the confluence of the Aspropotamos and Venetikos Rivers (1/20/8/A). Cherts from the Kokkina Litharia area (8+9/24/8) provided two contrasting ages of radiolarite (?Bajocian-Oxfordian based on *Eucyrtidellum* Sp) and Barremian-Coniacian (*Pseudodictyomitra lilyae*; Plate 4.15).

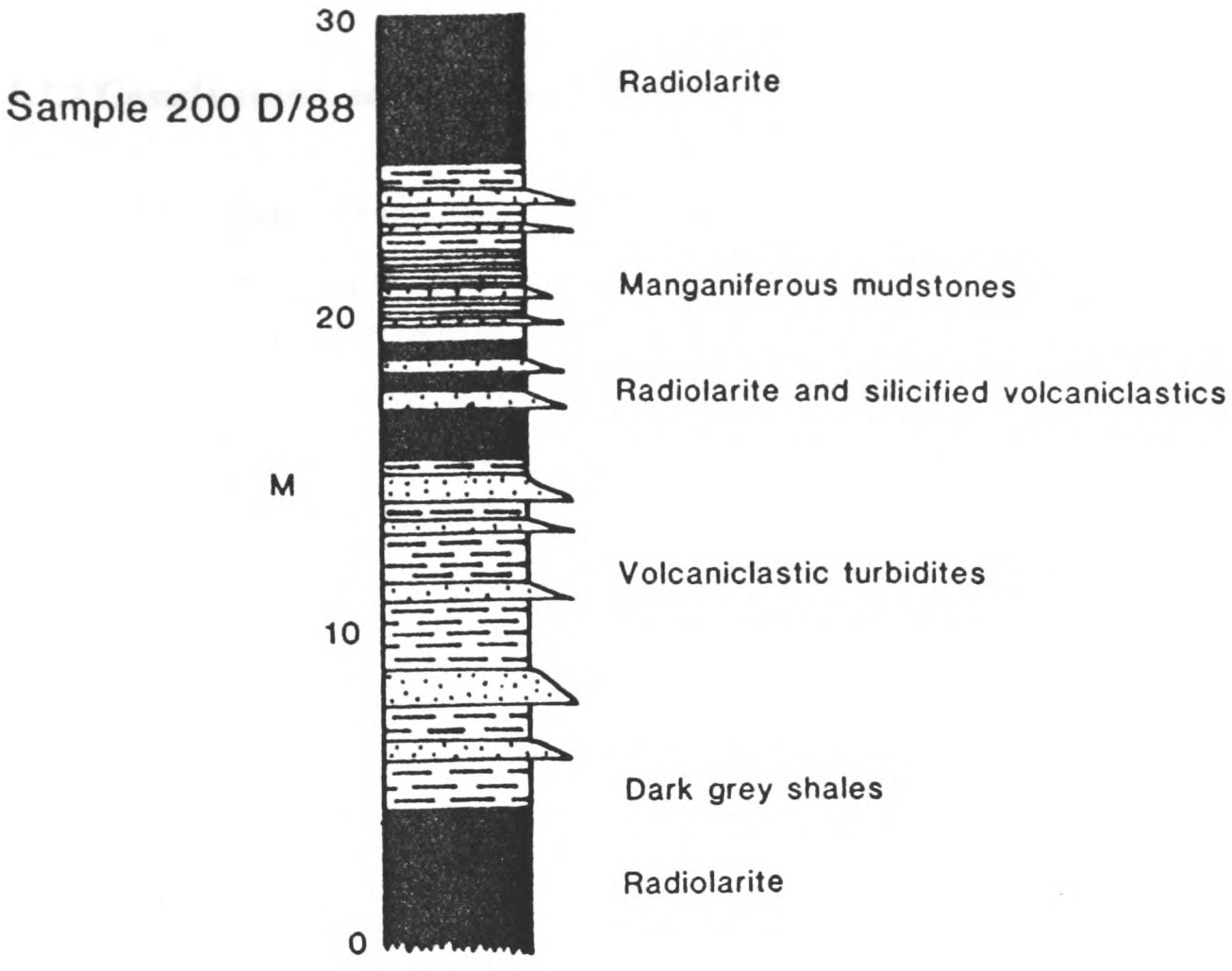

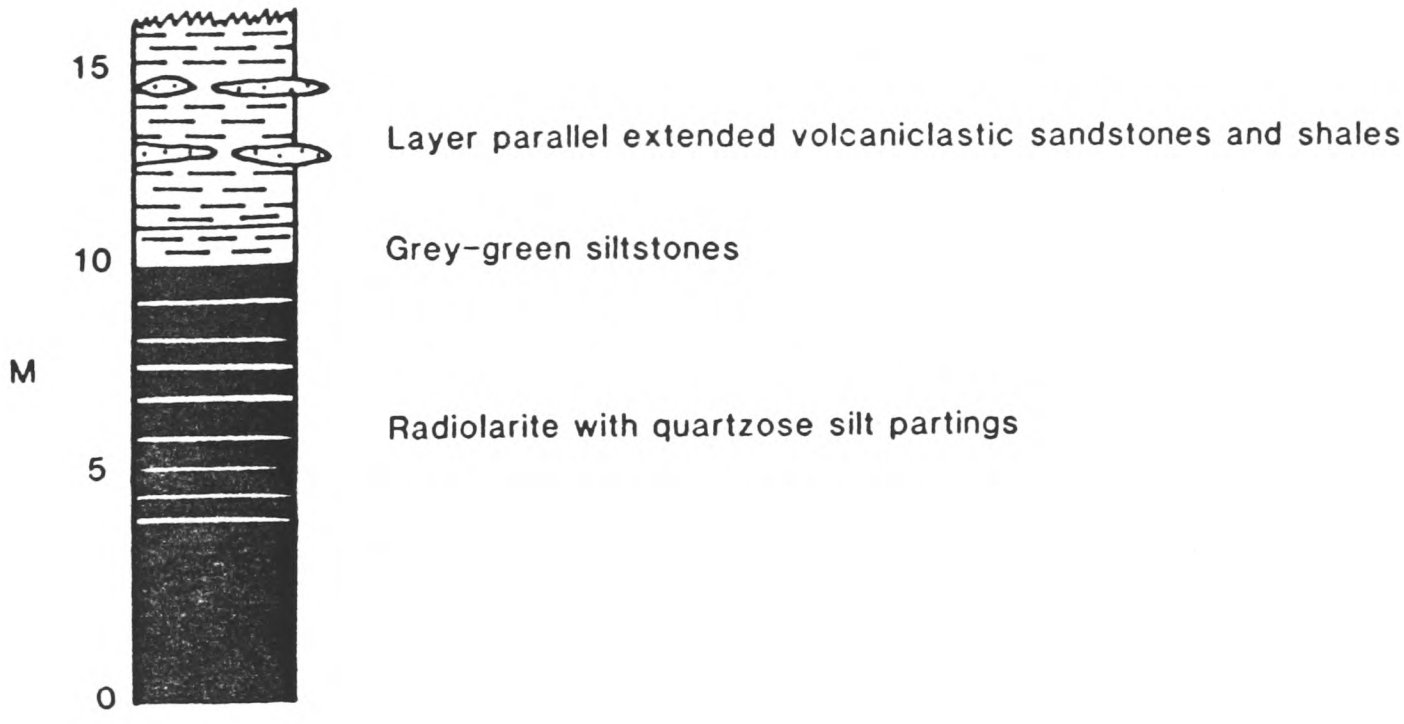

Fig. 4.15 Sedimentary log of turbidite sequences exposed on the north bank of the Potamouli River, 1 km N.W of Perivolaki Village. Note position of dated radiolarite sequence.

4.7.7 Conclusions, regional significance and synthesis of the age data

The data presented show that the Avdella Melange contains radiolarites of comparable ages to those of the Pindos and Sub-Pelagonian zones in central and southern Greece; ie. Late Triassic and Mid to Late Jurassic. This suggests that they all formed part of one interconnected ocean basin during the Mesozoic (Dercourt et al. 1986; Robertson et al. in press). However, in the north Pindos area, radiolarites occur within very different sedimentary sequences, particularly during the Mid to Late Jurassic. The abundance of mafic, and sometimes ultramafic detritus in the Avdella Melange sediments contrasts strongly with sediments of similar ages elsewhere. The data from the best constrained sequences (Perivolaki) suggest that radiolarite sedimentation first took place during the basin from Bathonian (also the time of formation of the metamorphic sole) at least until Oxfordian times, and possibly until the early Kimmeridgian. As Kimmeridgian sediments are found transgressing the emplaced Vourinos ophiolite (Mavrides et al. 1979), this data would seem to constrain the emplacement of the Pindos and Vourinos ophiolites to within the Kimmeridgian.

4.8 INTERPRETATION OF THE AVDELLA MELANGE

The Avdella Melange lithologies are interpreted as representing the Mid Triassic to Late Jurassic volcanic and sedimentary components of a Tethyan oceanic basin. This basin was finally closed during the Tertiary (Chapter 8), causing extensive deformation of these sequences (Chapter 7). Prior to this, however, the melange is believed to have been initially mixed as an accretionary complex at a destructive margin, during the formation of the Pindos ophiolite (Chapter 8). The following interpretation is based on a model of the Pindos ocean formed westward of the Pelagonian microcontinent. This westerly margin remained passive, until collapse prior to ophiolite obduction in the Late Jurassic. The sedimentary facies, coupled with the volcanic geochemistry and microfaunal age data, allow reconstruction of parts of this passive margin, and the more distal ocean basin settings which mainly comprise the melange. The melange is believed to have formed as the result of tectonic accretion within a subduction zone, which led to thrust-related deformation at low

temperatures and moderate pressures. The structural evolution of the melange is summarised in Chapter 7.

4.8.1 Triassic depositional environments

Triassic depositional environments, based on facies and age data summarised above, are represented in Fig. 4.16. The oldest sediments present in the melange may be quartzo-feldspathic turbidite sediments, associated with alkaline and transitional basalts, derived during the early stages of rifting by erosion of exposed continental basement, probably that of the Pelagonian Zone. Shallow-water carbonates (e.g. Megalodontid limestones) are interpreted to have formed on the margins of the Pelagonian microcontinent, where widespread platform carbonate deposition was taking place (Brunn 1956). Thickly-bedded, fine-grained carbonates (e.g. at Alatopetra) are believed to represent off-margin facies, intermediate between the carbonate platform and the true pelagic facies. These are sometimes overlain by ammonitico rosso-type limestones, interpreted as having formed within relatively shallow water depths (i.e. up to 800 m in the Greek area, assuming non-ideal subdidence, 1000-1500 m if ideal; Jenkyns 1980). They probably developed on subsiding horst blocks, evidenced by preserved palaeo-extensional faults, and may also have been the source of carbonate breccias and turbidites shed during this periodic faulting.

Thinly bedded pink and grey micritic carbonates (e.g. *Halobia* and ammonite-bearing limestones), commonly with replacement chert, formed a more distal facies, and may represent redeposited peri-platform ooze, or fine-grained carbonate turbidites (Robertson et al. 1990). Radiolarites probably formed in the deepest part of the basin (perhaps 2000-3000 m), and are found interbedded with the volcaniclastic turbidite sequences (e.g. Liagkouna, Kalivia Kerasias), sometimes with an intact volcanic basement. These Late Triassic turbidites are interpreted as having formed as a result of the initiation of oceanic spreading, at the centre of the developing Pindos ocean. This implies that a strong sea-floor topography was in existance through much of the Late Triassic and Early Jurassic. They may also have been partly derived by the collapse and redeposition of material from pre-existing carbonate-capped volcanic edifices or seamounts, during

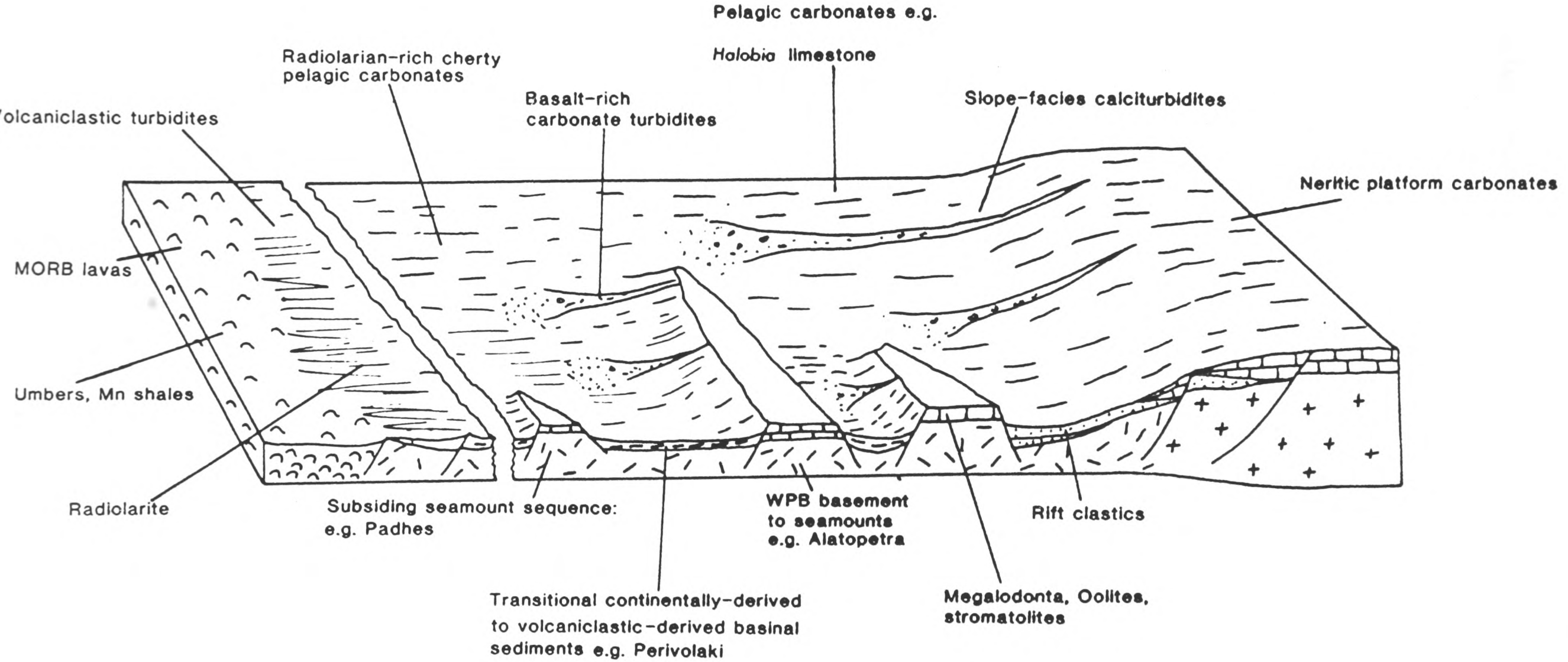

Fig. 4.16 Palaeogeographic reconstruction of the Pindos Ocean and Pelagonian continental margin during the Late Triassic-Early Jurassic, based on sedimentary facies present within the Avdella Melange.

extension. Volcaniclastic sediments of a similar age and inferred origin are present in the Godene Zone of the Antalya Complex (S.W. Turkey; Robertson and Woodcock 1981). Spreading processes at this time also account for the presence of metalliferous sediments, found in association with melange volcanic sequences (e.g. near Armata; Robertson and Varnavas 1990).

4.8.2 Jurassic depositional environments

The Jurassic facies of the melange (Fig. 4.17) show evidence of continued subsidence and deepening of the basin. Many of the Jurassic sediments are therefore of deep-water (i.e. several thousand m) origin. Fine-grained sediments, including red haematitic siltstones and grey and black mudstones are ubiquitous in the matrix, together with large volumes of coarser-grained turbidites. Fine-grained carbonates with thin radiolarite interbeds, probably represent distal marginal facies at this time (e.g. at Kalivia Kerasias; Fig. 4.1).

Off-margin "high" sequences originally located closer to the platform, such as that found at Alatopetra (see above) and Padhes (Chapter 3), record the subsidence of a carbonate shelf or shelf margin through the CCCD in the Jurassic. It is also possible that these sequences were developed on true oceanic seamounts far into the ocean basin. The sediments found at Alatopetra are particularly significant, as they preserve a stratigraphy not found elsewhere, but which is in some ways comparable to sequences found further south in central Greece, and northwards in Yugoslavia. Triassic carbonates passed into ammonitico rosso facies nodular limestones (?Latest Triassic-Early Jurassic), which show evidence of slow or non-deposition, away from any sediment source areas. Ammonitico rosso facies carbonates are common in the Argolis area of southern Greece (Clift and Robertson 1990), and within the Pindos nappes of central Greece. The following sediments include thin, redeposited and pelagic carbonates and radiolarites, recording eventual transgression of the blocks. These sediments may be similar to (much thicker) redeposited carbonates sequences found in the Othris area (Meterizia Formation of the Poulia sequence; Price 1977).

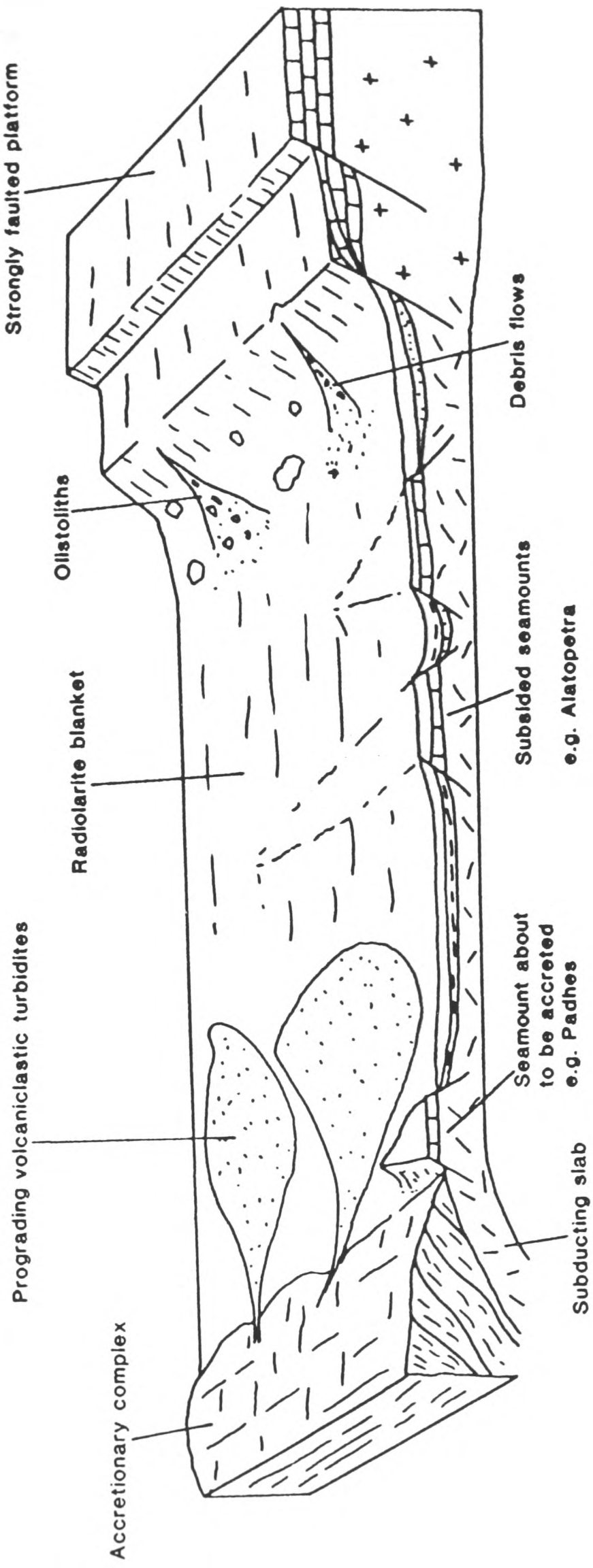

Fig. 4.17 Palaeogeographical reconstruction of the Pindos Ocean during the Mid to Late Jurassic, based on sediments from the Avdella Melange.

The overlying interval of manganiferous mudstones and cherty shales marks the end of carbonate sedimentation on these blocks. Manganiferous shales underlying radiolarites are also characteristic of the Pindos Zone sedimentary sequences of central Greece (Pelite de Kastelli, or Kastelli mudstone; Aubouin 1959; Fleury 1980; Baltuck 1982; Green 1983). The transition into radiolarites present in the south is not, in general, associated with a subsequent influx of volcaniclastic sediments, such as those found at Alatopetra. The Pindos Zone radiolarites probably range from Bathonian to Tithonian (De Wever and Cordey 1986), indicating a similar age for some of the melange volcaniclastic sequences. A remarkable variety of sediments are therefore recorded at Alatopetra, recording a complete, but perhaps somewhat atypical sequence, from Late Triassic to Late Jurassic times.

Elsewhere, thick volcaniclastic turbidite sequences dominate. This is well displayed at Smolikas, where extensive submarine fan sequences composed of ophiolitic detritus and radiolarite clasts are found. At certain localities, redeposited carbonates are also abundant in the Late Jurassic, rich in displaced shallow-water carbonate detritus, such as algae and corals (e.g. Kokkina Litharia). These usually conglomeratic carbonates typically occur as channelised bodies, and sometimes are seen to erode into volcaniclastic turbidites. They are interpreted as having been shed from within a relatively deep-water environment, perhaps from seamount-type features. They may alternatively have originated more proximally from off-margin highs, during collapse initiated by ophiolite obduction (Fig 4.18).

The basement of the Pindos ocean basin, as portrayed by the Avdella Melange is comprised of alkaline to tholeiitic basalts, of WPB, transitional to MORB and N-MORB chemistries (Kostpoulos 1989). These volcanics and intrusives record tectonic environments ranging from rifted continental through to oceanic ridges. In some places, this basement is still preserved beneath sedimentary sequences (e.g. Avdella, Alatopetra), but mostly it is interthrust and intersheared with the originally overlying sediments, losing the stratigraphic relationships in the process. At Tsouka, the first stages of advanced rifting, transitional to sea-floor spreading are documented. Basic dykes, of WPB and evolved MORB chemistry intrude Late Triassic pelagic sediments. Elsewhere, N-MORB volcanics present are

chemically indistinguishable from volcanics forming the basal units of the Pindos ophiolitic sequences (Kostopoulos 1989).

4.8.3 Model for the development of the Avdella Melange as a subduction-accretion complex

The Avdella Melange is believed to have developed by accretionary processes at a destructive plate margin, similar to modern day settings such as the Nankai Trough. One of the main reasons for this is the nature of the mixing of the melange lithologies, which are far more disrupted and tectonised than other thrust sheets. The melange also contains several deformational features which indicate that sediments were rapidly buried after deposition, and deformed at low temperatures (c.f. illite crystallinity studies) and moderate pressures (Chapter 7). The fact that the immediately overlying units of the Pindos ophiolite contain volcanic rocks which can only have developed above a subduction zone, also adds weight to an origin as an accretionary complex.

The type of situation in which the Avdella Melange may have been accreted is shown schematically in Fig. 4.18. The melange is essentially interpreted as representing oceanic basement (mainly basalts) and cover sediments, which were scraped from the downgoing slab during subduction. One interesting observation is that the melange basalts found immediately beneath the Aspropotamos Complex and its metamorphic sole, are distinctive pillow lavas with N-MORB and evolved MORB geochemical signatures. These lavas are interpreted as the first-accreted material during the initiation of subduction, and their chemistry suggests that this took place near a spreading ridge. At Samarina, these basalts are overlain by metalliferous sediments, and are associated with sheeted dykes. Subsequent accretion is believed to have progressively involved more oceanic crust and deep water sediments, particularly radiolarites, shales and redeposited carbonates, of both Triassic and Early Jurassic age. Resedimentation was also induced by this subduction, and some volcanic-radiolarite-pelagic limestone conglomerates and debris flows now found in the melange, may have developed as trench turbidites and slump deposits off the sediment prism (e.g. Valiara). Some sequences now found in the melange may also have been incorporated as seamounts during this

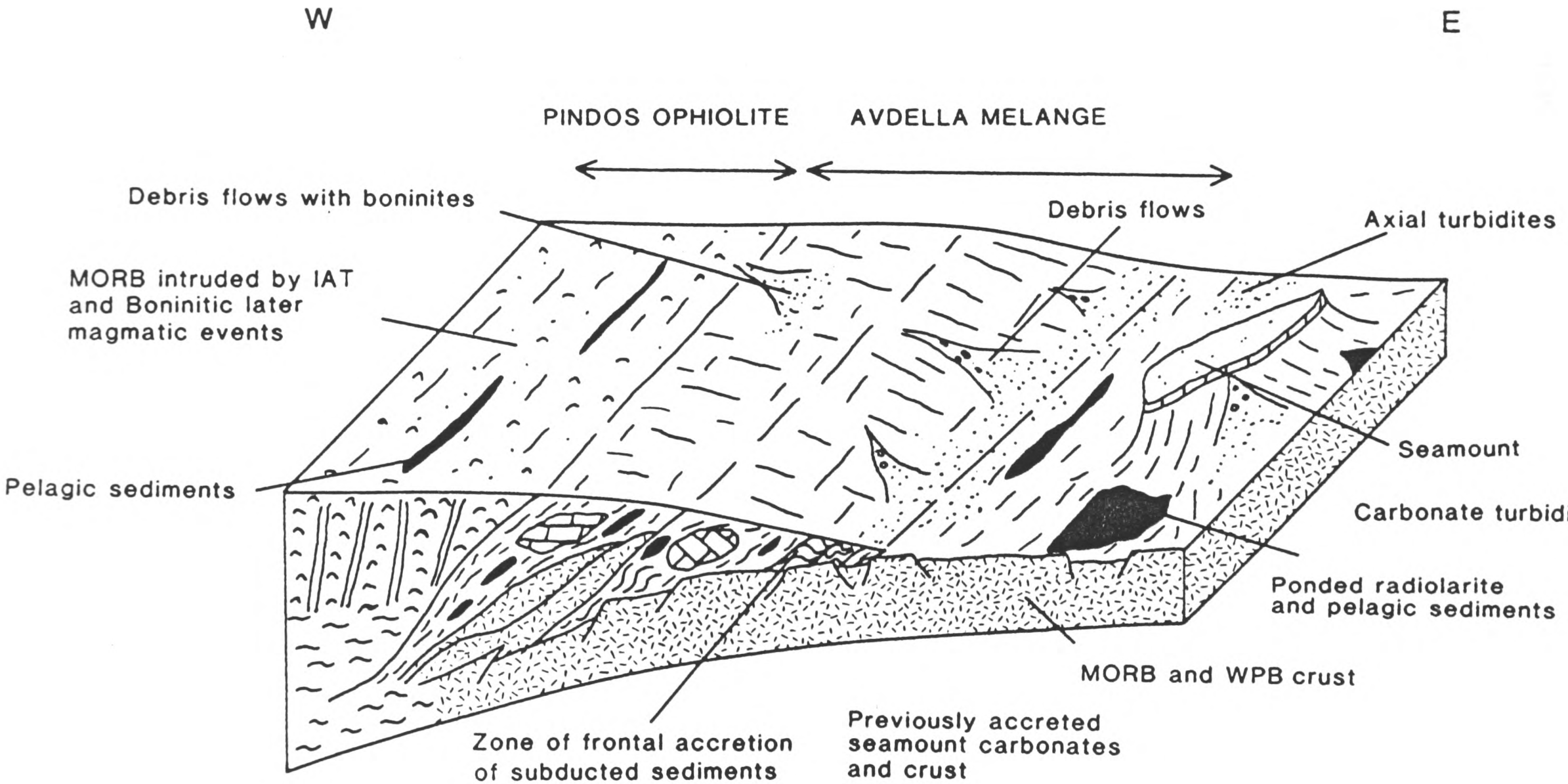

Fig. 4.18 Model for the accretion of the Avdella Melange at a destructive plate margin during the Early Mid Jurassic. See text for discussion (and also Chapters 4 and 8), and Chapter 7 for the deformational history of the melange.

phase (Fig. 4.18), shedding their cover sediments during break-up, similar to processes observed on the Daiichi-Kashima seamount in the Nankai trough (Lallement et al. 1989). Underthrusting eventually led to incorporation of sediments which were deposited closer to the continental margin, and more alkalic-type basalts (e.g. Alatopetra-type sequences). During initial ophiolite displacement, probably due to collision of the subduction zone with the continental margin, extensive volcaniclastic turbidite fans were shed off the rethrusted prism (e.g. Smolikas). Evidence that the ophiolite was also being eroded is found within these sediments. These turbidite fans were interbedded with the background sediments being deposited in the remainder of the basin at this time, i.e. radiolarian cherts (Mid-Late Jurassic).

4.9 Regional correlation of the Avdella Melange to similar units in Greece, Albania and Yugoslavia

Melange is present in the Sub-Pelagonian Zone in the Koziakas area, immediately south of the Avdella Melange, and partly in the Othris area of eastern central Greece. Melanges also occur within and beneath Triassic rocks at the base of the Pindos nappes of central and southern Greece, but these are thin and discontinuous in comparison to the Avdella Melange (De Wever 1982). In the eastern part of the Koziakas Mountains, west of Kalambaka, a thick harzburgite tectonite thrust sheet overlies a basalt and sediment-rich melange unit. This was studied by Ferriere (1982) from a stratigraphic viewpoint, and by Capedri et al. (1985) for the basalt geochemistry. The basalts from this melange are of MORB-type (normal, transitional and enriched; Capedri et al. op. cit.).

On the western side of the Koziakas range (S.E. of Metsovo; Fig. 4.14), observations by the author and Ferriere (1982) show that porphyritic andesitic lavas and radiolarites, similar to those of the Avdella Melange, occur imbricated at the base of a thick section of slope and pelagic carbonates, which contain fossils of Late Triassic age (Ferriere 1982).

Melanges of a very similar lithological and structural type to the Avdella Melange are found to the north in Albania and Yugoslavia, in the northerly equivalents of the Sub-Pelagonian tectonic belt. In Albania,

tectono-sedimentary melange includes thick radiolarite-spilite sequences, and is similarly transgressed by Late Jurassic pelagic carbonate (Shallo 1980).

In Yugoslavia, the "diabase-chert formation" (Schifer-Hornstein-Serpentinit-Schichen of Phillipson 1895) represents coloured melange of the type described. As in Greece, the melange belts are found as two distinct tectonic zones, in the Vardar Zone in the east and southeast, and in the "Southwestern Belt", the equivalent of the Avdella Melange (Karamata 1988). In both zones, the melange is associated with large tectonised ophiolite complexes (e.g. Zlatibor area). Karamata (op. cit.) distinguishes three main sedimentary associations in the Southwestern Belt: i) shallow water limestones; ii) continental slope terrigenous sediments and iii) cherts and mudstones. Igneous rocks within the melange include spilitic basalts, keratophyres, porphyrites and quartz-diorites, of Mid Triassic age. Rocks of eclogite facies are associated with amphibolites of the ophiolite metamorphic soles (Majer 1985). The diabase-chert formation is locally transgressed by Late-Jurassic to Early Cretaceous sediments of the Pogari series, which are only slightly deformed. The diabase-chert formation was similarly interpreted by Karamata (op. cit.) as the product of ophiolite obduction and subduction processes.

4.10 THE VOURINOS MELANGE

4.10.1 Introduction

The Vourinos ophiolite also possesses a basal melange (Moores 1969; Zimmerman 1972; Vergely 1976, 1977, 1984; Naylor and Harle 1976; Pichon and Brunn 1985), which was visited briefly during the present study, for comparison to the Avdella Melange. The melange is exposed beneath the Vourinos peridotite sheet, along its basal contact with the carbonate cover of the Pelagonian platform. The best localities for viewing the melange are to the north of Palaeokastro village, northwest and southeast of Chromion village, and in the Aliakmon River valley east and west of Zavordas Monastery (Fig. 4.19). Also, thin serpentinite is exposed near Metamorphosis and Siatista (Fig. 4.19). Locally, an amphibolite and

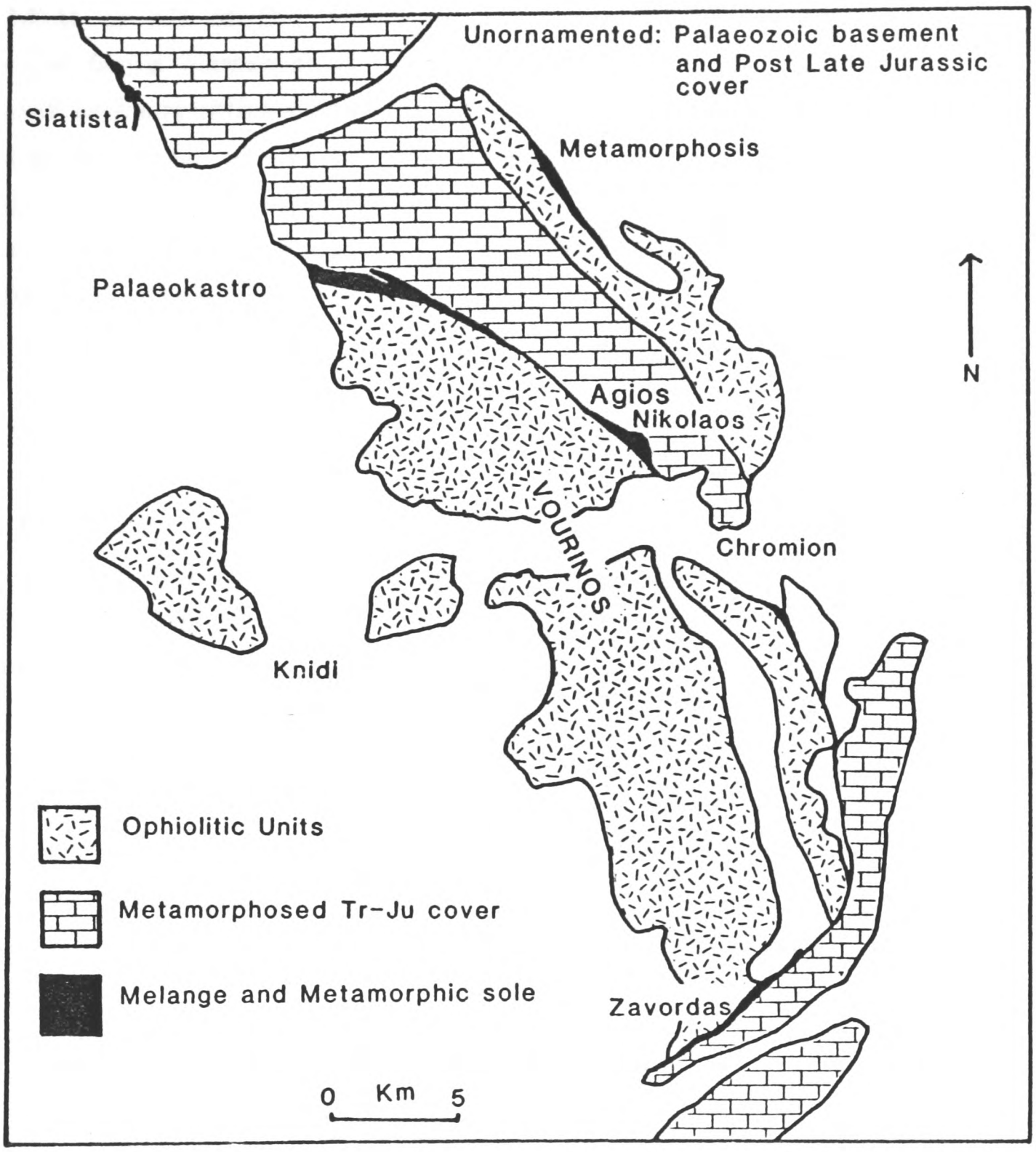

Fig. 4.19 Locality map for the Vourinos ophiolite, showing the occurrence of the sub-ophiolite melange and metamorphic sole (modified after Vergely 1984).

greenschist facies metamorphic sole is present along the contact (see Chapter 3).

Most or all of the Vourinos melange, where exposed, is of greenschist facies (Zimmerman 1972), consisting of marble, radiolarite, metabasalt and serpentinite blocks in a phyllitic matrix. It is uncertain how the melange relates to the greenschist part of the metamorphic sole, although it seems likely that they were metamorphosed synchronously. The Vourinos Melange is relatively thin compared to the Avdella Melange, reaching a maximum of 300-400 m.

4.10.2 Melange matrix

The matrix consists of generally light-grey to brown phyllites, which contain white mica, quartz and chlorite. A penetrative cleavage is developed, which in some areas is kink folded on a small scale (e.g. up to 10 cms wavelength, and plunging steeply S.E.; N. of Palaeokastro; Zimmerman 1972; this study). Zimmerman (1972) stated that the matrix consisted of metasiltstone and metatuff. This has been partly confirmed by chemical analysis of matrix phyllites near Zavordas Monastery (Chapter 3), which showed both metasedimentary and metabasic affinities (e.g sample 38/88; Appendix 5). The phyllites are commonly ferruginous, and pyrite and manganese was also found at one locality (N.E. of Palaeokastro; Fig. 4.19).

4.10.3 Melange blocks

The melange blocks are dominated by marbles, including dark-grey, shallow-water loferitic-type carbonates (Naylor and Harle 1976). The carbonate blocks are most abundant in the Palaeokastro and Agios Nikolaos valley localities, but they are also present elsewhere. These blocks are of variable dimensions, and range from pebble-grade up to 100 m long. Most of these blocks are wholly enclosed by the matrix, and are somewhat elongated into the foliation. In some cases, the carbonates are seen to be interbedded and interfolded with the matrix (e.g. Palaeokastro, Plate 4.16; Agios Nikolaos Valley; Fig. 4.19). The adjacent carbonate

platform, which consists of metamorphosed Triassic and Jurassic carbonates seems to be the logical source of the blocks. The marbles are sometimes found enclosed within the basal serpentinite of the Vourinos ophiolite (Plate 4.16; Moores 1969; Naylor and Harle 1976), which is well displayed in the Agios Nikolaos valley.

4.10.4 The Agios Nikolaos Valley

The Agios Nikolaos valley contains a thin sequence of melange type-lithologies sandwiched between the ophiolite to the west and platform marbles to the east. The structures within the melange at this locality have been the subject of some controversy (Vergely 1976, 1977, 1984; Naylor and Harle 1976), who interpreted southwestward and northeastward vergence respectively, from folds within the melange matrix. The folds in this valley appear to be mainly kink-type with sub-vertical axes. Inspection of the large-scale structure in the valley (Fig. 4.20), shows that a complex imbricate structure is present, with all major thrust contacts dipping to the west. The evidence presented here suggests that the ophiolite has been thrust over the platform towards the east-north-east, imbricating and metamorphosing parts of the platform and the melange during emplacement, similar to the model of Naylor and Harle (1976). The basal serpentinite also included and metamorphosed blocks of carbonate during emplacement, and serpentinite was also sheared and incorporated into the melange.

4.10.5 Zavordas Monastery

On the southern margin of the Vourinos ophiolite, the Aliakmon River has cut a deep east-west valley along the contact between marbles and basement to the south and east, and the ophiolite to the north. This contact zone exposes melange and metamorphic sole rocks (Fig. 4.21), and sections of highly deformed carbonate platform. The basal structures were studied previously by Vergely (1984), who suggested several phases of deformation, and Wright (1986), who interpreted the deformation present as resulting primarily from dextral shear along a wrench fault. However, consideration of the large scale structure shows that this margin is part of

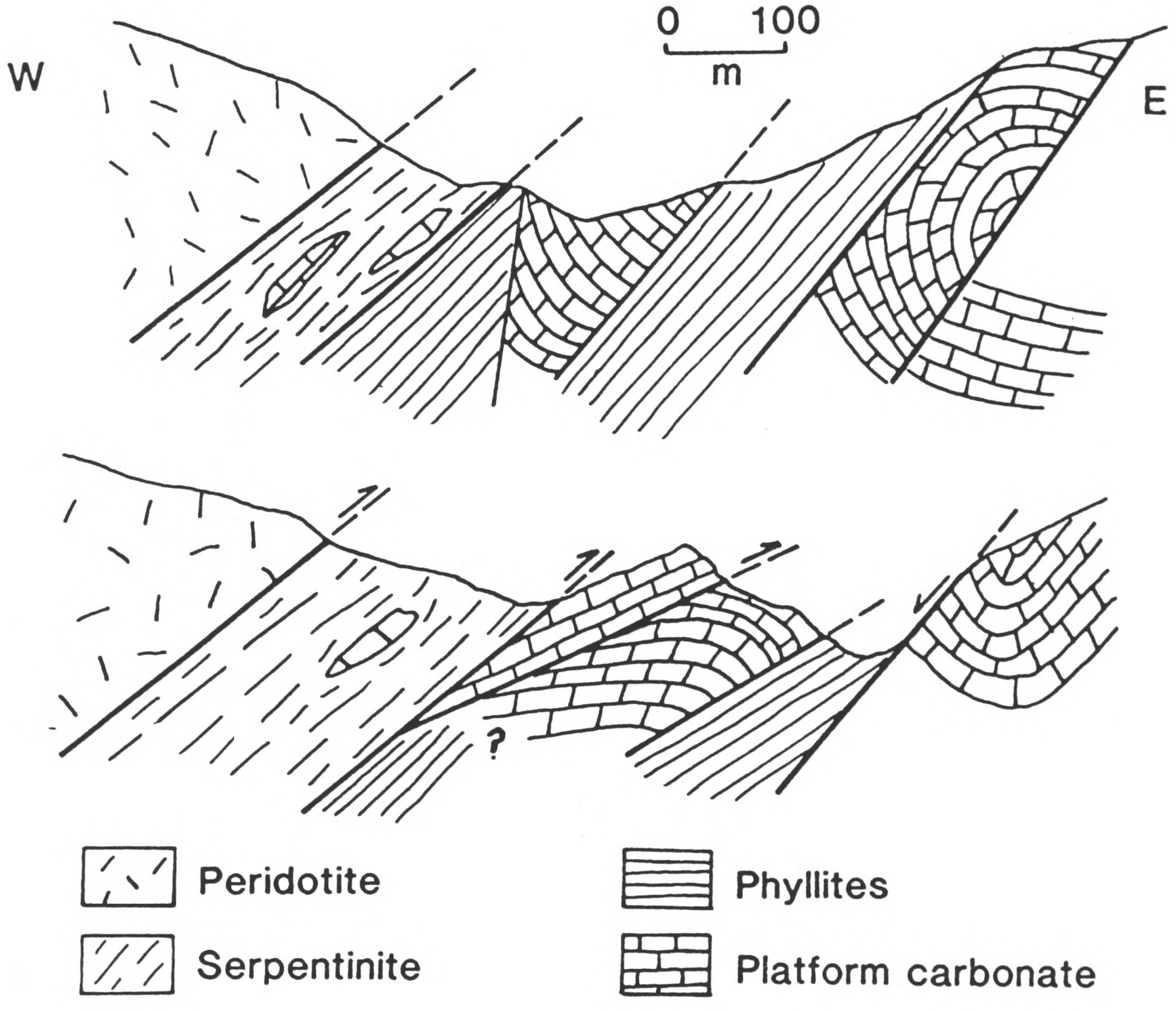

Fig. 4.20 a) Sketch sections of the structure beneath the Vourinos ophiolite at Agios Nikolaos, 5 km N.W. of Chromion Village (Fig. 4.19).

a major transform-type fault structure (Kastaniotikos transform of Lyberis et al. 1982), which marks the southern termination of the Pindos and Vourinos ophiolites, and currently dextrally offsets the Pelagonian platform some 20 km (Geological map of Greece 1987). This contact is therefore a major structural discontinuity along which multiple deformation has taken place, and possibly several hundred kilometers of movement has been accommodated (Robertson et al. in prep.).

A generalised cross-section is reconstructed here using data from the above sources and additionally that of Pichon and Brunn (1985; Fig. 4.21b). A reconnaisance survey of the Aliakmon River valley east and south of Zavordas Monastery confirms the high degree of deformation present. This is manifested within the platform carbonates by large-scale thrust imbrication and mylonite development. The mylonites are light and dark-grey crystalline rocks, banded on a centimetre scale. This banding may be spectacularly folded by high-temperature ductile folds (Plate 4.16). The platform carbonates become locally chert-rich (now jasper), and pass upwards conformably into phyllitic and tuffaceous interbeds, together with stretched pebble conglomerates. These are sometimes intruded by coarse-grained, amphibolite-facies gabbroic dykes, which are similarly metamorphosed and sheared (Plate 4.16). Structures visible within the river bed seem to generally indicate at least one phase of dextral shear, shown for example by boudinaged dolerite within a serpentinite matrix (Fig. 4.21a).

4.11 Interpretation of the Vourinos melange

From the localities studied, it is concluded that the Vourinos ophiolite was emplaced from the present day west towards the east, over a collapsing platform margin, or foreland basin, which is now represented by the melange (see Chapter 3 for illustrations). This is in disagreement with the findings of Vergely (1984), as discussed later (Chapter 8). The melange was deformed to greenschist facies by the residual heat of the ophiolite, and serpentinite was injected along tectonic contacts. The melange effectively represents the greenschist part of the metamorphic sole to the ophiolite, although this is coincidental, due to the close proximity of the platform and foreland basin during ophiolite

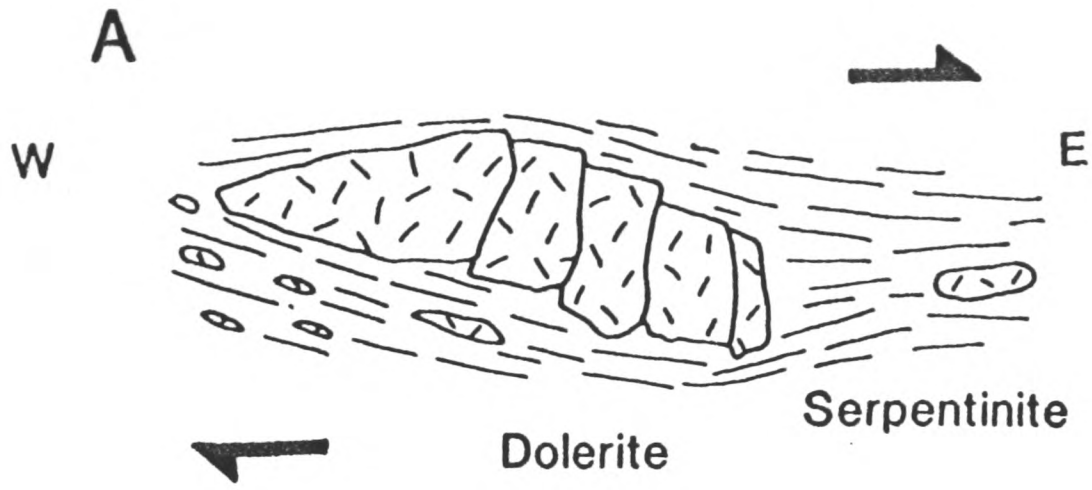

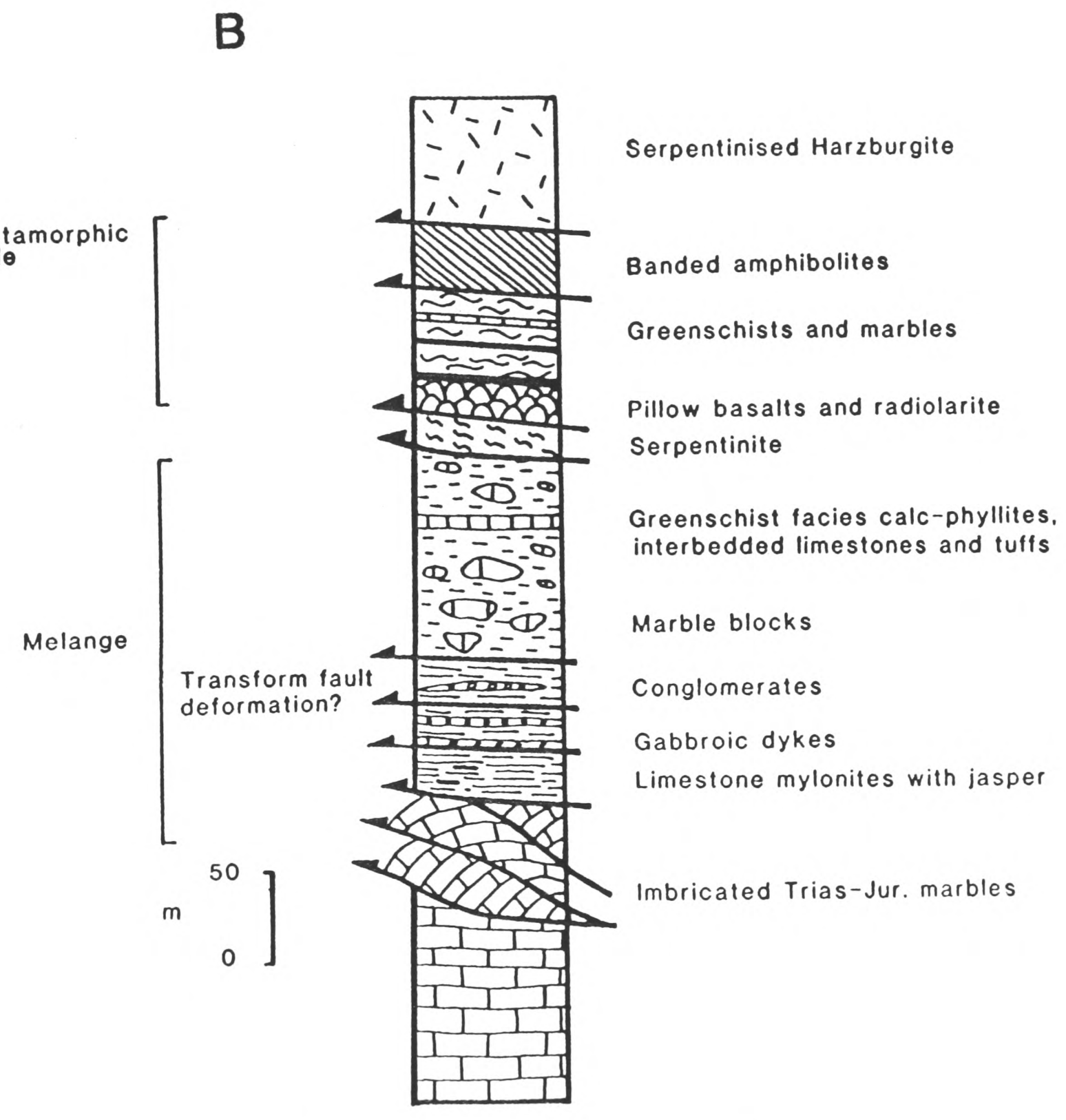

Fig. 4.21 a) Sheared dolerite boudin enclosed in serpentinte, indicating dextral motion. Aliakmon River Valley, at Zavordas Monastery. b) Reconstructed tectono-stratigraphic section of sequences beneath the Vourinos ophiolite on the S. margin of the Massif (Aliakmon River area). Partly after Brunn and LePichon (1985).

emplacement. The data presented by Mountrakis (1986), suggests that the Pelagonian platform carbonates were only low-grade metamorphosed during this overthrusting, supporting the suggestion that a steep geothermal gradient existed, similar to that found in other metamorphic sole sequences (see Chapter 2). The presence of shallow-water meta-carbonates within the Vourinos melange is comparable to the occurrence of carbonates described from the Loumnitsa Unit, also found mostly within the greenschist facies (Chapter 3). However, these are far less abundant than deep-water pelagic sediments and metabasites in the Loumnitsa Unit, and the Loumnitsa rocks are thus interpreted as having been accreted more distally within the ocean basin than those of the Vourinos melange. The chemistry of the Vourinos melange greenschist basalts was considered earlier (Chapter 3), but in summary, they are of MORB and IAT type, suggesting that they may have been eroded from the ophiolite and bulldozed ahead during emplacement. Alternatively, these basalts may have been part of the older Triassic crust, which may have contained basalts with anomalous IAT-type signatures such as those described earlier from the Avdella Melange.

The Vourinos melange shows good evidence of platform collapse, prior to ophiolite emplacement. The presence of abundant olistolith blocks of shallow-water limestones, and a conformable transition into phyllites and olistostromal conglomerates at Zavordas are the best indications of this. This collapse may have been accompanied by basic igneous activity, including gabbroic intrusions and tuffs, perhaps due to strong extension associated with platform collapse. Another possibility is that the igneous activity occurred at a much earlier stage, and was subsequently deformed.

The platform carbonates pass abruptly upwards into the metasiltstones, metatuffs and metaquartzites of the foreland basin. This indicates that platform collapse was rapid, and therefore that the ophiolite was also being rapidly emplaced. This is in good agreement with data from other ophiolites (e.g. Semail ophiolite; Lippard et al. 1986), which suggests that emplacement onto the continental margin occurred soon after ophiolite formation and displacement (displaced in the Bathonian, finally emplaced in the Kimmeridgian; approximately 20 Ma.). The abundance of marble blocks suggests a strongly faulted margin, with associated fault-induced topography. Most of the metasiltstones are

composed of quartzo-feldspathic debris, presumably derived from the Palaeozoic basement to the platform.

The southern limit of the ophiolite is bounded by a major transform fault, which has further deformed the platform and the melange along its length. The latest visible deformation is strong dextral shear, but the age of this is uncertain. It may be related to original emplacement of Vourinos during the Jurassic, as seems most likely, or by reactivation during Tertiary compression of the northern Hellenides.

Plate 4.1 a) Graded, calcite-cemented basalt breccia, Alatopetra. b) Nodular "ammonitico-rosso" type limestones, overlying massively bedded Triassic carbonates, Alatopetra. Note elongated carbonate nodules with stylolitic boundaries. c) Triassic carbonates, which overlie basalts and basalt breccias (see Plate 4.1a), containing palaeo-extensional faults (outlined). d) Transition (marked) from radiolarites with continentally-derived (quartz, muscovite, albite) shale interbeds, which pass into volcanic-derived shales and volcaniclastic turbiditic sandstones.

Plate 4.2 Melange basalt textures. a) Phenocrysts of pyroxene, now altered to chlorite (with alteration haloes), sit in a groundmass of micro-phenocrystic plagioclase (albite) altered chlorite, haematite and opaques (56/88, Alatopetra; x12 PPL). b) Chlorite-filled vesicle, in hyalopilitic plagioclase-chlorite-magnetite-haematite matrix (233/88, Stragopetra; x64 PPL). c) Basalt breccia, with calcite-cemented fractures (17/23/8, Avdella; x20 PPL). d) Glassy matrix now altered to chlorite, and abundant magnetite. Central calcite filled vein (218/88, Dio Dendra Valley; x18 PPL).

Plate 4.3 a) Ophitic gabbro with fresh clinopyroxene intergrown with albitised plagioclase (181/88, N.W. Perivoli; x18 XPL). b) Ophitic gabbro with clinopyroxene, plagioclase and magnetite. (2/26/8, N.W. Perivoli; field of view 6mm PPL). c) Quartz arenite, angular quartz and albite grains, set in a calcite cement. Large pyrite crystal has grown around the clasts (6/23/8, Avdella; 6 mm XPL). d) Coarse arenite, showing an abundance of polycrystalline quartz grains derived from a metamorphic source (6/24/8 Kokkina Litharia; 6 mm XPL).

Plate 4.4 a) Ammonitico rosso-type carbonates, Early Jurassic, Alatopetra. Note both carbonate rich and haematitic clay-rich patches are visible. b) Somewhat phosphatised hardground horizon from the top of the ammonitico rosso sequence, Alatopetra. Note fragment of belemnite guard (B) in the centre of the field of view (hammer handle for scale).

Plate 4.5 a) Calcirudite-calcarenite horizon overlying ammonitico rosso carbonates, Alatopetra. Note the parallel-lamination, sole structures (S) and grading in these sediments. b) Volcaniclastic mudstones and overlying ribbon radiolarites at Alatopetra.

Plate 4.6 Negative print of a thin section showing textures within a calcarenite from Alatopetra (see Plate 4.5). Abundant echinoid fragments (E), ooids (O), pellets (P), algal oncoids (A), trocholinid foraminifera (T) and cabonate intraclasts (I) can be seen in this rock. Note also the stylolitic contacts between carbonate grains (S).

Plate 4.7 a) Pillow basalts and massive flows, Tsouka Mountain, S.W. of Vovousa. b) Dyke (D) making a chilled margin aginst metamorphosed pink carbonates and radiolarites (L) of Late Triassic age, Tsouka, S.W. of Vovousa. c) Debrite containing clasts of pink and grey, recrystallised fine-grained carbonate, in a haematitic clay matrix. Also found are blocks of basalt, up to 1 m in length. d) Transgression of Late Jurassic Calpionellid limestone facies carbonates (CL) over the Avdella Melange (M), on the roadside between Metsovo and Milea, 8 km S. of Milea.

Plate 4.8 a) Turbidite fans of graded volcaniclastic arenites and fine rudites (prominent beds), with interbedded haematitic and chloritic shales. W. slopes of the Smolikas Mountains, N. of Padhes Village. b) Debris-flow rudite from the Valiara Valley, N.W. of Perivoli. Note low-angled thrust, with related weak cleavage. Blocks include marbles and fine-grained limestones, basalts, cherts and gabbros. These sediments are interbedded with radiolarites of Late Jurassic age. c) Late Triassic limestone from the Samarinotikos river valley (N. of Samarina), containing colonial corals and Megalodontid-type bivalves. Similar carbonates are also found in the metamorphic sole at this locality. d) Thin section photomicrograph (x64 PPL) of authigenic quartz crystals growing within micritised (shallow-water) carbonates, Kokkina Litharia melange block.

Plate 4.9 Photomicrographs showing Triassic carbonate microfacies within the Avdella Melange. a) Radiolarian micrite with clast of spalled pophyritic basalt. From 500 m N. of Avdella village (6mm XPL). b) Pervasively dolomitised pelagic carbonate, interthrust with basalts. Locality 500 m N. of Aspropotamos Bridge, Perivoli (8 mm PPL). c) Recrystallised valves of pelycypods, probably *Halobia* sp., disrupted by compaction. Stragopetra Mountain (6 mm XPL). d) Radiolaria and *Halobia* sp. in micrite matrix. Avdella village (6 mm PPL).

Plate 4.10 a) Melange block, slopes of Koleo Mountain, showing interbedded radiolarite and pelagic limestone. b) Carbonate debrite unit, Loumnitsa Valley, showing large clasts of pelagic limestone now compressed (whilst partly consolidated?), within a sparse matrix. c) Calcirudite, with variably sized rounded clasts of pink and grey recrystallised fine-grained carbonate (Aspri Petra; lens cap is 4 cms in diameter). d) Porcellanous pelagic limestone with replacement chert as nodules and more extensive layers at the centre of the beds.

Plate 4.11 Negative image photomicrograph from a thin section of volcaniclastic arenite, Perivoli. Note the great abundance of generally elongate clasts of chlorite (C) basalt (B), gabbro (G), microgabbro (M) and radiolarite (R). A chrome spinel (Cr) is found in a serpentinised mylonitic matrix. Quartz grains are also present (Q). Gross lamination of these clasts is visible. Grading is also present.

Plate 4.12 Negative image photomicrograph from a thin section of a redeposited calcarenite from Agios Nikolaos (Monahiti). The rock is classified as a oosparite, and contains trocholinid foraminifera (A), large ooids (B), composite ooids (C), with a cortex developed around a foraminifera, a previously formed ooid and an echinoid fragment. Also visible are echinoid plates (D). This rock is mildly metamorphosed and veined.

Plate 4.13 Triassic radiolaria from the Avdella Melange. a) Unidentified (x238; 48/89); b) *Xiphotheca cf karpenissionensis* (x 337; 143/88); c) *Capnuchosphaera* sp. (x252; 143/88) d) *Capnuchoshpaera* sp. (x252; 144/88) e) *Capnuchosphaera* sp (x252; 143/88) f) *Capnuchosphaera ?triassica* (x213; 60/88); g) Unidentified (x215; 143/88); h) Unidentified (x230; 36/89); i) Unidentified (x276; 37/89). All samples identified or confirmed by P. De Wever, 1990.

Plate 4.14 Jurassic radiolaria from the Avdella Melange; a) *Parahsuum* sp. (x428; 120/88); b) *Parvicingula* sp. (x155; 20/23/8); c) *Hsuum brevicostatum* OZVOLDOVA (x557; 200D/88); d) *Stichomitra* sp. (x337; 220d/88); e) *Unuma echinatus* ICHKAWA+YAO (x452; 23/23/8); f) *Triactoma blakeii* PESSAGNO sensu INTERRAD (x208; 200D/88) g) *Tricolocapsa plicarum*

YAO (x596; 25/23/8); h) *Triactoma* sp. (x278; 21/23/8); i) *Homeoparonella cf argolidensis* BAUMGARTNER (x224; 200D/88); j) Unindentified (*Paronella* sp.? x271; 200D/88); k) *Stuarloronche robusta* RUST sensu PESSAGNO (x229; 200D/88). l) *Homeoparonella* sp. (x271; 200d/88); m) Unidentified (*Acaeniotyle* sp.?; x178 224/88); n) *Podobursa triacantha* gp. (x337; 200D/88).

Plate 4.15 Jurassic (a-g) and Cretaceous (h-i) radiolaria from the Avdella Melange; a) *Parvicingula dhimenaensis* BAUMGARTNER (x574; 22/23/8); b) *Parvicingula dhimenaensis* BUAMGARTNER (x513; 25/23/8); c) *Archaeodictyomitra* sp. (x499; 20/23/8); d) *Hsuum aff. brevicostatum* OZVOLDOVA (x334; 200D/88); e) *Hsuum brevicostatum* OZVOLDOVA (x310; 200D/88); f) *Hsuum maxwelli* gr. PESSAGNO ((x339; 200D/88); g) *Hsuum maxwelli* PESSAGNO (x484; 20/23/8); h) *Sethocapsa cf uterculus* PARONA (x523; 8+9/24/8); i) *Pseudodictyomitra formosa* (x300; 8+9/24/8); j) *Pseudodictyomitra cf. lilyae* (x369; 8+9/24/8).

Plate 4.16 The Vourinos Melange and contact zones. a) Conformable marble horizon (2 m-thick) within a phyllite-rich melange meta-sedimentary sequence, Agios Nikolaos Valley, Chromion. b) Amphibolite-facies meta-gabbro, Aliakmon River at Zavordas Monastery. c) Folds within axial planar cleavage in carbonate mylonites at the top of the Pelagonian platform, Aliakmon River at Zavordas Monastery. d) Pelagonian marble block enclosed in basal serpentinite of the Vourinos ophiolite, Agios Nikolaos Valley, Chromion.

4.1

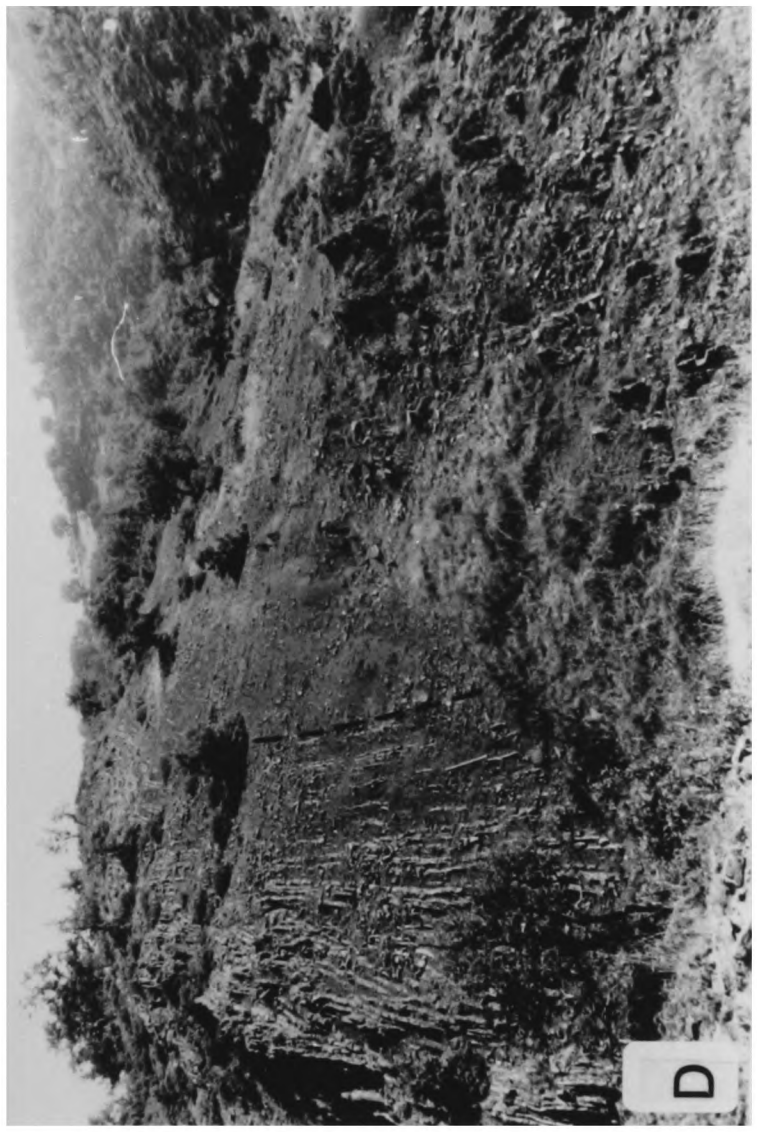

4.2

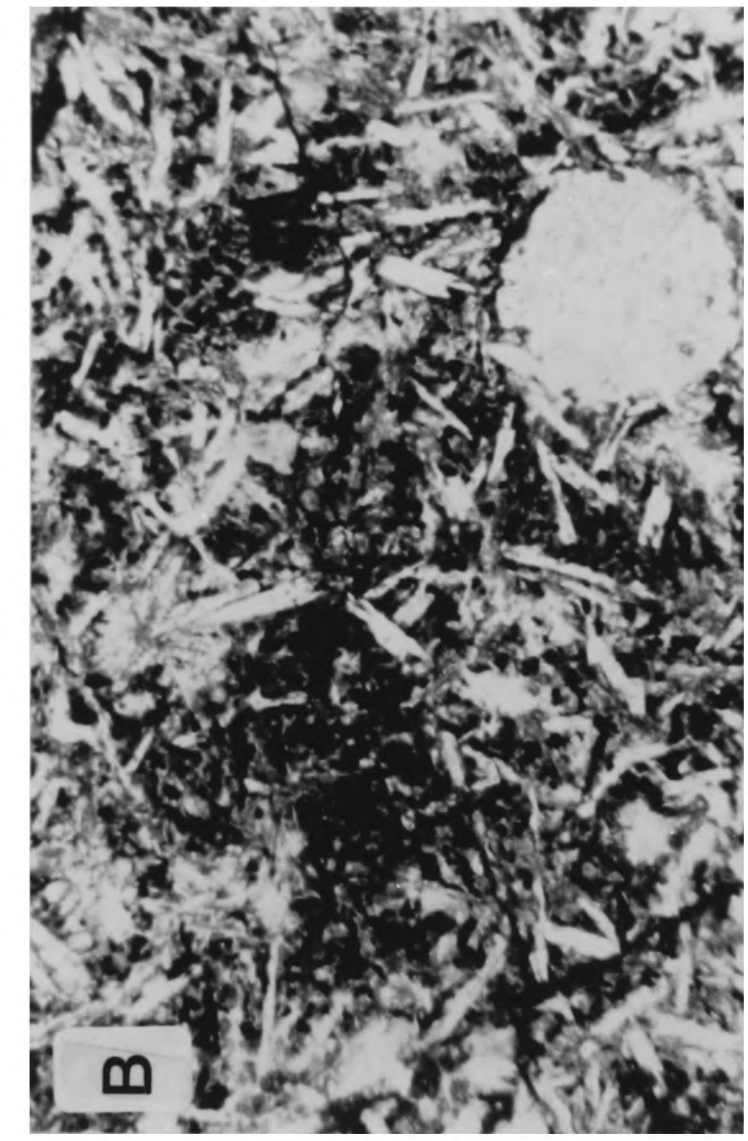

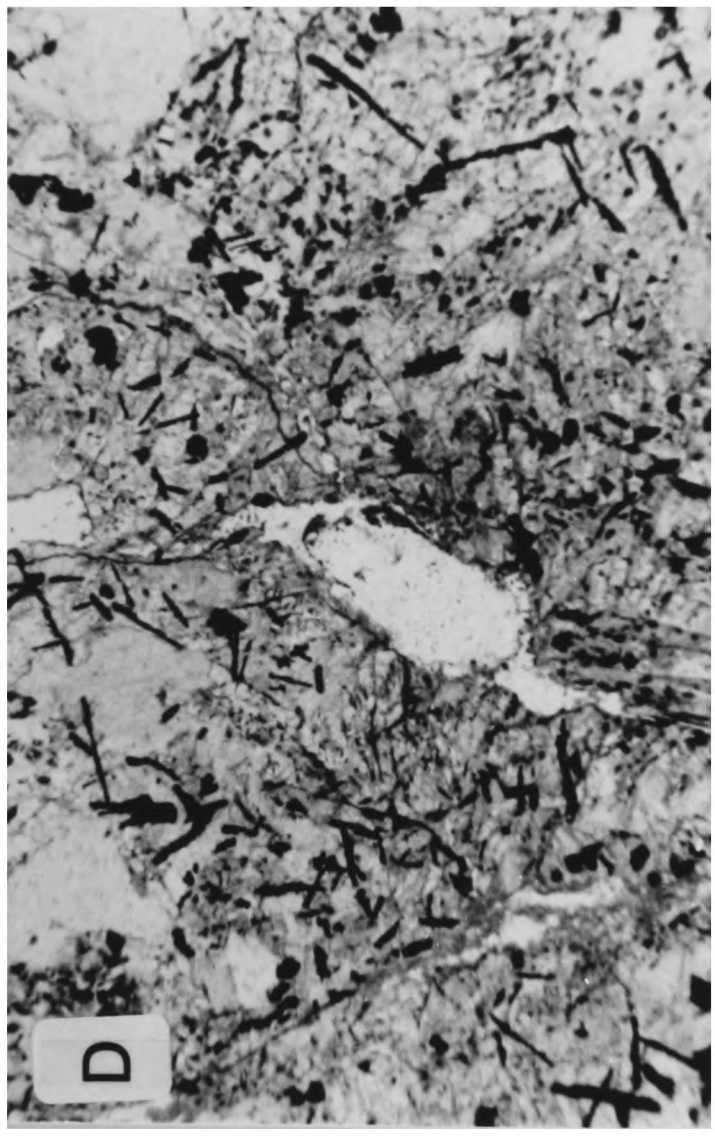

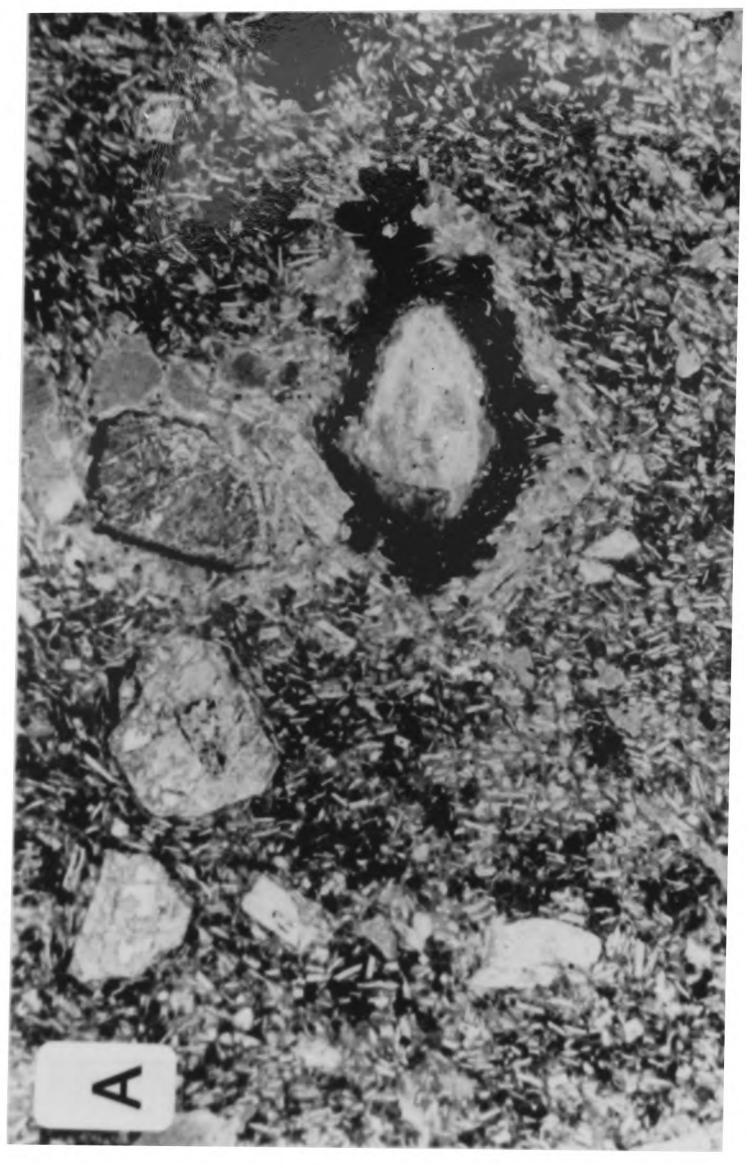

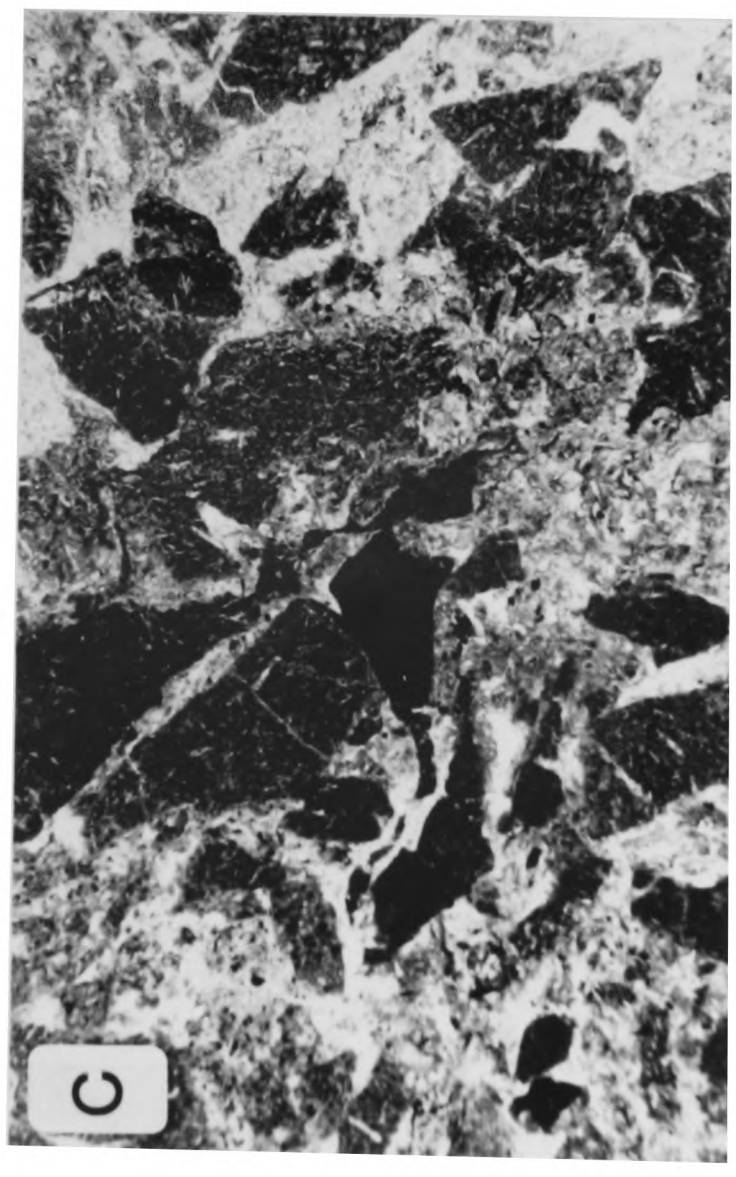

4.3

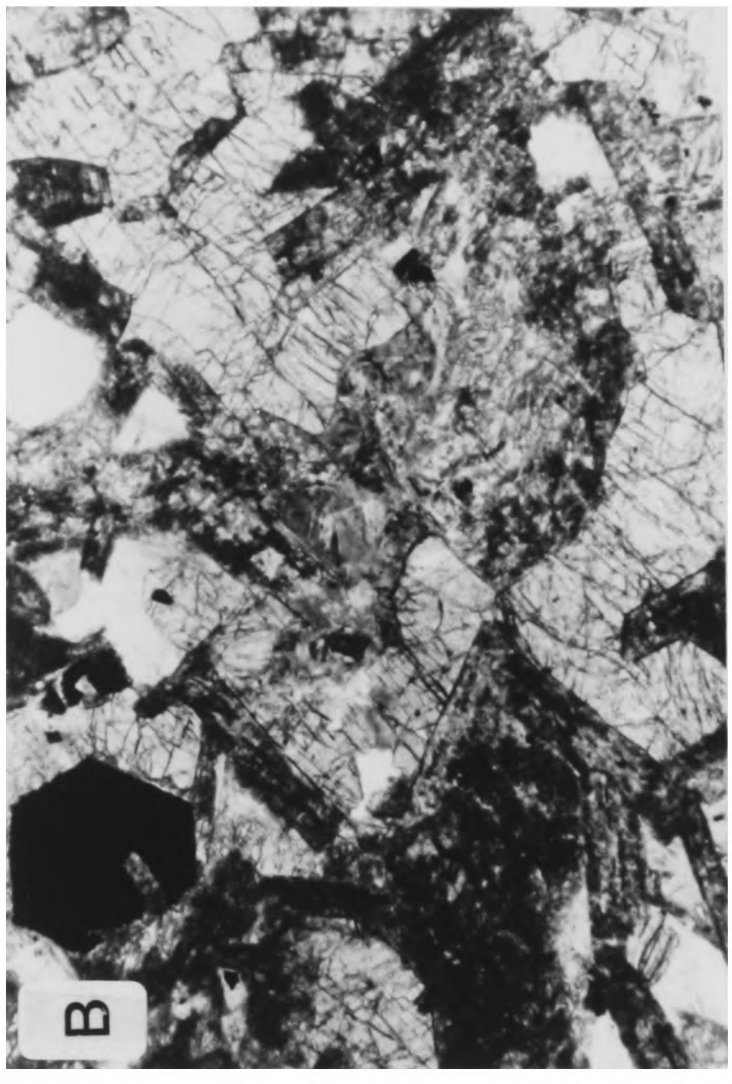

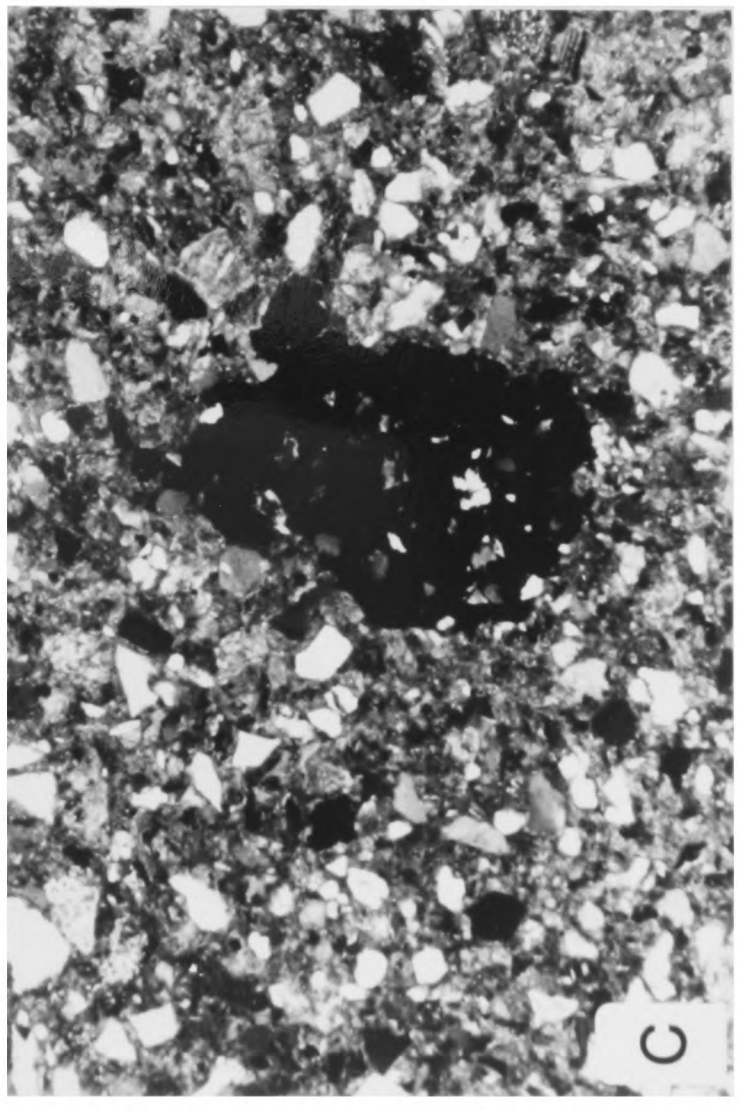

4.4

4.5

4.6

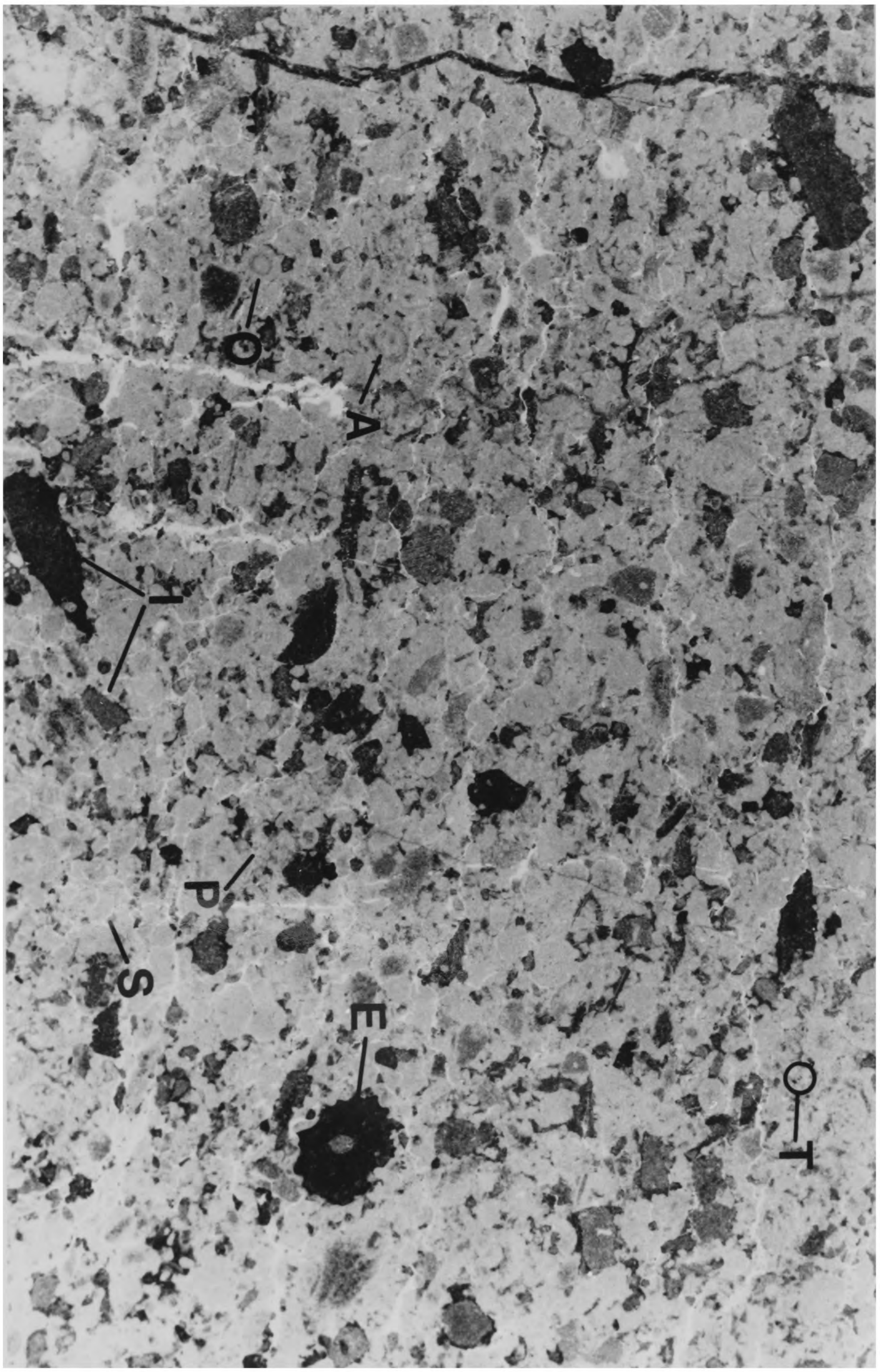

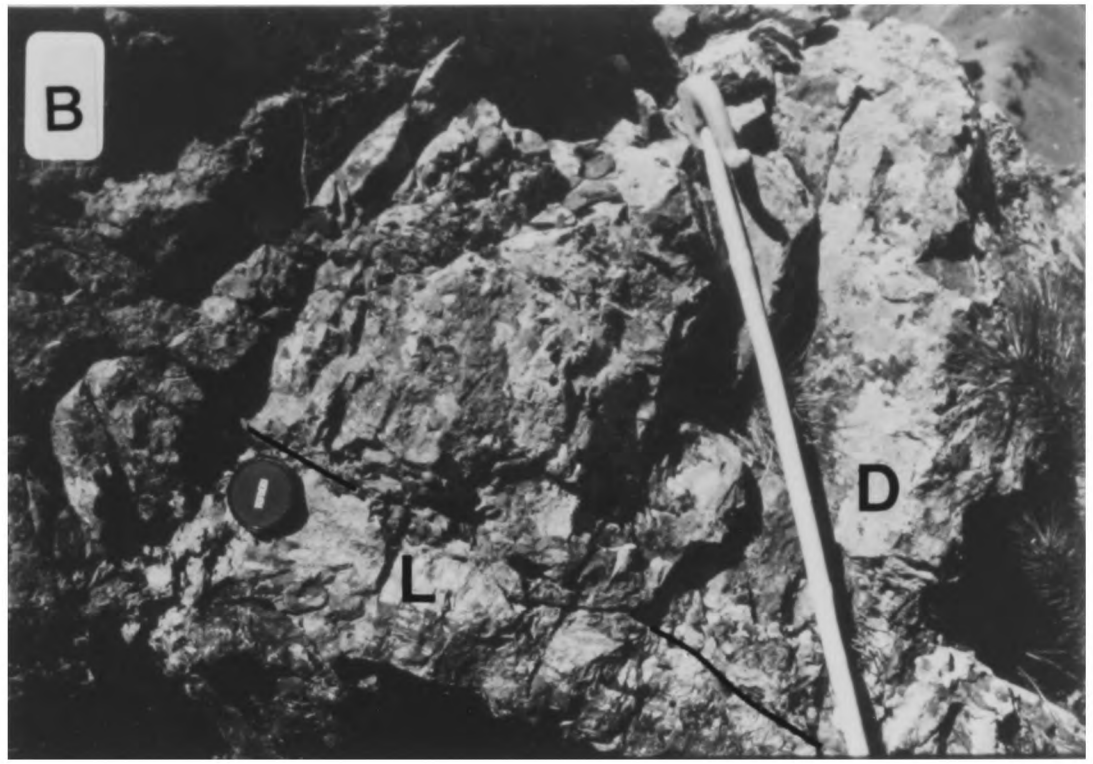

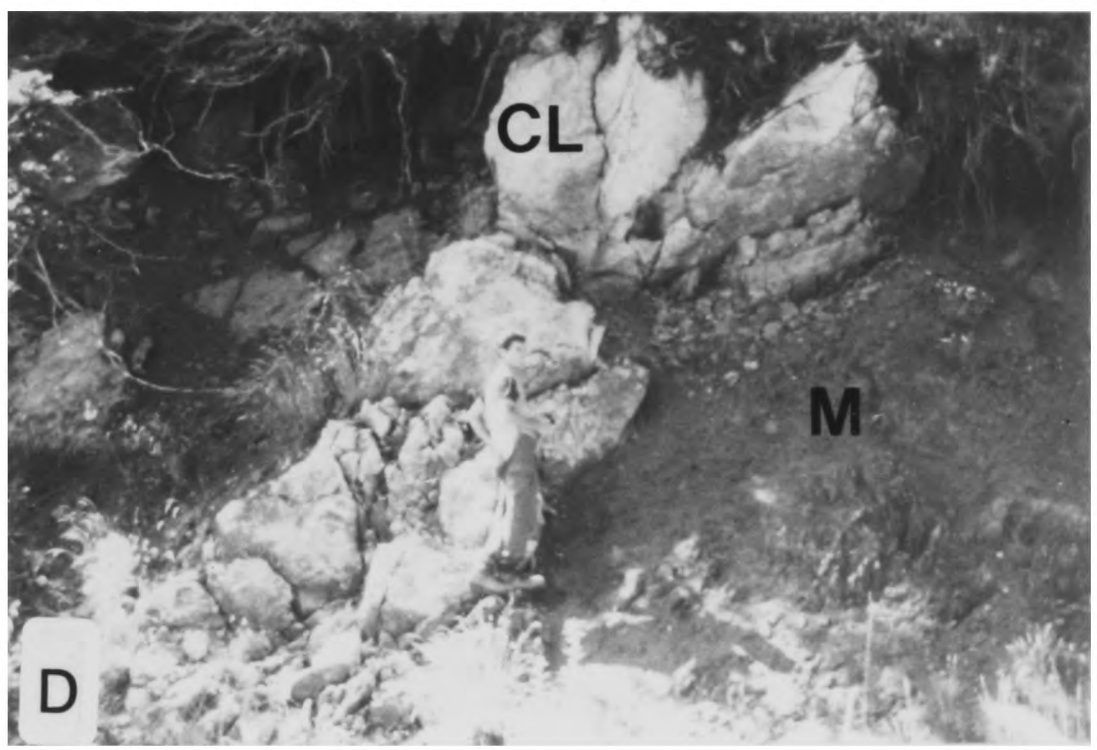

4.7

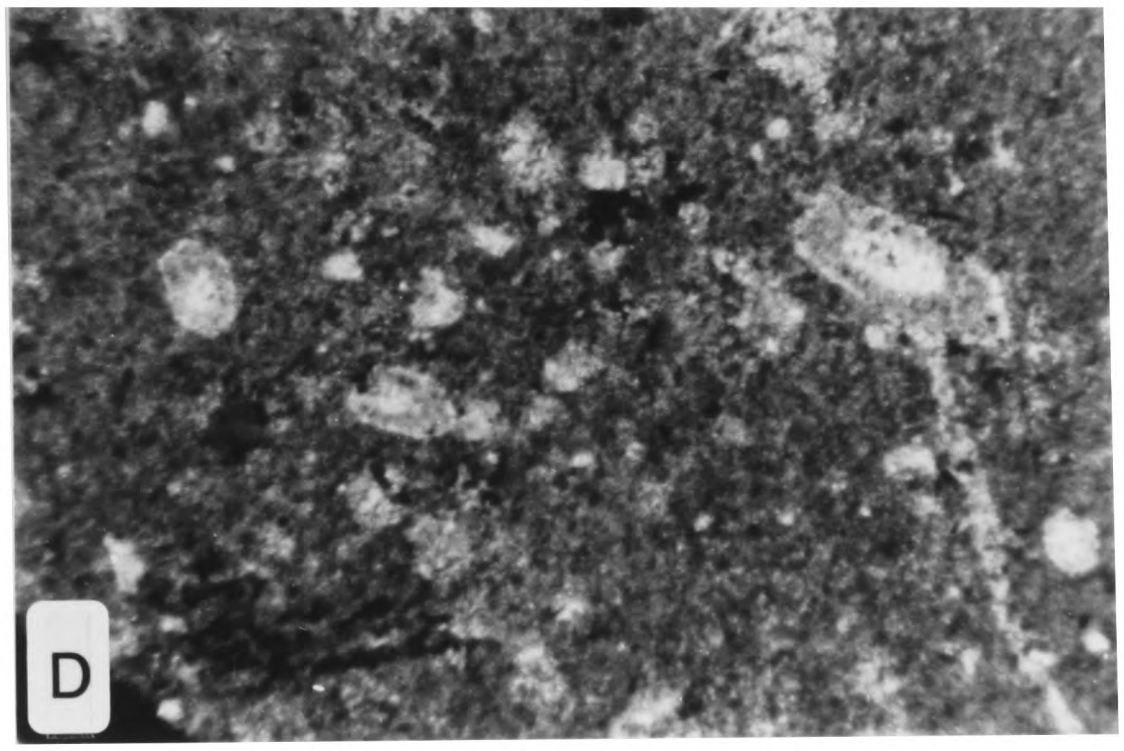

4.8

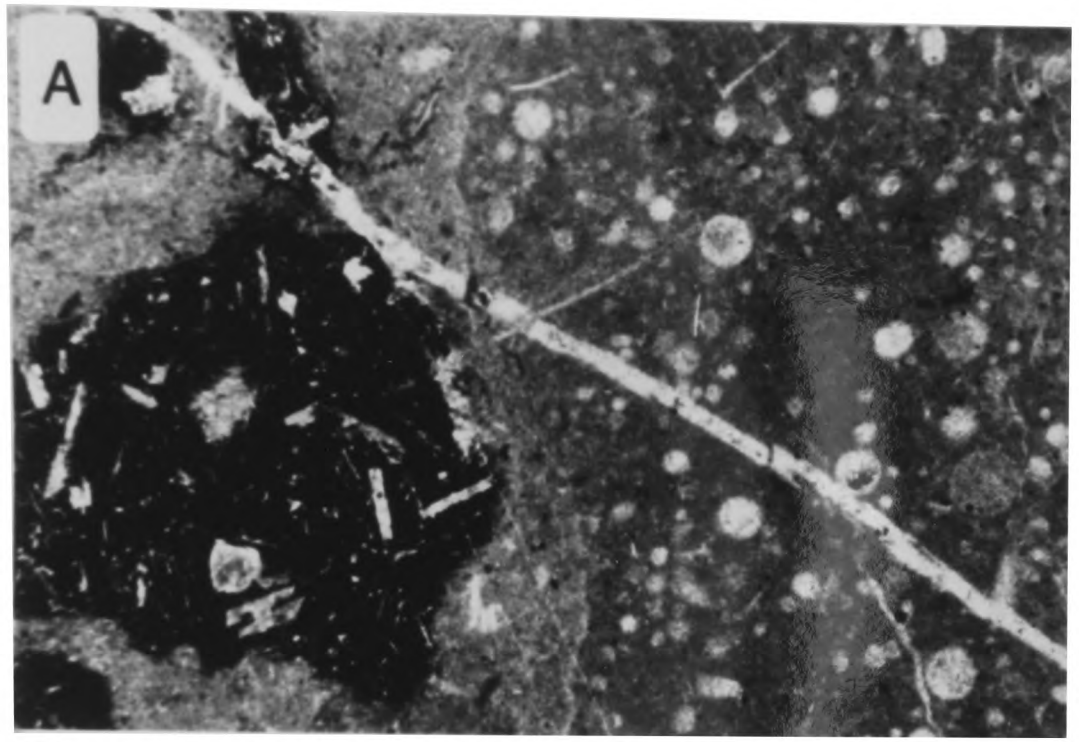

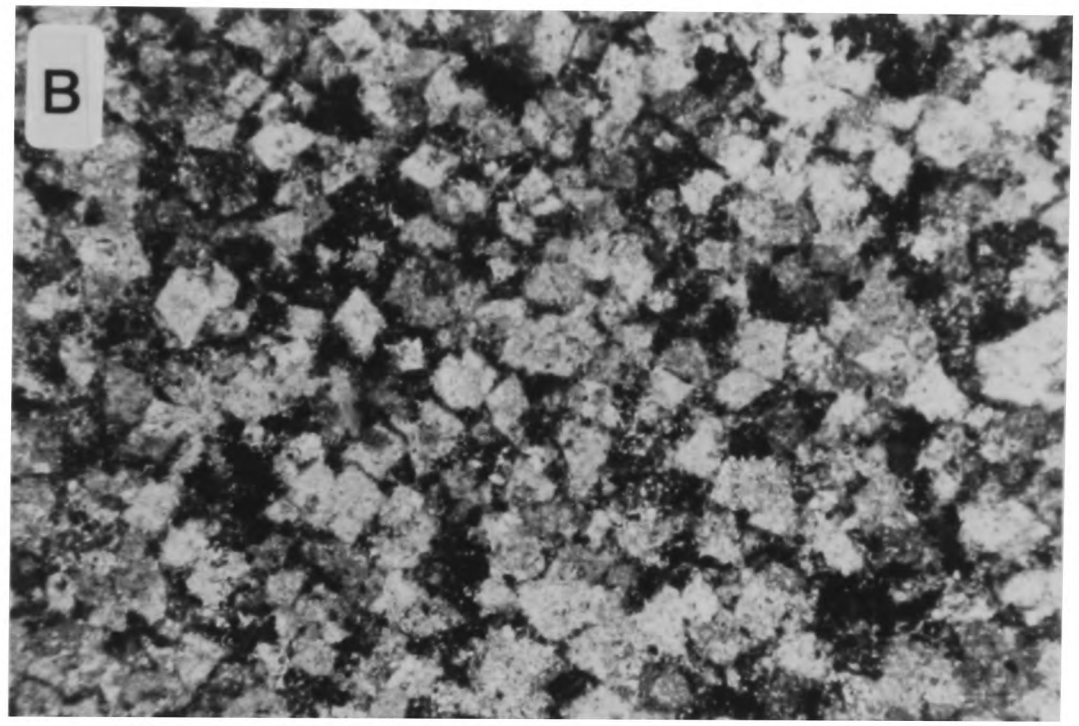

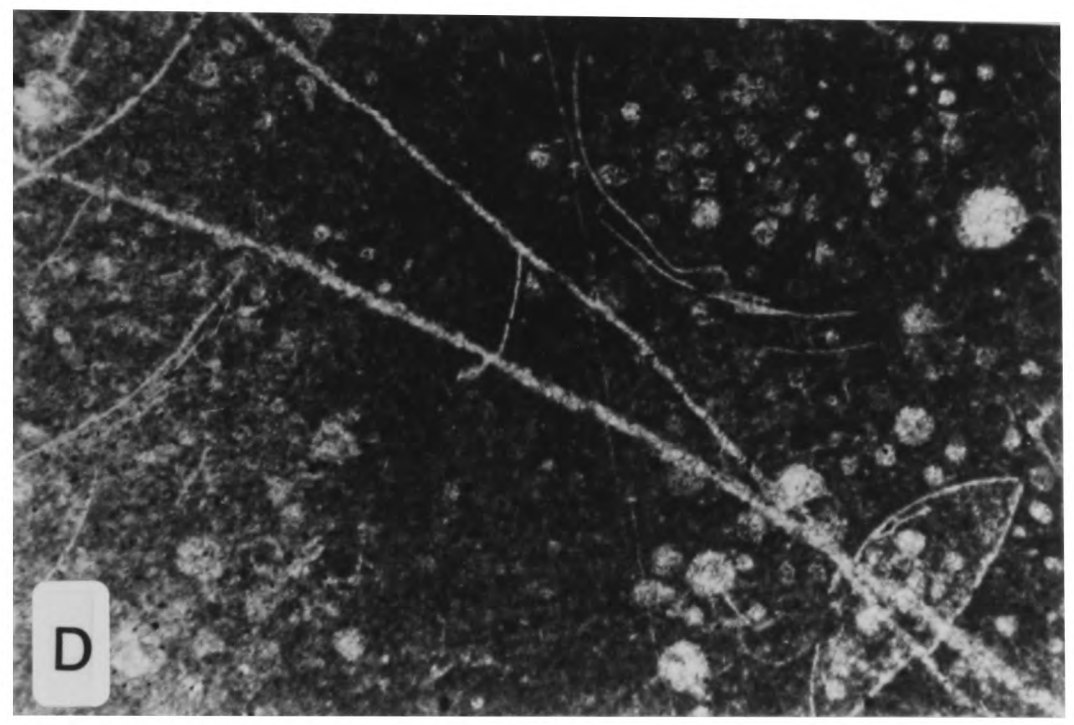

4.9

4.10

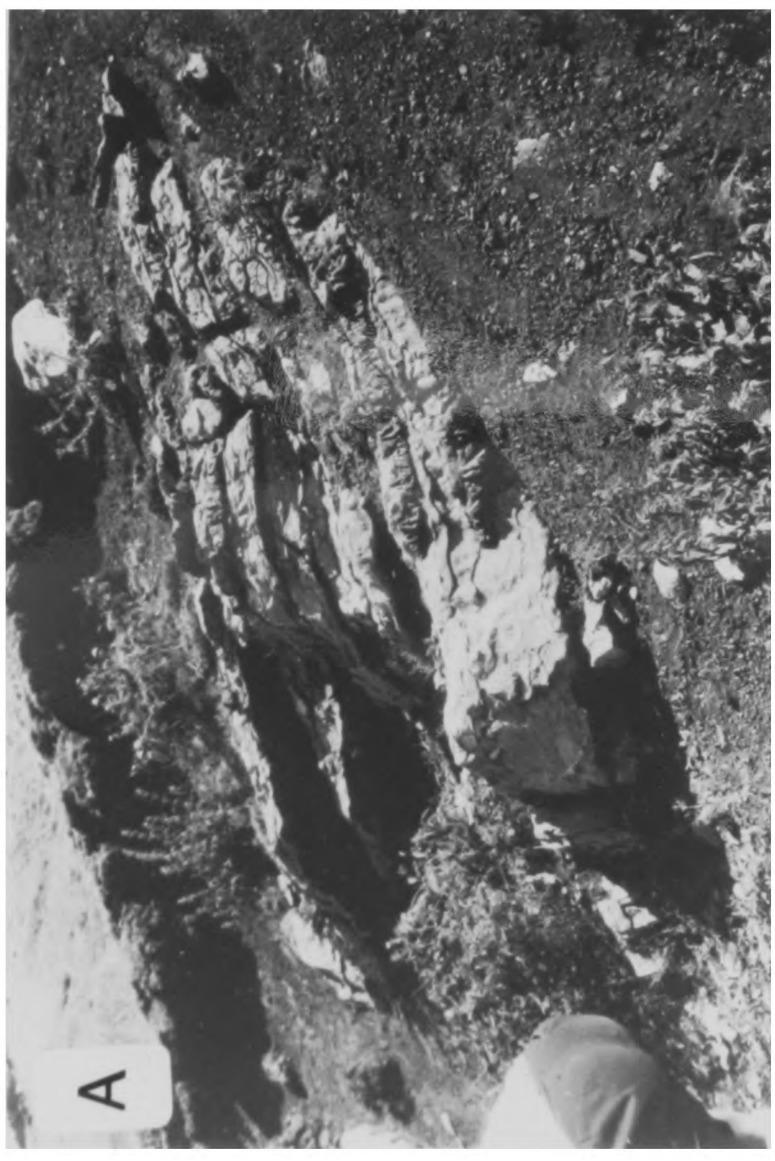

4.11

4.12

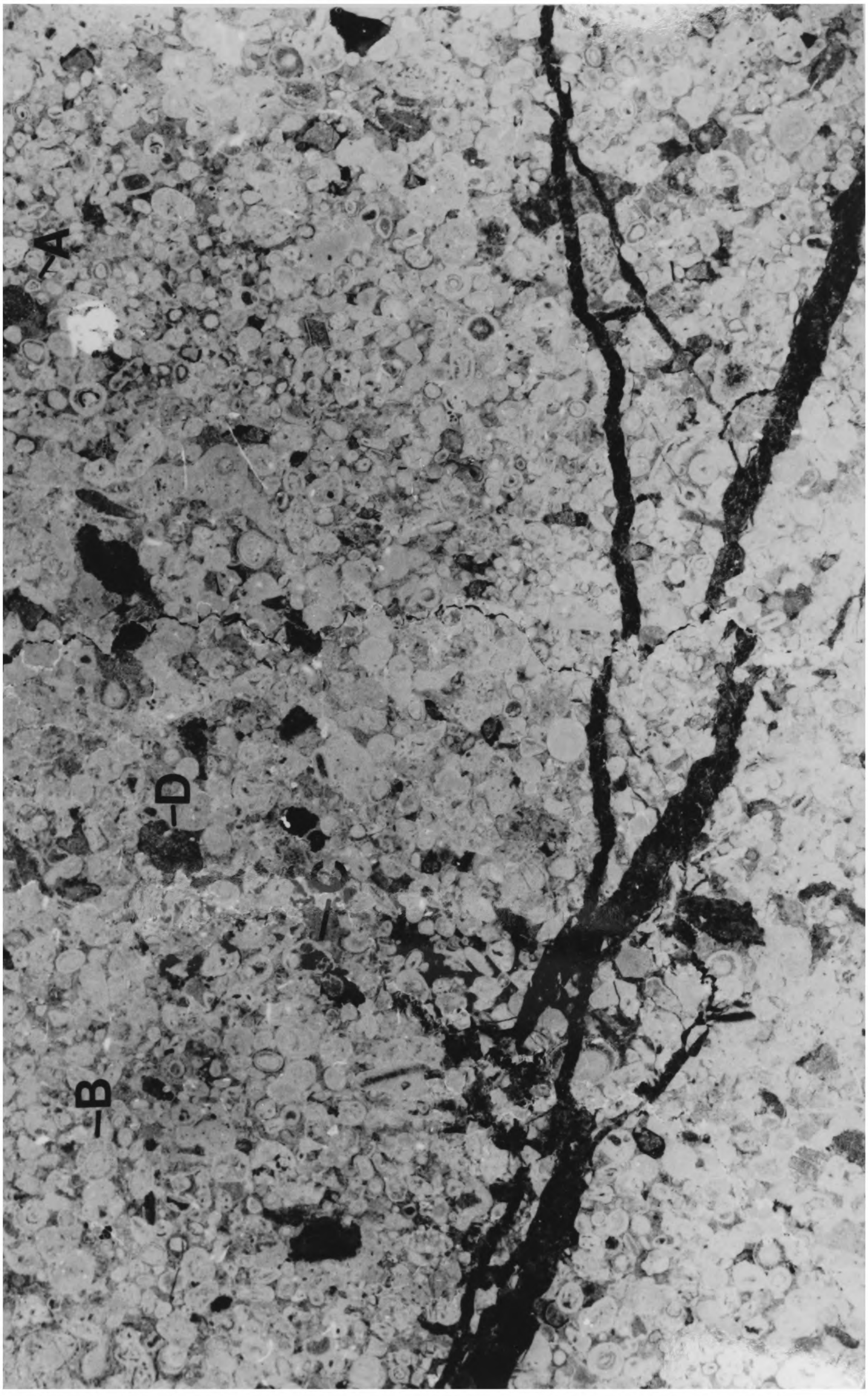

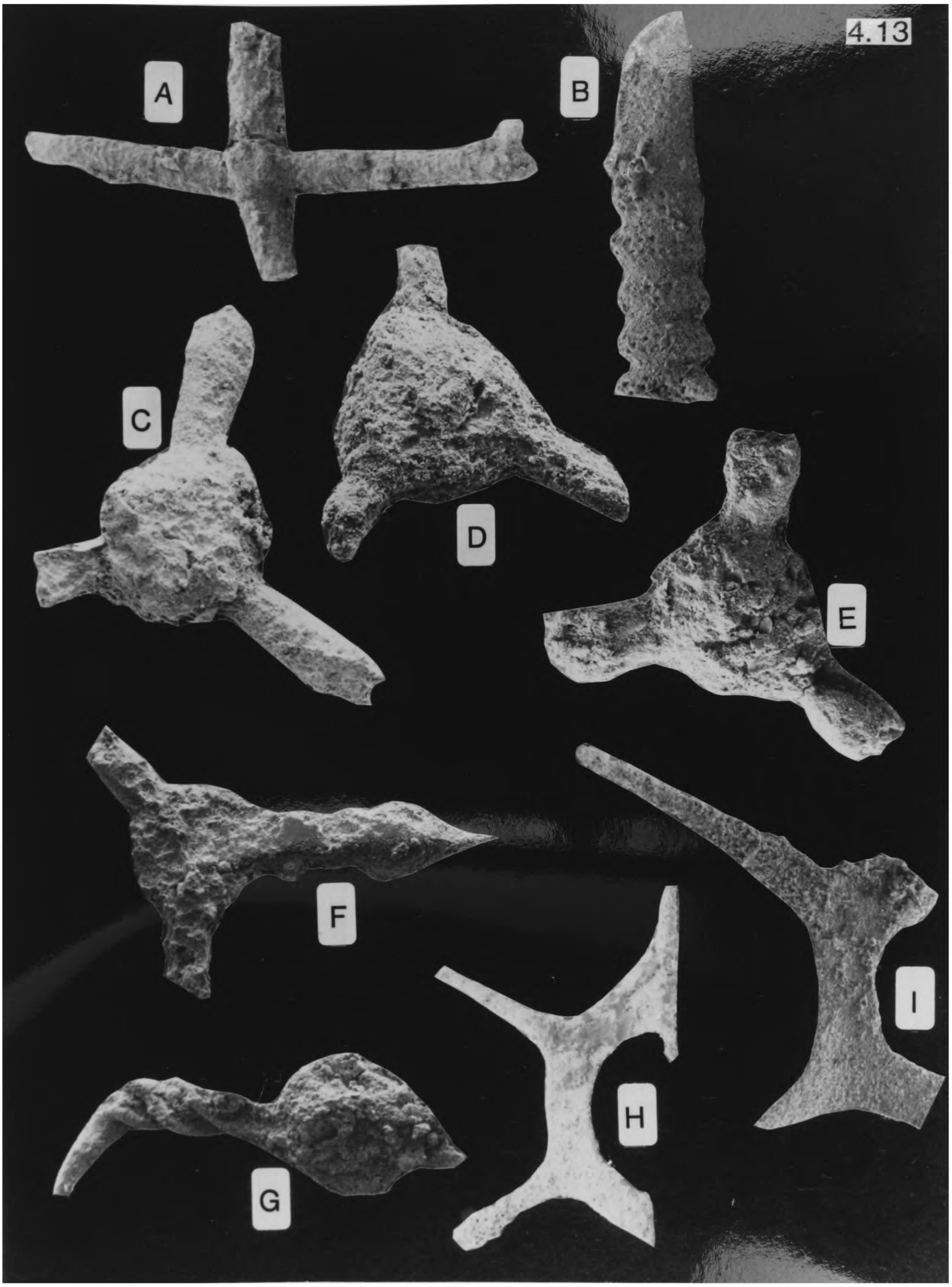
4.13
A
B
C
D
E
F
G
H
I

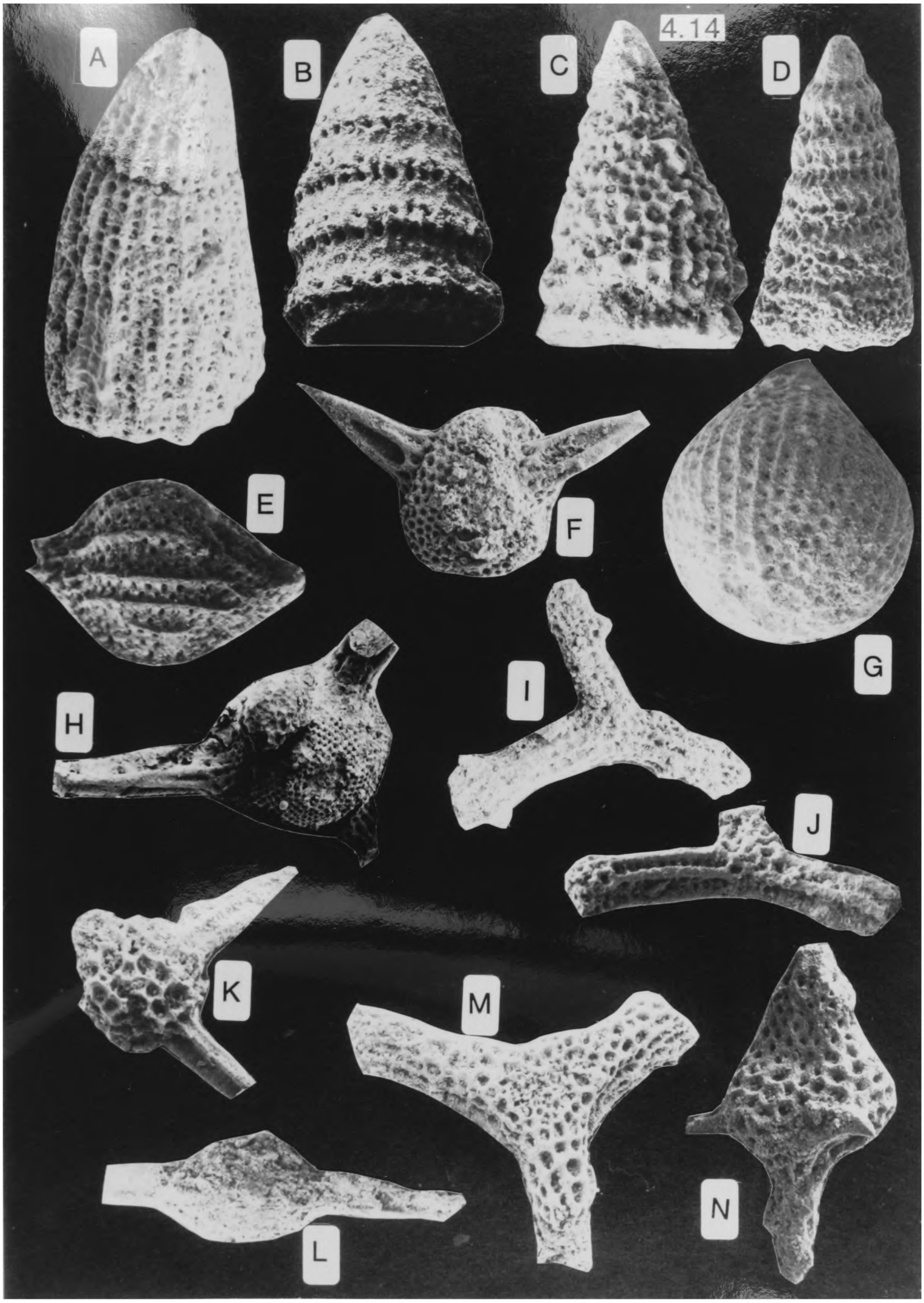
4.14
A
B
C
D
E
F
G
H
I
J
K
L
M
N

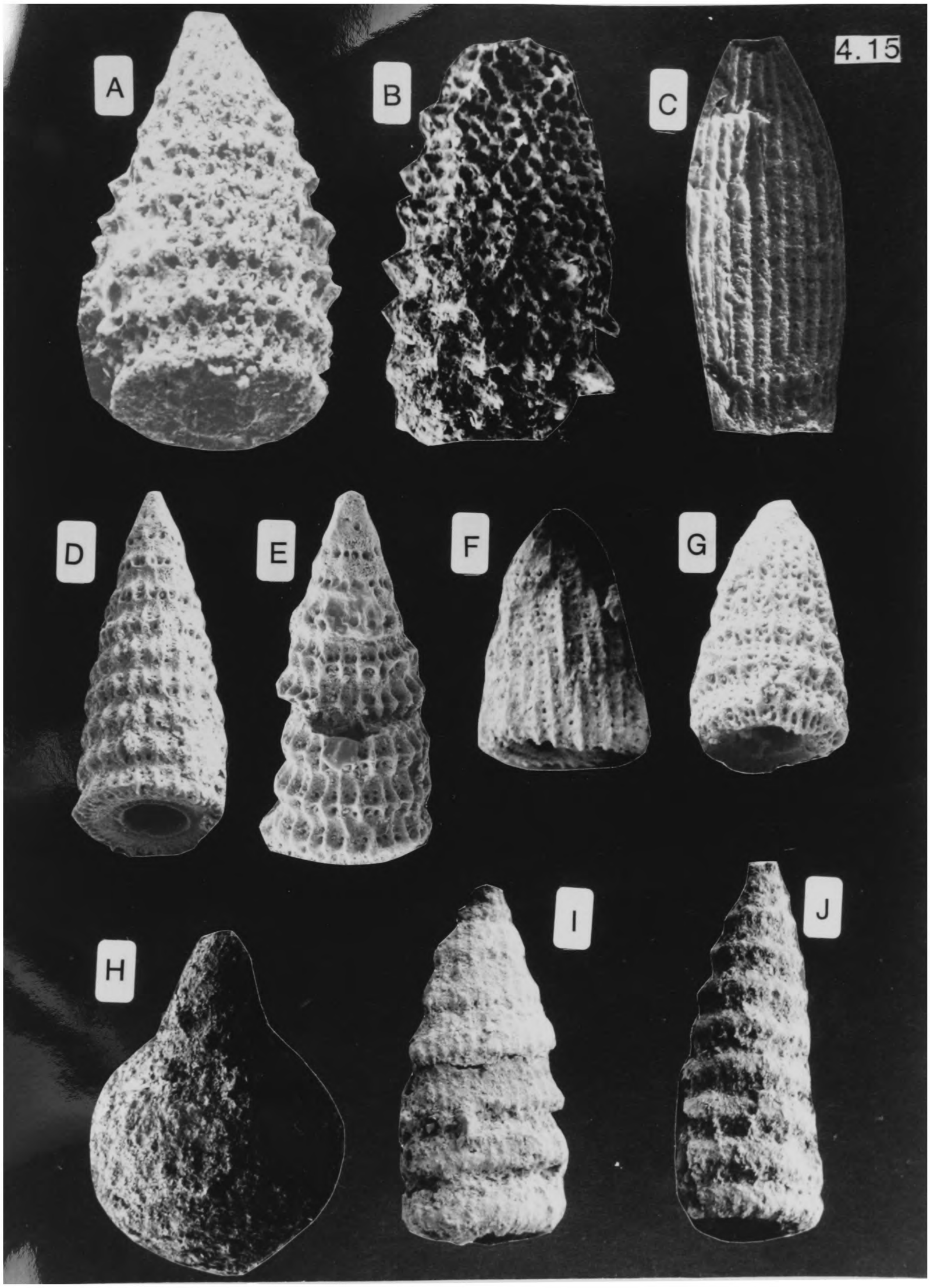
4.15
A
B
C
D
E
F
G
H
I
J

4.16

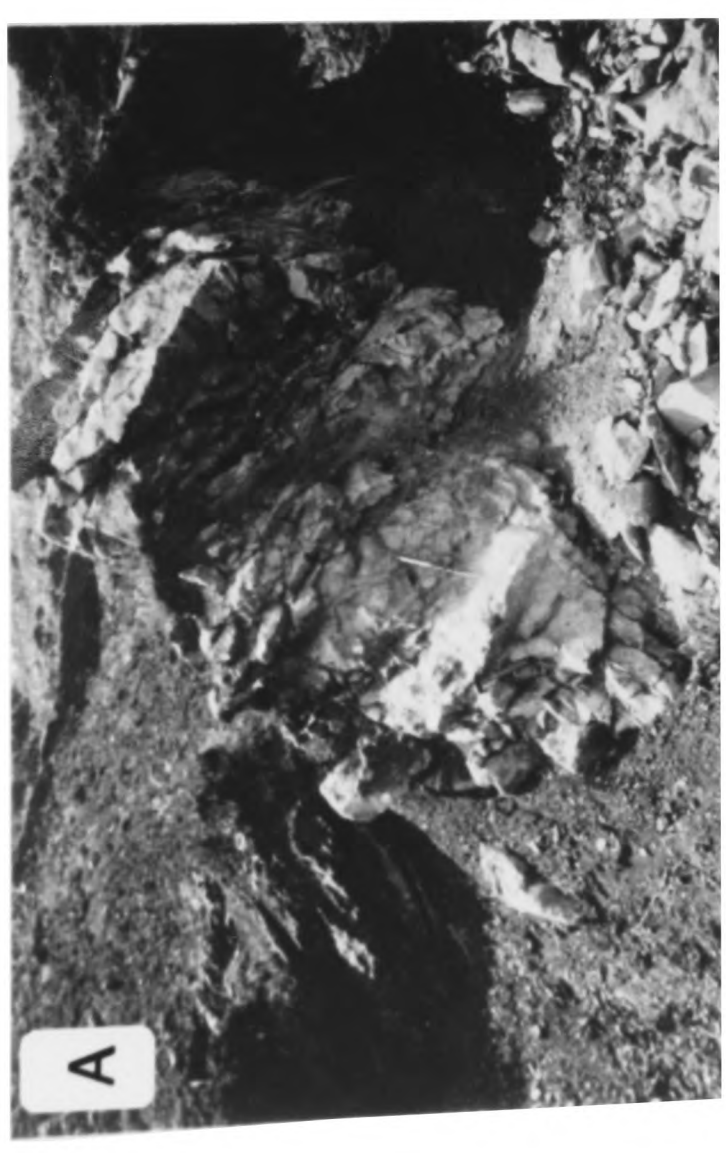

CHAPTER 5

CRETACEOUS SEDIMENTS OF THE NORTH PINDOS MOUNTAINS

5.1 THE DIO DENDRA GROUP: LATE JURASSIC TO LATE CRETACEOUS PELAGIC AND TURBIDITIC SEDIMENTS

5.1.1 Introduction

The Dio Dendra Group occurs as discontinuous, but extensively developed, sedimentary thrust sheets (Fig. 5.1) that are tectonically sandwiched between the Avdella Melange and the underlying Pindos Flysch (Kemp & McCaig 1984; Fig. 5.2). The group consists of four formations of Late Jurassic to Late Cretaceous age, which are mainly exposed in the Dio Dendra Valley within the central area of the north Pindos mountains (Fig. 5.3). From the oldest to youngest these are: a) the *Karamoula Formation;* b) the *Agios Nikolaos Formation;* c) the *Krevvati Formation;* and d) the *Zygourogreko Formation* (new names; see Appendix 1; Jones and Robertson in press).

Individual thrust sheets do not contain complete successions, but a composite lithostratigraphy has been pieced together by mapping and section logging. The sediments are poorly dated at most localities, although calpionellids have been utilised where present (Table 5.1). This means that some sections may perhaps be lateral facies equivalents of those placed in another formation. The Karamoula Formation is lithologically comparable to the widespread "Calpionellid Limestone" (Maiolica) facies of Alpine Tethys (Bernoulli & Jenkyns 1974). The Agios Nikolaos Formation may be partly equivalent to the Beotian Flysch (Celet et al. 1976; Ferriere 1976, 1982), and the First Flysch of the Pindos Zone (Aubouin 1959; Dercourt 1964; Fleury 1980). The Krevvati and the Zygourogreko Formations are possibly equivalent to the "Calcaires en Plaquette" of the Pindos Zone (Dercourt 1964; Ferriere 1982; Green 1983).

Table 5.1

LOCALITY AND FORMATION	SAMPLE	FAUNA
1) STRAGOPETRA (Karamoula Fm.)	104/89	*Calpionella alpina* *Tintinnopsella carpathica*
	105/89	*Calpionella alpina* *Crassicolaria parvula* *T. carpathica*
AGE: UPPER TITHONIAN		
2) KOKKINA LITHARIA (Karamoula Fm.)	157/88	*Calpionella alpina*
	158/88	*Calpionella alpina*
	159/88	*Calpionella alpina* *T. carpathica*
AGE: LOWER-MID BERRIASIAN		
3) PAPALIAPI BRIDGE (Karamoula Fm.)	1/29/A	*Calpionella alpina* *C. elliptica*
AGE: LOWER-MID BERRIASIAN		
4) KARAMOULA (Karamoula Fm.)	5/88	*Lorenziella?*
AGE: BERRIASIAN?		
5) MILEA ROAD (Karamoula Fm.)	104/88	*Crassicolaria parvula* *Saccocoma*
AGE: UPPER TITHONIAN		
6) KLEFI POTELAMOS (A. Nikolaos Fm.)	178/88	*Calpionella alpina*
AGE: UPPER TITHONIAN-MID BERRIASIAN		
7) LOUMNITSA VALLEY (A. Nikolaos Fm.)	162/88	*Calpionella alpina*
	163/88	*Calpionella alpina* *C. elliptica*

AGE: LOWER-MID BERRIASIAN

8) PERIVOLI VILLAGE (A. Nikolaos Fm.)	166/88	*Calpionella alpina* *C. elliptica?*
	167/88	*Calpionella alpina* *T. carpathica* *Calpionellopsis simplex*
	168/88	*Calpionella elliptica* *T. carpathica*

AGE: BERRIASIAN

9) PERIVOLI VILLAGE (Terry & Mercier 1971)	*T. carpathica?* *Calpionellites neocomiensis* *Calpionella elliptica*

AGE: MID-UPPER BERRIASIAN

10) AGIOS NIKOLAOS (Terry & Mercier 1971)	*T. carpathica* *Calpionella alpina* *Calpionellites neocomiensis* *C. dardeni* *Calpionellopsis sp.*

AGE: BERRIASIAN

11) FLEGGA MOUNTAIN (Terry & Mercier 1971)	*Calpionella alpina*

AGE: LATE TITHONIAN-MID BERRIASIAN

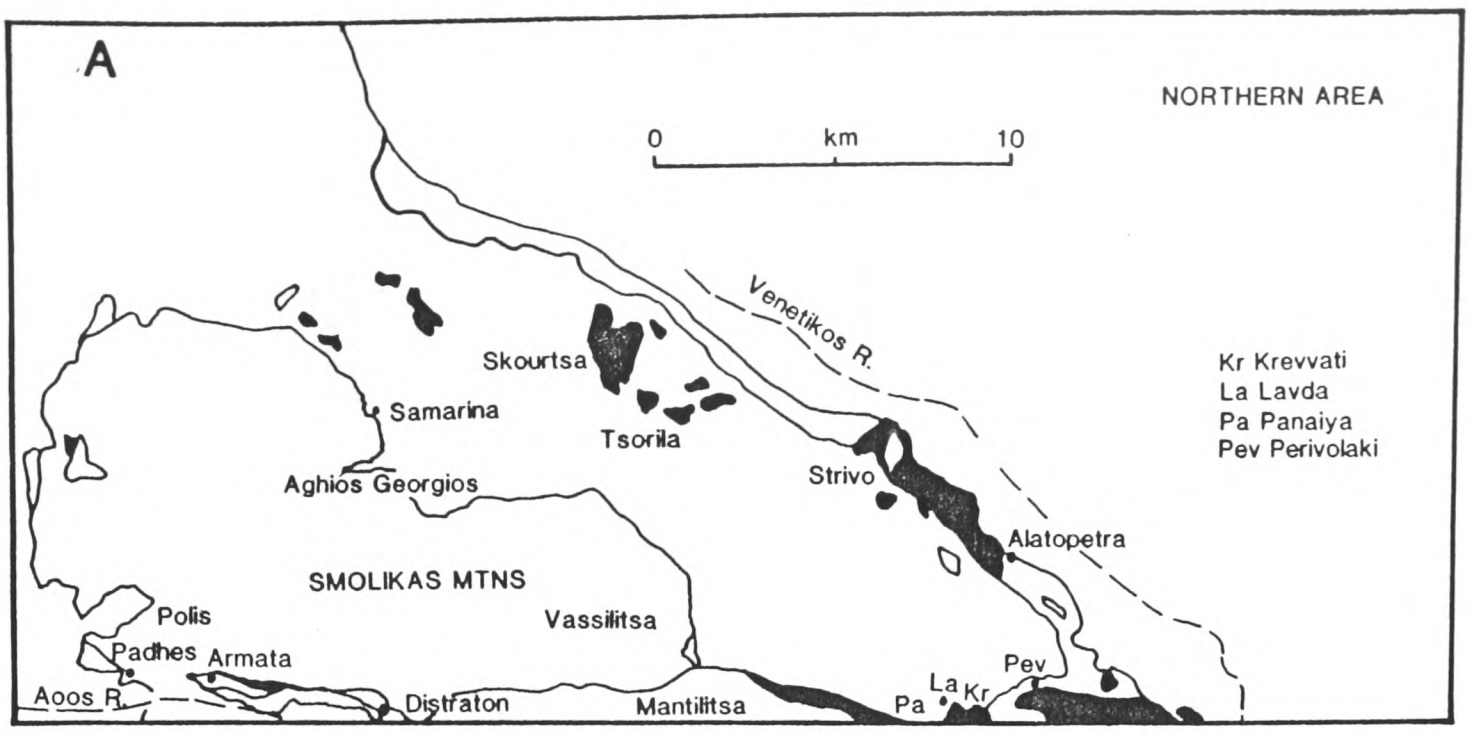

Fig. 5.1 Locality map for the Dio Dendra and Orliakas Groups.

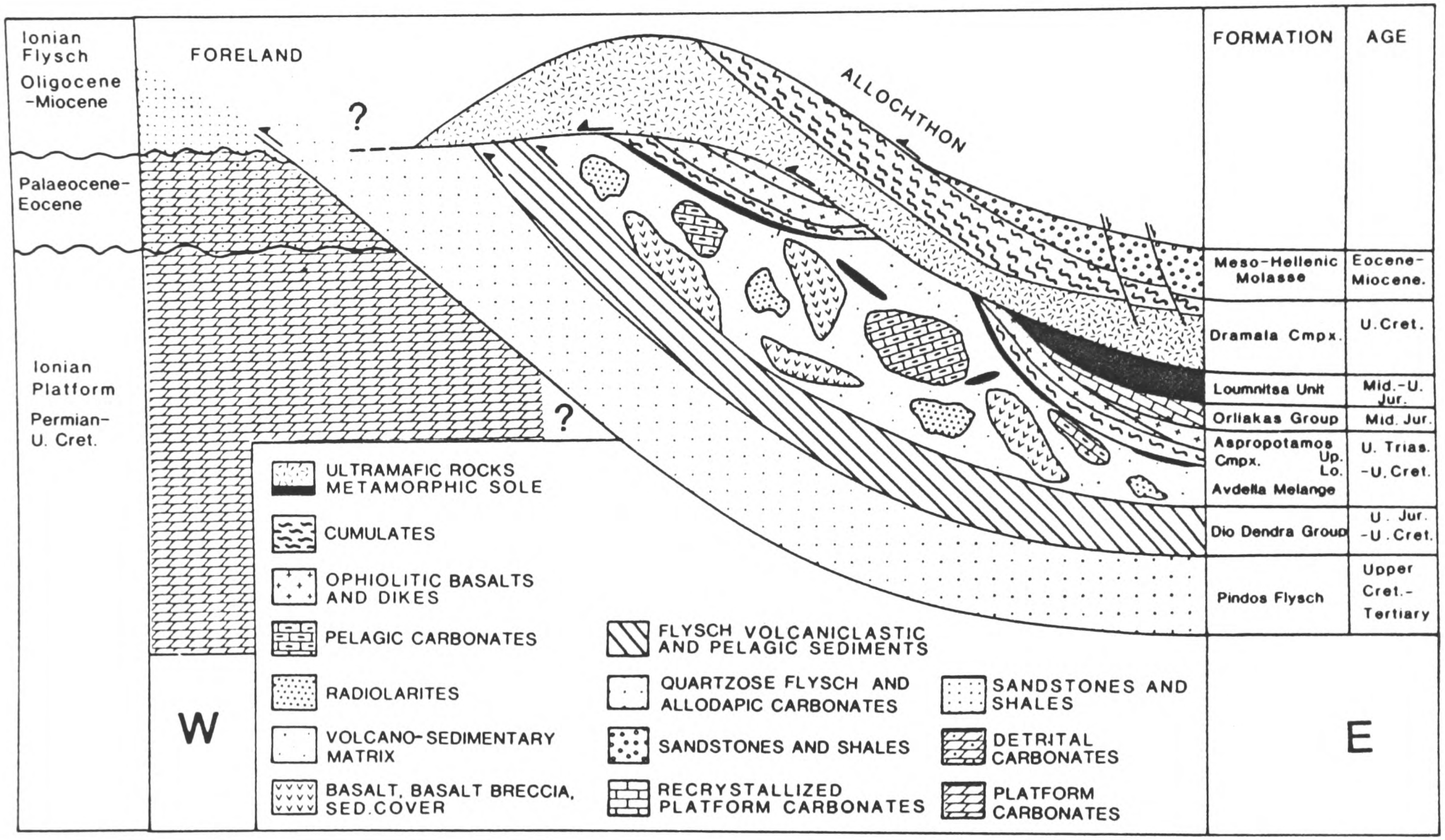

Fig. 5.2 Tectono-stratigraphy of the north Pindos Mountains. Note the position of the Dio Dendra Group consistently beneath the Avdella Melange and above the Pindos flysch. The Orliakas Group is in a less certain tectonic position, but definately overthrusts the Aspropotamos Complex of the Pindos Ophiolite Group.

5.2 PREVIOUS STUDIES

Following an initial description by Brunn (1956), some lithologies in the Dio Dendra Group were briefly described and dated as Berriasian (Early Cretaceous), in the Perivoli area, and north of Metsovo (Terry and Mercier 1971; Fig. 5.1). Kemp & McCaig (1984) described "a micrite rich to calc-arenite/calci-rudite rich transition" (i.e. Karamoula Fm.-Agios Nikolaos Fm.) near Perivoli, and noted the structural deformation present.

5.3 LITHOLOGICAL DESCRIPTION OF THE DIO DENDRA GROUP

The formations of the Dio Dendra Group are all composed of distal turbiditic and pelagic sediments (Fig. 5.4). They are carbonate-dominated, but some parts of the group have mixed carbonate-siliciclastic turbidite beds. The majority of clastic detritus is reworked mafic debris, although polycrystalline quartz grains compose a small, but significant part of some units.

5.3.1 The Karamoula Formation: pelagic and detrital sediments

The lowermost Dio Dendra Group formation (Fig 5.3) occurs as folded thrust slices, up to 500 m thick. Not all the lithologies of the formation are seen in any one section, and extensive thrust-and fold-related stratal disruption is common (e.g. at Perivoli; Fig. 5.1). The formation is not well dated, but is of probable Late Jurassic (Tithonian) to Earliest Cretaceous (Berriasian) age. This is based on the occurrence of calpionellids within pelagic and hemipelagic micritic carbonates (Table 5.1).

The Karamoula Formation is dominated by pelagic and hemipelagic, grey fine-grained carbonates and interbedded clastic sedimentary rocks (Plate 5.1). Fine-grained arenites, rich in basic igneous detritus and redeposited carbonate material, alternate with purple or olive-green calcareous shales and siltstones (Figs. 5.4, 5.5). At several localities, green or red-brown ribbon radiolarites and cherty mudstones, sometimes manganiferous or ferruginous, are also present. These often

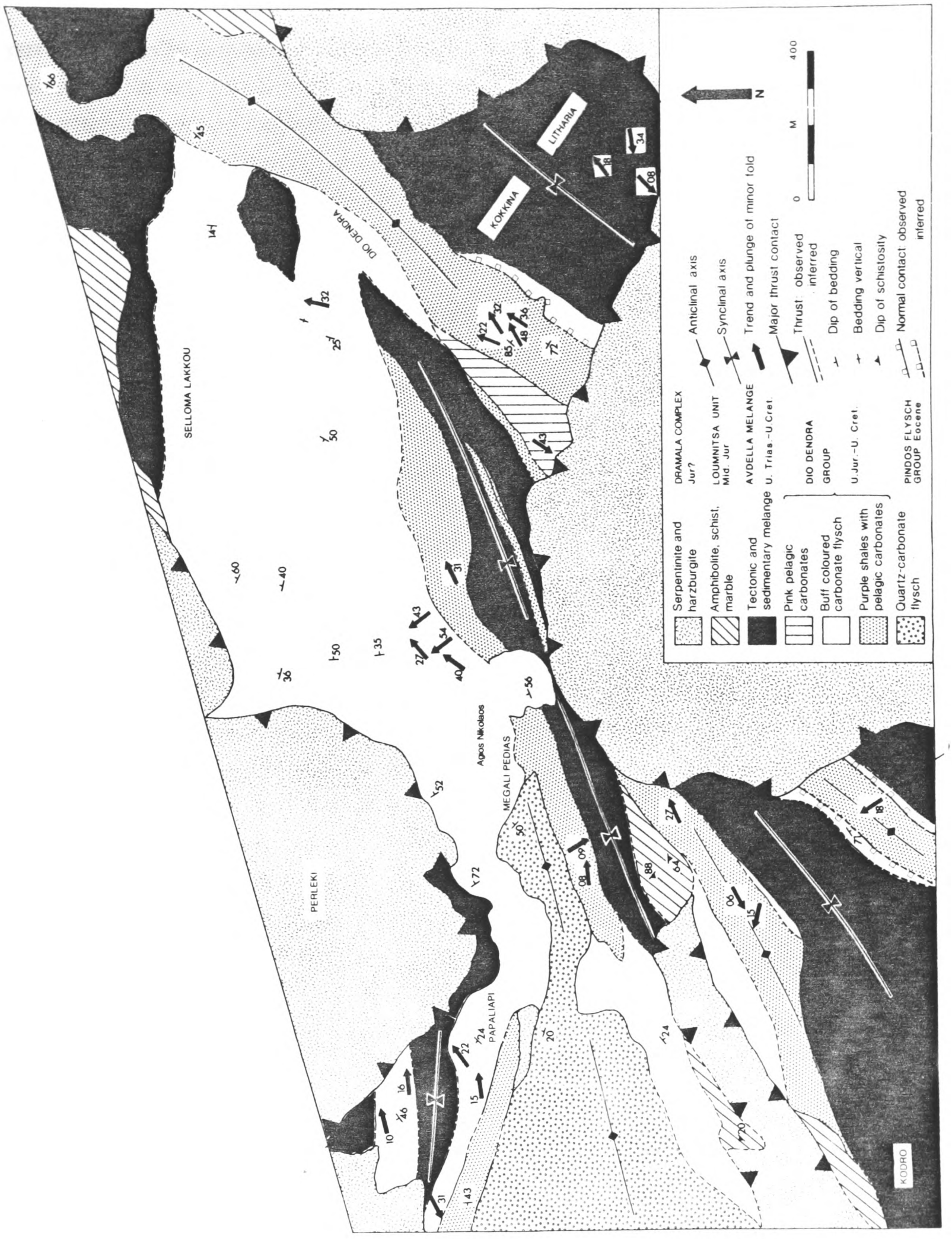

Fig. 5.3 Geological map of the Dio Dendra Valley, showing the locality of the main exposures of Late Jurassic and Cretaceous flysch of the Dio Dendra Group.

occur as cyclically deposited interbeds with the pelagic carbonates (e.g. at Karamoula, Dovas; Fig. 5.1; Plate 5.1). Both the pelagic carbonate and the radiolarite units are of extremely similar thickness (approximately 1.5 m), over an exposed thickness of several hundred metres (Fig. 5.4). Elsewhere (e.g. Stragopetra), true radiolarites are not common, but may occur as interbeds with brown cherty mudstones and purple shales (Fig. 5.5).

In some successions, towards the exposed top of the Karamoula Formation, redeposited fine calcirudites and calcarenites with volcanic detritus are found (e.g. N. Stragopetra, Fig. 5.5). These rocks are generally thin (Maximum 1.5 m), and are interbedded with distinctive purple coloured shales and siltstones, and light grey pelagic carbonates (Upper Tithonian; Table 5.1). Unusually, the base of the section at Stragopetra consists of greater than 100 m of purple-brown mudstones, cherty mudstones and manganiferous mudstones (Fig. 5.5). The redeposited carbonates are commonly parallel-laminated, containing up to 60 % altered basic volcanic material, particularly chloritised basalt, and also possibly degraded serpentinite. The carbonate fraction consists of a mixture of derived shallow-water carbonate clasts, and basinal material incorporated into the turbidites. A parallel-laminated calcarenite from Papaliapi (Fig. 5.5) is rich in clasts of non-ferroan dark-brown micritic carbonate, with diffuse clast boundaries (Plate 5.2). Clasts of shallow-water material also include partly micritised oosparites, pelsparites, brachiopod valves and several echinoderm plates (Plate 5.2). A ferroan carbonate matrix of finely crystalline sparry calcite (Plate 5.2) contains areas of secondary silicification. This rock also contains abundant altered basic material, particularly chloritised basalt, and angular to sub-angular fragments of radiolarite. Sponge spicules and radiolaria are present in abundance in some thin sections (Plate 5.2). Sub-angular to sub-rounded clasts of quartz and polycrystalline quartz are also present, but never abundant. Sedimentary structures are rare, but include parallel lamination, minor cross-lamination and wave-ripples.

Pelagic and hemipelagic carbonates are an important constituent of the Karamoula Formation (Plate 5.1, 5.3). Their bed thickness varies from 5-20 cm, but may reach 3 m in the case of some more massive beds. Nodules and bands of replacement chert also occur within the pelagic carbonates. These nodules typically occur towards the top of individual

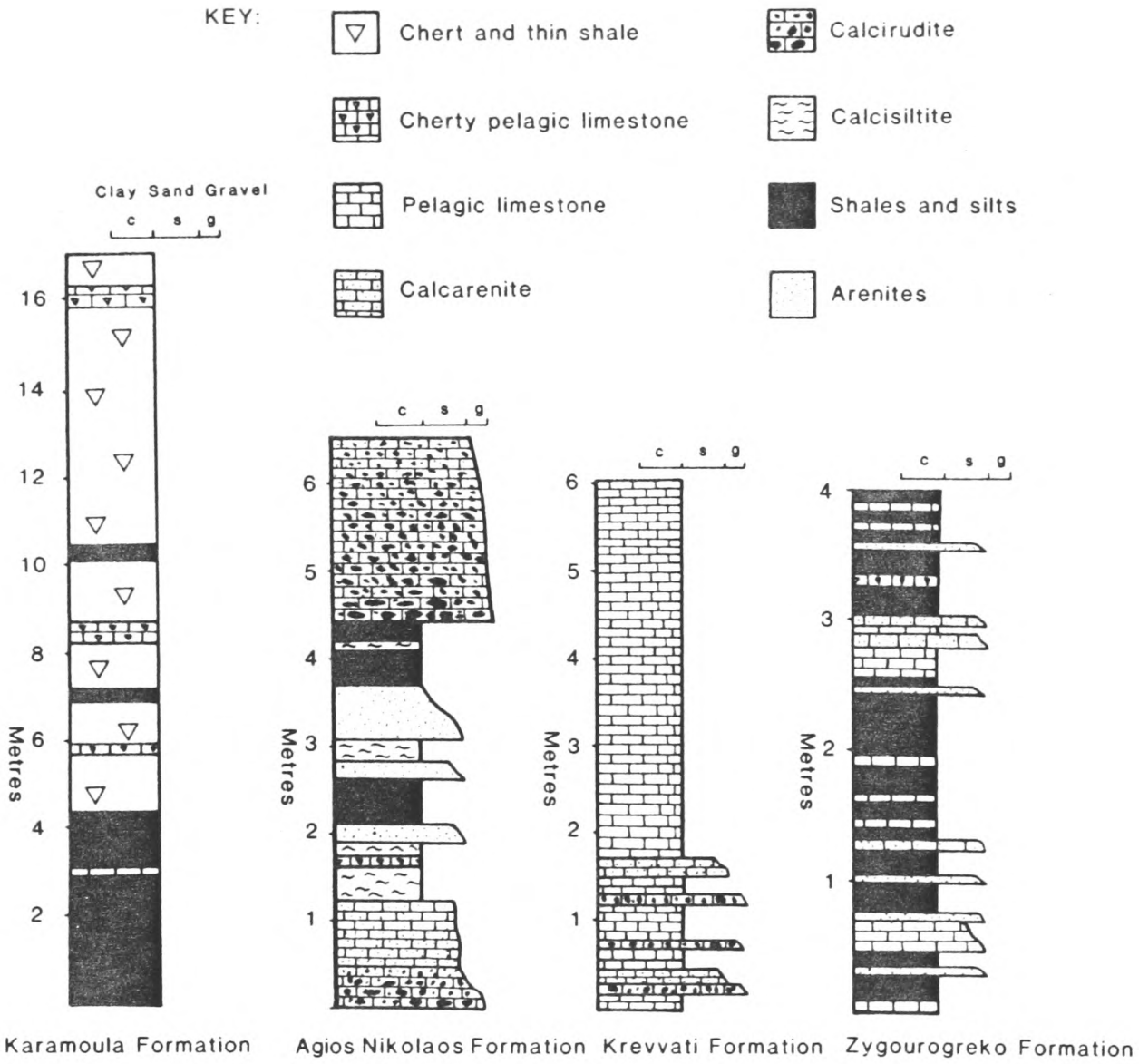

Fig. 5.4 Measured stratigraphic logs of the Dio Dendra Group, showing the typical lithologies encountered. a) measured at Karamoula; b) measured at Aspropotamos Bridge Perivoli (see also Fig. 5.6); c) measured at Krevvati Mountain; d) measured at Zygourogreko Hill.

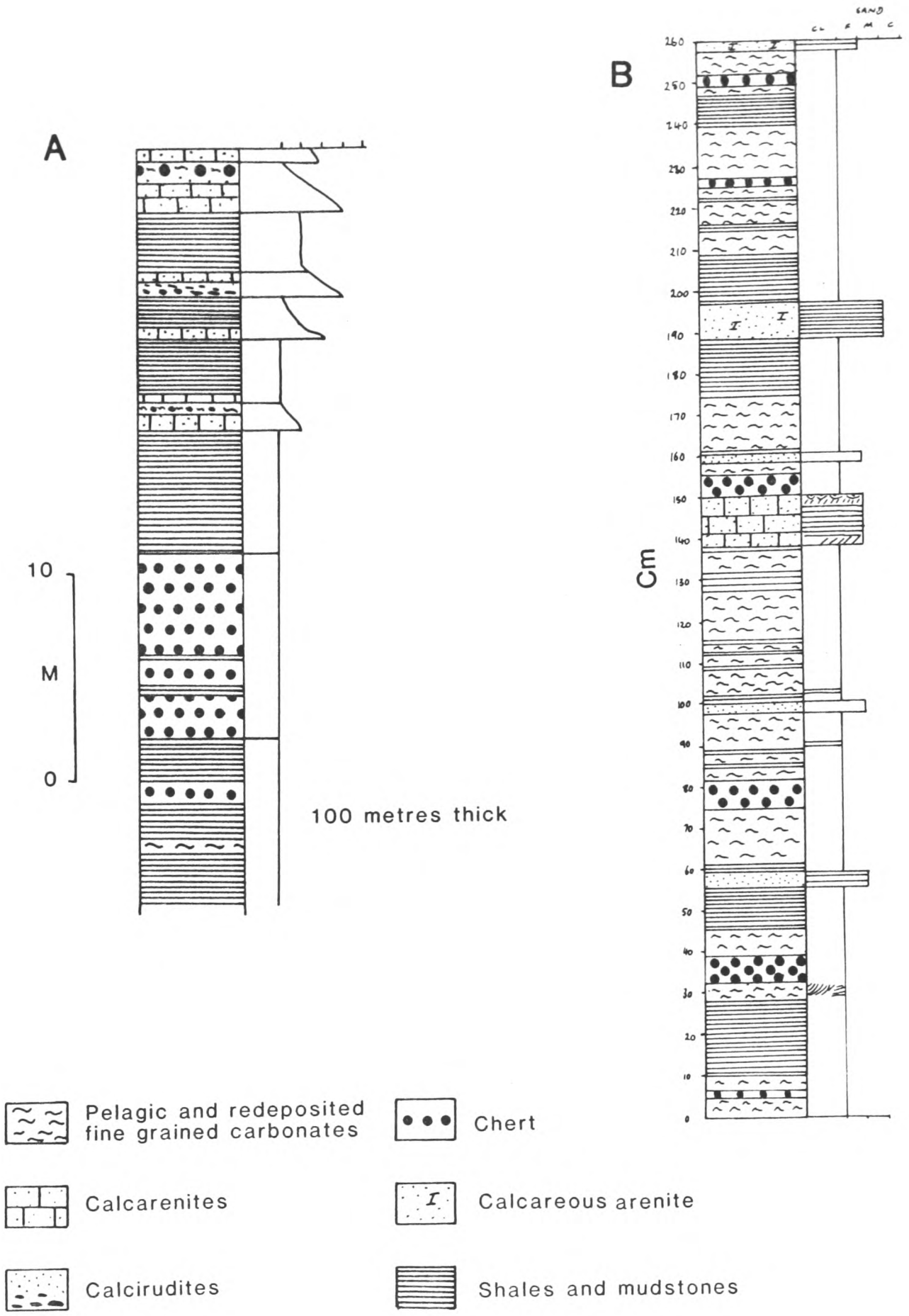

Fig. 5.5 Measured stratigraphic log of the Karamoula Formation; a) N. Stragopetra Mountain; b) Papaliapi bridge.

units, whereas the bands form in the centre. Some of these fine-grained carbonates are poorly graded, or may contain faint laminations and cross-laminations, indicating redeposition has taken place.

The contact between the Karamoula Formation below, and the Avdella Melange above, is a thrust, with the exception of one locality (S.W. of Milea, Fig. 5.1), where a conformable sedimentary contact was observed (see p165, Fig 4·8 and Plate 4·7). At this locality, a basal nodular pink carbonate, with corals and other bioclasts, passes into a pink and red micritic limestone and marl sequence, then into interbedded grey micrites and cherty shales (see Chapter 4). These basal carbonates contain the calpionellids *Tintinnopsella carpathica*, *Crassicolaria parvula* and the Late Jurassic pelagic crinoid, *Saccocoma*, dating the sequence as uppermost Tithonian (Table 5.1).

A Late Jurassic transgressive cover is also noted in the continuation of the Sub-Pelagonian Zone to the north in Albania (Mirdita Zone), where Late Jurassic/Early Cretaceous sediments transgress melange and ophiolite lithologies (Shallo 1980). Also, Kimmeridgian-Tithonian pelagic carbonates similar to those found at Milea transgress the Vourinos ophiolitic extrusives (Mavrides et al. 1979). Elsewhere, a transition from the Karamoula Formation upwards into the arenites and calcarenites of the overlying Agios Nikolaos Formation is preserved (e.g. Kokkina Litharia, Perivoli, Loumnitsa, Figs. 5.1, 5.3).

5.3.2 The Agios Nikolaos Formation: mixed carbonate-clastic turbidites

The Agios Nikolaos Formation conformably overlies the Karamoula Formation, above 2 m of transitional sediments. The contact is best exposed near Perivoli (Aspropotamos Bridge; Fig. 5.6), at Kokkina Litharia and in the Loumnitsa Valley (Fig. 5.1). The formation is mainly composed of carbonate and mixed carbonate-siliciclastic turbidite units, with interbedded pelagic and hemipelagic carbonates (Figs. 5.4, 5.6; Plates 5.3, 5.4), similar to those of the Karamoula Formation. The main distinguishing factor is that in the Agios Nikolaos Formation, purple mudstones become subordinate to buff-brown and olive-green arenites and mudstones. The Agios Nikolaos Formation also contains several graded turbiditic calcirudite horizons, each up to 3 m thick (Plate 5.4).

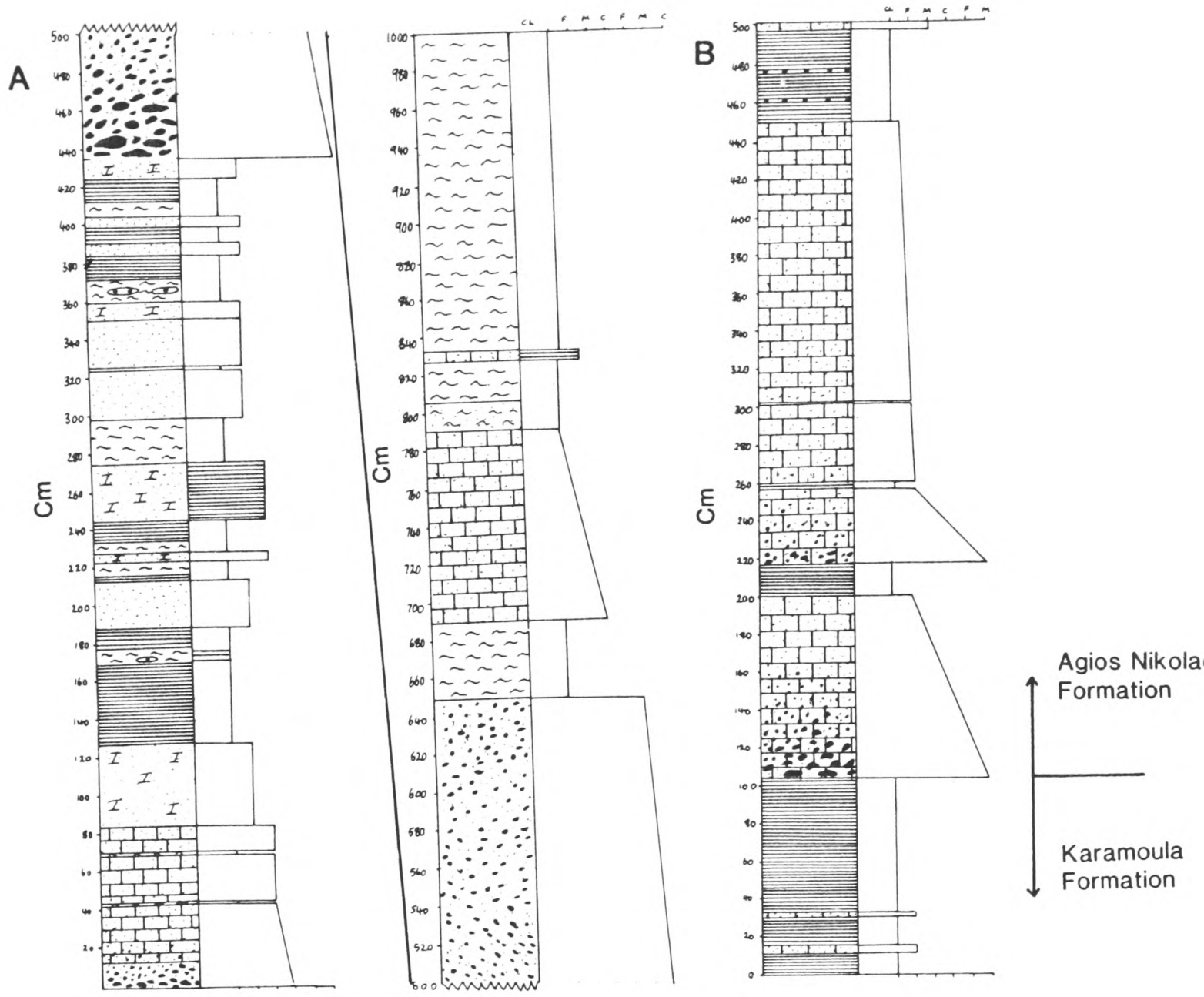

Fig. 5.6 Measured sections of the Agios Nikolaos Formation a) at Papaliapi Bridge; b) at the Aspropotamos Bridge, Perivoli, showing the transition from the Karamoula to Agios Nikolaos Formations.

The type section is located at the forestry station near Agios Nikolaos church (E. of Perivoli, Figs. 5.1, 5.3), and numerous other sections occur in the Dio Dendra Valley (Fig. 5.3), and elsewhere in the northern and southern areas (e. g. E. of Armata; Fig. 5.1). The maximum thickness is estimated as up to 350 m (e.g. N. Dio Dendra Valley). The flysch is believed to be mostly of Berriasian age based on the occurrence of calpionellids (Early Cretaceous; Terry and Mercier 1971; Table 5.1). No upper contact with younger formations was observed.

The Agios Nikolaos Formation is composed of thinly-bedded (5-50 cm), mixed carbonate-terrigenous turbidites, with interbedded pelagic carbonates. The turbiditic intervals consist of carbonate-cemented volcaniclastic rudites, arenites and siltstones containing variable mixtures of bioclastic carbonate material, chloritised and calcified basic igneous clasts, rare serpentine and quartz. The basic igneous clasts are mostly altered vesicular and/or plagioclase-phyric basalts. Gabbroic and ultramafic detritus is not at all common, and no opaques are seen. Much of the igneous detritus is highly degraded, and consists of patches of chlorite, serpentine and clay minerals which are often pervasively calcified. Crystals of altered pyroxene also may be found.

Clasts of chert and phosphatic chert are commonly calcified, and sometimes contain spherical patches representing dissolved radiolaria. The cherts are also observed to be micro-fractured, indicating that at least some calcification occurred prior to erosion. Other clasts observed include pink and white micritic limestones, usually composed of coarsely crystalline non-ferroan calcite. The rare presence of straight-shelled bivalves identifies these clasts as Triassic pelagic limestones. These clasts are common in sections exposed northwest of Perivoli, in the Koleo Mountain region (Fig. 5.1). Quartz clasts comprise up to 5 % of some sections studied. These are of metamorphic origin, polycrystalline clasts showing sutured grain boundaries and undulose extinction.

A large variety of carbonate detritus of shallow-water origin is present. Most abundant are buff-brown coloured micritic carbonate clasts, commonly containing euhedral authigenic dolomite and quartz crystals (Plate 5.2). Sometimes sparite-infilled fenestrae are also present in these

micrites. Also extremely abundant are algal carbonates, forming circular laminated oncoids, nucleated frequently on single quartz grains. Other clasts include oosparites, pelsparites and a variety of intraclasts. Echinoid plates and other echinoderm detritus are found frequently, as are brachiopod valves and spines. Calcisponges and corals are also distinguished in most thin sections. Trocholinid foraminifera occur rarely. Radiolaria are particularly abundant in the hemipelagic sediments.

Siltstones from the formation contain clasts similar to those described and, in addition, fragments of plant material. Hemipelagic micritic carbonates, with calcified radiolarians and calpionellids occur between turbidite units, in beds 3-8 cm thick. Pelagic grey micritic limestones, commonly partly silicified, together with olive-green mudstone form the inter-turbidite backgroung sediments. Common sedimentary structures within the turbidites include flute marks, well-developed parallel lamination, cross-lamination and wave-ripples (Plate 5.4). Many of the clasts present are elongated parallel to the lamination. The ratios of length to width sometimes reach 10 to 1. The basalt and chert clasts are also commonly oval to rounded on the corners, whereas the quartz clasts tend to have angular corners.

In the northern area, near Armata Village (Fig. 5.1; Plate 5.4), the Agios Nikolaos Formation is well-developed, but locally of a more distal facies. These units are made up of thinly-bedded (2-10 cm) brown, olive-green and purple mudstones, hemipelagic carbonates and marls. Thin calcarenites and volcaniclastic turbidite units are also present (Plate 5.4).

In the Dio Dendra Valley, thickly-bedded (3-5m), graded carbonate-rich turbidites occur, with chert, mudstone and basalt clasts at the base (1 mm-5 cm-sized grains), and calcilutite-grade carbonate at the top of each unit. At Agios Nikolaos (Fig. 5.3), the unit contains elongate rip-up clasts of mudstone and calcarenite (Plate 5.5), and comprises entirely carbonate clasts. Locally at Perivoli (Fig. 5.1), the equivalent unit also displays well developed sole structures (Plate 5.4). This unit contains displaced carbonate platform detritus, and is particularly rich in highly micritised bioclasts; algal oncoidal material, ooids, echinoids, bryozoa and bivalves; also calcified radiolaria and spicules. Thinner beds (5-15 cm) are

lithologically similar. In the Armata area, these are present as relatively thinly-bedded calcirudites, up to 2.5 m thick.

A cathodoluminescence study of a calcirudite from Papaliapi revealed calcite vein infills. An isopachous fringe cement with dull to black luminescence, passed outwards into coarse, prismatic, bright orange calcite spar, indicative of marine cements. The clasts of uniform poorly luminescent micrite indicate that they were formed separately under different diagenetic conditions, as expected. Pressure-solution stylolitic contacts occur between carbonate grains. Late Jurassic algae (*Clypeina* and *Salpingoporella* occur, probably within derived carbonate clasts. Small blue-luminescing feldspars occur within fragments of volcanic detritus.

5.3.3 Krevvati Formation: redeposited pelagic carbonates

The Krevvati Formation consists of redeposited and pelagic Late Cretaceous carbonate sediments, which are found as a component of the Dio Dendra Group. Other Late Cretaceous sediments are present within the Avdella Melange as olistolith blocks, and as separate thrust sheets, and are considered below. The Krevvati Formation consists predominantly of thin-bedded, and usually fine-grained (4-10 cm-thick) pelagic carbonates, with distinctive coarser redeposited horizons (Fig. 5.4; Plate 5.6). These horizons are similarly rich in chert and volcanic debris, together with an abundance of shallow-water carbonate clasts.

The formation crops out sporadically in the Dio Dendra Valley (Kokkina Litharia, Perivoli, Fig. 5.1), but is best developed in the Krevvati-Panaghia church area south of Lavda (Fig. 5.1), where it is up to 350 m thick. In the Katara Pass, lithologies typical of the Krevvati Formation are found conformably overlying volcanic extrusives of the Aspropotamos Complex.

The Krevvati Formation comprises distinctive grey, pink and red pelagic carbonates, sometimes rich in radiolaria and planktonic foraminifera. These sediments often have a large haematite content. Redeposited calcirudites and calcarenites are erosive into these pelagic carbonates (Plate 5.6), and contain basalt, occasional gabbro, and chert

grains, individually up to 6 mm in diameter. The basalts are again mostly highly chloritised, vesicular basalts and fine gabbros, sometimes plagioclase-phyric. Some beds do, however, contain basalt with relict pyroxene, and sometimes pyroxenes can be found in the matrix. Some of these better preserved basalts are petrographically comparable to island arc-type basalts found within the Pindos ophiolitic extrusives. They are particularly similar to basalts which underlie the Krevvati Formation in the Katara Pass. Also present are clasts of continental sandstone, similar to those present within the Avdella Melange, and grains of polycrystalline quartz, up to 1 mm in diameter. The carbonate components of the calcirudites and calcarenites include a large variety of shallow-water material, extremely similar to that found in the older Agios Nikolaos Formation. The carbonate clasts are mainly of micritic carbonate, but only rarely do they contain the dolomite crystals seen in the older clasts. Many types of carbonate are represented, including oosparite, pelsparite and ostracod-rich micrites (Plate 5.7). Coral, serpulid worm, algal and echinoid material is also common. Interbedded with these are red-brown stylolitic marls and shales. Several of these units contain the planktonic foraminifera *Globigerinelloides* sp., which ranges from Aptian to Maastrichtian. Ferruginous carbonate clasts within the calcirudites also contain this fossil.

Also present at several localities, including the type locality, are light grey calcirudites and coarse calcarenites, rich in comminuted rudist bivalve and other bioclastic debris. These sediments were also found to contain rare compressed rudist valves. They are probably related to the Late Cretaceous sediments of the Orliakas Group (see below).

A carbonate breccia horizon, up to 40 cm thick, is found at Zygourogreko (Fig. 5.1). The horizon has sub-angular to sub-rounded micritic limestone clasts, up to 3 cm in diameter at the base of the horizon. Laminated and cross-laminated calcarenites, and grey pelagic limestones are also present. Basaltic detritus is unusually rare in the succession at this locality.

Debris flow-type calcirudites, found locally as tectonic blocks associated with the Krevvati Formation (e.g. at Perivoli, Fig. 5.1), contain coralline material, oncoids, oosparite and fenestral micrite clasts with

equant dolomite crystals. The blocks are irregularly overlain by blue-grey calcareous arenites. Identical *Globotruncana*-bearing blue-grey calcareous arenites are also found as large clasts in a similar calcirudite debrite (e.g. at Kokkina Litharia, Fig. 5.3).

Further south, in the Katara Pass near Metsovo (Fig. 5.1; Brunn 1956), an inverted sucession of pink, thin-bedded redeposited and pelagic fine-grained carbonates ca. 50m thick, can be lithologically correlated with the Krevvati Formation. These carbonates overlie volcanics of island arc tholeiite (IAT) geochemical type, with an unconformable contact. Interbedded with the pelagic limestones is a 2.5 metre-thick rudaceous horizon, containing clasts of ophiolitic rocks up to 0.75 m in diameter, including basalt, gabbro serpentinite, chert, pelagic grey limestones, marble, and clasts of a coarse-grained augen gneiss. This sequence is interpreted as a large tectonic block within the Avdella Melange.

The Krevvati Formation is inferred to be Late Cretaceous based on common *Globotruncana* (e.g. the Katara Pass, near Panaghia, Fig. 5.1), and also on the occurrence of rudist bivalves, rarely as complete specimens, but more commonly as fragmented bioclasts in the coarser-grained units. No basal contact of the Krevvati Formation has been observed in the area, but it passes conformably upwards into the overlying Zygourogreko Formation at the type area of this latter unit (Fig. 5.1).

5.3.4 Zygourogreko Formation: clastic turbidites and pelagic sediments

The Zygourogreko Formation (see appendix 1; Fig. 5.4) is dominated by fine-grained and thinly-bedded carbonate turbidites and pelagic sediments (Plate 5.6), and forms the uppermost part of the Dio Dendra Group. So far, lithologies of this formation have been recognised only in one locality, south of Perivoli at Zygourogreko Hill, where it is ca. 250 m thick.

The succession comprises olive-green to buff-brown, parallel laminated, fine-grained arenites, siltstones and hemipelagic shales. These are interbedded with distinctive light gray, porcellaneous micritic pelagic carbonates in beds up to 30 cm thick, repeated on a metre scale (Fig. 5.4).

The carbonates are radiolarian-rich, and commonly contain benthic foraminifera. Basalt, chert and rare serpentinite fragments are present as clastic components.

At the type locality (Zygourogreko, Fig. 5.1), where it conformably overlies the Krevvati Formation, the formation apparently passes transitionally upwards into the Pindos Flysch. The transition is marked by the appearance of quartzo-feldspathic arenites and thick redeposited carbonate units containing nummulites.

Although an age diagnostic fauna have not yet been discovered, the base of the formation is assumed be Late Cretaceous, as it conformably overlies the Krevvati Formation. The uppermost part of the formation may extend to the Palaeocene or Eocene.

5.4 Facies and depositional environment of the Dio Dendra Group.

The Dio Dendra Group sediments are all of relatively deep-water facies. In general, a similar proportion of carbonate and clastic sediments is found within each formation, with the exception of the carbonate-rich Krevvati Formation. Depositional rates were low, with only somewhere in the order of 1500 m of sediment being deposited from the Late Jurassic to the Late Cretaceous (approx 70-80 Ma). The sediments were probably deposited within a Pindos ocean basin, remaining after emplacement of ophiolites onto the western Pelagonian margin, in the Late Jurassic (Chapter 8). The basin was apparently mostly infilled whilst above the carbonate compensation depth. This may not have been the case for the basal part of the group (Karamoula Formation), where interbedded radiolarites and pelagic carbonates are found. These cyclic deposits may have formed as a result of a fluctuating CCD, variations in the input of carbonate and clastic detritus, or due to alternating blooms of calcareous and siliceous nannoplankton.

A mixture of detritus from at least four different sources characterises all of these rocks: i) shallow-water carbonate material; ii) volcanic-chert clasts; iii) quartzose basement clasts and iv) intrabasinal background sediments. The derived material was transported mostly as

fine-grained turbidites, into a basin undergoing background pelagic sedimentation. The source area of this detritus must therefore include a carbonate platform or ramp, a metamorphic basement terrain, and the pre-existing oceanic basement and cover. The source of the extremely voluminous radiolarian chert and volcanic clasts, found throughout the Dio Dendra Group, could perhaps have been the Avdella Melange. The other possibility is that the Pindos ophiolite and its intact oceanic cover (presumably mainly radiolarites) formed at least part of the source. If so, it was the mostly volcanic sequence which was available for erosion, not deeper parts of the ophiolite.

By the Earliest Cretaceous, there is evidence that the melange was being eroded (e.g. the presence of Triassic limestone clasts, basalts and radiolarites in the Karamoula Formation). The ophiolite was also probably mostly available for erosion at this time, although how much was actually exposed above sea-level remains uncertain. By the Late Cretaceous, ophiolitic basement was certainly still partly submerged; pelagic carbonates of the Krevvati Formation directly overlie ophiolite volcanics in the Katara Pass. Furthermore, as the Karamoula Formation has been found transgressing the melange at one locality (S. of Milea), the melange must have been at least partly exposed on the sea-floor in the Late Jurassic. Evidence from the Vourinos ophiolite suggests that Kimmeridgian-Tithonian (Mavrides et al. 1979) pelagic and redeposited sediments overlie the island arc-type extrusives, indicating that the volcanic sequence remained exposed several hundred metres below sea-level after ophiolite emplacement. The platform which supplied detritus during and after the Early Cretaceous must have originated mainly after ophiolite emplacement (i.e. post-Kimmeridgian-Tithonian). This suggests that the platform was essentially the lateral equivalent of the Karamoula and Agios Nikolaos Formations, as it cannot have supplied material from beneath several kilometres thickness of ocean crust.

The more proximal sediments of the basin are probably not preserved today (but see below), an important conclusion for the structural evolution of the region. The Karamoula Formation consists mainly of pelagic and hemipelagic sediments, and contains more detrital material towards the top of the formation. It must be emphasised that the only conformable contact of Karamoula sediments with the infered

basement of the basin is preserved at Milea. Everywhere else, thrust om ission of sequence has occurred, and so the oldest sediments at other localities are almost certainly missing. In the western part of the basin, the Dio Dendra Group could theoretically have had Triassic basement, as it may have been deposited over sequences similar to those of the Pindos Zone. These have now been lost during Tertiary collisional processes.

The turbidites which were first deposited at the top of the Karamoula Formation, and are found throughout the Agios Nikolaos Formation, may have been part of a single developing carbonate submarine fan, although the intense deformation present in most sections precludes further investigation. The most relevant observation is the apparent northwards facies transition within the Agios Nikolaos Formation, into more distal thinly-bedded turbidites and mudstones than those found in the Dio Dendra Valley. Similar submarine carbonate fans have been described from the Upper Jurassic of the Betic Cordillera, southern Spain (Ruiz-Ortiz 1983), and from other parts of Greece (e.g. Othris; Price 1977). The sequences from Spain compare particularly well with those of the Agios Nikolaos Formation ("C" unit of Ruiz-Ortiz 1983). There, fan sediments are composed of rare calcirudites, abundant calcarenites (Bouma B-E divisions) and interbedded hemipelagic carbonates and radiolarites. Parts of the Hamrat Duru Group of the Oman Mountains of a similar age (Lower Cretaceous Sid'r Formation; Searle and Cooper 1986; Cooper 1988, 1990) also contains thinly bedded, silicified limestone turbidites, radiolarites and mudstones, somewhat comparable to the Karamoula Formation.

Several strong pulses of sedimentation took place during the deposition of the Agios Nikolaos Formation, resulting in the deposition of single, thick carbonate turbidite units. These units show good Bouma A-E turbidite sequence structures, whereas the other turbidites are usually missing the A and B units. They were derived almost entirely from a shallow-marine shelf-type source. They also contain clasts of radiolarite, basalt and mudstone, which must have been incorporated during the flow of the sediment. These units appear to have resulted from a significant tectonic event affecting the source area. This event is of Berriasian age, and therefore correlates to the Late-Jurassic to Early Cretaceous deformation of

the eastern margin of the Pelagonian continent (phase JE2b of Vergely 1984). This is discussed further below.

The Krevvati Formation sediments are carbonate-dominated, and turbiditic horizons are less common, but still rich in volcanic detritus. The presence of calci-turbidites composed of rudist bivalve fragments, suggests that a platformal source area still influenced basinal sedimentation. The Zygourogreko Formation sediments show facies which are essentially similar to the Karamoula and Agios Nikolaos Formations, and precede the thick turbidite sequences of the Pindos Flysch.

5.5 Tectonic setting of the Dio Dendra Group

The location of the source of the detritus for the Dio Dendra Group is uncertain. Several possibilities are considered here, taking into account the likely palaeogeography of the region during the Late Jurassic to Late Cretaceous (Robertson et al. in press). Generally, this is thought to be a time of tectonic quiescence on the western margin of the Pelagonian continent, although structural omissions and poor age dating places constraints on the inferences that can be made. Three main sources of shallow-water carbonate detritus are possible: the Pelagonian platform to the east, the Ionian platform to the west, and the Gavrovo-Tripolitza platform to the south. There may also be the possibility of an intra-basinal source, particularly from off-margin build ups thought to have been within the Pindos ocean (e.g. Olympos and Parnassos). This seems less likely however, from the available evidence. The platform that supplied the carbonate material must have been established for a considerable time period, as extensive diagenesis has affected the clasts prior to inclusion in the Dio Dendra Group sediments. However, much of the carbonate present does not contain evidence of a Jurassic age (i.e. characteristic Jurassic microfauna is missing), supporting the point made earlier that it was derived from a Late Jurassic-Early Cretaceous platform. The Ionian platform is the least likely source, as it was located too far to the west during the Cretaceous. The Pelagonian margin seems the most probable source area for all the components of the flysch, as it comprises carbonate platform with metamorphic continental basement, with emplaced

ophiolites and melange. However, the Gavrovo platform cannot be entirely discounted as a source, especially considering the south to north facies change present in the group. Again, in tectonic reconstructions, the Gavrovo platform may have been located many hundreds of kilometers to the south of the north Pindos area at this time, and is more likely to have supplied sequences of similar age in southern Greece.

The paucity of sedimentary structures, and the tectonised state of these sediments, means that palaeocurrent directions are unavailable. The favoured origin for these sediments is a faulted carbonate platform, developed on continental basement, which shed material from both of these sources into a basin, which had a basement of mafic basalts and their sedimentary cover. The original paleoslope may have faced to the north or northwest.

The Berriasian tectonic event perhaps responsible for the deposition of the thick limestone turbidites of the Agios Nikolaos Formation (the Je 2b event of Vergely 1976, 1982), was claimed to have mostly affected the Othris area of central Eastern Greece, and parts of the Vardar Zone (e.g. Almopias), according to Vergely (op. cit.). This event supposedly involved mainly southeastwards-directed backthrusting, but on the western Pelagonian margin northern Greece (i.e. the Vourinos area), little deformation occurred. Two lines of evidence suggest that this event may not, in fact have been related to the emplacement of Othris as interpreted by Vergely. Firstly, new age data for sediments at the top of the Pelagonian platform, onto which ophiolite emplacement occurred, shows a Late Jurassic emplacement was more probable in the Othris area (Ferriere et al. 1989). Secondly, suturing and major deformation of the Vardar Ocean is believed to be of Early Cretaceous age, not Late Jurassic (I. Sharpe and A.H.F. Robertson, pers. comm. 1990). It may therefore have been this Vardar closure-related deformation which triggered local faulting, and displacement of carbonate material westwards into the Pindos basin. As emphasised above, this carbonate seems to be mainly contemporaneous with the age of redeposition: reworked material with Jurassic fossils is very limited.

5.6 Comparison to synchronous sediments from southern and central Greece

Sediments similar to the Karamoula and Agios Nikolaos Formations of the Dio Dendra Group, are found in the Pindos and Beotian Zones of French nomenclature, in central and southern Greece (Aubouin 1959; Celet and Clement 1971; Celet et al. 1976). The Late Jurassic to Early Cretaceous sediments of the Pindos Zone (Aubouin 1959), comprise deep-water sediments similar to the Karamoula Formation (i.e. Calpionellid limestone facies), and to the Agios Nikolaos Formation (the "First Flysch"). These sediments also contain material said to have been derived from ophiolites; ie. basalt and radiolarite clasts. The sediments exposed in central Greece (i.e. within the Pindos Zone) include the Green sandstone member of Green (1983), which contains volcanic detritus also said to have been derived from an ophiolite, most likely to be the Othris ophiolite.

Celet and Clement (1971) and Celet et al. (op. cit.) compared all flysch outcrops of Late Jurassic to Early Cretaceous age, which crop out from the Peloponnessos to the North Pindos area, and packaged them as the Beotian Isopic Zone. The sediments of this age exposed to the east of the Parnassos platform and the Pindos Zone *sensu stricto*. According to Aubouin and Bonneau (1977) however, the Beotian Zone sediments were in "liason directe" with those of the Pindos Zone, and therefore formed part of the same basin. It seems unnecessary, considering these facts, to construct a separate Beotian Zone. Indeed, the distinction made by Celet et al. (op.cit.) is tectonic, and not palaeogeographic, a fact which has been pointed out by Papanikolaou and Sideris (1979). Furthermore, recent work (A.H.F. Robertson and P.J. Degnan, pers. comm. 1990) suggests that the Beotian Flysch of Celet et al. actually formed ahead of the emplacing ophiolite nappe as a foreland basin-type sequence (i.e. lateral equivalent to the Vourinos melange; see Chapter 4), and not in a post-tectonic flysch-type basin as envisaged for the Dio Dendra Group.

The "Beotian Flysch" of the Koziakas Mountains (Aubouin and Bonneau 1977; Jaeger and Chotin 1978) contains *Calpionella alpina*, and is located between the Triassic and Jurassic Koziakas sequence, and Late Cretaceous Thimiama Limestones. This sequence is probably comparable

to the Dio Dendra Group, and is similarly reported to contain radiolarite debris, and fragments of volcanic rocks.

According to the model of Vergely (1984), the "Beotian Flysch" (Clement 1971) now found to the east of the Parnassos and Olympos platforms, originated in an elongate narrow basin, formed ahead of the emplacing ophiolites and basement of the Pelagonian continent to the east. He attributes similar and synchronous sediments found to the west of the Parnassos and Olympos platforms (First Flysch of the Pindos Zone) as having been shed through divides in this barrier. As mentioned above, Robertson and Degnan (op. cit.) would interpret the "Beotian Flysch" as a foreland basin to ophiolites emplacing from west to east.

In the model adopted here (Chapter 8), the Olympos platform is located to the west of the Pelagonian within the Pindos ocean, and Parnassos is also interpreted as forming an outboard fragment of the continental margin of the Gavrovo platform to the southwest (Vergely 1984). This leads to a simple model of erosion of material from the western margin of the Pelagonian Zone, supplying the Pindos Zone during the Late-Jurassic and Early Cretaceous, when all tectonic events were taking place to the northeast. Considering all the evidence, there is little doubt that the Dio Dendra Group originated in a deep-water basin to the west of the Pelagonian Zone along the length of Greece. Similar post-tectonic flysch units are also present in Albania (Shallo 1980), and in Yugoslavia (Bosnian Flysch; Blanchet et al. 1969), indicating the considerable length, and probably width, of this basin.

5.7 THE ORLIAKAS GROUP: LATE CRETACEOUS PLATFORM AND SLOPE CARBONATES

The Late Cretaceous Orliakas Group (Fig 5.2; Appendix 1) is distinguished from the Late Cretaceous basinal sediments of the Dio Dendra Group because it consists mainly of platform and slope-type carbonates. The Orliakas Group also occupies a higher position within the thrust stack (definitely above the Avdella Melange, probably above the Aspropotamos Complex; Chapter 1). The group is exposed as a series of thrust sheets and tectonic blocks, best developed on the eastern margin of

the area studied (e.g. Orliakas Hills, Strivo Hills and their continuation to the N; Fig. 5.1). In the western and southern part of the Pindos Mountains, the group occurs as isolated olistolith blocks, up to 300 m in size, usually within the Avdella Melange (e.g. between Milea and Metsovo, Fig. 5.1; Brunn 1956).

5.7.1 Lithologies

The most common lithology is white or cream-coloured micritic carbonate, often containing isolated specimens of rudist bivalves, and less commonly, coral. Rare rudist reefs are preserved (e.g. Spileo road, Fig.5.1), locally in growth position (Plate 5.8). Rudists with individual valves up to 9 cm in diameter are found. Stromatolitic structures also occur in fine-grained carbonate (e.g. N. of Metsovo; Fig. 5.1). In thin section, these limestones typically contain benthic foraminifera, and a wide range of shallow-water allochems.

Redeposited carbonate units associated with the platformal units of the Orliakas Group include a variety of displaced shallow-water carbonate bioclasts (e.g. oosparite, dolomitised micrite, oncoids, echinoid plates, red algae etc.), and commonly contain a background component of chert, dolerite and basalt (Plate 5.7; Brunn 1956). The rocks are usually light grey and cream, coarse-to medium-grained, sometimes graded and laminated, with igneous debris present at the base of individual beds. Benthic foraminifera are abundant, and in some blocks rudist debris composes up to 100% of the rock. Occasionally, hemipelagic or pelagic units are interbedded with the redeposited material. Such units correlate with similar sediments present in the Krevvati Formation, which probably formed a lateral facies equivalent of the Orliakas Group.

Several carbonate sequences contain Late Cretaceous foraminifera, including *Globotruncana, Globigerina, Textularia and Orbitulina* (Brunn 1956). These, together with rudist bivalves date parts the Orliakas succession as Santonian-lower Campanian (P. Skelton pers. comm., 1988), and Coniacian (Brunn 1956). Hippuritid rudists are present within the Orliakas sequence at Spileo (Plate 5.8). At Monahiti (Fig. 5.1), isolated tectonic blocks with Radiolitid rudists are of Santonian age (Brunn 1956).

At Agios Dimitrios, west of Monahiti, quarried Late Cretaceous carbonates, exposed as a series of tectonic blocks, contain several interesting features. These include recrystallised platform-margin pink fine-grained limestones, containing abundant planktonic foraminifera. These blocks have narrow fissures and neptunian dykes (5-10 cms wide), infilled with angular clasts of the host carbonate, in a red haematitic clay matrix. Occasional small clasts of gabbro and dunite were also recovered. These sediments are overlain by reworked slope-type calcirudites, composed entirely of rudist debris. Other units contain more complete specimens.

In the region between Milea and Metsovo (Fig 5.1), blocks of Late Cretaceous carbonate are found as olistoliths within the Avdella Melange. These sediments were studied by Brunn (1956 pp 133), who obtained a number of Late Cretaceous foraminifera (e.g. *Globotruncana, Globigerina, Gumbelina, Textularia*). These carbonates are of several facies, including recrystallised and unrecrystallised fine-grained carbonate, calcirudites and calcarenites, typical of slope and platform-type environments. Sometimes, facies similar to the Krevvati Formation are seen, and volcanic detritus is present, but uncommon. Other blocks of similar age and facies are found in the Skourtza-Tsorila area, near the road to Samarina (Fig. 5.1). These contain *Orbitolina concava* within calcirudites, representing a Cenomanian age (Brunn 1956).

5.8 Facies and origin of the Orliakas Group

The Orliakas Group sediments are similar to shallow-water sediments present deposited throughout Greece in the Late-Cretaceous. The western Pelagonian margin ophiolite and basement sequences often have an extensive transgressive cover of Late Cretaceous carbonate (e.g. the Siatista carbonates, N. of Vourinos; Theopetra limestones, east of Kalambaka). The Orliakas Group is interpreted as forming part of this platform-slope sequence. The Orliakas Mountains themselves remain in a somewhat enigmatic structural position (see Chapters 1 and 7), and may have originally been deposited directly onto part of the Aspropotamos Complex and/or Avdella Melange. Further structural and sedimentological work is required to establish the precise palaeogeographic situation during their deposition. Work in the Vourinos

area has identified redeposited slope and off-reef talus deposits (e.g. Langadhakia, Poros and Metamorphosis villages), which may form lateral equivalents of similar units in the Orliakas Group.

Plate 5.1 Lithologies of the Karamoula Formation a) Cyclically interbedded green radiolarites, fine-grained limestone turbidites and hemipelagic carbonates, Karamoula. b) Purple shales and siltstones, interbedded with partly silicified pelagic carbonates, Perivoli Village. c) Redeposited calcarenites (C), interbedded with silicified hemipelagic carbonates, Papaliapi Bridge.

Plate 5.2 Photomicrographs of Karamoula Formation lithologies a) Calcarenite, showing micritised carbonate intraclasts (M), partly dolomitised (D), in a sparite cement (S). Also present is a radiolarite (R) clast (Papaliapi Bridge, 1/11/8; Field of view 3 mm PPL). b) Spicule-rich (S) calcarenite (Papaliapi, 7/11/8; 3 mm PPL). Photomicrographs from the Agios Nikolaos Formation. c) Agios Nikolaos; Calcirudite showing rounded shallow water clasts, including pelsparite (P) and echinoid plates (E), set in a micritic and microsparitic matrix (1/14/8; 6 mm XPL). d) Laminated micrite with calcified radiolaria and spines (Papaliapi, 5/14/8; 3 mm PPL).

Plate 5.3 Laminated calcareous arenite, rich in volcanic-radiolarite clasts, and interbedded hemipelagic carbonates, Agios Nikolaos Formation, N. of Papaliapi bridge. b) Recrystallised laminated marls, Kokkina Litharia, Agios Nikolaos Formation.

Plate 5.4 a) Thick, redeposited carbonate turbidite horizon, marking the transition from purple shales and pelagic limestones of the Karamoula Formation (right) into the Agios Nikolaos Formation (Aspropotamos Bridge, Perivoli). b) Sole structures at the base of the carbonate turbidite described above. c) Distal facies of the Agios Nikolaos Formation, exposed E. of Armata Village. Calcareous arenites, pelagic limestones, shales and marls, more thinly bedded than sequences found further to the S. d) Flute marks at the base of a calcareous arenite unit, Kokkina Litharia.

Plate 5.5 a) Carbonate rich turbidites, Agios Nikolaos Church, (Aspropotamos Valley, E. of Perivoli). b) Rip-up clasts of marl within the massive calcarenite bed shown in c). c) Well-bedded Agios Nikolaos Formation sediments at the type locality, Agios Nikolaos Church, Aspropotamos Valley, E. of Perivoli.

Plate 5.6 Krevvati formation sediments a) Deformed red haematitic marls at Panaghia church, 3 kms S.W. of Lavda Village (Pan on Fig. 5.1). b) Thin-bedded pink pelagic limestones, base of the Dio Dendra Valley at Kokkina Litharia. c) Erosive turbidite horizon within the marl sequence of b) above. This horizon contains angular clasts of radiolarite and altered basic volcanic rocks. d) Zygourogreko Formation, from the type locality, S.E. of Perivoli. Note the presence of porcellanous pelagic carbonates interbedded with calcareous arenites and shales.

Plate 5.7 Photomicrographs of Upper Cretaceous redeposited carbonates. a) Wide variety of shallow-water clasts, particularly dolomitised micrite and biosparite (B). Note also the presence of echinoid fragments (E), and oosparite (O), with other micritic debris (3/12/8/A, Perivoli; 12 mm PPL). b) Clast of coprolite limestone, and echinoid plates in carbonate debrite, associated with the Krevvati Formation (1/12/8/A, Perivoli, 6 mm PPL). c) Late Cretaceous debrite, base of Dio Dendra. Crinoid ossicles, other carbonate debris and the pelagic foraminifera *Globigerinelloides* (H) and *Globotruncana Sp* (I; 3 mm PPL). d) Carbonate block associated with the Orliakas Group, N.W. of Monahiti. Fragments of coral (D), gabbro (E) and basalt (F) set in a sparitic matrix (G; 3 mm PPL).

Plate 5.8 a) Rotallid rudist bivalves, from a melange block, 1 km N.W. of Monahiti. b) Hippuritid-type rudist bivalves, Agios Dimitrios, N.W. of Monahiti. c) Hippuritid rudist reef, road to Spileo, Orliakas Mountains. d) Close-up of rudist valves of c), weathered out on the limestone surface.

5.1

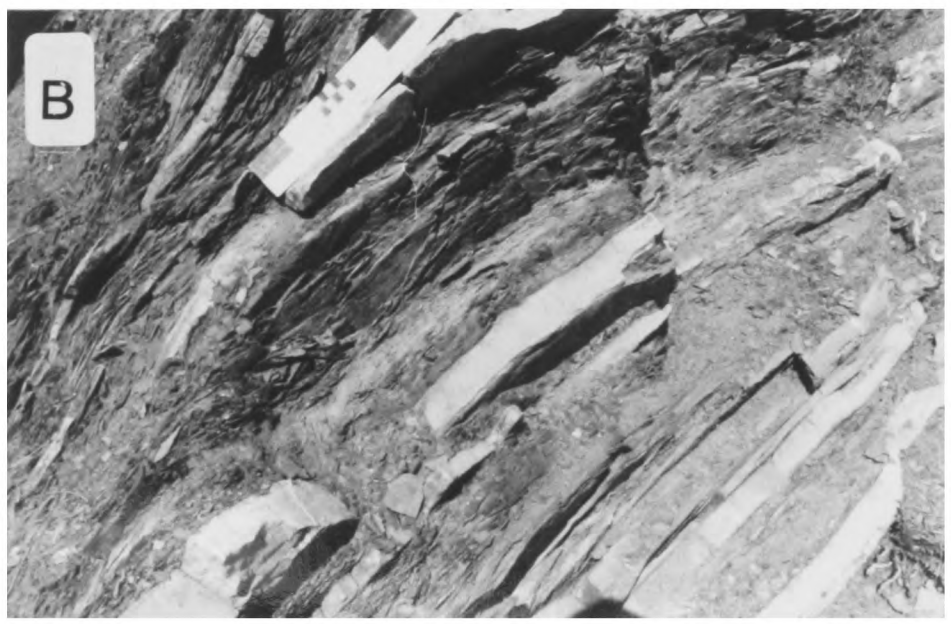

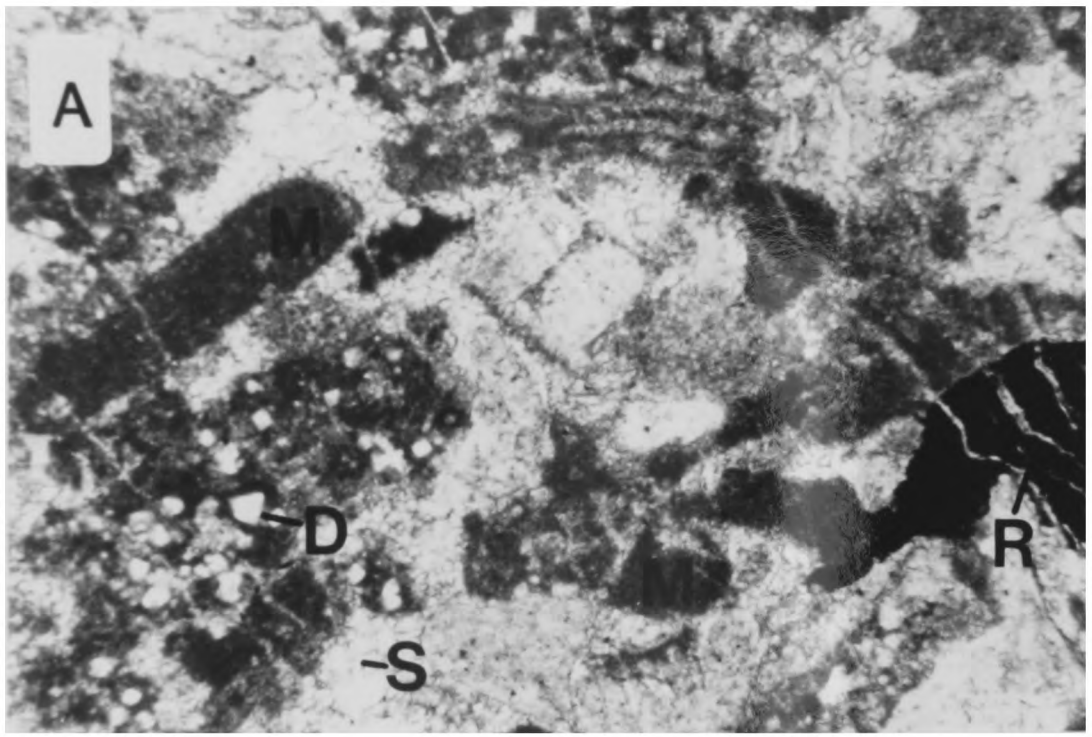

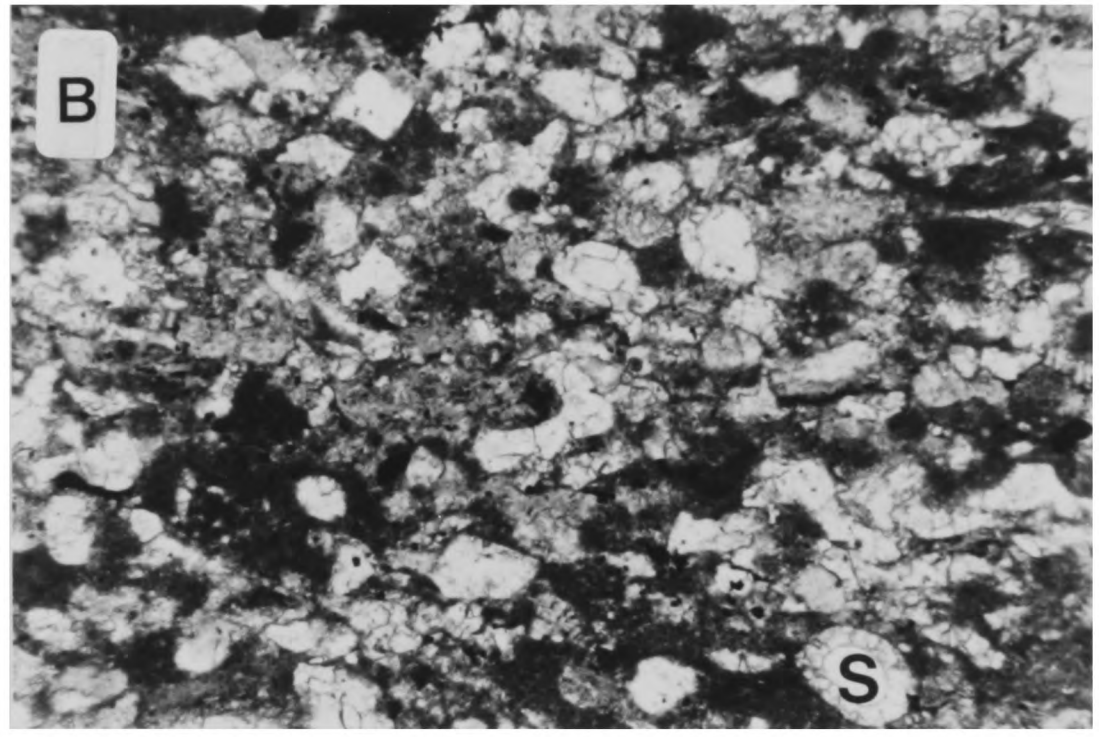

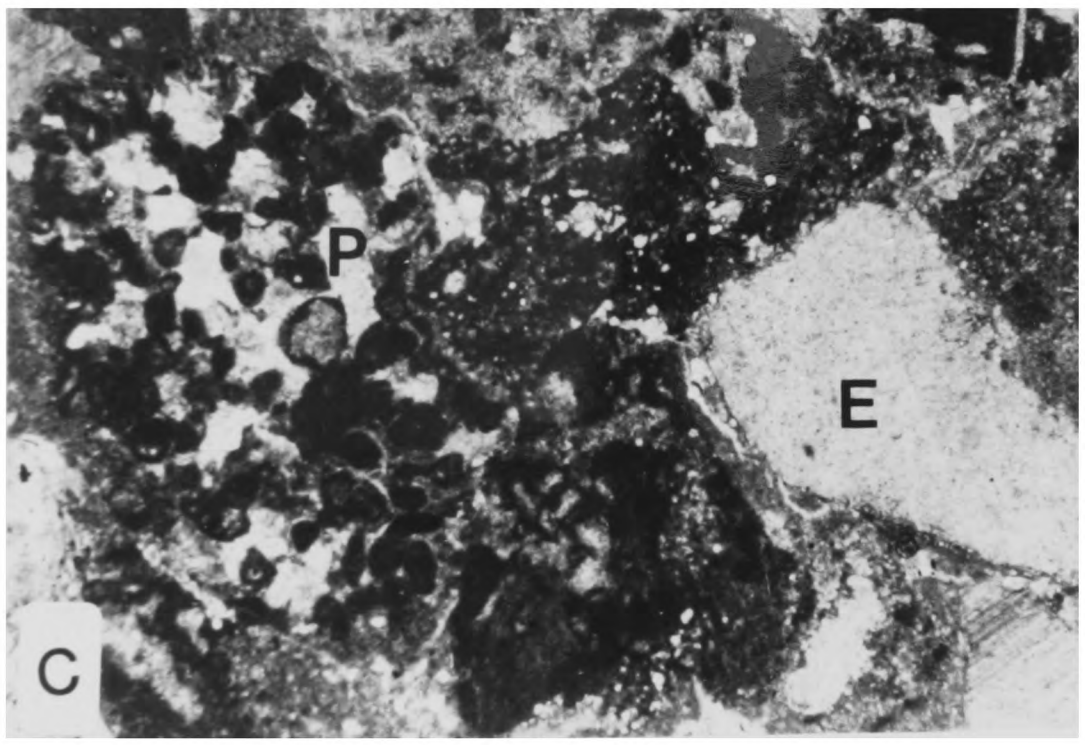

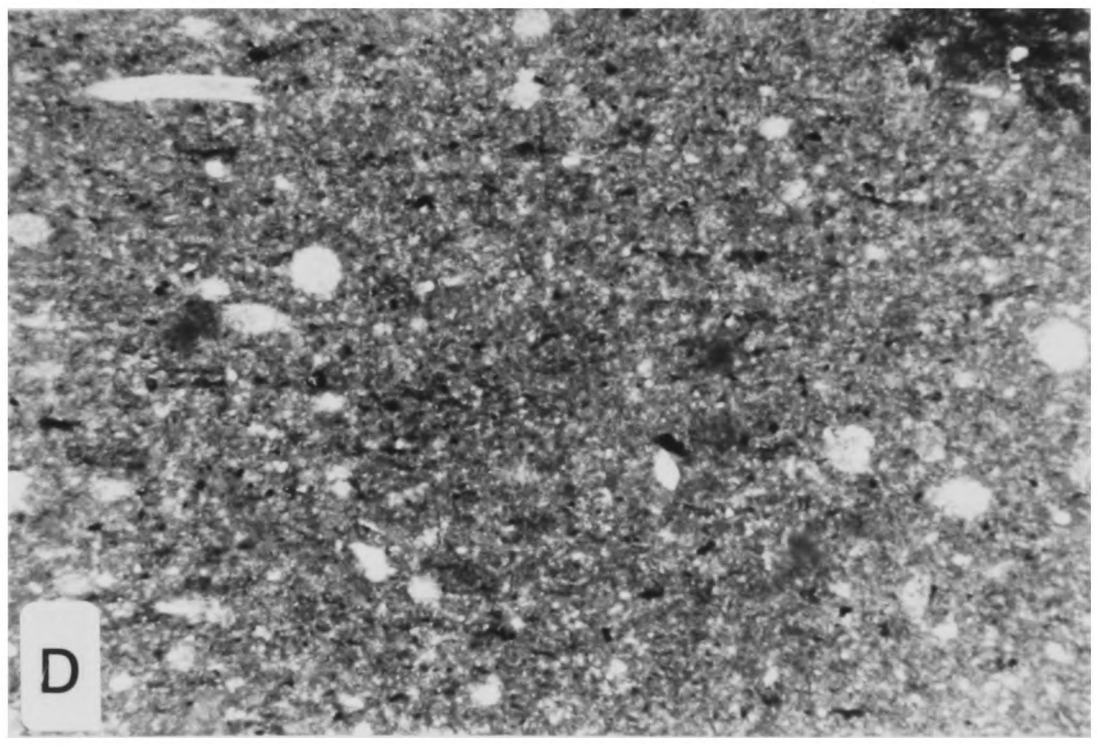

5.2

5.3

5.4

5.5

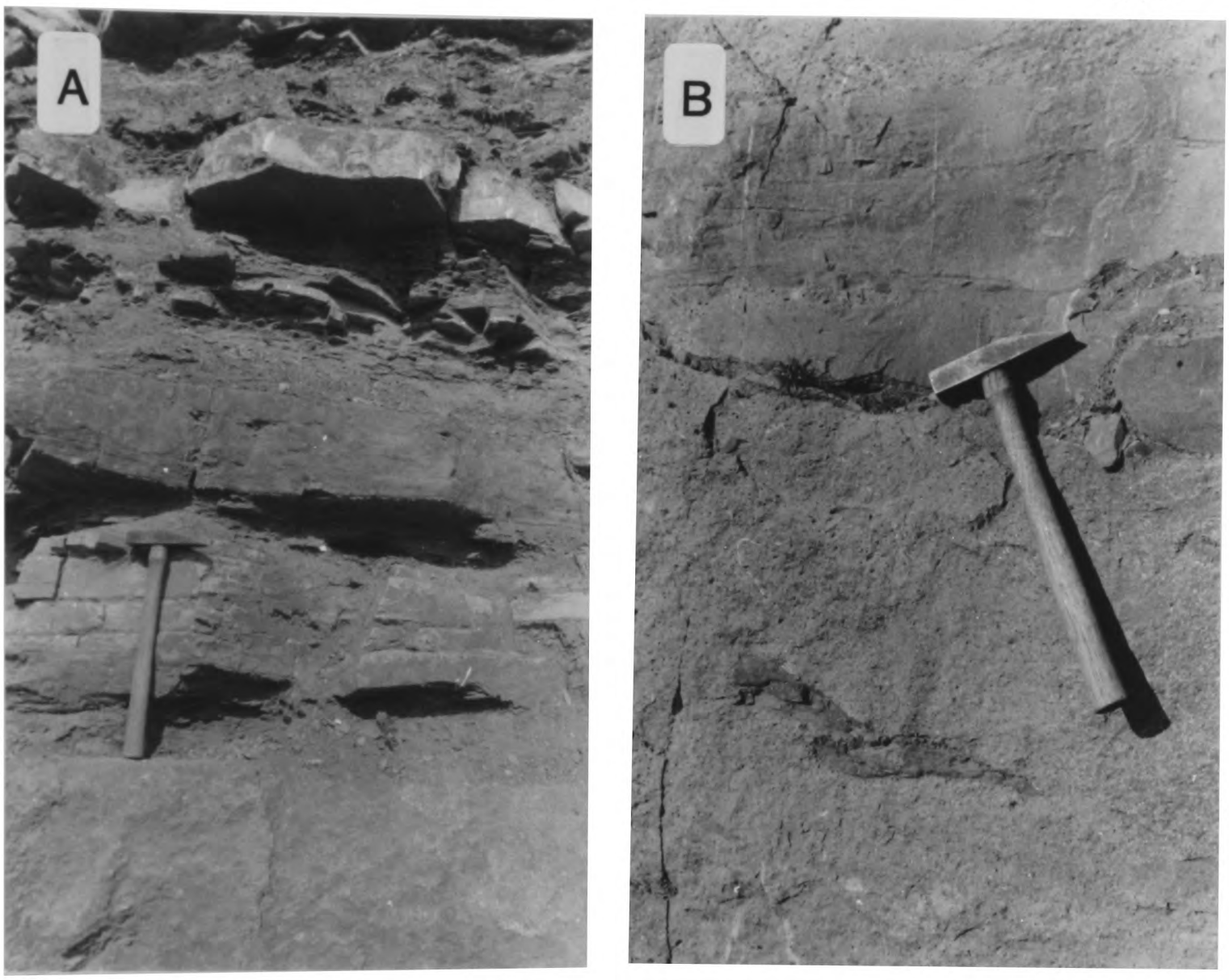

5.6

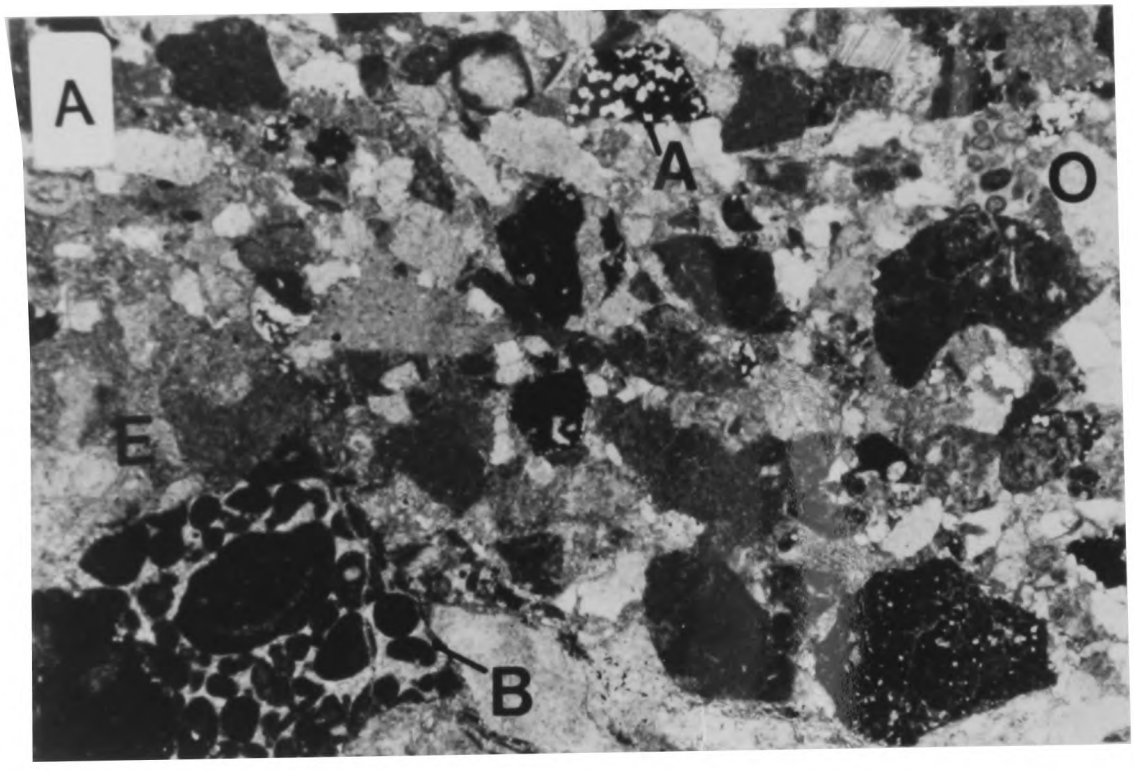

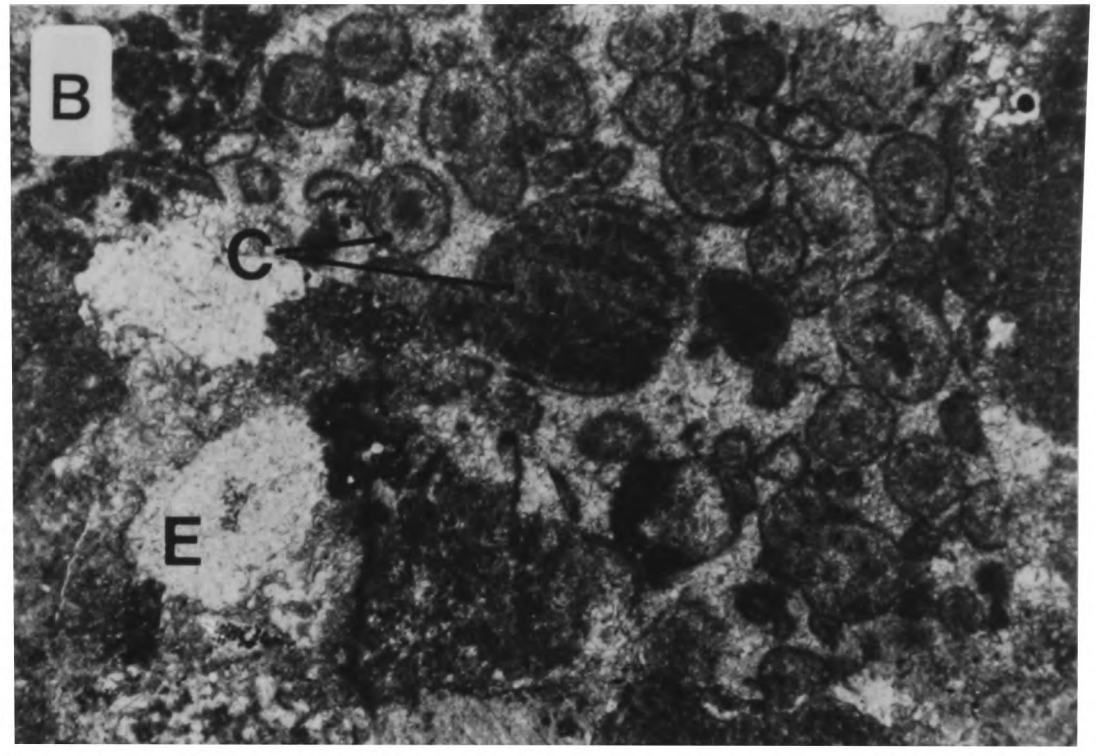

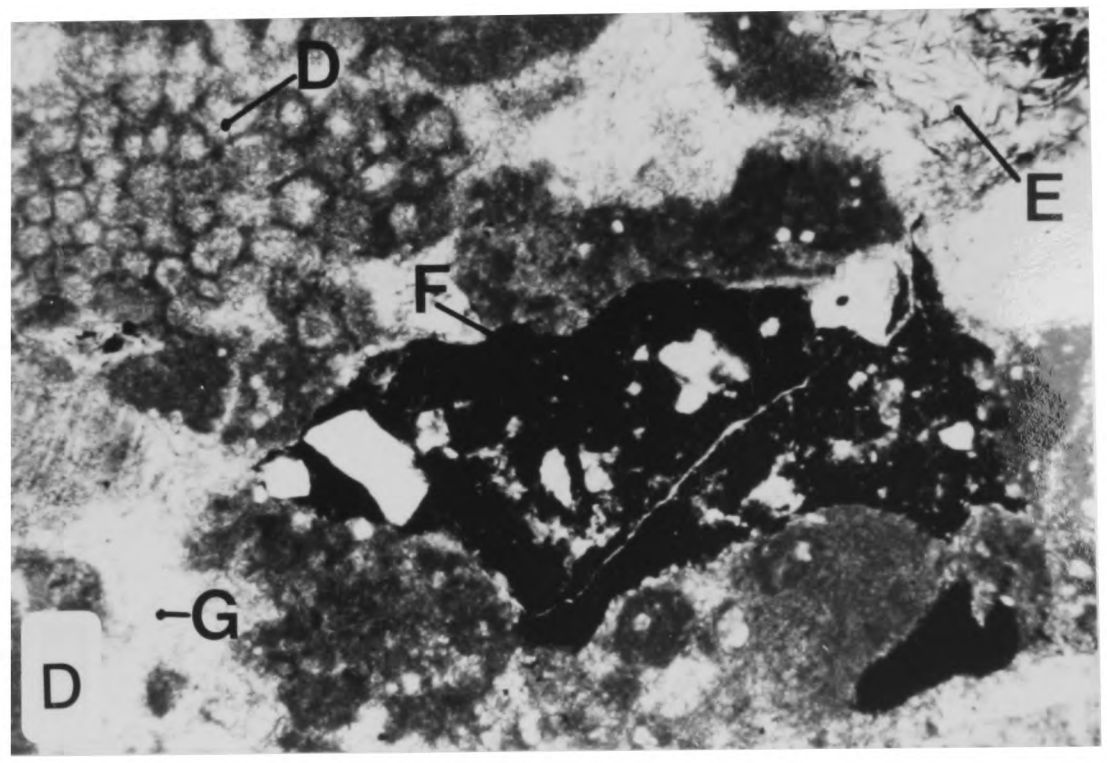

5.7

5.8

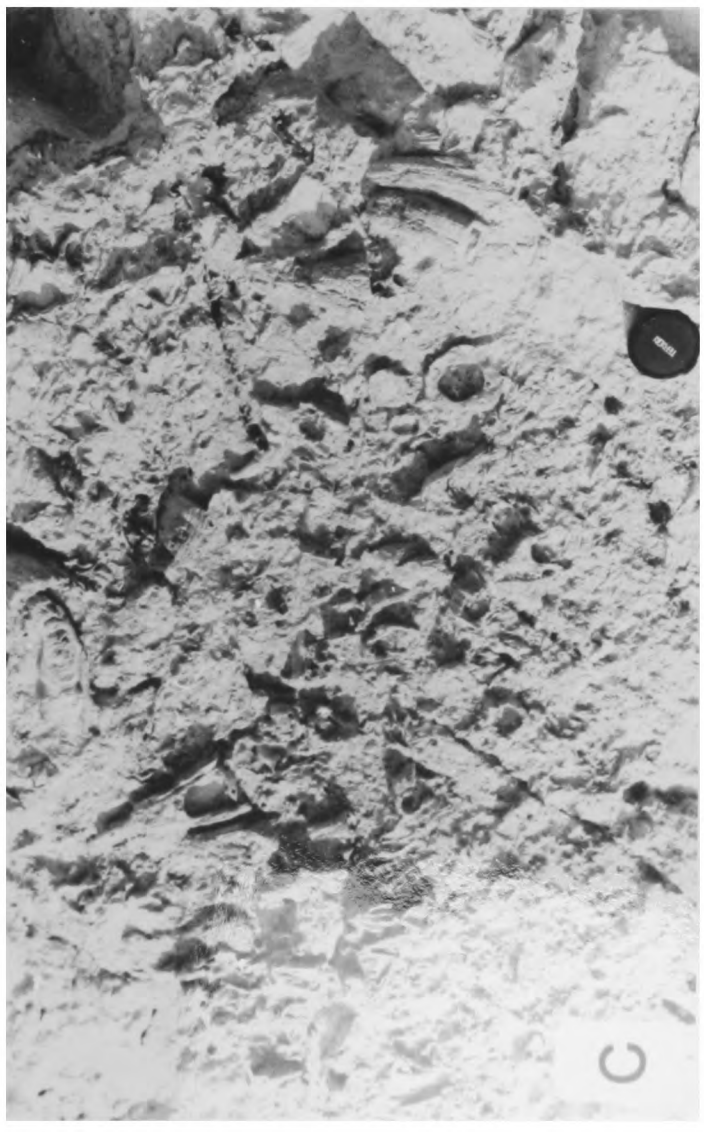

CHAPTER 6

TERTIARY TO RECENT SEDIMENTS OF THE NORTH PINDOS MOUNTAINS

6.1 Introduction

Tertiary sediments of the north Pindos Mountains are found in two highly contrasting tectonic positions in relation to the Early Tertiary deformation present in the region (Fig. 6.1). The Pindos Flysch is a pre- to syn-tectonic sedimentary sequence developed in a deep marine basin ahead (i.e. westwards) of the advancing Pindos thrust stack. The "molasse" sediments of the Meso-Hellenic trough found to the east, were deposited mainly after thrusting of the Pindos ophiolite was complete. This distinction is reflected in the nature of the sediments present, the Pindos Flysch being a predominantly deep-water marine turbidite sequence, and the molasse being of marine to fluvatile facies. The vast extent of the sedimentary basins in which these sediments were deposited can be seen on a sketch map of Greece and surrounding areas (Fig. 6.2). The Tertiary sediments of the Pindos Mountains were not studied in any detail during this project. However, during the course of regional and more detailed mapping, some observations were made within both these sequences, and are reported here.

6.2 The Pindos Flysch Group

The Maastrichtian to Eocene Pindos Flysch Group is known from both the North Pindos area (Brunn 1956; Lorsong 1977, 1979), and the Pindos Zone of central and southern Greece (Fig. 6.2; Aubouin 1959; Dercourt 1964; Green 1983). Additionally, similar sediments are found in an identical tectonic position, within both Albania and Yugoslavia (Papa 1970; Brunn 1979). The group crops out extensively in the area studied (Brunn 1956), forming the footwall of the thrust stack. Reconnaisance of the Pindos Flysch from Metsovo in the south through to Konitsa in the north (Figs. 6.2, 6.3) allows some broad conclusions to be drawn. Firstly, the flysch is everywhere more or less deformed. In the central region, beneath the Pindos ophiolite, this deformation is usually more intense, with the development of thrust-related shearing and cleavages, together with folding on several scales (see Chapter

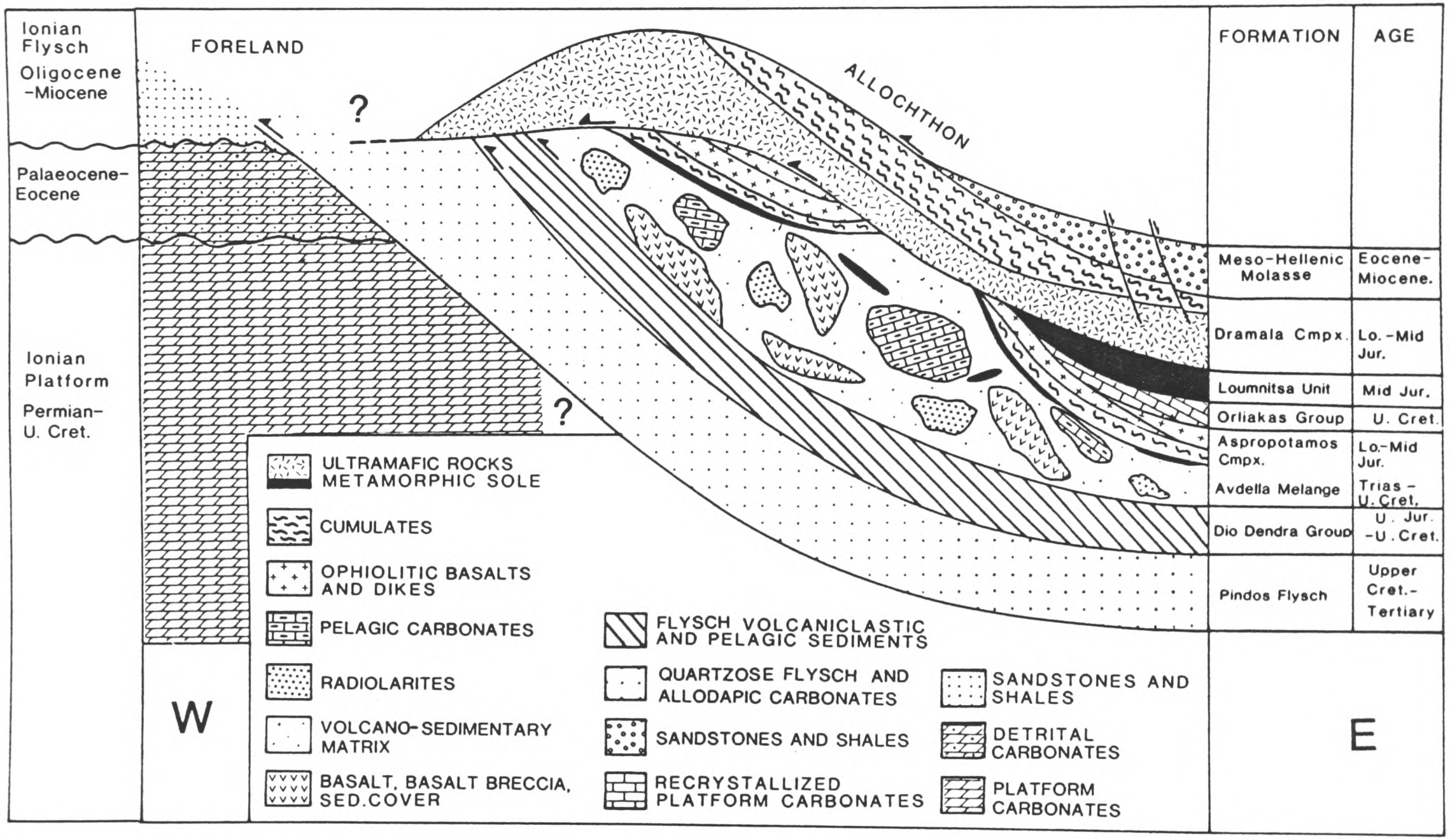

Fig. 6.1 Tectono-stratigraphy of the north Pindos Mountains showing the position of the Pindos Flysch at the base of the thrust stack. The Meso Hellenic molasse sediments may overlie all units of the thrust stack.

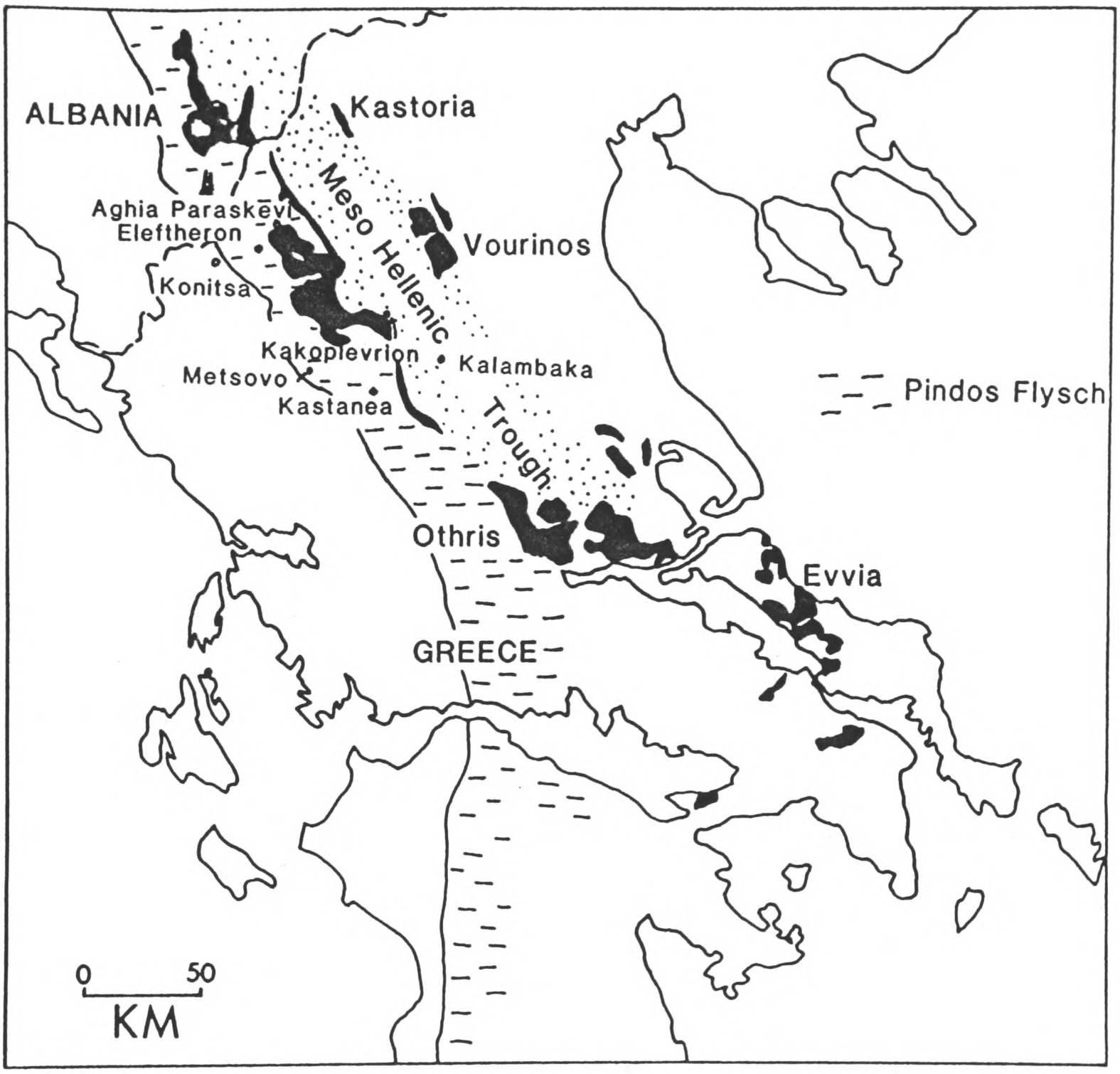

Fig. 6.2 Locality map showing the distribution of the Pindos Flysch and the Meso Hellenic trough molasse in central and northern Greece.

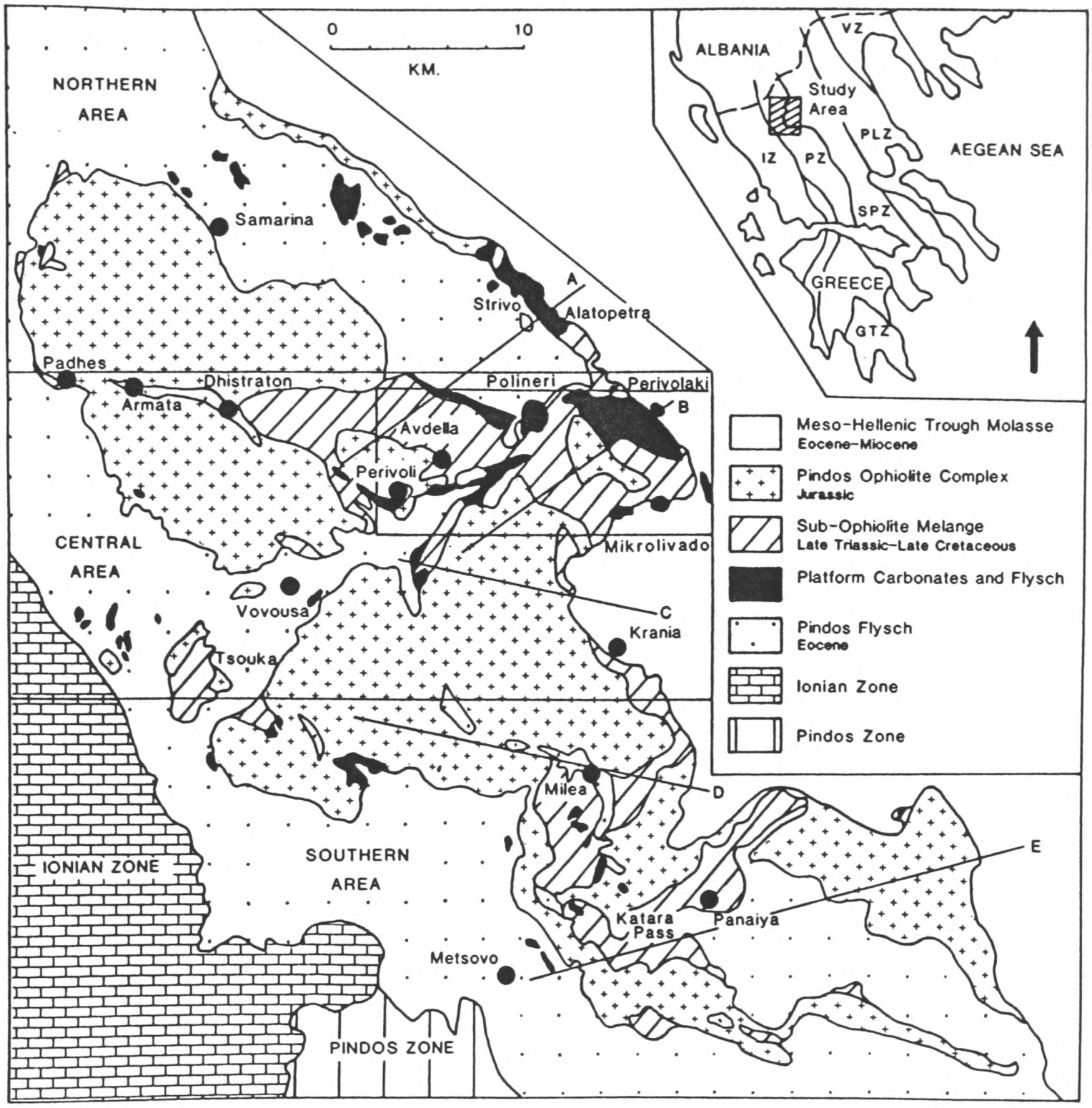

Fig. 6.3 Locality map for the Pindos Flysch and Meso Hellenic molasse in the study area.

7). Some sequences also display well-developed slump folds on several scales (Plate 6.1), indicating tectonism was coeval with sedimentation.

The second major feature of the Pindos Flysch, is that it apparently becomes of a more distal facies northwards. In the south, the flysch is comprised mainly of vast volumes of light brown and grey quartzose sand bodies, interpreted as representing a variety of deep-sea turbidite fan-type facies (Lorsong 1977). In the north, fan-type sediments are also common, but a considerable part of the sequence comprises anoxic black shales with pelagic and less common redeposited carbonates. A far greater proportion of fine-grained sediments are therefore found in the north, than in the southern and central areas. It is, however, uncertain how these sediments fit into the stratigraphy of the Pindos Flysch elsewhere, due to a lack of paleontological studies. Distal, mud-dominated sequences, are found exposed in the region north of Samarina village, and particularly between Aghia Paraskevi and Konitsa (Figs. 6.2, 6.3), where several hundred m-thick sections of folded and thrust sediments of this type occur.

The third main conclusion drawn is that ophiolite-derived material was only rarely shed into the Pindos Flysch basin during flysch deposition. A background component of fine-grained basalt and radiolarite clasts, is present within many of the flysch sandstone and siltstone sequences, but these only usually represent a few percent of the clasts in an average sediment. However, in the northern area, two distinctive clast-supported, disorganised conglomeratic horizons occur within the flysch (IGME Konitsa sheet 1978). These conglomerates are composed of debris undoubtedly derived from a Pindos ophiolite and Avdella Melange-type source. The clasts sampled from two areas where such conglomerates were discovered (E. flank of the Aoos Valley, 8 kms N. of Vovousa, Fig. 6.3; Elefthero Village, 8 kms W. of Konitsa, Fig 6.2), included fresh harzburgite and dunite, a variety of basic igneous rocks (including titanaugite-bearing basalts), marbles, quartz arenites and radiolarites. The clasts are mostly rounded to sub-rounded. These sediments are reported as being up to 500 m thick in total, and have a maximum clast size of approximately 25 cms (IGME Konitsa sheet 1987). According to IGME geologists (IGME Konitsa sheet op. cit.), these sediments comprise a lower unit rich in ophiolite debris, and an upper unit with rare ophiolite clasts.
The conglomerate discovered in the Aoos Valley was an individual carbonate channel (4 m thick), interbedded with sandstone turbidites, and contained

clasts up to 6 cms in diameter. No other such occurrences of ophiolitic detritus are known from several kilometres thickness of the Pindos Flysch.

The Pindos Flysch across much of the southern and central regions is composed of quartzo-feldspathic and micaceous, generally medium-to fine-grained turbidites, with common redeposited carbonates. In detail, a myriad of lithologies are present, representing a wide range of deep-water and redposited clastic-carbonate turbiditic sediments. The turbidites commonly show a wide range of sedimentary structures, particularly sole markings, load casts and bioturbation features. Cross-lamination and wave-ripples are found within finer-grained units, representing Bouma Tc-e sequences. Carbonate and terrigenous components vary within individual beds, as well as on a larger scale throughout the flysch sequences. Plant material becomes locally abundant within thin to medium-bedded micaceous sandstone turbidites (e.g. at Vovousa Village, Fig. 6.3).

In parts of the central area, redeposited carbonates are seen to erode distinctive channels into more quartzose terrigenous flysch units (e.g. Isomata Mountain, N.W. of Perivoli; Fig. 6.3). These carbonates (the "limestone breccias" of Kemp & McCaig 1984) form narrow (30-50 m) elongate (several hundred m visible, probably several km) channels which trend approximately west to east, despite suffering deformation. The carbonates consist of cyclically graded units dominated by calcirudites and fine calcarenites. These rocks are extremely rich in shallow-water carbonate detritus, which includes angular and rounded micritic limestone clasts, nummulitid foraminifera in abundance, red-green algae, bryozoa and corals (Plate 6.1). Quartz grains are common, even in these carbonate-dominated sediments.

6.3 Depositional environments of the Pindos Flysch

The Pindos Flysch clearly represents sedimentation which took place in a deep marine basin. Lorsong (1977, 1979), in a study of the Pindos Flysch of the Metsovo region (Fig 6.3), distinguished the following depositional environments, from base to top, for the turbidite sequences in this area (Politses Formation): basin plain, fan fringe and distal lobe, and proximal lobe. These sequences are repeated within thrust sheets. Clearly, deep-sea fan

turbidites dominate, and numerous sub-facies are discernable within the flysch as a whole.

6.4 Tectono-sedimentary evolution of the Pindos Flysch

The Pindos Flysch was deposited in a deep basin ahead of the advancing Pindos mountain front to the east, and the Apulian foreland to the west. The flysch was visualised as having formed within an accretionary complex Lorsong (1977), due to eastwards subduction of the continental margin of Apulia. Another interpretation is that the flysch was deposited in a flexurally-induced foreland basin, which formed on marginal or oceanic crust, which was subsequently overthrust by the Pindos ophiolite and related far-travelled thrust sheets. Perhaps the best compromise is a combination of these processes, firstly sedimentation in a flexural basin, followed by further compression, and partial subduction of the Ionian continental margin and platform sequences. The Ionian margin was certainly undergoing collapse during the Early Eocene, shedding volumes of shelf carbonate detritus, and even olistolith blocks.

One of the least well constrained problems is the derivation of the quartzose material which composes much of the Pindos flysch. Lorsong (1977, 1979) considers that this material had an eastern (i.e. Pelagonian) origin. This does indeed seem the most likely source, especially as there was large scale overthrusting of Pelagonian basement taking place to the east. However, a dominantly axial source is required for the detritus, to by-pass the ophiolite and melange also present to the east. Both Sub-Pelagonian (e.g. ophiolite-derived conglomerates) and Ionian sources (e.g. carbonate breccia channels) can be distinguished at particular times. However it is also possible that the quartzose material was derived from the basement of the Ionian zone, due to footwall collapse during continental collision. An understanding of both the sedimentary and tectonic evolution of the Pindos Flysch is required to fully answer this question.

6.5 Meso-Hellenic molasse: post-tectonic sediments

The Pindos thrust stack is overlain on the eastern margin by sediments of the Meso-Hellenic trough, a "molasse"-type basin. Sediments in this basin are of mainly Eocene to Miocene age (Brunn 1956; Soliman and Zygoyannis 1979; Fig. 6.2), and are several thousand metres-thick. These clastic sediments were deposited in a marine to alluvial-deltaic environment on top of, and behind, the Pindos thrust sheets. The molasse is conglomeratic at the base, with abundant ophiolitic debris (Plate 6.2), and fines-upwards, via thick channelised and coarse sheet sand sequences into shales, clays and marls. Some of these delataic sequences were studied in the Meteora area (Kalambaka, Fig. 6.2) by Ori and Roveri (1987).

The sedimentary facies seen mantling the Pindos Mountains include a variety of alluvial-deltaic and marine deposits. The basal sequences (e.g. in the Krania-Mikrolivado area, Fig. 6.3; Eocene, Brunn 1956) include thick conglomeratic alluvial fan sediments, locally derived from the surrounding ophiolite, and containing a contemporaneous matrix with marine fossils. These include large (50 cms) clasts of colonial corals, gastropods and bivalves, in particular. Elsewhere, locally derived harzburgite conglomerates are seen. Molasse-type sediments must have originally covered much of the eastern margin of the Mountains, and possibly topographically higher areas to the west.

6.6 Development of the Meso-Hellenic trough

The Meso-Hellenic trough formed as an extensional basin, probably whilst compression still occurred within the Pindos thrust stack to the west. The exact geometry of the basin is still poorly known, although it is clear that both margins have steeply dipping to vertical strata. As has been described previously (Chapter 7), sedimentation on the the southwestern margin of the basin has been strongly influenced by later deformation, perhaps related to transverse faulting. The basin is thought to be underlain by ophiolitic crust of the Pindos-Vourinos ophiolites. This is based mainly on sporadic outcrops of ophiolitic rocks, exhumed within central parts of the basin. Gravity data from the Meso-Hellenic trough do not prove the ophiolitic nature of the basement (R. Hipkin pers. comm. 1990), indicating that isostatic re-equilibration has

taken place, or that the sediment infill has masked the influence of the ophiolite on the gravity field. During Tertiary compressional deformation, a large volume of mafic and ultramafic material (Pindos Ophiolite Group) was thrust southwestwards out of the site of the Meso-Hellenic trough, possibly as a rootless sheet. This expulsion of ophiolitic material was almost certainly a result of underthrusting caused by subduction of the Ionian Platform to the west, leaving a void which was rapidly infilled with locally derived sediments.

Plate 6.1 a) Thickly-bedded turbiditic arenites and fine conglomerates, interbedded with finer-grained sediments, all part the Pindos Flysch, Katara Pass, E. of Metsovo. b) Slump-folded fine-grained carbonate horizon within siliciclastic sediments, road to Kastanea, S. of Metsovo. c) Carbonate breccia channel deposits, Isomata, N.W. of Perivoli. d) Photomicrograph of material from the carbonate breccia channels (11mm PPL), showing Eocene foraminifera and quartz clasts, typical of the mixed carbonate-siliciclastic material found in these sediments.

Plate 6.2 Sediments from the Meso-Hellenic trough; a) Coarse grained plutonic rocks from the Pindos ophiolite, in a muddy matrix, roadside 4 kms S. of Alatopetra. b) Polygenetic conglomerates, showing typically rounded clasts of ophiolitic and melange lithologies, Venetikos Valley, near Monahiti. c) Shales and conglomerates, rich in Tertiary marine fossils, complexly fault intercalated with basaltic rocks of the Aspropotamos Complex, roadside 6 kms N. of Mikrolivado.

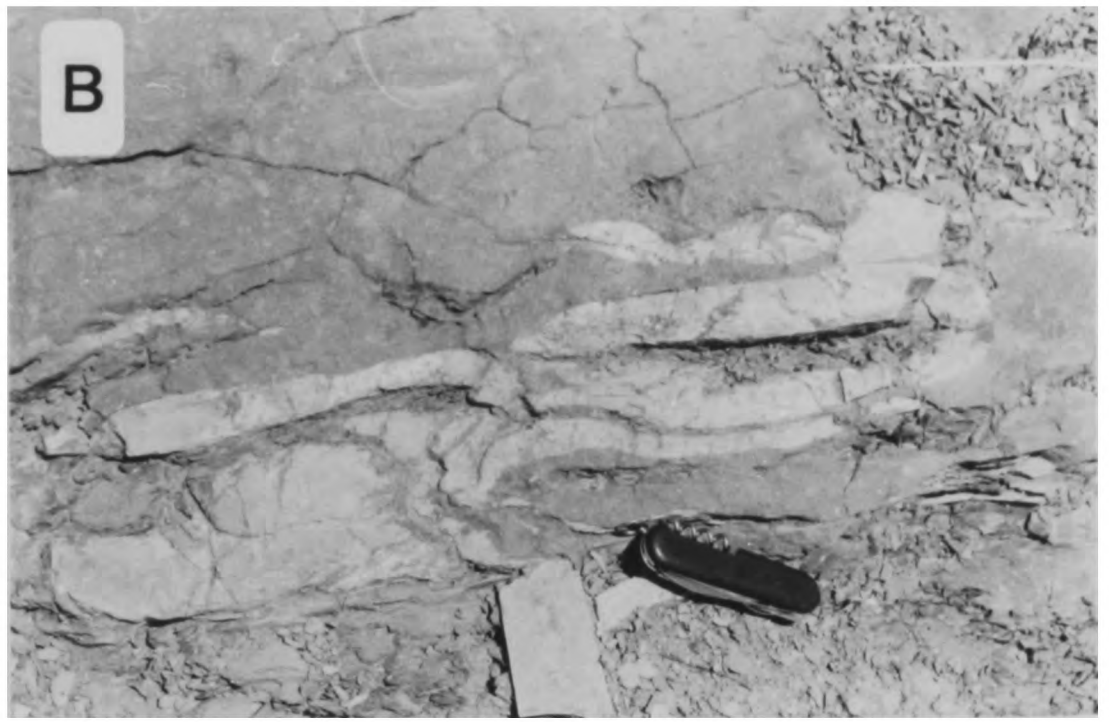

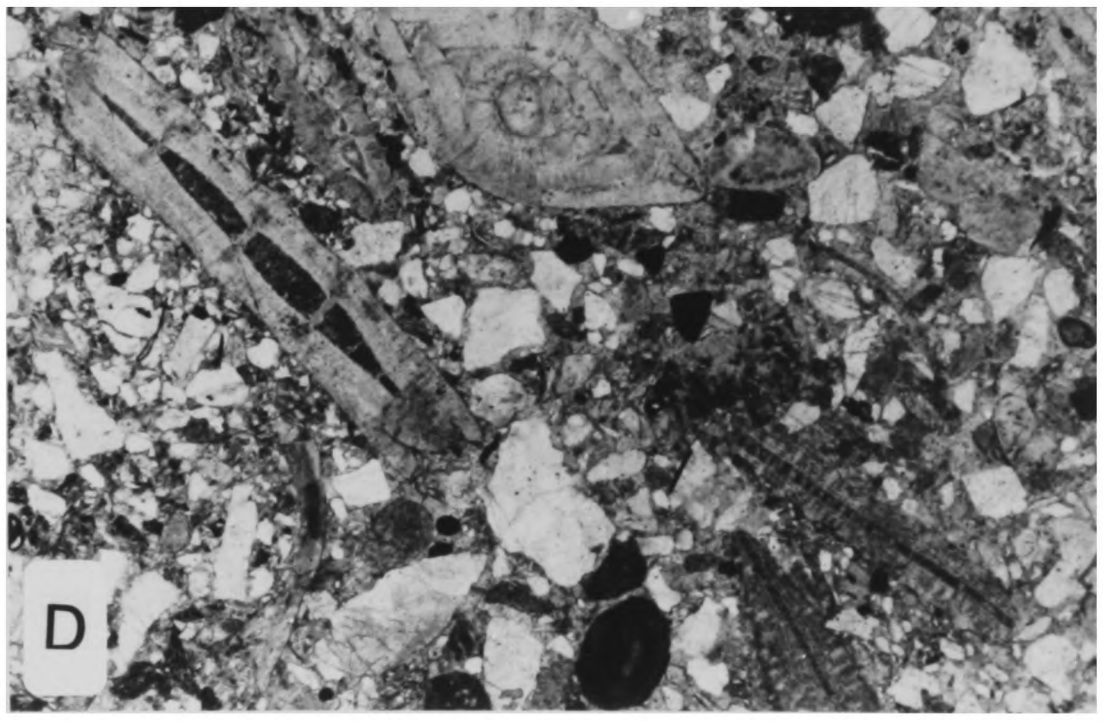

6.1

6.2

CHAPTER 7

STRUCTURAL GEOLOGY OF THE NORTH PINDOS MOUNTAINS

7.1 Introduction

The Pindos Mountains have experienced four main stages of tectonic deformation: i) Mid-Late Triassic (extensional); ii) Mid-Late Jurassic (compressional); iii) Early-Mid Tertiary (compressional and extensional); iv) Miocene to Recent (mainly extensional; Jones and Robertson 1990; Table 7.1). These events have resulted in the complex structural field relationships found at present, which are dominated by Tertiary compression and extension. Previous work on the structure of the area was limited (Brunn 1956; Kemp and McCaig 1984), and resulted only in an outline tectonic synthesis. Brunn (op. cit.) produced some sketch cross-sections of the region, based on his reconnaissance studies. This Chapter aims to document the structural history observed, based on both detailed mapping and general reconnaissance, and to present new structural cross-sections for the region.

7.2 Timing constraints on deformational phases

The age of the Mid-Late Triassic phase of deformation is constrained by the limited occurrence of syn-sedimentary extensional faulting within poorly-dated Triassic sediments, which are overlain by undeformed sediments of Early Jurassic age (e.g. at Alatopetra; N.W. Perivoli; Fig. 7.1). This faulting is thought to be part of a rifting event, which affected the Hellenides during the Mid to Late Triassic (Aubouin et al. 1970). The Jurassic phase is constrained by the youngest intact successions found in the melange (Oxfordian; Jones et al. in prep.), and the oldest transgressive sediments (Late Kimmeridgian carbonates; Mavrides et al. 1979). A further constraint is the inferred Bathonian age of the metamorphic sole (see Chapter 3), interpreted as representing the initiation of oceanic compression, leading to ophiolite emplacement.

TABLE 7.1

DEFORMATION STAGE	AGE
Rifting and extensional deformation, poorly displayed in the Pindos area but locally manifested by syn-sedimentary extensional faults within off-margin carbonates. Followed by formation of oceanic crust at a spreading centre.	MID-LATE TRIASSIC
Subduction-accretion related deformation of the Avdella Melange. Thrust-related deformation at moderate pressure and low temperature. Formation of Pindos and Vourinos high temperature mantle foliations. Internal deformation of ophiolite crustal sections.	LOWER JURASSIC
Formation of ophiolite metamorphic sole (Loumnitsa Unit), intra-oceanic thrusting and amphibolite metamorphism. Displacement of ophiolite sheet, with formation of associated high temperature mylonites and foliations, now found in ophiolite mantle sequences. (S.W. dipping foliation; in Pindos and Vourinos).	MID JURASSIC (probably Bathonian)
Further deformation and greenschist metamorphism of the Avdella Melange, during ophiolite emplacement to the northeast onto the Pelagonian margin. Formation and deformation of the Vourinos melange during margin collapse. Pelagonian platform metamorphism during ophiolite thrusting. Subsidence into remnant basin to the W?.	MID-EARLY LATE JURASSIC
Compressional deformation of northern Greek area, leading to large-scale southwest-vergent overthrusting, of ophiolites, accretionary complex, and Cretaceous and Early Tertiary basinal sediments. Formation of Pindos nappe stack. Initial large-scale folding of the thrust sheets along NW-SE axes, related to basement ramps, associated with N.E-S.W. wrench faulting. Followed by refolding of these	PALAEOCENE?-EOCENE

structures along perpendicular (NE-SW) axes, (e.g. Perivoli corridor), possibly by basement ramps, or by a separate compressional event. Possible age of NW-SE wrench faulting on the margin of the Meso-Hellenic trough?.	
Extensional deformation behind the thrust stack to the NE, forming the Meso-Hellenic trough. Wrench-fault related deformation and compression of molasse sediments?.	LATE EOCENE-MIOCENE
Neotectonic extensional faulting.	MIOCENE-RECENT

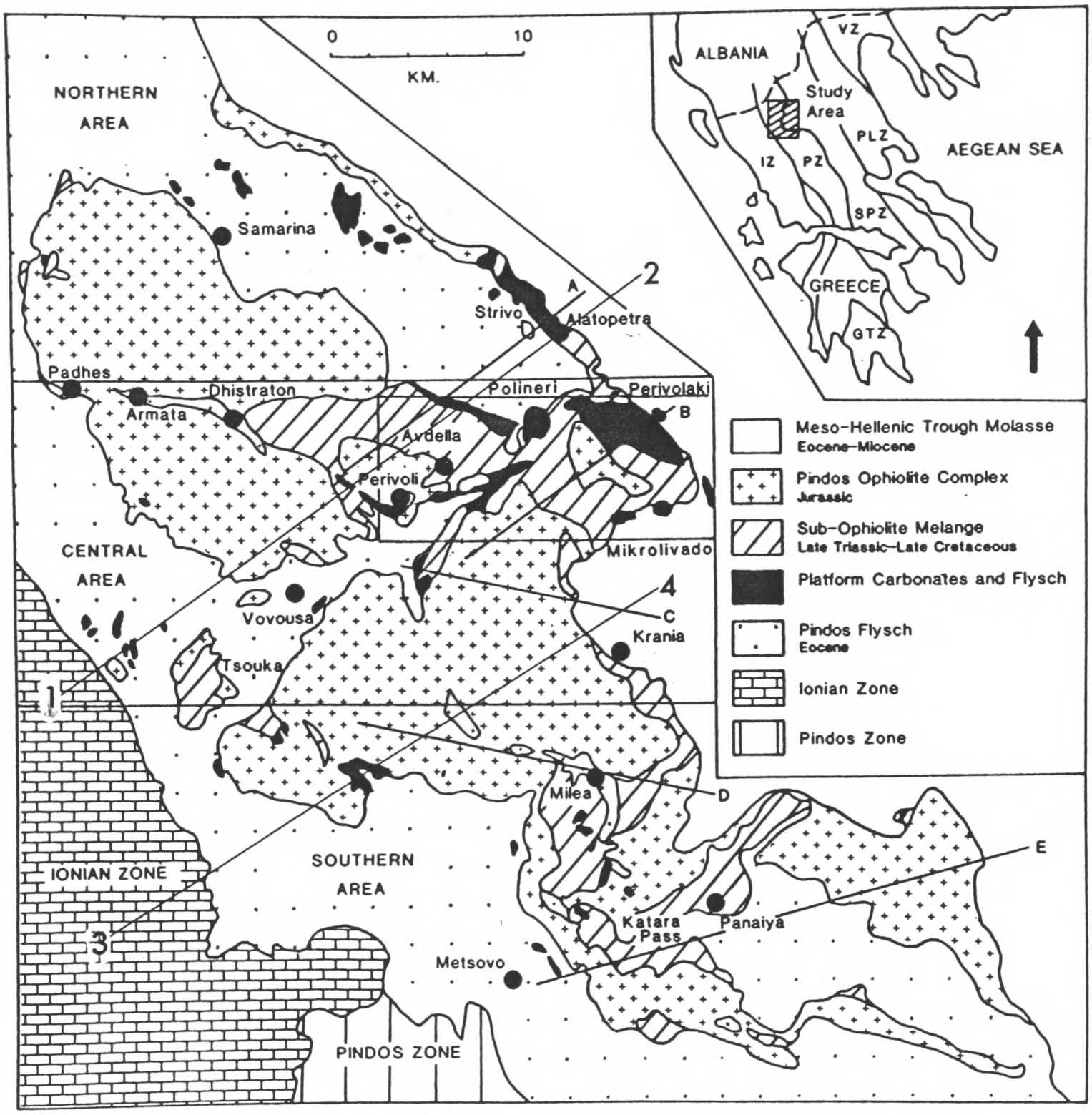

Fig. 7.1 a) Geological and locality map of the north Pindos Mountains, showing the main tectonic units present. Modified from Brunn (1956). Lines of section refer to Figs. 7.1.b. and Fig. 7.4. Northern, central and southern sectors are distinguished, Note also the outlined position of the more detailed map of the central area (Fig. 7.4). b) Sketch sections across the north Pindos Mountains, showing the main structural features present. Key as for 7.1.a.

B

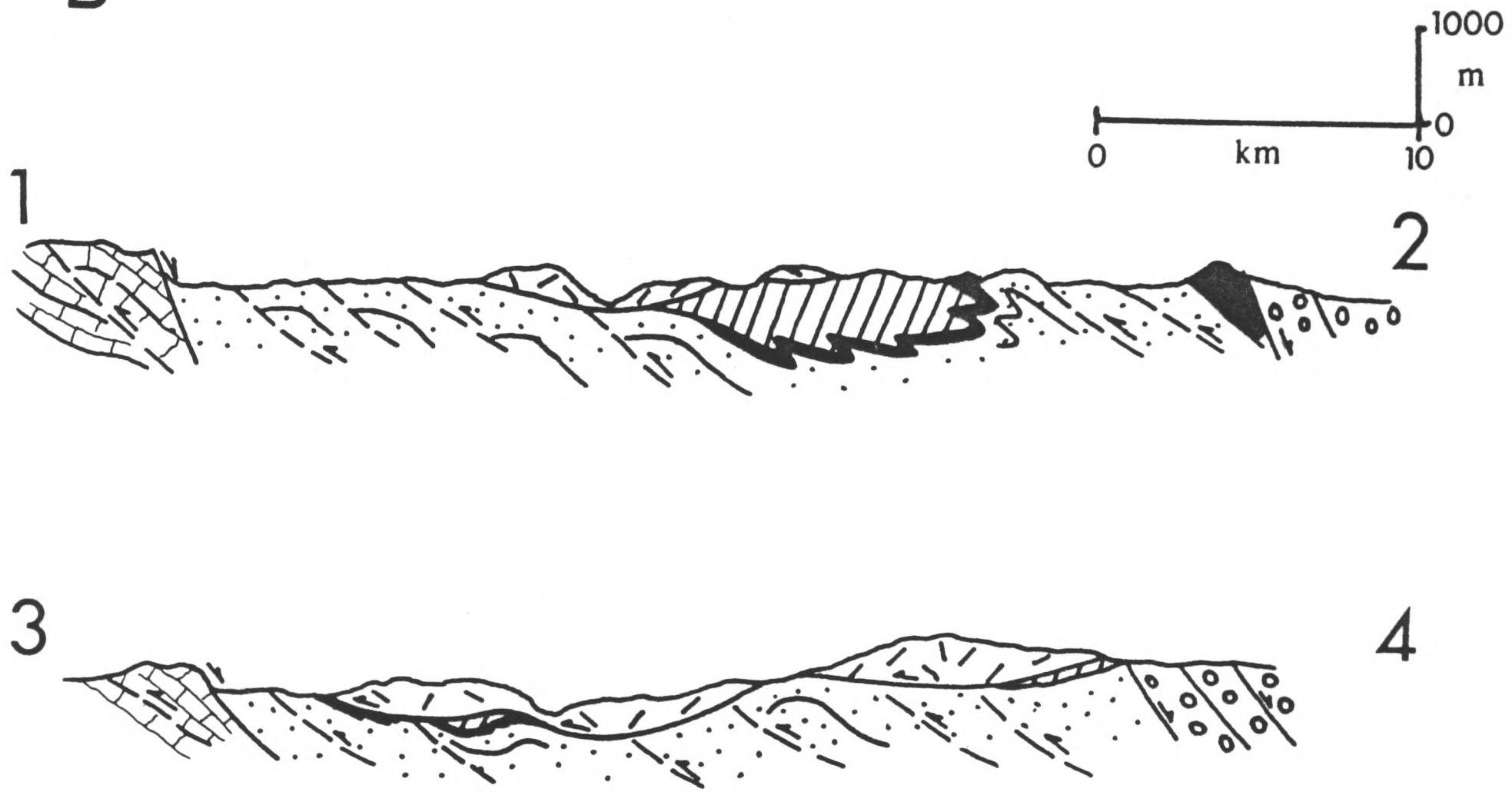

Early Tertiary compressional tectonism deforms poorly dated Maastrichtian-Eocene Pindos Flysch sediments (Brunn 1956), and was followed by Latest Eocene (Soliman and Zygoyannis 1979) extensional deformation, leading to formation of the Meso-Hellenic trough. The latest deformation is Neotectonic, related to subduction along the Aegean arc to the south of Greece, and to strike-slip motion associated with the western termination of the north Anatolian fault (MacKenzie 1984), which continues to the present day.

7.3 GENERAL STRUCTURAL FEATURES

7.3.1 Triassic deformation

As mentioned above, direct evidence for Triassic deformation is sparse, restricted only to some faulted blocks at Alatopetra (Fig. 7.1; Chapter 4), and to extensional structures in other melange sediments. However, indirect evidence (i.e. rift-type volcanism) suggests that during the Late Permian to Late Triassic, much of the Eastern Mediterranean underwent rift-related extension, leading to the extrusion of voluminous alkaline and tholeiitic lavas. In certain areas, including the north Pindos Mountains, this rifting appears to have lead directly to the formation of oceanic basement by Late Triassic times (Hynes 1974).

7.3.2 Jurassic deformation

Deformation considered to have taken place in the Jurassic includes foliation development, mylonite formation and isoclinal folding, which were associated with formation of the ophiolitic Dramala and Aspropotamos Complexes (Chapter 2). Deformation dated radiometrically as Mid Jurassic, resulted in formation of the metamorphic sole of the ophiolite (Loumnitsa Unit; Chapter 3). Other structures of possible Jurassic age within the Avdella Melange are discussed below.

7.3.3 Tertiary to Recent deformation

As mentioned in Chapter 1, the structure of the Pindos Mountains is dominated by southwestward-verging large-scale overthrusting, resulting from Early Tertiary compression (Brunn 1956; Kemp and McCaig 1984). The Tertiary emplacement vector was calculated by McCaig (unpublished data, 1978), as being approximately towards 214^{o}. Thrusts and shears are developed at all scales, and fault contacts are commonly marked by serpentinite. The gross tectonic stratigraphy is preserved across much of the region (see Chapter 1; Figs. 7.1, 7.2), but out-of-sequence thrusting is observed along the basal thrust of the main ophiolite sheet (Dramala Complex), and within the highly imbricated fold limbs of the Perivoli corridor (see below), with resultant omission of large thicknesses of section.

The major thrust contacts between tectonic units have been folded along northwest-southeast trending axes, and verge towards the southwest. A second fold trend has developed locally, parallel to the emplacement direction, and has led to refolding in a northeast-southwest direction (Fig. 7.3). This is particularly visible within the sub-ophiolitic flysch units. Fold interference has produced a number of Ramsay (1967) Type 2, ("mushroom-like") tectonic windows (e.g. in the Perivoli and Milea districts, Figs. 7.1, 7.3; see below).

Two major thrust culminations are visible from an inspection of the map of the main tectonic units. The first is the northwest-trending Armata-Milea corridor, as newly defined here (Fig. 7.3). This was first mapped by Brunn (1956), and was later interpreted by Kemp and McCaig (1984) as a frontal thrust ramp. This corridor is a major antiform within the exposed Pindos Flysch basement in the region. It is exposed as a series of individual tectonic windows, from the village of Armata in the north, through to the village of Milea in the south, and probably beyond. As mentioned above, this structure represents a frontal basement ramp, perpendicular to the southwestward-verging thrust sheets. Similar frontal ramps have been described, for example, from the Oman Mountains (e.g. the Jebel Akhdar culmination; Searle 1985).

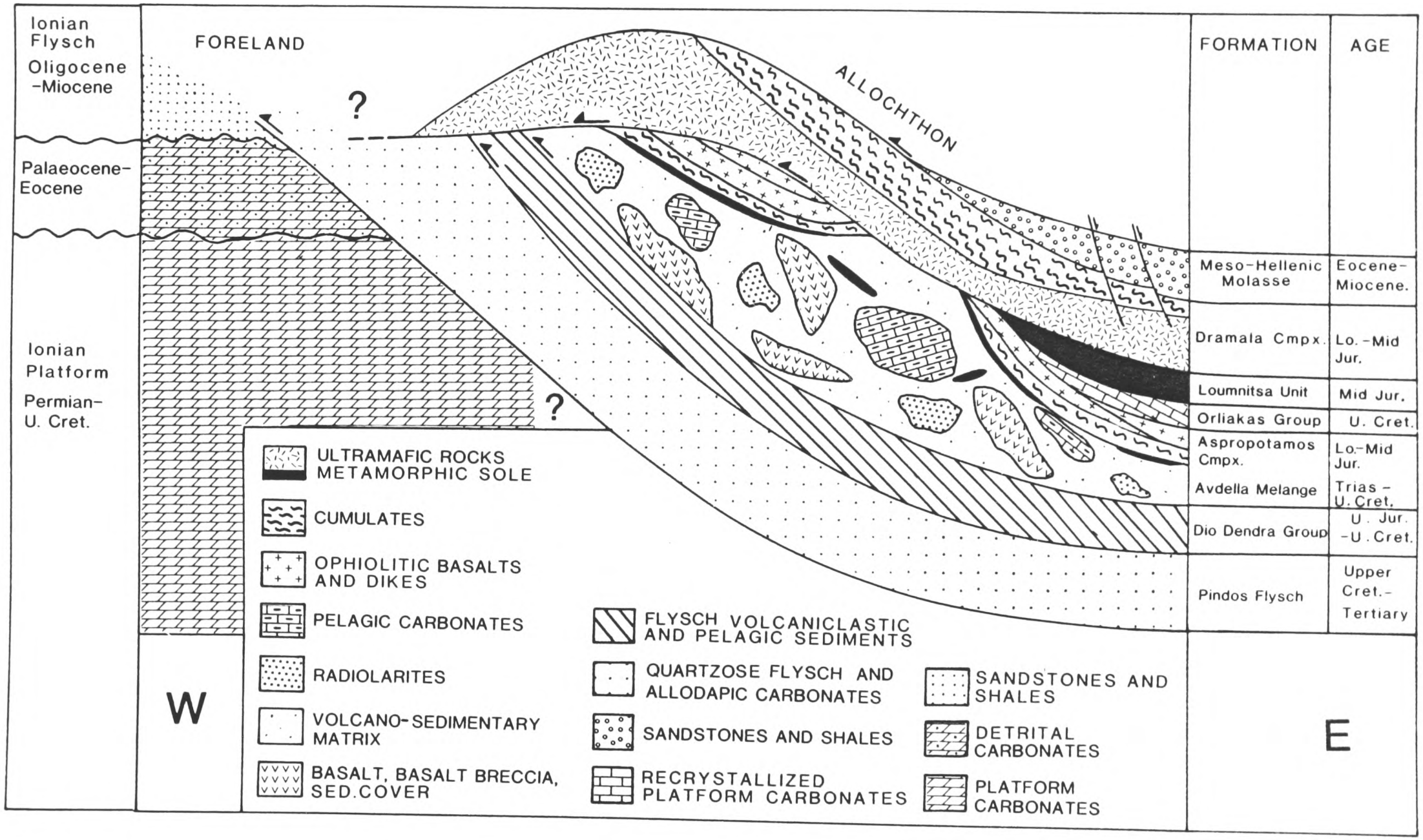

Fig. 7.2 Tectono-stratigraphy of the north Pindos Mountains (Jones and Robertson 1990). See Chapter 1 for details.

The second major thrust culmination present is the northeast-trending Perivoli corridor (Fig. 7.3, see below; Kemp and McCaig 1984), which refolds the Armata-Milea corridor about a northeast-southwest axis, and is therefore later-formed. On a regional scale, a number of smaller amplitude fold structures trend parallel to the Perivoli corridor, causing refolding of the Armata-Milea corridor (Fig. 7.3). All of the culminations fold the out-of-sequence Achladi thrust at the base of the Dramala Complex, and are therefore synchronous or later than this thrust (Fig. 7.4). The basal thrust of the entire stack, the Pindos Thrust (Lorsong 1977; Kemp and McCaig 1984) is apparently not folded, evidence which led Elliot and Johnson (1978, 1980) to propose the "piggy-back" sequence of thrusting elsewhere. It is this mechanism, whereby the thrusting propagates progressively towards the foreland carrying the older thrusts, which therefore appears to be applicable to the Pindos thrust stack.

In the southern area, the stacking order of the thrust sheets is well displayed along the main Kalambaka to Ioannina road, to the east of Metsovo (Fig. 7.1). The Dramala ophiolite overthrusts fragments of the Aspropotamos Complex, which are in turn interthrust with the Avdella Melange. All of these units overthrust Pindos Flysch, which is deformed into an antiformal structure, interpreted as the southerly extension of the Armata-Milea corridor (Figs. 7.3, 7.4).

Along the eastern border of the northern Pindos Mountains, complex extensional structures are developed at the boundary between the thrust sheets and the "molasse" sediments of the Meso-Hellenic trough (Fig. 7.4). The thrust units are presumed to have been downthrown towards the northeast to form the basement to this mainly post-orogenic sedimentary basin. Large-scale (100s of m) normal faults have accommodated this subsidence, and have led to further disruption of the thrust stratigraphy. These faults trend northwest-southeast, and are complemented by a further set of approximately east-west lateral faults in the Mikrolivado and Krania areas (Fig. 7.1), defining an "embayment" into the thrust stack, discussed further below.

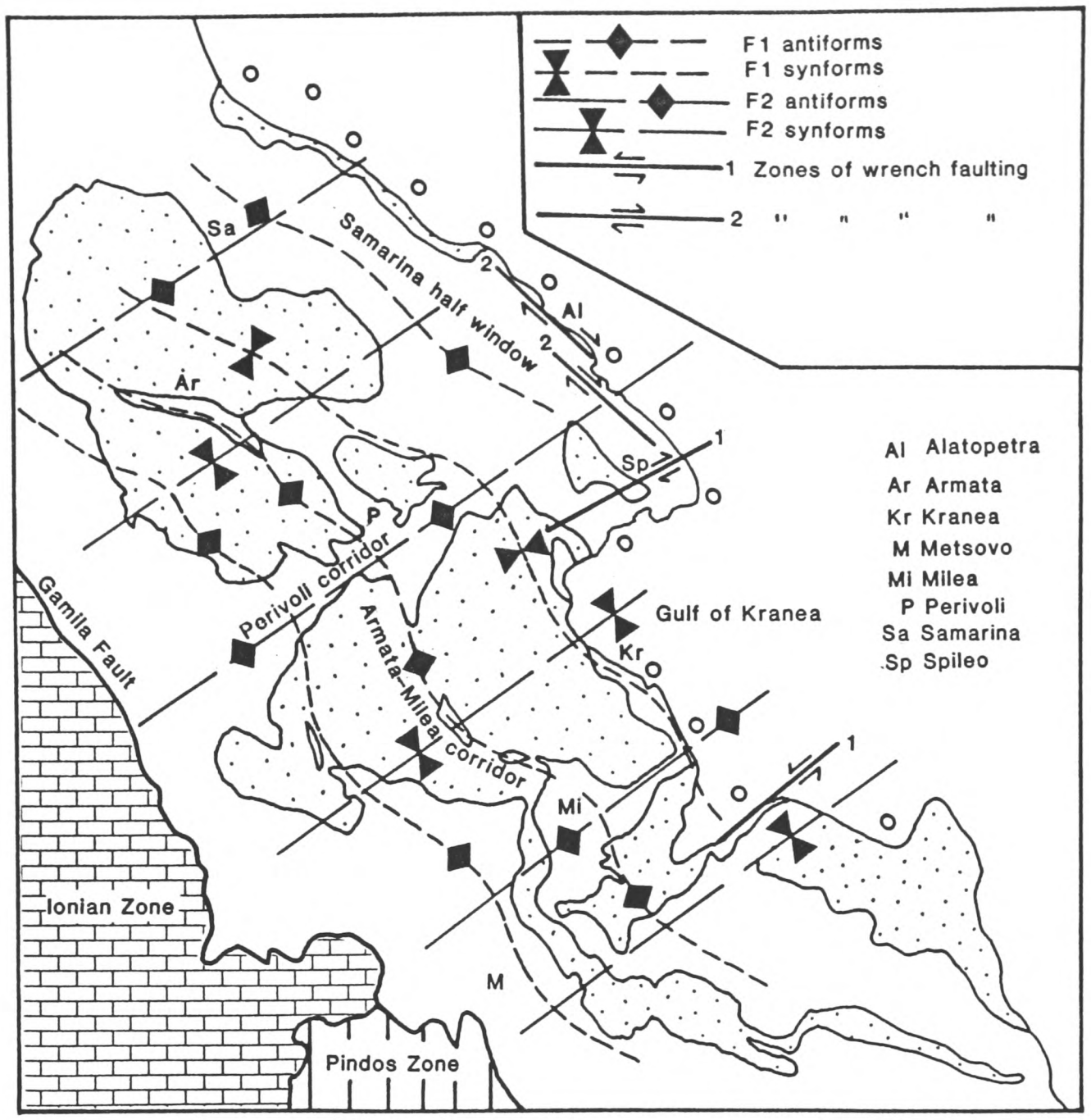

Fig. 7.3 Outline geological map of the north Pindos Mountains showing the major structural features present. Outline of the Pindos ophiolitic units is shown (stippled). Refer to Fig. 7.1 for more detailed geology. Note large-scale folding of the thrust sheets along northwest-southeast-trending axes (frontal ramps; e.g. Armata-Milea corridor), and then refolding along northeast-southwest axes, forming structures such as the Perivoli corridor (lateral ramps?). Zones of complex wrench faulting are shown as single lines, with the inferred sense of displacement indicated.

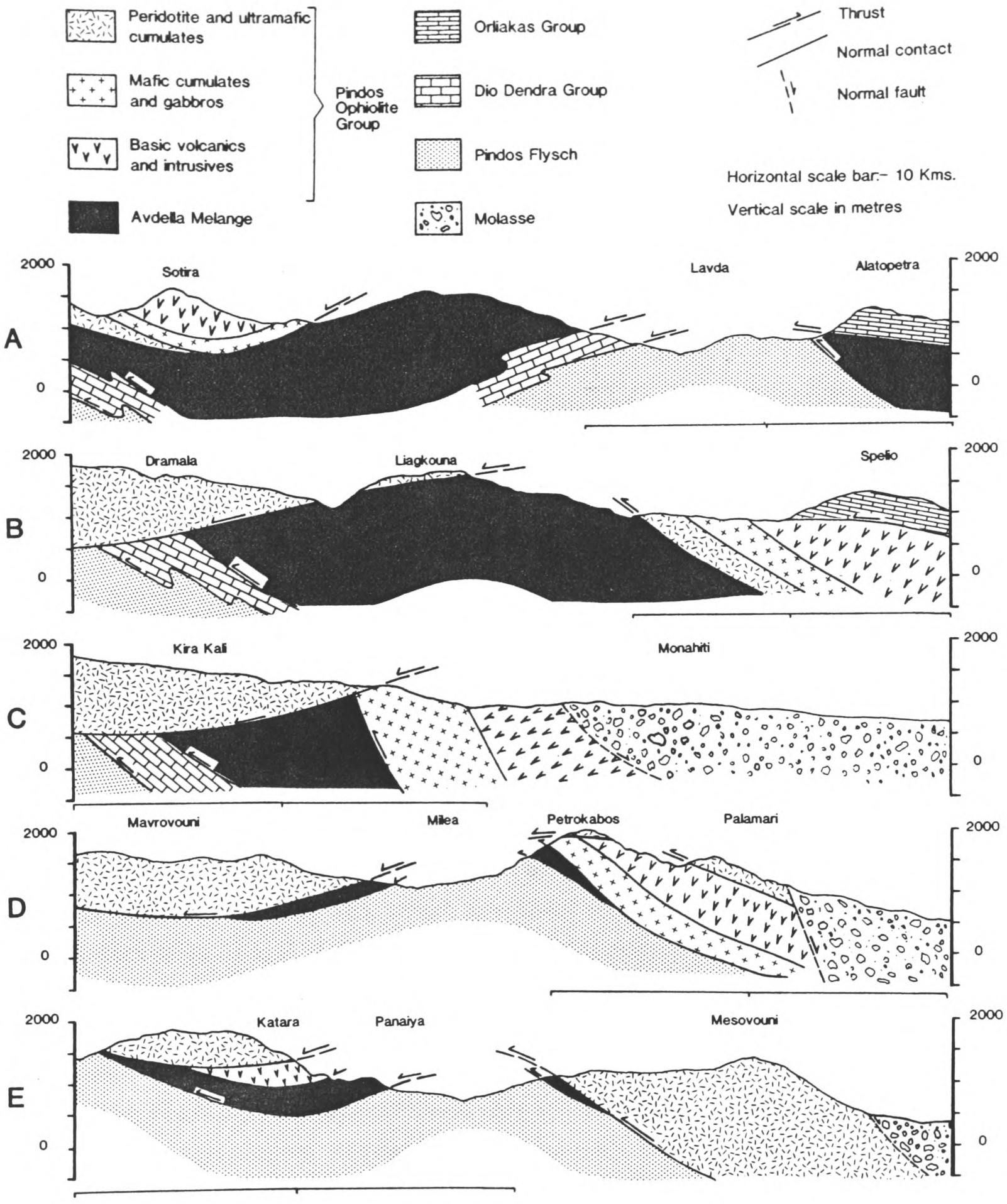

Fig. 7.4 Greatly simplified cross-sections across the eastern margin of the north Pindos Mountains. Only major tectonic contacts are shown. See Fig 7.1.a for lines of section.

7.4 THE PERIVOLI CORRIDOR

The Perivoli corridor (Fig. 7.3) is the name given to the largest tectonic window present within the north Pindos Mountains. The corridor is present within the central part of the studied area, the southwestern limit being the village of Vovousa, and the northeastern limit being the village of Perivolaki (Fig. 7.1). An outline cross-section of the central part of the corridor was produced by Kemp and McCaig (1984) in the Perivoli-Avdella region. The Perivoli corridor and the surrounding areas were mapped at 1:15000 scale as part of this study (Enclosure 1), and smaller areas were selected for detailed mapping (e.g. Dio Dendra Valley; Fig. 7.5). The sometimes poor exposure in the Perivoli corridor, together with later deformation, made mapping of these structures difficult. In areas of orthogonal refolding (Ramsay 1967), the map pattern expected depends on the level at which the structure is exposed, and may consist of complex dome and saddle-shaped areas. These features could not be distinguished during mapping.

The structure of the Perivoli Corridor is essentially that of an antiformal stack (e.g. Elliot 1976), folded orthogonally along both major fold axial trends (NE-SW and NW-SE), which produces the "mushroom-shaped" outcrop pattern (Figs. 7.1, 7.3). It is some 20 km in length, trends northeast-southwest (approximately N040E) and plunges towards the northeast at approximately 25-30 degrees (Kemp and McCaig 1984). The structure preserves the thickest sections of the Dio Dendra Formation (in the Dio Dendra Valley, Fig. 7.5; see Chapter 6), and due to the northeastward plunge, exposes progressively lower structural units towards the southwest. The Dramala Complex is an exception to this, as the Achladi thrust cuts down section so that it overlies the Pindos Flysch southwest of Perivoli, at the intersection of both major thrust stack fold axes (i.e. the Perivoli and Armata-Milea corridors; Fig. 7.3). The corridor is tightly folded along its northeast-trending axis in the northern Dio Dendra Valley, and broadens towards the southwest near Perivoli (Fig. 7.3), where the thrust sheets become highly imbricated and curved on the limbs of the structure, as described by Kemp and McCaig (op. cit). The northwest limb of the corridor is more shallowly dipping (approximately 45-50^{o}) than the steep to vertical southeast limb. Imbrication on the northern limb in the Perivoli area is intense, and involves

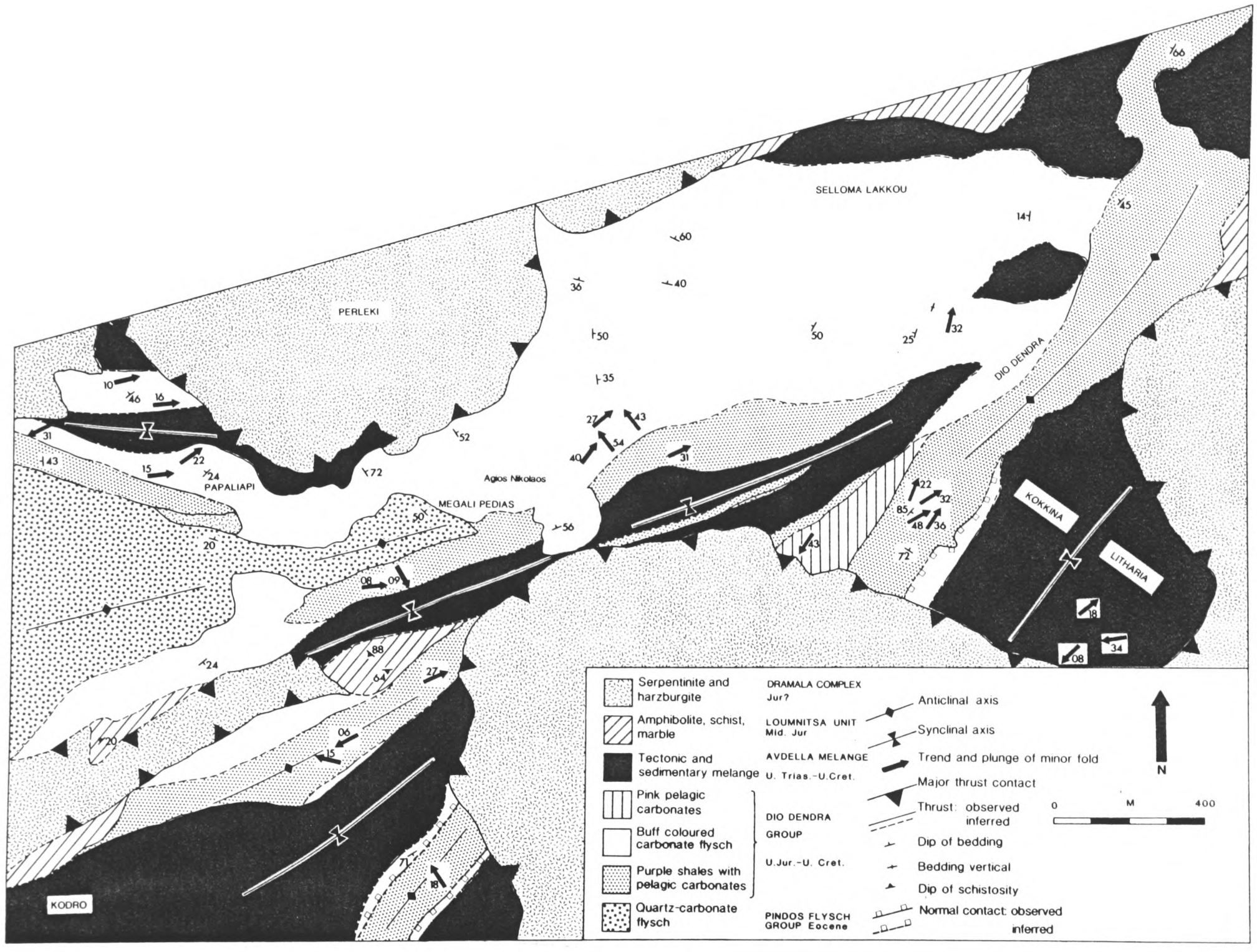

Fig. 7.5 Geological map of the central part of the Dio Dendra Valley. See Fig 7.6 for locality of the mapped area.

a significant amount of serpentinite, mobilised from the base of the immediately overlying peridotites.

In detail, the corridor displays a wide range of thrust-related structures, and individual thrust units are often highly deformed. The range of deformation present in the corridor is best observed in the road sections exposed north and south of Papaliapi Bridge, along the Aspropotamos River, and in the Loumnitsa Valley (Figs. 7.5; 7.6). Three dimensional exposures between Papaliapi bridge and Agios Nikolaos church at Megali Pedias, display the two main fold trends, and locally, well exposed refolds are present.

7.4.1 Northwest-southeast trending structures of the Perivoli corridor

Northwest-southeast-trending folds are developed perpendicular to the main transport direction of the thrust sheets (towards the S.W). These are exposed as minor folds on major structures, along the Dio Dendra Valley. At Agios Nikolaos church, these folds are chevron-type, with flat-lying axial planes (Plate 7.1). Nearby, at Megali Pedias, these folds are refolded by northeast-trending folds (Fig. 7.5; Plate 7.2, 7.3). The folds exposed in the far southwest of the Perivoli corridor, at the village of Vovousa (Fig. 7.1), are asymmetrical and southwest-verging, and occur within the Pindos Flysch.

7.4.2 Northeast-southwest trending structures of the Perivoli corridor

At Papaliapi bridge, exposures of Pindos flysch from the core of the antiformal structure, show that this unit is also affected by the deformation. Parts of the Dio Dendra Group at this locality (Karamoula Formation), on the northern limb of the corridor, show extensional deformation (Plate 7.2). This includes extreme layer-parallel extension of calciturbidite-mudstone interbeds, producing a block-in-matrix effect. However, some 500 m north of the bridge, spectacular thrust and fold-structures are seen within the Agios Nikolaos Formation. Here, on the northern limb of the corridor, refolds are well displayed (Fig. 7.7; Plates 7.2, 7.3). Northwest-trending fold axes are

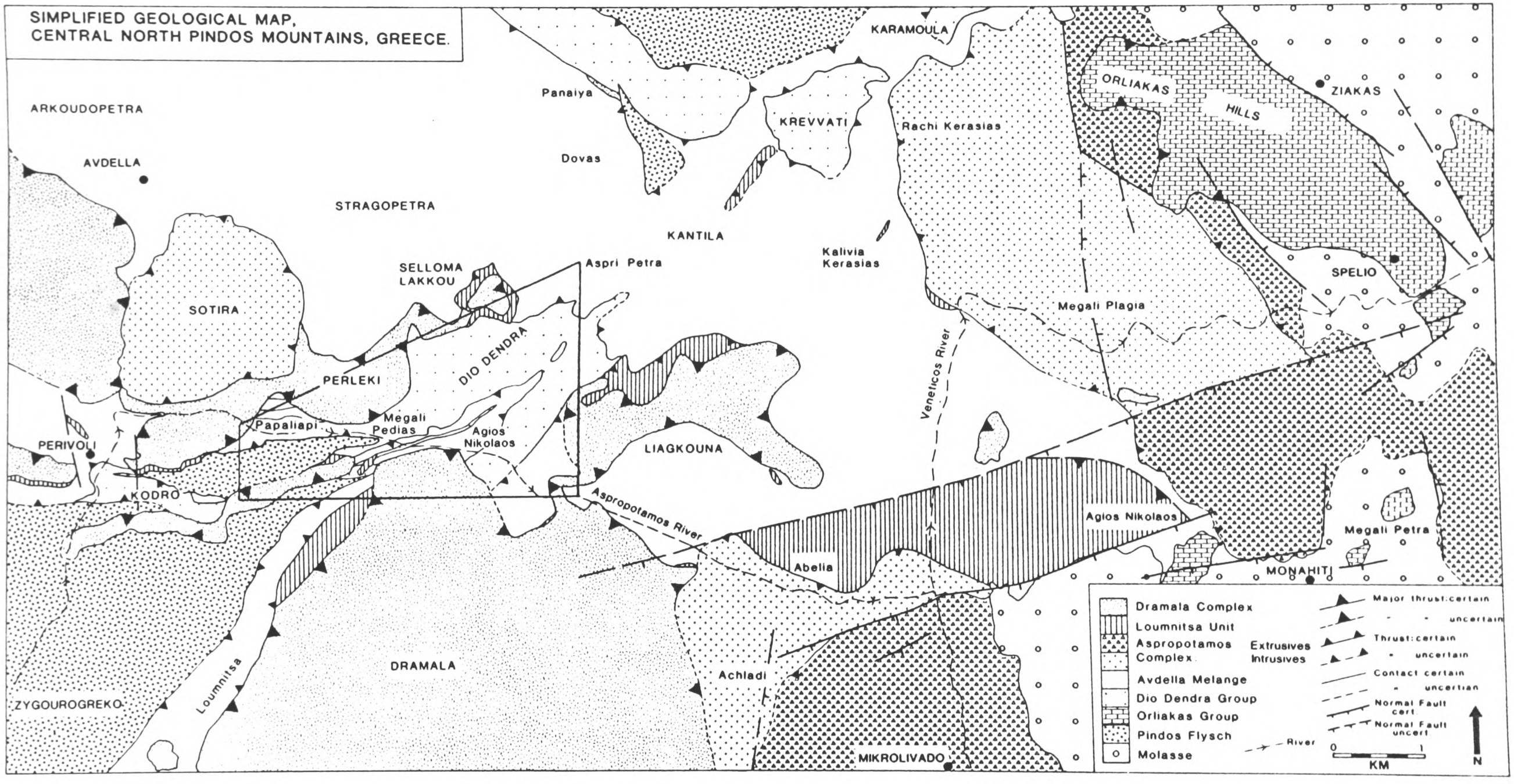

Fig. 7.6 Geological map of part of the central area (see Fig. 7.1). Boxed area indicates area of Fig. 7.5.

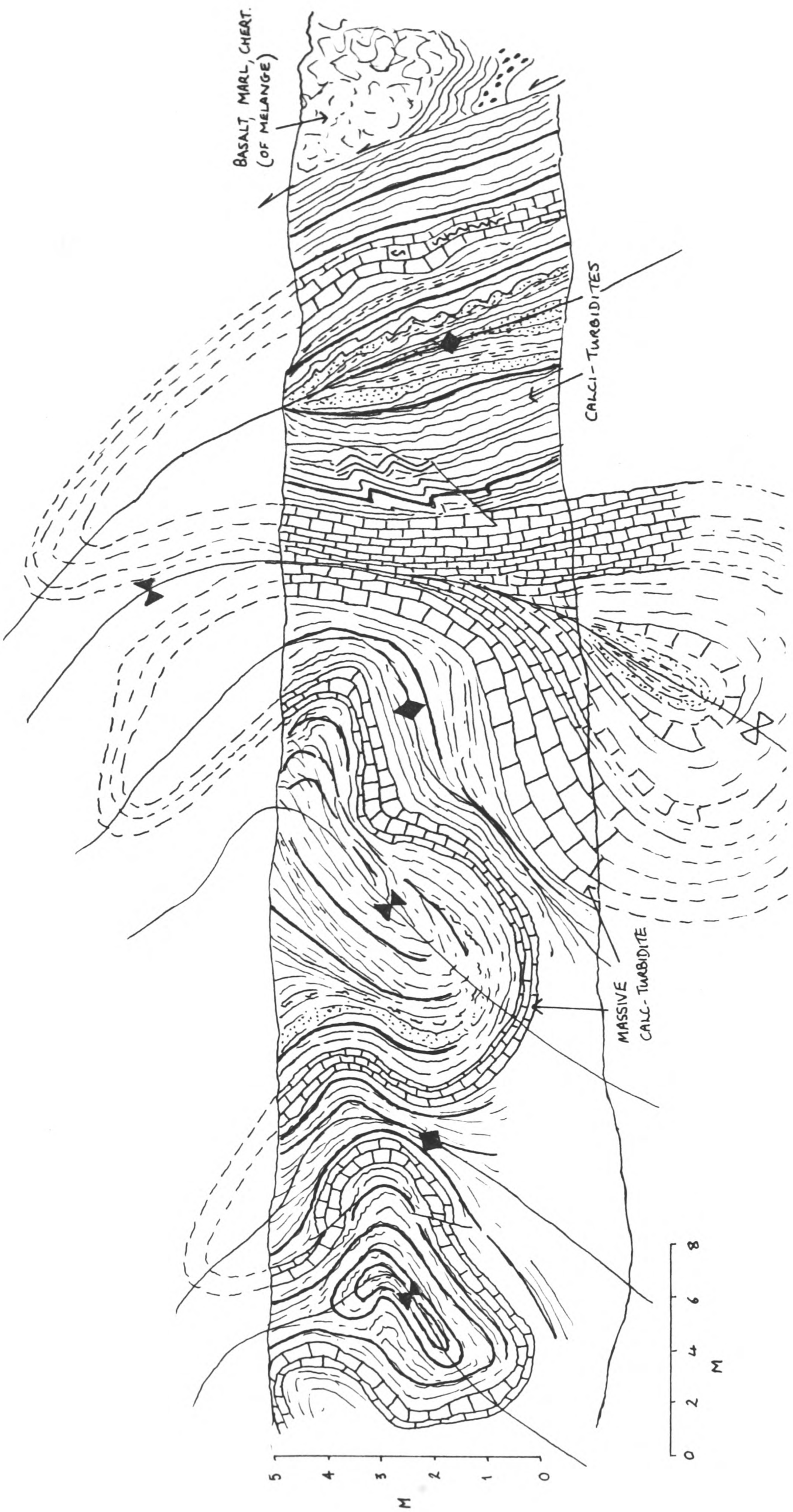

Fig. 7.7. Sketch of refolded fold structures within the Dio Dendra Group (Agios Nikolaos Formation), northern limb of the Perivoli corridor. Road section in the Aspropotamos Valley, 400 m N. of Papaliapi Bridge. (Fig. 7.5; based partly on Plate 7.3.a).

refolded along northeast-trending, northwest-dipping axes. The contacts between the individual thrust units are always poorly exposed, but are also assumed to be folded along northeast-trending axes.

On the southern limb of the structure, in the Aspropotamos Valley at Kokkina Litharia and within the Loumnitsa Valley, northeast-trending isoclinal folds are developed on the overturned limb of a major southwestward-verging, northwest-trending antiform (Fig. 7.8; Plates 7.3, 7.4).

7.4.3 Extensional structures

The Perivoli corridor experienced small-scale extension following northeast-trending refolding. The structure underwent extension on both limbs, leading to the development of normal faults, sometimes within individual thrust units, but also between units, along previous thrust contacts. This can be seen along the Aspropotamos Valley, near Papaliapi Bridge, where a number of northeast-trending, high-angled normal faults with variable displacements, cross-cut the tectonic units. This may lead to uncertainty where the contacts are poorly exposed, as there is no way of distinguishing out-of-sequence older thrusts from normal faults. At the northeastern end of the Perivoli corridor, juxtaposition of the Dio Dendra Group with high levels of the Avdella Melange may represent a major normal fault, downthrowing to the southeast. At Karamoula (Fig. 7.9), normal faults with minor displacements truncate southwestward-verging folds and thrusts within the Karamoula Formation, and appear to bound the exposure of this formation at both ends of the section.

7.4.4 Development of the Perivoli Corridor

Kemp and McCaig (1984) suggested that the Perivoli corridor developed as a lateral or oblique thrust ramp, with associated imbrication, during Tertiary thrust sheet emplacement. They quoted the example of the Dundonnell antiform within the Moine thrust belt of Scotland (Elliot and

Redeposited and pelagic carbonates

Calcarenites with volcanic detritus

Fine grained clastic sediments

Sheared mudstone

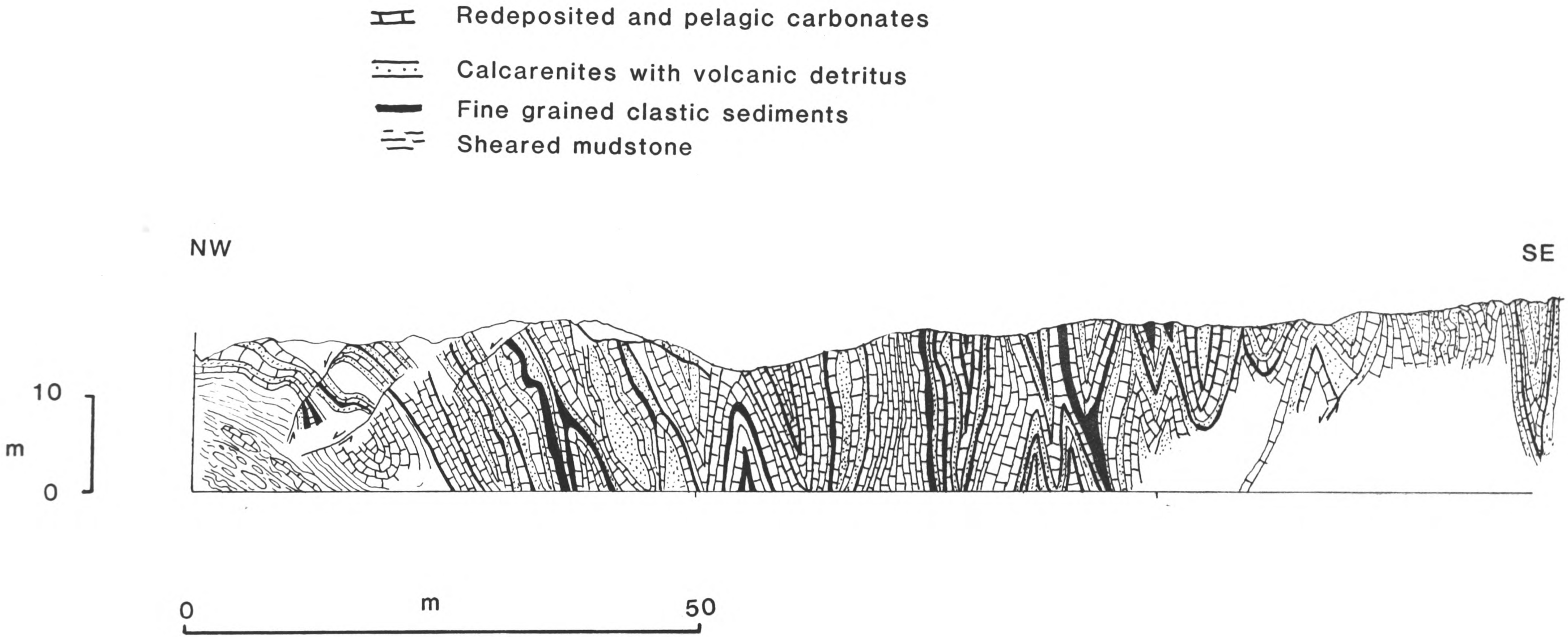

Fig. 7.8 Sketch section of isoclinal folds within the Dio Dendra Group (Karamoula and Agios Nikolaos Formations), on the southern limb of the Perivoli corridor. Roadside exposure at Kokkina Litharia, Figs. 7.5, 7.6).

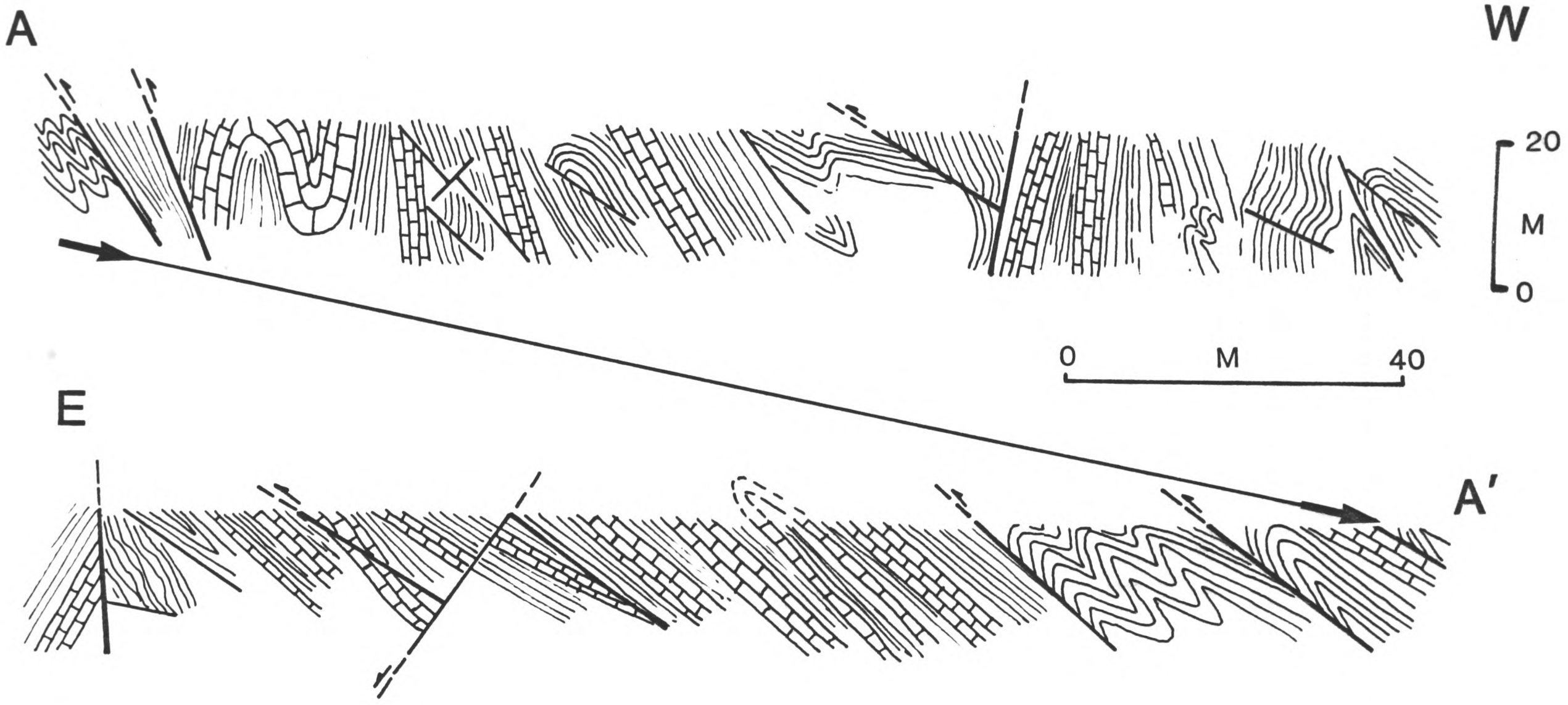

Fig. 7.9 Sketch section of roadside exposure located at Karamoula (Karamoula Formation of the Dio Dendra Group), showing styles of deformation within flysch sediments at this locality. Note the late stage extensional faults, probably related to collapse of the Perivoli corridor.

Johnson 1980), as a comparison for the oblique ramp model. Another area in which structures have been related to oblique ramps is the Oman Mountains. There, several major lateral ramp-type structures have been recognised bounding major tectonic windows such as the Hawasina window (e.g. Jebel Milh, Wadi Shafan; Searle 1985). Other so-called "transverse" structures are common throughout Oman (e.g. Hatta Zone, northern Oman; Robertson et al. 1990), and are interpreted as being related to basement topographies within the underlying carbonates.

The oblique ramp thought to be responsible for the formation of the Perivoli corridor imbricate structures, is interpreted as dipping steeply towards the southeast (as implied by Kemp and McCaig 1984), or even vertically, in the southwestern part of the corridor (S.W. of Perivoli). This area is also where the perpendicular-trending axis of the Armata-Milea corridor coincides with the Perivoli corridor axis, forming a double antiformal thrust culmination. The dip of the ramp in the northeast of the corridor is likely to be shallower, as the thrusts on the southern limb are thought to be more gently dipping.

It is possible that the major northeast-trending transverse structures which fold the thrust sheets were not caused by individual oblique basement ramps, but by late-stage northwest-southeast-trending compression of the entire thrust stack. Indeed, this is supported by the regional outcrop pattern, which shows an almost regular series of fold axes, on a wavelength of approximately 9 km. This wavelength appears to shorten towards the south, to nearer 5 kms. Interestingly, Lorsong (1977) interpreted curving thrust sheets within the Pindos Flysch northwest of Metsovo, first mapped by Brunn (1956), as having formed due to compressive stresses which acted on the Pindos Flysch probably after the Late Eocene (see below). Either of the above hypotheses, or a combination of both a series of oblique ramps and late compression appears to be possible at present, and further work is needed to establish the presence and causal mechanism of this possible northwest-southeast compressive phase.

7.5 STRUCTURAL FEATURES OF INDIVIDUAL TECTONIC UNITS

7.5.1 Introduction

A brief summary of the general structural disposition of the individual thrust units throughout the region is presented here. Summaries of the internal deformation present within the Dramala Complex, the Loumnitsa Unit, and the Avdella Melange have been presented in previous Chapters, and the discussion here is mainly restricted to large-scale, mainly thrust-related structures.

7.5.2 The Dramala Complex

The Dramala Complex is internally deformed, but essentially coherent on a regional scale. The Achladi thrust was the first-formed thrust, and separates mainly ophiolitic mantle lithologies, from the remainder of the thrust units. The thrust is an out-of-sequence thrust, as the overlying mantle rocks are relatively coherent, compared with the imbricated and deformed underlying thrust units. Also, the mantle lithologies of the Dramala Complex are found overlying all other thrust units, and the Achladi thrust apparently cuts down section to the west. There, it overlies the Pindos Flysch, thus eliminating large thicknesses of section (Figs. 7.1, 7.4). This thrust compares extremely well to the Semail thrust of the Oman Mountains (Glennie et al. 1974), which similarly acts as a major out-of-sequence discontinuity marking the base of ophiolitic mantle sequences. This thrust also cuts down section in the transport direction, eliminates large amounts of section and preserves a coherent mantle sequence above it (Searle 1985).

The regional outcrop pattern (Fig. 7.1), suggests that the Dramala Complex is broadly folded along the Achladi thrust. These broad scale folds of the Achladi thrust are further folded by later southwestward-verging overturned structures (e.g. at Liagkouna; Fig. 7.6; See Enclosure 2). The metamorphic sole is commonly best preserved within the cores of these overfolds. In addition, the Achladi thrust is imbricated by late-stage compressional faults associated with these folds (see Brunn 1956, pp 274),

which together have led to overturning of the basal peridotite mylonites and underlying metamorphics (Chapter 3 and Enclosure 2). Locally, these late imbricate structures have thrust the Avdella Melange over the metamorphic sole and peridotites.

Deformation within the complex has resulted in large-scale folding, imbrication and shearing of the peridotites and cumulates. Some of these features (i.e. those formed at high temperatures) are of Jurassic age, but lower temperature brittle structures formed then, are not always easily distinguished from later Tertiary structures (A. Rassios pers. comm. 1989).

7.5.3 Relationship of the Dramala and Aspropotamos Complexes.

There is no doubt that the Aspropotamos Complex, as defined here, represents crustal units once related to (i.e. overlying) the Dramala Complex. In general, it is thought that the Dramala Complex overthrusts the Aspropotamos Complex, as well as the remainder of the described units. However, the number of localities where this relationship can be well demonstrated is limited. This contact is probably best seen at Achladi (Fig. 7.6), where east-dipping isotropic gabbros (Aspropotamos Complex) are in tectonic contact with fresh mantle harzburgites. The contact is complicated by extensional faults, but was almost certainly originally a thrust. Otherwise, several hundred metres of westwards vertical downthrow of peridotite is required, in the opposite direction to the known regional extension (eastwards into the molasse basin). Another locality where this overthrust relationship is well seen is along the road between Perivoli and Avdella (Fig. 7.6). Here, intensely sheared sheeted dykes of the Aspropotamos Complex are similarly overthrust by mantle harzburgites, along a serpentinised basal contact.

At other localities, where such contacts are not present, complications may occur whilst attempting to classify the ophiolitic rocks into one or other of these units. Essentially, the known areas of exposed Aspropotamos Complex (i.e. Abelia area, Spileo area, Avdella, Katara Pass; Figs. 7.1, 7.6), in general, do not contain mantle sequence lithologies, and therefore usually

comprise cumulates, isotropic gabbros, sheeted dykes and volcanics. All of these are highly thrust deformed, and cover comparatively small areas, in contrast to the relatively coherent and extensive exposures of the Dramala Complex. The Dramala Complex also tends to form the topographically highest unit, capping many of the main peaks. Confusion may arise because metamorphic soles may be found in thrust contact with cumulate rocks from both Complexes, and often exposed areas of serpentinised ultramafic rocks with associated metamorphic soles cannot be assigned to either unit (e.g. N.W. Strivo Fig. 7.1).

In the Mikrolivado and Krania areas (Fig. 7.1), essentially along strike to the south of Achladi, Brunn (1956) and Parrot (1967) mapped a conformable contact between eastwards dipping peridotites and cumulates (part of the Dramala Complex; A. Rassios in prep.) and overlying crustal units. This contact was not observed during this study, and it is possible that this is not a major overthrust boundary, but indeed a conformable transition through into crustal rocks.

7.5.4 The Loumnitsa Unit metamorphic sole

The Loumnitsa Unit (Chapter 3) is found mainly at the base of both the Aspropotamos and Dramala ophiolitic units, although it is commonly detached into the underlying melange (e.g. Isomata Mountain, S.W of Perivoli; Enclosure 1). Imbrication of basal mylonite, amphibolites, greenschists and the melange occurs in several localities (e.g. in the Loumnitsa Valley; see Chapter 3).

7.5.5 The Orliakas Group

The Late Cretaceous Orliakas Group was folded and thrust during Early Tertiary emplacement. In the Orliakas Hills, near Spileo (Fig. 7.6), a stack of up to five separate thrust sheets occurs (Enclosure 2). The basal thrust of this stack is believed to overthrust the ophiolitic units of the Aspropotamos

Complex (see below). Recrystallisation of the carbonates has destroyed much of the original sedimentary fabric.

Reconnaissance studies of the structure of the Orliakas carbonates have failed to establish the original nature of the contact with underlying basalts in the west of the mountains. Here, the contact is mainly flat-lying, and it is possible that the basal carbonate units of the thrust stack were deposited as conformable sequences on the volcanic basement of the Aspropotamos Complex found here. The molasse sediments which are found mainly to the northeast of the mountains are obviously downfaulted to the northeast, but conformable drapes of molasse sediments are also present to the southwest of Spileo. The crest of the Orliakas Hills exposes a number of northwest-southeast trending linear valleys, probably representing major fault planes. Structures measured towards the western end of the hills suggest that some strike-slip motion may be present on these faults. For example, one fault zone exposed (trend 164/85/NE), contained a spaced fracture cleavage over a 20 m wide zone, and internal small-scale tear faults with a dextral sense of displacement.

At Strivo (Fig. 7.1), fold trains and discrete thrust planes deform the sequence. Serpentinite bodies are apparently found along the contact between the Orliakas Group and the Pindos Flysch at Strivo, and along strike to the north and south. At one locality (S.W. Skourtza hill, N.W. of Strivo; Fig. 7.1), the Late Cretaceous carbonate sequence is thrust over basal peridotite and metamorphic sole units, probably indicating that the entire ophiolite succession here has been omitted. Elsewhere (e.g. Monahiti, Fig. 7.6), individual detached blocks (up to several tens of metres in size), are locally unrecrystallised and internally intact.

7.5.6 The Aspropotamos ophiolite

The Aspropotamos Complex has been internally dismembered during emplacement over the Avdella Melange. Out-of-sequence thrusting has removed parts of the initial oceanic crustal sequence, and locally only the extrusive and upper intrusive sequences are preserved (e.g. Katara Pass, Fig.

7.1). Other sections have remained more internally coherent during emplacement (e.g. W. of Spileo, Fig. 7.6; Sotira, Fig. 7.6), but were disrupted by later high-angle extensional faulting, which also cuts out part of the section. In outcrop, units are often highly sheared and locally thrust imbricated, as seen especially within extrusive and sheeted dyke successions. Large-scale folding also affects the thrust slices (e.g. Sotira, Fig. 7.6), relating to either, or both of the main fold axial trends.

Consideration of the outcrop pattern of the Aspropotamos Complex in the eastern central area of the Pindos Mountains, shows two main outcrop areas of ophiolitic crustal rocks. The Aspropotamos Complex ophiolitic crustal rocks exposed west of Spileo Village, appear to correlate with those exposed in the Abelia-Achladi region, despite the deformation present (Fig. 7.6). Both areas expose cumulate rocks in the western part of their outcrops, and pass eastwards into progressively higher parts of the crustal section. The contacts within the crustal units (e.g. between sheeted dykes and lavas) also strike approximately northwest-southeast in both areas. Furthermore, the basal metamorphic sole sequence exposed in the Venetikos River Valley and the Agios Nikolaos (Monahiti) regions, appears to be abruptly truncated by a zone of deformation, within mainly basic volcanics. These factors lead to the proposal that a transverse fault separates these areas. This fault appears to trend west-south-west to east-north-east, have a dextral sense of displacement, and a visible lateral offset of approximately 6 km. This was previously believed to be a high angle normal fault (Kostopoulos 1989), but this is unlikely as little vertical offset has been observed. However, a number of structures trending parallel to this fault in the area, may have subsequently been re-activated as normal faults (e.g. Agios Nikolaos, Monahiti; Fig. 7.6). This transverse fault is believed to be essentially a Tertiary emplacement related structure, and is not therefore thought to have had any earlier (i.e. oceanic) history. Interestingly, however, the dominant MORB-type sheeted dyke trend in this area is approximately perpendicular to the fault.

High-temperature deformational features within the Aspropotamos Complex include the development of flaser structures and mylonites with shearing and alignment of chrome spinels, in the ultramafic and mafic cumulates. Serpentinisation of ultramafic cumulates generally increases

downwards towards the base of the Complex, where exposed. Localised sheets of serpentinite are found at the base of the cumulate lithologies (e.g. Sotira, Fig. 7.6), and imbricated within the underlying metamorphic sole sections (e.g. Abelia, Fig. 7.6).

7.5.7 The Avdella Melange

On a large scale, the Avdella Melange is folded into two large synformal structures in the central region, north (N.E. of Avdella, Figs. 7.1, 7.3) and south (Liagkouna-Kalivia Kerasias area, Fig. 7.6) of the northeast-southwest trending Perivoli corridor in the central area (Fig. 7.3; see cross-sections; Enclosure 2). The melange is also thinned on the limbs of this corridor (Kemp & McCaig, 1984), and imbricated beneath the Achladi thrust, sometimes occurring as tectonic slivers only several metres thick (Plate 7.5). Elsewhere, the melange is also reduced to only several tens to hunderds of metres (e.g. S. of Samarina; Tsouka, S.W. of Vovousa; Fig. 7.1). The melange lithologies are also tightly interfolded with other units, for example along the Dio Dendra Valley (Fig. 7.5).

A large expanse of melange is exposed in the region between Krania and Metsovo (Fig 7.1). In several areas, complex interthrusting with the ophiolite extrusives of the Aspropotamos Complex has occurred (e.g. in the Katara Pass Fig. 7.1), confusing the distinction between volcanics from each unit. In the Katara Pass, several large olistolith blocks, usually carbonates, are exposed within extensive melange. The structure in this area is dominated by another major fold structure trending parallel to the Perivoli corridor (i.e. N.E.-S.W.), the Metsovo corridor (new name).

At outcrop, metre-scale folding typically affects many lithologies, and is particularly visible within the more competent horizons; for example, radiolarite blocks commonly contain mesoscopic chevron, or concentric folds. Folds and related thrusts, are also widespread within thinly-bedded carbonate melange blocks.

7.5.7.1 Evidence for accretion-related deformation of the Avdella Melange within a subduction zone

The Avdella Melange also displays a number of features which are here interpreted as forming during accretion within a Jurassic subduction zone (Chapter 8). Many of these micro- to meso-scale structural features are found within drilled modern-day accretionary complexes, which therefore provide an ideal means of comparison (e.g. Barbados accretionary prism, Moore et al. 1986; Nankai trough; Karig 1986). Each of these structures will be dealt with in turn below. Accretionary complexes lead to a range of both extensional and compressional tectonic structures. The environment of formation of these features is dominated by underthrusting beneath an over-riding oceanic plate. This occurs within a low-temperature and moderate pressure volcanic and sedimentary wedge, in which water saturation and rapid burial commonly leads to high fluid pressures and therefore overpressuring. The direct results of such underplating and overpressuring are visible within the sediments of ancient and modern accretionary complexes, and have been recently well documented (e.g. Fransican Complex, California; Cloos 1982). Unlike some other on-land accretionary complexes, where high pressure metamorphism is evidenced by the formation of blueschists, deformation and metamorphism within the Avdella Melange took place at high structural levels.

a) *Thrust and fold-related deformation*

A pertinent question to consider is why the melange is considerably more disrupted and deformed than the other thrust sheets, despite a similar Tertiary thrust history? Much of the internal folding, thrusting and dismemberment of the Avdella Melange could, therefore, have resulted from accretion-related deformational processes during the Jurassic. In the Pindos Mountains, these structures are of course, almost impossible to distinguish from those formed during later stages of compressional deformation in the region. Such structures however are preserved within accretionary complexes from other areas of the world (e.g. Japan).

To try and distinguish Jurassic structures from Tertiary structures, part of the melange north of Avdella was studied. The area was chosen because the the dominant lithology was basalt, which would deform as relatively coherent sheets, and because the exposure was adequate. Thrust planes and steeper structures measured in these rocks dip in all directions (Fig. 7.10), probably due to refolding. However, where cross-cutting relations were visible, they showed a consistent chronology of displacement. Northwest-southeast trending, mainly northeast-dipping planes (?Tertiary thrusts) were truncated by steeply-dipping north-north-east trending planes (probably small tear faults, parallel to the emplacement direction; Fig. 7.10). Possible early structures (i.e. ?NE-SW-trending) were present, but their age relations with adjacent structures were unclear.

b) *Scaly fabrics*

Studies of drill cores has led to the recognition of a penetrative foliation within mudrocks from accretionary complexes, known as scaly fabric (e.g from the Middle America Trench, Baltuck et al. 1985). This fabric causes alignment of platy minerals within shales and clays, along anastomosing planes within the rock unit. In hand specimen this fabric appears as a smooth shiny surface found on all sides of a typical phacoidal sample of material, reminiscent of scaly serpentinite (Moore et al. 1986; Plates 7.6, 7.7). These fabrics are thought to develop as a result of strain processes in the wedge. A strong scaly fabric is developed in some of the turbidite and matrix-rich units at Alatopetra (Plate 7.6).

This scaly fabric is commonly associated with layer-parallel-extension features (e.g. elongation of sandstone beds; see below). Some of the turbidites with scaly fabrics developed, were previously deformed by soft-sediment deformation processes, particularly slump folding. This has also been recognised at Alatopetra, where radiolarite beds are folded into underlying shales.

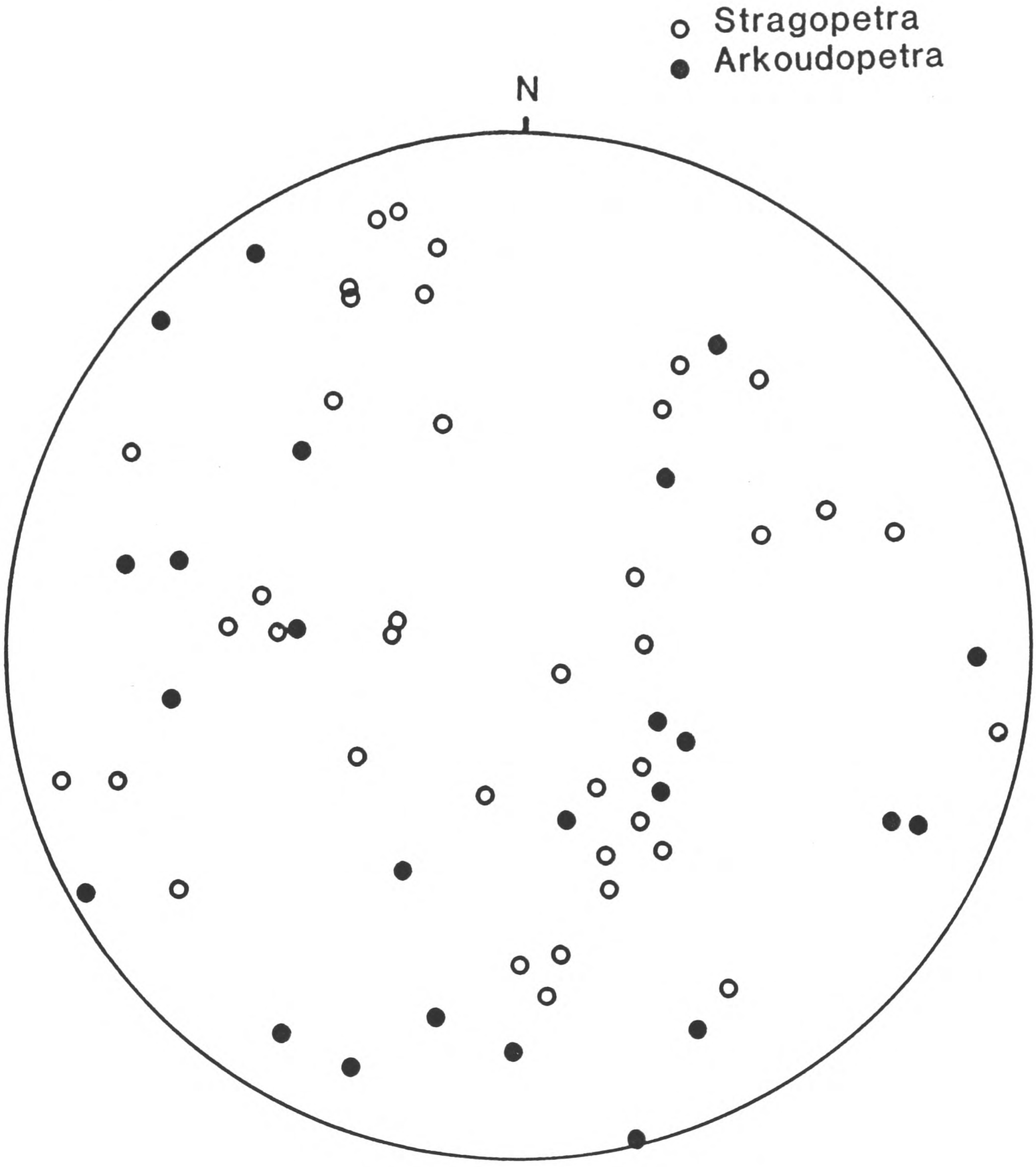

Fig. 7.10 Poles to thrust planes plotted on equal area, lower hemisphere, stereographic projection. Planes measured within melange extrusive thrust sheets, at N.W. Stragopetra and E. Arkoudopetra (Fig. 7.6). See text for discussion.

c) *Layer-parallel extension*

Many of the melange sequences show deformation whereby original competent sandstone beds have become extended and sometimes fractured, to form a series of blocks within a less competent matrix, usually of shale (Plate 7.6). Features like this can be seen within melange sequences at Alatopetra, Perivolaki, Armata and Liagkouna. Typically, a type of "chocolate-tablet" boudinage structure develops similar to that of medium grade-metamorphic rocks, but the more extreme cases display a block-in-matrix-type structure, which may be mistaken for an originally sedimentary fabric. A study of such features within the Shimanto Belt of Japan (Needham 1987), showed that they develop by ductile processes, under non-coaxial strains. Essentially these are shear bands developed within individual beds and packages of beds.

At Liagkouna (Fig. 7.6), elongate phacoidal sandstone beds are dismembered into interbedded siltstones and shales. A type of "pinch and swell" structure may form at first (Plate 7.6), developing into block-in-matrix structure with increasing deformation. These sediments were obviously part of an original bedded sequence, which has been firstly extended by up to 50 %, and subsequently folded into a series of concentric isoclines.

Sometimes, such layer-parallel extension can be seen to have affected units which have already formed as olistostromes. At Armata Village (Fig. 7.1; Plate 7.8), a number of highly sheared olistostromes, containing a wide variety of clasts, including sediment rafts of interbedded pelagic limestone and shales (up to 3 m long), blocks of harzburgite, gabbro, basalt, radiolarite. Clasts of marble breccia have overlying grey pelagic limestones, preserved in one block. The blocks are commonly phacoidal, and have smooth polished surfaces, particularly visible within quartz-rich sandstone blocks (Plate 7.6). These blocks sit in a matrix of sheared radiolarite, mudstone and quartzose shales and arenites.

d) *Compaction when unconsolidated*

Examples of sediments which have undergone compaction prior to lithification are common within the melange. These sediments typically comprise an originally compet nt lithology, such as carbonate, which was enclosed within incompetent shaly sediments. The competent layer has been extended whilst uncompacted, leading to the formation of tectonic blocks with folded or indented margins. The shales have flowed between the carbonate blocks, and subsequently the whole sequence has become further sheared. A good example of such deformation, where carbonate sediments are partly infolded into grey shales can be seen at Valiara (N.W. Perivoli; Plate 7.7).

e) *Fracturing and cleavage development*

Many lithologies display intense penetrative shear fabrics (e.g. Loumnitsa Valley; Fig. 7.6), associated with hydrothermal alteration, fracturing and vein infilling (usually carbonate). The vein structures are inferred to develop during thrusting within the accretionary complex, perhaps by rapid de-watering of sediments. Several generations of spaced cleavage affect the sandstone and shale turbidite units. These cleavages are often intense, and also affect basalts and other competant rocks, producing smooth surfaces similar to scaly fabrics.

f) *Formation of debris flows and olistostromes*

Several parts of the melange contain debris-flow-type units, containing blocks of basalt, chert, pelagic limestone and marble in a black shale matrix (Plate 7.8). Often, these sediments are deformed, and weak cleavage fabrics are developed within the matrix. The constituent clasts have become preferentially aligned during cleavage formation. A study of such aligned clasts from the Valiara Valley (2 km N.W. of Perivoli, Fig. 7.6; Kemp and McCaig 1984), showed that they were aligned along northwest trending axes (modal plane 134/30/NW).

7.5.7.2 Summary of internal deformation within the Avdella Melange

The melange has certainly been extensively deformed during Tertiary thrust emplacement, resulting in a wide range of compressional and extensional structures. Several aspects of the internal deformation of melange lithologies are also interpreted here as having been formed prior to Tertiary emplacement, within an active subduction zone. This interpretation is based on the styles of deformation present, the lithological associations and the overall tectonic interpretation for the setting of the Pindos ophiolite. Other supporting information includes the presence of clasts of bonititic basalt within these deformed seqences, rocks which are only known from oceanic destructive-margin settings.

The features described above formed in a range of environments within the accretionary complex system. Debris flows and olistostromes may have been formed by mass-wasting processes at the base of slope of the prism (e.g. Cowan 1985). Evidence suggests that some of these were previously indurated, cleaved and brecciated at the toe of the prism, and then uplifted and redeposited. Several sequences show evidence of structures formed under conditions of high pore fluid pressure, and also abundant evidence for deformation whilst unconsolidated. The extensive volcaniclastic turbidite sheets described from the Avdella Melange (Chapter 4) may have at least partly formed as trench-type turbidites, which were subsequently accreted and deformed by layer-parallel extensional processes.

7.5.8 The Dio Dendra Group

The mainly thin-bedded formations of the Dio Dendra Group, were deformed during their emplacement over the Pindos Flysch as a major thrust sheet. On a large scale (e.g. Dio Dendra Valley; Figs. 7.5, 7.6), the Group forms a broad anticlinorium plunging to the north-east, which defines the Perivoli corridor (see above). Outcrops to the north of Dio Dendra (e.g. Krevvati, Karamoula; Fig. 7.6), occur near the core of this fold structure. The Group also

forms a number of thin imbricate thrust slices, where tectonic complications are apparently caused by footwall ramps (e.g. Kodro; Fig. 7.6).

Outcrop-scale folds and thrusts are common. Two main fold axial trends are distinguished (NW-SE and NE-SW, Fig. 7.11). Both these fold phases are commonly of chevron type. In general, the folds are overturned or upright, tight to isoclinal (e.g. Kokkina Litharia, Fig. 7.8; Plates 7.3, 7.4). Minor folds are very well displayed in regularly bedded carbonates of the Krevvati Formation, sometimes associated with thrust planes. Several cleavages (up to five; S. Spencer, pers. comm. 1989) occur within the most tightly refolded sections (e.g. Kokkina Litharia, Fig. 7.5). Several thrust sheets have suffered stratal disruption. For example, layer-parallel-extension during refolding has given rise to "block-in-matrix"-type structure (e.g. Papaliapi, Fig. 7.5) formed under brittle conditions, and tectonic "broken formation" (e.g. Perivoli, Fig. 7.6; Plate 7.2), where fold hinges in competent lithologies may become isolated in a deformed matrix.

7.5.9 The Pindos Flysch Group

The Pindos Flysch is complexly deformed and tectonically "telescoped" beneath the other thrust sheets, forming several broad fold structures (e.g. "La demi-fenetre de Samarina" of Brunn 1956; Fig. 7.3). These structures are poorly understood, but clearly there has been extensive deformation, with cleavage, layer-parallel extension and intense imbrication developed. The Pindos Flysch forms the core of the Perivoli corridor in the Dio Dendra Valley (Figs 7.5, 7.6). The flysch also forms a major antiformal structure (Armata-Milea corridor; see above), which originated as a frontal ramp. Small-scale fold and thrust structures are also well developed, and large areas comprise "broken formation". This feature occurs particularly where antiformal fold crests coincide (e.g. S.W of Perivoli, Fig. 7.3). Folds within the unit, where structural complication is limited, verge mainly towards the southwest (e.g. at Vovousa; Fig. 7.1).

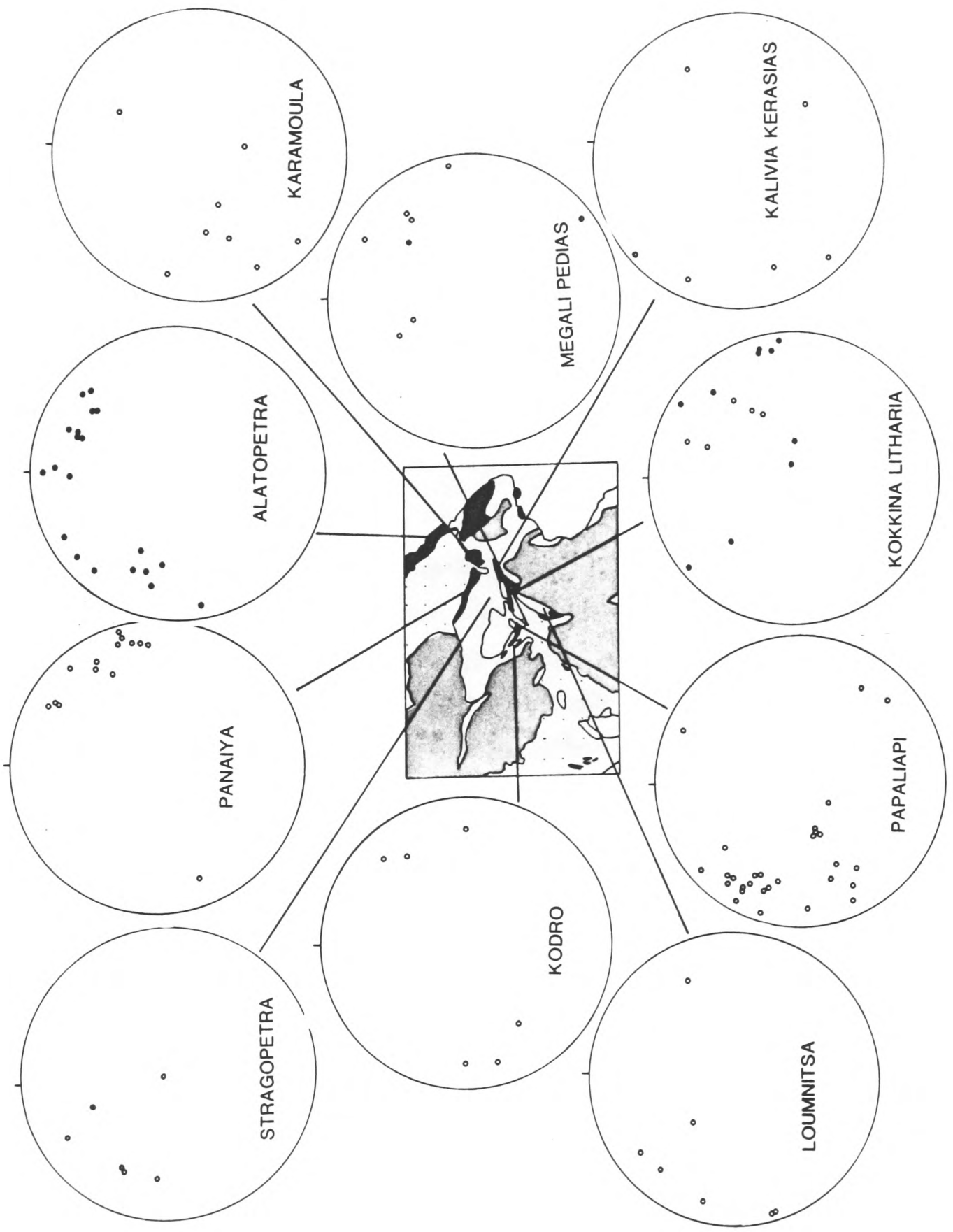

Fig. 7.11 Fold axial trends within the Dio Dendra Group and Avdella Melange at various localities around the Perivoli corridor, shown as lower hemisphere equal area stereographic projections. Note the occurrence of two fold trends at most localities. Refer to Figs. 7.1 and 7,3 for the position of the Perivoli corridor.

7.5.10 Meso-Hellenic molasse

The molasse sediments of the Meso-Hellenic trough are cut by large-scale extensional faults, downthrowing mainly to the northeast, which delineate the margin of the Meso-Hellenic trough (e.g. N. of Spileo; Fig. 7.6). An "embayment" within the thrust sheets (N. of Krania, S. of Monahiti, Figs. 7.1, 7.3; "Gulf of Krania" of Brunn 1956) contains sediments of Late Eocene age, the oldest so far discovered (Soliman & Zygoyannis 1979). This embayment is believed to be controlled by dextral strike slip faults (E-W trending), which occur on its northern and southern margins (S. of Spileo and S. of Krania; Fig. 7.3). This transverse faulting almost certainly took place during Tertiary emplacement, reflected by the occurrence of the Late Eocene sediments found there.

Structures within the molasse sediments in the Kranea-Spileo area include late-stage contractional faulting (S. Spencer, J. R. Underhill pers. comm. 1989). Outcrops of molasse conglomerates along the eastern central margin of the region, are often vertically dipping and sheared (e.g. at Alatopetra, Achladi; Figs. 7.3, 7.6). At Spileo, extrusives of the Aspropotamos Complex have an overlying molasse basalt-rich breccia, which now dips vertically. These structures, together with the evidence of local compressional structures along the margin, implies to the author that a second phase strike slip motion may have occurred during the final stages of compression. Evidence for a second phase of folding of the Pindos thrust sheets (forming the Perivoli corridor and similar structures) has already been presented. It is suggested here that the margins of the thrust belt were sheared to accommodate this compression (i.e. in a NNW-SSE direction). There is, at present, very little firm evidence (however see Orliakas Group, above), but it is suggested that these structures may have an overall dextral sense of displacement, and contain both extensional and compressional structures along their length. It is also possible that the "Gulf of Kranea" formed as a pull-apart basin within this system, but several other mechanisms may also have been in operation, during extensional collapse behind the thrust sheets.

7.6 Relationship of the thrust sheets to the foreland of the Ionian Zone

The Pindos Flysch overthrusts the Ionian platform sequence along a complex zone of deformation (the Pindos thrust; Lorsong 1977). In the southern area (Votonossi Village, W. of Metsovo; Fig. 7.1), this thrust is a low-angle zone of diffuse strain, in which sheared turbidites of the Pindos Flysch overthrust carbonates of the Ionian platform (Aubouin et al. 1977). In the central area (W. of Armata, Fig. 7.1), it is a high-angled feature, possibly representing a thrust that was re-activated as an extensional fault. In some parts of the northern area, the contact is marked by banded mylonitic carbonates of the Ionian platform which overthrust eastwards, back over the Pindos Flysch (this study; Brunn 1956). The Pindos Flysch beneath the thrust is spectacularly deformed into large kink folds (6 m wavelength). It is therefore clear that this contact is polyphase deformed, and represents one of the most fundamental tectonic lineaments in western Greece, worthy of much greater study.

The Ionian carbonate sequences exposed to the west of the overthrust belt of the Pindos Mountains form a classic fold and thrust imbricate sequence, formed by the progressive westward migration of the deformation front . It is assumed that the Ionian carbonate sequence is partially underthrust beneath the Pindos Flysch, as a result of Tertiary collision. The Pindos flysch probably also overlies a thick sequence of oceanic and continental margin sediments, deposited off the margin of the Ionian platform throughout the Mesozoic. The Pindos flysch may have accumulated as a foreland basin or an accretionary complex, as discussed in Chapter 6.

7.7 Relationship of the thrust sheets to the Pindos Zone of central Greece

On the southern margin of the region, there is a major structural discontinuity between the grossly overthrust northern Pindos Mountains terrain, as has been described here, and the comparatively less-deformed sequences of the Pindos Zone of central and southern Greece (Aubouin 1959; Fig. 7.1). South of the Metsovo corridor, compressional deformation has also

occurred, thrusting and folding the basinal sediments exposed. Displacement along the basal decollement of the Pindos Zone sediments may have been substantial. However, the displacement on individual thrusts is minimal, and the sedimentary sequences can be quite easily reconstructed, as shown by Green (1983). Separating these two areas is thought to be a major transform fault, the Kastaniotikos transform of Lyberis et al. (1982; see also Chapter 4). Such a structure is necessary to explain such an along strike variation within such a short distance. Consideration of the regional outcrop suggests that the present amount of visible offset is approximately 40 kms, the distance that the Pelagonian basement is displaced dextrally in the southern Vourinos area (Geological Map of Greece, IGME 1987). However, several hundred kilometers of motion may have taken place on this fault prior to this, and it therefore forms the most important transverse structure in the region.

7.8 Neotectonic deformation

Very little is known about the neotectonic deformation of the northern Pindos area. The region lies too far north of the Aegean arc to be significantly affected by subduction related extension behind the Hellenic trench, and too far west of deformation related to motion on the north Anatolian fault. The north Pindos mountains, and indeed much of northwestern Greece is presently thought to be tectonically stable, and no major earthquakes have occurred in the area for at least several hundred years. One major neotectonic extensional fault was, however, discovered in the eastern Smolikas Mountains, 8 kms N of Samarina (Fig. 1). There, a fault plane with a throw of some 20 m has been found, trending northeast-southwest, and downthrowing to the southeast. No other Recent faults were recognised during this study.

7.9 Summary of structural evidence

Following Mid to Late Triassic extension within the Pindos area, now recorded in the melange, deformation of the Dramala and Aspropotamos ophiolite complexes occurred during the ?Mid. Jurassic, related to their formation and susequent displacement within the ocean basin.

Metamorphism, folding and thrusting of the Loumnitsa Unit sole is dated as 165 3 ma (Bathonian). Deformation within the Avdella Melange is thought to be coeval, and continued until the Kimmeridgian-Tithonian. The next major deformational phase is Late Eocene compressional emplacement towards the present southwest. This involved major overthrusting and transverse faulting, and led to the formation of the Pindos thrust stack. The later stages of this event involved extensional faulting, downthrowing northeastwards towards the Meso-Hellenic trough (syn-or post-Late Eocene). Subsequently, northwest-southeast compression (post-Oligocene?) may have led to refolding of the thrust stack along northeast-southwest trending axes (e.g. Perivoli corridor). Strike slip faulting (dextral?) may have taken place on the eastern margin of the thrust belt to accommodate this compression, further deforming structures formed during the earlier compressional (and extensional?) structures. Further study is required to elucidate the exact timing of these events, particularly in relation to the formation of the Meso-Hellenic trough.

Plate 7.1 Flat lying chevron folds, viewed perpendicular to the direction of thrust transport (i.e. viewed to the N.W.) Within the central part of the Perivoli corridor, at Agios Nikolaos church (Perivoli).

Plate 7.2 Refolded fold structures at outcrop scale. a) Central Dio Dendra Valley, at Megali Pedias. b) as above. c) At the Aspropotamos bridge, Perivoli Village. Axial planes visible are marked. Cliff is 40 m high at its maximum extent.

Plate 7.3 a) Refolded fold in the Dio Dendra Formation, 500 m N.W. of Papaliapi Bridge (see also Fig. 7.7). Note circular fold closures within the turbidites. Limestone bed (centre left) is 2.5 m thick. b) Isoclinal chevron folds within purple shales and pelagic limestones of the Karamoula formation at Kokkina Litharia. 3 m high cliff section.

Plate 7.4 a) Isoclinal chevron fold in partly recrystallised calciturbidites, Kokkina Litharia. 10 m high cliff section. These folds are developed parallel to the emplacement direction of the thrust sheets. b) Close-up of the hinge of the above fold, plunging steeply towards the northeast.

Plate 7.5 a) Intense imbrication within the melange. Radiolarite (R; far left) and basalt (B; far right) in thrust contact with sheared serpentinite (S), possibly of pre-Tertiary origin. b) Imbrication on the northern limb of the Perivoli corridor. Amphibolites (A; far left) thrust against basalt (B; centre) and Cretaceous Flysch (F; right). c) Late Triassic radiolarites interthrust with basalts, confluence of the Aspropotamos and Venetikos Rivers.

Plate 7.6 Structures within melange sedimentary sequences. a) Quartzose turbidites with interbedded arenites and siltstones, showing pinch and swell structures in the arenite beds, due to layer parallel extension. Phacoids (A) showing pinching-in of bed boundary (B). S. Liagkouna Mountain, along roadside, N. bank of the Aspropotamos River. b) Phacoidal block of volcaniclastic arenite in sheared shale matrix, showing scaly fabrics, Alatopetra Village. c) Intensely deformed scaly shales, part of a volcaniclastic turbidite sequence, Alatopetra Village.

Plate 7.7 a) Soft-sediment deformed carbonate bed in a shale matrix. Fluidised shale has been injected into the carbonate bed during layer parallel extension under high fluid pressures, leading to fragmentation. Valiara Valley, N.W. of Perivoli. b) Shales showing polished surfaces (scaly fabric) and development of tectonic pebbles or phacoids. Turbidite block, Aspropotamos Bridge, Perivoli. c) Block within the debris flow shown in Plate 7.8 a. This block is of quartz arenite, which has completely polished and slickensided surfaces, indicating an earlier deformational history, prior to becoming incorporated into a debris flow. E. of Armata Village.

Plate 7.8 a) Sheared debris flow sequences, showing sediment rafts of pelagic limestone and shale, blocks of quartz arenite, mafic, ultramafic and radiolarite rocks. E. of Armata Village. Matrix is comprised of a finer mixture of smilar lithologies. Many of the clasts show pre-existing deformational histories. b) Sheared block-in-matrix sequence, S.W. Liagkouna Mountain. This sequence contrasts with the above, as it forms a continuous bedded sedimentary sequence. Note large quartz arenite blocks showing extreme layer-parallel extension, perhaps in excess of a factor of two. c) Melange olistostrome block, with a well developed penetrative cleavage, and small cross-cutting fractures (thrusts?).

7.1

7.2

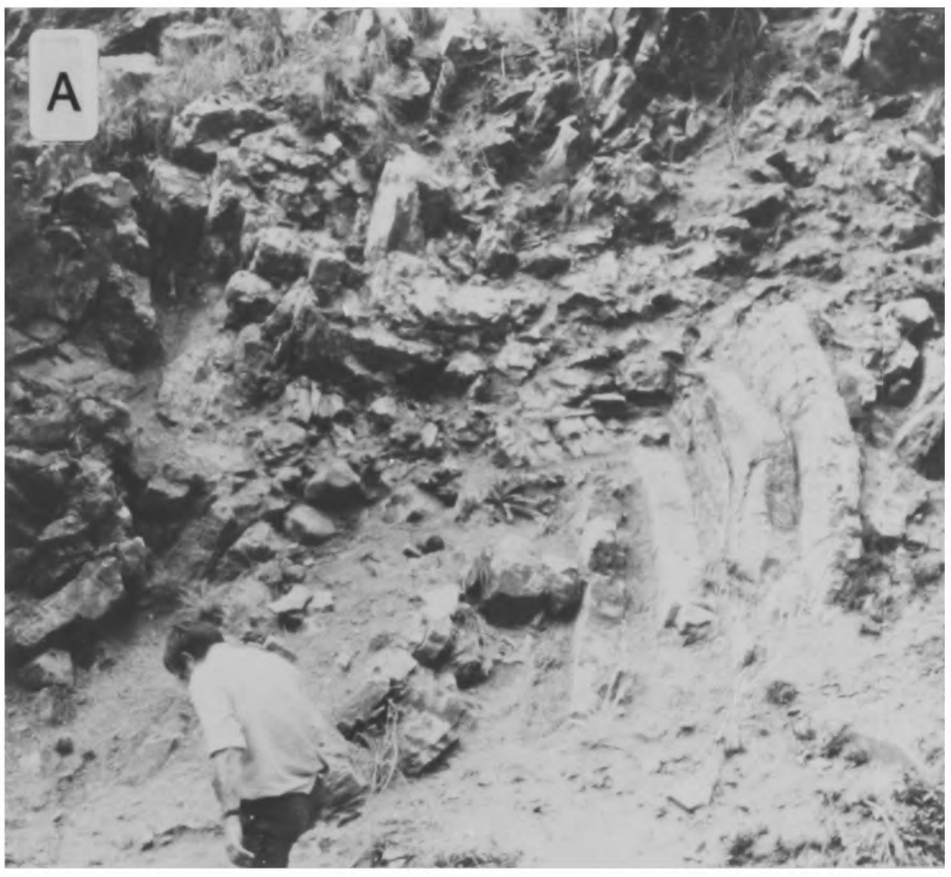

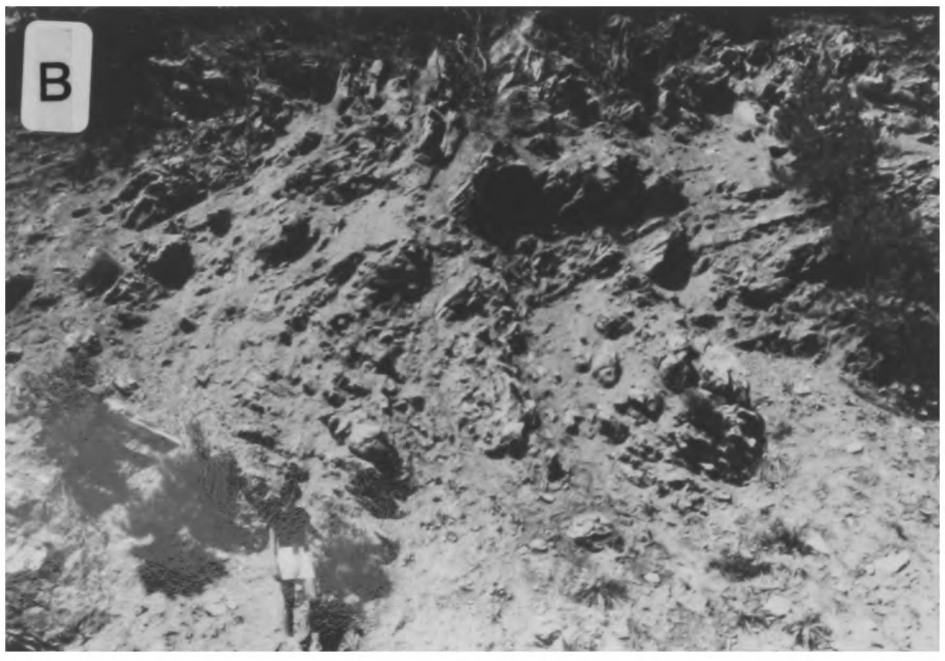

7.3


A


B

7.5

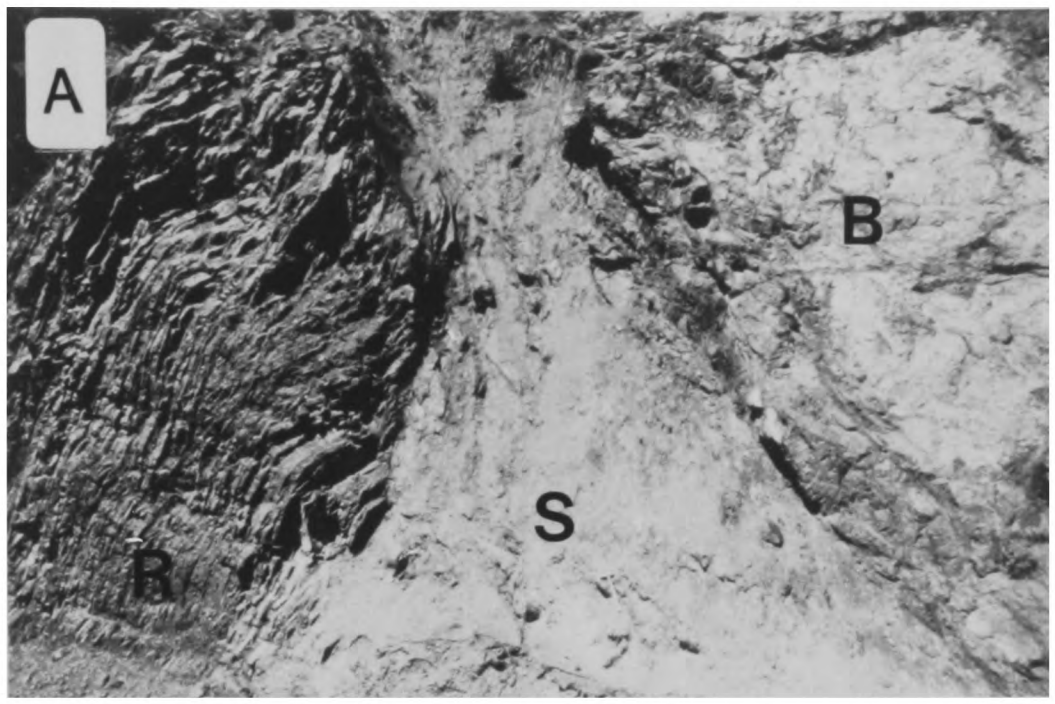

7.6

7.7

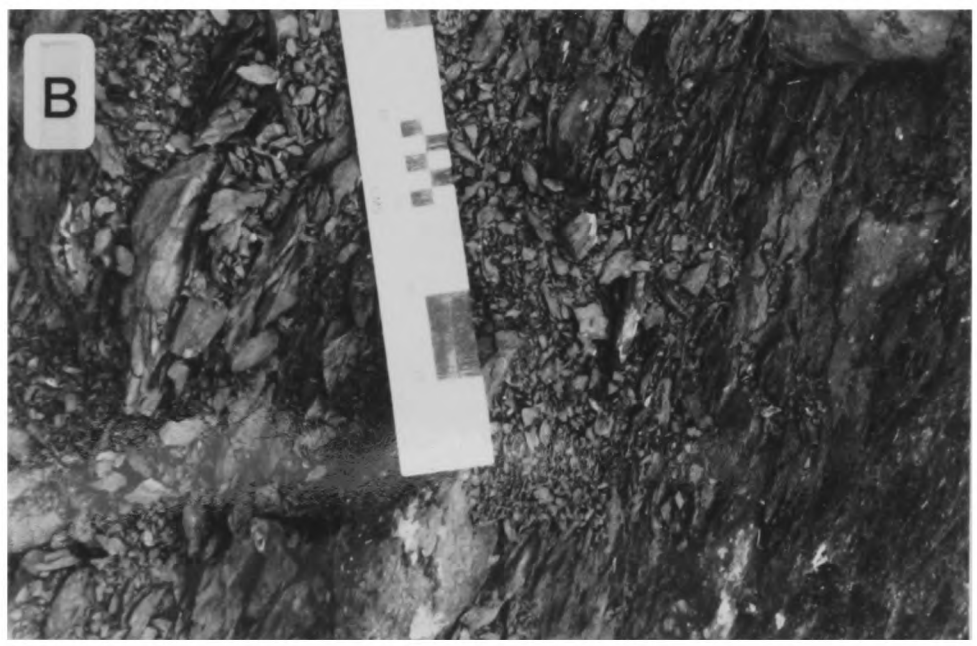

7.8

CHAPTER 8

CONCLUSIONS: THE TECTONIC AND SEDIMENTARY EVOLUTION OF THE PINDOS OCEAN BASIN IN NORTHERN GREECE

8.1 Introduction

A major aim of this project was to try to reconstruct the Mesozoic and Tertiary plate configuration of the external Hellenides in northern Greece. This relies heavily on an understanding of the processes of basin formation, oceanic crustal development, and continental margin sedimentation within the Tethys system. An essential part of this reconstruction is to establish the ages of the various igneous, tectonic and sedimentary events which have taken place since the Mesozoic. Despite extensive Tertiary deformation, the evolution of the north Pindos Mountains is quite well documented by the lithologies of the individual thrust sheets, as described in the preceding Chapters. The key points regarding the tectonic development of the area studied are: (1) that the Pindos Ophiolite Group developed above a subduction zone; (2) that the Avdella Melange represents a Jurassic subduction-accretion complex. The Pindos Neo-Tethyan basin was sited between the Apulian continental margin to the west, and an elongate micro-continental sliver, represented by the Pelagonian Zone (Fig 8.1), to the east. The initial stages of rifting of this basin are not well exposed in the area studied, but are evidenced indirectly by the large volumes of probable rift-related alkaline and tholeiitic basalts within the Avdella Melange. Elsewhere in the Hellenides, however (e.g. Othris: Hynes 1974; Smith et al. 1979; Peloponessos: Dercourt 1964; Pe-Piper 1982), rifting took place in the Early to Middle Triassic. In northern Greece (Kastoria area, Mountrakis 1984), continental margin sediments of Early to Mid Triassic age found on the western Pelagonian margin, include neritic limestones of the platform, passing westwards into sandstones, pelites and fine-grained limestones, considered transitional to sediments of the Avdella Melange.

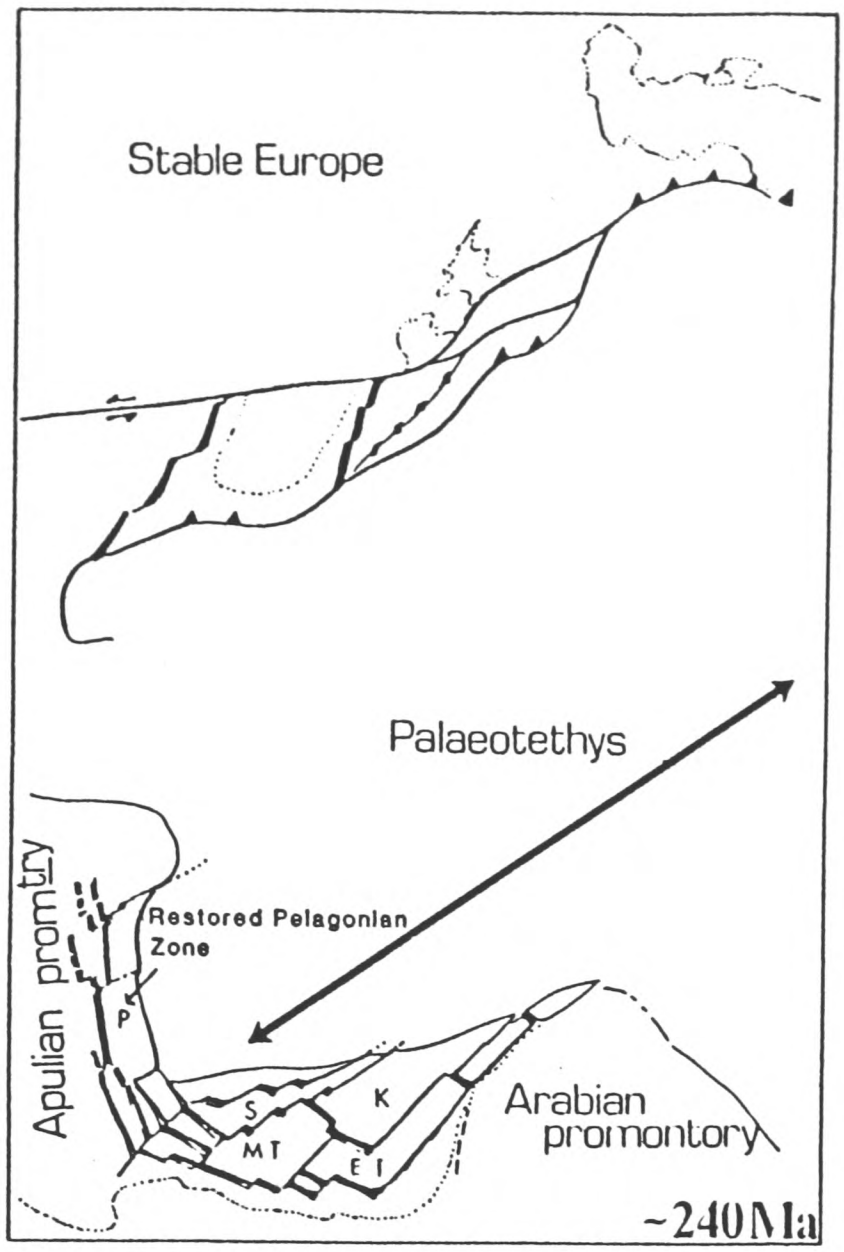

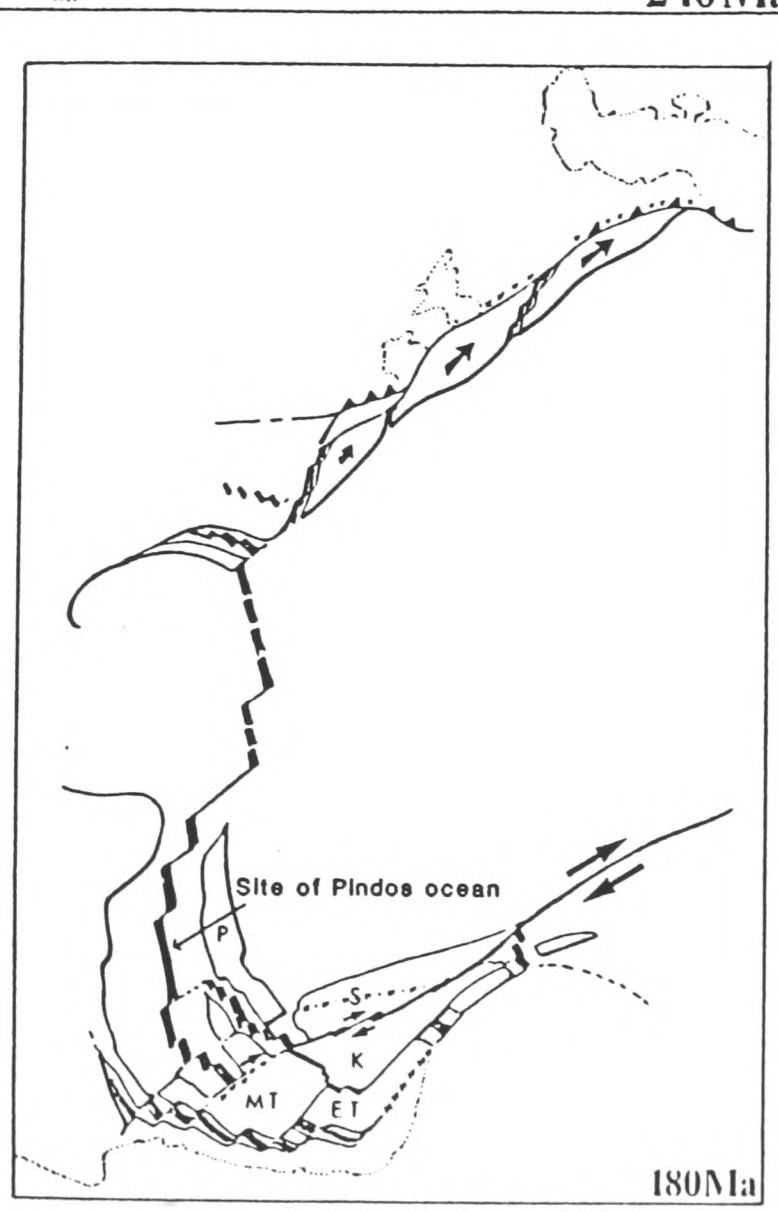

Fig. 8.1 Plate reconstructions of the Eastern Mediterranean area during the Triassic and Mid Jurassic, by J.E. Dixon (unpublished data). a) Note the position of the Pelagonian Zone, located at the margin of the Apulian promentory at this time, and the expanse of Palaeotethys to the northeast. b) Spreading of the Pindos ocean has occurred west of the Pelagonian Zone, note also other Neotethyan basins to the north and south. These may have developed by the partial subduction of Paleotethys towards the southwest.

8.2 Early spreading history: development of the Pindos Ocean

Final break-up of the Apulian Margin (Fig. 8.1) led to the formation of a Late Triassic small ocean basin, the Pindos ocean (Othris ocean of Smith et al. 1975; Fig. 8.1). In the north Pindos area, this is evidenced by the important occurrence of extrusives ranging from transitional to MORB to normal MORB, now dismembered within the Avdella Melange. This spreading took place to the north-east of a passive margin, now represented by the present day Pindos Zone. Other examples of igneous activity associated with the rifting phase are the intrusion of within-plate-type and transitional dykes. These dykes intrude both older basic volcanics of within-plate-type, and conformably overlying cover of pelagic limestones and radiolarites, dated as Late Triassic (P. De Wever pers. comm. 1990).

Deep-sea sediments related to rifting and early spreading include quartz-rich turbidites, which are perhaps some of the oldest sediments found in the area. Pelagic carbonate deposition as old as Mid Triassic has also been proven by the preserved ammonite fauna. Radiolarites, marls, and haematitic shales found within the melange also characterise the Late Triassic. A poorly preserved transition from quartzose turbidites into Late Triassic radiolarites marks the end of a continental influence on sedimentation. Turbidites of this age with abundant volcanic, gabbroic, radiolarite and pelagic limestone clasts may have formed when spreading started. The Triassic is seen as a time of strongly differentiated sea floor topography, leading to a variety of sedimentary facies, often with abundant evidence of redepositional processes having taken place.

Rare shallow water "exotic" blocks containing stromatolites, and current-sorted brachiopod-rich beds of Triassic age, must have originated close to, or at, the Pelagonian platform margin. Units of Late Triassic neritic carbonate, overlain by Early Jurassic condensed ammonitico-rosso sequences followed by radiolarites, are interpreted as continental margin seamounts (e.g. Alatopetra, Padhes). These formed near the continent-ocean boundary, and subsided after spreading began, falling eventually below the carbonate compensation depth, a similar history to that inferred for the Oman Exotics (Searle and Graham 1982). Basinal sediments were

also deposited adjacent to the inferred seamounts, from which carbonate material was apparently periodically displaced.

The Pindos ocean either developed as a Red Sea-type basin, or as a marginal basin formed above a subduction zone (e.g. Sea of Japan). The Late Triassic oceanic volcanics from the melange occasionally appear to show some supra-subduction zone chemical affinities, possibly inherited from an earlier subduction event. This fact, combined with similar evidence from central and southern Greece, leads to the interpretation of the Pindos ocean as a marginal basin, perhaps formed by subduction of parts of the Palaeotethys in areas further to the north east (Sengor et al. 1984). It is uncertain how much of the MORB-crust formed at this time (i.e. Late Triassic) is now preserved within the Aspropotamos Complex, but at least part of the basal volcanic unit (Abelia unit of Kostopoulos 1989), is conceivably a remnant of this phase of spreading. Supporting evidence for this interpretation is the low degree of partial melting apparently required for generation of these volcanics (5 %; Kostopoulos 1989). Also, in many other Tethyan ophiolites, the basal units of the sequence are usually of a more depleted nature than normal MORB, perhaps further indicating an earlier spreading event in the Pindos area. In the Pindos and Sub-Pelagonian Zones elsewhere in Greece, Late Triassic deep-water sedimentation was underway (e.g. radiolarites; De Wever 1989), and was accompanied by apparently synchronous volcanism of WPB and MORB type (Agrilia and Mirna lavas of the Othris area; Smith et al. 1975).

8.3 Supra-subduction zone spreading

During the Early-Mid Jurassic, convergence was initiated, apparently related to the opening of the North Atlantic (Smith and Spray 1984). In response to this induced relative eastward movement of Apulia, intra-oceanic subduction was thought to have developed within the Pindos ocean. One of the major unsolved problems is why one slab of oceanic lithosphere, apparently of the same structure, density and age as the adjacent lithosphere, should collapse to start subduction. Initiation of subduction by collapse of the previous ridge system following a slowing, or even cessation of the initial spreading phase has been previously

suggested (Robertson and Dixon 1985), as has an origin by underplating along transform faults (Casey and Dewey 1984).

One interesting possibility is that the metamorphic sole at the base of the Aspropotamos Complex, and related unmetamorphosed MORB-type crust found as thrust slices within the Avdella Melange immediately beneath the Aspropotamos Complex sole (e.g. at Avdella and Kopanes; Chapter 4), may represent the first crust accreted during the initiation of subduction (as in the model of Casey and Dewey 1984). One factor which argues against this interpretation is that the boninitic dykes of the Aspropotamos Complex do not cross-cut its sole, indicating a later stage of formation. However, this interpretation cannot entirely be disregarded, especially as no sole rocks with subduction-influenced chemistries have been found in metamorphic sole sections interpreted as being attached to the Aspropotamos Complex, as predicted by this model. Also, many of these soles appear to be lithologically dominated by rocks of mainly Late Triassic age (particularly lower amphibolite facies rocks from Kalivia Kerasias and the Venetikos Valley, Chapter 4), as sometimes proven by radiolarian age dating, possibly suggesting a comparatively early accretion history, before the Mid Jurassic date obtained (Spray et al. 1984). Only further detailed field mapping and sampling of these sections, with accurate radiometric age dating, may prove this origin. However, it should be noted that the Pindos ophiolite may be the best, and possibly only place, to test such hypotheses.

However first started, subduction subsequently gave rise to the Pindos and Vourinos ophiolites by supra-subduction zone spreading processes. This is evidenced particularly by the boninitic volcanics, which require the addition of material from the subducted slab to explain their chemical characteristics. This spreading could have occurred at a spreading axis, along a transform fault, or at a ridge-transform intersection, possibly related to a migrating triple junction (e.g. Smith and Spray 1984; Robertson and Dixon 1985).

The Pindos ophiolitic units are inferred to represent the mantle (Dramala Complex) and crustal (Aspropotamos Complex) sections of this developing supra-subduction-type tectonic setting (Fig. 8.2). In common with many Tethyan ophiolites, no true volcanic arc was formed. The

Pindos ophiolite was formed by a process which can best be described as pre-arc spreading, and was probably closed before an arc could form. The Dramala Complex is interpreted as representing mantle which was situated some distance away from the supra-subduction zone spreading axis when obduction occurred, as some lherzolite is preserved, and additionally the peridotites lack abundant massive chromites. Those present are elongate and thin, suggesting that mantle flow away from the ridge has streaked out the original chromite pods (Culeneer et al. 1988). By contrast, the Vourinos peridotites and crustal sequences are solely of supra-subduction zone type, with abundant podiform chromite, deformed mainly by Jurassic emplacement structures (Wright 1986). Vourinos is interpreted to represent the lateral equivalent of the Dramala Complex, probably preserved whilst located closer to the above-subduction zone spreading centre (Jones and Robertson 1990).

The Aspropotamos Complex demonstrates a clear influence of subduction (Pearce et al 1984a) in its sequential geochemical depletion of high field strength elements, and enichment in light rare earth elements, within the dyke and extrusive units (N-MORB, MORB/IAT, IAT; Kostopoulos 1989), culminating in the production of boninitic lavas and dykes, typical of modern day supra-subduction zone settings (e.g. Cameron et al. 1983). Interestingly, the Aspropotamos Complex contains intrusive and extrusive rocks of evolved MORB-type, which are thought to be indicative of formation at a propagating fast spreading ridge (e.g. East Pacific Rise; Pearce et al. 1986). These rocks may have formed during the initial stage of spreading during the Late Triassic, or during the early stages of secondary subduction-influenced spreading, during rapid progression through to more depleted volcanics. The original crustal thickness of the Aspropotamos Complex appears to have been anomalously thin (2-3 km), and is interpreted as thinned "fore-arc" crust, formed immediately adjacent to an active subduction zone (Kostopoulos 1989).

The volcanic stratigraphy of the Aspropotamos Complex is similar to that observed within the Oman ophiolite, where transitional MORB/IAT-type units (Geotimes Unit) are intruded and overlain by successively more depleted units (Lasail, Alley and Clinopyroxene-phyric Units; Alabaster et al. 1982). Also, the Troodos (Murton 1990) and Hatay

ophiolites (Piskin et al. 1986), similarly show more depleted extrusives, including boninites, towards the top of the succession, or related to well defined tectonic lineaments.

A possible analogue for the setting and volcanic chemistry of the Pindos ophiolite is the Eocene history of the Mariana-Bonin forearc (Natland and Tarney 1982), prior to Oligocene rifting (Fujioka et al. 1989), as discussed by Kostopoulos (1989). However, although the chemical range of rocks dredged from this area (boninites, MORB/IAT transitional and MORB; Bloomer and Hawkins 1987) is partly comparable to those of the Aspropotamos Complex, there is no choronological control for any of the rocks dredged there, and they could theoretically have formed in reverse order to those of the Aspropotamos Complex, during the transition to spreading in the Marianas back-arc basin (MORB-type).

8.4 Subduction-accretion processes

The olistolith blocks and dismembered thrust sheets of the Avdella Melange represent preferentially accreted Triassic and Jurassic Neo-Tethyan oceanic crust and associated sediments. Some of this material may have been scraped from the downgoing slab at the initiation of subduction (MORB and transitional to MORB basalts), which are now found closely associated with the fore-arc fragments and their metamorphic soles. It is also possible that an early stage of metamorphic sole formation also occurred then (discussed below). Seamounts composed of within plate basalts (WPB) capped by condensed carbonates, were preferentially accreted within the melange. These features are found both as little-deformed and unmetamorphosed sequences (e.g. Alatopetra), or as metamorphosed and thrust-accreted sequences, at the base of overlying ophiolite crustal and mantle lithologies (e.g. Padhes). These seamounts sometimes also show evidence of collapse and dismemberment, shown by carbonate debrites associated with radiolarites, and thrust sheets of WPB in the melange.

Deformational features related to tectonic accretion include low-grade metamorphism, folding, cleavage formation, shearing, soft-sediment deformation and stratal disruption. Extensional features are

pervasive and include normal faults and layer-parallel-extension of bedding. Together, these processes produced the block-in-matrix-type melange. Overpressuring of the prism, as inferred for the Barbados accretionary wedge (Lundberg and Moore 1986), was probably responsible for fracturing and vein infilling on all scales. Scaly fabrics, found within the melange sediments, are characteristic of modern day accretionary complexes, such as the Barbados prism and the Nankai trough (Moore et al. 1986; Moore and Lundberg 1986).

Turbidite and debris flow successions in the melange survived as coherent units, possibly because they were deposited in perched basins within the accretionary complex (e.g. trench-slope basins), or were never fully subducted. These turbidites are derived from the ophiolite, as evidenced by the occurrence of depleted ophiolitic volcanics as clasts, and are interbedded with Mid-Late Jurassic radiolarites (Jones et al. in prep.). They are interpreted as having formed both during accretion, and as turbidite fans ahead of the displaced ophiolite sheet.

Similar subduction-accretion settings are well documented, for example in the circum-Pacific area (e.g. Nankai trough; Moore and Lundberg 1986; Karig 1988), and on land (e.g. Franciscan Complex; Cloos 1984; Aleutian active margin; McCarthy and Scholl 1985).

8.5 Sub-ophiolite metamorphism

The Loumnitsa Unit metamorphic sole at the base of the Dramala peridotite, records the early Mid Jurassic (ca. 165±3 Ma; Spray et al. 1984) intra-oceanic displacement of the Neo-Tethyan oceanic crust and mantle (Woodcock and Robertson 1977). This displacement is believed to have resulted from collision of the subduction trench with the marginal oceanic and continental basement of the Pelagonian Zone. This seems to be a likely mechanism of ophiolite emplacement in much of the Tethyan area, i.e. a relatively simple model, whereby subduction faces away from the continental margin onto which emplacement finally occurs (Casey and Dewey 1984). This may be a particularly dominant mechanism in small ocean basins, where continental margins rapidly become involved during progressive subduction. Metamorphic sole formation may have taken

place in several tectonic settings, and at various times, during the history of subduction. One likely position for the formation of the Pindos metamorphic sole is along the boundary between the new crust formed at the above-subduction zone ridge, and the stranded crust found immediately above the subduction zone (with mainly older, remnant crust preserved) immediately to the east. The supra-subduction zone ridge itself may possibly have been the site of this thrust, but this situation is considered less likely in this case.

Additionally, the metamorphic sole at the base of the Aspropotamos Complex is believed to record the displacement of the ophiolite fore-arc along the basal thrust of the subduction zone, evidenced by thin, chemically heterogeneous crust with an attached metamorphic sole at cumulate level. This sole is thought to have formed by progressive overthrusting towards the continental margin. A further posssibility is that overthrusting was oblique, and occured along a pre-existing lineament such as a transform fault. The mainly WPB and MORB chemistry of the sole rocks is attributed to the over-riding of accreted material (Avdella Melange) by young, hot supra-subduction zone oceanic crust and mantle (Dramala and Aspropotamos Complexes). Supra-subduction zone-type chemistries are also present in the Loumnitsa Unit, and are related to the initial overthrusting within the newly formed supra-subduction zone crust and mantle, described above. This model is somewhat similar in outline to the mode of emplacement of the Semail ophiolite, Oman (Searle and Malpas 1980), and the Lower Palaeozoic Newfoundland ophiolites (Williams and Smyth 1973; Malpas 1979; Jamieson 1980, 1981).

8.6 Late Jurassic ophiolite emplacement

The progressive closure of much of the Pindos ocean is constrained as having taken place approximately during the Kimmeridgian stage of the Late Jurassic, based on palaeontological evidence presented here. A major ophiolite nappe overthrust the western Pelagonian margin in the Greek area, as well as to the north. The fore-arc and accretionary complex was overridden, during progressive thrusting towards the foreland. This

large-scale ophiolite nappe metamorposed the foredeep which had formed within the Pelagonian platform to the east, forming the Vourinos melange.

8.7 Cretaceous history: a relict ocean basin

This obduction and collision was followed by a period of comparative tectonic quiescence, after which platform and slope-type sedimentation was established on the Pelagonian margin, partly unconformably overlying the ophiolite sequence. This transgression took place at different times at different localities, from the Late Jurassic onwards.

The presence of a locally preserved Late Jurassic pelagic carbonate transgression over the melange (in both Pindos and Vourinos), and of widespread deep-sea sedimentation (Dio Dendra Group), indicates that the Pindos ocean in this area was not sutured, but remained as a relict small ocean (Fig. 8.2).

The Late Jurassic-Late Cretaceous sediments of the Dio Dendra Group record deposition in a deep marine basin above the carbonate compensation depth (CCD). The cyclically-bedded sequences of radiolarite and pelagic carbonate at the base of the Karamoula Formation (Late Jurassic-Early Cretaceous), may represent a fluctuating CCD, gravity input of peri-platform ooze and/or variations in primary plankton productivity. Each formation contains redeposited turbidites of mixed carbonate-clastic provenance: (1) quartzo-feldspathic and basic volcanic detritus; (2) detritus from older sediments, particularly radiolarian chert; (3) shallow-water carbonate material from a contemporaneous shelf sequence. The source of the basaltic and carbonate material may have been the Avdella Melange accretionary complex and post-tectonic cover to the east, and not necessarily the ophiolite itself, which was probably still submerged. Also, the quartzo-feldspathic detritus was derived from a continental area, presumably to the east or northeast within the Pelagonian Zone.

The absence of an identifiable westerly-derived source is consistent with accumulation of the Dio Dendra Group well away from the Apulian

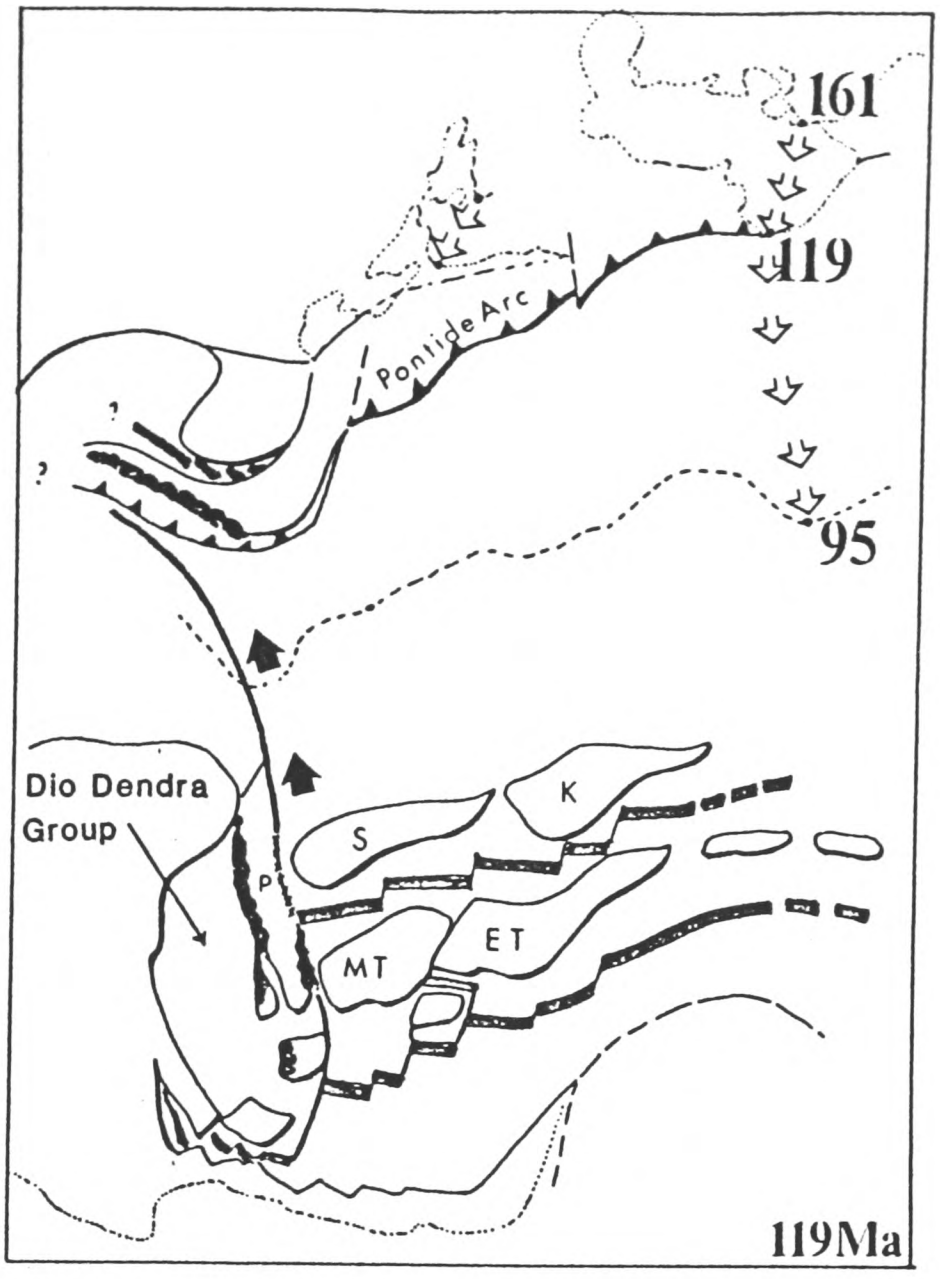

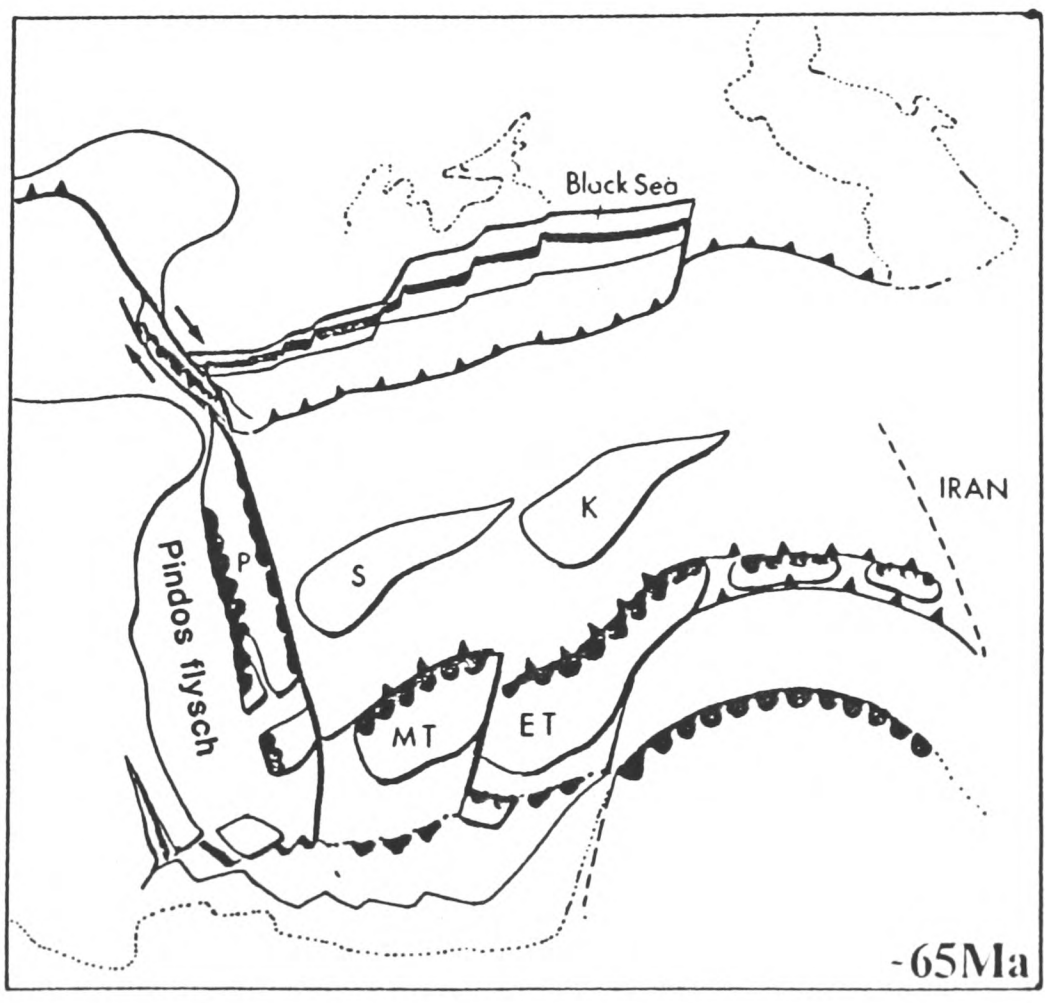

Fig. 8.2 Plate reconstructions for the Cretaceous and the Cretaceous-Earliest Tertiary, after J.E. Dixon (unpublished data). a) Late Lower Cretaceous, showing the emplaced ophiolites of the Pelagonian Zone (black serrated line), and the remnant Pindos ocean basin in which the Dio Dendra Group sequences were deposited. b) Late Cretaceous ophiolite emplacement has taken place to the east (e.g. Turkey), and the initiation of ther closure of the Pindos ocean basin is marked by the income of the terrigenous sediments of the Pindos Flysch (marked).

margin. During the Late Cretaceous, thick rudist-dominated carbonate build-ups developed (Orliakas Group), possibly controlled by an eustatic rise in sea level (Vail et al. 1977). Carbonate detritus was shed into the remnant ocean basin, as indicated by locally preserved slope and basinal facies of the Dio Dendra Group. The Late Cretaceous basinal sediments (Krevvati Formation) are carbonate-rich, and may possibly be the lateral equivalents of the Orliakas Group platformal sequence.

8.8 Early Tertiary emplacement

Early Tertiary regional compression resulted in final closure of the remnant Pindos ocean basin. As the thrust stack converged on the Apulian margin, the platform flexurally subsided and the Pindos Flysch accumulated (Fig. 8.2) in a distal foreland basin (e.g. Stockmal et al. 1986), and perhaps also partly as an accretionary body due to partial subduction of the Apulian plate at a later stage. This was followed by southwestward-directed thrusting, apparently over the Ionian platform sediments. It is uncertain as to whether the ophiolite itself was ever overthrust onto the present day exposed Ionian sequence. Thrusting is not believed to have been highly oblique relative to the footwall, which allows reconstruction of the tectonic stratigraphy on a gross scale. Extensive deformation during this phase included folding and thrusting of the Pindos Flysch as it was over-ridden, detachment of the Cretaceous deep-water successions from their basement, remixing of the Avdella Melange, and re-imbrication of the ophiolite sequences. Also, the metamorphic sole was detached from the ophiolite and intercalated with the melange, and the Orliakas Group platform units were partly incorporated as tectonic blocks.

The entire thrust stack was folded regionally, on several scales during Tertiary emplacement. The emplacement was onto a complicated footwall topography, probably reflecting original continental margin palaeogeography. These basement structures were particularly formed parallel to the emplacing thrust sheets, (e.g. Armata-Milea corridor), and led to out-of sequence type thrusting, and folding. The Dramala Complex overthrust all other units along a major out-of-sequence thrust, which was subsequently folded in a similar fashion. A number of large transverse structures also developed, (e.g. Perivoli corridor) possibly as lateral thrust

ramps (Kemp and McCaig 1984) over pre-existing continental margin transform offsets, or perhaps due to a late northwest-southeast directed compressive event. These caused large scale refolding of the thrust stack, and result in the complex outcrop pattern seen at present.

8.9 Post-emplacement events

Following thrusting onto the Ionian platform, extension was activated behind the thrust front to form the Meso-Hellenic trough, in which marine and continental sediments accumulated from Late Eocene to Miocene. Continuing tectonic activity is reflected in large scale normal faulting, as seen along the western margin of the basin; and, as yet poorly understood compressional deformation, perhaps involving basin margin strike-slip faulting. As in the Betic Cordillera of southern Spain (Platt and Vissers 1989), subsidence of the inner zones apparently began whilst thrusting still continued in the outer orogenic areas (i.e. Late Eocene).

8.10 Comparison of the Pindos and Vourinos ophiolites

The regional interpretation presented here has taken into account data from the Vourinos ophiolite (Moores 1969). Vourinos is believed to represent a fragment of essentially the same oceanic basement as that of the Pindos ophiolite, which probably also continues south to the Othris ophiolite (Smith 1979), and north to the Kastoria ophiolite (Mountrakis 1984, 1986), and into Albania. The Vourinos ophiolitic thrust sheet is relatively tectonically coherent (Moores 1969; Wright 1986), and has not suffered Tertiary re-imbrication.

Many lines of geochemical and structural evidence as presented, suggest that the Pindos and Vourinos ophiolites are of similar origin. Geochemically, the ophiolitic units are both of "supra-subduction zone" type (Pearce et al. 1984a). The Vourinos ophiolite displays geochemical trends similar to those of the more depleted parts of the Aspropotamos Complex (IAT and BSV). In both cases the mantle sequence rocks are highly depleted, represented by residual harzburgitic mantle tectonite (Roberts & Nesbitt 1987). An important point is that similar deformation

phases can be seen within the mantle sequences of the ophiolites, particularly high temperature foliations, which overall have the same present day orientation and dip in both mantle sequences (Ross & Zimmerman 1982; A. Rassios pers. comm. 1988). A critical observation is that ductile mylonites in the mantle sequences of both ophiolites have a similar sense of overthrusting, which is towards the present day north-north-east (Ross and Zimmerman 1982). Vourinos however, contains economic chromite deposits, whilst chromite is comparatively rare in the Pindos ophiolite. The Vourinos ophiolite also posesses a basal metamorphic sole, which is of almost identical age (169±4 Ma Spray et al. 1984) to that of the Pindos ophiolite.

The Vourinos ophiolite overlies a thin basal melange (Zimmerman 1972), or lies directly on the carbonate platform (Wright 1986). Unlike the Avdella Melange, the Vourinos melange is metamorphosed to greenschist and lower amphibolite facies. Underlying platform units have also experienced this metamorphism, and display an extreme high temperature ductile deformation near the contact with the overlying allocthonous units, possibly related to a major transverse fault (Kastaniotikos transform).

The accumulated evidence favours interpretation of the Vourinos ophiolite as a preserved fragment of supra-subduction zone oceanic crust and mantle, which appears to have shared a similar tectonic and chemical evolution to the the Pindos ophiolite until the Late Jurassic. One of the main differences from the Pindos ophiolite is the apparent lack of MORB-type extrusives as found in the Aspropotamos Complex, suggesting perhaps that Vourinos represents crust which was strongly influenced by supra-subduction zone spreading processes prior to obduction (i.e. in the Early-Mid Jurassic), and had no earlier history, as inferred for the Pindos Aspropotamos Complex crustal units. There is some evidence that Vourinos may represent a palaeo-spreading centre, as suggested by Harkins et al. (1980) and Ross et al. (1980), although this remains a questionable interpretation. It is interpreted here, however that the Vourinos crust and mantle was located closer to the supra-subduction zone spreading centre at the time of intra-oceanic displacement. The ophiolite was thrust towards the present N-NNE, whilst still within the oceanic environment (Ross et al. 1980; Ross and Zimmerman 1982), which

presumably also led to formation of the Vourinos metamorphic sole. An important line of evidence which suggests that the Pindos and Vourinos ophiolites were thrust over the Pelagonian margin is the presence of abundant neritic limestone blocks within the Vourinos melange. As outlined in Chapter 4, the Vourinos melange is interpreted as the greenschist facies part of the ophiolite metamorphic sole, implying that the Pelagonian platform was in comparatively close proximity to the emplacing Vourinos ophiolite sheet. Similarly, the greenschist facies sole of the Pindos ophiolite contains neritic sediments which must have originated as marginal sequences to the Pelagonian platform. This strongly suggests that both ophiolites were emplaced as part of the same sheet during collision with the continental margin.

8.11 Plate tectonic model

The construction of a regional plate tectonic model is essential as a framework for understanding the formation and temporal relationships of the units present. Alternatives already suggested, and an outline of the model favoured here, are shown in Fig. 8.3. The polarity of subduction in the Pindos ocean is not easily identified from studies in the Pindos Mountains. Based on a simple reconstruction of the tectono-stratigraphy, eastward intra-oceanic subduction within the Pindos ocean basin seems an attractive tectonic model (Jones et al. 1988). However, this model does not suggest a feasible mechanism for the eastward emplacement of ophiolites when viewed on an orogen-wide scale, including the Vourinos and Othris ophiolites in Greece, and the Albanian and Yugoslavian ophiolites further north.

Instead, it it perhaps more likely that the ophiolites of northwestern Greece originated above a single, Jurassic westward-dipping intra-oceanic subduction zone, which thus provides a mechanism for both the genesis and emplacement of the ophiolites. In this preferred model (Fig. 8.4), the Dramala and Aspropotamos Complexes originated above, and to the west of a subduction zone. The Aspropotamos Complex is assumed to represent the crust and mantle nearest the subduction zone. The Pindos and Vourinos ophiolites were originally part of the same oceanic system,

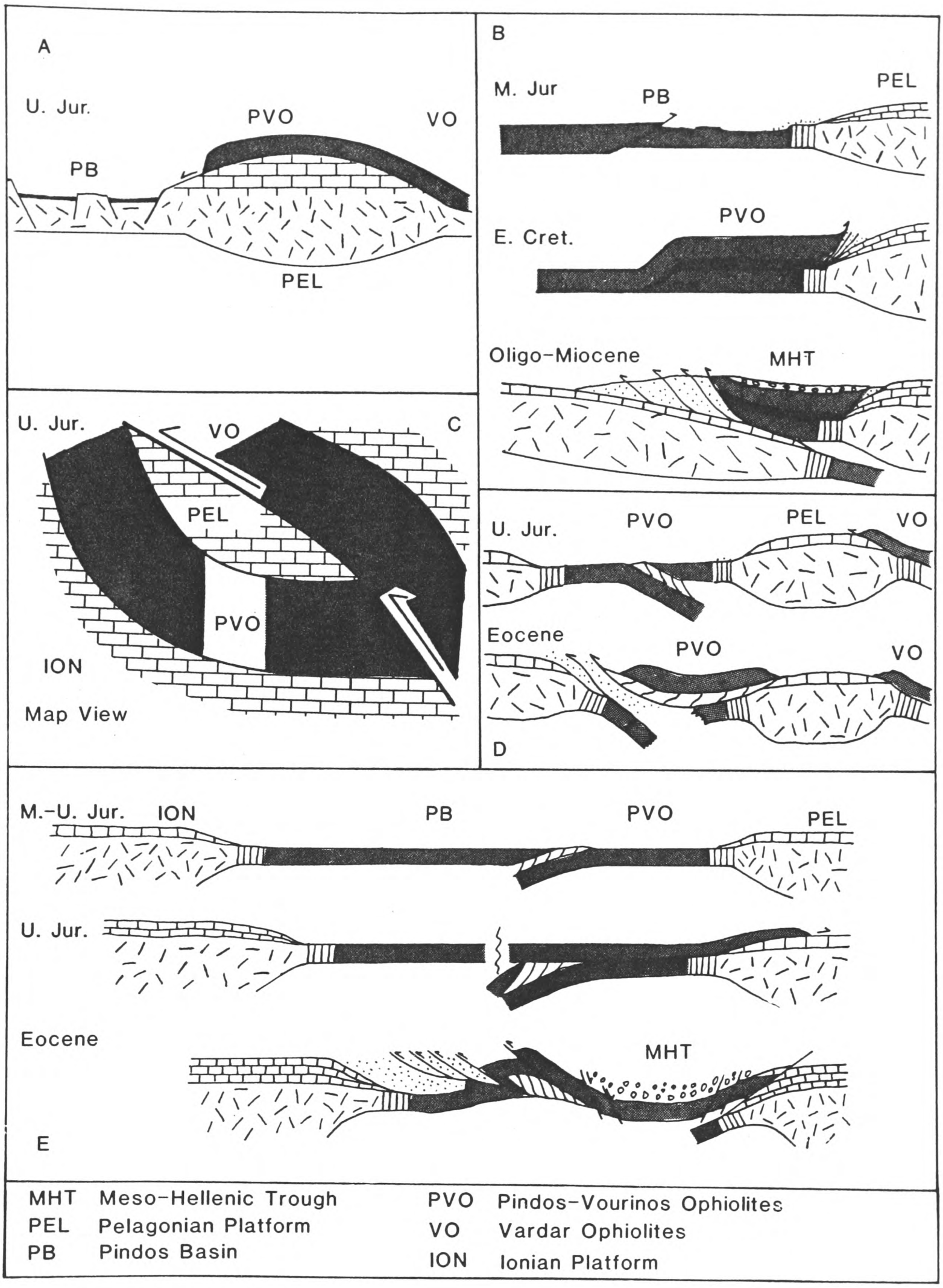

Fig. 8.3 Plate tectonic models for the Mesozoic and Early Tertiary evolution of the Pindos and Vourinos ophiolites and associated units. A-D from the literature: a) Vardar Zone origin for the ophiolites, subsequently emplaced westwards into the Pindos ocean during the Late Jurassic. (after Vergely 1976, 1977, 1984; Jacobshagen et al. 1978); b) Emplacement of a MORB-type ophiolite northeastwards (Kemp and McCaig 1984); c) Transform-type origin (Smith and Spray (1984); d) East-dipping subduction zone, (Jones et al. 1988); e) Preferred model of a west-dipping subduction zone (see Fig. 8.4 for further details).

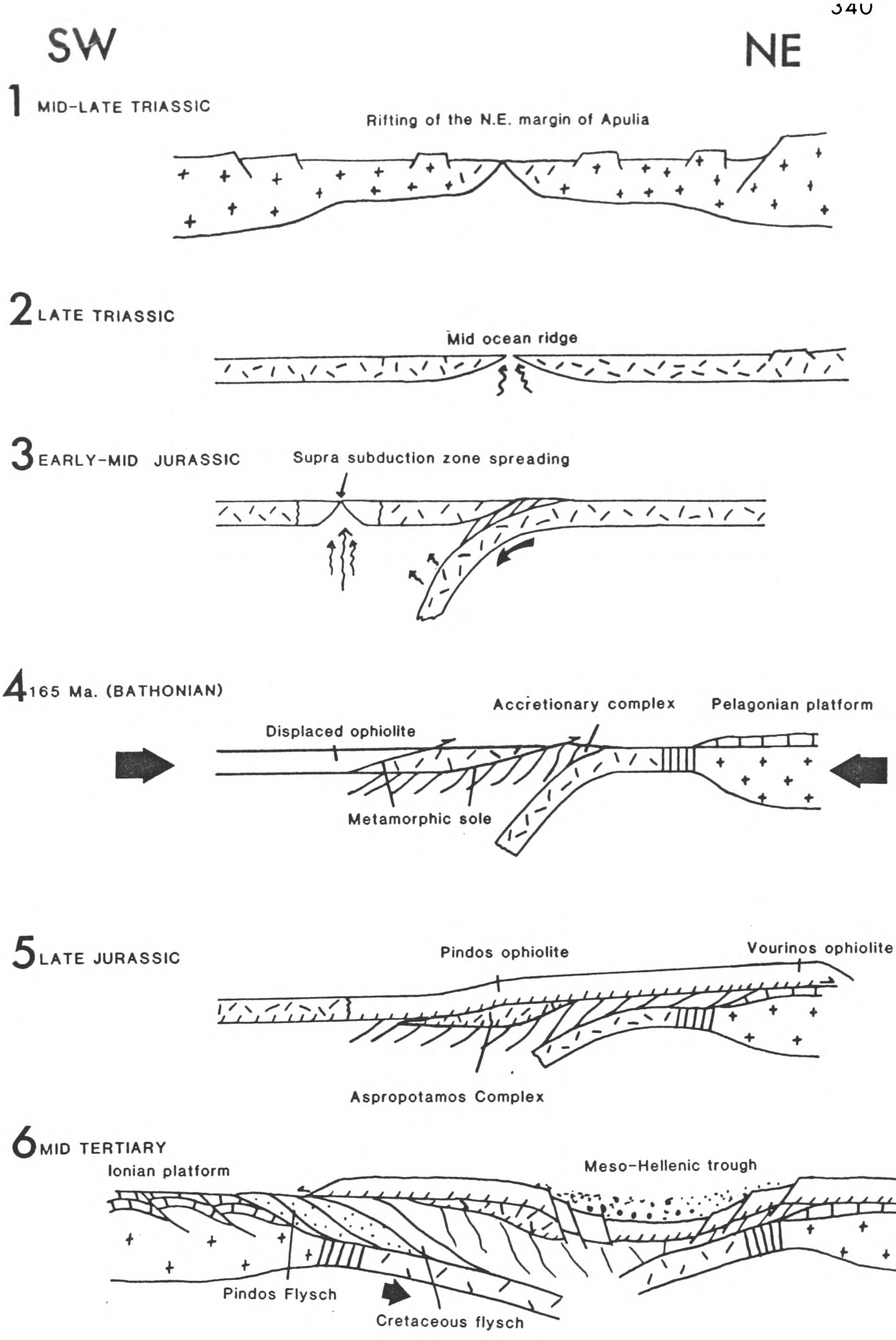

FIG. 8.4 Simplified two-dimensional tectonic model for the evolution of the Pindos ocean basin in northern Greece during the Mesozoic and Tertiary. 1) Rifting of the northeast Apulian margin, and subsequent drifting of the Pelagonian micro-continent. 2) Spreading of the Pindos Ocean during the Late Triassic to form oceanic basement. 3) Initiation of intra-oceanic subduction, and spreading to form the supra-subduction zone ophiolite. Note that the crust nearest to the subduction zone is isolated at this stage. Accretion takes place to form the Avdella Melange. 4) Collision of the subduction zone with the Pelagonian margin leads to ophiolite displacement and metamorphic sole formation. Note the position of the major intra-oceanic thrusts. 5) Ophiolite obduction onto the Pelagonian margin in the Late Jurassic, overthrusting the Aspropotamos Complex and the Avdella Melange. Cretaceous times saw the establishment of flysch sedimentation in a remnant basin, located to the west of the emplaced ophiolites 6) Final closure in the Early Tertiary was marked by major collision and overthrusting of the Ionian continental margin by the rethrust Pindos ophiolite and associated units.

and formed oceanic crust and mantle further from the subduction zone, i.e. to the west.

This model is in many ways compatible with the model of the Hellenides proposed by Vergely (1984; see Chapter 1). The main differences are with regard to the origin of the ophiolite bodies themselves, not with the other aspects of the tectonic and sedimentary evolution. Three possibilities discussed earlier (Chapter 1) include i) an origin of all present day Sub-Pelagonian Zone ophiolites from west of the Pelagonian Zone (Smith 1979; this study); ii) origin of the Pindos, Vourinos and Kastoria ophiolites from the Vardar Zone, and Othris from the Sub-Pelagonian Zone (Vergely 1984; Ferriere; iii) origin of the Pindos and Othris ophiolites from the Sub-Pelagonian Zone, and the Vourinos ophiolite from the Vardar Zone. Incontrovertible evidence supporting any one of these possibilities is absent, although Othris seems to have undergone a relatively simple Late Jurassic emplacement to the northeast, as agreed by all workers in that area (Smith et al. 1979; Ferriere 1982; Vergely 1984). The Pindos ophiolite has undergone extensive Tertiary deformation, and is presently not found in close association with the Pelagonian margin, and represents an unsuitable place to try and gain evidence for Jurassic emplacement vectors. However, in many ways, the Pindos ophiolite seems comparable to the Othris ophiolite, and it would seem probable that it underwent a similar Jurassic evolution. The Vourinos ophiolite is in many ways unique in the region, particularly in terms of its volcanic stratigraphy and apparently simple relationship with the Pelagonian platform. From the evidence presented here, aided particularly by studies of the peridotites of both ophiolites by A. Rassios, the Vourinos ophiolite is interpreted as also having originated west of the Pelagonian zone, as a different part of the same Pindos oceanic system. In the model of Vergely, such a conclusion is easily accommodated, by envisaging the ophiolites of northern Greece (north of the Kastaniotikos transform) as having developed in an northern extension of the Maliac basin, probably east or northeast of the Olympos platform. The interpretation of the ophiolites as forming above a west-dipping subduction zone made here, also simplifies Vergelys mode of emplacement for the Othris ophiolite, as complex backthrust emplacement from the Maliac basin due to east-dipping subduction is not required.

In the model presented here for the formation of the Pindos ophiolite (Fig. 8.5), oceanic spreading is envisaged to have taken place orthogonally to major north and northeast-trending (approximately 70^{o}) transform faults found in Greece (e.g. Kastaniotikos, Lyberis et al. 1982; Sperchios, Corinth, Ferriere 1982) and northwards in Yugoslavia (e.g. Scutari-Pec, Aubouin et al. 1970). These faults, probably representing Palaeozoic basement lineaments, are seen as the major controlling factor on microcontinental drifting and basin formation at the northern margin of Apulia (Fig. 8.5; Robertson et al. in press).

In the model of Kostopoulos (1989), the lower Aspropotamos Valley is interpreted as an oceanic transform fault, and is said to have been rotated 45^{o} clockwise since the Miocene, based on palaeomagnetic data measured within Tertiary flysch of the Ionian Zone (Kissel et al. 1985; i.e. originally trending at N70-80E, now at approximately 120^{o}, after rotation). This transform fault, according to Kostopoulos (1989), would then parallel the Kastaniotikos fault. However, the Kastaniotikos structure must have been rotated along with the "Aspropotamos fault", as rotation clearly far post-dates collision and assemblage of the structural belts of Greece. Therefore, isolated rotation of individual structures such as the "Aspropotamos fault" cannot have occurred. Furthermore, extensive MORB and more depleted sheeted dykes (at Spileo) strike orthogonally to the Kastaniotikos structure at the present time (NW-SE), and also to Tertiary high-angled emplacement wrench faults, and are thus far more likely to have been originally intruded at that orientation, and no rotation of individual faults is therefore required. It is considered more likely that the Kastaniotikos and similar transforms were originally north-northeast trending, and the whole northern Greek region was rotated (i.e. aproximately 45^{o} clockwise) after collision, during post-Miocene times.

The "Aspropotamos fault" is also claimed to have strongly influenced development of chemical trends within the ophiolite in that area (Kostopoulos 1989). However, further widespread chemical analyses, and mapping of the type area, suggests that the Aspropotamos Complex in the Abelia area forms a small part of a more extensive thrust sheet, which has collectively undergone an extremely similar chemical evolution, and was not related therefore, to localised tectonic influences. This also

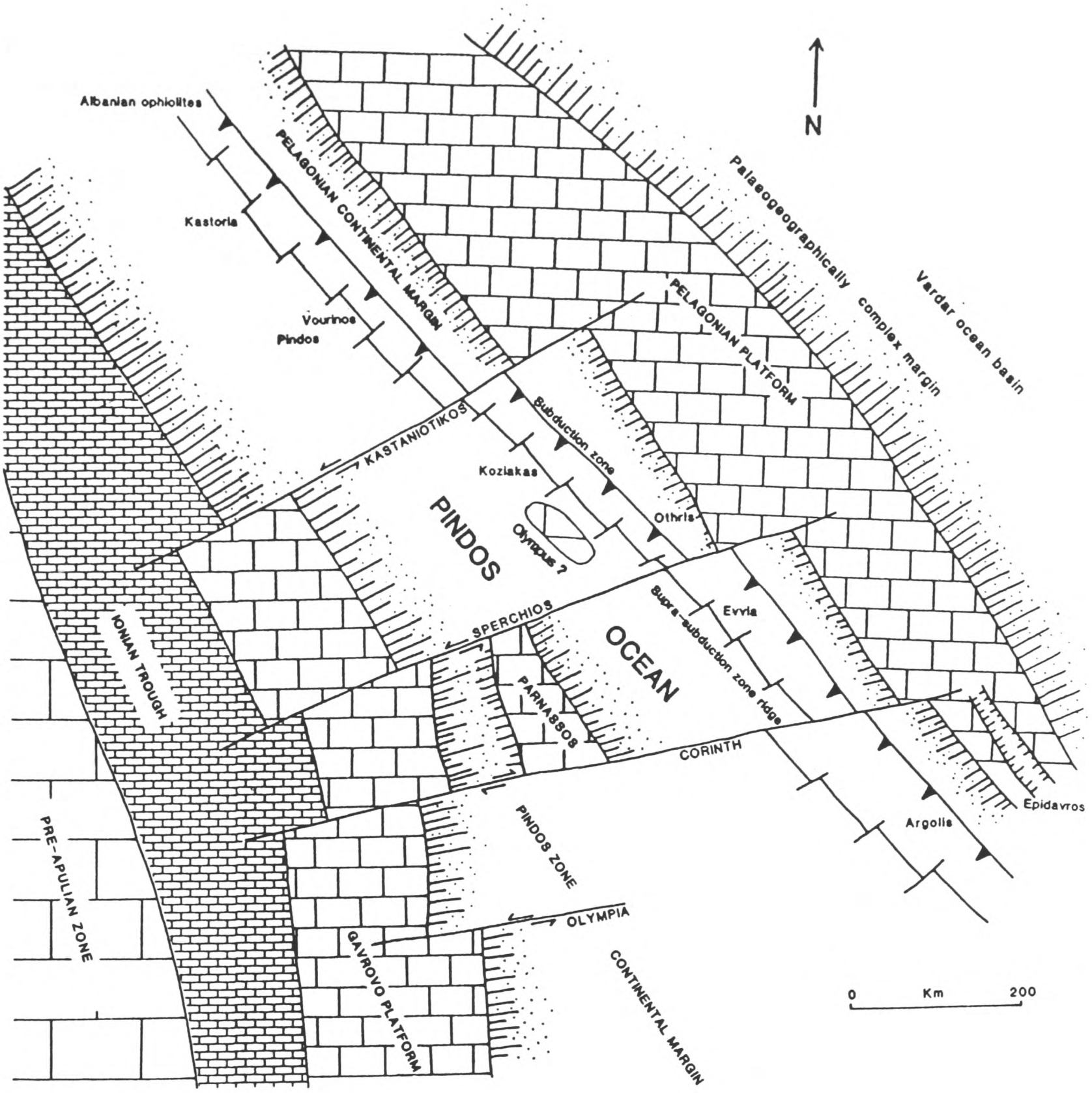

Fig. 8.5 Map view of the Pindos ocean basin in the Greek area during intra-oceanic subduction in the Lower to Mid Jurassic. Note the position of the Pindos and Vourinos ophiolites, and the Aspropotamos Complex. The Parnassos and Olympos platforms are interpreted as off-margin features, related to Apulia. From Robertson et al. (in press).

makes direct comparison to the Arakapas fossil transform sequence of Troodos by Kostopoulos (op. cit.) less tenable.

In addition to these points, no field evidence for oceanic transform-type deformation is present within the crustal lithologies of the Abelia area (e.g. lateral offsets, serpentinite intrusions, steeply-dipping foliations), the only large-scale deformation found is related to Tertiary fold and fault structures. A possible strike-slip fault does exist in the area (approximately E-W trending), representing the northern margin of a Tertiary embayment within the thrust sheets (i.e. the Gulf of Krania, Brunn 1956). In general, dyke trends within such deformed terrain are probably extremely unreliable, as a full understanding of block rotation during several stages of deformation is not possible.

The basis of the Open University model for the genesis and emplacement of the Oman ophiolite (Lippard et al. 1986) is that the ophiolite was first created by spreading above a subduction zone, followed by detachment and eventual emplacement when the Arabian continental margin collided with the trench. A similar model applies well to the formation of the Pindos and Vourinos ophiolites.

The Avdella Melange formed during progressive subduction by accretionary processes. Existing oceanic crust and sediment cover was either accreted or subducted from the eastern side of the basin. Apparently, only the higher levels of the Pindos accretionary complex are seen today, unlike some other accretionary complexes (e.g. Fransican).

Regional compression resulted from collision of the Pelagonian microcontinent to the east, with the Pindos intra-oceanic subduction zone (Fig. 8.4). At this stage, the supra-subduction zone slab was detached, and then over-rode the accretionary complex, forming the metamorphic sole (165 3 Ma; early Late Jurassic; see above). The initial detachment occurred within the Pindos supra-subduction zone crust and mantle, probably within the newly formed lithosphere at a mechanically weak boundary. Lateral detachment along ocean fracture-zone like segments is also hinted at by the occurrence of cemented ultramafic breccias. at the base of the Dramala Complex, indicating exposure of ultramafic rocks at the ocean floor as at rifted ridges or transform faults. The thin leading edge

(Aspropotamos Complex), was in turn dismembered and over-thrust. The remainder of the supra-subduction zone oceanic crust was emplaced northeastwards over the Pelagonian passive margin. This is consistent with early eastward-directed, high temperature fabrics measured in the Dramala Complex (A. Rassios pers. comm. 1989). Flexural subsidence of the Pelagonian margin ahead of thrust emplacement, gave rise to a foreland basin (Vourinos melange), into which shallow-water carbonate blocks were shed, and mixed with debris derived from the Pindos ocean. Locally, blueschists were also exhumed from the deeper parts of the accretionary complex. Final emplacement of the still hot ophiolite resulted in metamorphism of both the melange, and the underlying platform. The ophiolite may have been finally emplaced as a rootless sheet. Similarly, the Semail ophiolite thins and is probably detached beneath the Batinah coastal plain, from recent gravity and magnetic evidence (Lippard et al. 1986; Shelton 1990).

Before the end of the Jurassic, the Pindos ocean was sutured further north, in Albania and Yugoslavia (Karamata 1988). However, further south in the Hellenides, the Pindos remained as a remnant ocean basin during the Late Jurassic to Late Cretaceous-Early Tertiary. Evidence from the southern Pindos Zone, where similar sequences exist (Green 1983; Fleury 1980), suggests that the Dio Dendra Group sediments were deposited on oceanic crust (Green 1983).

In northern Greece, emplacement of the Vourinos and Kastoria ophiolites was soon followed by transgression of Kimmeridgian carbonates (West Krapa Hills, Vourinos; Mavridis et al. 1979), probably in response to flexural subsidence. Further west within the remnant Pindos ocean basin, Late Jurassic pelagic carbonates blanketed the Avdella Melange, where overlying ophiolitic rocks were locally absent. During the Late Cretaceous, a carbonate platform developed on the partly eroded Vourinos ophiolite (e.g. Siatista, Mikrokastron; Vourinos), while rudistid build-ups (Orliakas Group) were constructed further west along the eastern margin of the remnant Pindos basin.

During the Early Tertiary (?Palaeocene-Late Eocene), eastward subduction of the remnant Pindos ocean basin was initiated; the early Mesozoic oceanic basement was completely subducted, while the

overlying deep-water Cretaceous succession was underplated onto the base of the pre-existing thrust stack. The entire assemblage was finally emplaced westwards over the foreland basin represented by the Pindos Flysch, as a conventional "piggy-back" thrust sequence. The later stages of suturing were accompanied by collapse, to form the intermontane Meso-Hellenic molasse trough. More evidence from other ophiolite-related units in surrounding Neo-Tethyan areas, particularly in Albania and Yugoslavia, is now needed to test and develop this plate tectonic hypothesis.

8.12 Conclusions

This project has focussed on one of the least studied of the large Tethyan ophiolite bodies of the Eastern Mediterranean area. It is clear from the data collected that the present day situation of the Pindos ophiolite and associated tectonic units, is the result of Alpine collisional processes in the Early Tertiary. Despite considerable Tertiary deformation, reconstruction of the earlier history of these Mesozoic lithologies, using a combination of sedimentary, structural, palaeontological and geochemical techniques has revealed several regionally significant conclusions. Firstly, the Sub-Pelagonian and Pindos Zones formed the continental margin and distal oceanic parts respectively of a single oceanic basin, the Pindos ocean, during the Mesozoic, and both were floored by oceanic crust. Secondly, the Pindos and Vourinos ophiolites are likely to have originated as parts of the same fragment of oceanic lithosphere, a situation greatly confused by Tertiary deformation of the Pindos ophiolite, but reconstructed using several lines of evidence here. Thirdly, the well described Late Jurassic collisional event in Greece, probably resulted in emplacement of oceanic crust eastwards from the Pindos/Sub-Pelagonian Zones, onto the margin of the Pelagonian Zone in northern Greece, as well as in southern Greece (i.e. Othris-Argolis areas), as previously documented (Smith 1979; Vergely 1984; Clift and Robertson 1990). Fourthly, it is clear that the Pindos ocean was not completely sutured during the Late Jurassic collision, and remained as a basin of several hundred kilometers width.

An origin of the Pindos and Vourinos ophiolites as a completely allochthonous sheet transported from the eastern margin of the Pelagonian Zone (Vardar ocean), the traditional view of earlier Greek workers, cannot be discounted purely from evidence available from the north Pindos Mountains. The best evidence seems to come from structures formed during spreading and displacement preserved within the Pindos and Vourinos peridotites, which strongly support the model presented here. However the new data presented here, as well as recent findings in the Vardar Zone, indicate that a westerly origin for the Pindos and Vourinos ophiolites cannot be excluded on any grounds, and indeed in many ways seems the most attractive scenario.

8.13 Summary

1) The Pindos ocean of northwestern Greece, rifted during the Middle Triassic, splitting the Pelagonian microcontinent from Apulia (Gondwana).

2) Sea-floor spreading was initiated in the Late Triassic, and the Pindos ocean opened, possibly as a Red Sea-type basin, or a marginal basin. After break-up, Triassic marginal carbonate units subsided, and were later transgressed by radiolarian sediments.

3) Regional compression began during the late Middle Jurassic (ca. 165 Ma), activating intra-oceanic subduction, that was probably westerly-dipping.

4) The Dramala and Aspropotamos Complexes of the Pindos ophiolite, and the Vourinos ophiolite represent ocean crust and mantle, which were formed mainly by supra-subduction zone spreading. The Aspropotamos Complex is interpreted as having formed immediately above the subduction zone, the Vourinos and Dramala ophiolites further to the west, nearer to the supra-subduction zone spreading centre. Volcanics and sediments from the subducted slab, including seamount-type features, were accreted at a trench to form the tectono-sedimentary Avdella Melange.

5) The recently formed supra-subduction zone slab was displaced when the Pelagonian microcontinent to the east, collided with the subduction zone. Consequently, the new-formed oceanic crust and mantle (Vourinos and Dramala) were detached and thrust over the stranded crust nearest the subduction zone (Aspropotamos Complex), and then over the accretionary prism (Avdella Melange), forming the basal metamorphic soles of the firstly the Dramala and Vourinos ophiolites, and then the Aspropotamos Complex.

6) The Vourinos ophiolite was emplaced northeastwards over a foreland basin within the Pelagonian margin. The probably trailing Dramala ophiolite however, remained stranded along the eastern margin of the basin when compression ceased.

7) By the Kimmeridgian?, suturing was complete in the Albanian and Yugoslavian Neo-Tethys further northwest, while in the Hellenides, the Pindos ocean basin remained partly open.

(8) During the Late Jurassic (Kimmeridgian) to Late Cretaceous, turbidites and pelagic carbonates transgressed the remnant Pindos ocean basin and margins (Dio Dendra Group). Platformal units, with local rudistid build-ups developed on the eastern margin (Orliakas Group) in the Late Cretaceous.

19) During the Early Tertiary, renewed crustal compression initiated eastward subduction of the remnant Pindos ocean basin. Cretaceous deep-water sediments were thrust beneath the Jurassic deformed units; the whole assemblage was then thrust westwards over a foredeep/foreland basin (Pindos Flysch), and finally over the Apulian carbonate margin.

10) Final emplacement was associated with large-scale orogenic collapse and normal faulting to form the Meso-Hellenic trough. From Late Eocene to Oligocene this was infilled with marine, deltaic and alluvial sediments.

References

ABBEY, S. 1980. Studies in "standard samples" for use in the geochemical analysis of silicate rocks and minerals. Part 6, 1979 edition of "usable Values". Geol. Surv. Canada, paper 80, 14.

AUBOUIN, J. 1959. Contribution a l'étude géologique de la Gréce septentrional: les confins de l'épire et de la Thessalie. Ann. géol. pays héll. 10, 1-403.

_____, BONNEAU, M., CELET, P., CHARVET, J., CLEMENT, B., DEGARDIN, J.M., DERCOURT, J., FERRIERE, J., FLEURY, J.J., GUERNET, C., MAILLOT, H., MANIA, J.H., MANSY, J.L., TERRY, J., THIEBAULT, P., TSOFLIAS, P. and VERRIEX, J.J. 1970. Contribution à la géologie des Hellénides: le Gavrovo, le Pinde et la zone ophiolitique subpélagonienne. Ann. Soc. géol. Nord 90, 277-306.

_____, DESPRAIRIES, A. and TERRY, J. 1977. Le synclinal d' Epirè-Akarnanie, la nappe du Pinde-Olonos et la nappe ophiolitique. Réunion extraordianaire en Grèce, Bull. Soc. Géol. Fr. 7, t.X1X, (1), 20-27.

_____, and NDOJAJ, I. 1964. Régard sur la géologie de l'Albanie et sa place dans la géologie des Dinarides. Bull. Soc. Géo. Fr. 7 (6), 593-625.

_____, and BONNEAU, M. 1977. Sur la présence d'un affleurment de flysch éocretace (Béotien) au front des Unites du Koziakas (Thessalie, Grèce): la limite entre les zones externes et les zones internes dans les Hellenides. C. R. Acad. Sc. Paris 284, 2075-2078.

ALABASTER, T., PEARCE, J.A. and MALPAS, J. 1982. The volcanic stratig raphy and petrogenesis of the Oman ophiolite complex. Contrib. Min. Pet. 81, 168-183.

BALTUCK, M. Provenance and distribution of Tethyan pelagic and hemipelagic siliceous sediments, Pindos Mountains, Greece. Sed. Geology, 31, 63-88.

BARTON, C.M. 1976. The tectonic vector and emplacement age of an allochthonous basement slice in the Olympos area, Greece. Bull. Soc. Geol. Fr. 7, 18/2, 253-258.

BAUMGARTNER, P.O. 1984. A Middle Jurassic-Early Cretaceous low-latitude radiolarian zonation based on Unitary Associations, and age of Tethyan radiolarites. Eclogae geol. Helv. 77(3), 729-837.

BECCALUVA, L., OHNENSTETTER, D., OHNENSTETTER, M. and PAUPY, A. 1984. Two magmatic series with island arc affinities within the Vourinos Ophiolite. Contrib. Min. Pet. 85, 253-271.

BENN, K., NICOLAS, A. and REUBER, I. 1988. Mantle-crust transition zone and origin of wehrlitic magmas: evidence from the Oman ophiolite. Tectonophysics, 151, 75-85.

BERNOULLI, D. and LAUBSCHER, H. 1972. The palinspastic problem of the Hellenides. Eclgae geol. Helv. 65, 107-118.

_____, and JENKYNS, H.C. 1974. Alpine, Mediterranean and North Atlantic Mesozoic facies in relation to the early evolution of Tethys. In: DOTT, R.H. and SHAVER, R.H. (Eds) Symposium on modern and ancient geosynclinal sedimentation. Special Publication of the Society of Economic Mineralogists and Paleontologists 19, 129-160.

BERTOLANI, M., CAPEDRI, S. and GIACOBAZZI, G. 1982. Opaque phases in the ophiolitic rocks from the Aspropotamos valley (northern Pindos). Chemie der Erde 41, 103-110.

BLANCHET, R., CADET, J-P., CHARVET, J. and RAMPNOUX, J-P. 1969. Sur l'éxistance d'un important domaine de flysch Tithonique-crétace inferieur en Yugoslavie: l'unite du flysch bosniaque. Bull Soc. Géol. Fr, (7) XI, 871-880.

BLOOMER, S.H. and HAWKINS, J.W. 1987. Petrology and geochemistry of boninite series volcanic rocks from the Marianas trench. Contrib. Min. Pet 97, 361-377.

BOUDIER, F. and COLEMAN R.G. 1981. Cross-section through the peridotite in the Samail ophiolite, southeastern Oman Mountains. J. Geophys. Res. 86,

_____, NICLOLAS, A. and BOUCHEZ, J.L. 1982. Kinematics of oceanic thrusting and subduction from basal sections of ophiolites. Nature, 296 (58-60), 825-828.

_____, CULENEER, G. and NICOLAS, A. 1988. Shear zones, thrusts and related magmatism in the Oman ophiolite: Initiation of thrusting on an oceanic ridge. Tectonopysics, 151, 275-296.

BOYER, S.E. and ELLIOT, D. 1982. Thrust systems. Am. Ass. Pet. Geol. Bull., 1196-1230.

BRUNN, J.H. 1956. Contribution à l'étude géologique du Pinde septéntrional et d'une partie de la Macédonie occidentale. Ann. géol. pays héll. 7, 358p.

_____, 1960. Mise en évidence et différenciation de l'association pluto-volcanique du cortège ophiolithique. Rev. Geogr. phys. Gèol. dyn., 3, 115-132.

ÇAKIR, U., JUTEAU, T. and WHITECHURCH, H. (1978). Nouvelles préuves de l'écaillage intra-océanique précocé des ophiolites infra-peridotitiqués du massif Pozanti-Karsanti (Turquie). Bull. Soc. Géol. Fr. (7) 20, 61-70.

CAMERON, W.E., NISBETT, E.G. and DIETRICH, U.J. 1980. Petrographic dissimilarities between ophiolitic and ocean-floor basalts. In; PANAYIOTOU, A. (Ed) Proceedings of the International ophiolites symposium, Cyprus, 1979. 182-192.

_____, McCULLOCH, M.T. and WALKER, D.A. 1983. Boninite petrogenesis: chemical and Nd-Sr isotope constraints. Earth Plan. Sci. Lett. 65, 75-89.

CANN, J.R. 1979. Metamorphism in the ocean crust. In: TALWANI, M., HARRISON, C.G. and HAYES, D.E. (Eds) Deep drilling results in the Atlantic Ocean: ocean crust. Maurice Ewing Series, 2. Washington, American Geophysical Union, 230-238.

CAPEDRI, S., VENTURELLI, G., BOCCHI, G., DOSTAL, J., GARUTI, G. and ROSSI, A. 1980. The geochemistry and petrogenesis of an ophiolitic sequence from Pindos, Greece. Contrib. Min. Pet 74, 189-200.

_____, VENTURELLI, G., BEBIEN, J. and TOSCANI, L. 1981. Low and high Ti ophiolites in northern Pindos: petrological and geological constraints. Bull. Volcanologique 44 (3), 439-449.

_____, VENTURELLI, G. and TOSCANI, L. 1982. Petrology of an ophiolitic cumulate sequence from Pindos, Greece. J. of Geology 17, 223-242.

_____, LEKKAS, E., PAPANIKOLAOU, D., SKARPELIS, N. VENTURELLI, G. and GALLO, F. 1985. The ophiolite of the Koziakas range Western Thessaly (Greece). Nues Jarbuch Miner. Abh. 152 (1), 45-64.

CASEY, J.F. and DEWEY, J.F. 1984. Initiation of subduction zones along transform and accreting plate boundaries, triple junction evolution, and fore-arc spreading centres-implications for ophiolitic geology and obduction. In: GASS, I.G., LIPPARD, S.J. and SHELTON, A.W. (Eds) Ophiolites and Oceanic lithosphere. Geol. Soc. Lond. sp. pub. 14, 269-290.

CELET, P. 1962. Contribution à l'étude géologique du Parnasse-Kiona et d'un partie des régions méridionales de la Grèce continentale. Ann. geol. pays Hell. 13, 446pp.

_____, and CLEMENT, B. 1971. Sur le présence d'une nouvelle unité palaéogéographique et structurale en Grèce continental au Sud: l'unité de flysch béotien. C.R. somm. géol. Fr. 43-47.

_____, CLEMENT, B. and FERRIERE, J. 1976. La zone béotienne en Grèce: implications palaéogéographiques et structurales. Ecologae geol. Helv. 69, 577-599.

CLEMENT, B. 1971. Découverte du flysch éocretace en Béotie, (Grèce continentale). C. R. Acad Sc., Paris, 272, 791-792.

CLIFT, P.D. and ROBERTSON, A.H.F. 1990. Deep water basins within a Mesozoic carbonate platform, Argolis, Greece. J. Geol. Soc. Lond., in press.

CLOOS, M. 1984. Flow melanges and the structural evolution of accretionary wedges. Geol. Soc. Am. sp. pub. 198, 71-80.

COLEMAN, R.G. 1963. Serpentinites, rodingites and tectonic inclusions in Alpine-type mountaian chains. Geol. Soc. Am. sp. pap. 73.

_____, 1977. Ophiolites-ancient oceanic lithosphere? Springer-Verlag, Berlin 229 pp.

COOPER, D.J.W. 1988. Structure and sequence of thrusting in deep-water sediments during ophiolite emplacement in the south central Oman Mountains. J. Struct. Geol. 10 (5), 473-485.

_____, 1990. Sedimentary evolution and palaeogeographical reconstruction of the Mesozoic continental rise in Oman: evidence from the Hamrat Duru Group. In: ROBERTSON, A.H.F., SEARLE, M.P and RIES, A.C. (Eds). The Geology and Tectonics of the Oman Region. Geol. Soc. Lond. sp. pub. 49, 161-188.

CULENEER, G. and NICOLAS, A. 1985. Structures in podiform chromite from the Masquad district (Sumail ophiolite, Oman). Mineral. Depos. 20, 177-185.

_____, NICOLAS, A. and BOUDIER, F. 1988. Mantle flow patterns at an oceanic spreading centre: the Oman peridotites record. Tectonophysics, 151, 1-26.

CRAWFORD, A.J., BECCALUVA, L. and SERRI, G. 1981. Tectono-magmatic evolution of the West Philippine-Mariana region, and the origin of boninites. Earth Plan. Sci. Lett. 54, 346-356.

DEGNAN, P.J. and ROBERTSON, A.H.F. 1990. Tectonic and sedimentary evolution of the west Pindos ocean: evidence from the Pindos Zone, Peloponessos, Greece. Abstr. 5 th cong. Geol. Soc. Greece, Thessaloniki. 38-39.

DERCOURT, J. 1964. Contribution à l'étude géologique d'un secteur du Péloponnese septentrional. Ann. géol. pays héll. 15, 1-418.

_____, FLAMENT, J.M., FLEURY, J.J., MEILLEZ, F. 1973. Stratigraphié des couches situeés sous les radiolarites de la zone de Pindos-Olonos (Grèce). Ann. géol. Pays Hell. 25, 397-406.

_____, ZONENSHAIN, L.P., RICOU, L.E., KASMIN, V.G., LE PICHON, X., KNIPPER, A.L., GRANDJACQUET, C., SBORTSHIKOV, I.M., GEYSSANT, J., LEPVRIER, C., PECHERSKY, D.H., BOULIN, J., SIBUET, J-C., SAVOSTIN, L.A., SOROKHTIN, O., WESTPHAL, M. BASENOV, M.L., LAUER, J.P. and BIJU-DUVAL, B. 1986. Geological evolution of the Tethys belt from the Atlantic to the Pamirs since the Lias. Tectonophysics, 123, 241-315.

DE WEVER, P. 1982. Radiolaires du Trias et du Lias de la Tethys (Systematique, Stratigraphié). Soc. Géol. du Nord, Lille, Publication 7, 599pp.

_____, 1989. Radiolarians, radiolarites and Mesozoic palaeogeography of the Circum-Mediterranean Alpine belts. In; Hein, J.R., and Obradovic, J. (Eds), Siliceous deposits of the Tethyan Region. Springer-Verlag. 31-49.

_____, and ORIGLIA-DEVOS, I. 1982a. Datations nouvelles par les radiolaires de la série des radiolarites s.l. du Pindos-Olonos, Grèce. C. R. Acad. Soc. (Paris), 294(2), 1191-1198.

_____, and _____, I. 1982b. Datation par les radiolaires des niveaux siliceux du Lias de la série du Pinde-Olonos, (Présqu'ile de Koroni, Péloponese méridional, Grèce). Geobios (Lyon), 14(5), 577-609.

_____, and CORDEY, F. 1986. Datation directe par les radiolaires de la base et de la partie mediane des radiolarites s.s. de la seriè du Pinde-Olonos (en Grèce continéntale). In De Wever, P. (Ed), Eurorad IV. Mar. Micropalaeontology, 11(1-3), 113-127.

_____, SANFILLIPO, A., RIEDEL, W.R., GRUBER, B. 1979. Triassic radiolarians from Greece, Sicily and Turkey. Micropalaeontology 25 (1), 75-110.

DIMITRIJEVIC, M.D. and DIMITRIJEVIC, M.N. 1980. Structure and kinematics of the metamorphic aureole of the Zlatibor ultramafic massif. Vesnika (Beograd), 37, 101-121.

DIXON, J.E. and ROBERTSON, A.H.F. 1985. Asymmetrical ridge-collapse model for genesis of arc-type magmas in Ophiolites. Terra Cognita, 5, 127.

DUPUY, G., DOSTAL, C., CAPEDRI, S. and VENTURELLI, G. 1984. Geochemistry and petrogenesis of ophiolites from northern Pindos (Greece). Bull. Volcanologique, 47(1), 39-46.

ELLIOT, D. and JOHNSON, M.R.W., 1980. Structural evolution in the northern part of the Moine thrust belt, NW Scotland. Trans. Roy. Soc. Ed. (Earth Sci.), 71, 61-96.

FERRIERE, J. 1976. Sur la signification des séries du massif de l'Othrys (Grèce continental): la zone isopique maliaque. Ann. Soc. Géol. Nord 96 (2), 121-134.

_____, 1982. Palaéogeographie et tectoniques superposées dans les Hellénides internes: les massifs de l'Othrys et du Pélion (Grèce continental). Soc. Géol. Nord, Lille Publication 8, 1-970.

_____, BERTRAND, J., SIMANTOV, J, and DE WEVER, P. 1986. Comparaison entre des formations volcano-détritiques ("melanges") du Malm des Héllenides internes (Othrys, Eubeé); implications géodynamiques. Ann. géol. pays Hell. Athens, in press.

FITTON, J.G., and DUNLOP, H.M. 1985. The Cameroon line, west Africa, and its' bearing on the origin of oceanic and continental alkali basalts. Earth Plan. Sci. Lett. 72, 23-38.

_____, JAMES, D.E. and THIRLWALL, M.F. 1984. A users guide to the X-ray fluorescence analysis of rock samples. Unpublished report, 2nd edition, University of Edinburgh.

FLEURY, J.J. 1980. Les zones de Gavrovo-Tripolitza et du Pinde-Olonos (Grèce Continental), et Péloponesse du Nord. Evolution d'une plate-forme et d'un bassin dans leur cadre Alpin. Soc. Géol. de Nord, Lille Publication 4, 1-651.

FREY, M. (Ed) 1987. Low temperature metamorphism. Blackie, Glasgow. 351 pp.

FUJIAKA A., and leg 126 shipboard scientific party 1989. Arc volcanism and rifting. Nature, 342, 18-20.

GASS, I.G. 1968. Is the Troodos Massif of Cyprus a fragment of Mesozoic ocean floor? Nature, 220, 39-42.

____, 1980. The Troodos Massif: its role in the unravelling of the ophiolite problem and its significance in the understanding of constructive plate margin processes. In: PANAYIOTOU, A. (Ed), Proceedings of the International Ophiolite Symposium, Cyprus, 1979. Cyprus Geological Survey, 23-35.

_____, 1990. Magmatic processes at and nearconstructive plate margins as deduced from the Troodos (Cyprus) and Semail Nappe (N. Oman) ophiolites. In: SAUNDERS, A.D. and NORRY, M. J. (Eds), Magmatism in the ocean basins. Geol. Soc. Lond. sp. pub. 42, 1-16.

GEOLOGICAL MAP OF GREECE 1987. I.G.M.E., Athens.

GHENT, E.D. and STOUT, M.Z. 1981. Metamorphism at the base of the Samail ophiolite, southeastern Oman Mountains. J. Geophys. Res. 86, 2257-2571.

GLENNIE, K.W., BOUEF, M.G.A., HUGHES-CLARK, M.W., MOODY-STUART, M., PILAAR, W.F.H. and REINHARDT, B.M. 1974. The Geology of the Oman Mountains. Konin. Neder. Geol. Mijnbouw, Genoot. Verdh. 31, part 1 (text), part 2 (illustrations), Part 3 (enclosures).

GODFRIAUX, I. 1962. L'Olympe: une fenêtre tectonique dans les Hellenidés internes. C.R. Acad. Sci., Paris, 286, 555-558.

_____, and PICHON, J.F. 1979. Sur l'importance des énvènements tectoniques et metamorphiques de l' âge Tertiare en Thessalie séptentrional. (Olympe, Ossa, Flambouron). Ann. Soc. géol. Nord. 99 (1), 367-376.

_____, and SCHMITT, A propos du métamorphisme dans la fenêtre de l'Olympe (Grèce). 9 ième R.A.S.T., Paris, 282.

GRAHAM, G.M. 1980a Evolution of a passive margin and nappe emplacement in the Oman Mountains. In PANAYIOTOU, A. (Ed), Proceedings of the international ophiolite symposium, Cyprus 1979. 414-423.

_____, 1980b Structure and sedimentology of the Hawasina window, Oman Mountains. Unpublished PhD thesis, Open University. 458pp.

GRIVAS, E., RASSIOS, A., VACONDIOS, I. and VRHATIS, G. 1986. Structural traverses of Vourinos. In: The application of a multidisciplinary concept for chromite exploration in the Vourinos Complex, northern Greece. E.E.C. report, part 1. 258-283.

GREEN, T.J. 1983. The sedimentology and structure of the Pindos zone in southern mainland Greece. PhD thesis, University of Cambridge.

GREENLY, E. 1919. The Geology of Anglesey. Mem. Geol. Survey G.B. 980pp.

HARKINS, M.E., GREEN, H.G. and MOORES, E.M. 1980. Multiple intrusive events documented from th Vourinos ophiolite complex, northern Greece. Am. Jour. Sci. 280-A, 284-295.

HICKEY, R.L. and FREY, F.A. 1982. Geochemical characteristics of boninite series volcanics: implications for their source. Geochem. et Comochem. Acta, 46, 2099-2115.

HILBER, V. 1894. Geologische Reise in Nordgreichenland und Makedonien 1893 und 1894. Sb. k. k. Akad. M. N. Kl. 103, 575-600 and 616-623.

HOWELL, D.G. 1989. Tectonics of suspect terranes-mountain building and continental growth. Topics in Earth Sci. 3, Chapman and Hall. 232 pp.

HYNES, A.J. 1974. Igneous activity at the birth of an ocean basin in Eastern Greece. Can. J. Earth Sci. 11, 842-853.

IGME/IFP 1966. Etudé géologique de l'Epiré (Grèce nord-occidentale). Athens, 306pp.

INSTITUTE OF GEOLOGICAL AND MINERAL EXPLORATION, 1959. Metsovo sheet, 1:50,000 scale. Athens.

_____, 1987. Konitsa sheet, 1:50,000 scale. Athens.

_____, 1980. Panaighia sheet. 1:50,000 scale Athens.

JACKSON, E.D., GREEN H.W. and MOORES, E.M. 1975. The Vourinos ophiolite Greece: cyclic units of lineated cumulates overlying harzburgite tectonite. Bull. Geol. Soc. Am. 86, 390-398.

JACOBSHAGEN, V., ST. DURR, F., KOCKEL, K.O. and KOWALCZYK, G. 1978. Structure and geodynamic evolution of the Aegean region. In: CLOSS, J., ROEDER, D. and SCHMIDT, K. (Eds) Alps, Appenines, Hellenides. Schweizerbart, Stuttgart, 537-564.

JAEGER, P. and CHOTIN, P., 1978. La serié du flysch béotien (Tithonique-Berriasian superieur) au front du Koziakas (Mouzaki, Province de Karditsa, Grèce). C. R. somm. Soc. géol. Fr. 1, 28-31.

JAMIESON, R.A. 1980. Ophiolite emplacement as recorded in the dynamothermal aureole of the St Anthony complex north-western Newfoundland. In: PANAYIOTOU, A. (Ed) Proceedings of the International Ophiolite Symposium, Cyprus, 1979. Cyprus Geological Survey, 620-627.

_____, 1981. Metamorphism during ophiolite emplacement. The petrology of the St Anthony Complex. J. Geol. 22 (3), 297-449.

JENKYNS, H.C. 1974. Origin of red nodular limestones (Ammonitico Rosso, Knollenkalke), in the Mediterranean Jurassic. In: HSU, K.J. and JENKYNS, H.C. (Eds) Pelagic sediments: on land and under the sea. Sp. Pub. International Assoc. Sedimentologists 1, 249-271.

_____, 1980. Tethys: past and present. Proc. geol. Ass., 91, 107-118.

JENNER G.A., SWINDEN, H.S., DUNNING, G. SZYBINSKI, A. and KEAN, B. 1990. Tectonic setting and petrogenesis of central Newfoundland ophiolites: geochemistry and Sm/Nd isotopic constraints. In: Abstracts of the Symposium on ophiolites and oceanic lithosphere, Muscat 1990.

JONES, G., ROBERTSON, A.H.F., and DIXON, J.E. 1988. Tectonostratigraphic terranes in northwest Greece?. Terra, 1 (1), 56.

_____, and ROBERTSON, A.H.F. 1990. Tectonostratigraphy and evolution of the Pindos Mountains, northwest Greece. J. Geol. Soc. Lond., in press.

_____, ROBERTSON, A.H.F. and CANN, J.R. In press. Supra-subduction zone origin of the Pindos ophiolite, Northwest Greece. Proceedings of the Muscat symposium on Ophiolites and Oceanic Lithosphere, 1990.

_____, DE WEVER, P. and ROBERTSON A.H.F. In prep. Mesozoic radiolaria from the Pindos Mountains, northwest Greece.

JUTEAU, T., 1975. Les ophiolites des nappes d'Antalya (Taurides occidentales, Turquie). Petrologié d'un fragment de l' àncienne croûte océanique téthysienne. Sc. Terre, Mem. 32, 692 pp.

_____, 1980. Ophiolites of Turkey. Ofioliti (2) 199-237.

_____, ERNEWEIN, M., REUBER, I., WHITECHURCH, H. and DAHL, R. 1988. Duality of magmatism in the plutonic sequence of the Sumail nappe, Oman. Tectonophysics, 151, 107-135.

KARAMATA, S. 1975. Geological evolution of the Yugoslavian area from the Triassic to the Tertiary. Geol. anali. Balkanskog polustrva, XLII. 455-469. Beograd.

_____, 1988. The "Diabase-Chert Formation". Some genetic aspects. Bulletin T XCV de l'Academie Serbe des Science et des Arts. (Sciences naturelles), 28, 1-11.

KARIG, D. 1988. The framework of deformation in the Nankai Trough. In: KAGAMI, H., KARIG, D.E. et al. (Eds) Initial Reports, DSDP, Washington DC. US Government Printing Office 87, 927-940.

KEMP, A.E.S., and McCAIG, A. 1984. Origins and significance of rocks in an imbricate thrust zone beneath the Pindos ophiolite, northwestern Greece. In: ROBERTSON, A.H.F. and DIXON, J.E. (Eds) The Geological Evolution of the Eastern Mediterranean. Geol. Soc. Lond. sp. pub. 17, 569-580.

KIDD, R.G.W. and CANN, J.R. 1974. Chilling statistics indicate an ocean floor spreading origin for the Troodos Complex Cyprus. Earth Plan. Sci. Lett. 24, 151-155.

KISCH, H. J. 1987. Correlation between indicators of very low grade metamorphism. In; FREY, M. (Ed) Low temperature metamorphism. Blackie, Glasgow. 227-299.

KISSEL, C. LAJ, C. and MULLER, C. 1985. Tertiary geodynamical evolution of northwestern Greece: palaeomagnetic results. Earth Plan. Sci. Lett. 72, 190-204.

KOSTOPOULOS, D. 1989. Geochemistry and tectonic setting of the Pindos ophiolite, northwestern Greece. Unpublished PhD thesis, University of Newcastle-upon-Tyne.

LALLEMENT, S., CULOTTA, R. VON HEUNE, R. 1989. Subduction of the Daiichi-Kashima seamount in the Japan Trench. Tectonophysics, 160, 231-247.

LANPHERE, M.A., COLEMAN, R.G, KARAMATA, S. and PAMIC, J. 1975. Age of amphibolites associated with Alpine peridotites in the Dinaride ophiolite zone, Yugoslavia. Earth Plan. Sci. Lett. 26, 271-276.

_____, COLEMAN, R.G. and HOPSON, C.A. 1981. Sr isotopic tracer study of the Samail ophiolite, Oman. J. Geophys. Res. 86, 2709-2720.

LAURENT, Y-S, DIOU, C. and THIBAULT, Y. 1990. Structural and petrological features of peridotite diapirs from the Troodos ophiolite, Cyprus. In: Abstacts of the symposium on Ophiolites and oceanic lithosphere, Muscat, 1990.

LEKKAS, E. L. 1988. Geological structure and geodynamic evolution of the Koziakas Mountain range, (W. Thessaly). Geol. Monographs, 1, University of Athens. 281 pp.

LIPPARD, S.J., SHELTON, A.W. and GASS, I.G. 1986. The ophiolite of northern Oman. Geol. Soc. Lond. Memoir 11. 178 pp.

LIVERMORE, R. A. and SMITH, A.G. 1985. Some boundary conditions for the evolution of the Mediterranean. In; STANLEY, D.G. and WEZEL, F.C. (Eds), Geological evolution of the Mediterranean sea. Springer-Verlag, New York. 89-105.

LORSONG, J.A. 1977. Sedimentology and deformation of the Pindos and Ionian flysch, northwestern Greece. Unpublished PhD thesis, University of Cambridge.

_____, 1979. Stratigraphy of the Pindos Flysch in the Politses Mountains, northwestern Greece. In; 6th Colloquium on the geology of the Aegean Region. Institute of Geological and Mineral Exploration, Athens, 703-714.

LUNDBERG, N. and MOORE, J.C. 1986. Macroscopic structural features in DSDP cores from forearc regions. In: MORE, J.C., Structural fabrics in DSDP cores from forearcs. Geol. Soc. Am. Memoir 166, 13-44.

LYBERIS, N., CHOTIN, P. and DOUBINGER, J. 1980. Précisions stratigraphiques sur la serie du Pinde (Grèce): la durée de sedimentation des "radiolarites". C. R. Acad. Sci., Paris, 290 (D), 1513-1516.

_____, CHOROWICZ, J. and PAPAMARINOPOULOS, S. 1982. La palaeofaille transformante du Kastaniotikos (Grèce): téledètection, donnés de terrain et géophysiques. Bull. Soc. Géol. Fr. 7, t.24, no.1, 73-85.

MAJER, V. 1984. Metamorfne stijene u ofiolitnoj zoni Banije, Jugoslavija. I. metapeliti. Rad JAZU, 411. Zagreb.

MAKRIS, J. 1977. Geophysical investigations of the Hellenides. Hamburger Geophysikalische Einzelschriften 33, 128 p.

MALAPAS, J., STEVENS, R.K. and STRONG, D.F. 1973. Amphibolite associated with the Newfoundland ophiolites; its classification and tectonic significance. Geology, 1, 45-47.

_____, 1979. Dynamothermal aureole beneath the Bay of Islands Ophiolite in Western Newfoundland. Can. Jour. Earth Sci. 16, 2086-2101.

MAVRIDES, A., SKOURTSIS-CORONEOU, V. and TSALIA-MONOPOLIS, S. 1979. Contribution to the Geology of the Subpelagonian Zone (Vourinos area, West Macedonia). 6th Colloquium on the Geology of the Aegean Region. I.G.M.E., Athens, 175-195.

McCARTHY, J. and SCHOLL, D.W. 1985. Mechanisms of subduction accretion along the central Aleutian Trench. Bull. Geol. Soc. Am. 96, 691-701.

MERCIER, J-C and VERGELY, P. 1972. Les mélanges ophiolitiques de Macédonie (Grèce); décrochements d'âge ante-Cretacé superieur. Z. Desch. geol. Gest. 123, 469-489.

MOAT, T. 1990. Structure of the Vourinos peridotites, northwest Greece. Unpublished PhD thesis, University of Southampton.

MONTIGNY, R., BOUGAULT, H., BOTTINGA, Y. and ALLEGRE, C.J. 1973. Trace element geochemistry and genesis of the Pindos Ophiolite suite. Geochem. Cosmochem. Acta 37, 2135-2147

MOORE, J.C., ROESKE, S., LUNDBERG, N., SCHOONMACHER, J., COWAN, D.S., GONZALES, E. and LUCAS, S.E. 1986. Scaly fabrics from DSDP cores from forearcs. In: MOORE, J.C. (Ed) Structural fabrics in DSDP project cores from forearcs. Geol. Soc. Am. Bull. 166, 55-74.

_____, and LUNDBERG, N. 1986. Tectonic overview of DSDP transects of forearcs. In: MOORE, J.C. (Ed) Structural fabrics in DSDP project cores from forearcs. Geol. Soc. Am. Memoir 166, 1-12.

MOORES, E.M. 1969. Petrology and structure of the Vourinos Ophiolitic complex of Northern Greece. Geol. Soc. Am. sp. pap. 118, 74pp.

_____, AND VINE, F.J. 1971. Troodos massif, Cyprus and other ophiolites as oceanic crust:evaluation and implications. Phil. Trans. Roy. Soc. Lond. A268, 443-466.

MOUNTRAKIS, D. 1984. Evolution of the Pelagonian Zone in N.W. Macedonia. In: DIXON, J.E. and ROBERTSON, A.H.F. The Geological Evolution of the Eastern Mediterranean. Geol. Soc. Lond. sp. pub. 17.

_____, 1986. The Pelagonian Zone in Greece: a polyphase deformed fragment of the Cimmerian continent and its role in the geotectonic evolution of the eastern Mediterranean. J. Geol. 94, 335-347.

MURTON, B.J. 1986. Anomalous oceanic crust formed in an oceanic transform fault: evidence from the Western Limassol Forest Complex. J. Geol. Soc. Lond. 143, 845-854.

_____, 1990. Tectonic controls on boninite genesis. In Saunders, A.D., and NORRY, M.J. (eds), 1989. Magmatism in the ocean basins, Geol. Soc. sp. pub. 42, 347-377.

NATLAND, J.H. and TARNEY, J. 1982. Petrological evolution of the Mariana arc and backarc basin system, a synthesis of drilling results in the South Phillipine Sea. Initial Reports of the Deep Sea Drilling Project, United States Government Printing Office, Washington DC 60, 877-908.

NAYLOR, M.A. and HARLE, T.J. 1976. Palaeogeographic significance of rocks and structures beneath the Vourinos Ophiolite, northern Greece. J. Geol. Soc. Lond. 132, 667-676.

NEEDHAM, D.T. 1987. Asymmetric extensional structures and their implication for the generation of melanges. Geol. Mag. 124 (4), 311-318.

NEUMAYR, M. 1880. Der geologische Bau des westlichen mittel griechenland. Dk. k. Ak. d. Wiss. M. N. Kl. 40, 91-128.

NICOLAS, A. and LE PICHON, X. 1980. Thrusting of young lithosphere in subduction zones with special reference to structures in ophiolitic peridotites. Earth Plan. Sci. Lett. 46, 397-406.

_____, REUBER, I., and BENN, K. 1988a. A new magma chamber model based on structural studies in the Oman ophiolite. Tectonophysics, 151, 87-105.

_____, A. CULENEER, G. BOUDIER, F. and MISSERI, M. 1988b. Structural mapping in the Oman ophiolites: mantle diapirism along an oceanic ridge. Tectonophysics, 151, 27-56.

NOIRET, G., MONTIGNY, R., and ALLEGRE, C.J. 1981. Is the Vourinos Complex an island arc ophiolite? Earth Plan. Sci. Lett. 56, 375-386.

ORI, G.G. and ROVERI, M. 1987. Geometries of Gilbert type deltas and large channels in the Meteora Conglomerate, Meso-Hellenic Basin (Oligo-Miocene), Central Greece. Sedimentology 34, 845-859.

PALLISTER, J.S. 1981. Structure of the sheeted dyke complex of the Semail ophioplite near Ibra, Oman. J. Geophys. Res. 86, 2661-2672.

_____, and KNIGHT, R.J. 1988. Obduction dykes: geochemistry and emplacement constraints for the Oman ophiolite. Geol. Assoc. Canada Program with abstracts, 13, pp A94.

PAMIC, J. 1983. Considerations on the boundary between the lherzolite and harzburgite subprovinces in the Dinarides and northern Hellenides. Ofioliti, 8 (1), 153-164.

_____, SCAVNICAR, S. and MEDJIMOREC, S. 1973. Mineral assemblges of amphibolites associated with Alpine-type ultramafics in the Dinaride ophiolite zone (Yugoslavia). J. Petrol. 14, 133-157.

PAPA, A. 1970. Concéptions nouvelles sur la structure des Albanides (présentation de la carte tectonique de l'Albanie au 500 000). Bull. Geol. Soc. Fr. 7 (xii), 6, 1096-1109.

PAPANIKOLAOU, D., and SIDERIS, C. 1979. Sur la signification des zones "ultrapindique" et "béotienne", d'aprés la géologie de la région de Karditsa: l'unite de Thessalie Occidentale. Eclogae Geol. Helv. 72 (1), 251-261.

PARROT, J.F. 1967. Le cortége ophiolithique du Pinde séptentrional (Grèce). Cahiers ORSTOM sér. Géol. 114p.

_____, 1969. Etude d'une coupe de réference dans le cortège ophiolithique du Pinde Septentrional: la valeé de l'Aspropotamos. Cahiers ORSTOM sér. Géol. 1. 35-59.

_____, 1973. Petrologié de la coupe du Djebel Moussa, massif basique-ultrabasique de Kizil Dag, (Hatay, Turquie). Sciénce de la Terre, (Nancy), 18, 143-172.

_____, 1974. L'assemblage ophiolitique du Baer-Bassit (Nord-Ouest de la Syrie): ètude petrographique et géochemique du complexe filonien, des laves en coussins qui lui sont associées, et d'une partie des formations effusives du volcano-sedimentaire. Cah. ORSTOM sér. Géol. 6, 97-126.

_____, and VERDONI, P-A. 1976. Conditions de formations de deux assemblages ophiolitiques Mediterraneens (Pinde et Hatay) d'apres l'étude des mineraux constituifs. Cah. O.R.S.T.O.M., sér. Géol. 8 (1), 49-68.

PEARCE, J.A. 1975. Basalt geochemistry used to investigate past tectonic environments on Cyprus. Tectonophysics, 25, 41-67.

_____, 1980. Geochemical evidence for the genesis and eruptive setting of lavas from Tethyan ophiolites. In; PANAYIOTOU, A. (Ed), Proceedings of the International Ophiolite Symposium, Cyprus, 1979. 261-272.

_____, 1982. Trace element characteristics of lavas from destructive plate boundaries. In THORPE, R.S. (Ed), Andesites. J. Wiley. 525-548.

_____, Unpublished manuscript. A users guide to trace element discrimination diagrams.

_____, and CANN, J.R. 1973. Tectonic setting of basic volcanic rocks determined using trace element analyses. Earth Plan. Sci. Lett. 19, 290-300.

_____, and WANMING, D. 1988. The ophiolites of the Tibetan Geotraverses, Lhasa to Gholmud (1985) and lhasa to Kathmandu. Phil. Trans. R. Soc. Lond. A 327, 215-238.

_____, ALABASTER, T., SHELTON, A.W. and SEARLE, M.P. 1981. The Oman Ophiolite as a Cretaceous arc-basin complex: evidence and implications. Phil. Trans. Roy. Soc. Lond. Series A, 3, 299-317.

_____, LIPPARD, S.J. and ROBERTS, S. 1984a. Characteristics and tectonic significance of supra-subduction zone ophiolites. In: KOKELAAR, B.P. and HOWELLS, M.F. (Eds) Marginal Basin Geology. Geol. Soc. Lond. sp. pub. 16, 77-89.

_____, HARRIS, N.B.W. and TINDLE, A.W. 1984b. Trace element discrimination diagrams for the tectonic interpretation of granitic rocks. J. Petrol. 25 (4), 956-983.

_____, ROGERS, N. TINDLE, A.J. and WATSON, J.S. 1986. Geochemistry and petrogenesis of basalts fron Deep Sea Drilling Project Leg 92, Eastern Pacific. In LEINEN, M. REA, D.K. et al. (Eds) Initial Reports of the Deep Sea Drilling Project 92, 435-457.

PE-PIPER, G. 1982. Geochemistry, tectonic setting and metamorphism of mid-Triassic volcanic rocks of Greece. Tectonophysics 85, 253-272.

PESSANGNO, E.A. Jr. and NEWPORT, R.L. 1972. A new technique for extracting radiolaria from radiolarian cherts. Micropalaeontology 18 (2), 231-234.

PHILLIPSON, A. 1895. Reisen und forschungen in Nord-Griechenland. Zeitschr. d. Ges. f. Erdk. 30, 135-226.

PIPER D.J.W., and PE-PIPER, G. 1989. Geologic significance of tectonic slices containing igneous rocks at the base of the Pindos Nappe, External Hellenides, Greece. In press.

PICHON, J.F. and BRUNN, J.H. 1985. An inverted metamorphism beneath the Vourinos Ophiolitic suite, Greece. Ofioliti 10, (2/3), 363-374.

PICKERING, K.T., AGAR, S.M. and OGAWA, Y. 1988. Genesis and deformation of mud injections containing chaotic basalt-limestone-chert associations: examples from the southwest Japan forearc. Geology 16, 881-885.

PISKIN, O, DELALOYE, M., SELCUK, H. and WAGNER, J.J. 1986. Guide to Hatay Geology. Ofioliti 11, 87-104.

PLATT, J.P. and VISSERS, R.L.M. 1989. Extensional collapse of thickened continental lithosphere- a working hypothesis for the Alboran Sea and Gibraltar Arc. Geology 17, (6), 540-543.

PRICE, I. 1977. Carbonate sedimentology in a pre-Upper Cretaceous continental margin sequence, Othrys, Greece. Bull. Soc. Geol. Fr. 7 (18/2) 321-335.

RAMSAY, J. 1967. Folding and fracturing of rocks. McGraw-Hill.

RICHARD, P. and ALLEGRE, C.J. 1980. Neodimium and strontium isotope study of ophiolite and orogenic lherzolite petrogenesis. Tectonophysics, 47, 65-74.

RASSIOS, A., BECCALUVA, L., RASSIOS, A., BORTOLOTTI, V., MAVRIDES, A. and MOORES, E.M. 1983. The Vourinos Ophiolitic complex. Ofioliti 8 (3), 275-292.

_____, and ROBERTS, S. 1986. Results of the chromite research program, Vourinos, Greece (1984-1986): a synthesis. In: The application of a multidisciplinary concept for chromite exploration in the Vourinos Complex, northern Greece. European Economic Community Report, part 1.

_____, In prep. Internal structure of the Dramala peridotite, Pindos ophiolite, Greece.

RAUTENSCHLEIN, M.F.M. 1985. Geology and geochemistry of Akaki Volcanics, Cyprus. Unpublished PhD thesis University of Bochum. pp 222.

RAYMOND, L. and TERRANOVA, T. 1984. Prologue- the melange problem: a review. Geol. Soc. Am. Sp. Pub. 184, 1-5.

RENZ, C. 1928. Zur Geologie des thessalischen Pindos. Eclog. geol. Helv. 21 (1), 135-153.

ROBERTS, S. RASSIOS, A., WRIGHT, L., VACONDIOS, I., VRACHATIS, G., GRIVAS, E., NESBITT, R.W., NEARY, C.R. MOAT, T. and KONSTANTOPOLOU, L. 1988. Structural controls on the location and form of the Vourinos chromit deposits. In: BOISSONNAS, J. (Ed) Mineral deposits within the Eurpoean Community. Sp. pub. Soc. geol. applied to mineral deposits, 6, 249-266.

_____, and NESBITT, R.W. 1987. Geochemistry of a residual mantle sequence from the Vourinos complex, N. Greece: complications for magma genesis in a supra-subduction zone ophiolite. Abstracts of papers accepted for oral and poster presentation; Symposium, Troodos 87, Ophiolites and Oceanic Lithosphere, Nicosia, Cyprus. 4-10 Oct. 1987. Geological Survey Department, Nicosia, Cyprus.

ROBERTSON, A.H.F. 1989. Palaeoceanography and tectonic setting of the Jurassic Coast Range Ophiolite, Central California. Evidence from the extrusive rocks and the volcaniclastic sedimentary cover. Mar. Petrol. Geol. 6, 194-220.

_____, and WOODCOCK, N.H. 1980. Godene Zone, Antalya Complex: volcanism and sedimentation along a Mesozoic continental margin. Geol. Rundschau 70 (3), 1177-1214.

_____, and DIXON, J.E. 1984. Introduction: aspects of the geological evolution of the Eastern Mediterranean. In: DIXON, J.E. and ROBERTSON, A.H.F. (Eds) The Geological Evolution of the Eastern Mediterranean. Geol. Soc. Lond. sp. pub. 17, 1-74.

_____, and VARNAVAS, S. 1990. Metalliferous sediments associated with the Pindos ophiolite, northwest Greece. Colloquium of the Aegean Region. Abstacts, 5th cong. Geol. Soc. Greece, Thessaloniki, 1990.

_____, KEMP, A.E.S., REX, D.C., and BLOME, C.D. 1990. Sedimentary and structural evolution of a transform lineament; the Hatta zone, northern Oman Mountains. in ROBERTSON, A.H.F., The geology and tectonics of the Oman region. Geol. Soc. Lond. sp. pub. 49, 285-306.

_____, DEGNAN, P.J. CLIFT, PD. and JONES, G. 1990. In press. Palaeoceanography of the Greek Neotethys. Proceedings of the I.G.C. congress, Washington, 1990.

ROBINSON P.T., MELSON, W.G., O'HEARN, T. and SCHMINKE, H-U, 1983. Volcanic glass compositions of the Trooodos ophiolite Cyprus. Geology, 11, 400-404.

RODDICK, J.C., CAMERON, W.E. and SMITH, A.G. 1979. Permo-Triassic and Jurassic Ar-Ar ages from Greek ophiolites and associated rocks. Nature 279, 788-790.

ROSS, J.V., MERCIER, J-C.C., AVE LALLEMENT, H.G., CARTER, N.L and ZIMMERMAN, J. 1980. The Vourinos ophiolie complex, Greece: the tectonite suite. Tectonophysics, 70, 63-83.

_____, and ZIMMERMAN, J. 1982. The Pindos ophiolite complex, Northern Greece: evolution and significance of the tectonic suite. Abstract in: DIXON, J.E. and ROBERTSON, A.H.F. (Eds) 1982. The Geological Evolution of the Eastern Mediterranean. Conference Abstracts, Edinburgh 1982, p.95.

RUIZ-ORTIZ, P.A. 1983. A carbonate submarine fan in a fault controlled basin of the Upper Jurassic, Betic Cordillera, southern Spain. Sedimentology, 30, 33-48.

SEARLE, M.P. 1980. The metamorphic sheet and underlying volcanic rocks beneath the Semail ophiolite in the northern oman Mountains of Arabia. Unpublished Ph.D thesis, Open University.

_____, and COOPER, D.W. 1986. Structure of the Hawasina window culmination, central Oman Mountains. Trans. Roy. Soc. Ed. (Earth Science), 77, 143-156.

_____, and MALPAS, J. 1980. Structure and metamorphism of rocks beneath the Semail Ophiolite of northern Oman and their significance in ophiolite obduction. Trans. Roy. Soc. Ed. (Earth Sciences) 71, 247-262.

_____, and _____, 1982. Petrochemistry and origin and sub-ophiolite metamorphic and related rocks in the Oman Mountains. J. Geol. Soc. Lond. 139, 5-24.

_____, and GRAHAM, G.M. 1982. The "Oman Exotics"- oceanic carbonate build-ups associated with the early stages of continental rifting. Geology, 10, 43-49.

SENGÖR, A.M.C., YILMAZ, Y. and SUNGURLU, O. 1984. Tectonics of the Meditteranean Cimmerides: nature and evolution of the western termination of Palaeo-Tethys. In Dixon, J.E. and Robertson, A.H.F. (Eds). The Geological Evolution of the Eastern Mediterranean. Geol. Soc. Lond. sp. pub. 17, 77-112.

SHALLO, M. 1978. Amphibolites et micaschists dans l'exocontact sud-est du massif ultrabasique de Puka. Permb. Stud., 2, Tirana.

_____, 1980. Petrology of magmatic rocks from the central Mirdita zone, Albania. Unpublished Ph.D thesis, Tirana University.

SHELTON, A.W. 1990. The interpretation of gravity data in Oman: constraints on the ophiolite emplacement mechanism. In: ROBERTSON, A.H.F., SEARLE, M.P. and RIES, A.C. The geology and tectonics of the Oman region. Geol. Soc. Lond. sp. pub. 49, 459-472.

SHERVAIS, J.W. and KIMBROUGH, D.L. 1985. Geochemical evidence for the tectonic setting of the Coast Range Ophiolite, a composite island arc-oceanic crust terrane in the West Pacific. Geology 13, 35-38.

SIMANTOV, J., ECONOMOU, C. and BERTRAND, J. 1988. Metamorphic rocks associated with the central Euboea ophiolite (southern Greece). Some new occurrences. In press.

SIMONIAN, K.O. and GASS, I.G. 1978. The Arakapas Fault belt, Cyprus: a fossil transform fault. Bull. Geol. Soc. Am., 89, 1220-1230.

SMITH, A.G., 1979. Othris, Pindos and Vourinos Ophiolites and the Pelagonian Zone. 6th Colloquium on the Geology of the Aegean Region. Institute of Geological and Mineralogical Exploration, Athens. 1369-1374.

_____, and MOORES, E.M. 1972. The Hellenides. In; SPENCER, (ed) Mesozoic-Cenozoic orogenic belts, data for orogenic studies. Geol. Soc. Lond. sp. pub. 4, 159-185.

_____, A.G., and SPRAY, J.G. 1984. A half-ridge transform model for the Hellenic-Dinaric ophiolites. In: DIXON, J.E. and ROBERTSON, A.H.F. The Geological Evolution of the Eastern Mediterranean. Geol. Soc. Lond. sp. pub. 17, 629-644.

_____, A.G., HYNES A.J., MENZIES, M., NISBET E.G., PRICE I., WELLAND, M.J. and FERRIERE, J. 1975. The stratigraphy of the Othris Mountains, eastern central Greece: a deformed Mesozoic continental margin sequence. Eclogae geol. Helv., 68, 463-481.

_____, A.G., WOODCOCK, N.H. and NAYLOR, M.A. 1979. The structural evolution of a Mesozoic continental margin, Othris Mountains, Greece. J. Geol. Soc. Lond. 146, 589-603.

SMITH, C.H. 1958. The Bay of Islands igneous complex, western Newfoundland. Geol. Surv. Canada Mem., 290, 1-132.

SOLIMAN, H.A. and ZYGOYANNIS, N. 1979. Foraminiferal assemblages from the Eocene of Mesohellenic Basin, northern Greece. 6th Colloquium of the geology of Greece, Athens. p

SPRAY, J.G. and RODDICK, J.C. 1980. Petrology and 40Ar/39Ar geochronology of some Hellenic sub-ophiolite metamorphic rocks. Contrib. Min. Pet. 72, 43-55.

_____, BEBIEN, J., REX, D.C. and RODDICK, J.C. 1984. Age constraints on the igneous and metamorphic evolution of the Hellenic-Dinaric ophiolites. In: DIXON, J.E. and ROBERTSON, A.H.F. The Geological Evolution of the Eastern Mediterranean. Geol. Soc. Lond. sp. pub. 17, 619-627.

_____, 1990. Upper mantle segregation processes: evidence from Alpine-type peridotites. In SAUNDERS, A.D. and NORRY, M.J. (Eds), Magmatism in the ocean basins. Geol. Soc. Lond. sp. pub. 42, 29-40.

STOCKMAL, G.S., BEAUMONT, C. and BOUTILIER, R. 1986. Geodynamic models of convergent margin tectonics: transition from rifted margin to overthrust belt and consequences for foreland basin development. Am. Ass. Petrol. Geol. Bull. 70 (2), 181-190.

TERRY, J. P. 1971. Sur l'âge Triassique de laves associées a la nappe ophiolitique du Pinde séptentrional (Epiré et Macédonie, Grèce). C. R. somm. Soc. géol. Fr. 384-385.

_____, 1974. Ensembles lithologiques et structures internes du cortège ophiolitique du Pinde séptentrionale (Grèce), construction d'un model pétrogenetique. Bull. Soc. Géol. Fr. 16, 204-213.

_____, 1975. Echo d'une téctonique jurassique: les phenomènes de résedimentation dans le secteur de la nappe des ophiolites du Pinde séptentrional (Grèce). C. R. somm. Soc. géol. Fr. 49-51.

_____, 1979. Distinction géochemique de plusieurs groupes dans les ensembles volcaniques de la nappe ophiolitique du Pinde séptentrional (Grèce). Bull. Soc. Gèol. Fr. 21(6), 727-735.

_____, and MERCIER, M. 1971. Sur l'éxistence d'une serie détritique bèrrasienne intercalée entre la nappe des ophiolites et le flysch Eocene de la nappe du Pinde (Pinde septentrional, Grèce). C. R. somm. Soc. géol. Fr. 71-73.

TILTON G.R., HOPSON, C.A., WRIGHT, J.E. 1981. Uranium-lead isotopic ages of the Seamail ophiolite Oman, with applications to Tethyan sea ridge tectonics. J. Geophys. Res. 86, 2763-2776.

THUIZAT, R., WHITECHURCH, H., MONTIGNY, R. and JUTEAU, T. 1981. K-Ar dating of some infra-ophiolitic metamorphic soles from the Eastern Mediterranean: new evidence for oceanic thrustings before obduction. Earth Plan. Sci. Lett. 52, 302-310.

TURKU, I. 1986. Les métamorphites prés du massif ultrabasique de Kukes. Bull. Shekenc. Gjeol. 3, Tirana.

VAIL, P.R., MITCHUM, R.M. and THOMSON, S. 1977. Seismic stratigraphy and global changes of sea level. iv. Global cycles of relative changes of sea level. In: PAYTON, C. (Ed), Seismic stratigraphy: applications to hydrocarbon exploration. Am. Ass. Petrol. Geol. Memoir 26, 83-97.

VERGELY, P. 1976. Origine "vardarienne" chevauchement vers l'ouest et rétrocharriage vers l'est des ophiolites de Macedonie (Grèce) au cours du Jurassique supérieur-Eocrétace. C. R. Acad. Sci. Paris D280, 1063-1066.

_____, 1977. Discussion of the palaeogeographic significance of rocks beneath the Vourinos ophiolite, Northern Greece. J. Geol. Soc. Lond. 133, 505-507.

_____, 1984. Téctonique des ophiolites dans les Hellénides internes. Consequences sur l'évolutions des regions Téthysiennes occidentales. Thèse de l'Université de Paris-Sud, Orsay. 661pp.

WEBER, K. 1972. Notes on the determination of illite crystallinity. Nues Jb. Mineral. Mh. 267-276.

WHITECHURCH, H. and PARROT, J.F. 1978. Ecailles métamorphiques infraperidotitiques dans le Pinde séptentrional (Grèce): croûte oceanique, métamorphisme et subduction. C. R. Acad. Sci. Paris t.286, 1491-1494.

WILLIAMS, H. 1975. Structural succession, nomenclature and interpretation of transported rocks in western Newfoundland. Can. J. of Earth Sci. 1874-1894.

_____, and SMYTH, W.R. 1973. Metamorphic aureoles beneath ophiolite suites and Alpine peridotites: tectonic implications with West Newfoundland examples. Am. J. Sci. 273, 594-621.

WINCHESTER, J.A. and FLOYD P.A. 1976. Geochemical magma type discrimination: application to altered and metamorphosed basic igneous rocks. Earth Plan. Sci. Lett. 28, 459-469.

WOOD, D.A., JORON, J-L, and TREUIL, M. 1979. A re-appraisal of the use of trace elements to classify and discriminate between magma series erupted in different tectonic settings. Earth Plan. Sci. Lett. 45, 326-336.

WOODCOCK, N.H. and ROBERTSON, A.H.F. 1977. Origins of some ophiolite-related metamorphic rocks of the "Tethyan" belt. Geology 5, 373-76.

WRIGHT, L. 1986. The effect of deformation on the Vourinos Ophiolite. In: The application of a multi-disciplinary concept for chromite exploration in the Vourinos Complex, N Greece. European Economic Community report, part 1, Athens, 1986. 156-214.

ZIMMERMAN, J. 1972. Emplacement of the Vourinos Ophiolite complex, Northern Greece. Memoirs Geol. Soc. Am. 132, 225-239.

APPENDIX 1

NEW STRATIGRAPHICAL NAMES		TYPE SECTION LOCATION	PREVIOUS NAME(S)
PINDOS OPHIOLITE GROUP	DRAMALA COMPLEX	Dramala Mountain, 5km east of Perivoli Village. Numerous road and hillside exposures (up to 5km thick)	"Dramala Peridotite"; Rassios (in Prep.) Dramala Unit; (D. Latin, D. Edwards, 1986. Unpublished data).
	ASPROPOTAMOS COMPLEX	Aspropotamos River valley near Ambelia hill area, and the Venetikos-Aspropotamos confluence (up to 4km thick).	"Aspropotamos Sequence". (Parrot, 1967, 1969; Montigny et al., 1973). "Aspropotamos series" (Capedri et al., 1981). Sotira Complex. (D. Latin, 1986. Unpublished data). Aspropotamos Complex (Kostopoulos 1989).
	LOUMNITSA UNIT	Loumnitsa valley, on the west side of Dramala Mountain. Sections located on both sides of the valley, approximately 3km S. of Megali Pedias, passing S. into Dramala Complex. Roadside exposures (up to 0.4km thick).	"Schistes Cristallins" (Brunn, 1956) Kodro Unit (D. Latin, D. Edwards, 1986. Unpublished data).
AVDELLA MELANGE		Avdella village. Section located 1km N.E. of village. Roadside and hillside exposures, along river valley (up to 1.5km thick).	Perivoli Complex; (Kemp & McCaig, 1984). Avdella Unit; Stragopetra Unit (D. Latin, 1986. Unpublished data). Avdella Unit; (D. Edwards, 1986. Unpublished data). Anilion Complex: Lorsong 1979a, 1979b Valiara Melange, Isomata Chert Formation; (A. McCaig, 1978. Unpublished data).

DIO DENDRA GROUP	KARAMOULA FORMATION	Karamoula hill area. Roadside exposures 6km west of Zakas village, on main road to Perivoli (up to 0.5km thick).	Papaliapi Unit (Karamoula & Agios Nikolaos Fmns equivalent; D. Latin, 1986. Unpublished data). Dio Dendra Unit, Panaiya Unit (Karamoula, Agios Nikolaos and Krevvati Fmn. equivalents D. Edwards, 1986. Unpublished data).
	AGIOS NIKOLAOS FORMATION	Roadside exposures, and exposures in small valley 30m to the N.E. of Agios Nikolaos church, near Forestry Station (Perivoli) (up to 0.35km thick).	White River Limestone Formation (A. McCaig, 1978. Unpublished data. Karamoula & Agios Nikolaos Fm. equivalents).
	KREVVATI FORMATION	Krevvati hill, 3km S.W. of Lavda Village. Stream and road side sections east of Panaiya church (up to 0.35km thick).	"Niveaux detritiques" (Brunn, 1956).
	ZYGOUROGREKO FORMATION	Hillside and limited roadside sections at Zygourogreko, 4km S. of Perivoli Village. Exposures around triangulation point at Zygourogreko (Up to 0.25km thick).	New name
ORLIAKAS GROUP (Undivided)		At the Orliakas hills, on the road to Spileo Village, from Ziakas, and West of Spileo Village. Hill and roadside sections. (up to 0.4km thick)	Calcaires à Rudistes; Calcaires à Orbitoides; Calcaires très lités à Petits Foraminiferes; Calcaires bréchiques à orbitolines. (Brunn, 1956).

APPENDIX 2: X-ray fluorescence techniques

Whole rock chemical analysis of samples collected in the north Pindos Mountains was undertaken by X-ray fluorescence at Edinburgh University. The samples were analysed on Philips PW 1450/20 and PW 1480 spectrometers. The analyses were calibrated using USGS and CRPG international standards, described in Abbey (1980). Typical accuracy, i.e. a measure of the absolute quality of the analysis, is presented in Table 1 (Fitton et al. 1984). Major elements were analysed from fused glass discs. These were prepared using the standard technique of Fitton and Dunlop (1985). A measured quantity of Lithium flux (Johnson-Mathey Spectroflux), was added to the residue. Trace elements were measured on pressed powder pellets. Further details are presented in Fitton et al. (1984).

TABLE 1

Weight %	Mean (n=5)	1σ	
SiO_2	43.80	0.09	0.22
Al_2O_3	14.06	0.05	0.12
Fe_2O_3	12.46	0.03	0.05
MgO	8.31	0.03	0.08
CaO	10.62	0.03	0.05
Na_2O	3.61	0.04	0.06
K_2O	1.412	0.005	0.02
TiO_2	3.165	0.006	0.01
MnO	0.215	0.007	0.01
P_2O_5	1.030	0.003	0.01
p.p.m.			
Ni	170.9	0.3	4.3
Cr	380.5	2.9	11.0
V	236.6	3.5	11.5
Sc	18.2	0.3	2.4
Cu	48.4	0.4	5.3
Zn	113.9	1.1	5.0
Pb*	-1.8	1.6	4.0
Sr	1129.7	4.0	9.6
Rb	46.7	0.5	3.5
Zr	366.0	1.0	14.8
Nb	92.2	0.5	2.4
Ba	718.4	5.6	39.0
Th	16.6	1.2	2.8
La	78.9	0.8	5.6
Ce	156.7	1.6	13.5
Nd	66.2	0.6	3.6
Y	33.2	0.4	3.4

* Below detection limit. 6 determinations (by MFT) of Pb in andesite MT45 gave a mean concentration of 9.6 p.p.m. with a σ of 0.8 p.p.m.

DYKES

	7SP2	7SP4	7SP6B	7SP10	7SP11	7SP14	7SP15	56/89	60/89	62/89	106/89	107/89	77/89	78/89	79/89	80/89	7SP13	7VE15	7VE29
SiO2	51.86	46.85	55.22	48.17	50.33	49.32	48.89	47.12	48.48	47.27	56.46	55.76	63.70	55.17	56.09	50.74	51.92	65.26	54.89
Al2O3	10.57	14.62	13.92	13.47	12.88	14.36	13.44	15.17	15.31	15.02	14.90	14.07	12.19	13.97	15.61	14.32	11.80	14.41	13.48
Fe2O3	8.74	12.71	11.36	14.04	13.71	10.83	13.33	10.10	10.11	9.82	10.15	11.79	9.64	9.40	11.99	8.23	14.09	7.68	9.09
MgO	12.05	8.14	6.68	7.19	5.80	8.67	6.35	9.14	7.83	9.35	4.09	3.80	4.15	5.26	4.70	6.80	6.69	2.53	4.25
CaO	9.91	10.27	6.78	9.70	8.92	9.77	10.49	12.14	8.95	12.69	4.40	3.44	1.49	4.72	3.86	6.86	6.17	3.51	5.85
Na2O	1.29	3.03	0.65	3.20	4.07	2.95	2.98	2.36	4.15	2.00	5.57	5.64	4.06	4.66	5.93	4.30	5.20	6.00	4.20
K2O	0.112	0.088	0.012	0.066	0.052	0.061	0.062	0.039	0.065	0.064	0.032	0.047	0.031	0.109	0.038	0.021	0.029	0.075	0.123
TiO2	0.614	1.840	0.228	2.319	2.185	1.290	2.266	1.034	0.212	0.835	0.927	1.237	0.300	0.269	1.120	0.454	2.371	0.820	0.202
MnO	0.166	0.176	0.149	0.240	0.228	0.219	0.238	0.180	0.178	0.182	0.162	0.192	0.126	0.131	0.165	0.207	0.220	0.093	0.158
P2O5	0.017	0.172	0.021	0.222	0.227	0.099	0.236	0.086	0.018	0.072	0.087	0.098	0.029	0.027	0.083	0.040	0.247	0.103	0.022
LOI								2.63	3.84	2.06	3.24	4.40	4.58	6.07	4.20	7.91	1.48		
TOTAL	94.883	97.901	95.020	98.606	98.391	97.560	98.286	99.996	99.138	99.355	99.726	100.484	100.289	99.790	103.776	99.877	100.226	100.476	92.271
Ni	167.8	145.5	62.6	110.2	98.5	128.0	85.1	109	76.7	131.5	16.3	12.6	21.6	38.8	10.5	41.1	78.5	22.3	48.3
Cr	855.6	304.2	104.9	240.8	224.2	402.3	126.8	395.3	127.5	455.1	10.9	9.0	59.9	44.5	0	44.6	229.5	0	56.2
V	224	337.3	302.4	435.5	415.1	303.7	419.8	275.4	287.4	284.8	303.8	336.6	332.3	304.9	400.9	230.3	392.5	193.2	297.8
Sc	44.4	34.4	39.7	37.8	37.0	33.5	37.6	49.5	67.7	52.1	39.7	39.6	57.8	61.99	42.0	43.8	55.7	22.4	42.1
Cu	3.7	44.2	88.8	56.3	20.8	146.7	50.8	86	155.0	68.3	76.8	171.2	213.1	113.4	132.6	14.0	10.1	6.4	210.0
Zn	58.6	106.7	102.8	114.6	146.3	111.6	119.2	79.1	101.1	73.1	126.6	129.5	102.8	80.4	52.7	49.9	127.1	20.3	82.3
Sr	43.8	129.1	104.0	94.2	144.7	91.9	108.4	143.6	30.9	106.9	40.3	35.0	18.9	65.1	54.4	44.2	25.2	45.6	55.1
Rb	0.6	0.7	0	0	0	0	00	0	0	0	0	0	0	0	0	0	0	0	0.8
Zr	8.0	132.3	12.8	166.4	148.3	78.5	163.9	62.7	20.1	44	55.4	62.0	16.5	13.5	51.8	21.6	161.3	78.5	11.0
Nb	1.6	3.5	2.3	5.0	4.0	2.3	4.1	1.1	0.8	1.8	2.0	2.2	0.9	0.9	1.8	1.5	4.2	3.6	1.9
Ba	11	0	0	31.8	4.6	5.4	12.4	3.5	16.4	18.8	13.5	1.9	8.4	15.7	6.0	0	0	0	0
Pb	2.1	2.2	4.6	2.6	1.0	2.5	0.8	0.3	2.0	0	1.4	0	2.0	0.9	1.0	1.5	0.3	2.3	3.8
Th	0.6	0.2	0.5	0	0	0.2	0	0	0	0	0	0	0.1	0	0.4	0.2	0	0	0.2
La	0	12.2	5.6	9.7	15	12.3	14.9	0.6	2.7	0	4.7	3.4	9.7	3.6	4.3	0.9	3.3	17.6	8.8
Ce	0.6	6.2	1.2	15.9	16.2	6.7	17.2	0	0	0	4.0	0	0	0.2	2.3	0	13.1	14.8	1.5
Nd	0	6.3	0	13.0	9.7	7.3	16.3	2.9	0	4.0	4.3	1.0	0	0	3.3	1.4	13.7	2.8	0
Y	5.9	40.9	8.2	54.2	52.6	31.0	52.9	23.1	6.6	18.4	24.3	26.4	9.8	8.3	21.8	12.5	53.4	30.3	6.4
TiO2 ppm	3684	11040	1368	13914	13110	7740	13596	6204	1272	5010	5562	7422	1800	1614	6720	2724	14226	4920	1212
Ti/Y	624.41	269.93	166.83	256.72	249.24	249.68	257.01	268.57	192.73	272.28	228.89	281.14	183.67	194.46	308.26	217.92	266.40	162.38	189.38
Nb/Y	0.271	0.085	0.280	0.092	0.07	0.074	0.07	0.04	0.12	0.09	0.08	0.08	0.09	0.10	0.08	0	0.07	0.11	0.29
Zr/Y	1.35	3.23	1.560	3.073	2.81	2.53	3.09	2.71	3.04	2.39	2.27	2.34	1.68	1.62	2.37	1.72	3.02	2.59	1.71
Ce/Y	0.102	0.151	0.146	0.293	0.30	0.216	0.32	0	0	0	0.16	0	0	0.02	0.10	0	0.24	0.48	0.23
Zr/Nb	5	37.8	5.565	33.28	37.1	34.13	39.97	57	25.12	24.4	27.7	28.18	18.33	15	28.77	14.4	38.40	5.78	6.21

BASALTS

	108/89	86A/89	87A/89	89/89	90/89	92/89	93/89	67/89	68/89	188/88/A	189/88/A	190/88/A	191/88/A	7VE2	7VE4	7VE7A	7VE36	7VE37	7AV3	7AV13
SiO2	56.76	63.84	59.40	48.23	48.45	44.85	47.41	50.75	50.92	48.959	48.147	43.686	41.987	68.15	54.14	53.09	48.94	46.71	58.83	49.25
Al2O3	14.97	13.89	13.03	14.67	12.98	14.76	15.78	13.54	14.92	15.586	15.511	15.023	14.311	13.92	15.14	16.12	15.58	14.91	13.75	13.90
Fe2O3	8.08	6.56	8.24	10.09	9.18	10.51	11.62	13.30	9.60	8.947	9.017	9.492	9.804	5.96	9.38	9.25	7.95	10.46	7.44	8.73
MgO	4.61	2.86	3.69	6.58	10.76	5.06	5.02	4.58	4.32	7.923	6.621	9.307	7.981	1.74	5.60	5.40	7.27	6.42	7.81	7.33
CaO	4.50	6.44	4.32	8.71	10.88	13.01	11.47	5.69	7.00	8.797	10.627	10.167	13.265	1.01	3.88	2.96	10.72	10.92	1.78	12.12
Na2O	6.55	3.98	5.54	4.68	2.31	3.53	3.44	5.92	4.27	4.348	4.250	3.327	2.922	6.02	4.92	6.07	2.37	3.42	4.24	3.66
K2O	10.13	0.178	0.191	0.381	0.707	0.721	0.963	0.049	1.894	0.038	0.031	0.078	0.237	0.151	0.669	0.075	1.733	0.914	0.057	0.013
TiO2	0.289	0.288	1.187	2.159	1.070	1.085	1.219	2.435	0.608	1.144	1.176	1.250	1.180	0.517	0.780	0.738	1.058	1.067	0.627	1.347
MnO	0.095	0.087	0.104	0.231	0.198	0.714	0.186	0.165	0.184	0.150	0.136	0.175	0.211	0.125	0.180	0.179	0.165	0.180	0.153	0.186
P2O5	0.033	0.033	0.279	0.232	0.183	0.136	0.164	0.254	0.082	0.126	0.136	0.090	0.095	0.118	0.067	0.064	0.123	0.154	0.068	0.128
LOI	1.93	1.32	3.56	3.59	3.88	6.35	3.26	3.03	6.20											
TOTAL	98.824	99.482	99.538	99.554	100.606	100.177	100.528	99.708	99.998	96.02	95.65	92.59	91.99	97.704	94.755	93.956	95.907	95.170	94.760	96.665
Ni	58.6	25.2	19.0	67.3	158.3	90.5	99.4	32.9	24.8	77.3	64.5	235.5	330.4	16.2	25.3	23	155.6	96.7	41.5	91.5
Cr	86.9	12.2	43.0	240.8	505.6	345.0	391.9	45.9	14.7	225.9	137.9	489.3	704.0	0.1	4.7	7	347.4	372.6	146.5	351.3
V	290.0	297.7	143.9	334.2	305.5	315.1	362.9	458.6	270.4	294.1	317.8	210.0	211.8	20.6	268.3	231.1	284.0	294.3	229.6	278.6
Sc	55.0	48.2	27.3	52.7	52.3	43.0	50.3	51.6	45.5	36.2	36.6	30.9	29.4	16.0	28.7	25.6	35.1	37.8	29.1	34.4
Cu	25.0	118.4	26.1	88.0	103.7	24.8	32.6	45.4	104.8	69.8	65.1	80.1	56.1	26.1	69.7	59	52.9	45.7	118.2	47.8
Zn	64.9	50.7	150.1	88.8	61.8	91.3	108.4	126.2	62.6	63.1	67.3	62.8	79.6	95.5	78.4	96.2	69.0	78.9	74.7	74.5
Sr	87.9	200	50.7	63.7	380.4	159.0	112.2	66.8	105.9	622.9	134.9	708.4	246.5	69.3	91.3	51.9	190.3	223.0	72.8	56.4
Rb	6.0	3.8	0.6	2.4	7.6	10.2	12.6	0	20.0	0	0	0	3.0	0.2	5.0	0	23.0	18.7	0	0
Zr	15.2	11.3	381.2	162.4	67.3	57.4	64.0	182.5	38.5	113.5	76.8	137.7	94.8	123.7	42.3	39.3	57.8	55.6	49.2	99.7
Nb	1.6	0.5	16.3	8.6	19.6	7.5	8.0	4.1	1.7	6.9	7.3	1.9	2.5	4.8	2.7	2.6	9.3	9.4	3.4	2.6
Ba	57.8	26.0	33.8	52.0	116.9	38.9	75.9	17.4	198.7	28.4	37.5	5.8	28.2	19.0	87.7	14	313.1	66.5	5.5	0
Pb	2.2	3.0	2.3	0.2	1.3	1.3	0	0.4	0	0.5	2.1	0	0	4.1	3.7	3.4	2.1	3.4	4.2	2.4
Th	0.7	0	2.8	64.4	64.5	0	0	0	0	0	0.6	0	0	0.1	0	0.3	0	0	1.3	0
La	1.4	3.8	26.8	13.3	20.6	4.2	8.7	7.2	4.7	2.1	8.9	2.0	0.3	14.3	7.5	12.9	12.8	10.4	9.6	10.2
Ce	0	0	51.9	13.7	17.6	8.5	6.9	18.0	4.0	17.8	12.8	8.7	13.1	20.2	0	0	9.0	13.3	4.0	16.6
Nd	0.2	0.4	28.1	9.7	8.0	7.1	6.0	15.5	3.0	4.9	9.8	8.0	7.1	7.0	0	0	4.5	4.6	0	10.4
Y	8.3	8.9	75.6	34.0	15.2	24.8	28.2	57.6	14.6	21.1	22.5	24.6	24.2	37.9	17.3	14.3	26.2	26.6	18.4	29.3
TiO2	1734	1728	7122	12954	6420	6510	7314	14610	3648	6864	7056	7500	7080	3102	4680	4428	6348	6402	3762	8082
Ti/Y	208.92	194.16	94.21	381.00	422.37	262.50	259.36	253.65	249.86	325.31	313.60	304.88	292.56	81.85	270.52	309.65	242.29	240.68	204.46	275.84
Nb/Y	0.19	0.05	0.2156	0.25	1.28	0.30	0.28	0.07	0	0.32	0.32	0.077	0.10	0.12	0.15	0.1	0.35	0.35	0.18	0
Zr/Y	1.83	1.26	5.04	4.77	4.40	2.31	2.26	3.16	2.63	5.37	3.41	5.59	3.91	3.26	2.44	2.74	2.20	2.09	2.67	3.40
Ce/Y	0	0	0.68	0.40	1.15	0.34	0.24	0.31	0	0.84	0.56	0.35	0.54	0.53	0	0	0.34	0.5	0.21	0.56
Zr/Nb	9.5	22.6	23.38	18.88	3.43	8	44.51	22.64	16.44	10.52	72.47	37.92	25.77	15.6	15.11	21.80	5.91	14.47	38.34	39.92

	7AV16	7AV18	7AV20	7AV22	53/89	54/89	33A/89	35/89	38/89	39/89	97/88	98/88	99/88	99/A/88	70/89	7AD8	95/89	96/89	57/89	58/89	61/89	63/89	64/89
SiO2	47.54	47.78	48.93	50.08	48.02	47.18	41.41	57.18	50.17	50.68	60.713	59.710	49.504	59.493	49.31	52.50	54.54	58.12	49.67	48.17	46.90	46.77	50.53
Al2O3	13.22	13.74	14.16	14.05	15.56	15.27	15.31	13.79	14.34	13.83	13.398	13.839	13.302	12.691	14.38	17.13	13.03	14.71	13.45	13.77	14.31	15.58	13.96
Fe2O3	11.97	11.00	9.09	8.61	8.48	8.78	7.90	7.65	10.06	9.85	8.981	9.128	13.194	10.329	9.98	7.92	7.23	9.26	12.01	11.80	10.95	9.22	9.84
MgO	6.97	9.23	6.28	8.32	8.69	8.69	5.12	7.76	8.75	8.94	4.801	4.794	7.047	3.336	7.92	8.09	11.08	6.27	8.15	7.51	7.25	9.71	8.60
CaO	7.14	9.92	13.04	10.57	8.84	8.44	11.57	3.93	6.85	7.58	2.743	3.167	8.942	9.077	9.96	10.87	6.39	2.18	10.17	10.52	9.80	11.04	11.09
Na2O	5.68	3.02	3.52	3.92	3.92	4.72	5.29	3.94	4.66	4.66	4.998	4.925	3.127	0.185	3.77	1.16	4.57	4.76	3.38	3.21	3.49	2.65	2.99
K2O	0.057	0.412	0.026	0.024	0.549	0.253	0.215	0.642	0.212	0.122	0.277	0.343	0.202	0.272	0.316	0.362	0.050	0.024	0.080	0.050	0.071	0.051	0.042
TiO2	1.663	1.345	0.838	0.900	1.105	1.156	0.849	0.514	1.479	1.345	0.383	0.392	1.716	0.350	1.349	0.187	0.299	0.489	1.714	1.801	1.754	0.966	1.034
MnO	0.209	0.200	0.164	0.166	0.142	0.158	0.519	0.509	0.179	0.174	0.132	0.136	0.230	0.124	0.166	0.118	0.184	0.117	0.206	0.193	0.174	0.157	0.188
P2O5	0.138	0.107	0.077	0.064	0.099	0.109	0.080	0.047	0.135	0.111	0.028	0.023	0.150	0.030	0.091	0.016	0.032	0.037	0.167	0.172	0.176	0.081	0.069
LOI					4.50	4.76	12.28	3.57	3.07	2.74					2.79		3.12	4.04	1.34	2.14	2.01	3.43	1.92
TOTAL	94.579	96.756	96.131	96.705	99.903	99.529	100.543	99.536	99.906	100.034	96.452	96.638	97.413	95.888	100.026	98.354	100.616	100.008	100.342	99.332	96.871	99.666	100.353
Ni	69.9	108.0	73.9	150.7	132.1	131.0	174.2	66.3	100.1	84.3	19.5	19.3	65.1	14.6	70.2	41.0	176.2	12.4	130.1	137.4	135.0	135.5	113.6
Cr	143.4	391.4	204.7	442.3	333.7	341.2	491.0	137.1	307.7	332.2	28.9	26.3	139.5	15.1	358.4	60.9	530.5	0.8	293.7	303.1	308.2	362.3	297.3
V	335.9	321.2	296.2	256.1	230.8	242.7	106.6	160.8	276.3	263.1	252.8	266.7	411.6	524.0	267.0	214.2	205.0	303.5	340.6	344.6	326.9	227.2	301.1
Sc	31.9	35.6	27.9	35.7	41.3	43.4	32.9	43.1	50.0	49.7	34.9	36.7	42.0	41.3	44.6	41.9	43.0	45.6	54.5	55.1	50.8	45.0	55.0
Cu	53.9	75.9	67.3	12.4	67.1	71.1	36.1	9.9	68.0	82.5	121.8	116.2	30.4	35.0	75.6	46.3	1.0	966.5	14.0	104.8	114.5	69.6	47.2
Zn	94.2	79.1	57.1	71.3	59.8	67.1	90.9	54.5	60.5	70.3	67.0	66.8	92.5	63.5	79.8	22.8	59.9	82.9	108.0	85.5	82.2	76.7	81.9
Sr	56.2	191.1	71.1	78.6	263.2	200.3	189.2	106.1	339.9	209.7	46.3	79.2	291.7	32.7	217.4	64.9	99.8	49.1	181.0	121.8	122.4	150.0	107.0
Rb	0	2.3	0	0	0.6	1.3	4.7	19.9	1.1	0.5	1.2	2.2	0.4	1.0	6.3	1.5	0	0	0.1	0.2	0	0	0
Zr	107.8	85.5	49.0	42.6	72.1	73.5	56.0	33.7	98.2	82.7	19.5	22.9	116.8	17.8	70.2	10.4	22.1	22.8	119.9	125.6	63.5	60.5	45.4
Nb	2.7	2.2	2.7	2.1	1.1	1.1	1.7	1.4	1.5	1.4	1.1	0.9	2.7	1.5	1.7	1.9	2.2	1.9	2.7	3.3	6.3	1.0	1.1
Ba	0	83.5	0	0	36.9	6.0	43.2	58.2	84.6	39.9	58.6	99.4	52.8	7.9	17.0	34.0	14.6	0	40.9	27.2	13.5	13.0	14.4
Pb	1.5	3.1	2.1	2.6	1.1	1.3	2.3	4.3	0.3	1.0	2.0	1.7	1.5	3.3	0	2.6	0.6	0.8	1.1	2.1	1.3	0	0
Th	0.2	0	0.3	0	0	0	0	0	0	0.2	0	0	0	0	0	0	0	0	0	0	0	0	0
La	11.5	8.5	7.7	11.9	2.1	4.2	7.6	7.2	4.0	3.5	2.1	3.3	4.4	0	3.3	0	1.6	3.6	3.2	1.4	2.8	2.1	1.4
Ce	11.6	0	8.6	0	2.5	6.3	19.4	2.4	8.2	5.4	3.1	0	9.8	0	2.0	0.9	0	0	1.9	9.5	11.9	2.5	1.8
Nd	8.9	4.0	5.3	2.5	6.0	6.0	11.4	0.5	7.4	6.6	5.1	0	7.8	0.1	6.1	1.4	0	0	5.1	7.3	11.7	5.5	4.3
Y	39.4	32.9	23.0	27.1	24.1	24.2	22.4	12.2	29.7	28.6	10.0	10.5	40.8	11.4	30.7	8.0	8.7	11.6	37.1	37.9	34.0	19.7	23.3
TiO2	9978	8070	5028	5400	6630	6936	5094	3084	8874	8070	2298	2352	10296	2100	8094	1122	1794	2934	10284	10806	10524	5796	6204
Ti/Y	253.25	245.29	218.61	199.26	275.10	286.61	227.41	252.79	298.79	282.17	229.80	224.00	252.35	184.21	263.65	140.25	206.21	252.93	277.20	285.12	309.53	294.21	266.27
Nb/Y	0.06	0.06	0.11	0.07	0.04	0.04	0	0.14	0.05	0.04	0.11	0.08	0.06	0.13	0	0.23	0.25	0.16	0.07	0.08	0	0.05	0.04
Zr/Y	2.73	2.59	2.13	1.57	2.99	3.03	2.5	2.76	3.30	2.89	1.95	2.18	2.85	1.56	2.28	1.3	2.54	1.96	3.23	3.31	1.86	3.07	1.94
Ce/Y	0.29	0	0.37	0	0.10	0.26	0	0.19	0.27	0.1	0	0	0.24	0	0	0.11	0	0	0.05	0.25	0	0.12	0.077
Zr/Nb	38.86	18.14	20.28	65.54	66.81	32.94	24.07	65.46	59.07	17.72	25.4	43.25	11.86	41.29	5.47	10.04	12	8.30	44.40	38.06	10.07	60.5	41.27

PLAGIOGRANITES

	7AD1	7AD2	7AD3	7AD5	65/89	66/89
SIO2	73.89	64.11	75.94	74.43	77.02	70.61
Al2O3	12.53	17.28	12.18	12.07	13.00	12.78
Fe2O3	1.53	1.03	1.62	2.13	3.49	4.58
MgO	1.47	1.79	1.26	2.29	0.83	0.97
CaO	2.64	5.41	2.47	1.74	3.37	2.76
Na2O	5.26	7.83	4.63	3.96	5.30	5.42
K2O	0.483	0.433	0.379	0.407	0.148	0.263
TIO2	0.404	0.659	0.498	0.542	0.411	0.515
MnO	0.033	0.021	0.015	0.025	0.030	0.035
P2O5	0.062	0.128	0.026	0.024	0.105	0.119
LOI					0.95	1.10
TOTAL	98.398	98.688	99.013	97.633	104.791	99.162
Ni	11.5	34.0	5.8	9.1	9.1	11.4
Cr	20.8	0	0	0	0.2	5.0
V	22.6	35.0	38.6	74.1	85.6	57.5
Sc	6.1	14.4	4.7	24.9	16.0	16.3
Cu	0	0	0	4.6	1.9	1.4
Zn	4.6	2.9	5.9	9.4	8.1	14.9
Sr	144.2	184.0	100.3	74.4	102.6	93.2
Rb	4.1	3.1	1.0	1.4	0	1.2
Zr	27.4	37.7	57.5	42.9	98.3	111.6
Nb	3.3	3.7	6.5	4.9	2.9	4.1
Ba	11.2	14.7	25.3	29.1	30.9	45.3
Pb	2.7	1.8	2.3	3.2	2.0	1.6
Th	0.8	0	1.6	1.6	0.1	0.8
La	0	0	0	0	0.8	4.9
Ce	12.4	15.6	11.2	6.8	4.8	2.7
Nd	3.4	10.8	2.5	0.4	4.2	4.2
Y	15.7	33.0	13.1	24.6	20.2	24.8
TIO2	2424	3954	2988	3252	2466	3090
TI/Y	154.39	119.82	228.09	132.20	122.08	124.60
Nb/Y	0.21	0.11	0.49	0.19	0.14	0.165
Zr/Y	1.74	1.14	4.38	1.74	4.86	4.5
Ce/Y	0.78	0.47	0.85	0.27	0.23	0.10
Zr/Nb	10.18	8.84	8.75	33.89	27.21	0

AMPHIBOLITES

	3.23/8	4.26/8	1.20.8	1.27/8	2.27/8	3.27/8	4.27/8	5.27/8	15/88	19/88	20/88	103/88	109/88	123/88	124/88	126/88	127/88	183'88	186/88	33'89	69/89
SIO2	47.21	43.06	49.84	48.71	45.04	42.48	46.51	48.13	49.16	50.50	45.17	50.56	45.91	49.03	47.66	47.65	45.61	44.10	38.70	54.51	42.82
Al2O3	15.68	15.21	15.24	14.72	14.97	14.98	14.57	16.23	15.73	14.48	14.24	13.95	14.94	15.04	14.66	16.47	14.22	15.94	14.63	12.75	13.73
Fe2O3	12.55	12.14	11.19	8.25	6.40	11.42	10.85	10.00	9.31	9.56	8.58	11.05	11.05	10.78	7.66	11.19	9.15	5.25	11.14	8.11	11.08
MgO	5.78	6.22	7.47	7.49	6.58	14.08	10.85	9.01	7.87	9.24	8.70	7.71	6.89	6.82	7.77	8.21	8.77	12.05	13.24	8.92	11.71
CaO	10.80	18.26	12.16	16.04	23.03	13.00	12.72	11.70	10.54	8.57	18.03	7.96	11.47	8.57	16.15	15.47	16.39	18.70	13.36	7.36	8.09
Na2O	3.71	1.12	2.09	2.31	0.28	2.02	1.94	2.90	3.41	3.47	0.65	4.50	2.88	3.53	2.23	2.39	1.76	0.48	0.82	5.24	2.97
K2O	0.86	0.61	0.31	0.55	0.10	0.13	0.67	0.34	0.49	1.15	0.23	0.50	1.14	1.85	0.30	0.35	0.17	0.01	0.05	0.119	0.210
TIO2	2.24	2.06	1.31	.85	.69	1.12	1.07	.95	1.13	1.03	.82	1.74	2.2	2	.73	1.29	.9	0.25	1.23	.657	1.613
MnO	0.17	0.18	0.16	0.16	0.23	0.17	0.17	0.15	0.14	0.16	0.15	0.15	0.15	0.15	0.14	0.16	0.15	0.11	0.18	0.148	0.171
P2O5	0.33	0.32	0.13	0.09	0.07	0.02	0.09	0.07	0.12	0.08	0.09	0.25	0.33	0.29	0.07	0.14	0.08	0	0.11	0.049	0.278
LOI																				1.92	5.91
TOTAL	99.32	99.17	99.89	99.16	97.39	99.42	99.44	99.47	97.91	98.24	96.67	98.36	96.75	98.15	97.38	103.31	97.18	96.89	93.45	99.875	96.581
Ni	80	73	111	119	149	399	169	158	156	133	173	174	104	110	134	119	115	227	337	144	321
Cr	95	124	361	409	376	722	501	424	415	472	479	423	251	250	435	390	325	705	590	483	495
V	243	235	309	254	228	276	318	290	278	273	255	215	228	215	229	319	264	166	295	216	187
Sc	28	33	45	37	20	46	44	42	40	43	37	27	26	25	34	43	38	38	47	41	28
Cu	54	20	81	58	18	121	76	55	19	81	43	111	64	42	34	30	17	17	73	55	74
Zn	111	114	85	64	62	131	82	49	66	83	68	94	94	96	57	88	46	27	78	62	76
Sr	459	129	137	145	167	65	171	256	197	455	36	252	143	222	93	137	92	74	68	122	445
Rb	10	2	6	8	1	0	9	7	5	23	4	6	15	29	4	3	1	0	0	1	3
Zr	169	129	90	49	36	34	42	44	79	85	42	136	168	165	45	80	48	12	52	28	105
Nb	24	23	5	3	4	4	4	3	3	3	3	15	25	21	3	5	2	1	4	3	23
Ba	193	77	0	115	38	45	275	22	60	456	26	408	139	257	71	29	39	21	47	39	97
Pb	1	4	1	0	4	1	1	0	2	1	2	3	2	3	3	2	2	3	1	1	0
Th	0	5	0	0	0	0	0	0	0	0	0	1	2	1	0	0	0	0	0	0	0
La	19	26	10	0	0	5	0	0	0	0	1	14	25	18	0	0	0	0	4	13	19
Ce	47	46	8	4	0	4	17	2	0	0	1	33	44	42	0	1	0	0	5	23	34
Nd	20	21	9	10	4	3	13	2	3	1	5	16	20	21	5	11	5	0	6	9	16
Y	26	26	29	21	17	24	25	24	26	24	20	21	23	21	18	29	21	7	26	19	20
TIO2ppm	13440	12360	7860	5100	4140	6720	6420	5700	6780	6180	4920	10440	13200	12000	4380	7740	5400	1500	7380	3942	9678
TI/Y	516.92	475.38	271.03	242.86	243.53	280.00	256.80	237.50	260.77	257.50	246.00	497.14	573.91	571.43	243.33	266.90	257.14	214·28	283.85	209.68	488.79
Nb/Y	0.92	0.88	0.17	0.14	0.24	0.17	0.16	0.13	0.12	0.13	0.15	0.71	1.09	1.00	0.17	0.17	0.10	0·14	0.15	0.14	1.17
Zr/Y	6.50	4.96	3.10	2.33	2.12	1.42	1.68	1.83	3.04	3.54	2.10	6.48	7.30	7.86	2.50	2.76	2.29	1·71	2.00	1.47	5.28
Ce/Y	1.81	1.77	0.28	0.19	0.00	0.17	0.68	0.08	0.00	0.00	0.05	1.57	1.91	2.00	0.00	0.03	0.00	00·0	0.19	1.22	1.73

GREENSCHISTS

	8AN5	8AN7A	8AN7B	8AN8	8AN9	8AN10	8AN11	1/89	15/89	40/89	6-27/8	1/20/8/D	22/88	1/20/8/E	1/25/D	13/24/8	85/88	131/88
SIO2	44.52	50.73	49.52	46.97	49.63	41.93	46.94	44.09	50.27	45.56	49.52	49.96	49.08	49.59	46.94	49.34	50.43	46.70
Al2O3	13.28	13.50	13.41	17.31	16.64	13.63	17.23	13.05	13.55	15.85	17.16	13.38	17.12	13.35	15.31	15.13	15.53	20.61
Fe2O3	15.80	12.13	13.42	8.97	15.89	15.06	8.48	9.59	8.95	12.13	12.40	13.19	9.20	13.06	11.80	11.58	8.11	11.13
MgO	6.40	6.38	6.00	7.66	3.41	8.97	7.10	5.44	3.44	5.92	5.89	7.12	7.58	7.30	4.40	7.63	1.81	3.44
CaO	6.43	8.14	8.63	9.19	2.82	9.19	10.97	13.75	8.64	8.62	5.55	10.87	4.51	10.87	14.01	11.62	8.57	4.57
Na2O	3.86	3.64	3.34	3.49	4.09	0.31	3.35	2.99	0.88	3.35	3.19	2.48	4.71	2.57	2.19	2.41	6.97	2.28
K2O	0.03	1.33	1.359	0.624	2.402	0.369	0.294	0.092	3.122	1.082	1.64	0.24	0.98	0.25	1.87	0.19	0.53	2.74
TIO2	2.76	1.58	1.596	1.087	1.895	1.89	1.092	1.764	.646	2.4	2.67	1.8	1.74	1.72	2.18	1.48	2.37	3.3
MnO	0.23	0.18	0.193	0.192	0.189	0.228	0.164	0.205	0.158	0.197	0.21	0.19	0.14	0.19	0.17	0.18	0.13	0.19
P2O5	0.26	0.16	0.164	0.097	0.372	0.422	0.097	0.308	0.129	0.336	0.40	0.16	0.32	0.15	0.38	0.14	0.57	0.91
LOI								8.70	9.69	2.73								
TOTAL	93.58	97.79	97.638	95.588	97.339	91.994	95.701	99.972	99.480	99.171	98.64	99.40	95.37	99.05	99.25	99.69	95.12	95.96
Ni	35	56	57	132	340	172	113	144	53	88	98	64	115	66	86	96	93	145
Cr	30	154	148	320	769	296	251	260	83	122	85	157	201	169	126	290	77	69
V	460	381	390	195	183	197	186	194	115	251	210	421	178	409	224	329	121	188
Sc	34	35	37	29	22	13	24	24	18	33	24	48	20	49	32	47	13	15
Cu	61	52	45	131	116	62	65	43	44	48	42	135	41	195	75	76	39	27
Zn	148	97	107	57	256	138	59	81	173	140	154	151	89	177	138	89	118	274
Sr	81	234	175	606	259	637	274	379	82	560	172	137	332	136	299	173	311	156
Rb	0	21	23	6	55	14	1	0.8	108	14	32	2	8	1	24	2	9	121
Zr	206	90	90	76	127	168	75	136	138	177	211	114	222	106	170	103	294	557
Nb	8	11	10	3	28	30	3	16	11	22	26	4	9	3	21	5	42	95
Ba	21	566	452	122	214	44	66	44	224	294	200	38	219	25	242	22	99	562
Pb	3	1	0	0	3	6	1	2	26	3	7	4	3	1.00	4	2	10	23
Th	0	0	0	0	0.2	0	0	0.6	12	0.6	3	0	0	0	2	0	6	16
La	19	16	16	17	31	33	10	40	34	21	33	7	13	6.00	49	7	51	119
Ce	26	17	12	15	36	58	9	43	74	48	56	3	34	7.00	38	13	96	202
Nd	17	10	11	8	16	21	7	18	34	24	32	8	19	13.00	21	5	47	91
Y	56	35	35	23	22	25	22	21	29	24	33	42	30	40	26	32	28	35
TIO2ppm	16596	9528	9576	6522	11370	11340	6552	10584	3876	14400	16020	10800	10440	10320	13080	8880	14220	19800
TI/Y	296.36	272.23	273.60	283.57	516.82	453.60	297.82	504.00	133.66	600.00	485.45	257.14	348.00	258.00	503.08	277.50	507.86	565.71
Nb/Y	0.14	0.31	0.29	0.13	1.27	1.20	0.14	0.76	0.38	0.92	0.79	0.10	0.30	0.08	0.81	0.16	1.50	2.71
Zr/Y	3.68	2.57	2.57	3.30	5.77	6.72	3.41	6.48	4.76	7.38	6.39	2.71	7.40	2.65	6.54	3.22	10.50	15.91
Ce/Y	0.46	0.49	0.34	0.65	1.64	2.32	0.41	2.05	2.55	2.00	1.70	0.07	1.13	0.18	1.46	0.41	3.43	5.77

VOURINOS

	26/88	27/88	28/88
SIO2	50.56	51.46	46.95
Al2O3	14.84	13.88	14.87
Fe2O3	11.84	11.48	12.61
MgO	6.58	6.52	7.54
CaO	7.90	9.37	10.66
Na2O	2.99	2.77	2.35
K2O	0.09	0.05	0.09
TIO2	1.43	1.24	1.28
MnO	0.13	0.16	0.18
P2O5	0.14	0.11	0.13
LOI			
TOTAL	96.50	97.04	96.75
Ni	73	67	85
Cr	151	114	181
V	362	342	362
Sc	47	48	47
Cu	76	78	65
Zn	122	90	102
Sr	160	136	193
Rb	1	0	1
Zr	90	78	90
Nb	4	4	3
Ba	59	29	43
Pb	3	2	2
Th	0	0	0
La	2	1	4
Ce	14	12	0
Nd	9	7	3
Y	35	30	33
TIO2ppm	8580	7440	8280
TI/Y	245.14	248.00	250.91
Nb/Y	0.11	0.13	0.09
Zr/Y	2.57	2.60	2.73
Ce/Y	0.40	0.40	0.00

PINDOS PERIDOTITES

	30/88	36/88	37/88	38/88	39/88	125/88	184/88	185/88	187/88
SIO2	49.04	50.24	48.88	46.94	46.73	44.36	37.06	39.43	38.36
Al2O3	16.17	15.12	14.34	15.23	11.04	1.01	16.40	0.81	1.86
Fe2O3	9.85	8.38	8.13	8.52	5.93	9.39	4.36	7.46	9.30
MgO	8.30	7.34	2.56	5.58	2.08	43.41	13.21	37.79	37.34
CaO	6.21	9.93	15.64	10.33	18.81	1.14	22.78	0.27	0.13
Na2O	4.93	4.44	3.46	4.78	3.60	0	0	0.08	0.03
K2O	0.08	0.08	0.15	0.06	0.12	0	0	0	0
TIO2	1.41	1.1	.92	1.58	.53	0.01	0.13	0.02	0.09
MnO	0.15	0.14	0.18	0.17	0.15	0.13	0.12	0.06	0.11
P2O5	0.13	0.11	0.11	0.22	0.07	0	0	0	0.01
LOI									
TOTAL	96.27	96.87	94.36	93.42	89.16	99.43	94.03	85.92	87.23
Ni	97	93	58	88	40	2548	476	2281	2151
Cr	326	316	327	266	203	2985	2506	2242	2199
V	263	216	240	229	166	80	116	32	36
Sc	32	29	29	33	14	9	21	6	8
Cu	69	29	26	68	23	14	44	0	16
Zn	69	50	68	79	48	48	29	33	41
Sr	165	287	55	88	88	3	9	8	7
Rb	1	1	3	0	2	0	0	0	0
Zr	106	96	53	144	42	0	3	1	4
Nb	2	2	2	6	2	0	1	0	0
Ba	64	53	79	52	20	32	36	0	11
Pb	2	2	3	5	3	2	1	2	2
Th	0	0	0	0	0	0	0	0	0
La	1	1	5	8	1	0	0	13	3
Ce	2	0	10	26	15	0	0	0	0
Nd	4	2	7	18	8	0	0	0	0
Y	31	25	25	33	19	2	5	1	2
TIO2ppm	8460	6600	5520	9480	3780				
TI/Y	272.90	264.00	220.80	287.27	198.95				
Nb/Y	0.06	0.08	0.08	0.18	0.11				
Zr/Y	3.42	3.84	2.12	4.36	2.21				
Ce/Y	0.06	0.00	0.40	0.79	0.79				

METASEDIMENTS

	16/88	121/88	24/88	25/88	132/88	182/88	17/88	14/24/8	1/25'C
	79.29	85.44	76.49	66.05	69.98	4.00	61.46	28.24	62.35
	10.15	6.29	9.23	15.78	14.56	1.82	17.40	8.21	16.86
	3.59	3.10	5.22	6.36	5.05	1.25	7.74	5.77	8.17
	0.94	2.17	3.32	2.17	1.52	1.35	2.47	1.92	2.40
	0.89	0.42	0.42	0.44	0.77	50.51	1.31	50.75	2.29
	1.25	0.41	0.04	0.63	0.98	0	1.32	0.16	3.69
	1.36	1.54	1.88	3.74	2.92	0.02	3.80	1.96	1.85
	0.44	0.29	0.37	0.67	0.65	0.11	0.89	0.42	1.23
	0.11	0.07	0.26	0.31	0.14	0.05	0.56	0.12	0.39
	0.25	0.04	0.07	0.13	0.12	0.02	0.19	0.07	0.43
	98.28	99.77	97.30	96.27	96.68	59.10	97.15	97.82	99.64
	30	40	61	106	36	9	85	29	80
	59	34	49	98	87	7	99	45	124
	72	48	111	141	111	11	144	65	130
	6	5	10	19	9	0	12	0	16
	21	10	101	65	41	11	83	129	114
	49	55	84	100	84	16	119	84	109
	65	34	9	18	96	1612	92	396	206
	42	37	67	129	95	0	119	73	54
	125	60	70	140	198	158	179	95	224
	8	7	8	13	10	2	30	9	34
	193	121	208	515	396	24	457	242	301
	18	10	7	16	22	0	21	14	42
	9	6	6	12	13	0	15	5	13
	17	16	16	20	12	0	35	18	45
	29	30	28	48	52	24	81	54	98
	15	11	10	17	11	16	26	28	32
	18	13	18	24	16	7	26	21	26

	1/21/8	42/88	33/88	1/23/8	18'88
SIO2	63.91	65.22	67.48	66.16	57.39
Al2O3	18.91	14.00	13.29	16.64	22.66
Fe2O3	7.74	6.86	5.88	7.05	7.96
MgO	2.03	4.28	3.04	2.78	1.97
CaO	0.92	0.85	1.40	1.27	0.38
Na2O	1.34	0.64	0.07	1.11	1.30
K2O	3.99	3.11	3.88	3.49	3.86
TIO2	0.71	0.71	0.70	0.67	0.85
MnO	0.21	0.29	0.05	0.41	0.28
P2O5	0.12	0.13	0.06	0.11	0.13
LOI					
TOTAL	99.89	96.09	95.85	99.68	96.79
Ni	84	197	53	94	62
Cr	101	225	77	110	110
V	146	137	112	165	170
Sc	20	18	12	16	19
Cu	75	69	111	113	42
Zn	123	94	82	122	94
Sr	97	12	21	116	105
Rb	137	109	133	94	137
Zr	189	121	137	132	176
Nb	24	14	15	13	14
Ba	436	376	421	597	474
Pb	36	7	5	30	32
Th	18	11	13	15	20
La	37	29	34	22	36
Ce	42	56	75	95	86
Nd	27	23	27	27	36
Y	28	24	23	25	35

BASALTS + DYKES

	55/88	56/88	57/88	147/88	181/88	204/88	218/88	219/88	233/88	234/88	11/89	17/89	18/89	25/89	28/89	29/89	30/89	42/89	45/89	46/89	47/89	50/89
SiO2	51.47	50.81	50.20	43.93	47.15	50.58	46.35	38.95	50.42	48.39	53.16	47.37	51.04	37.04	49.10	50.14	50.74	43.29	45.02	44.84	46.91	52.95
Al2O3	17.12	17.54	17.37	12.25	16.11	17.41	16.21	13.61	12.55	13.54	12.62	14.17	11.70	14.72	14.33	15.20	13.28	15.83	15.68	15.21	16.00	19.21
Fe2O3	5.09	5.52	5.74	8.25	9.63	8.14	12.90	12.33	15.26	12.95	9.82	11.93	9.56	10.94	13.20	11.69	13.22	12.68	5.19	8.08	9.88	5.07
MgO	1.55	2.18	2.22	2.82	8.34	8.05	9.34	1.39	5.51	4.59	7.74	8.02	6.40	5.32	5.38	6.33	5.71	8.71	4.92	6.70	5.63	3.11
CaO	7.80	7.11	7.62	13.32	10.00	6.96	3.40	14.81	6.48	8.51	8.30	9.98	10.88	12.86	7.61	4.68	6.66	4.62	10.62	10.69	9.16	5.98
Na2O	5.97	5.68	5.53	4.72	3.41	2.85	3.19	3.66	4.34	4.28	3.72	3.07	3.24	3.56	5.10	4.91	5.63	4.61	5.41	3.31	4.39	5.75
K2O	2.32	2.40	2.46	0.36	0.19	3.089	0.29	1.77	0.03	0.47	0.149	0.365	0.031	0.154	0.213	0.032	0.215	0.403	1.053	2.203	0.430	1.562
TiO2	0.53	0.59	0.70	1.77	1.27	1.024	2.10	1.65	2.19	2.29	0.998	1.781	1.343	1.527	2.029	2.152	2.047	2.924	1.984	1.932	2.806	2.758
MnO	0.08	0.06	0.06	0.28	0.15	0.149	0.29	0.11	0.21	0.20	0.183	0.196	0.181	1.599	0.185	0.150	0.236	0.252	0.168	0.117	0.283	0.794
P2O5	0.58	0.35	0.36	0.61	0.12	0.090	0.41	0.23	0.23	0.30	0.085	0.183	0.129	0.128	0.180	0.179	0.187	0.345	0.478	0.371	0.544	0.414
LOI						2.90					3.74	3.43	5.86	11.72	2.44	4.31	1.92	6.91	9.37	6.81	3.97	3.37
TOTAL	92.70	92.35	92.24	88.31	96.36	101.243	94.47	88.52	97.22	95.53	100.497	100.504	100.183	99.558	99.758	99.784	99.857	100.575	99.897	100.269	99.921	99.955
Ni	15	14	17	11	185	88	173	133	41	38	55.7	86.0	54.6	86.9	49.3	22.6	73.2	92.7	135.6	119.8	36.7	128.9
Cr	41	27	37	15	281	391.9	131	266	44	37	166.4	238.4	127.2	293.4	95.8	25.7	56.9	198.2	110.2	158.9	35.0	268.0
V	110	245	251	118	217	214.6	125	154	418	340	277.0	401.2	314.2	363.4	417.8	387.3	385.9	377.5	180.8	206.6	259.0	273.3
Sc	7	10	9	10	30	39.1	14	15	42	42	47.0	59.0	49.5	56.7	59.0	48.2	49.3	58.1	35.7	25.8	26.5	42.4
Cu	27	4	5	24	66	74.1	60	13	58	22	88.1	59.0	47.7	58.1	15.2	44.4	57.3	39.9	33.0	39.57	49.6	78.7
Zn	46	60	62	77	72	64.8	124	94	126	119	76.3	108.4	90.3	93.2	119.4	99.1	119.0	93.1	68.8	71.0	90.5	158.6
Sr	86	135	136	222	268	295.0	262	229	105	179	136.2	189.7	81.5	119.7	135.3	108.5	204.4	188.6	175.2	242.7	305.7	235.8
Rb	50	46	47	7	3	96.9	4	52	0	9	0	6.1	0	0.6	2.9	0	2.9	3.1	6.6	9.9	2.2	26.4
Zr	149	159	157	243	90	58.0	212	122	132	142	58.8	113.3	83.8	87.1	132.1	139.2	133.1	216.4	306.1	201.2	323.6	282.5
Nb	15	16	15	45	5	1.3	29	13	12	13	1.7	5.1	4.3	0.9	2.3	2.5	2.5	7.4	11.9	9.8	15.1	9.7
Ba	36	40	50	92	41	373.8	171	189	53	69	36.1	82.4	20.2	160.2	58.7	30.4	63.2	89.3	84.3	99.5	81.0	164.7
Pb	4	4	4	5	2	0	5	3	2	2	0.1	0.4	1.4	3.8	1.0	1.0	0	3.1	2.8	0	0	3.4
Th	5	4	4	5	0	0	3	0	0	0	0	0	0	0	0	0	0	0	0.3	0	0	0
La	30	18	17	44	4	3.4	22	13	13	13	1.4	6.4	2.7	6.6	4.8	6.7	4.8	11.8	18.8	8.3	20.8	16.4
Ce	63	39	48	85	0	2.2	47	31	18	22	0	12.2	5.2	17.1	10.9	10.1	7.9	34.1	47.6	31.3	52.7	34.3
Nd	34	25	23	36	7	5.1	25	16	14	16	0	10.2	8.6	8.3	11.4	12.0	10.1	18.7	27.0	19.6	32.0	28.0
Y	40	30	30	29	22	22.5	26	17	41	45	23.3	43.0	29.0	30.9	47.7	50.1	51.3	40.3	35.6	33.1	53.0	53.3
Ti ppm	3780	4140	4200	10620	7620	6144	12600	9900	13140	13740	5988	10686	8058	9162	12174	12912	12282	17544	11904	11592	16836	16548
Ti/Y	94.50	138.00	140.00	366.21	346.36	273.07	484.62	582.35	320.49	305.33	257.00	248.51	277.86	296.50	255.22	257.72	239.42	435.33	334.38	350.21	317.66	310.47
Nb/Y	0.38	0.53	0.50	1.55	0.23	0.06	1.12	0.76	0.29	0.29	0.07	0.12	0.15	0.03	0.05	0.05	0.05	0.18	0.33	0.30	0.28	0.18
Zr/Y	3.73	5.30	5.23	8.38	4.09	2.58	8.15	7.18	3.22	3.16	2.52	2.63	2.89	2.82	2.77	2.78	2.59	5.37	8.60	6.08	6.11	5.30
Ce/Y	1.58	1.30	1.60	2.93	0.00	0.10	1.81	1.82	0.44	0.49	0.00	0.28	0.18	0.55	0.23	0.20	0.15	0.85	1.34	0.95	0.99	0.64

GABBROS

	52/89	85/89	86/89	87/89	82A/89	102/89	124/89	21/88	22/88	75 88	76/88	148/88	149/88	150/88	151/88	192/88	193/88
SIO2	47.84	47.85	48.53	47.35	47.69	45.82	44.83	47.40	49.08	47.10	47.15	47.80	43.00	47.30	40.67	45.32	50.17
Al2O3	17.10	13.82	13.81	14.01	13.63	14.80	16.63	15.87	17.12	16.18	16.55	13.76	13.51	13.29	14.96	16.68	18.19
Fe2O3	7.57	8.99	10.43	11.17	9.60	10.58	15.49	10.31	9.20	10.83	10.68	10.91	10.82	10.63	11.89	9.58	5.31
MgO	5.22	5.47	7.46	7.90	8.36	5.89	2.55	8.33	7.58	9.17	8.50	4.88	4.67	4.52	2.41	4.92	3.73
CaO	7.18	9.57	12.58	9.71	12.84	8.71	8.44	5.11	4.51	6.85	7.05	6.70	9.41	8.67	10.75	7.57	11.39
Na2O	4.86	5.76	3.11	4.71	2.82	4.52	4.74	4.17	4.71	3.61	3.58	4.44	4.41	4.66	5.46	5.90	4.12
K2O	1.642	0.283	0.251	0.424	0.089	1.523	0.150	0.88	0.98	0.44	0.52	0.14	0.14	0.05	0.06	0.18	0.19
TIO2	1.784	1.216	0.893	1.334	1.256	1.952	2.769	2.00	1.74	0.85	0.88	1.50	1.51	1.54	1.36	1.47	0.77
MnO	0.284	0.139	0.133	0.202	0.167	0.266	0.270	0.15	0.14	0.18	0.18	0.49	0.59	0.54	0.74	0.13	0.10
P2O5	0.531	0.188	0.109	0.108	0.126	0.241	0.364	0.29	0.32	0.05	0.06	0.15	0.16	0.15	0.47	0.38	0.07
LOI	5.26	7.20	2.77	3.50	2.07	6.93	3.28										
TOTAL	99.374	99.476	100.065	100.423	98.644	101.240	99.520	94.51	95.37	95.26	95.15	90.77	88.21	91.34	88.78	92.13	94.15
Ni	103.1	154.2	96.2	46.6	124.3	69.4	78.0	88	115	272	206	51	73	72	11	155	55
Cr	170.8	267.7	236.1	95.3	275.8	95.9	78.4	228	201	360	277	203	206	207	3	176	175
V	189.8	202.8	324.3	308.2	287.5	307.7	513.6	209	178	168	171	259	292	313	93	83	143
Sc	29.1	41.5	55.1	57.5	55.5	59.7	64.1	28	20	27	25	32	32	35	19	12	21
Cu	19.1	61.5	0	90.1	1.2	82.1	43.6	39	41	100	100	33	51	46	36	43	37
Zn	58.2	71.6	29.9	80.3	51.8	107.0	195.9	93	89	70	69	75	86	66	96	80	40
Sr	442.7	123.1	344.1	105.1	128.6	205.4	210.8	290	332	648	622	218	266	216	92	529	157
Rb	51.8	2.0	1.6	4.1	0	10.6	2.6	7	8	5	6	4	4	0	1	1	1
Zr	190.1	92.1	31.1	77.1	57.6	160.0	171.7	189	222	104	104	125	127	122	154	210	67
Nb	98.6	9.1	2.9	1.2	5.6	7.4	14.1	8	9	2	1	4	4	4	8	29	2
Ba	670.7	42.0	48.5	87.5	28.5	243.0	51.2	175	219	75	90	1491	134	134	66	319	15
Pb	5.7	1.5	0	0.1	1.0	0.3	0	1	3	1	1	2	3	4	17	3	3
Th	16.1	0	0	0	0	0	0	0	0	0	0	0	0	0	1	1	0
La	115.6	8.0	2.6	4.2	5.5	8.0	10.2	10	13	0	4	9	7	3	13	29	2
Ce	178.6	20.9	4.2	0	11.8	18.8	20.3	40	34	4	7	17	20	15	33	48	3
Nd	50.9	10.9	4.6	4.6	8.7	15.2	14.6	21	19	4	3	12	13	5	26	24	5
Y	24.6	22.6	20.8	30.3	24.9	35.8	52.2	28	30	21	22	31	34	32	55	20	13
Tl ppm	10704	7296	5358	8004	7536	11712	16614	12000	10440	5100	5280	9000	9060	9240	8160	8820	4620
Tl/Y	435.12	322.83	257.60	264.16	302.65	327.15	318.28	428.57	348.00	242.86	240.00	290.32	266.47	288.75	148.36	441.00	355.38
Nb/Y	4.01	0.40	0.14	0.04	0.22	0.21	0.27	0.29	0.30	0.10	0.05	0.13	0.12	0.13	0.15	1.45	0.15
Zr/Y	7.73	4.08	1.50	2.54	2.31	4.47	3.29	6.75	7.40	4.95	4.73	4.03	3.74	3.81	2.80	10.50	5.15
Ce/Y	7.26	0.92	0.20	0.00	0.47	0.53	0.39	1.43	1.33	0.19	0.32	0.55	0.59	0.47	0.60	2.40	0.23

APPENDIX 6: X-ray diffraction techniques

1) Standard X-ray technique for clay mineral identification

Standard X-ray diffraction techniques were carried out on fine-grained sedimentary rocks. A fully automated Philips PW 1808 diffractometer was utilised during the study, which additionally has a computer based databank of several thousand different clay minerals and organic compounds. Scans were taken from 2 to $40^{o}\theta$, using a Cu K alpha source. A small fraction of rock was crushed with a pestle and mortar with a little acetone, and then pipetted evenly onto a glass slide. The slide was then placed into the sample loading system of the diffractometer and automatically measured. Results were transferred automatically to the data storage system. The diffractogram was then called to the computer screen, and the trace compared to the best fit produced from the databank. A further manual comparison with the peaks produced was also undertaken, especially where poor initial matches were produced.

2) Illite "crystallinity" evaluation technique

a) Preparation

Samples were initially broken up in a jaw crushing mill. The aim of the following steps was to produce a sample of consistent grain size, which otherwise may influence an effect on the measured crystallinity. The crushed material was then placed in the bottom of a test tube, and filled up near to the top with distilled water. This was then centrifuged for 2 minutes at 2000 revolutions per minute. Clays in suspension were then pippeted from the top of the tube, and placed into another tube, and the process repeated. The material remaining at the base of this tube was then pipetted onto glass discs and measured.

b) Running conditions

Samples were placed into the Philips automated diffractrometer. The samples were scanned from $7\text{-}22^{o}\theta$, at steps of $0.2^{o}\theta$ (total running time 25 minutes per sample). All diffractograms were produced as hard copies using a

a standard plotter. A pure quartz standard was run at the beginning and end of the measuring of samples.

c) Method

The illite peaks at 10 A were measured by hand on the hard copy, and corrected to the standard using the technique of Weber (1972). This defines an illite crystallinity parameter Hb_{rel}, where Hb is the height at half width of the peaks concerned:

$$Hb_{rel}=\frac{Hb\ (001)\ illite\ x\ 100}{Hb\ (100)\ quartz}$$

A number of samples contained indistinct illite peaks or no illite, and were disregarded. All the data used had distinct single peaks at 10 A. This data was then plotted on a locality basis.

APPENDIX 7: Radiolarite extraction and sample localities

1) Radiolarian extraction from siliceous rocks

Most of the collected samples were impure radiolarian cherts, usually highly siliceous and hard. The samples collected were initially screened in the field to establish the presence of radiolaria. They were then crushed in the laboratory into small chips (approximately 1 cm diameter), and placed in polythene beakers. The carbonate rich samples were then subjected to a weak solution of HCl, and left to react for several days, to remove any excess carbonate present on surfaces or in veins. Next, the samples were washed, and then subjected to HF solutions of decreasing concentration, starting at 10% for a few hours, followed by removal and addition of progressively more dilute acid over longer time periods (5% for a day, 2% for two days, 1% for 4 days; P. De Wever, pers. comm. 1988). After three or four treatment stages, the acid was neutralised by successive decanting, and the residue sieved through coarse and fine sieves (300 mesh and 70 mesh), and finally the material collected was washed into small containers. The residue was then pipetted onto a glass slide, dried, and individual specimens picked using a 000 sable paint brush.

The specimens collected were picked onto metal stubs, which were then gold coated and studied under a scanning electron microscope (Cambridge Instruments), at the Department of Botany, University of Edinburgh. A photographic record of the best preserved specimens was obtained.

Description of the localities sampled for radiolaria

1) Aspropotamos Bridge, Perivoli Village

Localities: A melange block, situated 15 m to the west of the Aspropotamos River bridge, immediately east of Perivoli Village (samples 22+23/23/8), and tectonic slices of radiolarite between basalts, 500m north of the bridge (samples 20+21/23/8).

General tectonic position: Thin (<20m) thrust slices of melange, imbricated tightly with Cretaceous and Tertiary flysch beneath the overthrust ophiolitic lithologies, mainly serpentinite, exposed on Kodro Mountain to the immediate east.

Lithologies: The melange block exposes some 30 m^2 of interbedded ophiolitic turbidites and radiolarite, and samples were collected from a horizon at the top of the measured sequence. The associated turbidites are composed of large volumes of altered serpentinite, gabbro, basalt, and reworked radiolarian chert clasts, and range from fine rudite to siltstone grade. The thin (approx 1 m) radiolarite interbeds yielded the fauna.

2) East of Perivolaki Village

Locality: Exposed melange sequence to the north of the Potamouli River, 2 km east of Perivolaki Village (sample 200/D/88).

General tectonic position: Large scale (1 km+) northwesterly-plunging fold within the melange, in tectonic contact with Tertiary Pindos Flysch. The sampled section froms part of a locally folded and thrust turbidite and pelagic sedimentary sequence, which is, however relatively coherent over several hundred metres.

Lithologies: The base of this sequence exposes folded radiolarite with interbeds of continentally-derived (quartz and white-mica) rich siltstones and shales (see Chapter 4). These pass upwards sharply into volcaniclastic turbidites, which show layer parallel extension of the fine rudite and arenite horizons. These turbidites include interbeds of hemipelagic black shale, manganiferous mudstone, and towards the top of the sequence, radiolarite. Two well-defined radiolarite horizons are present (approximately 3 m thick and 6 m thick respectively), the uppermost horizon of which yielded the radiolarian fauna.

3) Venetikos River valley

Localities: 1 km north of the confluence of the Aspropotamos and Veneticos Rivers, and 25 m north of the confluence.

General tectonic position: The radiolarites occur as thin (up to 8 m) thrust-bounded packets which are isoclinally folded, thrust imbricated and low-grade metamorphosed (samples 143, 144, 145/88). Sample 1/20/8/A was collected from a metamorphosed and folded radiolarite-marl sequence, imbricated between basalts. This locality is situated some 600 m S. of the previous locality. These radiolarites are interpreted as being part of the greenschist-facies metamorphic sole of the Pindos ophiolite.

Lithologies: Well-bedded, dark-red radiolarites, exposed together with greenschist-facies metamorphosed basalts (MORB and WPB; Jones and Robertson 1990) red-brown haematitic shales and pink, nodular ammonitico-rosso-type carbonates. These sediments were originally overlying the basalts.

4) Milea-Metsovo Road

Locality: 10 km southwest of Milea village, roadside section on the Metsovo road (samples 100/88+107/88).

General tectonic position: Block-in-matrix tectonic melange, beneath a transgressive cover sequence.

Lithologies: Sample 100/88 was collected beneath a cover of Calpionellid limestone, which transgresses the melange at the southern extremity of this locality (Jones and Robertson 1990). The individual melange radiolarite blocks are associated with fine grained clastic sediments, quartzose turbidites, basalts and gabbros. At the northern end, further blocks of radiolarite (sample 107/88) occur beneath a thrust separating the Calpionellid limestone from the melange.

5) Kandila Hillside and Liagkouna

Localities: 1 km north of the mountain of Liagkouna, on the southwestern slopes of Kandila hill, 50 m northwest of the Perivoli-Grevena road (60/88), and on the northwest slopes of Liagkouna itself.

General tectonic position: The radiolarites (sample 60/88) are considered to be part of a melange turbidite sequence, which is quite extensively exposed in the Liagkouna-Kandila area. These turbidites are tectonised and locally poorly exposed.

Lithologies: Bedded radiolarite blocks (6 m-thick), found as a disrupted but laterally continuous (over 20 m) sequence. The exact nature of the contact with adjacent basalt and limestone-rich rudites, shales and carbonate blocks is unknown.

6) Kodro Mountain

Locality: Kodro Mountain, situated immediately east of Perivoli village (sample 120/88). Sample was colected on the southeast side of the mountain, 200 m southeast of the church, at a roadside exposure.

General tectonic position: Imbricate thrust slices of the major tectonic units above a postulated basement thrust ramp.

Lithologies: Carbonate and siliciclastic turbidites and hemipelagic sediments of the Dio Dendra Group are found in tectonic contact with a tectonic slice of radiolarite (4 m thick).

7) Kokkina Litharia

Locality: Roadside exposure, 6 km along the Perivoli-Mikrolivado road, on the north side of the Aspropotamos River valley (samples 8+9/24/8).

General tectonic position: Extensive thrust sheets of melange on the north west limb of a synform.

Lithologies: A sequence of melange basalts, redeposited limestones and shales are locally layer-parallel sheared and disrupted. At the easterly end of this locality, thrust slices of radiolarite appear, before a major contact with deformed continentally-derived, sandstone-shale turbidites.

8) Megali Pedias

Locality: Aspropotamos River valley, at Agios Nikolaos church, 4.5 km east of Perivoli village (sample 25/23/8).

General tectonic position: Core of the Perivoli corridor, a complex NE-SW-trending antiformal stack

Lithologies: Several large blocks of basalt, limestone and radiolarite within a block-in-matrix melange. The radiolarite block is spatially associated with a large carbonate turbidite block.

9) Armata-Dhistraton Road

Locality: East of the village of Armata, in the north central part of the mountains. Roadside exposure of several metres of pure radiolarite.

General tectonic position: Thrust slices of melange, beneath thick ophiolitic peridotite.

Lithologies: Associated with basalts, basalt breccias and locally, sheeted dykes (MORB-type).

10) Tsouka, S.W. Vovousa

Locality: Mountain located northwest of the Vovousa-Elatochorion road, 7 km SW of Vovousa.

General tectonic position: Extensive melange, and thin Cretaceous flysch thrust sheets, partly internally deformed, overlying the Pindos flysch.

Lithologies: The radiolarites occur as interbeds and overlying, pillowed and massive basalts, which pass downwards into dyke swarms. The dykes locally intrude the cover sediments. A wide variety of carbonate and siliciclastic units are present overlying this basement,

APPENDIX 8: LOCALITIES FOR CHEMICALLY ANALYSED ROCKS

A) Loumnitsa Unit metamorphic rocks

1) Amphibolites and greenschists

3/23/8500 m N.E. of Avdella Village.
18/23/8/ as above

4/26/8 Aoos Valley, 12 km N.W. of Perivoli.

1/27/8 N. side of Kodro Mountain.
2/27/8 as above
3/27/8 as above
4/27/8 as above
5/27/8 as above
6/27/8 as above

1/20/8/D Venetikos/Aspropotamos river confluence.

15/88 N.W. side of Liagkouna Mountain.
19/88 as above
20/88 as above
22/88 as above

186/88 S.W. side of Liagkouna Mountain.
183/88 as above

103/88 Roadside 800m south of Milea Village.
109/88 as above

123/88 E. side of the Loumnitsa Valley.
124/88 as above
126/88 as above
127/88 as above

33/89 100m W. of Padhes Village.

69/89 Venetikos Valley, 500m N of the confluence with the Aspropotamos River.
8AN5 as above
8AN7A as above
8AN7B as above
8AN8 as above
8AN9 as above
8AN10 as above
8AN11 as above

1/89 Olistostrome clast, 1 km S.W. of Alatopetra Village.

ɔ

15/89 250m N.W. of Agios Georgios, 5 km S.W. of Samarina.

40/89 E. side of Vassilitsa Mountain, near the ski centre.

1/20/8/D Agios Nikolaos Church, near Venetikos River.
1/20/8/E as above
13/24/8 as above

1/25/D Isomata Mountain, 5 km W. of Perivoli Village.

85/88 Korydhalos, N.W. of Panaiya Village, E. of Metsovo.

131/88 S.W. Selloma Lakkou.

2) Pindos Ultramafic rocks

125/88 E. side of the Loumnitsa Valley.
184/88 as above
185/88 as above
187/88 as above

3) Pindos metasediments

16/88 N.W. Liagkouna mountain.
17/88 as above
18/88 as above

1/25/C Isomata Mountain, 5 km W. of Perivoli.
121/88 as above

1/23/8 500m N.E. of Avdella Village.
18/23/8 as above

132/88 Selloma Lakkou.

14/24/8 Agios Nikolaos Church, near Venetikos River.

182/88 Klefi Potelamos, 6 Km N.W. of Perivoli.

1/21/8 N. side of Kodro Mountain.

4) Vourinos metabasites

26/88 3 km N.E. of Zavordas Monastery.
27/88 as above
28/88 as above

30/88 Aliakmon River bed, 3 km E. of Zavordas.
36/88 as above

37/88 Agios Nikolaos Valley, 5 km N.W. of Chromion.
38/88 as above
39/88 as above

5) Vourinos Metasediments

24/88 200m N. of Zavordas monastery.
25/88 as above

42/88 Agios Nikolaos Valley, 4 km N.W. of Chromion.

33/88 Aliakmon River valley, 3 km E. of Zavordas Monastery.

B) Avdella Melange basic rocks

1) Basalts

55/88 100m S.W. of Alatopetra Village.
56/88 as above
57/88 as above

147/88 S. side of Liagkouna Mountain.

181/88 Klefi Potelamos, 6 km N.W. of Perivoli Village.

204/88 3 km S.W. of Alatopetra Village.

218/88 Dio Dendra Valley.
219/88 as above

11/89 N.W. of Agios Georgios, S. of Samarina.
17/89 as above
18/89 as above

25/89 W. side of Smolikas Mountains, at Polis.
28/89 1 km N.W. of Armata Village.
29/89 as above
30/89 as above

42/89 Tsouka Mountain, 7 kms S.W. of Vovousa (basalt).
45/89 as above (basalt)
46/89 as above (dyke)
47/89 as above (dyke)
50/89 as above (basalt)
52/89 as above (basalt)

85/89 150 m N. of Aspri Petra.

86/89 S.W. side of Kandila.
87/89 as above

82A/89 100 m N.W. of Alatopetra Village.

102/89 W. side of Stragopetra Mountain.
124/89 as above
233/88 as above
234/88 as above

2) Melange gabbros and coarse-grained basalts

21/88 N.W. Liagkouna Mountain.
22/88 as above

75/88 500m N.E. of Avdella Village.
76/88 as above

148/88 S. Liagkouna mountain, N. side of Aspropotamos River.
149/88 as above
150/88 as above
151/88 as above

192/88 Agios Nikolaos Church, near Monahiti.
193/88 as above

C) Aspropotamos complex

1) Dykes

7SP2 Track 2 km west of Spileo Village.
7SP4 as above
7SP6B as above
7SP10 as above
7SP11 as above
7SP13 as above
7SP14 as above
7SP15 as above
56/89 as above
60/89 as above
62/89 as above

106/89 3.5 Kms W. of Zakas, road to Perivolaki.
107/89 as above

77/89 5 kms S.W. of Zakas, main road to Perivoli.
78/89 as above
79/89 as above
80/89 as above

7VE15 S. of Aspropotamos-Venetikos confluence.

7AD8 S.W. of Avdella Village, road to Perivoli.

2) Basalts

57/89 Track, 2 km W. of Spileo Village.
58/89 as above
61/89 as above
63/89 as above
64/89 as above

108/89 Roadside 1.5 km W. of Zakas Village.

86/A/89 200 m S. of Paroreio Village.

87/A/89 S. of Venetikos bridge at Trikomon.
88/89 as above

188/A/88 150 m E. of Venetikos bridge at Trikomon.
189/A/88 as above
190/A/88 as above
191/A/88 as above

89/89 25 m N. of Venetikos bridge at Trikomon.
90/89 as above

92/89 1.5 km W. of Venetikos bridge, Trikamon-Monahiti road.
93/89 as above

67/89 Stream section, W. side of Krania village.
68/89 as above

7VE2 300 m South of the Venetikos-Aspropotamos confluence.
7VE4 as above
7VE7A as above
7VE29 as above

7VE36 At the Aspropotamos Venetikos confluence.
7VE37 as above

7AV3 5 km N. of Vovousa, Aoos River valley.
7AV13 as above
7AV16 as above
7AV18 as above
7AV20 as above
7AV22 as above

53/89 6 km S. of Vovousa, road to Elatochori.
54/89 as above

33/A/89 1 km E. of Armata Village.
35/89 as above

38/89 3 km E. of Armata, Dhistraton road.
39/89 as above

97/88 Katara Pass, roadside 3 kms E. of snow station.
98/88 as above
99/88 as above
99/A/88 as above

70/89 1 km S.W. of Malakasia Village, Katara Pass.

95/89 1.5 km S.W. of Avdella Village.

96/89 4 kms S.W. of Avdella Village, Avdella-Perivoli Rd.

3) Plagiogranites

7AD1 500 m S of Avdella Village, Avdella River.
7AD2 as above

7AD3 1.5 kms S.W. of Avella, road to Perivoli.
7AD5 as above

65/89 2 kms W. of Spileo Village.
66/89 as above

APPENDIX 9 Cathodoluminescence microscopy

Cathodoluminence studies are based on the emission of light from any given material due to bombardment by electrons. Energy from impacting electrons excites one or more electrons in the atom to a higher energy level. The return of this electron to its original energy level results in the emission of a given quantity of energy as electro-magnetic radiation (observed as visible light in this case).

Upon excitation by an electron beam, it is sites of crystal imperfection which are most liable to absorb energy from the beam and luminesce, rather than the adjoining lattice. Such luminescent centres come in two varieties; (a) Intrinsic, i.e. irregularities in the lattice independant of composition, (b) extrinsic, which are impurity related defects in the lattice.

Electrons were produced from a cold cathode (tungsten/steel) source to which a voltage of up to 30 kV was applied relative to a collimated anode, a hole in which provides the source of the electron beam. A Nuclide Corporation ELM-2B Luminoscope was utilised, in which an electron beam, of 0.7-0.9 mA current was accelerated to 13-14 kV and fired horizontally into a sealed chamber, under partial vacuum (0.55-0.95 millitorr), into which the specimen was placed. The beam was then deflected on to the specimen by the action of two, adjustable, permanant magnets. The specimen was viewed using a Nikon Optiphot microscope fitted with a FX 35WA camera and Nikon microflex UFX-II photographic operating system. Double polished thin sections were used, as the partial vaccuum means there are always sufficient positive ions in the vicinity of the specimen to prevent it from acquiring a space charge.

APPENDIX 10 Scanning Electron Microscopy

A *Cambridge* scanning electron microscope (S90B), was used for study of radiolaria at high magnifications. The samples were mounted on stubs, and then sputter coated with gold prior to observation. They were then bombarded under a vaccuum and viewed remotely with a monitor. Photographs were taken from the video image using a Nikon camera.

APPENDIX 11

AVDELLA MELANGE

LOCALITY	SAMPLE NO.	LITHOLOGY	FAUNA	AGE
Aghios Nikolaos (200m NW of church)	11/24/8/An	oosparite	Protopeneroplis striata Thaumatoporella sp. Nauticolina sp. Textularidae	Dogger-Malm
	12/24/8/An	oobiosparite overlying basalts		
(1.5 Km NW of Monahiti)	97/89	oobiosparite interbedded with radiolarites	Labyrinthia sp. Protopeneroplis striata Cayeuxia sp. Valvulinidae	?Dogger-Malm
Alatopetra (W of village)	9/25/8	Nodular, fine grained lst. from hardground	Nodosaria sp. Ammonoidea	Late Triassic
	232/88 233/88	Redeposited and calci-rudite overlies above	Sigmolinia sp. Labyrinthia sp.	Liassic?
	84/88	Pink lst	Halobia? sp Radiolaria	Late Triassic
Aspri Petra	81/89	Fine redepo-sited calcirudite from olistolith	Algae	Late Triassic
Avdella (0.5 Km NE)	16/23/8	Nodular haematitic carbonate	Halobia, Radiolaria	Late Triassic

Dovas	4/88	Fine calc-arenite from large lst olistolith	Thaumatoporella sp, Radiolaria	Late Triassic
Kalivia Kerasias	242/88	Oobiosparite	Cladocoropsis mirabilis Salpingoporella sp. Thaumatoporella sp. Valvulinidae	Dogger-Malm
Kokkina Litharia	152/88	Biomicrite	Daonella sp. Halobia sp. Radiolaria	Late Triassic ,,
	220/88	Biomicrite,	Radiolaria	Late Triassic
	221/88	Biomicrite	Radiolaria	Late Triassic
Liagkouna (NW side)	77/88, 78/88 79/88	Calcirudites with rare mafic, detritus in conformable turbidite	Duostomina sp: derived Miliolipora sp: '' Brachiopoda Bivalvia	Late Triassic?
	82/88	Calcarenite, found as a clast in a turbidite sequence	Protopeneroplis Cayeuxia moldavica Pianella sp.? Textularidae	Dogger-Malm
(SW flanks)	137/88 138/88 139/88	Calcilutite '' ''	Radiolaria Halobia? Radiolaria	Late Triassic ''

	140/88	Calcarenite, overlies above	Radiolaria	,,
Panaghia, Nr Metsovo	71-73/89	Biosparite, biomicrite from olistolith	Miliolipora cuvillieri Stromatolites Brachiopoda	Late Triassic (Nor-Rhaet)
Tsouka Rossa (SW of Vovousa)	44/89	Biomicrite	Posidonia sp.? Radiolaria	Liassic?
	51/89	Biomicrite	Posidonia?	Liassic?

DIO DENDRA GROUP

LOCALITY	SAMPLE NO.	LITHOLOGY	FAUNA	AGE
Katara Pass (Krevvati Formation)	93/88	Pink biomicrite	Globotruncana stuartiformis?	Sant-Maastr
	94/88	''	Globotruncana stuarti?	Camp-Maastr.
	96/88	''	Globotruncana stuarti	Camp-Maastr.
Megali Pedias (Krevvati Formation)	1/24/8	Pink biomicrite	Globigerinelloides sp.	Alb-Maastr.
	2/24/8	Blue-grey calcarenite clast in debris flow	Globotruncana gr. linneana	Camp-Maastr.
	129/88	Pink laminated biomicrite	Globotruncana sp.	Senon.
Panaghia (Krevvati Formation)	4/30/A	Calcirudite	Rudists Corals	Late Cr.
	209/88	Biosparite	Rudists	''
	213/88	Biomicrite	Globotruncana sp. Globotruncanita sp.	Senon.
	214/88	Biomicrite	Globotruncana sp. Globotruncanita sp.	''
	99/89	Calcirudite	Rudists	Late Cr.

Zygourogreko (Krevvati Formation)	169/88	Laminated micritic lst	Radiolaria	Late Cr.
	170/88	Calcarenite with basalt and chert	Red algae	,,
(Zygourogreko Formation)	171/88	Biomicrite	Globogerinelloides sp.	,,

ORLIAKAS GROUP

LOCALITY	SAMPLE NO.	LITHOLOGY	FAUNA	AGE
Agios Dimitrios (Monahiti)	98/89	Biomicrite	Miliolidae Rudists	Late Cr.
Milea (Metsovo Rd)	111/88	Calcareous arenite, from olistolith block	Orbitoides? sp.	Camp-Maastr.
Monahiti (Aghios Nikolaos Rd)	2/3/8/D	Calcirudite, with basalt and chert clasts	Miliolidae Globotruncana sp. Neoiraqia sp?:-derived Orbitolina sp:-derived	Senon.
	2/3/8/G	Calcarenite with basalt and chert clasts	Globotruncana sp. Globigerinelloides sp. Rudists	Senon.
Skourtza	5/89	Biosparmicrite from olistoliths	Orbitoides sp. Halimeda sp Ostracoda Gastropoda	Camp-Maastr.
	6/89	Calcirudite	Rudists Miliolidae	Late Cr.
	7/89	Biosparmicrite	Halimeda sp. Leptorbitodes sp.	Camp-Maastr.
	8/89	Biomicrite	Rudists	Late Cr.
Spileo	108/89	Calcirudite	Rudists	''